Functional Analysis of the Rac-Binding Protein POSH

Anne Louise Bishop

A thesis submitted to the University of London
for the degree of Doctor of Philosophy

April 2001

MRC Laboratory for Molecular Cell Biology
University College London
Gower Street
London WC1E 6BT

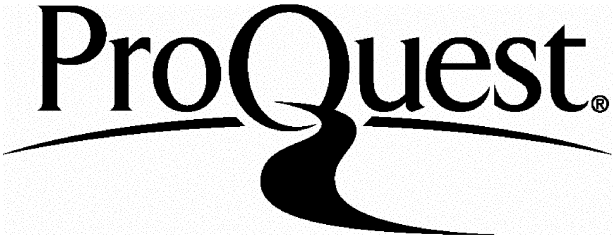

ABSTRACT

The scaffold protein POSH (Plenty of SH3s) was discovered to be an effector for the GTPase Rac using the yeast-two-hybrid system. Rac regulates numerous cellular processes including actin reorganisation and the control of gene transcription (JNK and p38 MAP kinase pathways and NF-κB and SRF transcription factors). It was previously shown that POSH, like Rac, is able to activate both JNK and NF-κB. Unlike Rac, POSH was also shown to induce apoptosis when over-expressed. The induction of apoptosis by POSH provided the starting point for the functional analysis of POSH described in this thesis.

Data is presented here showing that the Rac-binding domain of POSH contributes to apoptosis, by inhibiting Rac, and that activated Rac rescues POSH-expressing cells by providing a survival signal that is independent of binding to POSH. The whole of the N-terminus of POSH (containing two SH3 domains and a RING finger) was also found to be required, in addition to the Rac-binding domain, for POSH-induced apoptosis. Investigation of the binding partners for POSH N-terminus revealed that the major binding partner was dynamin, a GTPase required for endocytosis. The two N-terminal SH3 domains of POSH were sufficient and necessary for binding of POSH to dynamin and POSH constructs containing this region inhibited endocytosis, suggesting both a physical and a functional link between POSH and dynamin. The RING finger of POSH was essential for apoptosis and increased the potency of POSH inhibition of endocytosis. Initial data suggests that POSH, like many other RING finger-containing proteins, is itself ubiquitinated and may be involved in the ubiquitination of other, as yet unknown, protein substrates.

Overall, the data presented here suggests the existence of a novel POSH-dependent link between Rac activity and endocytosis (or another less well characterised dynamin-dependent process), which is regulated by ubiquitin-dependent protein degradation.

TABLE OF CONTENTS

TABLE OF FIGURES

CHAPTER 1
INTRODUCTION

This thesis describes the characterisation of a protein named POSH (plenty of SH3s) first identified as a binding partner for the small GTPase Rac. The introduction to this thesis, therefore, covers: (1) the Ras superfamily, of which the Rho family is a part; (2) the Rho family, of which Rac is a member, the general characteristics of these GTP-binding proteins, their regulators and their interactions with effector proteins; (3) the specific functions of Rac and Rac-binding proteins that may mediate these functions; (4) the information already available about POSH itself. Results presented in this thesis suggest that POSH not only binds to Rac, but also to dynamin, a much larger GTPase that is essential for the regulation of endocytosis. Finally, therefore, the introduction ends with a description of endocytosis in general and the specific roles that dynamin and its binding partners are thought to play.

1.1 THE RAS SUPERFAMILY OF GTP-BINDING PROTEINS

Ras proteins were first identified as the transforming principal of two murine retroviruses, Harvey Sarcoma Virus and Kirsten Sarcoma Virus (reviewed in [Olson, 2000]). Human cellular homologues of these viral proteins were subsequently identified (Ha-Ras and Ki-Ras) as well a third member of the family, named N-Ras [Hall, 1983]. Ras proteins function as monomeric 20-30kDa GTP-binding proteins, which cycle between an active GTP-bound form and an inactive-GDP-bound form [Bos, 1989]. This cycle is regulated by GTPase activating proteins (GAPs), which accelerate the slow intrinsic GTPase activity of Ras, and Guanine nucleotide exchange factors (GEFs), which catalyse exchange of GDP for GTP (discussed below).

In the active state Ras proteins exert their cellular effects by interacting with effector molecules. Structural analysis and mutational studies have revealed that a region of Ha-Ras between amino acids 30-40 is essential for its GTP-dependent interaction with effector proteins (reviewed in [Wittinghofer, 1996]). A major cellular role for Ras is to regulate the ERK1/2 (Extracellular Regulated Kinase) MAP (Mitogen Activated Protein) kinase pathway by directly interacting with an upstream kinase, a MAPK kinase kinase, c-raf [Marshall, 1996]. Other Ras effectors include phosphatidylinositol-3-OH kinase (PI3K) [Rodriguez-Viciana, 1994].

Since the discovery of Ras, a large number of Ras-related proteins have been identified. These can be divided into six subfamilies, Ras, Rho, Rab, Arf/Sar, Ran and Rad, on the basis of amino acid similarities, see figure 1.1. The members of the subfamilies are also related with respect to their cellular functions. Ras controls growth, differentiation and survival [Olson, 2000] [Downward, 1998]. The Rab and Arf/Sar family proteins are implicated in regulation of vesicle

transport (reviewed in [Chavrier, 1999]). Ran is involved in nuclear transport and has been implicated in mitotic spindle assembly [Azuma, 2000]. Members of the Rho family control primarily the actin cytoskeleton and gene transcription (for reviews see [Van Aelst, 1997] and [Bishop, 2000]). The most recently identified members of the Ras superfamily are the Rad-related proteins, which are unusual in that for many members of the family their expression is under transcriptional control, but their functions are as yet unclear (see for instance [Maguire, 1994] and [Finlin, 1997]). There are also multiple pathways mediating cross-talk between members of different Ras subfamilies, as well as between members of the same subfamily, that are gradually becoming evident (reviewed in [Kjoller, 1999] and [Bar-Sagi, 2000]).

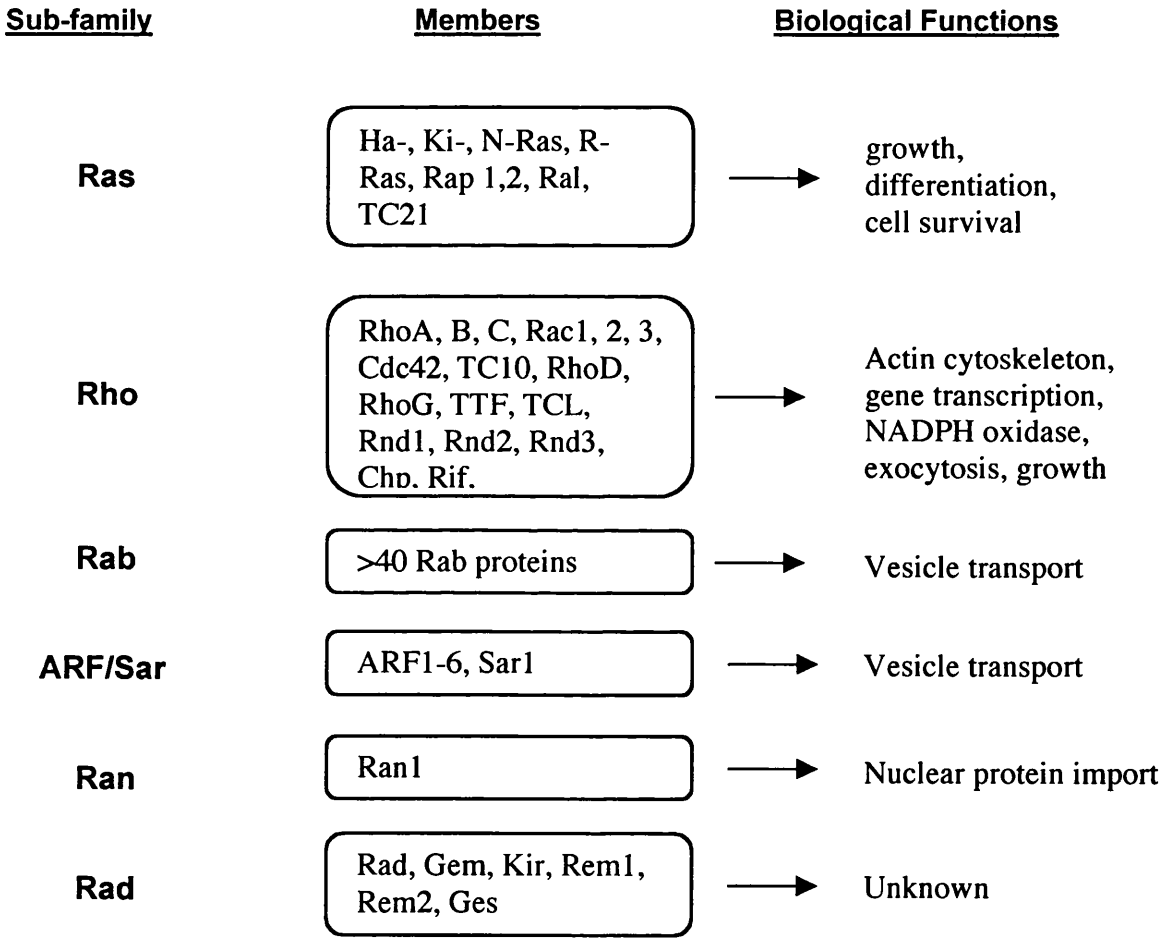

Figure 1.1 Members of the Ras superfamily of GTP-binding proteins

1.2 THE RHO FAMILY

1.2.1 Rho family members

Rho GTPases are members of the Ras superfamily of GTP-binding proteins. Seventeen mammalian Rho GTPase genes have been identified to date: Rho (A, B, C), Rac (1, 2, 3), Cdc42 (Cdc42Hs and G25K splice forms), Rnd1/Rho6, Rnd2/Rho7, Rnd3/Rho8/RhoE, RhoD, RhoG, TC10, TTF/RhoH, Chp, TCL and Rif ([Aronheim, 1998], [Ellis, 2000a] [Vignal, 2000] and reviewed in [Ridley, AJ, 2000]). These proteins are about 30% homologous to Ras and 50-55% to each other [Hall, 1994]. Chp contains N- and C-terminal extensions not seen in other Rho GTPases, a proline-rich sequence towards the N-terminus and extra residues involved in binding to the effector protein Pak2 towards the C-terminus [Aronheim, 1998]. The most extensively characterised members of the mammalian Rho family are RhoA, Rac1 and Cdc42. RhoA was serendipitously discovered by homology to Ras, whereas Rac1 was found as a toxin substrate and Cdc42 as a genetic mutant involved in cell division in *S. cerevisiae*.

Most Rho GTPases are ubiquitously expressed, exceptions are the brain-specific splice forms of Cdc42, mouse Cdc42Mmb and human G25K [Marks, 1996] [Munemitsu, 1990], TTF, which is only expressed in haematopoietic cells [Dallery, 1995]. Also, two of the three Rac proteins are not ubiquitously expressed: Rac2 is only expressed by haematopoietic cells [Shirsat, 1990]; Rac3/ Rac1B, at least in chick embryos, is only expressed in the developing nervous system [Malosio, 1997].

Changes in levels of Rho GTPase proteins have also been observed, although the significance of such regulation is poorly understood: RhoB transcription is induced by stress-inducing agents such as UV light [Fritz, 1997] and by growth factors [Jahner, 1991]; RhoG and Rac3 genes are also growth factor inducible [Vincent, 1992] [Haataja, 1997].

This thesis describes the characterisation of a Rac-binding protein and the three known mammalian Rac gene products are shown in figure 1.2. Residues that are not identical between Rac1 and Rac2 or Rac1 and Rac3 are underlined; Rac2 is 94% identical to Rac1; Rac3 is 96% identical to Rac1. The differences between the three Rac proteins are mainly substitutions of similar amino acids, such as phenylalanine instead of tyrosine or vice versa. A notable exception is Rac residue 150 within effector loop 2, a region implicated in Rac activation of effectors such as p65PAK (p21-activated kinase) and the phagocyte NADPH oxidase complex [Diekmann, 1995]. Residue 150 is a glycine in Rac1 and Rac3, but is an aspartate in Rac2. The consequences, if any, of this difference to Rac2-effector interactions are unknown.

Figure 1.2 Sequence alignment of Ha-Ras with RhoA, Cdc42 and Rac1-3

The motifs essential for GTP binding and hydrolysis in all GTPases, as defined in [Bourne, 1991], are shown in green. Mutations that create constitutively active or dominant negative mutants of Rho and Ras GTPases are indicated. The C-terminal "CAAX" boxes, essential for prenylation, are shown in red. Switch I (effector loop 1), and switch II, which change conformation upon GTP hydrolysis, are shown in blue. An α-helical region (the insert region) present in Rho GTPases, but not in Ha-Ras, is shown in purple. A second effector region in Rac1-3, required for activation of a subset of effectors, is shown in grey [Diekmann, 1995]. Rac1 residues that are not identical in Rac2 or 3 are underlined. Swiss Prot accession numbers for the human Rho GTPases shown are as follows: Ha-Ras NP_005334; RhoA NP_001655; Cdc42 NP_001782; Rac1 NP_008839; Rac2 NP_002863; Rac3 NP_005043.

1.2.2 Post-translational modification of Rho GTPases

Ras and Rho GTPases all undergo a post-translational lipid modification called prenylation, which is important for their ability to bind to membranes (reviewed in [Cox, 1992]). A C-terminal CAAX box motif (where X is any amino acid and A is usually a small aliphatic residue), shown in red in figure 1.2, is the target for prenylation. Prenylation involves three steps: (1) the cysteine residue within this motif is linked to the lipid via a thioether linkage; (2) the three C-terminal amino acids are removed by a prenylation-dependent endoprotease, which has been identified in yeast, but not in mammals [Ashby, 1992]; (3) the carboxyl-group of the prenylated cysteine is methylated [Clarke, 1992].

The nature of the "X" residue in this motif broadly determines the type of isoprenoid modification received by a CAAX box-containing protein (reviewed in [Cox, 1992]). For the majority of Rho GTPases, including Rac1, 2 and 3 (see figure 1.2), "X" is leucine, isoleucine or phenylalanine and these proteins are modified with a 20 carbon geranylgeranyl lipid. When "X" is serine or methionine, as in Ha-Ras (see figure 1.2) and the Rho GTPases Rnd1-3, this has been shown to result in modification of Ha-Ras and Rnd3 with a 15 carbon farnesyl lipid [Hancock, 1989] [Foster, 1996]. It has been demonstrated that if the terminal serine of Ha-Ras is mutated to leucine then the protein is now geranylgeranylated [Seabra, 1991]. In some cases, however, residues in addition to the "X" position contribute to the type of isoprenoid modification. For instance, RhoB has a C-terminal leucine residue, but can be modified by either a farnesyl or a geranylgeranyl group [Adamson, Marshall, 1992]. A cysteine adjacent to the CAAX box appears to be important to the balance between addition of C20 or C15 lipids to RhoB [Adamson, Marshall, 1992].

In addition to being farnesylated, Ha-Ras and N-Ras are palmitoylated at additional cysteines close to the CAAX box (see figure 1.2), which increases their membrane association [Hancock, 1989]. RhoB also has two cysteines adjacent to the CAAX box, both of which been shown to be palmitoylated [Adamson, Marshall, 1992]. Ki-Ras has no cysteines adjacent to the CAAX box, instead there is a poly-basic region that contributes to membrane localisation [Hancock, 1991]. Most Rho GTPases also contain a poly-basic region, containing 3-6 arginine or lysine residues, adjacent to their CAAX box. Rac1-3 differ in the number of basic amino acids immediately upstream of the CAAX box (Rac1 has 6, Rac2 has only 3 and Rac3 has 4, see figure 1.2), whether this variation reflects a difference in affinity for membranes, or for protein binding partners, is unknown.

Rho GTPases can also be covalently modified by a number of bacterial toxins, reviewed in [Aktories, 2000] and discussed further below. The only other post-translational modifications reported for Rho GTPases are phosphorylation events. RhoA has been reported to be

phosphorylated by PKA, at serine 188, which is a residue that is not conserved in RhoB or RhoC [Lang, 1996]. Phosphorylation of RhoA by PKA in natural killer cells resulted in a loss of RhoA from the membrane, where it is active, and an increase in the amount of RhoA associated with its cytosolic partners the Rho guanine nucleotide dissociation inhibitors (discussed below) [Lang, 1996]. *In vitro* Rac1 can be phosphorylated at serine 71, which is conserved in Rac2 and 3, by Akt/PKB and this inhibits its ability to bind GTP [Kwon, 2000].

1.2.3 The Rho GTPase GDP/ GTP exchange cycle

Rho GTPases act as molecular switches, cycling between active GTP-bound and inactive GDP-bound states, see figure 1.3. When in the GTP-bound form Rho proteins are competent to interact with effector or target molecules to initiate downstream signals (figure 1.3 step 3). Each biological response induced by a Rho GTPase requires the action of one or more effector proteins. Intrinsic GTPase activity returns Rho proteins to their GDP-bound state, to complete the cycle and terminate signal transduction (figure 1.3 step 4). Additional proteins that regulate this cycle are discussed below.

1.2.3.1 Guanine nucleotide exchange factors and Rac activation

Guanine nucleotide exchange factors (GEFs) facilitate release of GDP, which is replaced by GTP due to the high intracellular GTP/GDP ratio, thereby activating Rho GTPases (figure 1.3 step 2), reviewed in [Whitehead, 1997]. Over fifty Rho GTPase GEFs have been identified (reviewed in [Stam, 1999]), some due to their transforming activity, such as Dbl and Vav1, [Ron, 1988] [Katzav, 1989]. Others were identified due to the presence of other catalytic domains or interactions with proteins other than Rho GTPases. For instance, son of sevenless (Sos) that was identified as a GEF for Ras is also a Rho GEF [Bowtell, 1992], Trio was isolated as a protein binding to the phosphatase LAR and harbors two Rho GEF domains [Debant, 1996] and recently an APC (adenomatous polyposis coli)-binding protein was cloned, termed Asef, which contains a GEF domain [Kawasaki, 2000]. In a few cases Rho GEFs have been identified due to their implication in specific processes. For instance, in *Drosophila* a screen for genes involved in axon morphology during synapse maturation lead to the identification of a GEF called *Still life* (Sif) [Sone, 1997]. The mammalian homologue of Sif is the T cell tumour invasive gene product, Tiam-1, which was identified in a screen of invasive T-lymphoma variants induced by proviral insertions [Habets, 1994]. Recently another mammalian Rac-specific Sif and Tiam-1-like exchange factor, Stef, was cloned by PCR due to homology with Sif and Tiam-1 [Hoshino, 1999].

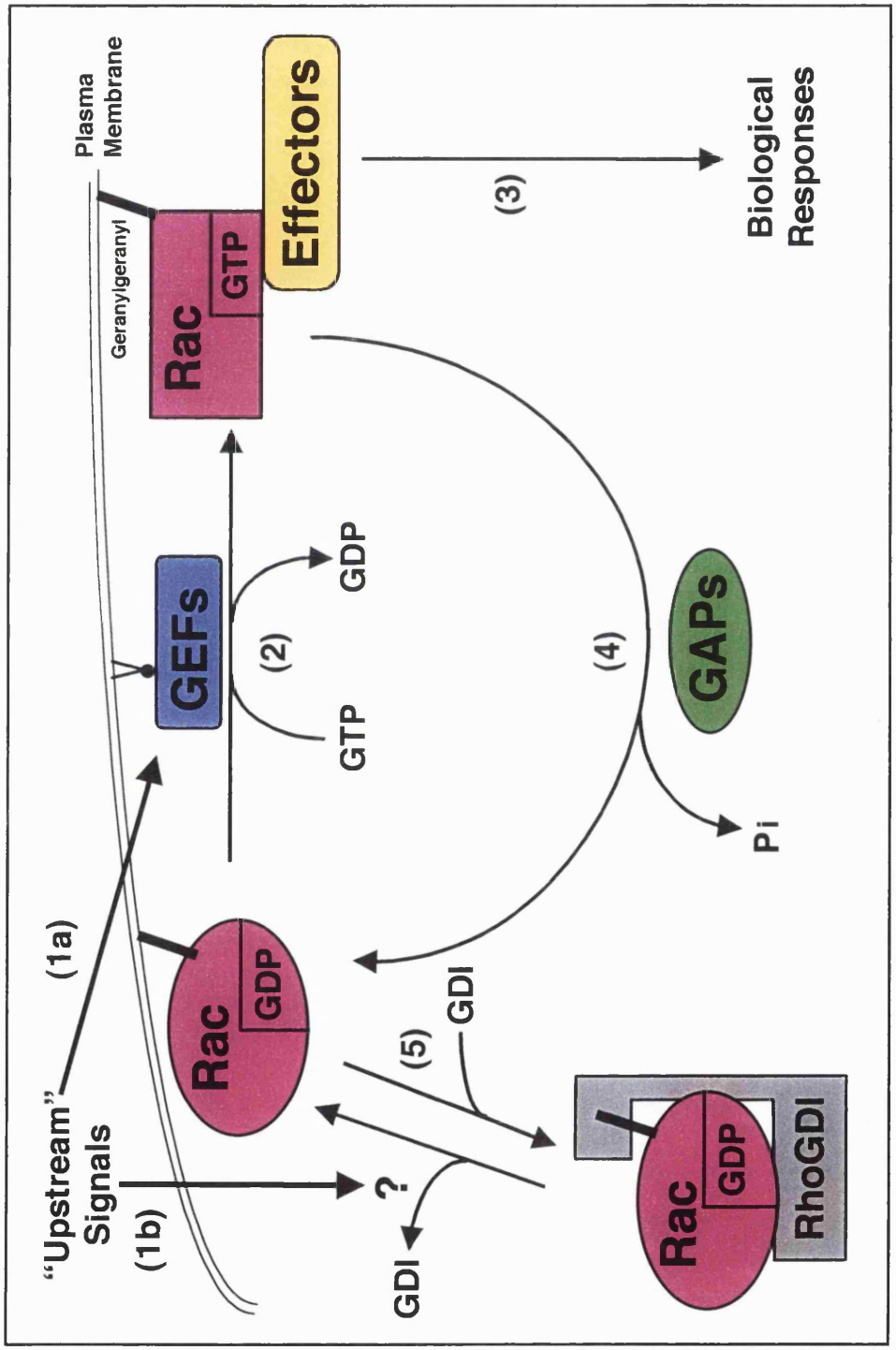

Figure 1.3 The Rho GTPase GDP/GTP Exchange Cycle (see text for discussion)

All Rho GEFs contain a Dbl-homology (DH) domain that encodes the catalytic activity ([Hart, 1994] and reviewed in [Cherfils, 1999]) and an adjacent pleckstrin homology (PH) domain. The PH domain is thought to mediate membrane localisation through lipid binding [Zheng, Zangrilli, 1996] [Rameh, 1997]. In addition to bindng of lipids, binding of proteins, such as Gβγ subunits and filamentous actin, to some PH domains has been reported [Touhara, 1994] [Yao, 1999]. Recently it was found that the first PH domain within Trio's two DH-PH modules not only binds to lipids [Liu, 1998], but is also responsible for localisation of the Trio to the actin cytoskeleton by binding to the actin cross-linking protein filamin [Bellanger, 2000]. Tiam-1 and RasGRF contain additional PH domains (outside of their DH-PH motifs) essential for their membrane association and activation [Michiels, 1997] [Buchsbaum, 1996]. In many cases it appears that domains outside of the DH-PH motif negatively regulate the activity of the GEF. Activated mutants of GEFs are often produced by deletion of regulatory domains, to create a constitutively active DH-PH module. For example, truncation of the N-terminus of Dbl, Vav2 or Tiam-1 makes these proteins more potent oncogenes than the full-length protooncogenes in NIH3T3 cell transformation assays [Ron, 1989] [Schuebel, 1996] [van Leeuwen, 1995].

Rho GEFs are activated by a wide variety of "upstream" signals (figure 1.3 step 1a), ranging from G protein-coupled receptors and receptor tyrosine kinases to integrins, reviewed in [Kjoller, 1999]. Protein-lipid and protein-protein interactions as well as protein phosphorylation events have all been shown to contribute to the activation of different Rho GEFs, as discussed below.

Activation of Rac GEFs by the lipid products of PI3K

Binding of phosphatidylinositol-4,5-bisphosphate (PI-4,5-P_2) to the PH domain of Vav1 inhibits its GEF activity, whereas phosphatidylinositol-3,4,5-triphosphate binds more strongly and stimulates Vav1 [Han, J, 1998]. The PH domains of Rho GEFs Tiam-1 and Sos also bind to the lipid product of PI3K, PI-3,4,5-P_3 [Rameh, 1997] and see [Leevers, 1999] for a review of PI3K. The DH-PH domain of Sos becomes active against Rac via a mechanism that is dependent upon Ras activation of PI3K [Nimnual, 1998]. A GEF called αPIX, which associates with PAK (a Rho GTPase effector) and Nck (an adaptor protein), is also activated in a PI3K-dependent manner [Yoshii, 1999]. In *S. cerevisiae* the exchange factor ROM2 activates Rho1 and Rho2 in response to activity of the phosphatidylinositol kinase TOR2 [Schmidt, A, 1997]. Ras activates PI3K [Rodriguez-Viciana, 1996] and both growth factors, such as PDGF, activate Rac in a PI3K-dependent manner [Nobes, Hawkins, 1995] [Hawkins, 1995]. One link between Ras and Rac activation may therefore be the indirect activation of specific Rho GEFs via PI3K (reviewed in [Bar-Sagi, 2000]).

Protein-protein interactions and phosphorylations involved in GEF activation

Vav is synergistically activated by a combination of lipid binding and phosphorylation by the Src family member Lck, so requires two signal inputs for full activation [Han, 1997] [Han, J, 1998]. Some GEFs appear to be activated by direct interaction with other proteins. For instance, p115RhoGEF is activated via interaction with the $G\alpha_{13}$ heterotrimeric G protein subunit [Hart, 1998] [Kozasa, 1998] [Mao, 1998] and Asef is stimulated in a cell cycle-dependent manner by binding to APC [Kawasaki, 2000].

GEFs implicated in the activation of Rac

The specificity of GEFs for particular Rho GTPases can be determined using a combination of *in vitro* and *in vivo* assays. *In vitro* GEF assays are carried out using recombinant proteins and radiolabelled nucleotides. *In vivo* specificity of GEF is often assayed using fibroblasts, in which induction of actin structures and gene transcription events reminiscent of the activity of a certain Rho GTPase can be detected, and the ability to inhibit these events with a dominant negative version of that GTPase can be tested.

Some DH proteins appear to be highly specific both *in vitro* and *in vivo*, such as FGD1, which acts only upon Cdc42 *in vitro* and when over-expressed induces only actin microspike structures reminiscent of Cdc42 activity [Olson, 1996] [Zheng, Fischer, 1996]. Other GEFs *in vitro* are capable of activating a number of different GTPases, for instance Vav1 and Tiam1 activate RhoA, Rac1, Rac2 and Cdc42 *in vitro* [Michiels, 1995] [Olson, 1996]. *In vivo*, however, Tiam1 only induces actin-rich structures that are similar to those induced by activated Rac and are inhibited by dominant negative Rac [Michiels, 1995]. The structure of Tiam1's DH-PH module with Rac1 reveals contacts with many switch I and II residues that are also present in Rho GTPases other than Rac, but also with amino acids (3, 41, 43, 52 and 56) that are more specific to Rac1-3 (see figure 1.2) and may be important to the *in vivo* specificity of Tiam1 for Rac [Worthylake, 2000]. *In vivo* using fibroblasts Vav1, unlike Tiam1, still appears to activate RhoA, Rac1 and Cdc42 [Olson, 1996]. The fibroblast system, however, may not truly reflect the *in vivo* situation, as GEFs such as Vav1 are only expressed in certain cell types and may have cell type specific activities. Vav1 appears to be a specific activator of Rac in lymphoid cells where it is actually expressed [Crespo, 1996] [Crespo, 1997]. The more ubiquitously expressed Vav2 appears also to be active against RhoA, Rac1 and Cdc42 *in vitro* and *in vivo* in fibroblasts [Abe, 2000] and the specificity of Vav3, also widely expressed, has not yet been determined [Trenkle, 2000]. The domain structures of GEFs that have shown to be active against Rac are shown in figure 1.4.

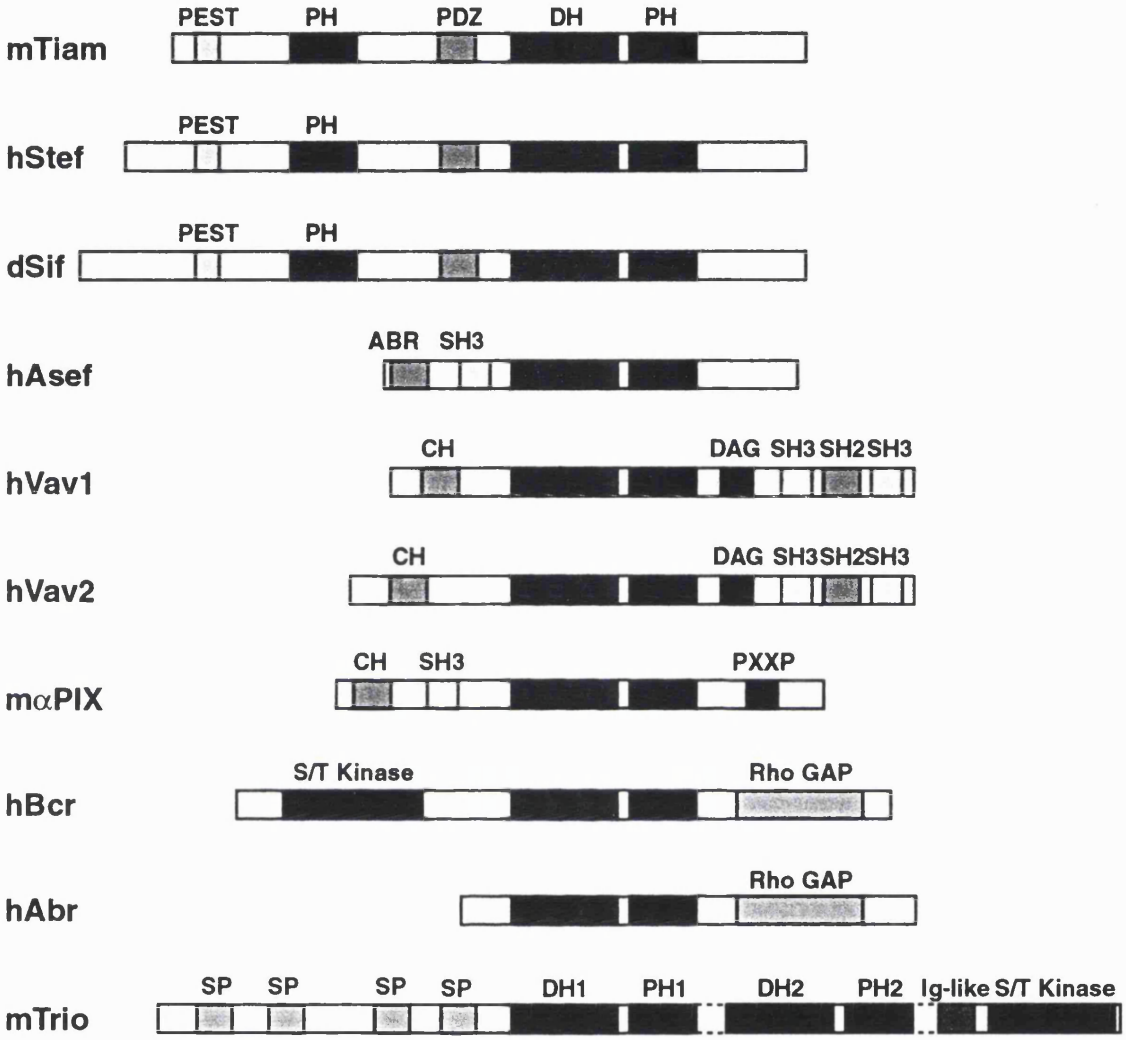

Figure 1.4 Guanosine nucleotide exchange factors (GEFs) that act upon Rac

Domains: Dbl-homology (DH); Pleckstrin-homology (PH); Src-homology 3 (SH3); Src-homology 2 (SH2); Region rich in amino acids P,E,S,T, according to the single letter amino acid code, implicated in protein stability (PEST); spectrin-like domain (SP); Diacyl-glycerol-binding (DAG); APC-binding region (ABR); GTPase activating protein (GAP); Region containing SH3 domain-binding motifs (PXXP, where P is proline and X is any amino acid); calponin-homology domain (CH); serine/threonine (S/T) Kinase; immunoglobulin- (Ig) like. Abbreviations for GEF names and accession numbers: human (h); mouse (m); *Drosophila* (d); T-lymphoma invasion and metastasis (Tiam-1), U05245; Sif/ Tiam-1-like exchange factor (Stef), AAF03902; Still life (Sif), splice variant 2 D86546; Adenomatous polyposis coli-stimulated guanine nucleotide exchange factor (Asef), AB042199; Vav, sixth letter the Hebrew alphabet, Vav1 NP_005419, Vav2 NP_003362; Pak-interactive exchange factor (αPIX); breakpoint cluster region (Bcr) gene product, P11274; Active Bcr-related (Abr) gene product, U01147; three catalytic domains (Trio), U42390.

GEFs that appear to be specific to Rac both *in vitro* and *in vivo* are the Tiam-1-related family (Stef, Sif and Tiam-1 itself), the newly identified ASEF and possibly Vav1 in haematopoietic cells (discussed above). Kalirin/P-CIP10a was shown to bind specifically to Rac1, but is not included in figure 1.4 as exchange activity has not been shown [Alam, 1997]. αPIX appears to activate Rac *in vivo*, so is included in figure 1.4, but recombinant αPIX and βPIX are poor GEFs *in vitro*, suggesting a requirement for additional activating factors, possibly lipids [Manser, 1998] [Yoshii, 1999]. Vav2, Bcr and Abr activate RhoA, Rac1 and Cdc42 *in vitro*, and also *in vivo* for Vav2, [Chuang, 1995] [Abe, 2000]. Trio is an unusual GEF, in that it contains two DH-PH modules; the C-terminal one has been shown to be a RhoA GEF and the N-terminal one activates Rac1 [Debant, 1996]. Trio has been included as a Rac GEF in figure 1.4, however, recently it was reported that Trio activation of Rac may not be direct, but may occur through RhoG [Blangy, 2000]. Trio has become of particular interest because it has been implicated in axon guidance in *Drosophila* and was genetically linked to Rac, Pak and dock (homolog of the scaffold protein Nck) in this process [Awasaki, 2000] [Newsome, 2000] [Bateman, 2000]. The IgG domain of Trio has also been shown to bind to activated RhoA, suggesting that Trio, which also contains a kinase domain and spectrin-like regions, is both a GEF and an effector for RhoA [Medley, 2000].

In addition to these mammalian Rac GEFs, *Salmonella typhimurium* produces a protein called SopE that acts as a GEF that activates Cdc42 and Rac. SopE is injected into host cells via a type III secretion system and triggers actin changes that enable the bacterium to be engulfed into a normally non-phagocytic cell [Rudolph, 1999].

At first glance it seems that there are a surprisingly large number of Rho GEFs compared with the number of Rho GTPases. It is becoming increasingly clear that variations in the expression profiles, GTPase specificities and modes of activation (reflected in the domains present in each Rho GEF outside of the core DH-PH motif) of Rho GEFs enable Rho GTPases to be activated in different combinations, in specific cell types and in response to a variety of signals.

1.2.3.2 GTPase-activating proteins

Rho GTPases have a relatively slow intrinsic rate of GTP hydrolysis that can be stimulated by GTPase activating proteins (GAPs), which thus inactivate Rho GTPases (see figure 1.3). At least fifteen Rho GAPs have been identified, reviewed in [Lamarche, 1994] and [Van Aelst, 1997]. There are three blocks of homology between Rho GAPs, each consisting of 30-40 amino acids and spread over around 150-200 amino acids. The human genome sequencing project reveals that chromosome 22 alone encodes eight potential Rho GAPs [Dunham, 1999].

A comparison of the crystal structures of a ground state complex between RhoGAP and Cdc42.GMPPNP (GMPPNP is a non-hydrolysable GTP analogue) and a transition state-mimicking complex of RhoGAP with RhoA.GDP.AlF_4^-, along with NMR analysis of a Cdc42 RhoGAP complex, has provided insight into the mechanistic details of GAP-facilitated GTP hydrolysis [Rittinger, Walker, Eccleston, Nurmahomed, 1997] [Rittinger, Walker, Eccleston, Smerdon, 1997] [Nassar, 1998] and reviewed in [Scheffzek, 1998]. The most striking feature is that a 20° rotation between GTPase and GAP, from ground state to transition state, allows an arginine residue in the GAP protein, the "arginine finger", to enter the GTPase active site and participate in the stabilization of the transition state.

Although GAPs often exhibit GTPase activating activity towards several Rho GTPases *in vitro* their specificities *in vivo*, assessed according to their ability to inhibit actin changes characteristic of a particular Rho GTPase, appear to be more restricted. GAPs that appear to act preferentially upon Rac *in vivo* include three that are predominantly expressed in the brain: Bcr, the product of the breakpoint cluster region gene, the translocation breakpoint in Philadelphia chromosome-positive chronic myeloid leukaemias [Diekmann, 1991]; Abr, the product of the active Bcr-related gene [Tan, 1993]; N-chimaerin [Diekmann, 1991]. Other Rac GAPs include the testis-restricted β-chimaerin [Leung, 1993] and the more ubiquitous 3BP-1 [Cicchetti, 1995]. The GAP domains of N- and β-chimerins prevent both Rac and Cdc42-induced actin changes [Diekmann, 1991] [Leung, 1993] [Kozma, 1996]. Surprisingly injection of full-length N-chimerin, and a mutant lacking GAP activity, actually induced formation of actin structures that could be inhibited by dominant negative Rac and Cdc42, suggesting that this protein is both a GAP and an effector [Kozma, 1996]. Interestingly, *Salmonella typhimurium* not only activates Rac1 and Cdc42, by introducing the SopE protein into host cells, but also introduces a GAP-like protein, SptP, to attenuate the Rho GTPase response [Fu, 1999]. *Yersinia pseudotuberculosis* also produces a cytotoxin, called YopE, that also acts as a Rho GAP [Von Pawel-Rammingen, 2000].

Interactions with other proteins and binding to lipids may regulate both the catalytic activity of GAPs and their association with membrane-associated activated Rho GTPases.. For instance, myosinIXb and Myr5 (5^{th} unconventional myosin from rat) bind to actin and act as GAPs for RhoA [Muller, 1997] [Post, 1998]. As mentioned above, Bcr and Abr contain both a Rho GAP and a Rho GEF domain and their GAP domains are active against Rac1, Rac2 and Cdc42 [Diekmann, 1991] [Tan, 1993] [Chuang, 1995]. N-chimaerin contains a zinc finger that binds to phospholipids and phorbol esters and lipid binding positively regulates chimerin GAP activity *in vivo* [Ahmed, 1991] [Ahmed, 1993]. In general the mechanisms by which GAPs are regulated remain poorly understood.

1.2.4.3 Rho guanine nucleotide dissociation inhibitors and the sub-cellular localisations of Rho GTPases

Ha-, N- and Ki-Ras are exclusively localised to the plasma membrane [Hancock, 1991]. In contrast most Rho GTPases, such as RhoA, RhoC and Rac1, are mainly cytoplasmic, but translocate to membrane fractions upon activation [Abo, 1991] [Adamson, Paterson, 1992] [Bokoch, 1994]. For example, Rac was found to enter the membrane fraction of eosinophils and neutrophils in response to phorbol myristate acetate stimulation [Quinn, 1993] [Lacy, 1999] and association with neutrophil membranes was seen for Rac in a cell-free system in response to non-hydrolysable GTPγS [Bokoch, 1994].

Only three Rho GTPases have been reported to have different subcellular localisations to that of RhoA, RhoC and Rac1: Cdc42 has been observed to be associated with the ER and Golgi apparatus (see for instance [Abo, 1998]); RhoB was localised to an endosomal compartment [Adamson, Paterson, 1992]; Rnd3 was found in the cytoplasm, but was also associated with "worm-like" structures at the plasma membrane [Foster, 1996].

The cytoplasmic pools of prenylated Rho GTPases can be isolated as soluble complexes with a protein called RhoGDI (guanine nucleotide dissociation inhibitor), reviewed in [Olofsson, 1999]. Three mammalian RhoGDI proteins have been identified: ubiquitously expressed GDI-1/RhoGDIα [Ohga, 1989] [Leffers, 1993]; haematopoietically expressed GDI-2/RhoGDIβ/LyGDI/D4 [Leffers, 1993] [Lelias, 1993] [Scherle, 1993]; GDI-3/RhoGDIγ, preferentially expressed in brain and pancreas [Adra, 1997]. The three GDIs appear to differ in their Rho GTPase-binding specificity. Using microanalytical liquid chromatography to separate GDI-1 and GDI-2 complexes from a myelomonocytic cell line, GDI-1 was found to be associated with Cdc42, RhoA, Rac1 and Rac2, whereas none of these proteins were found complexed with GDI-2 [Gorvel, 1998]. GDI-3 appears to be preferentially associated with RhoB, reviewed in [Olofsson, 1999].

GDI-1 is proposed to sequester GDP-bound Rho GTPases in the cytoplasm and inhibit their spontaneous GDP/GTP exchange activity, but the precise role of the GDIs is still poorly understood (reviewed in [Olofsson, 1999]). Binding of RhoA to GDI-1 requires that RhoA be prenylated [Hori, 1991], suggesting that interactions with Rho GTPase geranylgeranyl or farnesyl groups may contribute to the ability of GDI to retain Rho GTPases in the cytoplasm despite their hydrophobic lipid modifications. NMR and crystal structures of GDI alone and crystal structures of RhoA.GDI-1 and Cdc42.GDI-1 complexes all agree on the following points: binding of GDI to a Rho GTPase occurs mainly through an immunoglobulin-like C-terminal domain of GDI; a hydrophobic pocket in this C-terminal domain can accommodate the geranylgeranyl lipid; a

flexible N-terminal domain inhibits GDP/GTP exchange [Keep, 1997] [Gosser, 1997] [Longenecker, 1999] [Hoffman, Nassar, 2000]. Cytoplasmic RhoGDI is capable of extracting Rho GTPases from membranes. For instance, recombinant GDI-1 has been observed to extract endogenous RhoA and Cdc42, but not RhoB or Ha-Ras, from kidney brush border membranes [Bilodeau, 1999]. Cerione's group have reported the use of fluorescence energy resonance transfer (FRET) to follow the removal of Cdc42 from membranes by GDI-1 in real time [Nomanbhoy, 1999]. They detected two phases, which appear to represent a rapid membrane-associated GTPase-GDI binding step followed by a slow transfer of the geranylgeranyl moiety from membrane to GDI-1. It should be noted that GDI-3 is membrane-associated not cytoplasmic [Zalcman, 1996], so must regulate Rho GTPases using a slightly different mechanism to GDI-1 and GDI-2.

The GDP/GTP exchange cycle (figure 1.3) raises interesting questions about how the transfer of a GTPase between its binding partners is co-ordinated. In particular, the activation of Rho GTPases must involve not only GEF activation (figure 1.3 step 1a) and GEF exchange activity towards Rho GTPases (figure 1.3 step 2), but also removal of RhoGDI from the Rho GTPase (figure 1.3 step 1b). Exactly how and when RhoGDI is removed from Rho GTPases during their activation remains unclear, but some suggestions have been put forward, reviewed in [Olofsson, 1999]. **(1)** ERM (Ezrin/ Radixin/ Moesin) proteins may remove GDI from Rho GTPases. GDI-1 was isolated from BHK cells in a complex with ERM proteins [Hirao, 1996] and the N-terminus of ERM proteins was found to bind weakly to GDI-1 *in vitro* [Takahashi, 1997]. **(2)** Lipids may disrupt binding of GDI to Rho GTPases, as biologically active phospholipids have been reported to enhance the release of RhoGDI from Rac *in vitro* [Chuang, 1993]. Also, the Rac-GDP.GDI-1 complex can bind to both diacylglycerol kinase and a type I phosphatidylinositol-4-phosphate 5-kinase [Tolias, 1995] [Tolias, 1998], leading to the suggestion that the products of these enzymes may facilitate dissociation of RhoGDI from Rho GTPases. **(3)** Phosphorylation of GDIs may regulate their affinity for Rho GTPases. Phosphorylation of GDI-1 has been shown to stabilise RhoA-GDI-1 complexes in the cytosol of neutrophils [Bourmeyster, 1996], in Jurkat T cells GDI-2 was found to be threonine phosphorylated in response to phorbol ester treatment [Scherle, 1993] and in a later study phorbol esters were found to induce phosphorylation of GDI-2 in a myelomonocytic cell line (U937) [Gorvel, 1998].

1.2.4 Experimental tools used to study Rho GTPases

The biological activities of individual Rho GTPases have been elucidated using a variety of methods. These include transfection or injection of activated and dominant negative GTPase mutants, treatment with bacterial toxins that inhibit or activate Rho GTPases and use of RhoGDI as a general inhibitor of Rho family members (the latter is discussed in [Olofsson, 1999]).

Based upon transforming mutations in Ras [Bos, 1989], amino acid substitutions of glycine to valine at codon 12 or glutamine to leucine at codon 61 (Rac numbering, see figure 1.2) have been extensively used to generate constitutively active Rho GTPases. These mutations prevent intrinsic and GAP-induced GTP hydrolysis. The crystal structure of RhoGAP complexed with RhoA.GDP.AlF_4^- confirms an essential role for glutamine 63 (equivalent to Rac glutamine 61) in stablizing the γ-phosphate during GTP hydrolysis [Rittinger, Walker, Eccleston, Smerdon, 1997]. The crystal structure of a V14RhoA.GTPγS (V14Rho is equivalent to the valine 12 mutant of Rac) showed how the larger valine side chain forces glutamine 63 away from the γ–phosphate, so preventing it from facilitating GTP hydrolysis [Ihara, 1998]. Rnd1-3 and TTF Rho family members do not contain glycine and glutamine at the equivalent positions to Rac amino acids 12 and 61 respectively and thus are constitutively GTP-bound [Foster, 1996] [Nobes, 1998]. This raises interesting questions as to how these proteins are regulated, but so far nothing is known.

A threonine 17 to asparagine amino acid substitution (Rac numbering) allows this mutant GTPase to compete with the corresponding endogenous GTPase for binding to cellular GEFs, but this leads to a non-productive complex unable to generate a downstream response [Feig, 1999]. These dominant negative proteins appear to be rather specific for individual Rho GTPases, despite the complexity of the RhoGEF family (see [Whitehead, 1997]).

A variety of bacterial toxins have been used to modify the activity of Rho GTPases, reviewed in [Aktories, 2000]. The exoenzyme C3 transferase, an ADP-ribosyltransferase from *Clostridium botulinum*, is relatively specific and inactivates only RhoA, RhoB and RhoC [Aktories, 1997]. Cytotoxic nectotizing factor 1 (CNF-1) from *Escherichia coli* activates RhoA, Rac1 and Cdc42 by deamidation of the essential glutamine 63 residue of RhoA (glutamine 61 in Rac/Cdc42) [Schmidt, G, 1997] [Lerm, 1999], so can be used to identify cellular processes that can be activated by these Rho GTPases. *Clostridium difficile* toxin B inactivates most, if not all, members of the Rho GTPase family and is useful to broadly assess the involvement of Rho GTPases in a biological process [Aktories, 2000]. There is no known toxin that specifically activates or inactivates Rac. The prevalence of Rho GTPase modifications by bacterial toxins illustrates the fundamental importance of these proteins to cellular regulation.

GST-fusion protein pull-down assays have now been developed in order to extract the GTP-bound fractions of endogenous Rho GTPases from cell lysates. These assays make use of the fact that effector proteins bind selectively to the activated forms of Rho GTPases (see step 3 of the GTPase cycle in figure 1.3), by using GST-fusions of activated Rho GTPase-binding domains from effector proteins as bait. GTP-Rho can be isolated with a GST-rhotekin Rho-binding domain and GTP-bound Rac and Cdc42 can be isolated with a GST-PAK1 CRIB construct. This

pull-down approach has successfully demonstrated agonist activation of RhoA, Rac1 and Cdc42 (see for instance [Leeuwen, 1997] [Benard, 1999] and [Kranenburg, Poland, 1999]).

A technique called FLAIR (fluorescence activation indicator for Rho proteins) has recently been development to enable the spatial and temporal dynamics of activated Rho GTPases to be visualised in living cells [Chamberlain, 2000]. The principal is that a fluorescent-tagged wild type Rho GTPase protein is injected into cells along with a fluorescent-tagged effector domain peptide like those used for the pull-down assays described above. The effector will only bind to the GTPase when it is active and the close proximity of fluorescent markers can be detected at these sites of activated GTPase. FLAIR, has been successfully used to visualise the localisation of activated Rac1 in living cells, using a PAK CRIB construct as the activation state-specific binding partner [Kraynov, 2000]. This revealed precise spatial control of growth factor-induced Rac activation, in membrane ruffles and in a gradient of activation at the leading edge of motile cells.

Attempts to visualise the localisation of endogenous activated Rho GTPases *in vivo* have so far proved fruitless. Even so, the ability to visualise activation of over-expressed GTPases in live cells with FLAIR, and the ability to biochemcally isolate endogenous activated GTPases with pull-down assays, are exciting technical developments that are enabling new progress to be made in the Rho GTPase field.

1.2.5 Binding of Rho GTPases to effector proteins

More than thirty potential effectors for Rho, Rac and Cdc42 have been identified (see [Bishop, 2000] and Rac effectors in figure 1.7), primarily using affinity chromatography and the yeast-two-hybrid system. Most of these proteins interact only with the GTP-bound form of the GTPase, as one would expect from an effector protein (see figure 1.3). Exceptions are DAGK and PI-4-P5K that interact with GDP and GTP-bound Rac, but are only activated by GTP-bound Rac [Tolias, 1998] [Tolias, 1995]. A comparison of the RhoA.GDP and Val14RhoA.GTPγS crystal structures has revealed that the conformational differences between the GTP and GDP-bound forms are restricted primarily to two surface loops, named switch regions I and II (Cdc42/Rac amino acids 26-45 and 59-74 respectively, see figure 1.2), [Wei, 1997] [Ihara, 1998]. Effector proteins must utilise these differences to discriminate between the GTP and GDP-bound forms, as well as interacting with residues specific to a particular GTPase, within or outside of the switches, in order to discriminate say Rac from Rho.

1.2.5.1 Use of Rho GTPase mutants to identify effector binding sites

Numerous point mutations have been introduced into Switch I of Rho, Rac and Cdc42, often referred to as effector region I, and have rather interesting effects preventing the binding of some, but not all, target proteins, see for instance [Joneson, 1996] [Lamarche, 1996] [Sahai, 1998]. In the case of Rac in particular numerous effector region point mutations have been made, some of which knock out binding to certain targets. For example, the interaction of PAK with Cdc42 or Rac is blocked by a tyrosine 40 to cysteine mutation (Y40C), but not by a phenylalanine 37 to alanine mutation (F37A) [Lamarche, 1996]. Whereas the interaction of Mlk2 (mixed lineage kinase 2) with Rac is blocked by either of these mutations [Tapon, Nagata, 1998]. Substitution of different amino acids at the same position in switch I can also have varied effects upon target protein binding, for instance, C40Rac can bind to p67phox (a component of the NADPH oxidase complex), whereas K40Rac cannot [Lamarche, 1996]. Such results suggest that different effectors interact with different residues even within the switch I region of a single GTPase, in this case Rac.

Further studies using GTPase mutants and chimeras have implicated regions outside of switch I, often different regions for Rho, Rac and Cdc42, in the binding of certain effectors. For instance, Rac/Rho chimeras indicate that a region close to the C-terminus of Rac (amino acids 143-175, shown in grey in figure 1.2), termed effector loop II, is required for activation of the phagocyte NADPH oxidase (phox) complex and for binding to p65PAK [Diekmann, 1995]. For Rho amino acids just C-terminal to switch II appear to be important for Rho binding to the effector proteins PRK2 and ROK [Zong, 1999]. This same region of Rac (amino acids 74-90, shown in pink in figure 1.2), has been implicated in binding to GAPs [Diekmann, 1995]. An overlapping region of Cdc42 (amino acids 84-120) is involved in binding to WASP and IQGAP, but not to PAK1 [Li, 1999]. There is an α-helical region present in all Rho family GTPases (except *Drosophila* RhoL), but not in Ras, referred to as the "insert region" (Rac amino acids 123-135, shown in purple in figure 1.2). This region was also required for Rac activation of the NADPH oxidase complex and for binding to IQGAP, but not for Rac interaction with PAK [Nisimoto, 1997] [McCallum, 1996]. So far there are no known examples of Rho effectors requiring this insert region for binding. Diacylglycerol kinase and phosphatidylinositol-4-phosphate 5-kinase are unusual effectors in that a C-terminal region of Rac is necessary and sufficient for binding to Rac *in vitro* and (mentioned above) these effectors can bind to GDP- as well as GTP-bound Rac [Tolias, 1998].

1.2.5.2 Binding of Cdc42 and Rac to CRIB-containing effectors

Data obtained from many mutational studies has lead to a complex, and sometimes contradictory, picture of Rho GTPase-effector interactions. NMR structures of Cdc42 bound to peptides from activated Cdc42-associated tyrosine kinase, ACK, (amino acids 504-545) [Mott, 1999], Wiskott-

Aldrich-syndrome protein, WASP, (amino acids 230-288) [Abdul-Manan, 1999], PAK1, (amino acids 65-108) [Gizachew, 2000] and αPAK (amino acids 75-118) [Morreale, 2000] have been solved. These structures have provided a clearer understanding of the interface between Cdc42 and the subset of its effectors that contain a CRIB (Cdc42/Rac-interactive binding) motif. The CRIB sequences for three PAKs, ACK, WASP and the related N-WASP are shown in figure 1.5. For proteins such as WASP [Rudolph, 1998], PAK [Guo, 1998] [Thompson, 1998], ACK [Manser, 1993] and Mlk3 [Bock, 2000] the CRIB motif has been shown to be necessary, but not sufficient, for strong binding to Rho GTPases.

CRIB domains

L	S	A	Q	D	I	S	Q	P	L	Q	N	S	F	I	H	T	G	H	G	D	S	D	hAck	(505-527)
I	S	K	A	D	I	G	A	P	.	.	S	G	F	K	H	V	S	H	V	G	W	D	hWASP	(233-253)
L	T	K	G	D	I	G	T	P	.	.	S	N	F	Q	H	I	G	H	V	G	W	D	hN-WASP	(198-218)
K	E	R	P	E	I	S	L	P	.	.	S	D	F	E	H	T	I	H	V	G	F	D	hPak1	(65-85)
K	E	R	P	E	I	S	P	P	.	.	S	D	F	E	H	T	I	H	V	G	F	D	hPak2	(64-84)
K	K	R	V	E	I	S	A	P	.	.	S	N	F	E	H	R	V	H	T	G	F	D	hPak4	(6-26)
			*	I	S	*	P	.	.	*	*	F	*	H	*	*	H	*	G	*	D	CRIB consensus	

Figure 1.5 Sequences of Cdc42/Rac-interactive binding (CRIB) motifs

Cdc42/Rac-interactive binding (CRIB) motif sequences are shown from the human (h) versions of the cdc42 effector proteins Ack, WASP and N-WASP and the Cdc42 and Rac effector proteins PAK1, 2 and 4. CRIB consensus residues, as defined by [Burbelo, 1995], are shown in red; (*) indicates less conserved residues within the CRIB motif.

Comparison of these PAK, ACK and WASP CRIB-containing peptides bound to Cdc42 has revealed a number of clues as to how GTPase binding specificity may be achieved via CRIB-GTPase interactions, including the following observations.

(i) In all three cases aspartate 38 in Switch I interacts with the two histidine residues conserved in many CRIB proteins (see figure 1.5). Switch I and II are very similar in Rho, Rac and Cdc42, but position 38 is aspartate in Rac/Cdc42 and glutamate in Rho (see figure 1.2). Mutation of Cdc42 aspartate 38 to glutamate decreased the affinity for mPAK3, which binds to both Rac and Cdc42, by 50 fold [Leonard, 1997] and mutation to alanine destroyed interactions of Cdc42 with PAK, Ack and WASP [Owen, 2000]. Such data suggested that aspartate 38 may be important to all CRIB-Rac/Cdc42 interactions.

(ii) PAK1 binds with similar affinity to Rac and Cdc42 [Manser, 1994], whereas ACK and WASP are relatively selective for Cdc42 [Manser, 1993] [Symons, 1996]. In order to

achieve this selective binding, ACK and WASP must interact with amino acids that differ between Cdc42 and Rac, and contacts with residues specific to Cdc42 were indeed revealed in the NMR studies. Cdc42 leucine 174 and valine 42 have been shown to form strong hydrophobic contacts with both ACK and leucine 174 is also important to the interaction with WASP. The equivalent residues in Rac are arginine 174 (within Rac effector loop II) and alanine 42, which should weaken these interactions (see sequences in figure 1.2). The PAK1 peptide did in fact make contacts with both leucine 174 and valine 42, however, mutation of neither Cdc42 valine 42 nor leucine 147 to alanine significantly disrupted binding to PAK, showing that these interactions are not essential [Gizachew, 2000]. Instead, contacts between the hydrophobic portion of PAK lysine 48 and Cdc42 leucine 177 (conserved in Rac), in addition to some contribution from leucine 174 and the hydrophobic portion of glutamate 178, form the dominant hydrophobic interface. The CRIB residues of ACK that interact with leucine 174 and valine 42 of Cdc42 are leucine 505 (the equivalent residue in WASP is an isoleucine, which also contacts leucine 174) and isoleucine 519 respectively. The equivalent residues in PAK1 are lysine 65 and glutamate 77 (see CRIB sequences in figure 1.5), which should not pack well against leucine 174 and valine 42. It is only the hydrophobic portions of these PAK1 residues that are seen to make any contribution to the interface with Cdc42 leucine 174 and valine 42.

(iii) From the NMR data PAK tyrosine 40 within switch I of Cdc42, which when mutated to cysteine in either Cdc42 or Rac prevents binding to PAK [Lamarche, 1996], can be seen to be essential for GTPase binding. The hydroxyl of tyrosine 40 makes contact with the carboxylate group of glutamate 77 and additional hydrophobic contacts are made with glutamate 77 and tyrosine 79. Tyrosine 40 is conserved in Rac and may contribute to the ability of PAK to bind to both Rac and Cdc42.

(iv) A further insight gained from these NMR structures is that the GTPase induces significant conformational changes in PAK, ACK and WASP. The CRIB-containing fragments of ACK and WASP used in these experiments have no discernible structure in solution, but when bound to Cdc42 they form a tight intermolecular β-sheet across GTPase switch regions I and II. Presumably Cdc42 stabilises this key conformation, which is only one of many that the free peptide can adopt in solution. Equally, the switch regions of free Cdc42 in solution are flexible, but become rigid when bound to an effector.

1.2.5.3 Interactions of Rac with non-CRIB proteins

This NMR data has certainly provided much insight into how CRIB motif-containing proteins in general may interact with Cdc42, and how they may achieve specificity for binding to Cdc42 or to Cdc42 and Rac. Even so, not all Rac effector proteins contain a classic CRIB domain, infact of

the 25 or so known potential Rac effectors (shown in figure 1.7) only 6 have a full CRIB motif, so cannot be assumed to bind to GTPases in the same way as Ack, WASP and PAK.

Some Rac and Cdc42 effectors appear to have partial CRIB domains that may act along with other regions of the protein to facilitate GTPase binding. The MAP kinase kinase kinase MEKK4, for instance, contains a partial CRIB motif with only 6 of the potential 8 conserved residues of a full CRIB motif [Fanger, G. R., 1997]. Recently it was found that the mammalian version of *C. elegans* PAR6 polarity determination gene product requires both a partial CRIB sequence, plus regions remote to this motif (a PDZ domain in particular), for its interaction with GTP-Cdc42. The full CRIB motif alone is sometimes sufficient for a strong interaction between classic CRIB-containing proteins and Rac or Cdc42 and is certainly sufficient for a weak interaction (see for instance [Rudolph, 1998] and [Guo, 1998]). For PAR6 the PDZ domain is required for even weak binding to Cdc42, but deletions or mutations within the partial CRIB indicate that it plays an essential part in the interaction [Joberty, 2000] [Lin, 2000] [Qiu, 2000]. It will be interesting to see whether sequence analysis of proteins thought to be non-CRIB Rac or Cdc42 effectors may also reveal partial CRIB motifs that mediate GTPase binding in combination with additional regions of the protein.

The p67phox component of the NADPH oxidase is one of the non-CRIB-containing Rac effectors (see figure 1.7). Based upon the sequence and circular dichroism studies it was suggested that the Rac-binding domain of p67phox folds into four tetratricopeptide repeat (TPR) motifs, each comprised of a pair of antiparallel α-helices, [Koga, 1999]. The structure of the p67phox Rac-binding domain (amino acids 1-203) along with GTP-Rac has now been solved [Lapouge, 2000]. The TPR repeats can be seen to form a platform on which a β-hairpin insertion sits. This β-hairpin, along with a few surface residues from TPR3 and TPR4, makes the majority of contacts with Rac. When p67phox binds to Rac it does not appear to mask the GAP-binding region of Rac, which includes switches I and II plus amino acids 75-90 (shown in pink in figure 1.2) [Diekmann, 1995] [Rittinger, Walker, Eccleston, Nurmahomed, 1997] [Rittinger, Walker, Eccleston, Smerdon, 1997]. In contrast, these regions are hidden in the PAK1-Cdc42 structure [Gizachew, 2000]. These data suggest that Rac may be turned off by a GAP even when bound to p67phox, resulting in a very transient interaction compared with effectors, like PAK, that compete more efficiently with GAPs.

1.2.6 Activation of effectors by Rho GTPases

The structural analysis of Rho GTPase-effector interactions has, so far, made use of discrete binding domains derived from effectors. When considering how a GTPase might regulate the

activity of a target protein, and how these proteins subsequently transduce signals to the cell, the whole effector protein must be considered.

1.2.6.1 Relief of autoinhibitory interactions by Rho GTPases

The most common mechanism of effector activation by Rho GTPases appears to be the disruption of autoinhibitory intramolecular interactions, to expose functional domains within the effector protein (see step 1 of the model shown in figure 1.6). For example, the Rac/Cdc42 targets PAK1-3 are Ser/Thr kinases, which contain a regulatory domain that inhibits kinase activity. Upon GTPase binding, the autoinhibitory sequence is displaced leaving the kinase domain free to bind to substrates [Tu, 1999] [Bagrodia, 1999]. A more distantly related PAK family member, PAK4, does not contain an autoinhibitory domain, and is not significantly stimulated by GTPase binding [Abo, 1998].

In agreement with the model a peptide from the PAK1 regulatory region (amino acids 83-149) can be used as an inhibitor of PAK activity both *in vitro* and *in vivo* and mutants of the PAK inhibitory domain have constitutive kinase activity [Zhao, 1998] [Frost, 1998]. Cleavage of PAK-2 by caspases during apoptosis also removes its regulatory domain and creates a constitutively active protein [Tang, 1998]. A crystal structure of the two autoinhibitory regions of PAK1 (amino acids 70-149 and 249-545) surprisingly showed an intermolecular dimer, mediated by the N-terminal fragments, which also sterically hinders kinase activity and adds to intramolecular autoinhibitory interactions to stabilise the inactive state of PAK [Lei, 2000].

A similar activation principal has been observed for some of the scaffold-like targets of Rho GTPases, such as the Cdc42 effectors WASP and N-WASP. In these cases, rather than directly masking a catalytic site, the intramolecular autoinhibitory interactions mask binding sites for other proteins that are required to initiate downstream signaling. The regions of WASP that bind to each other were identified, using a tryptophan fluorescence quenching assay, as the N-terminal GTPase-binding domain (amino acids 230-310) and a cofilin-homology region at the C-terminus (amino acids 461-492) [Kim, 2000]. Cdc42-GTP competes with WASP C-terminus for binding to the N-terminus and induces a conformational change in the WASP N-terminus quite different from its conformation when autoinhibited [Kim, 2000]. NMR analysis of WASP's autoinhibitory regions fused to each other has suggested that the acidic region, which binds to the Arp2/3 complex that is essential for WASP activity [Machesky, Mullins, 1999] [Rohatgi, 1999], is masked making the protein inactive [Kim, 2000].

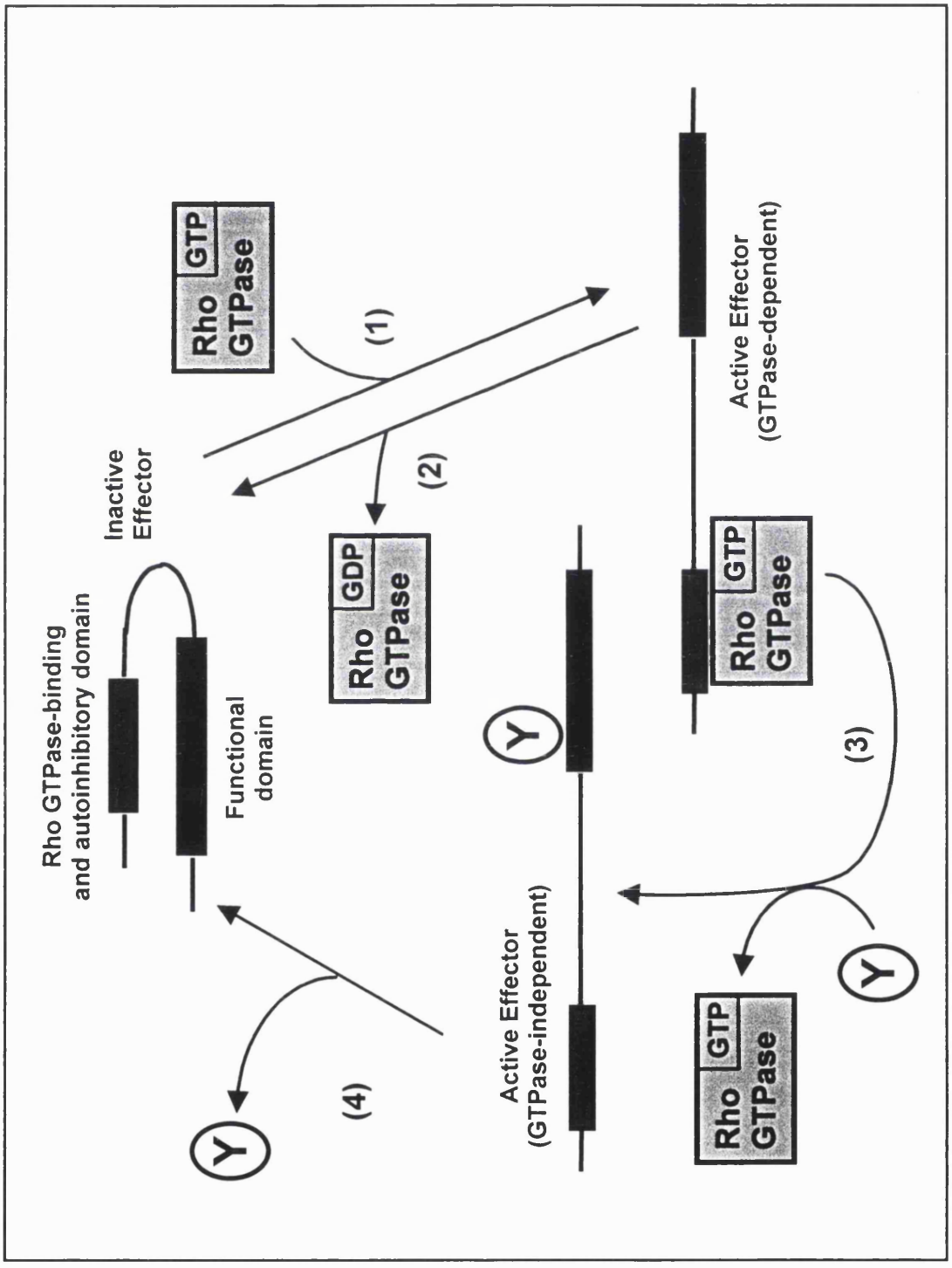

Figure 1.6 Model for activation of Rho GTPase effector proteins by relief of autoinhibitory interactions

Recently it has been shown that Arp2/3 can in fact bind to inactive N-WASP, priming it for activation, but that a region adjacent to the Rac-binding domain inhibits its activity until intramolecular interactions are disrupted [Prehoda, 2000]. In this same study it is shown that both Cdc42-GTP and lipids, which bind to the same site that forms inhibitory contacts with Arp2/3, are required for full activation of the N-WASP-Arp2/3 complex [Prehoda, 2000]. In light of these data co-activators, that cooperate with GTP-bound GTPases to induce effector activation, could be added to step 1 of the effector activation model in figure 1.6.

Once an effector has been activated by binding to a GTP-bound Rho GTPase (figure 1.6 step 1), inactivation of the GTPase by a GAP will cause the effector to dissociate from the Rho GTPase, leaving an inactive effector protein (figure 1.6 step 2). Alternatively, a second event can allow the effector to dissociate and yet remain active even in the absence of an active GTPase (figure 1.6 step 3). For example, once the kinase PAK has been activated by its interaction with GTP-bound Rac or Cdc42 it then autophosphorylates. This both reduces its affinity for GTPase (freeing the GTPase to bind to more effectors or to be inactivated by GAPs) and maintains PAK in an activated conformation even when dissociated from the GTPase [Manser, 1994].

Similar mechanisms may exist to control the duration of activation for scaffold-like effectors, but a separate kinase activity would be needed if effector activity is to be maintained by phosphorylation. WASP may be an example of this, as it is a substrate for two tyrosine kinases, Lyn and Btk [Guinamard, 1998] [Baba, 1999] and shows increased tyrosine phosphorylation in the presence of constitutively active Cdc42, indicating that Cdc42 may recruit WASP to the site of Lyn and Btk activity [Guinamard, 1998]. The tyrosine residue phosphorylated by Btk (tyrosine 291) [Baba, 1999] is predicted to disrupt the autoinhibited fold of WASP N-terminus, so may stabilize WASP in an active conformation even in the absence of Cdc42 [Kim, 2000].

The presence, or not, of kinases that phosphorylate scaffold-like effectors (figure 1.6 step 3), and the activity of phosphatases that may dephosphorylate both activated kinase and scaffold types of effectors (figure 1.6 step 4), may prove to be a general mechanism for regulating the kinetics of effector activity. Interestingly protein phosphatase 2A co-precipitates with PAK1 and another Rho GTPase effector, p70S6 kinase, so may be involved in their inactivation (figure 1.6 step 4) [Westphal, 1999]. In keeping with the model, binding of other proteins to an activated effector, in addition to or instead of phosphorylation, could stabilize effectors in an active conformation after GTPase dissociation (figure 1.6 step 3), although no clear example of an effector that utilises such a mechanism has yet been identified.

1.2.6.2 Regulation of effector proteins by sub-cellular localisation

Almost all Rho GTPase effectors have multiple domains, which, in addition to Rho GTPase binding, may regulate their activity. They could, for instance change the subcellular localisation of the effector. For example, a number of effectors contain PH domains, which may mediate membrane-association: the Cdc42 effectors WASP, N-WASP and MRCKα/β and the RhoA effectors ROK, citron and citron-kinase. For N-WASP a point mutation that reduces lipid binding by the PH domain destroys the ability to support actin microspike formation seen for the wild type protein [Miki, 1996].

Protein-protein, as well as protein-lipid, interactions can regulate the subcellular localization of GTPase effectors. For example, PRK2 (but not the related PKN/PRK1), WASP and PAK all contain PXXPXR (where X is any amino acid, P is proline and R is arginine) SH3 domain-binding motifs which have been reported to bind to the adaptor Nck [Quilliam, 1996] [Rivero-Lezcano, 1995] [Bokoch, Wang, 1996] [Galisteo, 1996]. Nck also has an SH2 domain so it could recruit these effectors to activated receptor tyrosine kinases. PAK also interacts with another SH3-containing protein, αPIX (also known as Cool-2), though this interaction is via a non-classical SH3 domain-binding region of PAK (amino acids 175-206) [Obermeier, 1998] [Manser, 1998]. αPIX, which is a Cdc42/Rac GEF, can potentially activate PAK and can also localize the kinase to specific sites within the cell (reviewed in [Bagrodia, 1999]). For example, paxillin recruits Cat/Git/Pkl to focal contacts which, in turn, binds to PIX [Turner, CE, 1999]. Binding of PAK to Nck and Pix is inhibited upon activation, as are PAK autoinhibitory interactions, creating a dynamic cycle of PAK kinase activity and protein localisation [Zhao, Manser and Lim, 2000].

1.3 BIOLOGICAL ACTIVITIES AND EFFECTORS OF RAC

1.3.1 Potential Rac Effector Proteins

Around 25 effectors for Rac1 have been identified to date. These are listed in figure 1.7, along with key references. Rac effector proteins fall mainly into three broad types. **(1)** serine/ threonine kinases Mlk2, MEKK1 and 4, PAK1-3 and p70S6 kinase, all of which also bind to Cdc42, Prk2 that binds to RhoA as well as Rac but in a nucleotide-independent manner and Mlk3 that binds to Rac and Cdc42, but has been functionally linked only to Cdc42. **(2)** cytoplasmic scaffold proteins POSH, POR-1, p67phox, p140Sra-1, IRSp53 (possibly also a Cdc42 effector, Krugman and Hall unpublished data) and IQGAP1 and 2 and PAR6, which have all been reported to bind to activated Rac and Cdc42, but have been functionally linked only to Cdc42. **(3)** lipid modifying enzymes phosphatidylinositol-3 kinase (PI3K), phospholipase D (PLD), phospholipase C-β2 (PLC-β2), synaptojanin2 (Sac1-like phosphatidylinositol phosphatase),

diacylglycerol kinase (DAG) and phosphatidylinositol-4-phosphate 5-kinase (PI-4,5-P5K), the latter two effectors appear to bind both to GDP and GTP forms of Rac, but their activation by Rac is GTP-dependent. Rac effectors that fall outside of these categories are the Rho GAP N-chimaerin, which in one report was implicated as an effector for Rac and Cdc42 as well as a GAP, and the axon guidance semaphorin receptor plexin B1.

Of the potential Rac effectors shown in figure 1.7 only a small number (PAK1-3, Mlk2, Mlk3, Plexin-B1, PAR6 and MEKK4) contain CRIB motifs (mentioned above) that are essential, although not sufficient, for their interaction with activated Rac. The CRIB domain was identified as a motif that was similar between murine p65PAK and ACK and formed the most minimal Cdc42 binding site within p65PAK [Burbelo, 1995]. Alignment of this domain with proteins in the GenBank™ data base revealed potential CRIB domains in a number of proteins that were subsequently found to bind to GTP-bound Rac and Cdc42 *in vitro* [Burbelo, 1995] [Teramoto, 1996] [Nagata, 1998]. Of the non-CRIB effectors only the GTPase-binding region of p67phox has been well characterised [Lapouge, 2000].

Rac effectors identified using the yeast-two-hybrid system

The scaffold proteins POR-1 and POSH were identified as potential Rac effectors using constitutively active Rac mutants as bait in yeast-two-hybrid screens [Van Aelst, 1996] [Tapon, Nagata, 1998]. POR1 has been found to interact with Arf6 via the same region that binds to Rac, and is proposed to act as a co-ordinator of actin reorganisation at the plasma membrane in response to both GTPases [D'Souza-Schorey, 1997].

Figure 1.7 Potential effector proteins for the Rho family GTPase Rac

* denotes proteins that are activated only by the GTP-bound GTPase, but the interaction is GTP-independent. + denotes proteins that have been functionally linked to a GTPase, but a direct interaction has not been shown. ( ) denotes a GTPase for which an *in vitro* interaction has been demonstrated, but there is no known functional link. Note that Rho inhibits DAG, whereas the other target proteins are activated by Rho GTPases. Where an effector function has been reported this is noted, but in many cases these are far from clear. Abbreviations: the Cdc42/Rac-interactive binding (CRIB) motif; the tetratricopeptide (TPR) motif; Mixed lineage kinase (Mlk); p21-associated kinase (Pak); phosphatidylinositol phosphate (PIP); phosphatidic acid (PA); phospholipase (PL); diacylglycerol (DAG); kinase (K); insulin receptor substrate (IRS); plenty of SH3s (POSH); Wiskott-Aldrich syndrome protein-like verponin-homologous protein (WAVE); Specific Rac1-associated protein (Sra); partitioning-defective (PAR).

Potential Rac Effector	Type of protein	Functions	Selectivity of GTPase binding			GTPase binding motif	Key References
p70 S6 kinase	Ser/Thr kinase	Cell cycle control via translation regulation	Rac	(Cdc42)			[Chou, 1996]
Mlk2	Ser/Thr kinase	JNK	Rac	(Cdc42)		CRIB	[Nagata, 1998]
Mlk3	Ser/Thr kinase	JNK/ p38	(Rac)	Cdc42		CRIB	[Teramoto, 1996] [Bock, 2000]
MEKK1, 4	Ser/Thr kinase	JNK	Rac	Cdc42		Partial CRIB for MEKK4	[Fanger, Johnson 1997]
Prk2	Ser/Thr kinase	Actin organisation	Rac		Rho *		[Vincent, 1997]
PAK1, 2, 3	Ser/Thr kinase	JNK/ actin organisation	Rac	Cdc42		CRIB	Reviewed in [Bagrodia, 1999]
PI-4-P5K	Lipid kinase	PIP_2 levels/ actin	Rac *		(Rho * +)		[Tolias, 1995] [Ren, 1996] [Tolias, 2000]
PI3K	Lipid kinase	PIP_3 levels	Rac	Cdc42			[Zheng, 1994] [Tolias, 1995] [Bokoch, Vlahos 1996]
DAGK	Lipid kinase	PA levels	Rac *		Rho +		[Tolias, 1998] [Houssa, 1999]
PLD	Lipase	PA levels	Rac	Cdc42	Rho		[Malcolm, 1996] [Hess, 1997] [Han, JS 1998] [Bae, 1998]
PLC-β2	Lipase	DAG/IP_3 levels	Rac				[Illenberger, 1998]
Synaptojanin2	Lipid phosphatase	PIP_2/PIP_3 levels/ actin	Rac				[Sakisaka, 1997] [Nemoto, 1997] [Malecz, 2000]
Plexin-B1	Transmembrane receptor	Receptor for semaphorin axon guidance signals	Rac			CRIB	[Vikis, 2000] [Driessens, 2001]
PAR6	Scaffold	Polarity	(Rac)	Cdc42	(TC10)	Partial CRIB + PDZ	[Joberty, 2000] [Lin, 2000] [Qiu, 2000]
IRSp53	Scaffold	Actin organisation via WAVE	Rac	(Cdc42)			[Miki, Suetsugu 1998] [Miki, 2000]
POSH	Scaffold	Unknown	Rac				[Tapon, Nagata 1998]
POR-1	Scaffold	Actin organisation	Rac		Arf6		[Van Aelst, 1996] [D'Souza-Schorey, 1997]
p67phox	Scaffold	NADPH oxidase	Rac			TPR motifs + β-hairpin	[Abo, 1991] [Diekmann, 1994] [Lapouge, 2000]
IQGAP1,2	Scaffold	Actin/ cell-cell contacts	(Rac)		Cdc42		[Brill, 1996] [Erickson, 1997] [Fukata, 1997] [Fukata, 1999]
p140Sra-1	Scaffold	Actin organisation	Rac				[Kobayashi, 1998]
N-chimaerin	GAP for Rac/Cdc42	Actin organisation	Rac		Cdc42		[Kozma, 1996]

Figure 1.7 Potential effector proteins for the Rho family GTPase Rac

Very recently synaptojanin2, the ubiquitious and constitutively membrane-bound form of a Sac1-like phosphatidylinositol lipid phosphatase implicated in regulation of endocytosis [Nemoto, 1997], was found in a yeast-two-hybrid screen to be a binding partner for Rac [Malecz, 2000].

Mouse PAR6 was identified as a Cdc42 or TC10-binding protein in yeast-two-hybrid screens by two groups [Joberty, 2000] [Qiu, 2000]. Another group working on the PAR6-PAR3 complex in mammalian cells noticed the PAR6 partial CRIB and this lead them directly to check for Rho GTPase binding [Lin, 2000]. Each of the three groups reported different results for binding of the four known mammalian PAR6 isoforms (A-D) to Rac: two groups found that mouse PAR6C binds to Rac [Lin, 2000] [Qiu, 2000], whereas Joberty et al reported that only PAR6A bound to Rac [Joberty, 2000]. In *Caenorhabditis elegans* PAR6 is involved in embryonic polarity [Hung, 1999], as is Cdc42 in many organisms [Johnson, 1999], therefore it seems likely that Cdc42 is the functional partner for PAR6 *in vivo*.

Rac effectors identified biochemically

For many other effectors an interaction with, and activation by, Rac was discovered biochemically. IQGAP1 had been initially identified as a protein that has some sequence homology to a yeast RasGAP and binds to calmodulin, via an IQ domain, hence its name [Weissbach, 1994]. IQGAP1 was subsequently isolated by two groups as a protein, from cell lysates [Hart, 1996] or rat brain lysate [Kuroda, 1996], that associated with Cdc42Hs-GTP. As a recombinant protein both groups found that IQGAP1 bound directly to both Rac and Cdc42 in a GTP-dependent manner. The very similar IQGAP2 was also shown to bind to both Rac and Cdc42 [Brill, 1996]. More recent experiments showing a complex between IQGAP1, actin and Cdc42 did not address whether Rac can also form such a complex [Erickson, 1997] [Fukata, 1997], whereas sudies of IQGAP1 and regulation of cell-cell contacts showed effectes with both Cdc42 and Rac [Fukata, 1999]. Kaibuchi's group, who were one of the groups to isolate IQGAP1 with Cdc42, also isolated p140Sra-1 from rat brain cytosol using GTPγS-GST-Rac1 as bait [Kobayashi, 1998].

Rac, complexed with RhoGDI, was purified as a cytosolic fraction required for NADPH oxidase activation [Abo, 1991]. Subsequently the p67phox component of the complex was identified as the direct binding partner for Rac1 [Diekmann, 1994] [Prigmore, 1995].

Mouse p65PAK (homolog of human PAK1) was first isolated as a Rac and Cdc42-binding protein from rat brain [Manser, 1994]. When Prigmore et al identified p67phox as a binding partner for Rac in neutrophils they also observed that Cdc42 was associated with a 68kDa protein from neutrophil cytosol that turned out to be a PAK family member [Prigmore, 1995]. Mammalian PAK3 was identified by sequence homology with PAK1 and was shown also to bind

to GTP-Rac and GTP-Cdc42 *in vitro* [Bagrodia, Taylor, 1995]. There now known to be are at least four mammalian PAK family proteins, three of which bind to both Rac and Cdc42.

Prk2 was first identified as a protein from a bacterial expression library that bound to Nck adaptor protein SH3 domain, and was subsequently shown to bind to RhoA [Quilliam, 1996]. Prk2 was later identified as the major RhoA-associated kinase in many tissue extracts and was shown to be activated by both activated Rac and Rho, but the interaction with RhoA was GTP-independent [Vincent, 1997].

A fraction from neutrophil cytoplasm that contained a Rho family GTPase and LyGDI was found to activate PLC-β2 and using recombinant Rho GTPases and PLC-β2 it was shown that activated Rac and Cdc42 both stimulate PLC-β2 directly *in vitro* [Illenberger, 1998].

Rac effectors identified because of known links with Rac-dependent processes

Due to links between actin reorganisation, Rho GTPases and lipid signaling lipid modifying enzymes in addition to PLC-β2 (PI-4-P5K, DAG, PLD and PI3K) were tested *in vitro* and *in vivo* and were found to bind directly to Rac [Tolias, 1995] [Bokoch, Vlahos, 1996] [Hess, 1997] [Tolias, 1998].

p70S6 Kinase was identified as a binding partner for Rac and Cdc42 because of previous observations that PI3K mediates activation of both p70S6K and Rac in response to growth factors such as PDGF [Chung, 1994] [Ridley, Paterson, 1992] [Hawkins, 1995], which lead Chou and Blenis to test for a direct interaction between Rho GTPases and p70S6 Kinase [Chou, 1996].

Recently a direct interaction has been shown between Rac and a member of the plexin family (B1) [Vikis, 2000]. Plexins act as receptors and co-receptors for semaphorins; some semaphorins (such as Sema3A/collapsin) bind directly to neuropilins, but signal through plexin co-receptors, while Sema4D/CD100 binds directly to plexins such as plexin B1 [Takahashi, 1999] [Tamagnone, 1999]. Previous reports implicating Rac in axon guidance downstream of semaphorins [Jin, 1997] [Kuhn, 1999] lead Vikis et al to test for a direct plexin-Rac interaction [Vikis, 2000], whereas Driessens et al identified a B-type Plexin as a binding partner for Rac using the yeast-two-hybrid system [Driessens, 2001].

1.3.2 Biological activities of Rho, Rac and Cdc42

The most studied function of Rho GTPases is to regulate the assembly and organization of the actin cytoskeleton [Hall, 1998]. The effects of Rho, Rac and Cdc42 were initially described using quiescent Swiss3T3 fibroblasts, a cell line in which serum starvation creates a very low

background of organised F-actin structures. Addition of lysophosphatidic acid (LPA) induces the formation of contractile actin-myosin stress fibres and associated focal adhesions, and this can be blocked by C3 transferase [Ridley and Hall, 1992]. Growth factors, such as PDGF, insulin or EGF induce the formation of actin-rich lamellipodia and membrane ruffles, associated with focal contacts, and the dominant negative N17Rac specifically inhibits this response [Ridley, Paterson, 1992]. Thirdly, bradykinin induces the formation of peripheral microspikes or filopodia, which are also associated with focal contacts, and this can be inhibited by expression of dominant negative N17Cdc42 [Kozma, 1995] [Nobes and Hall, 1995]. These types of experiment have lead to the conclusion that Rho, Rac and Cdc42 regulate three signal transduction pathways linking various membrane receptors to the assembly of actin-myosin filaments, lamellipodia and filopodia respectively.

It is not surprising, therefore, that Rho GTPases have been found to play a role in a variety of cellular processes that are dependent on the actin cytoskeleton, such as cytokinesis [Mabuchi, 1993] [Drechsel, 1997], phagocytosis [Cox, 1997] [Caron, 1998], pinocytosis [Nobes, 1999]□, cell migration [Allen, 1998] [Nobes, 1999], morphogenesis [Settleman, 1999] and axon guidance [Luo, L, 1997].

	Actin	SRF	JNK/ p38	NF-κB	NADPH oxidase	G1 cell cycle progression	cell-cell contacts	secretion	cell polarity	Transfo-rmation
Rho	+	+	-	+	-	+	+	+	-	+
Rac	+	+	+	+	+	+	+	+	-	+
Cdc42	+	+	+	+	-	+	+	?	+	+

Figure 1.8 Summary of cellular processes that involve Rho, Rac and Cdc42

The activities shown refer to biological pathways that can be induced by the activated Rho GTPases indicated and can be inhibited by dominant negative constructs of the appropriate Rho GTPases. SRF (serum response factor) and NF-κB (nuclear factor-κB) are both transcription factors; JNK (c-jun N-terminal kinase) and p38 are MAP Kinase pathways; the NADPH oxidase complex is present only in professional phagocytic cells; secretion has only been shown to involve Rho GTPases in mast cells.

In fibroblasts injection of activated Cdc42 protein induces filopodia, but also lamellipodia, which are Rac-dependent. Also, within 5min of treatment, growth factor-induced Rac stimulation causes lamellipodia formation, but at later time points (20-30min) stress fibres, which are inhibited by the Rho inhibitor C3, have been observed [Nobes and Hall, 1995]. These data indicate that in fibroblasts there is a GTPase cascade from Cdc42 to Rac and then Rho. In other cell types, however, it appears that Rac and Cdc42 activity inhibits Rho, see for instance [Sander, 1999] and [Noren, 2000]. RhoG has also been shown to activate both Rac and Cdc42 [Gauthier-Rouviere, 1998]. The mechanistic links between these Rho GTPases are poorly understood.

In addition to their effect on the actin cytoskeleton, the Rho family also regulate a variety of other biochemical pathways (see figure 1.8) including: SRF and NF-κB transcription factors [Hill, 1995] [Perona, 1997]; the JNK and p38 MAP Kinase pathways [Coso, 1995] [Minden, 1995]; the phagocytic NADPH oxidase complex [Abo, 1991]; G1 cell cycle progression [Olson, 1995]; the assembly of cadherin-containing cell-cell contacts (for Rac this may be actin-dependent) [Kaibuchi, 1999] [Braga, 1999]; secretion in mast cells [Norman, 1996]; cell polarity [Johnson, 1999]; and cell transformation [Van Aelst, 1997]. Although Rho GTPases are best characterised for their effects on the actin cytoskeleton there is now much interest in their abilty to affect cell proliferation and gene transcription. The contributions of all of these Rho GTPase activities to malignant transformation is a particularly important field of study. The involvement of Rac and its effector proteins in a broad range of biological processes is discussed in the following sections.

1.3.3 Biological activities of Rac and links to downstream effectors

1.3.3.1 Rac-induced actin reorganisation and focal contact formation

Rac induces actin web-like structures called lamellipodia at the periphery of cells, which often fold back onto the cell and are then termed ruffles. These structures appear in fibroblasts in response to constitutively active Rac and stimulation by growth factors such as insulin, epidermal growth factor and platelet-derived growth factor. Rac-induced lamellipodia are essential for the migration of many cell types in response to various stimuli. For example, migration of primary rat embryo fibroblasts at a wound edge [Nobes, 1999], migration of the Bac1 macrophage cell line in response the chemoattractant colony stimulating factor-1 [Jones, GE, 1998] and neurite outgrowth in response to inhibition of Rho [Kozma, 1997] are all Rac-dependent events. During development a number of cell movements and morphological changes have been shown to be both actin- and Rac-dependent. During *Drosophila* development a dominant inhibitory DRac transgene interferes with the appropriate migration of a subset of follicle cells called border cells [Murphy, 1996], inhibits actin-dependent epidermal cell shape changes required for dorsal closure [Harden, 1995] and interferes with motor neuron axon guidance [Kaufmann, 1998]. In mammalian systems the growth cone collapse response of neurons to the Sema3/collapsin axon

guidance cue is also inhibited by dominant negative Rac [Jin, 1997] and by Rac switch I and PAK CRIB cell permeable peptides [Vastrik, 1999]. Recent observations that Rac binds directly to the cytoplasmic tail of the Sema3 receptor Plexin B1 [Vikis, 2000] and that Rac is localised to actin-rich vacuoles and membrane ridges induced by Sema3 provide interesting links between Sema3 signaling and Rac [Fournier, 2000].

Rac has been linked not only to actin reorganisation, but also to associated focal complex (FC) formation, reviewed in [Ridley, A, 2000]. In fibroblasts Rac-induced ruffles are accompanied by the appearance of small FCs [Nobes and Hall, 1995]. Also, adhesion to fibronectin requires Rac activity, in fibroblasts and T cells [Price, 1998] [D'Souza-Schorey, 1998], and in fibroblasts can be seen to induce transient Rac activation [del Pozo, 2000]. Spreading on a thrombospondin-1 matrix also activated Rac and Cdc42, but in a more prolonged way than on fibronectin [Adams, 2000]. At least two FC-associated Rac-activating protein complexes have been reported that could locally activate Rac at sites of FC formation: the Rac/Cdc42 GEF αPIX binds to Pkl/Git, which binds to the focal adhesion component paxillin [Turner, CE, 1999]; the focal adhesion kinase-p130^{Cas}-CrkII-DOCK180 complex is regulated by integrin adhesion and the DOCK180 component binds to and somehow activates Rac, possibly via the Rac GEF Vav [Kiyokawa, 1998].

1.3.3.2 Effectors of Rac implicated in actin reorganisation

There are very few examples of unique Rac effectors that have been implicated in actin reorganisation. POR-1 (Partner of Rac) has been implicated in Rac-induced lamellipodia formation, since POR-1 truncations act as dominant negative constructs [Van Aelst, 1996] [D'Souza-Schorey, 1997] and p140Sra-1 (Specific Rac1-associated protein) co-sediments with F-actin, implying a role in Rac-induced actin reorganisation [Kobayashi, 1998]. Little more is known about the cellular functions of these two proteins.

A target of Rac that is better characterised is PI-4-P5K, see figure 1.9. Many observations point to a role for lipids, particularly phosphatidylinositol-4,5-bisphosphate (PI-4,5-P_2), in actin cytoskeleton rearrangements. For instance, the binding of PI-4,5-P_2 to capping proteins, such as gelsolin, can induce their release from actin filament barbed ends, providing a mechanism whereby PI-4,5-P_2 could increase actin polymerization [Janmey, 1987]. Over-expression of PI-4-P5K, (to produce PI-4,5-P_2, induces massive actin polymerization in COS7 cells [Shibasaki, 1997]. Also, the PI-4,5-P_2 phosphatase synaptojanin, now known itself to be a Rac target although poorly characterised as yet [Malecz, 2000], when over-expressed reduced PI-4,5-P_2 levels, resulting in a reduction in actin structures [Sakisaka, 1997].

Rac interacts directly with PI-4-P5K and although this interaction is not GTP dependent the activation of PI-4-P5K by Rac is dependent upon GTP [Tolias, 1998]. A GTP-independent interaction of RhoA with PI-4-P5K has also been detected, however, unlike for Rac, this has not been shown to be direct [Ren, 1996]. It has been established, using permeabilised platelets, that thrombin-induced actin filament assembly requires actin filament uncapping, which is absolutely dependent upon an increase in PI-4,5-P_2 levels, and this is now known to be mediated by Rac activation of a type I (PI-activated) PI-4-P5K [Hartwig, 1995] [Tolias, 2000]. PI-4,5-P_2 also binds to vinculin, increasing its talin-binding ability, which could induce focal adhesion formation [Gilmore, 1996]. PI-4-P5K could, therefore, provide a link between Rac and the stimulation of both new actin polymerization and of focal complex assembly.

At least three other effectors of Rac have also been implicated in actin-reorganisation: IRSp53, via binding to a WASP family member, WAVE, (WASP proteins being Cdc42 effectors); IQGAPs, which are also potential Cdc42 effectors; PAKs, which are again also Cdc42-binding proteins. These proteins shall be discussed below.

The WASP family of Rac and Cdc42-regulated proteins

WASP is a Cdc42 effector protein that is expressed only in haemoatopoietic cells and is the product of the X-linked immunodeficiency gene found in Wiskott-Aldrich syndrome [Derry, 1994] [Kirchhausen, 1996]. The more ubiquitously expressed (neuronally enriched) N-WASP, like WASP, also binds to Cdc42 [Aspenstrom, 1996] [Kolluri, 1996] [Miki, 1996]. WASP and N-WASP each contain an N-terminal PH domain, followed by a WASP-homology domain 1 (WH1), a CRIB domain, an SH3-binding proline-rich sequence, a WH2 domain containing verprolin-like sequences and an acidic C-terminus to which Arp2/3 binds (see below). Over-expression of N-WASP plus Cdc42 induces very long microspikes, like an exaggeration of Cdc42 activity [Miki, Sasaki, 1998], suggesting that these proteins may be involved in the formation of filopodia downstream of Cdc42. N-WASP binds to profilin, which binds to actin, and WASP and N-WASP bind directly to actin monomers through their verprolin-like WH2 domains [Machesky, 1998] [Miki and Takenawa, 1998] [Suetsugu, 1998].

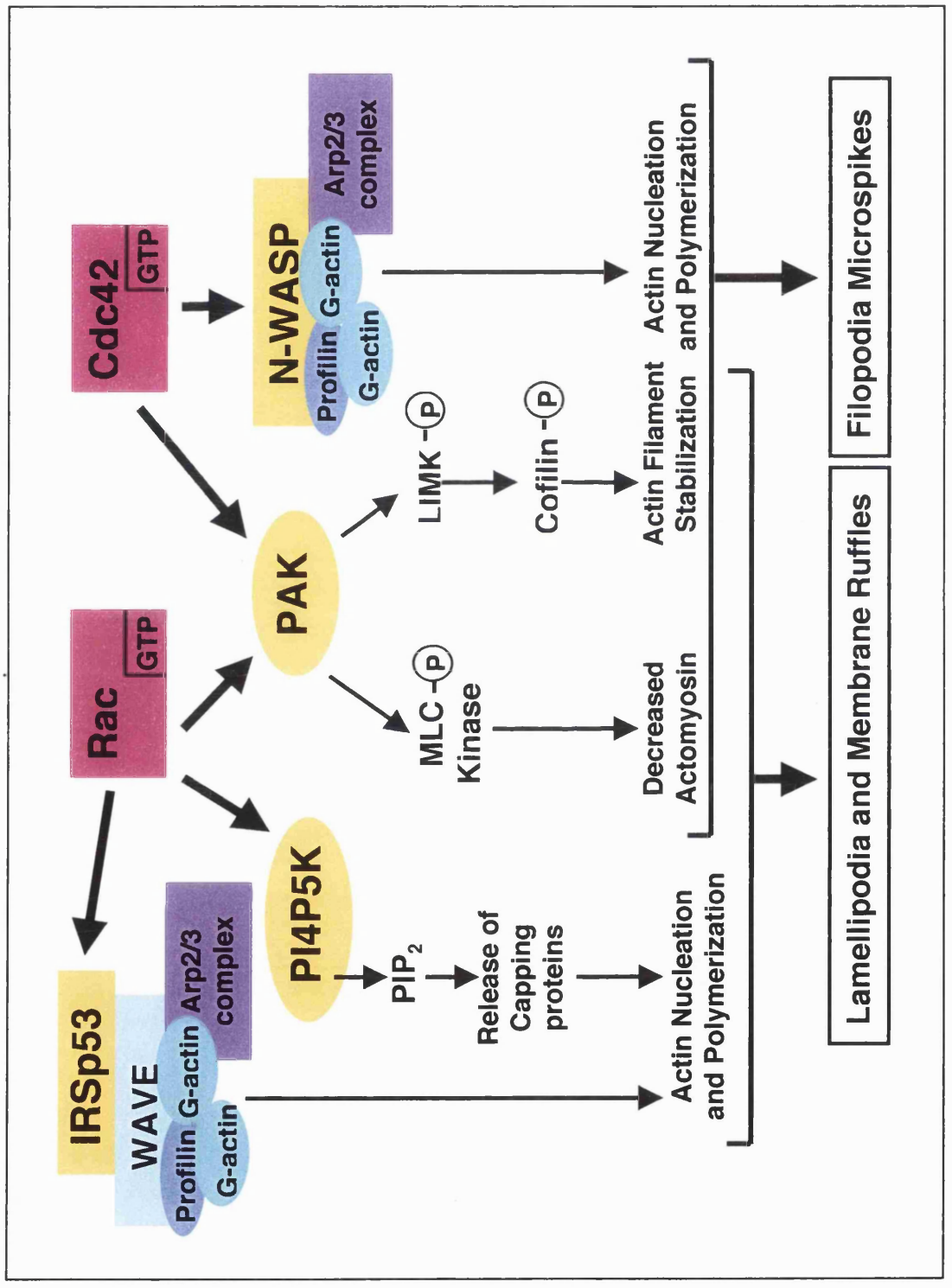

Figure 1.9 Signal transduction pathways induced by Rac and Cdc42 thought to contribute to the formation of actin-containing structures
GTPase effector proteins are shown in yellow (based upon [Bishop, 2000])

A WASP-like Verprolin-homologous protein (WAVE, also known as Scar) has beeen shown to precipitate with Rac [Miki, Suetsugu, 1998]. This interaction is not direct, but has recently been reported to occur through a scaffold protein called IRSp53 (insulin receptor substrate), which binds to both activated Rac (via an N-terminal non-CRIB binding site) and WAVE (via a C-terminal SH3 domain) [Miki, 2000]. WAVE was localised to membrane ruffles, and its over-expression caused actin clusters, an activity that required the profilin-binding and verprolin-homology (actin-binding) domains; a verprolin-homology domain mutant of WAVE inhibited Rac-induced ruffling, further suggesting an *in vivo* link between Rac and WAVE [Miki, Suetsugu, 1998]. WAVE/Scar, like WASP and N-WASP, interacts with and activates the Arp2/3 complex through its C-terminal acidic domain (see figure 1.9) [Machesky, 1998] [Machesky, Mullins, 1999]. The Arp2/3 complex binds to actin monomers and acts as a nucleation site for new actin polymerization [Machesky and Gould, 1999] [Welch, 1999]. By recruitment of actin, profilin and Arp2/3 and binding, directly or indirectly, to a Rho GTPase WASP family members appear to create GTPase-activated actin nucleation complexes involved in actin reorganisation downstream of both Rac and Cdc42 (see figure 1.9).

PAK kinases and Rac-dependent regulation of actin and focal contacts

PAK1, 2 and 3 (called α, β and γ in mouse) are Ser/Thr kinases, related to yeast Ste20, which have received a great deal of detailed attention [Manser, 1994] [Manser, 1995] [Bagrodia, Taylor, 1995] and reviewed in [Bagrodia, 1999]. *In vitro* PAK1 and 3 bind equally well to Cdc42 and Rac, though Cdc42 stimulates PAK1 activity more strongly than does Rac [Manser, 1995]. PAK2 only inhibits the intrinsic GTPase activity of Rac, and not Cdc42, suggesting that it may be a Rac target [Zhang, B, 1998]. It is difficult to be sure whether PAK1,2,3 are targets for Rac, Cdc42 or both *in vivo* from these *in vitro* interactions.

There have been conflicting reports linking PAKs to actin changes. Activated mutants of PAK1 have been reported to induce both filopodia and membrane ruffles in Swiss3T3 cells, to increase NIH3T3 cell migration and to cause neurite outgrowth in PC12 cells, similar to the affects of constitutively active Cdc42 and Rac [Sells, 1997] [Daniels, 1998] [Sells, 1999]. PAK1 has also been seen to localize to membrane ruffles, as well as phagocytic actin-containing cups, in N-formyl-methionyl-leucyl-phenylalanine (fMLP) stimulated neutrophils [Dharmawardhane, 1997]. Other groups, however, have failed to find any effects of PAK over-expression on the actin cytoskeleton [Lamarche, 1996] [Joneson, 1996].

A variety of substrates for PAKs have been identified that could affect the actin cytoskeleton. Rac and Rho both induce phosphorylation of LIM Kinase (LIMK), when phosphorylated LIMK is able to inhibit (by phosphorylation) cofilin, leading to stabilization of filamentous actin structures (see scheme in figure 1.9) [Arber, 1998] [Bamburg, 1999] [Maekawa, 1999]. The Rac

target PAK1 (*in vitro*) and the Rho target ROK (*in vitro* and *in vivo*) have been shown to phosphorylate LIMK [Maekawa, 1999] [Edwards, 1999], also, an inactive form of LIMK has been shown to inhibit both Cdc42 and Rac induced actin changes [Yang, 1998]. These data suggest that cofilin phosphorylation may be required in a number of Rho GTPase signaling pathways that lead to actin reorganisation (see scheme in figure 1.9).

PAK has also been reported to phosphorylate and inactivate myosin light chain (MLC) kinase, thus decreasing MLC phosphorylation [Sanders, 1999]. Phosphorylation of MLC occurs at Ser19, which stimulates the actin-activated ATPase activity of myosin II and promotes the assembly of actomyosin filaments [Bresnick, 1999], therefore a decrease in MLC phosphorylation causes disassembly of actomyosin filaments. RhoA has the opposite affect, it increases MLC phosphorylation, thereby increasing actomyosin filament assembly and contraction. This activity of RhoA is mediated by its effector protein ROK, which phosphorylates both myosin light chain phosphatase, inactivating the enzyme, and myosin light chain itself [Amano, 1996] [Kawano, 1999]. There has also been a report of Rac-induced phosphorylation of Myosin II Heavy Chain (MHC), which potentially would also lead to loss of actomyosin filaments [Bresnick, 1999] [van Leeuwen, 1999]. Dominant negative PAK inhibited MHC phosphorylation, but active PAK did not reconstitute the effect, suggesting that multiple effectors may mediate this activity of Rac [van Leeuwen, 1999].

Interestingly, PAK-induced actin cytoskeletal changes are partly independent of its kinase activity, but require membrane targeting [Sells, 1997] [Daniels, 1998] [Lu, 1997]. PAK is recruited to the plasma membrane by binding to the receptor tyrosine kinase-associated adaptor protein Nck [Bokoch, Wang, 1996] [Galisteo, 1996]. At the plasma membrane PAK can be recruited to focal contacts by binding to PIX, which forms part of a paxillin-associated GIT-PIX complex [Turner, CE, 1999]. GIT has been shown to induce focal contact dissassembly when over-expressed [Zhao, Manser, Loo, 2000]. PAK autophosphorylation disrupts its interactions with Nck and PIX, so PAK dissociates from these membrane-associated complexes upon activation [Zhao, Manser and Lim, 2000]. In *Drosophila* a Nck homologue (Dock) is required for projection of photoreceptor cells to the optic ganglia and membrane-targeted PAK can rescue the loss of Dock [Hing, 1999]; Rac and its activator Trio have now been genetically linked with this Pak-dependent signaling pathway [Newsome, 2000]. In PC12 cells over-expression of kinase dead β-PAK lead to increased neurite outgrowth [Daniels, 1998]. The ability of activated Rac to translocate to the membrane and to activate PAK is somehow reduced in non-adherent fibroblasts [del Pozo, 2000], suggesting again that the activities of Rac and Pak and the presence of cell-matrix contacts are highly co-ordinated. The build-up of such data has lead to a proposal that the primary function of PAK is to regulate focal contact turn over, particularly in the context of axon guidance.

IQGAP and actin reorganisation by Rac and Cdc42

IQGAP1 and 2 are binding partners for Rac and Cdc42 and have been linked to Cdc42-dependent actin polymerization [Hart, 1996] [McCallum, 1996] [Brill, 1996]. IQGAP has been detected in a complex with F-actin and Cdc42, which was enhanced by EGF and disrupted by dominant negative Cdc42 (Rac was not mentioned in these experiments) [Erickson, 1997]. IQGAP is able to oligomerize and to cross-link F-actin *in vitro*, an activity that is enhanced by GTPγS-GST-Cdc42 (again Rac was not mentioned) [Fukata, 1997]. Calmodulin inhibits the binding of IQGAP to actin and to Cdc42 [Joyal, 1997]. It has, therefore, been suggested that IQGAP oligomers may form upon binding to GTPase (probably Cdc42 and possibly Rac) after dissociation of calmodulin, and that somehow this facilitates cross linking of F-actin, reviewed in [Johnson, 1999].

1.3.3.3 Rac and modification of cell-cell contacts

Cadherins form homophilic calcium-dependent contacts between cells, which inside the cells are anchored to the actin cytoskeleton via proteins called catenins (reviewed in [Yap, 1997]). β-catenin binds to cadherin cytoplasmic tails and to α-catenin, which is linked directly and indirectly to actin filaments (see for instance [Oyama, 1994] and [Rimm, 1995]). E-cadherin and P-cadherin are essential to establish and maintain the differentiated phenotype of epithelial cells, reviewed in [Gumbiner, 1996]. E-cadherin also performs a tumour supressor role by influencing both the physical links between cells and their differentiation state (reviewed in [Christofori, 1999]).

RhoA and Rac1, and also Ras, have been identified as key regulators of cadherin-mediated adhesiveness and Rac regulation of cell-cell contacts is thought to be primarily due to actin-dependent events (reviewed in [Braga, V, 2000b]). For primary human keratinocytes Rac is required for both the establishment and the maintenance of E-cadherin mediated cell-cell contacts, both of which are inhibited by dominant negative N17Rac [Braga, 1999] and also by high levels of activated L61Rac [Braga, VM, 2000]. Activated Ras also disrupts E-cadherin-mediated cell-cell contacts and this appeared to be dependent on the activity of Rac [Braga, VM, 2000]. Using keratinocytes in low calcium, without contacts formed, Rac was seen to be required for recruitment of actin to beads coated with antibodies to E-cadherin [Braga, 1999], suggesting an actin-dependent role for Rac in cell-cell contact formation. Using mutants in effector domain II (in particular A147A148L61Rac and A162A163L61Rac) the disrupting effects of activated L61Rac upon cell-cell contacts were found to be separate from the ability of L61Rac to induce lamellipodia [Braga, VM, 2000], indicating a possible actin-independent effect.

The effects of dominant negative N17Rac upon cell-cell contacts depend on the cell type and the cadherins tested: VE-cadherin in endothelial cells is not disrupted by N17Rac, but VE-cadherin is disrupted by N17Rac in CHO cells; E-cadherin is disrupted by N17Rac in keratinocytes, but not in L cells (fibroblasts) [Braga, 1999]. In the MDCK epithelial cell line activated Rac (or its activator Tiam-1) increased, rather than disrupting, cell-cell contacts [Sander, 1998]. Both activated and dominant negative mutants of Rac were also observed to be concentrated with actin at sites of cell-cell contacts in MDCK cells [Jou and Nelson, 1998].

One Rac effector implicated in modulation of cell-cell adhesion is IQGAP1. IQGAP1 binds to β-catenin-cadherin complexes, apparently in competition with α-catenin [Kuroda, 1998]. Binding of Rac or Cdc42 to IQGAP reduces its interaction with β-catenin, so shifting the balance back to α-catenin-β-catenin complex formation [Fukata, 1999]. Although IQGAP binding to β-catenin does not visibly disrupt E-cadherins it is thought to render the cadherins less adhesive [Kuroda, 1998]. IQGAP is, however, an actin-binding protein itself, so could potentially replace α-catenin at sites of cell-cell contact [Fukata, 1997].

Cell-cell adhesion can influence motility [Huttenlocher, 1998]; upon formation of cell-cell contacts migration rates of cells are decreased and both microtubule and actin dynamics are reduced [Waterman-Storer, 2000]. Rho proteins are essential to both cell motility and cell-cell adhesion, making them likely co-ordinators of the balance between these two processes (reviewed in [Braga, V, 2000a]). One possible mechanism of co-ordinating Rac activity in cell migration with cell-cell adhesion may come from the ability of a cadherin-associated catenin (p120 catenin) to activate Rac and Cdc42, possibly via Vav2, and to down-regulate RhoA [Noren, 2000]. This is not the only report of Rac activation being linked to Rho inactivation, RhoA downregulation has also been observed in NIH3T3 cells in response to Tiam-1 or activated Rac [Sander, 1999].

Interestingly, one report shows that activated and dominant negative Rac are also able to disrupt ZO-1-containing tight junctions in polarised epithelial cells [Jou, Schneeberger, 1998].

1.3.3.4 The role of Rac in endocytic processes

Clathrin-dependent endocytosis

Activated Rac has been reported to inhibit clathrin-mediated transferrin receptor endocytosis in transfected HeLa cells and using a perforated A431 cell assay [Lamaze, 1996]. It is possible, however, that these effects are due to changes in the actin cytoskeleton induced by Rac that indirectly affect endocytosis [Lamaze, 1997].

Clathrin-independent endocytic events

Macropinocytosis and phagocytosis are both actin-dependent, and clathrin-independent vesiculation events, but they can be distinguished by the size of their cargo and the stimuli that induce them. Macropinocytosis and phagocytosis in some contexts are dependent upon Rac, which may act at the level of actin recruitment or possibly of vesicle closure (reviewed in [Nobes, 2000]).

Macropinocytosis

Rac-induced ruffling is often accompanied by the production of large plasma membrane, extracellular fluid-containing, vesicles (>0.2μm in diameter) that are separate from the clathrin-dependent pool of endocytic vesicles [Racoosin, 1992] [Hewlett, 1994] [Damke, 1995] [Araki, 1996]. These large vesicles are termed macropinosomes, and can be seen in small numbers in fibroblasts stimulated by injection of activated L61Rac [Ridley, Paterson, 1992]. In professional phagocytes appearance of macropinosomes is hugely increased by stimuli such as diacylglycerols and phorbol myristate acetate for neutrophils [Keller, 1990] and macrophage colony-stimulating factor for macrophages [Racoosin, 1992] [Araki, 1996]. In dendritic cells Rac-dependent macropinocytosis occurs constitutively in immature cells, for the purpose of gathering antigens for MHC class II presentation [West, 2000]. In one study using BHK-21 cells activated Rac was reported to induce ruffling without associated pinocytosis, whereas activated Ras induced both ruffling and pinocytosis [Li, 1997]. This Ras-induced pinocytosis was inhibited by a dominant negative mutant of Rab5, another small GTPase that stimulates early endosome fusion in the process of clathrin-mediated endocytosis [Bucci, 1992] [West, 2000]. Constitutively active Rab5 has also been shown to induce Rac-independent ruffles (full of filopodia) in fibroblasts [Spaargaren, 1999]. Membrane ruffling and associated-macropinocytosis, therefore, are not always Rac-dependent.

Phagocytosis

Phagosomes will enclose large particles that can be coated in opsins (such as IgG or complement fragments) and engage specific receptors on the cell surface (such as the FcγR and CR3), reviewed in [Sansonetti, 2000]. Professional phagocytes, such as macrophages, require Rac for phagocytosis in response to the binding of IgG-opsinised particles to the Fc-γ receptor, but require Rho to internalize C3bi-opsinised particles bound to the CR3 receptor [Cox, 1997] [Massol, 1998] [Caron, 1998].

Links between Arf6 and Rac and regulation of cortical actin and pinocytosis

One Rac effector, POR-1, also interacts with Arf6 [D'Souza-Schorey, 1997], a member of the Ras superfamily that has been implicated in membrane traffic and in remodeling of cortical actin and

cell spreading [Radhakrishna, 1997] [Song, 1998]. Arf6 is required for Rac-dependent phagocytosis in macrophages [Zhang, Q, 1998]. Arf6 has also been implicated in Rac-induced ruffling in HeLa cells and in macrophages in response to activated Rac or colony stimulating factor-1 [Radhakrishna, 1999] [Zhang, 1999]. Studies in living cells suggest that actin may be recruited to newly formed pinosomes and may be involved in their movement away from the plasma membrane [Merrifield, 1999]. Recently Arf6 has been shown to induce actin and Arp2/3-dependent pinosome motility in living cells [Schafer, 2000]. Others have shown that another potential Rac effector, the type I PI-4-P5K, may be involved in actin-dependent movement of vesicles [Rozelle, 2000] and in the formation of ruffles that were dependent upon Arf6 and phosphatidic acid (produced by phospholipase D that is also a potential Rac effector) [Honda, 1999].

1.3.3.5 Rac and exocytosis in mast cells

In permeabilized mast cells recombinant Rac protein was seen to enhance secretion induced by various agents, while dominant negative Rac could inhibit secretion induced by calcium and non-hydrolysable GTP analogues [Price, 1995] [Brown, 1998]. Rac was also purified from mast cells as a factor that can enhance secretion [O'Sullivan, 1996] and in natural killer cells dominant negative Rac inhibited polarised granule exocytosis [Billadeau, 1998]. Exocytosis in mast cells is strongly correlated with actin reorganisation, however, cytochalasin, which disrupts the filamentous actin structures, did not affect secretion induced by activated Rac, suggesting that cytoskeletal reorganisation and exocytosis occur by separate parallel pathways [Norman, 1996].

1.3.3.6 Activation of transcription from the serum response element

The first indication that Rho GTPases are able to regulate activity of transcription factors came from studies on the serum response element (SRE) of the c-*fos* gene promoter. Activity of the SRE is dependent upon binding of a ubiquitous transcription factor, the serum response factor (SRF), which in the case of the c-fos promoter forms a complex with members of the ternary complex factor (TCF) family of transcription factors, shown in the model in figure 1.10.

Activated mutants of RhoA, Rac1 and Cdc42 have all been shown to activate transcription from SRF-dependent reporter constructs and Rho is required for lysophosphatidic acid (LPA) activation of these constructs [Hill, 1995]. Cdc42 and Rac do not require Rho for their affects on SRF [Hill, 1995]. Cdc42, but not Rac or Rho, is able to induce endogenous c-*fos* gene transcription from a chromosomally integrated reporter construct [Alberts, 1998]. In the case of Rho a second signal that causes hyperacetylation of histone H4, which can be induced by Cdc42 via JNK-dependent or JNK–independent pathways, was required for activation of chromosomal SRE-containing genes [Alberts, 1998], see figure 1.10.

The Ras-induced ERK pathway regulates c-fos SRE by targeting the TCF family protein Elk-1. Rac and Cdc42, via Pak, may also contribute to this ERK-dependent pathway of SRE activation [Frost, 1997], see figure 1.10, whereas Rho does not contribute to SRE via the ERK pathway [Hill, 1995]. Elk-1 can be activated by JNK as well as by ERK [Whitmarsh, 1995], leaving open the possibility that activation of the JNK MAPK pathway downstream of Cdc42 or Rac may also contribute to TCF activation, as depicted in the model in figure 1.10. The biological significance of SRF activation by Rac, and the mechanism by which this occurs, still remains unclear.

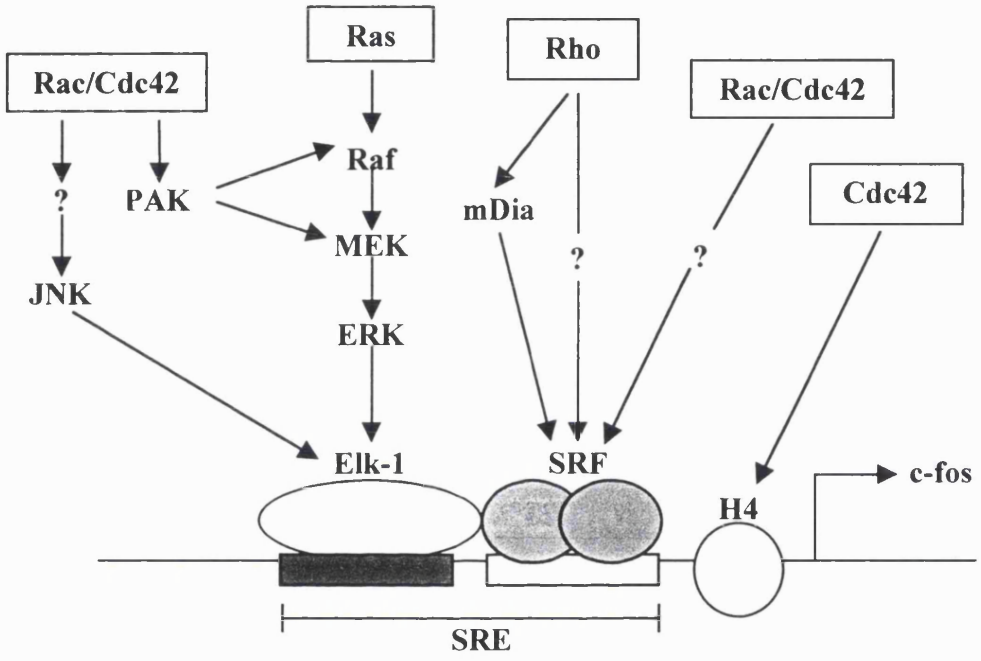

Figure 1.10 Activation of the c-fos gene Serum Response Element (SRE)

A model, based upon [Bar-Sagi, 2000], showing how transcription factors at the c-fos SRE are thought to be targeted by Ras and Rho signaling pathways. The model is based primarily on data from studies using transfected SRE or SRF reporters. Chromosomally integrated SRF reporters can not be activated solely by Rho-induced signals, but also require the hyperacetylation of histone H4, which occurs via signals induced at least in part by Cdc42. JNK MAPK pathway, as well as ERK, can activate Elk-1; Rac and Cdc42 activate JNK, but whether this contributes to SRE activation *in vivo* is unclear. Activation of the SRE is a prime example of integration of signaling cascades downstream of Ras and Rho GTPases.

1.3.3.7 MAP kinase pathway activation

Mitogen activated protein kinase (MAPK) pathways are conserved modular kinase cascades that mediate signal transduction events in all eukaryotes [illegible] (reviewed in [Marshall, 1994] and [Kyriakis, 1996]). There are at least three MAPK pathways in mammalian cells: the prototypical Ras-controlled ERK1/2 pathway; the c-jun N-terminal kinase (JNK)/stress activated protein

kinase (SAPK) pathway; the p38/reactivating kinase (RK) pathway. Kinases known to be involved in the three MAPK pathways in mammalian cells, MAPK kinase kinases (MAPKKKs), MAPK kinases (MAPKKs) and the MAPKs themselves, and their transcription factor targets are summarised in figure 1.11.

Growth factors activate the ERK pathway, but are mostly poor activators of JNK and p38. An exception is the Epidermal Growth Factor (EGF), which activates JNK as well as ERK in HeLa cells [Minden, 1995]. The JNK and p38 pathways are activated in response to cellular stresses such as ultraviolet irradiation, heat or inflammatory cytokines, such as interleukin-1 (IL-1) or tumour necrosis factor α (TNFα). JNK and p38 are, therefore, thought to be important regulators of inflammatory responses, reviewed in [Kyriakis, 1996] and [Davis, 1998]. More recently JNK has been implicated in regulation of development (particularly in *Drosophila*), cell proliferation and apoptosis (discussed below), reviewed in [Davis, 1998].

Constitutively active versions of both Rac and Cdc42 have been shown to activate JNK and p38 MAPK pathways in COS, NIH3T3 and HeLa cells [Bagrodia, Derijard, 1995] [Coso, 1995] [Minden, 1995] [Zhang, S, 1995]. In 293T cells p38 and JNK are activated by Cdc42 and Rho, but not by Rac [Teramoto, 1996]. Mutations in Rac and Cdc42 effector regions have shown that lamellipodia and filopodia formation, cell cycle progression and transformation occur independently of JNK activation [Joneson, 1996] [Lamarche, 1996] [Westwick, 1997].

In some cases agonist stimulation of JNK has been shown to be dependent upon Rho GTPases. IL-1-induced JNK and p38 are partially inhibited by dominant negative N17Rac and N17Cdc42 in COS cells [Bagrodia, Derijard, 1995] [Zhang, S, 1995] and by dominant negative Rho, Rac or Cdc42 in CHO cells [Whitmarsh, 1995]. Transforming Growth Factor β-induced JNK can be inhibited by N17Rac, and partially by N19RhoA and N17Cdc42 [Atfi, 1997]. In COS cells EGF- and TNFα-induced JNK activation have been reported to be partially inhibited by N17Rac and N17Cdc42 [Coso, 1995]. In contrast, in HeLa cells N17Rac partially blocked EGF-induced JNK, but had no affect on TNFα-induced JNK [Minden, 1995] and in NIH3T3 cells N17Cdc42 inhibited actin changes induced by TNFα and IL-1, but did not affect JNK activation [Puls, 1999]. Dependence upon Rho GTPases for JNK activation downstream of different stimuli, therefore, appears to be highly cell type-dependent.

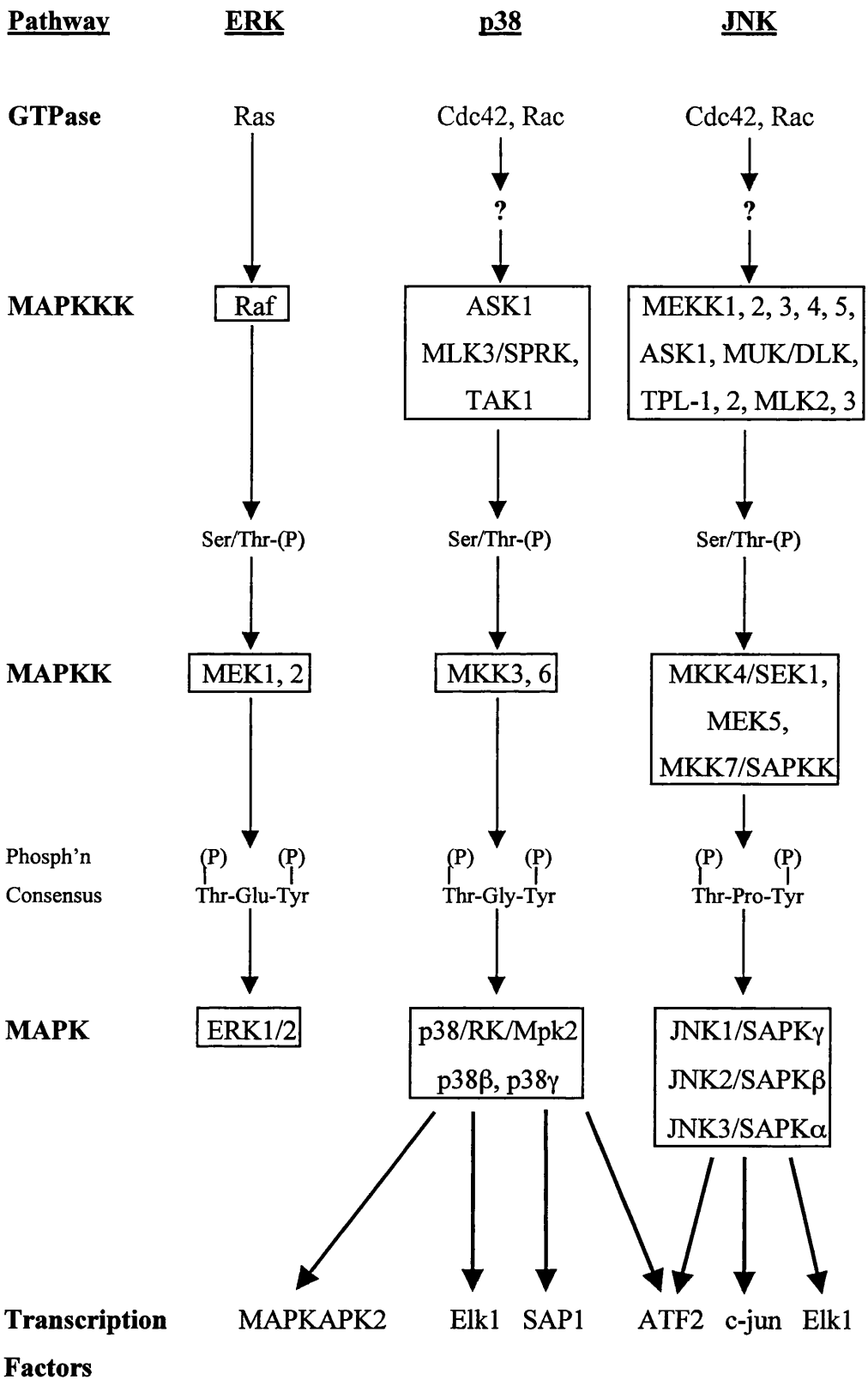

Figure 1.11 Mammalian mitogen activated protein kinase (MAPK) pathways

Comparison of the kinases that constitute the ERK, p38 and JNK MAPK pathways and examples of transcription factors regulated by JNK and p38. Consensus phosphorylation motifs for dual phosphorylation of each type of MAPK by upstream MAPKKs are shown, using the ~~single~~ three letter amino acid code and (P) to denote phosphorylation.

Once activated JNK and p38 MAPKs control gene transcription via a variety of proteins, some of which are shown in figure 1.11 and are reviewed in [Treisman, 1996]. JNK activates the AP1 complex by directly phosphorylating c-jun, which results in increased transcription of genes containing TPA response elements (TREs) in their enhancer regions [Pulverer, 1991]. *In vivo* evidence that JNK is important for AP1 activity has been provided by knock-out mice, such as the JNK3-/- mouse, which can not respond to excitotoxic stress in tissues that normally express JNK3 [Yang, 1997]. ATF-2 can be activated by both JNK and p38 [Gupta, 1995], although cross-linking studies show that, in response to TNFα, physical interactions occur only between ATF2 and p38, and between JNK and c-jun [Read, 1997]. p38 and JNK also activate the Ternary Complex Factor (TCF) proteins Elk-1 and SAP-1 [Gille, 1995] [Whitmarsh, 1997]. TCF associates with SRF to induce transcription through SREs and this may contribute to activation of the c-fos SRE by Rac and Cdc42, see figure 1.10. In addition p38 activates another kinase, MAPK-activated protein kinase-2, which phosphorylates the transcription factor CREB (cAMP Response Element Binding protein) and other substrates including the actin polymerisation-modulating heat shock protein hsp27 [Rouse, 1994]. Phosphorylation by JNK also inhibits NFAT4 transcription factor, but not the closely related NFAT1, 2 and 3 [Chow, 1997].

Rac, via activity of its serine/threonine kinase effector PAK, has also been shown to synergise with Ras to activate the ERK MAP kinase pathway at the levels of both Raf (serine 338 phosphorylation) [King, 1998] [Chaudhary, 2000] and MEK1 (serine 298 phosphorylation) [Frost, 1997]. Integrin-mediated activation of ERK in COS7 cells required PI3K, Rac and the Rac effector protein PAK [King, 1998] [Chaudhary, 2000], whereas in Rat-1 cells PAK appears to be activated by Akt, another serine/threonine kinase activated by PI3K, and Rac is not required [Tang, Y, 2000].

1.3.3.8 Effectors implicated in Rac-induced JNK activation

The MAPKKKs MEKK1, MEKK4, Mlk2/MST and Mlk3/SPRK all activate JNK, by phosphorylation of the MAPKKs MKK4 or MKK7, see figure 1.11, [Fanger, G.R., 1997] [Gerwins, 1997] [Hirai, 1997]. These MAPKKKs also bind to Rac and Cdc42, so could potentially be effector proteins involved in Rac/Cdc42-induced JNK activation [Teramoto, 1996] [Fanger, G. R., 1997] [Nagata, 1998]. Kinase dead MEKK1 or MEKK4 can inhibit Rac or Cdc42-induced JNK activation, indicating that they may indeed act downstream of these Rho GTPases to activate JNK [Fanger, G. R., 1997]. Mlk3 has recently been shown to be phosphorylated *in vivo* in response to activated Cdc42 [Bock, 2000].

Members of the Ste20 Ser/Thr kinase family (PAK, GCK, HPK, NIK, KHS and GLK) activate JNK via unknown mechanisms that do not appear to involve the direct phosphorylation of MAPKKKs or MAPKKs [Diener, 1997] [Fanger, G.R., 1997] [Su, 1997] [Tung, 1997].

Although the mechanism of action of these Ste20 homologs has not been defined, it appears that binding to other components of the JNK signaling pathway, and to adaptor/scaffold-like proteins, may be critical for their function. For example, HPK1 binds to Mlk3 and to Grb2 adaptor [Kiefer, 1996] [Anafi, 1997] and NIK binds to MEKK1 and to Nck adaptor [Su, 1997].

Ste20-like proteins have been implicated as effectors for Rac and Cdc42 involved in JNK activation. In the yeast pheromone response pathway Ste20 appears to coordinate Cdc42 activity (note that there is not Rac homolog in yeast) with activation of a MAPK cascade, although the physical binding of Ste20 to Cdc42 is not essential for MAPK activation [Leberer, 1992] [Peter, 1996] and reviewed in [Leberer, 1997]. The mammalian Ste20-like proteins p21-activated kinases (PAKs 1-3) are Rac and Cdc42 effectors [Manser, 1994]. PAK1 was observed to enhance p38 activation when co-expressed with Rac and Cdc42, and constitutively active PAK1 and 3 were reported to activate JNK in COS cells [Zhang, S, 1995] [Brown, 1996]. Other groups, however, have failed to find activation of p38 or JNK by PAK or to find any requirement for PAK binding to Rac and Cdc42 for activation of JNK [Joneson, 1996] [Lamarche, 1996] [Westwick, 1997] [Tapon, Nagata, 1998]. In *Drosophila* a PAK-like protein has genetically been shown to be an essential component downstream of Rac/Cdc42 and upstream of JNK in the developmental process or dorsal closure: *Djun*, *basket* (a JNK) and *hemipterous* (a JNKK) have all been shown genetically to be required for dorsal closure [Glise, 1997]; *DRac1* and *DCdc42* have been linked both biochemically and genetically to Dorsal closure upstream of the JNK cascade [Harden, 1995] [Glise, 1997]; thirdly, the *Drosophila* PAK-like kinase *misshapen* was shown genetically to lie between Rac/Cdc42 and *hemipterous* [Su, 1998].

1.3.3.9 Activation of the transcription factor NF-κB

Activated mutants of RhoA, Rac and Cdc42 have all been reported to activate the transcription factor NF-κB (nuclear factor-κB) in COS cells [Perona, 1997]. RhoA and Cdc42, but not Rac1, were found to participate in NF-κB activation by TNFα [Perona, 1997]. Dominant negative Rac1, on the other hand, inhibits NF-κB activation downstream of activated Ras and in response to interleukin-1β [Sulciner, 1996]. In one report antioxidants were found to prevent NF-κB activation by constitutively activate V12Rac and increases in intracellular reactive oxygen species were detected following V12Rac1 expresssion [Sulciner, 1996]. This is not the only report suggesting that reactive oxygen species may act as second messengers to induce NF-κB activation. For instance, in T cells antioxidants were found to inhibit NF-κB activation by stimuli such as TNFα, IL-1 and phorbol ester [Schreck, 1991].

The NF-κB/Rel family of transcription factors is composed of five members (RelA, RelB, c-Rel, p52 and p50), which form homo- and hetero-dimers, interact with inhibitory proteins (including

IkBα, β, γ, δ, ε and Bcl-3) and can enter the nucleus and bind to DNA once released from these regulatory proteins (the structure of an NF-κB/IκB complex is described in [Huxford, 1998] and for a review of IκB and NF-κB family members see [Baldwin, 1996]). Phosphorylation of IκBα, β or ε, the only IκB family members that contain a defined regulatory domain, leads to their targeting for ubiquitination and subsequent degradation by the proteasome (reviewed in [Karin, 2000]). NF-κB itself is also phosphorylated, in some cases by the same kinases that induce phosphorylation of IκB, which appears to increase NF-κB transcriptional activity (reviewed in [Mercurio, 1999]).

Many stimuli activate NF-κB, including proinflammatory cytokines such as TNFα and IL-1, double-stranded RNA, bacterial lipopolysaccharide (LPS), physical and chemical stresses, viral infection and T- and B-cell mitogens, reviewed in [Li, 2000]. A multisubunit kinase (IKK), which contains a heterodimer of two catalytic subunits (IKK-1 and IKK-2) phosphorylates (at Ser32 and Ser36 for IκBα) IκB in response to stimuli such as IL-1 and TNFα [Chen, 1996] [Mercurio, 1997]. IKK itself is activated by phosphorylation and in some cases kinases that activate IKK downstream of certain stimuli have been identified, reviewed in [Mercurio, 1999]. For instance, in response to both IL-1 and TNFα an NF-κB-inducing kinase (NIK) is activated, NIK is physically associated with IKKα *in vivo* and phosphorylates IKKα *in vitro*, also kinase dead NIK inhibits NF-κB activation by a number of stimuli [Malinin, 1997] [Ling, 1998]. TNFα treatment also activates MEKK1 and kinase dead MEKK1 can inhibit NF-κB activation [Lee, 1997], however MEKK1-/- stem cells are still able to activate NF-κB, but not JNK, in response to various stimuli including TNFα, suggesting that MEKK1 is not essential for NF-κB activation [Xia, 2000]. Rac and Cdc42 interact with MEKK1 [Fanger, G. R., 1997], but there is no evidence that these GTPases require MEKK1 for activation of NF-κB.

A few kinases have been shown to activate NF-κB by phosphorylation of IκB at the same serine residues phosphorylated by IKK: double stranded RNA-dependent protein kinase (PKR) can phosphorylate IκB *in vitro* [Kumar, 1997]; mitogen-activated ribosomal S6 protein kinase $p90^{rsk}$ phosphorylates IκB *in vitro* and *in vivo* [Ghoda, 1997] [Schouten, 1997]. NF-κB activation that does not involve serine phosphorylation has also been reported: hypoxia induces phosphorylation of IκBα at Tyr-42 and leads to IkBα degradation that is proteasome-independent and PI3K-dependent [Beraud, 1999]; short wavelength UV radiation induces IκBα degradation by the proteasome via an unknown mechanism [Li, 1998].

An SCF type of ubiquitination complex recognises serine-phosphorylated IκB and tags it with ubiquitin, thus targeting it for proteasomal degradation, reviewed in [Laney, 1999]. The recognition component of this complex, a so called E3 enzyme, is an F-box/WD-domain-

containing protein that was isolated from HeLa cells by virtue of its phosphorylation-dependent interaction with the NF-κB-IκB complex and was termed the pIκBα-E3 receptor subunit ($E3RS^{I\kappa B}$) [Yaron, 1998].

The genes regulated by the NF-κB family are diverse and include those involved in immune function, inflammatory response, cell adhesion, growth control and survival signals, reviewed in [Baldwin, 1996] and [Baichwal, 1997]. IκB itself, although not the IκBβ isoform, is regulated by NF-κB, and this newly synthesised IκB enters the nucleus to down-regulate the NF-κB response, [Cheng, 1998] and reviewed in [Baldwin, 1996].

1.3.3.10 Cell cycle progression

Rac has been shown to stimulate cell cycle progression through G1 and to be necessary for serum-induced DNA synthesis in quiescent Swiss3T3 cells [Olson, 1995]. Dominant negative Rac also reduced cell proliferation induced by the non-receptor tyrosine kinase v-Abl [Renshaw, 1996]. The ability of Rac, and Cdc42, to induce cell cycle progression and to contribute to transformation (see below) has been suggested to be linked to their ability to activate E2F, leading to expression of cyclin D1, a key regulator of the cell cycle [Gjoerup, 1998]. Binding of Rac to PAK does not appear to be required for induction of DNA synthesis in Swiss3T3 cells [Lamarche, 1996].

p70S6kinase regulates the translational machinery by phosphorylation and has been reported to bind to and to be activated by Rac [Chou, 1996]. p70S6 kinase is involved in the G1-S cell cycle transition; p70S6kinase-neutralising antibodies inhibit serum-induced DNA synthesis [Proud, 1996]. Furthermore, p70S6 kinase is activated by oncogenes and by numerus mitogenic stimuli [Chou, 1995]. p70S6 kinase may, therefore, link Rac with induction of G1 cell cycle progression.

1.3.3.11 Rac and cancer – transformation and invasion

Activated mutants of Ras are frequently found in tumour cells [Bos, 1989], but activated Rho GTPase mutants have never been found in cancer cells. In one case high levels of wild type Rac3 activity were detected in a highly proliferative human breast cancer-derived cell line and in tumor tissues [Mira, 2000]. Activating mutations in Rho GTPase exchange factors have occasionally been identified as transforming factors in actual cancers and many Dbl family members were identified in NIH3T3 fibroblast transformation assays, reviewed in [Cerione, 1996]. Activated mutants of RhoA, RhoB, RhoG, Rac1 and Cdc42 are also weakly oncogenic when introduced into certain rodent fibroblast cell lines and can contribute to malignant transformation by the Ras oncogene [Prendergast, 1995] [Qiu, 1995] [Lebowitz, 1997] [Qiu, 1997] [Roux, 1997]. In the case of Rac an activated mutant synergises with activated, membrane targeted, RafCAAX (a Ras

effector protein) to transform Rat-1 fibroblasts, and dominant negative Rac inhibits activated Ras transformation [Qiu, 1995].

The transforming potential of Rac mutants and a number of GEFs appears to correlate with their ability to stimulate transcription of cyclin D1, via activation of E2F, implying that this ability is critical to the involvement of Rac and Cdc42 in both cell cycle control and transformation [Westwick, 1997] [Westwick, 1998]. Whether other changes in gene transcription (SRF, JNK, p38, ERK, or NF-κB) also contribute to transformation, and whether actin reorganisation or modulation of cell-cell contacts by Rac (discussed above) contribute to other stages of tumourigenesis such as invasion remains unclear.

A study using Rac-Rho chimeras suggested that an interaction with PAK is not essential for Rac's contribution to transformation [Westwick, 1997]. In contrast, proliferation of the breast cancer cell line found to have hyperactive Rac3 was inhibited by kinase dead PAK, but was independent of JNK [Mira, 2000]. Also, transformation of Rat-1 fibroblasts by activated Ras or Rac could be inhibited by dominant negative PAK [Tang, Y, 1997] [Tang, 1999]. Such data suggests that PAK, but not JNK, may in some cases be involved in Rac-induced transformation. Rac mutants and chimeras have suggested that actin reorganisation and JNK activation can be separated from transformation, and that the insert region is important for transforming potential [Westwick, 1997] [Joneson, 1998]. Rac stimulation of the production of oxygen radicals, which also required the insert region, has been linked to transforming activity [Joneson, 1998]. Oxygen radicals have also been shown to be required for Rac activation of NF-κB [Sulciner, 1996] and NF-κB has been implicated in cell survival (reviewed in [Baichwal, 1997]), so may contribute to transformation by preventing apoptosis.

Rac has been implicated in tumour invasion, as well as in the control of proliferation contributing to transformation. Tiam-1, a Rac GEF, was identified in a screen for T cell invasion-inducing genes [Habets, 1994] and both Tiam-1 and activated V12Rac induce an invasive phenotype in non-invasive T-lymphoma cell lines [van Leeuwen, 1995]. The downstream proteins involved in Tiam-1-Rac-induced invasion are not yet known, but could be acting to modify actin dynamics, cell-matrix contacts or cell-cell contacts.

1.3.3.12 NADPH oxidase complex activation

In phagocytic cells Rac has been shown to positively regulate the phagocytic NADPH oxidase complex (phox), reviewed in [Segal, 1993]. This enzyme complex uses NADPH as an electron donor to generate superoxide radicals, which play a crucial role in the killing of phagocytosed pathogens by professional phagocytic cells. The complex consists of two membrane-bound

cytochrome b558 catalytic subunits (gp91phox and gp21phox) and two cytosolic regulatory proteins (p67phox and p47phox). Absence of any of these components results in Chronic Granulomatous Disease (CGD), a disease resulting in immuno-compromised patients [Casimir, 1992]. An additional regulatory component of the oxidase complex was purified and found to be a Rac1/RhoGDI complex [Abo, 1991]. Rac2, also present in hematopoietic cells, also activates the NADPH oxidase complex [Knaus, 1991]. Oxidase activity can be reconstituted *in vitro* using recombinant p67phox, p47phox, gp91phox, gp21phox and GTP-bound Rac [Abo, 1992]. The target of Rac in the oxidase complex is p67phox, which interacts directly with Rac in a GTP-dependent manner [Diekmann, 1994]. Rac and p67phox both translocate to the membrane upon activation, although translocation of p67phox is not thought to be Rac-dependent [Heyworth, 1994]. Instead Rac, by binding to p67phox, appears to act as an allosteric regulator of the complex [Nisimoto, 1997].

The NADPH oxidase complex components discussed above are only expressed by professional phagocytic cells. However, recently non-phagocytic gp91phox homologues have been cloned [Suh, 1999], [De Deken, 2000] and reviewed in [Lambeth, 2000]. The production of reactive oxygen species in non-phagocytic cells has been implicated in mitogenic signaling and cancer. In the case of Rac-induced transformation the production of reactive oxygen species has been implicated [Joneson, 1998]. One of the gp91phox-like proteins, Mox1, expressed in a number of cell types, was shown to transform NIH3T3 cells and cells expressing Mox1 produced tumours in athymic mice [Suh, 1999]. The cloning of a family of gp91phox-like proteins leads us to believe that non-phagocytic phox-like complexes may exist, which may also be regulated by Rac and will require as yet unidentified p67phox-like Rac-binding components.

1.4 THE RAC-BINDING PROTEIN POSH

1.4.1 Identification of POSH as a novel Rac-binding protein

Nicolas Tapon, a former member of the Hall Laboratory, set out to identify novel effectors for the Rho family GTPase Rac1. He took a yeast-two-hybrid approach, using the activated L61 mutant of Rac1 as the bait, with an additional cysteine to serine mutation in the CAAX box to prevent targeting to the plasma membrane. The principals and protocols for yeast-two-hybrid screening are described in the methods and in [Aspenstrom, 1995]. Using an integrated bait a cDNA library derived from Ras-transformed NIH3T3 mouse fibroblasts was screened. One novel Rac-binding clone (clone 4) was identified in this screen [Tapon, Nagata, 1998]. *In vitro* analysis using recombinant proteins showed that clone 4 was specific in its interaction with L61Rac, being unable to bind to L63Rho or L61Cdc42, and also bound specifically to GTP loaded, and not to GDP loaded, wild type Rac [Tapon, Nagata, 1998].

Sequencing of clone 4 (named here Y2H POSH) revealed that it was 1803 base pairs long (including the stop codon) and the 600 amino acid protein for which it coded contained two SH3 domains (see figure 1.12). Clone 4 was not necessarily a full-length cDNA, so 5' RACE PCR was carried out in an attempt to isolate any upstream sequence elements. A 1.4kbp major RACE product was isolated, which contained a Kozak sequence around the first methionine and proved to have upstream in-frame stop codons, suggesting it was a full-length clone [Tapon, Nagata, 1998]. Sequencing of the full-length cDNA revealed that it encoded a protein containing two more SH3 domains, so the protein was named POSH, standing for Plenty of SH3s.

1.4.2 The domain structure of the scaffold-like protein POSH

POSH appears to be a scaffold-like protein, containing no catalytic site detectable from the protein sequence, but including four SH3 domains and a RING type of zinc finger as well as the Rac-binding region. The domain structure of full-length mouse POSH is shown in figure 1.12 and an alignment of *Drosophila* and mouse POSH protein sequences in figure 1.13.

Figure 1.12 The domain structure of POSH

The yeast-two-hybrid clone of POSH (Y2H POSH) contained amino acids 292 to the end (892), as indicated. Abbreviations used for domain names are: src-homology 3 (SH3) domain; RING type of Zn finger (RING); Rac-binding domain (RBD).

Scaffold proteins act by bringing together multiple components of a signaling pathway into close proximity in a specific subcellular location, reviewed in [Whitmarsh and Davis, 1998] and [Burack, 2000]. This can provide specificity to the signaling pathway, for instance the JNK-interacting protein JIP-1 binds to a certain subset of JNK MAPK pathway components (Mlk3, MKK7, JNK1 and JNK2) [Whitmarsh, Cavanagh, 1998] [Yasuda, 1999]. Scaffolds can also co-ordinate a specific stimulus with activation of a particular response. For instance N-WASP brings together actin, profilin-actin and the Arp2/3 actin nucleating complex, but this actin polymerising machinery is held inactive by N-WASP until it also binds to the activators Cdc42-GTP and lipids [Prehoda, 2000]. Bringing signaling components into close proximity also has the capacity to enhance the efficiency of signal propagation. This is true of mammmalian MAPK scaffolds such as JIP-1 and MP1, which binds to components of the ERK pathway (MEK1 and ERK1) [Schaeffer, 1998]. Like these scaffold proteins POSH would be expected to bind to proteins that act together to induce a signal transduction pathway.

1.4.2.1 POSH proteins from different organisms

POSH was cloned from a mouse fibroblast cell line cDNA library, this protein is termed here mPOSH. There is now known to be a POSH homologue in *Drosophila* (dPOSH) and a partial clone is currrrently available from the human genome project. There does not appear to be a POSH homologue in yeast or in *C. elegans*. The human POSH protein (hPOSH) is encoded by at least five exons close together on chromosome 4 (Ensembl peptide clones AC027716, four predicted exons, and AC021151, second predicted exon). The start of the hPOSH gene sequence, up to and including sequence encoding the Rac-binding region, is present in clone AC027716 and the final SH3 domain is endoded by clone AC021151 (see figure 1.13). The central portion (including SH3 domain three) either is not present in the human clone or is not yet available through the Ensembl search engine. The 364 predicted amino acids (aa) of hPOSH clone AC027716 are 93% identical to mPOSH aa 1-362 and clone AC021151 second predicted exon is 98% identical to mPOSH aa 840-892.

A full alignment of dPOSH with mPOSH is shown in figure 1.13, with identical amino acids marked by vertical lines, and regions identical between mPOSH and hPOSH are also indicated with horizontal lines. The N-terminal RING finger and the four SH3 domains appear to be highly conserved between the two POSH homologues and in hPOSH at least three of the SH3 domains and the RING finger are almost identical to mPOSH. The Rac-binding region appears to be more variable between dPOSH and mPOSH, but is very similar between mPOSH and hPOSH and a potential Rac-binding sequence (a partial Cdc42/Rac-interactive binding motif) within this region is more conserved between dPOSH and mPOSH.

Figure 1.13 Alignment of mouse and *drosophila* POSH protein sequences

Mouse (m) and *Drosophila* (d) POSH protein sequences (accession numbers AAC40070 and AAF37265 respectively) aligned using the ClustralW pairwise method (EMBL Outstation, European Bioinformatics Institute) and Blasts2 to refine alignment of specific domains (National Centre for Bioinformatics Information). Identical amino acids are marked with a vertical line; a horizontal line above marks regions identical between mPOSH and the predicted peptides encoded by two clones that form part of the human POSH gene (Ensembl AC027716 and AC021151). Domains: green-RING finger; red-SH3 domains; blue-Rac-binding domain, with a partial Cdc42/Rac interactive motif underlined; pink-PXXP sequences noted in the text.

Four potential SH3 domain-binding motifs, PXXP (where X is any amino acid), three of which are overlapping, just C-terminal to the Rac-binding region of mPOSH were previously noted (shown in pink in figure 1.13) [Tapon, Nagata, 1998]. These PXXP motifs, however, are not accompanied by positively charged residues found in the majority of SH3 domain-binding peptides (see discussion of SH3 domains and their ligands below), and are not conserved between mPOSH and dPOSH. These PXXP motifs are, therefore, unlikely to be important for POSH function. Another interesting feature of the mPOSH sequence is an alanine-rich region, amino acids 419-433. This was suggested to create a low complexity region that could act as a flexible linker within the POSH protein. Again this region is not conserved in the dPOSH protein, this whole section is in fact missing from dPOSH (and possibly from hPOSH), suggesting that it is not important to POSH function.

1.4.2.2 The Rac-binding region of POSH

Using GST-fusion proteins of POSH truncations in a dot blot assay with L61Rac protein the Rac-binding domain of POSH was narrowed down to a region of 71 amino acids at the extreme N-terminus of the Y2H POSH construct (amino acids 292-362 of full-length POSH, see figure 1.13). This short polypeptide, as a GST-fusion protein, appeared to bind to L61Rac *in vitro* just as well as a GST-fusion of the full Y2H clone [Tapon, Nagata, 1998]. This is the minimal region of POSH, found to date, which is able to interact with activated Rac.

Possible TPR motifs within POSH Rac-binding domain

Within the Rac-binding domain of POSH a short stretch of regularly spaced small (A, S, G, V or P, green in figure 1.1) and large (W, V, L, I, F, Y, H or M, red in figure 1.1) hydrophobic amino acids were noted by Koga et al. They suggested that these regions could form two repeats of a structure termed a tetratricopeptide repeat (TPR) motif, comprised of a pair of antiparallel α-helices [Koga, 1999], these regions are shown in figure 1.14. Four such motifs are present within the Rac-binding domain of another Rac effector protein p67phox (see figure 1.14), the first three of which appear to be required for binding to Rac [Koga, 1999]. In most TPR-containing proteins the TPR motifs together create a super-helical twist with a groove suitable for binding of peptides in an extended conformation. The structure of a TPR-containing adaptor protein, Hop, plus peptides from Hsp79 and Hsp90 showed such an interaction [Scheufler, 2000]. The structure of p67phoxTPR (amino acids 1-203) with Rac-GTP has recently been solved and shows that the TPR domains do not directly bind to Rac, but act as a platform to present a short β-hairpin insertion between TPR3 and TPR4 that forms the direct Rac-binding interface [Lapouge, 2000].

The mPOSH hydrophobic residues suggested to facilitate formation of two TPR motifs do not appear to be conserved in dPOSH (see figure 1.14): of the 7 critical residues in each mPOSH TPR

motif only 2 or 3 are similar in dPOSH. This suggests that the TPR fold is not essential to the binding of POSH to Rac. Residues of p67phox whose side chains make essential contributions to the binding of Rac are underlined in figure 1.14. These are mainly within the small β-sheet insertion loop between TPR motifs 3 and 4, but also within TPR2 [Lapouge, 2000]. There are no extra amino acids available to form a similar insertion loop between the two potential TPRs of mPOSH (see figure 1.13), and the end of mPOSH TPR2 is outside of the minimal region of POSH found to bind to Rac [Tapon, Nagata, 1998]. From sequence analysis alone it seems unlikely that POSH TPR motifs act in exactly the same way as those of p67phox, as a platform to present a loop that forms the major interface with Rac. Only structural analysis of POSH Rac-binding domain will truely clarify whether POSH and p67phox bind to Rac in a similar manner.

```
SLTMANKSSQGSQN--RHSMEISPPVLISSSNPTA   mPOSH    (307-339) TPR1
TPGSSNSSSTSSSNNCSPNHQISLPNTPQHVVASG   dPOSH    (305-339)
AARISELSGLSCSA--PSQVHISTTGLIVTPPPSS   mPOSH    (340-372) TPR2
SASVRFRDKGAKEK--RHSLNALLGGGAPLSLLQT   dPOSH    (340-372)
AISLWNEGVLAAD---KKDWKGALDAFSAVQDPH    p67phox  (6-36)    TPR1
SRICFNIGCMYTI---LKNMTEAEKAFTRSINRDKHL p67phox  (37-70)   TPR2
AVAYFQRGMLYYQ---TEKYDLAIKDLKEALIQLRGN p67phox  (71-104)  TPR3

QLIDYKILGLQFKLFA              p67phox (105-120) inter-TPR β-sheet

SRICFNIGCMYTI---LKNMTEAEKAFTRSINRDKHL p67phox  (121-154) TPR4
```

Figure 1.14 Potential TPR motifs within POSH Rac-binding domain

Shown is an alignment of the two potential tetratricopeptide (TPR) motifs of mPOSH, the equivalent regions of dPOSH and the four TPR motifs of mp67phox, plus a β-sheet region between TPR3 and 4, as defined in [Koga, 1999] and [Lapouge, 2000]. The small (green) and larger (red) hydrophobic residues required to make up each TPR motif are indicated. Within the POSH sequence a potential partial CRIB motif (see text and figure 1.19 below) is underlined and within the p67phox sequence residues whose side chains are important for binding to Rac [Lapouge, 2000] are also underlined. Abbreviations: plenty of SH3s (POSH); phagocyte NADPH oxidase (phox); mouse (m); *Drosophila* (d).

A partial CRIB motif within POSH Rac-binding domain

The classic Cdc42/Rac interactive binding (CRIB) motif present in a number of Rac and/or Cdc42 effector proteins (see figure 1.7) is discussed above. This motif appears to be required for binding of a number of proteins to activated Rac or Cdc42. The classic CRIB motif contains eight residues that are highly conserved in effector proteins such as WASP, Ack, Mlk2 and PAK (see figure 1.15).

Recently a novel effector for Cdc42 has been identified as the mammalian homologue of the *C. elegans* cell polarity-determining protein PAR6 [Joberty, 2000] [Lin, 2000]. Within all known PAR6 proteins (from mouse, rat, human *drosophila* and *C.elegans*) there is a conserved partial CRIB motif just N-terminal to a PDZ domain, which is also conserved [Joberty, 2000]. Five of the classic CRIB consensus residues are present in mPAR6 partial CRIB (see figure 1.15). It appears that this region is necessary, but not sufficient, for binding of activated Cdc42 to PAR6. Deletion of the conserved proline residue within PAR6 CRIB motif (position 140 for PAR6C), in a PAR6 CRIB-PDZ-GST fusion protein, almost entirely destroyed binding to transfected V12Cdc42 [Lin, 2000]. Integrity of both the partial CRIB and the neighbouring PDZ domain appears to be required for the interaction of PAR6 with Cdc42 according to PAR6 truncations tested in the yeast-two-hybrid system [Joberty, 2000]. MEKK4 also contains a partial CRIB, shown in figure 1.15, that is required but is not sufficient for its interaction with Rac and Cdc42 [Fanger, G. R., Johnson, 1997].

Classic CRIB domains (6-8 consensus residues)

L	S	A	Q	D	I	S	Q	P	L	Q	N	S	F	I	H	T	G	H	G	D	S	D	**hAck** (505-527)
I	S	K	A	D	I	G	A	P	-	-	S	G	F	K	H	V	S	H	V	G	W	D	**hWASP** (233-253)
K	E	R	P	E	I	S	L	P	-	-	S	D	F	E	H	T	I	H	V	G	F	D	**hPak1** (70-90)
E	G	G	S	H	I	S	L	P	-	-	S	G	F	E	H	K	I	T	V	Q	A	S	**hMlk2** (469-489)
				*	I	S	*	P	-	-	*	*	F	*	H	*	*	H	*	G	*	D	**CRIB consensus**

Partial CRIB domains (3-5 consensus residues)

R	P	P	L	L	I	S	L	P	-	-	H	D	F	R	Q	V	S	S	V	I	-	D	**hPAR6C** (132-146)
					C	D	T	P	-	-	K	S	Y	D	N	V	M	H	V	G			**mMEKK4** (1311-1324)
				*	I	S	*	P	-	-	*	*	F	*	H	*	*	H	*	G	*	D	**CRIB consensus**

Potential Partial CRIB domains

R	H	S	M	E	I	S	P	P	-	-	V	L	I	S	S	S	N	P	T	A	A	A	**mPOSH** (321-341)
S	P	N	H	Q	I	S	L	P	-	-	N	T	P	Q	H	V	V	A	S	G	S	A	**dPOSH** (321-341)
				*	I	S	*	P	-	-	*	*	F	*	H	*	*	H	*	G	*	D	**CRIB consensus**

Figure 1.15 The potential partial CRIB domain of POSH

Classic Cdc42/Rac interactive binding (CRIB) domains, containing at least 6 of the 8 consensus CRIB residues defined in [Hoffman and Cerione, 2000], are shown from the Cdc42-binding proteins WASP and Ack, the Rac-binding protein Mlk2 and the Rac and Cdc42 binding protein PAK1. These CRIB motifs are essential for the interaction of these effectors with their Rho GTPase partners. The partial CRIB motif of PAR6C contains only 5 of the 8 CRIB consensus residues and mediates binding to Cdc42 only in combination with a PDZ motif [Joberty, 2000] [Lin, 2000]. Only 4 of the potential 8 CRIB consensus residues are conserved in MEKK4 partial CRIB and this region is required, but is not sufficient, for binding to Rac and Cdc42 [Fanger, G. R., Johnson, 1997]. An partial CRIB sequence with even less identity to the conseneus motif is shown that lies within the Rac-binding domain of mPOSH (only 3 CRIB consensus residues) and dPOSH (5 CRIB consensus residues). Consensus CRIB motif residues are shown in red; (*) represents less conserved residues within the CRIB motif. Abbreviations used: human (h); mouse (m); *Drosophila* (d).

Within POSH Rac-binding region an even less conserved CRIB motif, with only three CRIB consensus amino acids in mPOSH and five in dPOSH, was noted by myself and S. Krugman (see figure 1.15). That this partial CRIB domain is not totally conserved between mPOSH and *d*POSH implies that this motif may not be essential for POSH binding to Rac. It could be, however, that the three N-terminal CRIB residues conserved in mPOSH and dPOSH (I, S and P) are the most important part of the partial CRIB motif; the conserved proline in PAR6 did appear to be important for binding of Cdc42 [Lin, 2000]. If POSH is anything like PAR6 then its partial CRIB will only form part of the interface with Rac and other sequence elements within the Rac-binding region, possibly the TPR repeats that over-lap with the partial CRIB motif (see figure 1.14), may act in concert with the partial CRIB to facilitate binding of POSH to Rac.

1.4.2.3 POSH SH3 domains

POSH contains four Src-homology 3 (SH3) domains. The SH3 domain is an autonomously folding protein module that consists of approximately 60 residues and mediates protein-protein interactions [Pawson, 1992]. SH3 domains can be found in a large number of eukaryotic proteins. These proteins can be kinases (such as tyrosine kinases Src, Abl and Fyn), scaffolds (such as Grb2, Nck and Crk), lipid modifying enzymes (such as phospholipase-Cγ and the regulatory, p85, subunit of PI3K). Some GAPs, such as p50RhoGAP [Barfod, 1993] and Graf [Hildebrand, 1996], and Rho GEFs, such as Vav1-2 (see figure 1.4) and hPEM-2 [Reid, 1999] also contain SH3 domains. POSH is not the only SH3 domain-containing protein that is an effector for a Rho GTPase. The mammalian kinase Mlk2 and the NADPH oxidase component p67phox are also SH3 domain-containing effectors for Rac [Diekmann, 1994] [Nagata, 1998]. The yeast scaffold protein Bem-1 that co-ordinates Cdc42 activity with MAPK signaling also contains SH3 domains, reviewed in [Leberer, 1997].

Structures of isolated SH3 domains have been solved, for example SH3 domains from Fyn [Noble, 1993] and p85PI3K [Booker, 1993], and in some cases SH3 domains with their ligands, for example SH3 domains from c-Crk [Wu, 1995] and Src [Feng, 1994]. These data showed that the SH3 domain folds into a compact, five-stranded, anti-parallel β-barrel on which a number of conserved hydrophobic residues are displayed. Side-chains from these residues form a hydrophobic surface against which key protein ligand residues pack.

Figure 1.16 shows an alignment of the SH3 domain from c-Src against the four SH3 domains from *Drosopila* and mouse POSH and SH3 domains from other Rac-binding proteins (Mlk2, p67phox, BEM-1). Key conserved hydrophobic SH3 domain residues are shown in bold.

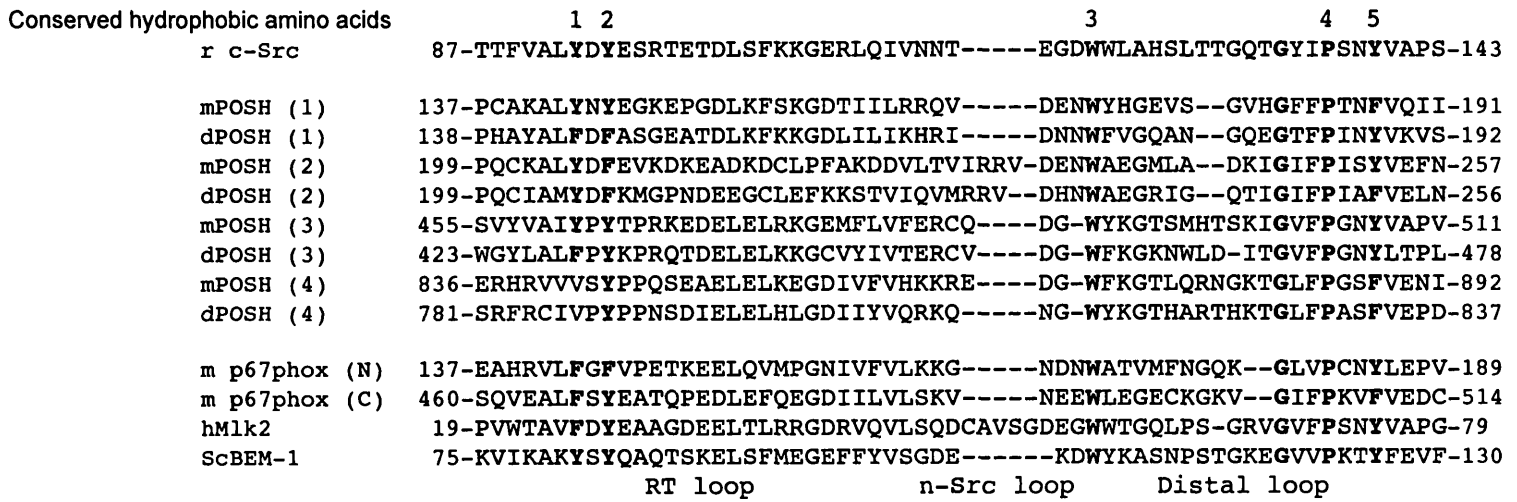

Figure 1.16 Alignment of mouse and *drosophila* POSH SH3 domains with SH3 domains from other Rac effectors

Conserved hydrophobic amino acids required in all SH3 domains for packing against proline-rich peptides are shown in bold and numbered above for reference purposes. Regions that form loops in the SH3 domain structure (reviewed in [Cohen, 1995]) are named according to nomenclature from [Noble, 1993] and [Wu, 1995]. Abbreviations: rat (r); mouse (m); *Drosophila* (d); human (h); *Saccharomyces cerevisiae* (Sc); N-terminal SH3 domain (N); C-terminal SH3 domain (C); Plenty of SH3s (POSH); phagocyte NADPH oxidase complex (phox); mixed lineage kinase 2 (Mlk2). Accession numbers for the proteins whose SH3 domain sequences are shown: r c-Src AF157016; mPOSH AAC40070; dPOSH AAF37265; m p67phox NP_000424; hMlk2 Q02779; ScBEM-1 NP_009759.

So what are the ligands for SH3 domains? There is now a large body of evidence showing that proline-rich regions are the ligands for SH3 domains, specifically proline-rich regions that are able to form a type II poly-proline helix (reviewed in [Cohen, 1995]), see figure 1.17. The most basic requirement for binding to an SH3 domain is a PXXP motif. The type II poly-proline helix can lie in one of two orientations in the SH3 domain hydrophobic pocket ([Feng, 1994] and reviewed in [Cohen, 1995]). Class I ligands contain the motif RXXPXXP and sit in the opposite orientation to class II ligands, that contain the motif XPXXPXR, where the residues underlined pack against the SH3 domain surface (see figure 1.17). There is a general preference for more prolines in the X positions, as they promote the formation of the type II helix [Yu, 1994]. This is especially true of residues that face away from the SH3 domain surface, where a bulky proline can be more easily accommodated: positions 2 and 5 in class I ligands and 3 and 6 in class II ligands, numbered as in figure 1.17. In most SH3 domains there appears to be at least one negatively charged patch (for example see [Owen, Wigge, 1998]). This charge patch often includes an aspartate (D) found between conserved hydrophobic residues 1 and 2 (numbering as in figure 1.16) in many SH3 domains and further acidic residues in the RT loop (see figure 1.16) [Yu, 1994]. This region binds strongly to positively charged amino acid side chains, usually arginine (R) and occasionally lysine (K). This creates a preference for R, or K, at position 1 in class I ligands and position 7 in class II ligands (numbered as shown in figure 1.17) [Feng, 1994].

The SH3 domains of POSH contain most of the conserved hydrophobic residues expected in an SH3 domains (shown in bold and marked as 1-5 in figure 1.16). POSH SH3 domain 4 is unusual in lacking one conserved hydrophobic residue, which is usually a tyrosine (1 in figure 1.16). For the binding of class I ligands this tyrosine, plus conserved W, P and Y (or sometimes F) residues (figure 1.16 conserved residues 3-5), interact with the proline at position 4 [Yu, 1994] (numbered as in figure 1.17). The second conserved residue marked in figure 1.16, also usually a tyrosine, is important for binding to the proline at position 7 in a class I ligand [Yu, 1994] (numbered as in figure 1.17). For class II ligands the proline and non-proline positions are reversed in the type II helix (see figure 1.17) and instead these conserved hydrophobic residues contact prolines at positions 5 and 2 [Feng, 1994].

There is little specificity to be had from hydrophobic interactions. On either side of the hydrophobic pocket are loops termed the n-Src and RT loops, nomenclature according to [Noble, 1993] and [Wu, 1995] (see figure 1.16). The length of loops and the presence or not of charged amino acids within them, along with regions outside of the SH3 domain itself, are thought to determine the specificity of ligand binding [Cohen, 1995].

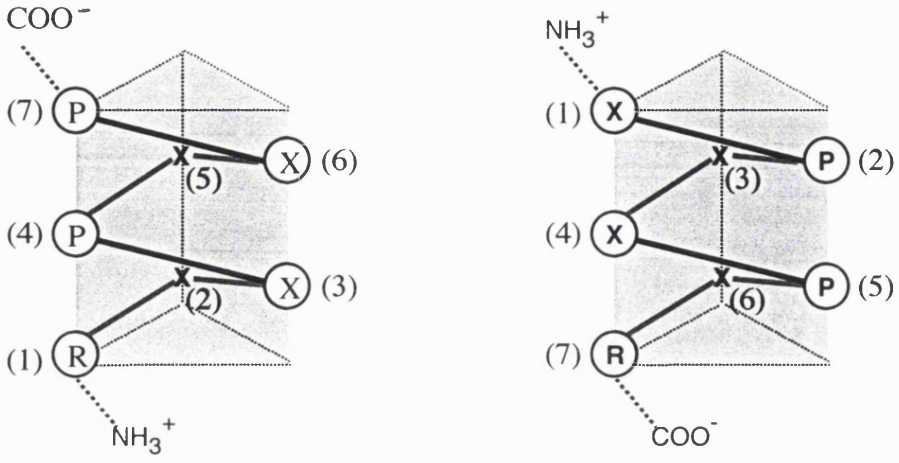

(a) Class I SH3 domain ligands (RXXPXXP)

(b) Class II SH3 domain ligands (XPXXPXR)

Figure 1.17 Diagram illustrating the type II helix formed by SH3 domain ligands

The type II helix formed by proline-rich peptides (residues numbered from the N-terminus) that bind to SH3 domains is depicted here with the SH3 domain surface towards the reader (adapted from diagrams of Src-binding ligands in [Yu, 1994]).

1.4.2.4 The POSH RING type of zinc finger

At the extreme N-terminus of the POSH protein (mPOSH and dPOSH amino acids 12-52, see figure 1.18) there is a RING type of zinc finger. In almost all zinc fingers the side chains from four cysteine or histidine residues tetrahedrally ligate a zinc ion.

Zinc fingers were originally identified as DNA-binding motifs, and have also been found as binding partners for RNA (reviewed in [Klug, 1987]). It has become increasingly clear that zinc fingers can also mediate protein-protein interactions, including binding to other zinc finger proteins (reviewed in [Mackay, 1998]). In some cases multiple zinc fingers within a single protein can bind to DNA or to other proteins. For instance, LIM double zinc finger domains, often seen within homeobox transcription factors, have been proposed to mediate DNA binding via their C-terminal zinc finger and homo- and hetero-dimerization between LIM domains via their N-terminal zinc finger [Schmeichel, 1997].

All known protein kinase C (PKC) isoforms appear to contain at least one zinc finger-like sequence, in many cases this has been shown to be responsible for phorbol ester binding, this is true of PKCα for instance [Zhang, G, 1995]. In the case of the atypical PKC λ/ι isotype its single zinc finger motif binds, in the yeast two-hybrid-system, to another protein called LIP [Diaz-

Meco, 1996]. A similar motif in the MAP Kinase kinase kinase Raf-1 appears to mediate interactions with its upstream activator Ras [Luo, Z, 1997]. The FYVE-type of zinc finger (an acronym for proteins containing this finger, Fab1, YOTB, Vac1, EEA1) is known to be involved in binding to lipids, specifically phosphatidylinositol-3-phosphate (reviewed in [Stenmark, 1999]). Zinc fingers, therefore, appear to be very versatile in their interactions, binding to proteins, lipids and nucleotides.

There are several types of zinc finger, categorised by the nature and spacing of their zinc-chelating residues, cysteines and/or histidines (reviewed in [Mackay, 1998]). Some zinc finger domains contain eight zinc chelating residues in close succession, which are able to chelate two zinc ions, such domains here are termed double zinc fingers. The consensus sequences for the four known types of double zinc finger motif, LIM domains, FYVE fingers, PKCλ/ι /Raf-like zinc fingers and RING fingers, are shown in figure 1.18 A. It is interesting to note that most nuclear zinc finger proteins contain multiple separate zinc fingers, whereas cytoplasmic zinc finger proteins usually contain just one, although this is sometimes a double zinc finger, such as a FYVE finger or RING finger.

The zinc fingers of mouse and *Drosophila* POSH conform only to the RING finger consensus sequence, see figure 1.18 A and C. The number of eukaryotic proteins known to have RING fingers has grown in the last few years, interestingly there do not appear to be any RING fingers in prokaryotic proteins [Saurin, 1996]. RING fingers always contain cysteine residues at zinc-chelating residue positions 1-3 and 6-8 (numbered as in figure 1.18 C), position 4 is always a histidine and 5 may be a histidine or a cysteine, as indicated in the RING finger consensus sequence shown in figure 1.18 (A and C). RING fingers are termed either HC, if they contain a histidine only at the 4^{th} zinc-chelating residue position, or H2, if they have histidines at both positions 4 and 5. Examples of other RING finger protein sequences, HC and H2, are shown aligned with POSH RING finger in figure 1.18 C. The mouse and *Drosophila* POSH zinc fingers are HC RING fingers.

(A) Consensus sequences for double zinc finger motifs

FYVE finger [Stenmark, 1999 #1068]

Consensus **C-X_2-C-X_{12}-C-X_2-C-X_4-C-X_2-C-X_{16}-C-X_2-C**

LIM domain [Perez-Alvarado, 1994 #1071] [Schmeichel, 1997]

Consensus **C-X_2-C-X_{16-23}-H-X_2-C-X_2-C-X_2-C-X_{16-21}-C-X_{2-3}-C/H/D**

PKCλ/ι and Raf-like ring finger [Diaz-Meco 1996] [Luo 1997]

Consensus **H-X_{12}-C-X_2-C-X_{9-13}-C-X_2-C-X_4-H-X_2-C-X_7-C**

RING finger [Saurin, 1996 #983]

Consensus **C-X_2-C-X_{9-39}-C-X_{1-3}-H-X_{2-3}-C/H-X_2-C-X_{4-48}-C-X_2-C**

(B) Representation of the ligation scheme employed by RING fingers

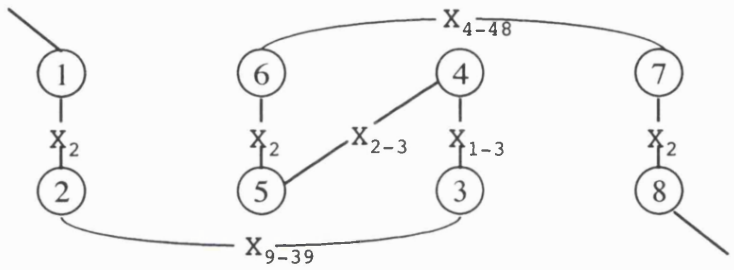

(C) Alignment of POSH RING finger with RING fingers from other proteins

```
              1  2                    3 4  5  6                      7  8
m POSH    12- CPVCLER-----LDASAKVLPCQHTFCKRCLLGIVGS-------RNELRCPEC-52
d POSH    12- CSVCLER-----LDTTSKVLPCQHTFCRKCLQDIVAS-------QHKLRCPEC-52
h RING1   19- CPICLDM-----LKNTMTTKECLHRFCSDCIVTALRS--------GNKECPTC-58
h PML    381- CKICAEN------DKDVKIEPCGHLMCTSCLTSWQES--------EGQGCPFC-419
Sc Far1  381- CLICEESISSTFTGEKVVESTCSHTSHYNCYLMLFET---LYFQGKFPECKIC-251
Sc Ste5  177- CTLCDEPISNRRKGEKIIELACGHLSHQECLIISFGTTSKADVRALFPFCTKC-230
```

Figure 1.18 Double zinc finger motifs

(A) shows consensus sequences for four categories of double (ligating two zinc atoms) zinc finger motifs. X can be any amino acid, although there are often preferences for certain types of amino acid at particular positions (see references). **(B)** shows schematically how RING fingers ligate two zinc ions in a "cross-brace" fashion, taken from [Saurin, 1996 #983]. **(C)** shows an alignment of POSH RING finger with RING fingers from a number of other proteins. The conserved zinc-chelating cysteine and histidine residues within each RING finger are shown in bold and are numbered 1-8. Abbreviations: mouse (m); *Drosophila* (d); human (h); *Saccharomyces cerevisiae* (Sc).

RING finger NMR structures have been solved for the acute promyelocytic leukaemia proto-oncoprotein (PML) [Borden, 1995], the immediate-early EHV-1 protein from equine herpes virus (IEEHV) [Everett, 1993] RING fingers and for the RING finger protein Cbl bound to a ubiquitin ligase called UbcH7 [Zheng, 2000]. A central β-sheet was the most conserved secondary structure element in these RING fingers and the inter-zinc distance was observed to be consistently 14Å. From such structures it appears that the first and third pair of chelating residues act together to tetrahedrally ligate one zinc atom and the second and fourth pair ligate the second zinc (see figure 1.18 B). This creates a cross-brace structure in which the two zinc-binding sites are folded into an integrated domain. The correct nature and spacing of zinc-chelating residues (numbered 1-8 and shown in bold in figure 1.18 C) is essential for the formation of such a structure.

Really Interesting New Gene 1 (RING1) was identified back in 1993 proximal to the major histocompatibility complex region of chromosome six. The product of this gene, a nuclear protein of unknown function, contained a novel cysteine-rich region termed RING finger or C3HC4 finger [Lovering, 1993], RING1 RING finger sequence is shown in figure 1.18 C. RING fingers generally appear to mediate protein-protein interactions and have been found to be involved a wide variety of cellular processes (reviewed in [Saurin, 1996] and [Freemont, 2000]). For instance, the RING-H2 motif within the adaptor protein Ste5 (sterile 5), a component of the yeast pheromone response pathway, is responsible for the interaction of Ste5 with Ste4 (the yeast Gβ subunit) [Inouye, 1997]. The TNFα-receptor associated proteins TRAF1 and 2 also contain RING fingers, which are required for TNF receptor signaling [Takeuchi, 1996], as do their binding partners IAP-1 and 2, which are inhibitors of apoptosis [Rothe, 1995].

Recently a number of cases have been identified where a RING finger is required for the ability of a protein to act as an E3 ubiquitin ligase (reviewed in [Freemont, 2000]). The RING fingers of a number of these E3 enzymes have been shown to be required for direct binding of an E2 ubiquitination enzyme, from which the ubiquitin moiety is transferred. This is true of proteins such as Cbl [Joazeiro, 1999], HHAR1 [Moynihan, 1999] and A07 [Lorick, 1999]. It is possible that the RING finger of POSH also links it to an E2 ubiquitinating enzyme, something that is investigated in chapter 6.

A number of oncogenic proteins are among the RING finger-containing E3 ubiquitin ligase group. MDM2 RING-containing E3, for instance, inhibits the tumour supressor p53 by ubiquitination [Honda, 2000]. Also c-Cbl mediates ubiquitination of a number of receptor tyrosine kinases (such as the EGF receptor [Waterman, 1999]), which is required for internalisation of these receptors, and is oncogenic (v-Cbl) when its RING finger is deleted

[Blake, 1993]. Two other RING finger-containing proteins have been linked to ubiquitination-related processes and are also oncogenes. The product of the breast cancer susceptibility gene BRCA1 utilises its RING finger for binding to a ubiquitin hydrolase [Jensen, 1998]. PML uses its RING finger to bind to an E2 enzyme UbcH9 whose substrate is not ubiquitin but the ubiquitin-like polypeptide SUMO-1 [Duprez, 1999]. Other proteins localised to PML nuclear bodies (also called oncogenic domains) have also been observed to contain RING fingers, such as Herpes simplex virus type 1 immediate-early protein Vmw110 [Everett, 1995] and mammalian Ret-finger protein (Rfp) [Cao, T, 1998]. The RING finger of PML, and SUMO-1 attachment to PML, are required for PML nuclear body formation [Borden, 1995] [Zhong, 2000].

1.4.3 Known activities of POSH

1.4.3.1 POSH is not implicated in actin reorganisation

Two mutants of activated L61Rac, characterised by Nathalie Lamarche in the Hall lab, appear to separate Rac functions: A37L61Rac is unable to induce actin changes but is able to activate JNK; C40L61Rac is unable to activate JNK or NF-κB, but can still induce actin reorganisation [Lamarche, 1996] [Tapon, Nagata, 1998]. The POSH yeast-two-hybrid clone (Y2H POSH) was found to bind, in the yeast-two-hybrid system and *in vitro*, to A37L61Rac and not to C40L61Rac [Tapon, Nagata, 1998]. This implicated POSH in the activation of JNK and NF-κB downstream of Rac and suggested that POSH was not essential for lamellipodia formation. In agreement with this full-length POSH or Y2H POSH injected into serum starved Swis3T3 cells did not induce actin reorganisation [Tapon, 1998b].

1.4.3.2 JNK activation

Activated Rac and Cdc42 can activate JNK, as discussed above in section 1.3.3.7 [Coso, 1995] [Minden, 1995]. No effector protein has been convincingly shown to be required for this Rac activity in mammalian cells, although PAK is clearly downstream of Rac and upstream of JNK in the *Drosophila* dorsal closure signaling pathway [Su, 1998] [Glise, 1997] and discussed in section 1.3.3.8 above.

In the light of the POSH interaction with A37L61Rac, which activates JNK, it seemed possible that POSH could be a Rac effector essential for JNK activation. Using transfected COS1 cells it was shown that full-length POSH, but not POSH C-terminus without the Rac-binding domain (C POSH, amino acids 352-892), could weakly activate JNK (5.6 fold as opposed to 11 fold for L61Rac), implicating POSH in JNK activation downstream of Rac [Tapon, Nagata, 1998]. C POSH was unable to interfere with Rac-induced JNK activation [Tapon, Nagata, 1998]. If C POSH were involved in JNK activation downstream of Rac then it would be expected to act as a

dominant negative protein by binding to downstream signaling components in non-productive complexes. As this was not shown to be the case this suggesets that POSH C-terminus is not involved in JNK activation. The ability of POSH N-terminus to activate JNK was not tested.

1.4.3.3 NF-κB activation

As discussed in section 1.3.3.9 above, a constitutively active mutant of Rac can activate the NF-κB transcription factor [Perona, 1997] and this signaling pathway appears to be dependent upon reactive oxygen species [Sulciner, 1996]. No known effector proteins have been shown to be required for Rac-induced NF-κB activation.

Full-length POSH and C POSH DNAs were injected into serum-starved quiescent Swiss3T3 cells, which have a low basal level of nuclear NF-κB, and were found to activate NF-κB, implicating the C-terminal end of POSH in NF-κB activation downstream of Rac [Tapon, Nagata, 1998]. C POSH expression occasionally had an autocrine NF-κB-stimulating effect upon uninjected neighbouring cells [Tapon, Nagata, 1998]. This could be due to new gene transcription (NF-κB induces transcription of NF-κB-activating cytokines such as IL-1 and TNFα, reviewed in [Baldwin, 1996]) or to a diffusable second messanger (such as the oxygen radicals suggested to be involved in Rac-induced NF-κB activation [Sulciner, 1996]).

1.4.3.4 Induction of apoptosis

Apoptosis, also known as programmed cell death, is the cell-autonomous system used as a self-destruct mechanism that avoids the production of pro-inflammatory signals released by cells that die by necrotic cell death. Apoptosis is an important process during embryogenesis and lymphoid cell development as it allows selective elimination of cells from the body (reviewed in [Jacobson, 1997]). If a cell detects its own DNA damage, which could lead to lesions and possibly contribute to cancer formation, the p53 transcription factor is activated. This phosphoprotein can cause cell-cycle arrest in order to give the cell time to fix the damage, if this fails then p53 can trigger apoptosis via a combination of mechanisms [Sheikh, 2000]. Some bacteria hijack the apoptosis machinery to kill host immune cells, so avoid immune detection, or to inhibit cell death in cells they have invaded (reviewed in [Gao, 2000]). In addition some pro-inflammatory cytokines, such as TNFα, induce apoptosis in non-haematopoietic cells. Professional phagocytes recognise apoptotic cells, phosphatidyl-serine (PS) is revealed on the surface of apoptotic cells and recently a phagocyte receptor for PS has been identified [Fadok, 2000], allowing them to clear apoptotic cell debris (reviewed in [Messmer, 2000]).

Apoptosis is characterised by a series of morphological features, such as: shrinkage of the cell body; condensation of the nucleus (called a pyknotic nucleus); fragmentation into membrane-

bound apoptotic bodies; rapid phagocytosis by neighbouring cells. All of these features contribute to preventing unnecessary inflammatory responses that may be induced by necrotic cell death (reviewed in [Nicotera, 1999]). Mechanistically apoptosis, but not necrosis, relies upon the activation of cysteine proteases called caspases, a cascade of which play a major role in the execution of apoptosis (reviewed in [Earnshaw, 1999]). These proteases selectively cleave vital cellular substrates, which results in apoptotic morphology and internucleosomal fragmentation of DNA by selectively activated DNases. In response to several pro-apoptotic signals mitochondria release caspase-activating factors, in particular cytochrome c, which initiate an escalating caspase cascade and commit the cell to die, see for instance [Goldstein, 2000]. Members of the Bcl-2 oncoprotein family control mitochondrial events and are able to prevent or induce apoptotic cell death (reviewed in [Desagher, 2000]).

When transfecting full-length POSH it was observed that over-expressed protein yields were low and could be increased by including a general caspase inhibitor in the transfection, suggesting that the cells were undergoing caspase-dependet apoptosis [Tapon, Nagata, 1998]. In the JNK kinase assays described above this caspase inhibitor had to be included in order to keep cells alive during full-length POSH transfections. By injection of POSH into NIH3T3 cells and filming them over an 8h time-course, using time lapse video microscopy, expressing cells were seen to exhibit classic signs of apoptosis, such as membrane blebbing followed by cell body retraction [Tapon, 1998a]. Staining of nuclei with Hoechst showed a pyknotic nuclear morphology associated with late stages in apoptosis [Tapon, Nagata, 1998].

1.5 CLATHRIN-DEPENDENT ENDOCYTOSIS

Whilst characterising the activities of POSH a link with endocytosis, specifically with the large GTPase dynamin, was discovered. The following sections introduce clathrin-dependent endocytosis in general and go on to highlight the roles of dynamin and its binding partners.

1.5.1 Introduction to clathrin-mediated endocytosis

The term endocytosis broadly refers to invagination of the plasma membrane (PM) to create internalised sealed vesicles. These vesicles carry with them membrane-associated proteins and extracellular fluid. The non-selective internalisation of fluid-phase material is often referred to as pinocytosis. The most extensively studied form of endocytosis is clathrin-dependent endocytosis. A specialised form of clathrin-mediated endocytosis occurs at nerve terminals, where very rapid endocytosis recovers synaptic vesicle membranes (reviewed in [Cremona, 1997] and [Hannah, 1999]). Endocytosis plays a part in some disease states, for instance, some viruses hijack the endocytic machinery in order to invade host cells [DeTulleo, 1998] [Oldridge, 1998] and some leukaemias contain DNA translocations involving components of the endocytic machinery (reviewed in [Floyd, 1998]). One of the first links discovered between receptor-mediated endocytosis and disease came from studies of the low density lipoprotein receptor (LDLR). Individuals with familial hypercholesterolaemia were found to have mutations in the cytoplasmic tail of the LDLR that prevented it from being incorporated into clathrin-coated pits and internalised, leading to a high incidence of atherosclerosis (reviewed in [Goldstein, 1985]).

In addition to clathrin-mediated endocytosis at the PM clathrin-independent endocytic pathways can also be detected, such as macropinocytosis and phagocytosis (discussed above), caveolae formation (reviewed in [Anderson, 1998]) and non-clathrin-dependent vesiculation events at the neuronal synapse (reviewed in [Palfrey, 1998]). The mechanisms of these clathrin-independent processes are poorly understood in comparison with clathrin-mediated endocytosis.

Clathrin coats are involved both in endocytosis at the PM and in budding of vesicles from the trans-Golgi network (TGN). The major constituents of these coats are clathrin itself plus adaptor proteins: AP2 (a $\alpha\beta2\mu2\sigma2$ heterotetramer) at the PM and AP1 (a $\gamma\beta1\mu1\sigma1$ heterotetramer) at the TGN. The overall scheme of events thought to be required for the formation of a clathrin-coated vesicle at the PM is summarised in figure 1.19 and reviewed in [Schmid, 1997]. The potential protein-protein interactions that occur between the many components of a clathrin coated pit are depicted in figure 1.20 and reviewed in [Marsh, 1999]. Ways in which the interactions (shown in figure 1.20) are thought to facilitate the different steps in coated pit formation (shown in figure 1.19) are described below.

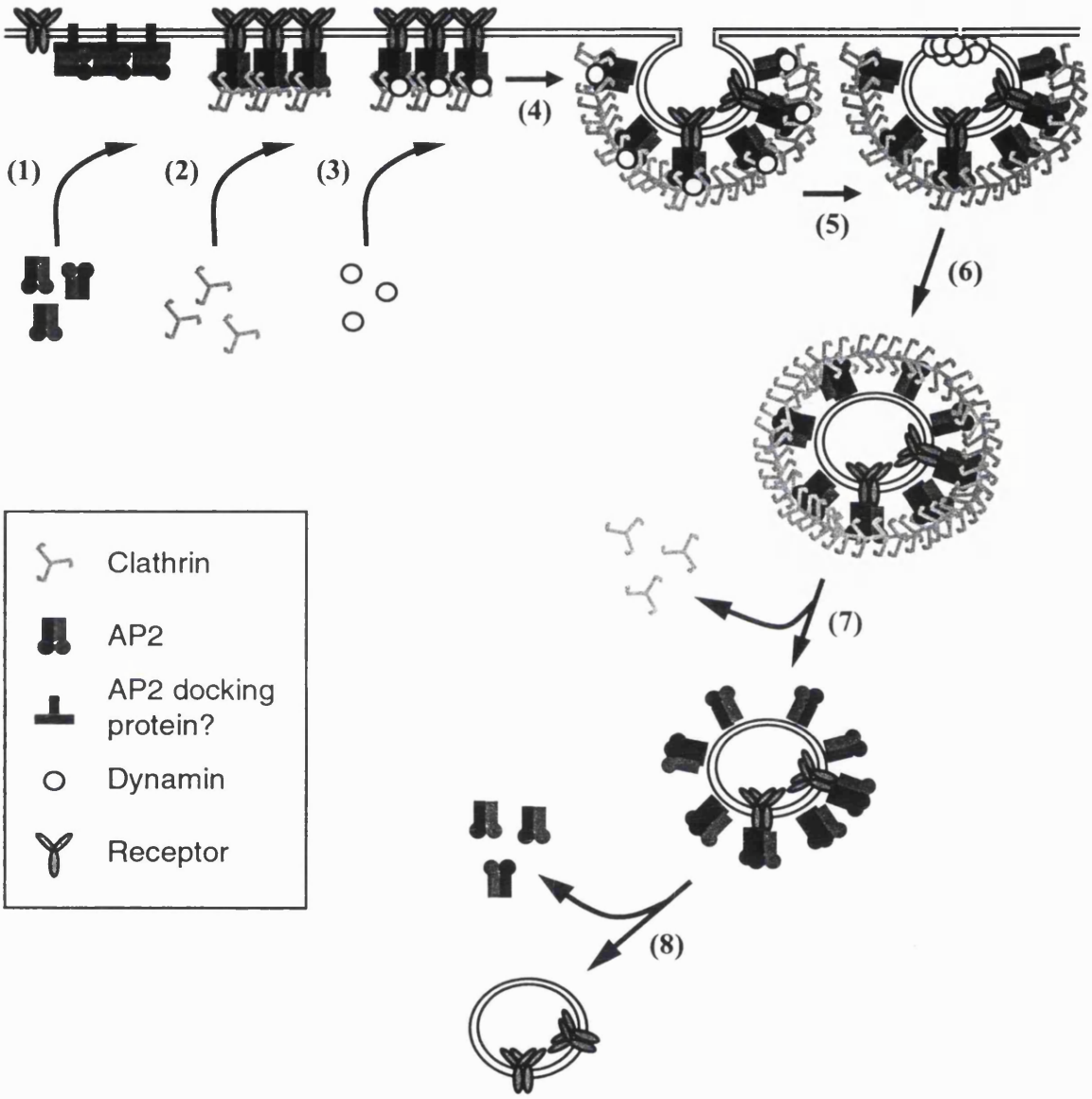

Figure 1.19 The clathrin-coated vesicle cycle that drives receptor-mediated endocytosis
The following steps are depicted and are described in the text: (1) recruitment of AP2, which in turn recruits receptors; (2) clathrin coat assembly; (3) recruitment of dynamin; (4) coated pit invagination; (5) coated pit constriction, requiring GTP-dynamin action and re-distribution to the neck of the coated-pit; (6) coated vesicle budding, requiring fission of the membrane and dynamin GTP hydrolysis; (7) clathrin release; (8) AP2 release. Based upon [Schmid, 1997].

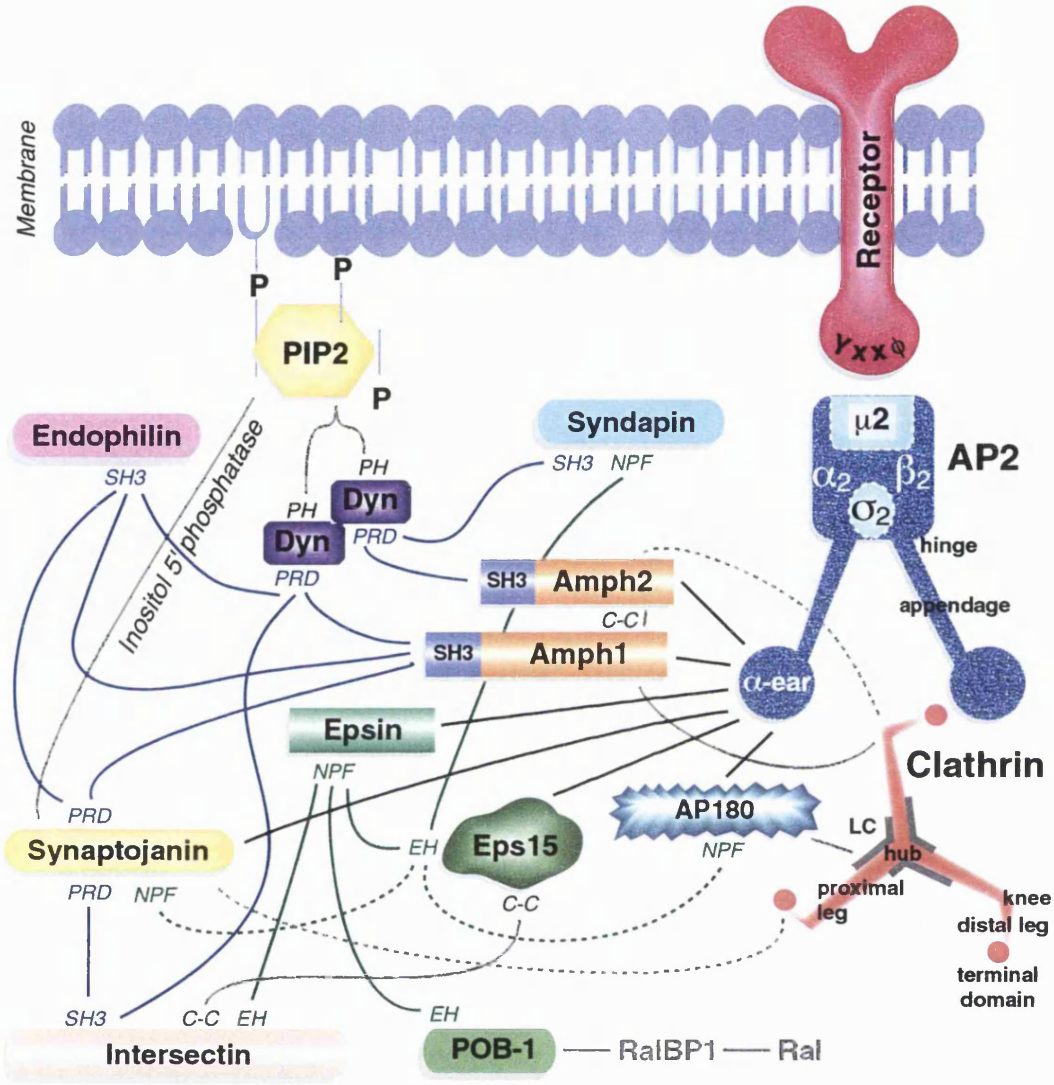

Figure 1.20 Schematic representation of the structures of clathrin and AP2 and the potential protein-protein interactions that can occur between these proteins and other components of a clathrin-coated pit (based on [Marsh, 1999])

Lines between proteins signify direct interactions. Dotted lines signify interactions that only occur for certain protein isoforms: 170kDa synaptojanin1, but not the 145kDa splice form binds to Eps15 and clathrin; NPF motifs for binding to Eps15 are present in the non-neuronal AP180-like protein CALM but not in AP180 itself; only certain splice forms of amph2 are able to bind to clathrin. Black lines: binding of proteins to the AP2 α-ear mediated by DPF motifs. Green lines: EH domain-NPF motif interactions; Note that intersectin's EH domains are depicted as binding to epsin, but may also interact with other NPF motif-containing proteins and syndapin NPF motifs are shown to interact with Eps15, but this is currently only a prediction and this region of syndapin may also bind to other EH domain-containing proteins. Blue lines: SH3 domain-mediated interactions. Abbreviations: pleckstrin homology (PH) domain; Eps15 homology (EH) domain; Src homology 3 (SH3) domain; NPF and DPF are tripeptide motifs named according to the single letter amino acid code; dynamin (Dyn); amphiphysin (Amph); adaptor protein (AP); clathrin light chain (LC); phosphatidylinositol-4,5-bisphosphate (PIP_2) coiled-coil (C-C); x = any residue; ϕ = bulky hydrophobic residue.

1.5.2 Receptor recruitment into clathrin-coated pits

Some receptors, such as the transferrin receptor (TfnR), are constitutively endocytosed and spend much of their time at the plasma membrane (PM) clustered in coated pits (reviewed in [Goldstein, 1985]). Other receptors, such as the EGF receptor (EGFR), are only recruited into clathrin-coated pits after activation (step 1 in the scheme shown in figure 1.19), enabling them to be specifically internalised after ligand binding, reviewed in [Trowbridge, 1993]. This ligand-mediated endocytosis can serve to attenuate the signal from an activated receptor and, in some cases, may be required to place an activated receptor in an appropriate sub-cellular location where it can encounter downstream signalling molecules (reviewed in [Ceresa, 2000]). Adaptor proteins facilitate receptor recruitment into clathrin-coated pits by binding to both clathrin and activated receptors (depicted in step 1 of figure 1.19). At the PM the adaptors are primarily AP2 and β-arrestins (reviewed in [Kirchhausen, 1999]). Purified AP2 tetramers visualised using freeze-etch electron microscopy (EM) have a dense trunk and appendages that are protease-sensitive, as shown schematically in figure 1.20 [Heuser, 1988].

1.5.2.1 Peptide signals for sorting of receptors into coated pits

Formation of clathrin-coated vesicles is initiated at the PM by AP2 recruitment (figure 1.19 step 1). Evidence suggests that AP2 is somehow able to interact, directly or indirectly, with the PM where it recruits clathrin. The best characterised interactions between AP2 and PM components are those between AP2 and peptide motifs within the cytoplasmic tails of many receptors, reviewed in [Kirchhausen, 1999].

The first receptor sorting motif identified for the clathrin pathway was the NPXY motif (where X is any amino acid) within the cytoplasmic tail of the LDL receptor [Anderson, 1977] [Lehrman, 1985]. However, despite being the first endocytosis sorting-signal to be identified it is still unclear how the NPXY motif is recognised.

The YXXϕ motif (where X is any residue and ϕ is a residue with a bulky hydrophobic side chain) was first identified as a sorting signal within the cytoplasmic tail of the transferrin receptor (TfnR) [Collawn, 1990], depicted in figure 1.20. YXXϕ motifs have now been found in many proteins, including receptors that are constitutively present in clathrin-coated pits, such as the TfnR itself, and receptors that undergo ligand-induced endocytosis, such as the EGFR. Using the yeast-two-hybrid system, followed by confirmation of the results with *in vitro* binding assays, it was found that the μ2 subunit of AP2 bound to YXXϕ–containing peptides [Ohno, 1995]. Crystal structures of YXXϕ peptides from EGFR, TGN38 or P-selectin bound to the signal recognition portion of μ2 (amino acids 158 or 160 to 435), have now been solved [Owen and Evans, 1998] [Owen, 2001]. EGFR and TGN38 peptides took on a "two-pinned plug"

conformation, where residues Y and ϕ fitted into pockets within the μ2 "socket" [Owen and Evans, 1998]. The P-selectin peptide formed a "three pinned plug" type of conformation, where a residue N-terminal to the YXXϕ motif formed the "third pin" that was just as important for binding to the μ2 "socket" as were interactions between μ2 and P-selectin Y and ϕ residues [Owen, 2001]. For other transmembrane proteins additional interactions may also occur between AP2 and regions outside of their YXXϕ motifs. For instance, a mutant μ2 that was unable to bind to YXXϕ motifs (N176A W421A) blocked TfnR internalisation, but not EGFR internalisation, implying that additional contacts were made between the EGFR and AP2 [Nesterov, 1999].

The third sorting motif recognised by AP complexes is a di-leucine motif of the general form D/ExxxLL (where x is usually polar and L can sometimes be replaced with I or M). LL motifs control traffic through both the endocytic and secretary pathways.

1.5.2.2 Sorting of seven-transmembrane receptors into coated pits

The only other adaptor proteins made by mammalian cells, in addition to AP2, that are thought to be involved in receptor recruitment into clathrin-coated pits at the PM are the β-arrestins. There are at least six arrestin family members, β-arrestins are expressed in many tissues, whereas visual arrestin (α-arrestin) is only expressed in the retina (reviewed in [Ferguson, 1996]). β-arrestins bind to the phosphorylated activated form of certain seven-transmembrane receptors such as the β_2-adrenergic receptor [Goodman, 1996] and interact with clathrin with high affinity *in vitro* [Krupnick, 1997]. β-arrestins have also been reported to interact with the AP2 β2 subunit, indirectly linking them to the clathrin lattice [Laporte, 1999]. Under conditions where AP2 promotes clathrin cage assembly (see below) β-arrestins do not show any such activity [Goodman, 1997]. AP2 is, therefore, unique in its ability to bind to both receptors and clathrin at the PM and to be able to promote clathrin cage assembly.

1.5.3 Docking of AP2 at the plasma membrane

Purified AP2 can bind to PM preparations in the absence of clathrin and clathrin binding is dependent upon the presence of AP2 [Mahaffey, 1990]. The initial recruitment of AP2 to the PM, therefore, appears to be the first step in coated pit formation (figure 1.19 step 1). Binding of adaptors to the short peptide sequences within activated receptors, described above, is essential for recruitment of these receptors into coated pits, forming part of step 1 in figure 1.19. These interactions alone, however, are not strong enough to account for recruitment of AP2 into the high-affinity sites detected with membrane-binding assays [Mahaffey, 1990].

Lipid binding may help to facilitate AP2 recruitment to the PM. The α subunit of AP2 binds to phosphatidyinositol lipids, with highest affinity for phosphatidylinositol-4,5-phosphate (PI-4,5-

P_2), via residues 5-80 [Beck, 1991] [Gaidarov, 1996]. This lipid-binding site is close to a region of the α subunit implicated in membrane targeting of AP2 [Page, 1995]. Work by West et al provided further evidence that PI-4,5-P_2 and also phosphatidic acid (PA) may regulate AP2 membrane targeting. GTPγS was observed to cause mislocalisation of AP2 to endosomal membranes, which was blocked by an inhibitor of exchange factors that activate Arf GTPases, Brefeldin A [Seaman, 1993]. Arf1 and PI-4,5-P_2 synergistically activate phospholipase D, which hydrolyses phosphatidyl choline to produce PA, which in turn can activate phosphtidylinositol-4-P 5-kinase to produce more PI-4,5-P_2 [Jenkins, 1994] [Hammond, 1997]. Such a positive feedback loop could rapidly lead to local increases in both acidic phopholipids. West et al showed that activated Arf1 or exogenous PLD, like GTPγS, also cause mis-localisation of AP2 to endosomal membranes *in vitro* [West, 1997]. Neomycin, which inhibits PI-4,5-P_2-dependent processes, had no effect upon GTPγS-induced AP1 recruitment to TGN membranes, but blocked both the mis-localisation of AP2 to endosomal membranes in response to GTPγS and recruitment of AP2 to its natural docking site at the PM [West, 1997]. The neomycin effect on AP2 recruitment was stronger than its effect on PLD activity, suggesting that PI-4,5-P_2 plays additional roles in AP2 recruitment that are independent of PLD activation [West, 1997]. These data suggest that PA and PI-4,5-P_2 may contribute to docking of AP2 at the PM.. Arf1 mediates AP1 docking, but does not appear to mediate normal AP2 PM docking, but a different Arf family member or other small GTPase may be involved in PLD activation and AP2 recruitment to the PM. Possible candidate small GTPases include Arf6, which is the only known constitutively membrane-bound and BFA-insensitive Arf and is localised to the PM and endosomal membranes and Rho GTPases, as RhoA and Rac1 are known to be activators of PLD [Hammond, 1997].

There is some evidence to suggest that unknown docking proteins may also aid in the recruitment of AP2 to the PM (depicted as a hypothetical component of step 1 in figure 1.19). Binding of AP2 to membranes, where it recruits clathrin coats, is saturable, implying that it binds to discrete sites at the PM that must somehow be marked, possibly by both proteins and acidic phospholipids [Moore, 1987] [Mahaffey, 1990]. Indeed "hot-spots" for clathrin-coated pit assembly have been observed *in vivo* in real time with GFP-clathrin [Gaidarov, Santini, 1999] and at synaptic nerve terminals [Estes, 1996]. A fraction able to bind to AP2, and to prevent it from interacting with membranes, was isolated from the cytoplasmic face of the PM by limited elastase treatment. Affinity purification of AP2-binding peptides from this fraction yielded a collection of peptides dominated by a 45 kDa species, which has yet to be further characterised [Peeler, 1993].
In neurons synaptotagmin was suggested as a potential AP2 docking site, based mainly on its presence at the plasma membrane in neurons and its ability to interact with AP2 *in vitro* [Zhang, 1994]. More recently it has been shown that peptides containing tyrosine-based sorting motifs that bind to AP2 increase the interaction of synaptotagmin with AP2 [Haucke, 1999]. Also, over-

expression of the AP2-binding region of synaptotagmin increased recruitment of AP2 to the plasma membrane, whereas over-expression of a binding partner for synaptotagmin (synprint) inhibited transferrin endocytosis [Haucke, 2000]. These reports provide the first functional data supporting a role for synaptotagmin in AP2 recruitment. Identification of docking proteins that bind to AP2 and facilitate coated-pit formation at discrete PM sites has been a key goal and it appears that synaptotagmin may be one such protein.

1.5.4 AP2 recruitment of clathrin

The major coat constituent, clathrin, is comprised of three heavy chain subunits each bound to one of two possible light chains (LCa or LCb). The clathrin polypeptide is shaped like a triskelion (shown schematically in figure 1.20), its three legged appearance can be viewed with negative staining, rotary shadowing or deep etching EM techniques [Kirchhausen, 1986]. Purified clathrin has been observed, using deep etching EM, to form polyhedral cages *in vitro* [Heuser, 1987]. Structural comparison of the barrels formed by purified clathrin alone or combined with AP2 suggest that AP2 promotes clathrin coat assembly *in vitro* and forms an inner layer inside of the clathrin lattice [Vigers, 1986] [Smith, 1998].

AP2 binds to two sites within clathrin heavy chain, the proximal hub region of the triskelia and the distal terminal domains (clathrin structure is shown schematically in figure 1.20) [Keen, 1991] [Murphy, 1992]. Evidence suggests that the β2 subunit is important for clathrin binding: recombinant β2 alone supported cage assembly *in vitro* [Gallusser, 1993] and deletion mutagenesis of β2 suggested that residues within the hinge region, amino acids 616-663, are essential for this activity [Shih, 1995].

1.5.5 Recruitment of additional coated pit components by AP2

AP2 not only binds to membranes, receptors and clathrin but also interacts, via the α-ear, with clathrin-coated pit components containing DPF/W tri-peptide motifs (see figure 1.20). These include: amphiphysin (1 DPF), which is a dynamin-binding protein that is discussed below; auxilin (3 DPFs), which is required for coat disassembly [Ungewickell, 1995]; AP180 (2 DPFs), which also binds to clathrin and facilitates clathrin-coat formation, size and shape, reviewed in [McMahon, 1999]; Eps15 (13 DPFs) and its binding partner epsin (9 DPWs), discussed below. The strength of α-ear binding appeared to be proportional to the number of DPF/W repeats [Owen, 1999].

1.5.6 The balance of multiple potential protein-protein interactions

Many protein-protein interactions have been found to occur between multiple binding partners within the coated pit, as can be seen in figure 1.20. In the recent review by Pearse et al [Pearse,

2000] it is pointed out that small repeated motifs and low affinity interactions (such as DPF/W-α-ear interactions) are common within the clathrin-coated pit. This should enable rapid exchange of binding partners and make the whole system dynamic. Different DPF/W-motif containing proteins are implicated in very different stages in endocytosis. AP2 must somehow utilise these potential interactions at the appropriate stages during the cycle shown in figure 1.19. Exactly how this is achieved remains unclear, but some general theories are developing.

The spatial and temporal control of coated-pit assembly, coated-vesicle formation and disassembly may actually depend upon the existence of what appears, at first sight, to be excessive numbers of combinations of protein-protein interactions (see figure 1.20), reviewed in [Marsh, 1999]. For instance, proteins could be selectively retained within micro-domains where their overall affinity for the coated-pit is maximised by binding to the greatest number of potential partners. Equally, proteins may be retained or lost from the pit over time according to the recruitment and accessibility of their multiple binding partners. Some of the potential interactions shown in figure 1.20 are in fact mutually exclusive, so could not occur all at once. For instance, clathrin binds to amphiphysin, but is displaced by dynamin, although these interactions are mediated by separate domains of amphiphysin [McMahon, 1997].

1.5.7 Regulation of coated pit assembly by lipids and by phosphorylation

Further levels of regulation for coated pit assembly, in addition to protein-protein interactions, are provided by protein and lipid phosphorylation events and by protein-membrane interactions.

In a resting nerve terminal dynamin1, synaptojanin1 and amphiphysin1 are all serine/threonine phosphorylated by PKC, which inhibits amphiphysin1 binding to AP2 and clathrin and dynamin1 and synaptojanin1 binding to amphiphysin1 [Slepnev, 1998]. The phosphorylated pool of dynamin1 is apparently unable to associate with coated pits [Liu, Powell, 1994].

In non-neuronal cells tyrosine phosphorylation of dynamin2 has been reported to enhance dynamin activity in response to stimuli such as carbachol, insulin and lysophosphatidic acid [Baron, 1998] [Kranenburg, Verlaan, 1999b] [Werbonat, 2000], although exactly how this affects dynamin activity is unclear. Src has been shown to mediate phosphorylation of dynamin2 and to be required for internalisation of the seven-transmembrane (7TM) receptors, the M1 muscarinic acetylcholine receptor [Werbonat, 2000] and the β2-adrenergic receptor [Ahn, 1999]. The adaptor protein β-arrestin1 binds directly to c-src, so could be responsible for recruiting src to 7TM receptors [Miller, 2000]. Src also phosphorylates clathrin in response to EGF and this was shown to be required for EGF receptor internalisation [Wilde 1999]. Epsin and Eps15 are also phosphorylated, which is discussed below.

A number of proteins involved in endocytosis, AP2, β-arrestins AP180, amphiphysin and dynamin, have been found to bind to phosphatidylinositol lipids *in vitro*, suggesting that phospholipids may regulate their activities *in vivo* (reviewed in [Corvera, 1999]). As mentioned above, the AP2 α subunit binds to phosphatidylinositol lipids, in particular PI-4,5-P_2, at a site close to that required for membrane association and this phospholipid binding reduces the ability of AP2 to bind to clathrin [Beck, 1991] [Page, 1995] [Gaidarov, 1996]. An N-terminal region of AP180 binds strongly to PI-3,4,5-P_3 and lipid association inhibits clathrin assembly mediated by the C-terminal domain [Ye, 1995] [Hao, 1997]. At least two β-arrestins also have high affinity binding sites for both PI-4,5-P_2 and PI-3,4,5-P_3 and the lipid binding site of β-arrestin2 was shown to be critical for the concentration of β-arrestin2-receptor complexes into clathrin-coated pits [Gaidarov, Krupnick, 1999]. The interactions of phosphatidylinositol lipids with these adaptor proteins may somehow help to co-ordinate clathrin coat assembly and receptor recruitment into forming clathrin-coated pits (steps 1 and 2 shown in figure 1.19).

Evidence that PI-4,5-P_2 plays a particularly important role in clathrin-mediated endocytosis *in vivo* came from observations that endocytosis in a perforated cell system can be inhibited by pleckstrin homology (PH) domains that bind to PI-4,5-P_2, but not those that bind to PI-3,4-P_2 [Jost, 1998]. The binding of AP2 to PI-4,5-P_2 is described above. Dynamin is a key clathrin-coated pit component that also binds specifically to PI-4,5-P_2, in this case via a PH domain, and this is essential for its function in endocytosis [Achiriloaie, 1999] [Lee, A, 1999] [Vallis, 1999]. Both dynamin and its binding partner amphiphysin are able to bind directly to protein-free liposomes *in vitro* [Takei, 1998] [Takei, 1999]. Amphiphysin binds to membranes via a region separate from the AP2, clathrin and dynamin binding sites [Ramjaun, 1999], whether this is a phospholipid-binding site is unclear. The interaction of dynamin, and other PI-4,5-P_2-binding proteins involved in endocytosis, with membranes may be down-regulated by a protein called synaptojanin. Synaptojanin is a Sac family phosphatidylinositol 5-phosphatase, which reduces the levels of PI-4,5-P_2, by converting it into PI-4-P [McPherson, 1996] [Hughes, 2000]. The importance of the phosphatase activity of synaptojanin to endocytosis, in particular to the uncoating of synaptic vesicles, has been confirmed using mutations that destroy its phosphatase activity. These mutants, made for both mammalian synaptojanin1 and *C. elegans* unc-26 (the synaptojanin ortholog), act as dominant negative proteins that inhibit endocytosis [Cremona, 1999] [Harris, 2000]. Synaptojanin, like dynamin, contains a PRD and binds to some of the same PRD-binding partners as dynamin (see for instance [McPherson, Czernik, 1994] [Micheva, Kay, 1997] [Nemoto, 1997]), so may also regulate dynamin function by competing for these binding partners.

Phospholipid-protein interactions are not the only way that lipids can regulate endocytosis. Localised regulation of lipid composition of the donor membrane bilayer may be required to induce changes in membrane curvature needed for the fusion and fission events that occur during vesicle budding, reviewed in [Burger, 2000]. One report has suggested that the ability of a dynamin-binding protein, endophilin1, to transfer arachidonate to LPA may be important for synaptic vesicle endocytosis. This activity of endophilin1 is thought to change the local membrane topology, inducing the extra membrane curvature needed for vesiculation [Schmidt, 1999] and reviewed in [Barr, 2000].

1.5.8 The AP2-binding proteins Eps15 and epsin and the regulation of endocytosis by ubiquitination

Two particularly interesting AP2 α–ear binding partners, in terms of potential cross-talk between endocytosis and other cellular processes including ubiquitination, are Eps15 (and the related Eps15R [Coda, 1998]) and its binding partner epsin. The few known links between endocytosis and ubiquitination are of particular interest because investigation of POSH has suggest that it may be involved both with dynamin in endocytosis and in ubiquitination.

Eps15 is an EGF receptor tyrosine-phosphorylated substrate [Fazioli, 1993], hence its name, and its binding partner epsin has also been reported to bind directly to clathrin [Drake, 2000]. Eps15 is amongst a number of proteins that contain EH (Eps15-homology) domains, which allow them to bind to NPF repeats within proteins such as epsin ([Wong, 1995] and reviewed in [Mayer, 1999]). Two EH domains are also present in the dynamin-binding protein intersectin/Ese, which forms a complex with Eps15 via coiled-coil regions in both proteins [Sengar, 1999]. Eps15 is the strongest known binding partner for the AP2 α-ear [Benmerah, 1996] [Owen, 1999]. Over-expression of full-length Eps15 inhibits endocytosis, whereas a mutant defective in AP2 binding does not [Benmerah, 1998], showing the importance to endocytosis of proteins (including Eps15 and epsin) that interact with the α-ear. Intriguingly Eps15 has been shown to co-localise with clathrin and AP2 at coated pits, but does not require AP2 or clathrin for PM localisation [van Delft, Schumacher, 1997]. This raises the possibility that Eps15 is involved in AP2 recruitment to the PM (figure 1.19 step 1).

Recruitment of Eps15 and epsin to coated pits is highly regulated. Eps15 and epsin are both phosphorylated in response to mitotic signals, which has been reported to inhibit their binding to AP2, and are de-phosphorylated in response to membrane de-polarisation in nerve terminals, which increases their binding to AP2 [Chen, H, 1999]. Eps15 phosphorylation, in response to stimuli such as EGF or TGFα, is required for EGFR, but not TfnR, internalisation [Confalonieri, 2000].

Eps15, epsin and some receptors provide interesting links between endocytosis and the process of ubiquitination. Once phosphorylated Eps15 is then mono-ubiquitinated [van Delft, Govers, 1997]. In *Drosophila* the gene encoding a de-ubiquitinating enzyme (*fat facets*) has been genetically linked to a gene encoding an epsin-like protein (*liquid facets*), as well as to a proteasome component [Huang, 1995] [Cadavid, 2000]. A number of mammalian and yeast receptors, transporters and channels have been reported to undergo ligand-dependent ubiquitination, which is required for their internalization, reviewed in [Hicke, 1999]. For the yeast α-factor receptor the in-frame fusion of a single ubiquitin to the receptor allows this chimera to be internalised [Terrell, 1998]. In the case of the mammalian growth hormone receptor one study suggests that the region of the receptor that binds to the ubiquitination machinery, but not the actual ubiquitination sites, is required for endocytosis to proceed [Govers, 1997]. In a few cases the E3 ubiquitin ligase, which binds to both the receptor substrate and E2 ubiquitinating enzymes, has been identified. For instance, Cbl binds to activated receptor tyrosine kinases via its SH2 domain and an E2 enzyme via its RING finger (discussed above) and Cbl ubiquitination activity is required for internalisation of the receptors to which it binds [Joazeiro, 1999]. The classic role for multi-ubiquitination is to target a protein for degradation by the proteasome, reviewed in [Weissman, 1997]. The role of the proteasome in ubiquitination-dependent internalisation of mammalian receptors, assessed using proteasome inhibitors, seems to vary from one receptor to another, reviewed in [Strous, 1999]. Mono-ubiquitination, or recruitment of the ubiquitination machinery without ubiquitination itself, is not sufficient to target a protein for proteasomal degradation, which requires a multi-ubiquitin chain [Chau, 1989]. The transient multi-ubiquitination of epsin in *Drosophila*, mono-ubiquitination of Eps15 in mammalian cells and ligand-dependent mono-ubiquitination of some receptors have instead been suggested to act as signals, recognised by unknown receptors, that may mediate processes other than degradation.

Epsin, via its NPF motifs, can bind to another EH domain-containing partner called POB1 [Morinaka, 1999], which in turn interacts with RalBP1 (Ral-binding protein 1), an effector for Ral (shown in figure 1.20). Mutants of Ral, RalBP1 and POB1 were able to inhibit EGF and insulin internalisation, but not transferrin receptor endocytosis [Morinaka, 1999] [Nakashima, 1999]. Phosphorylation of Epsin and POB1 in response to mitogenic signals was shown to reduce recruitment of the Epsin/POB1/RalBP complex to coated pits by inhibiting binding of epsin to AP2 and to POB1 [Kariya, 2000].

A number of links between Eps15 or epsin and nuclear shuttling have been observed (reviewed in [Di Fiore, 1999]). Eps15, epsin and AP180 all contain FG (single letter amino acid code) repeats that could allow them to bind to members of the importin family in order to enter the nucleus. One report showed that a transcription factor called promyelocytic leukemia zinc finger protein

(PLZF) binds to a region towards the N-terminus of epsin that is separate from the AP2, clathrin and Eps15-binding domains [Hyman, 2000]. Eps15 binds to NUMB, which is degraded by the nuclear proteasome and is also thought to be involved in endocytosis, and Rab/hRip, which has been linked to the control of nuclear export [Salcini, 1997].

Despite a wealth of information the *in vivo* function(s) of Eps15 and epsin still remain unclear, but they are certainly at the heart of the endocytic machinery, as can be seen schematically in figure 1.20.

1.5.9 Coated pit invagination, constriction and budding

Once AP2, activated receptors (figure 1.19 step 1) and a clathrin-lattice (figure 1.19 step 2) have been recruited, the plasma membrane becomes invaginated (figure 1.19 step 4) and then constricted (figure 1.19 step 5). A constricted pit is plasma membrane-associated via a narrow neck, but enters a state where receptor-bound ligands are sequestered from bulky probes (such as avidin); in contrast invaginated pits are fully open to the extracellular environment, including bulky probes [Schmid, 1990]. Clathrin-coated pits, composed mainly of pentameric clathrin units, appear to invaginate from the edges of a flat clathrin lattice, composed mainly of hexagonal clathrin units, that is observed on the cytoplasmic face of the PM and can be artifically induced to invaginate by cytoplasmic acidification [Heuser, J, 1989].

Constriction is inhibited *in vitro* by ATP depletion, but exactly how constriction occurs, and the identity of the ATPase involved, remains unknown [Schmid, 1990]. GDPβS, but not GTPγS can also interfere with constriction suggesting a role for a GTP-bound GTPase in this process [Carter, 1993]. The large GTPase dynamin is at least one GTPase that has been implicated in coated pit constriction (see [Sever, 2000a] and further discussion below). Recruitment of dynamin is predicted to occur once AP2 and clathrin are assembled, as depicted in figure 1.19 (step 3), and to be mediated by association of a protein called amphiphysin with all three components (reviewed in [Wigge, 1998] and [Sever, 2000b] and discussed below).

The transition from an invaginated to a constricted pit can be inhibited by injection of anti-endophilin1 antibodies into a tonically stimulated synapse [Ringstad, 1999] or by treatment of perforated A431 cells with GST-endophilin1 SH3 domain [Hill, 2001]. These data implicate endophilin1, a dynamin and synaptojanin-binding protein, in these early stages of endocytosis. Inhibition of endocytosis in the perforated A431 cell assay was associated with a drop in PI-4,5-P_2 levels and loss of AP2 staining [Hill, 2001]. This suggests that inhibition of endocytosis resulted from the inappropriate activation of the endophilin-binding partner synaptojanin (a phosphatidylinositol 5-phosphate phosphatase), however, an excess of neither synaptojanin nor dynamin could rescue endocytosis inhibition by endophilin SH3 domain [Hill, 2001].

The constricted pit must somehow pinch-off from the membrane to form a separated vesicle (figure 1.19 step 6). This process is dependent upon both ATP and GTP hydrolysis *in vitro* [Carter, 1993] and requires a membrane fission event initiated on the external leaflet of the plasma membrane. The exact mechanism of pinching-off is a matter of great debate, but the GTPase dynamin is though to be crucial (reviewed in [Hinshaw, 2000] and [Sever, 2000a] and discussed below).

The uncoating stages of the clathrin-coated vesicle cycle (figure 1.19 steps 7 and 8), removal of clathrin and then of AP2, are also ATP-dependent. The ATPase involved is the chaperone hsp70c in combination with its binding partner auxillin, which also binds to AP2 (see above) [Ungewickell, 1995] [Holstein, 1996]. In a synaptojanin deficient mouse cortical neurons exhibited increased number of clathrin-coated vesicles and high PI-4,5-P2 levels [Cremona, 1999]. This and other studies suggest that synaptojanin is involved in the process of uncoating.

1.6 INTRODUCTION TO DYNAMIN

Dynamin is a large (100kDa) GTPase that was first isolated from calf brain as a putative microtubule-associated motor protein [Shpetner, 1989]. There is no evidence that mammalian dynamin interacts with microtubules *in vivo*, but the localisation of a dynamin-like protein in plants, phragmoplastin, appears to be dependent upon microtubules [Gu, 1997]. The first clue that dynamin may function in endocytosis came from *Drosophila shibire^{ts}* mutant flies, which were identified in a screen for mutants that exhibited temperature-sensitive paralysis [Grigliatti, 1973]. In the *shibire^{ts}* fly paralysis was caused by a block in endocytosis, which prevented synaptic vesicle recycling and caused a build-up of coated pits at the nerve terminal [Koenig, 1989]. At a non-permissive temperature many cell types in the *shibire^{ts}* fly were shown to be deficient in endocytosis [Kosaka, 1983b] [Kosaka, 1983a] [Kessell, 1989]. The *shibire^{ts}* gene was later identified as the single *Drosophila* dynamin gene with mutations in the GTP-binding domain [van der Bliek, 1991] [Chen, 1991]. These mutations were outside of three essential GTP-binding motifs found in all GTPase domains, [Bourne, 1991] and see figure 1.22: *shibire^{ts1}* and *shibire^{ts2}* alleles were mutated at residues equivalent to rat dyn2 amino acids 273 and 147 [van der Bliek, 1991]. This may account for the temperature-sensitive phenotype of the *shibire^{ts}* flies, as mutations within the essential GTP-binding motifs often create proteins that act as potent dominant negatives (discussed below).

In mammalian cells, as in *Drosophila*, it appears that dynamin has a GTPase-dependent role in clathrin-mediated endocytosis. Transfection of COS7 or HeLa cells with dominant negative GTPase-deficient dynamin mutants, such as K44E, K44A K206D and S45N point mutants within the essential GTP-binding motifs shown in figure 1.22 [van der Bliek, 1993] [Herskovits,

Burgess, 1993], blocked clathrin-mediated endocytosis. Endocytosis was also blocked when synaptosome preparations were treated with GTPγS [Takei, 1995]. Dynamin has been localized to clathrin-coated pits in both neuronal [Damke, 1994] and non-neuronal cells [Bauerfeind, 1997]. A wealth of such data suggests that dynamin, and dynamin's GTPase activity in particular, is essential for endocytosis both at nerve terminals and in non-neuronal cells.

1.6.1 The domain structure of mammalian dynamins 1, 2 and 3

Three mammalian dynamin genes have been identified to date (Dyn1,2,3), each with at least four splice forms, see figure 1.23. Dyn1 was the first of the dynamins to be cloned, it is expressed only in neuronal tissues and has 8 splice variants [Nakata, 1991] [Robinson, 1993] [van der Bliek, 1993] [Cao, H, 1998]. Dyn2 is the ubiquitously expressed form of dynamin and has 4 splice variants [Cook, 1994] [Robinson, 1994] [Sontag, 1994]. Dyn3 is expressed only in brain, heart, lung and testis and each of its 13 splice variants are expressed in different subsets of these tissues [Nakata, 1993] [Cook, 1996] [Cao, H, 1998].

The three mammalian dynamin proteins share the same overall domain structure, shown in figure 1.21. The N-terminus contains the most conserved domain (see % identities of domains shown in figure 1.21), the GTPase domain. This includes the highly conserved tripartite motif essential for GTP binding and hydrolysis indicated in figure 1.21 and shown in detail in figure 1.22. The dominant negative dynamin GTPase mutations mentioned above were made by homology with Ha-Ras. K44E or K44A is equivalent to Ha-Ras K16N and would be predicted to bind poorly to any nucleotide, whereas S45N corresponds to Ha-Ras S17N and would be predicted to bind to GDP but not to GTP [Feig, 1986]. These mutants act as dominant negatives, presumably by forming non-productive complexes with endogenous dynamin and its binding partners.

In addition to the highly conserved GTPase domain dynamins1-3 also contain a pleckstrin homology (PH) domain, a GTPase effector (GED) domain and the C-terminal proline-arginine-rich region (PRD), which is the least conserved region between dynamins1-3 (see figure 1.21). The many splice forms of dynamins 1-3 affect a number of domains, see figure 1.23, and the significance of these variations (if any) is only just beginning to be studied, see for instance [Cao, H, 1998]. The functions of dynamin and the roles of each domain in controlling the function of dynamin in endocytosis shall be discussed below. Known differences between neuronal dynmain1 and the ubiquitous dynamin2 (little is currently known about dynmain3) are noted.

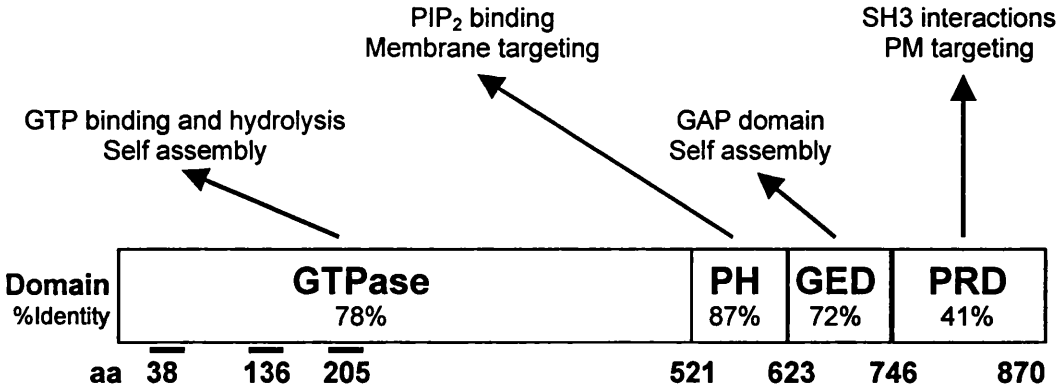

Figure 1.21 Schematic representation of the domain structure of dynamin

Amino acid (aa) numbers shown are for dynamin2ba and signify the start of a motif or domain. The % aa identities within each domain were calculated for rat dynamins 1ab, 2ba and 3bab and excluded extra aa's that extend the start of a domain (dyn3 aa's 521-526 and dyn1 aa's 629-632 and 639-640). The lines below the GTPase domain indicate the positions of the three GTP-binding motifs shown in detail in figure 1.22. The roles played by each domain are summarised above and are discussed further in the text. Domain names: GTP-binding domain (GTPase); pleckstrin homology domain (PH); GTPase effector domain (GED); proline/arginine-rich domain (PRD).

	Element I								**Element II**				**Element III**			
Consensus	**G**	**X**	**X**	**X**	**X**	**G**	**K**	**S/T**	**D**	**X**	**X**	**G**	**N/T**	**K**	**X**	**D**
r Dyn 1-3	G	G	Q	S	A	G	K	S^{45}	D	P	Q	G^{139}	T	K	L	D^{208}
h Ha-Ras	G	A	G	G	V	G	K	S^{17}	D	T	A	G^{60}	N	K	C	D^{118}
h Rac 1	G	D	G	A	V	G	K	T^{17}	D	T	A	G^{60}	T	K	L	D^{118}

Figure 1.22 The tripartite motif required by GTPases for GTP-binding

GTP-binding consensus sequence elements are shown at the top [Bourne, 1991]. The sequences for these conserved regions within the small GTPases human (h) Ha-Ras and Rac 1 and within rat (r) dynamins 1-3 are shown below. X = any amino acid.

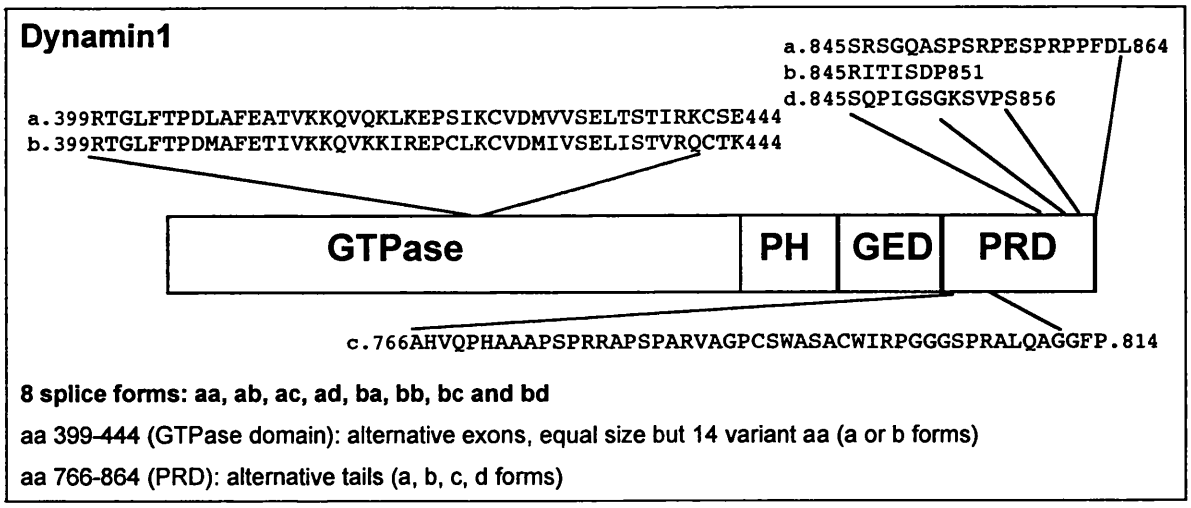

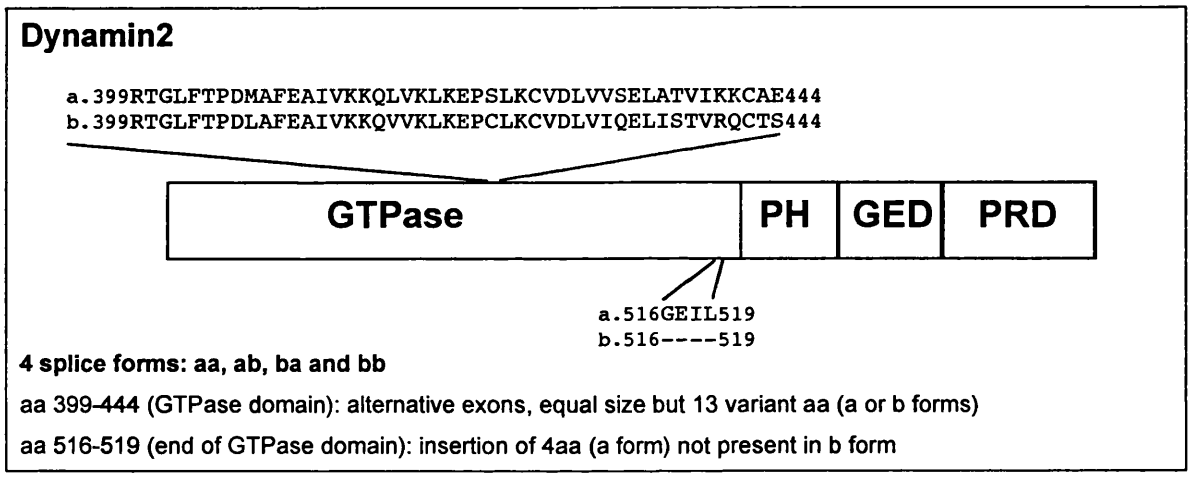

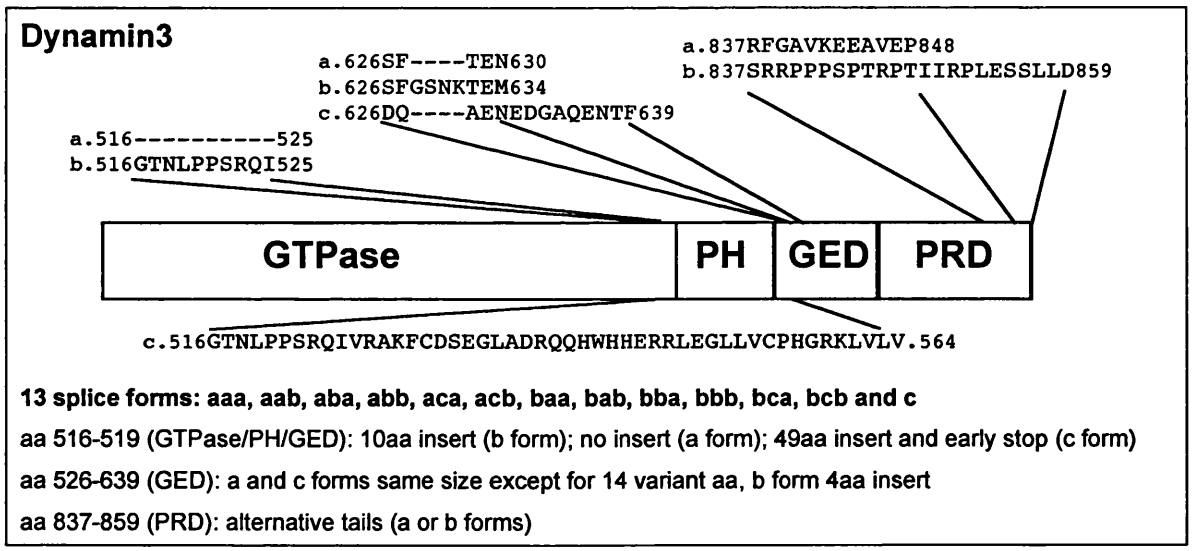

Figure 1.23 Schematic representation of the 25 different dynamin proteins produced by alternative splicing of the three rat dynamin genes

Abbreviations used: amino acid (aa), except where indicated to be an isoform name; GTP-binding domain (GTPase); pleckstrin homology domain (PH); GTPase effector domain (GED); proline/arginine-rich domain (PRD). In dynamin1 second splice site c form and dynamin3 third splice site c form a premature stop codon severly truncates the protein. Adapted from [Cao, H, 1998].

1.6.2 Endocytic events in which dynamin has been implicated

Constriction and fission stages of clathrin-coated pit endocytosis at the PM

Analysis of HeLa cells transfected with the K44A dynamin1 mutant (predicted to be mostly nucleotide-free) revealed that the normal sequestration of large probes, such as avidin, was prevented just as much as that of small probes, such as the sodium salt of 2-mercaptoethane sulphonic acid (MesNa) [van der Bliek, 1993]. EM analysis of transferrin receptors, on HeLa cells stably transfected with K44A dynamin1 showed normal receptor recruitment into pits, but an increase in invaginated pits apparently blocked before the constriction stage [Damke, 1994]. Such data suggests a role for dynamin in the constriction of pits (figure 1.19 step 4). Constricted pit formation can be inhibited by GDPβS, but not by GTPγS, suggesting that GTP-binding, possibly GTP binding by dynamin, but not hydrolysis is required for this step [Carter, 1993]. In contrast, the later event of vesicle budding (figure 1.19 step 5) is inhibited by GTPγS [Carter, 1993], suggesting a requirement for GTP hydrolysis (probably by dynamin) at the budding stage of endocytosis. A recent study using perforated cells showed that a dynamin mutant that is able to bind to GTP, but is deficient in GTP hydrolysis (dyn1 T65S), inhibited endocytosis at a late invagination/constriction stage [Hill, 2001]. In contrast with previous studies, this suggests that dynamin GTP hydrolysis may in fact play a role in coated-pit constriction. Models proposed to explain how dynamin may facilitate the constriction and scission stages of endocytosis are described below.

Budding from the TGN

Evidence has suggested a role specifically for dynamin2 "aa" and "ab" splice forms in budding from the TGN. A GFP-fusion protein of Dyn2aa was localised partly to the plasma membrane and partly to the TGN [Cao, H, 1998] and a dominant negative (K44A) mutant of Dyn2aa was seen to disrupt Golgi structure and inhibited VSVG exit from the Golgi [Cao, H, 2000]. Immuno-depletion of dynamin also blocked budding from the TGN *in vitro* [Jones, SM, 1998].

Caveolae internalisation and phagocytosis

It has also been proposed that dynamin2 is required for some clathrin-independent vesiculation events. Internalisation of cholera toxin B by caveolae in hepatocytes was inhibited by anti-dynamin antibodies [Henley, 1998] and the actin-dependent internalisation of large particles by macrophages, termed phagocytosis can be inhibited by K44A dynamin2, but not by K44A dynamin1, [Gold, 1999].

These potential roles for dynamin2 outside of clathin-dependent endocytosis at the plasma membrane remain controversial.

1.6.3 The GTPase domain of dynamin

Dynamin, like any GTPase, can exist in a GTP-bound state, a GDP-bound state and an empty state. For small GTPases such as Ras the rates of both GTP hydrolysis and release of GDP are slow (see figure 1.24) and are increased by the action of GAPs and GEFs respectively, discussed above and reviewed in [Bourne, 1991]. Dynamin's biochemical properties are unusual, besides its relatively high molecular weight (around 100kDa) dynamin has a low affinity for GTP and a high basal rate of GTP hydrolysis, see figure 1.24 ([Shpetner, 1992] and reviewed in [Sever, 2000b]). The kinetic parameters of dynamin's GTPase cycle, shown in figure 1.24, and the high levels of intracellular GTP (1mM) mean that dynamin should exist only transiently (1-10ms) in an empty or GDP-bound state unless accessory proteins stabilised these states *in vivo*.

Despite dynamin's high basal rate of GTP hydrolysis a number of factors can further stimulate dynamin's GTPase activity *in vitro*, acting like the GAPs for small GTPases (see above). These factors include: oligomerization of dynamin itself [Tuma, 1994] [Warnock, 1995] [Warnock, 1996]; binding of dynamin PRD to microtubules [Shpetner, 1992]; association of dynamin PH domain with anionic phospho-lipids (liposomes) [Tuma, 1993]; interaction of dynamin PRD with SH3 domain-containing proteins, see for instance [Herskovits, Shpetner, 1993] and [Gout, 1993]. Some of these GTPase-activating factors can act synergistically. For instance, binding of lipids to dynamin PH domain stimulates oligomerization, both of which increase GAP activity, and this stimulation can be further enhanced synergistically by addition of the PRD-binding protein Grb2 [Tuma, 1993] [Barylko, 1998].

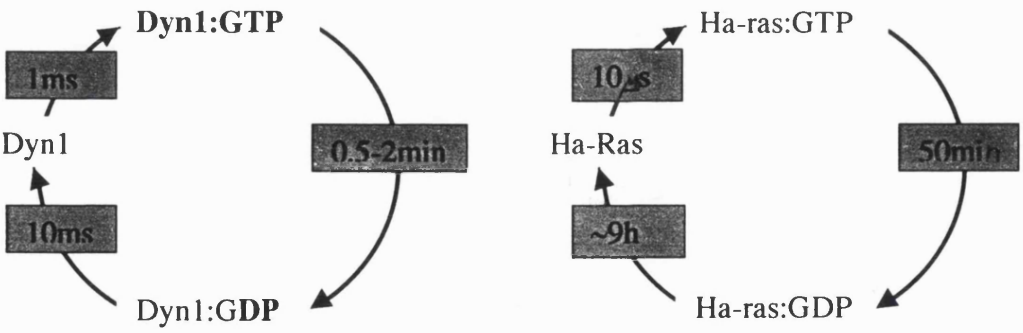

	GTP dissociation	GTP hydrolysis	GDP dissociation
Ha-Ras	$1.4 \times 10^{8}\ M^{-1}s^{-1}$	$3.4 \times 10^{-4}\ s^{-1}$	$3 \times 10^{5}\ s^{-1}$
Dynamin1	$7 \times 10^{5}\ M^{-1}s^{-1}$	$8\text{-}30 \times 10^{-3}\ s^{-1}$	$93\ s^{-1}$

Figure 1.24 The GTPase cycles of dynamin1 (Dyn1) and Ha-Ras

The half-times for each step in the GTPase cycle in the absence of other factors are shown (taken from [Sever, 2000b]). The rate constants from which these half-times were calculated are also shown.

Except for dynamin itself all known protein dynamin binding-partners, shown in figure 1.27 and discussed below, interact with the PRD. The observation that many of these SH3 domain-containing dynamin-binding proteins act as GAPs does not rule them out as also being transient effector proteins acting downstream of GTP-bound dynamin. There is at least one Rac GAP, n-chimaerin, that binds to GTP-Rac and appears both to inactivate Rac by stimulating its GTPase activity and to act synergistically with activated GTP-bound Rac to induce actin-reorganisation [Kozma, 1996].

Differences have been reported between the GTP cycles and regulation of cycling for dynamins 1 and 2. Dynamin2 has an even higher intrinsic GTPase activity, affinity for GTP and stimulated GTPase activity than dynamin1 [Warnock, 1997]. These differences between dynamins 1 and 2 may reflect their concentrations in the cell; dynamin is at much higher levels in neuronal tissues, where dynamin1 is expressed, than in any other tissue [Warnock, 1997]. The smaller pool of dynamin2 may need to re-prime more rapidly, which would be facilitated by a very fast GTPase cycle. The differences in dynamin 1 and 2 GTPase cycles may also reflect their different functions, synaptic membrane recycling and receptor-mediated endocytosis respectively.

Dynamin1, but not dynamin2, GTPase activity has been reported to be regulated by phosphorylation, reviewed in [Turner, KM, 1999]. Dynamin1 is phosphorylated in resting nerve terminals by PKC, at Ser-795 within the PRD *in vitro* [Powell, 2000], and this may be facilitated by the adaptor protein RACK-1 (a receptor for activated C-kinase) [Rodriguez, 1999]. *In vitro* PKC phosphorylation enhances dynamin1 GTPase activity up to 12-fold [Robinson, 1993]. In contrast direct binding of dynamin1 to calcium and de-phosphorylation by calcineurin, which is activated by calcium influx during synaptic membrane depolarization (reviewed in [Turner, KM, 1999]), have both been reported to inhibit dynamin1 GTPase activity [Liu, Sim, 1994] [Liu, 1996].

There are no known examples of proteins that further enhance dynamin's extremely rapid basal GDP/GTP exchange activity, acting as GEFs, neither are there known to be any GDI-like molecules that could prevent futile cycling of dynamin.

1.6.4 The GTPase effector domain (GED) of dynamin and oligomerization

The GTPase effector domain (GED) of dynamin is a coiled-coil region. Coiled-coil domains are often involved in protein-protein interactions [Lupas, 1996] and indeed dynamin GED interacts with the GTPase domain, so facilitating dynamin oligomerization [Muhlberg, 1997] [Sever, 1999] [Smirnova, 1999]. The isolated GED also stimulates unassembled dynamin GTPase activity by 50-fold, suggesting that the GED provides the GAP activity induced by oligomerization [Sever, 1999].

Purified dynamin in the absence of membranes forms tetramers [Muhlberg, 1997] or possibly dimers [Tuma, 1995]. These self-assemble into higher order oligomers forming rings or spirals under low ionic salt conditions [Hinshaw, 1995] or, at physiological ionic strength, when treated with GDP plus metallofluorides (this combination induces a transition state-like conformation) [Carr, 1997]. Artificial templates, such as microtubules or acidic phospholipids, can also induce assembly of multimeric dynamin structures [Shpetner, 1989] [Tuma, 1994]. Electron microscopy (EM) analysis of nerve terminals in *shibire*^{ts} flies revealed a build-up of pits, sometimes clathrin-coated, encircled by rings of electron-dense material [Kosaka, 1983a] [Kessell, 1989]. These rings were of similar dimensions to the dynamin structures seen *in vitro* and the striations seen on synaptosomes treated with GTPγS [Takei, 1995]. It was suggested that these structures, termed collared pits, could represent an enlarged, stabilised form of a normally transient endocytosis intermediate.

In contrast, when endocytosis has been inhibited by dominant negative dynamins in mammalian cells EM analysis has never revealed electron-dense dynamin collars. This may be due to the lack of a neuron-specific component in non-neuronal cells that enables collars to be visualised by thin-sectioning techniques. In support of this, it has been shown that only when neuronal amphiphysin1 is present with dynamin are striated patterns seen on lipid tubes [Takei, 1999]. Whether the more ubiquitous amphiphysin2 splice forms (amphiphysins are reviewed in [Wigge, 1998]) localise to the necks of coated pits *in vivo* and whether they can form striations with dynamin and lipid tubes *in vitro* remains to be determined.

Point mutation analysis of the GED indicated that residues K694 and R725 are important for stimulating GTPase activity in the presence of a microtubule template [Sever, 1999]. It was thought that R725 may act as a classical arginine finger seen in other GAPs, but mutation of this residue was recently shown not to effect dynmain GTPase activity [Marks, 2001]. K694 within the GED domain plays a structural role in dynamin's GED to GTPase domain self-assembly interactions [Sever, 1999]. Surprisingly mutants of either of these residues, despite being unable to stimulate dynamin GTPase activity *in vitro*, stimulated transferrin endocytosis when transfected into cells [Sever, 1999]. This lead to a re-assessment of the mechanism by which dynamin may contribute to endocytosis, resulting in a new model discussed below and shown as model 5 in figure 1.25.

1.6.5 The PH domain of dynamin and the sub-cellular localisations of dynamins 1 and 2

Although the actual budding event driven by dynamin is dependent upon GTPase activity, binding of dynamin to membranes is independent of GTPase activity. This is reflected in the localisation of a dynamin mutant deficient in nucleotide binding and GTPase activity (K44A), which is still found to be enriched in the membrane fraction of transfected cells [van der Bliek,

1993]. Re-localisation of membrane-associated dynamin to the neck of a coated pit (shown in figure 1.9 step 5) may require GTP; in the presence of GDP dynamin is membrane bound but uniformly distributed throughout the clathrin lattice, whereas in the presence of GTPγS dynamin is localised to the neck region [Warnock, 1997].

The dynamin PH domain bound preferentially to PI-4,5-P_2 *in vitro* and, of the phospholipids tested, PI-4,5-P_2 gave the highest stimulation of dynamin's GTPase activity [Salim, 1996]. The PH domain of dynamin is essential for its function in endocytosis; a dynamin PH domain deletion mutant (ΔPH) and a point mutant in this region (K535A) failed to bind to lipids and acted as a dominant negative proteins in transferrin endocytosis assays [Vallis, 1999].

Additional factors may be required for recruitment of dynamin to the plasma membrane and for strong dynamin-membrane association. Binding of amphiphysin to dynamin's PRD has been proposed to be important for dynamin recruitment to clathrin-coated pits, reviewed in [Wigge, Kohler, 1997] and discussed below. Also, binding of the PH domain of dynamin to phospholipids has been reported to be increased by oligomerization [Klein, 1998], suggesting that dynamin will bind co-operatively to membranes once it begins to self-assemble into rings at the neck of a coated pit. The dynamin PH domain has also been shown to bind to the βγ subunits of heterotrimeric G proteins in stimulated neuroendocrine cells [Liu, 1997], possibly through WD40 repeats in the Gβ subunit [Wang, 1995]. In contrast to phospholipid binding the interaction with Gβγ inhibited dynamin GTPase activity [Lin, 1996]. The PH domain of β-adrenergic receptor kinase requires both lipids and Gβγ-association for binding to membranes [Pitcher, 1995]. Dynamin may also utilise Gβγ for strong membrane association in cases where 7TM receptors are activated. Excess Gα subunits, which "mop up" and inhibit free Gβγ subunits, have been shown to inhibit transferrin and LDL endocytosis [Lin, 1998], further suggesting a role for Gβγ in endocytosis, possibly in association with dynamin.

The PKC-phosphorylated pool of dynamin1 in nerve terminals is cytosolic, calcium-dependent de-phosphorylation of dynamin1 increases its presence in the membrane fraction, separating it physically from cytoplasmic pools of PKC [Liu, Powell, 1994] [Powell, 2000]. It has been suggested that this segregation of phosphorylated dynamin1 from the de-phosphorylated protein may be partly due to an inhibition of dynamin1 binding to PI-4,5-P_2, which was observed in response to dynamin1 phosphorylation by PKC *in vitro* [Powell, 2000]. A reduced affinity of phosphorylated dynamin1 for protein binding partners, in particular amphiphysin, has been observed and may also contribute to its sub-cellular localisation [Slepnev, 1998].

Although the PH domain is thought to mediate membrane-association of both dynmain1 and dynamin2, evidence suggests that dynamin1 may contain additional targeting information that directs it more efficiently to the apical membrane of polarised cells. For instance, transfection of K44A dominant negative dynamin mutants of both dynamin1 and dynamin2 into polarised epithelial MDCK cells blocked baso-lateral endocytosis, but dynamin1 K44A was a more potent inhibitor of apical endocytic events [Altschuler, 1998]. The axon membrane is the site for synaptic activity and is the neuronal equivalent of the apical plasma membrane, so this kind of sorting information could be vital for the observed localisation of dynamin1 to nerve terminals (see for instance [Takei, 1995]).

Different dynamin2 and 3 splice forms appear to vary in their sub-cellular localisations, as assessed using GFP-fusion proteins of each splice form [Cao, H, 1998]. The dynamin2 second splice site, for instance, seemed to influence whether or not the protein is targeted to the TGN as well as to the PM: the a-form was seen partly at the TGN, whereas the b-form was only at the PM [Cao, H, 1998]. A number of splice variants of dynamins 1 and 3 affect the PRD domain and dynamin3c is alternatively spliced within the PH domain (see figure1.23), changes to either of these domains are likely to influence the protein's cellular distribution.

1.6.6 Proposed mechanisms for induction of membrane fission by dynamin

Dynamin GTPase activity has been implicated in the pinching-off of clathrin-coated pits, for instance dynamin GTPase mutants inhibit this stage of endocytosis, but exactly how dynamin induces membrane fission is still a matter for debate [Sever, 2000b]. At least five models have been proposed, which are depicted in figure 1.25 and discussed below.

Model 1 – Dynamin as a molecular garrotte

The first model proposed to explain dynamin function in endocytosis is depicted as model 1 in figure 1.25. In this model GDP-bound or nucleotide-free dynamin is targeted to coated pits. GTP-binding leads to a conformational change that causes dissociation of dynamin from the clathrin lattice and promotes its self-assembly into a helical collar that forms a constriction at the neck of the coated pit. Co-ordinated GTP hydrolysis by the assembled dynamin ring triggers a second conformational change tightening the collar and severing the vesicle from the plasma membrane, like a garrotte strangling the neck of the coated pit. The strongest evidence that dynamin could act as a molecular garrotte comes from the observation (made with EM) that pure dynamin protein forms helical spirals around phosphatidylserine liposomes and converts these liposomes to tubules, which then fragmented into small vesicles upon addition of GTP [Sweitzer, 1998]. A GTP hydrolysis-induced conformational change was required for vesiculation, as GTPγS or K44A dynamin1, which is defective in GTP-binding and hydrolysis, could not support vesiculation.

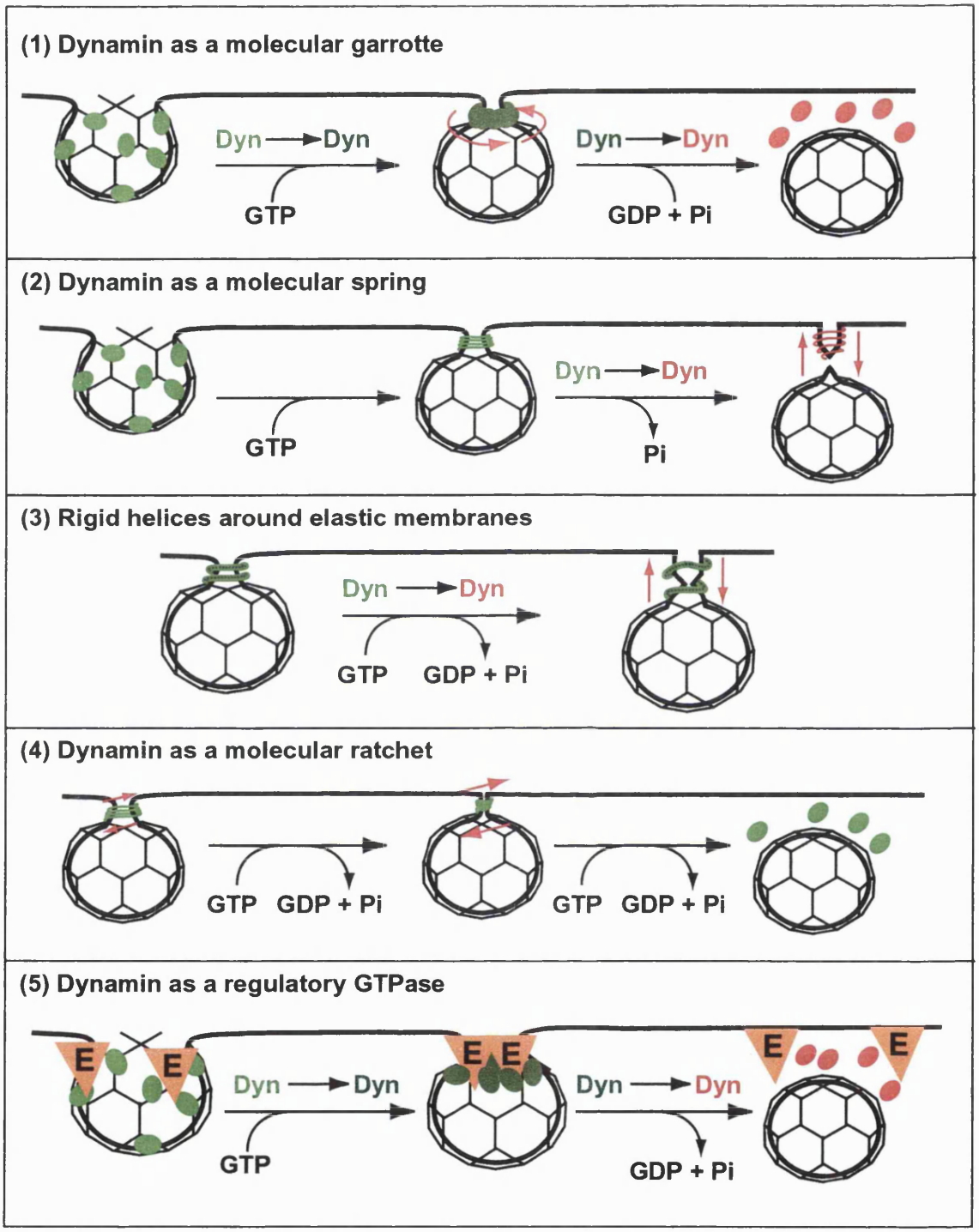

Figure 1.25 Current models for dynamin function in endocytic coated vesicle formation
Stages at which dynamin binds and hydrolyses GTP are indicated. In model 5 "E" designates an unknown effector molecule, see text. A change in dynamin colour indicates a conformational change. Red arrows indicate motion that accompanies dynamin's conformational changes. The dotted lines in model 3 indicate the line of dynamin attachment to underlying lipids required by the model. Based upon [Sever, 2000].

Model 2 – Dynamin as a molecular spring

A different model to explain how fission could be induced by a GTPase-dependent conformational change in dynamin has been suggested by Stowell et al. Rings of dynamin were seen to form *in vitro* on nanotubes formed from a mixture of lipid components [Stowell, 1999]. The pitch of the dynamin rings was nucleotide-dependent: when GTPγS or GDP:AIF4- were added a tightly packed stack of rings formed with a pitch of 11±1.5nm; in the presence of GDP dynamin formed a looser helix with a pitch of 20±3nm. This showed that assembled dynamin could adopt at least two conformations. When GTP hydrolysis was triggered by addition of $MgCl_2$ to dynamin pre-assembled onto nanotubes in the presence of 1mM GTP the dynamin spirals loosened, acquiring the pitch seen in the presence of GDP. These observations lead to the suggestion that dynamin acts as a mechno-spring, which undergoes an abrupt increase in pitch resulting from a conformational change induced by concerted GTP hydrolysis. The force from this molecular spring is thought to be sufficient to sheer the membrane at the neck of the coated pit [Stowell, 1999].

Model 3 – Rigid helices around elastic membranes

A mathematical model (model 3 in figure 1.25) has been proposed to explain how an increase in the pitch of a dynamin helix (the basis for model 2) could lead to vesicle formation [Kozlov, 1999]. This model was based upon the known physical properties of model lipid membranes and the following assumptions. (1) dynamin must assemble into a rigid helix around a tubular lipid neck. (2) the dynamin spiral must be tightly bound to the membrane along a single narrow line and lipid domains between these points of contact must be freely mobile. (3) lipids along the attachment line must not be freely exchangeable, thus dynamin must act as a barrier for lipid exchange. (4) the conformational change driven by GTP hydrolysis must be abrupt and concerted. Although dynamin's behaviour on pre-formed nanotubes, [Stowell, 1999] and discussed above, supports most of these assumptions it is not clear whether dynamin can act as a barrier for lipid exchange.

Model 4 – Dynamin as a molecular ratchet

This model suggested that dynamin induces constriction and membrane fission by a ratcheting mechanism, with one rung of dynamin molecules moving over another (depicted as model 4 in figure 1.25), similar to the way that myosin moves along actin filaments. This model was proposed in the light of yeast-two-hybrid data that showed multiple dynamin-dynamin interactions [Smirnova, 1999]: GED with GED; GED with middle domain, which is towards the C-terminus of the GTPase domain as depicted in figure 1.21; GED with GTPase domain. The GED-GTPase domain interaction was also seen to be nucleotide-dependent, being strongest with mutants that are predicted to be GDP-bound or nucleotide-free [Smirnova, 1999]. In this model the GTPase cycle would drive rounds of dynamin-dynamin attachment and detachment to tighten

a collar of dynamin around the membrane. For this model to work an anchor point, possibly provided by a protein such as amphiphysin, would be needed to prevent futile spiralling of dynamin along the neck of the coated pit.

Model 5 – Dynamin as a regulatory GTPase

A very different mechanism for dynamin activity to those described above has recently been proposed. It has been suggesting that, like the small GTPases discussed above, GTP-bound dynamin recruits one or more separate target proteins that are responsible for effecting coated pit constriction and membrane fission (figure 1.25 model 5). In this model it is the GTP-bound form of dynamin that is active and GTP hydrolysis causes dissociation of dynamin from its effector protein(s), terminating dynamin activity.

This model was proposed when it was observed that dynamin GED mutants defective in assembly-induced GTPase activity did not to inhibit endocytosis, but instead stimulated it [Sever, 1999]. The R725A mutation reduced the GED's GAP activity and K694A reduced assembly-dependent GTPase activity by inhibiting self-assembly, yet both mutants increased transferrin endocytosis [Sever, 1999]. Further analysis showed that both mutants increased the rate of the constriction phase of endocytosis, which appears normally to be the rate-limiting step, backing up previous observations suggesting that constriction is dynamin-dependent [Sever, 2000a]. The R725A mutant, although enhancing constriction, also appeared to slow down fission, turning this stage of endocytosis into the rate-limiting step ~~y into long spirals. This may sterically hinder the normal process of membrane fission, as was suggested for the R725A GAP-defective mutant~~ [Sever, 2000a].

One dynamin-binding protein that could provide an effector activity relevant to membrane invagination, constriction and fission is the PRD-binding protein endophilin and its lysophosphatidic acid acyl transferase activity that was mentioned above [Schmidt, 1999].

To date the majority of evidence seems to support models such as 1-4, where dynmain requires its GTPase activity and oligomerization properties to induce coated pit constriction and scission.

1.6.7 The proline/ arginine-rich domain of dynamin

The proline/ arginine-rich domain (PRD) of dynamin, as its name suggests, is rich in proline and basic residues. The PRD is the region that varies most between mammalian dynamins 1-3 (see figures 1.21 and 1.26). There are a number of class I and class II potential SH3 domain-binding motifs within the PRD sequences (SH3 domain-proline-rich sequence interactions are discussed above in section 1.4.2.3). These motifs allow dynamin's PRD to bind to the SH3 domains of a number of proteins that are discussed below.

Figure 1.26 The proline/ arginine-rich domains of dynamins 1, 2 and 3

(a) Rat dynamin1aa (see splice forms in figure 1.23) PRD sequence. Class I potential SH3 domain binding motifs, of the form RXXPXXP (where X is any amino acid), are shown in bold. Class II potential SH3 domain binding motifs, of the form PXXPXR, are underlined. Note that class II motifs 2 and 3 (numbering from the N-terminal end of the PRD) overlap with each other and with the second class I motif. The region specific to the second splice site a-form is shown in red.

(b) Rat dynamin2ba (see splice forms in figure 1.23) PRD sequence, labels as in (a). Note the additional 5^{th} class II motif, at the extreme C-terminus of the PRD, and a class I motif, overlapping the 4^{th} and 5^{th} class II motifs, which are not present in dynamin1 PRD.

(c) Rat dynamin3bab (see splice forms in figure 1.23) PRD sequence, labels as in (a). Like dynamin2 (b) the dynamin3 PRD contains one additional class I (3^{rd}) and one class II (5^{th}) motif not present in dynamin1. The region specific to the third splice site b-form is shown in red.

(d) Schematic representation of dynamin1 and 3 splice forms that effect potential SH3 domain binding motifs within the PRD. The positions of class II motifs (underlined in (a)-(c)) are shown in red and class II motifs (bold in (a)-(c)) in green. The 5^{th} class II and 3^{rd} class I motifs are only present in dynamins 2 and 3, while the 1^{st} class I motif is only present in dynamin1 PRD, so are shown in brackets. Dynamin1 or 3 splice variants that do not contain potential SH3 domain binding sites present in other splice forms are indicated.

(a) The sequence of dynamin1aa PRD (amino acids 750-864)

```
     750–V  STPMPPPVDD  SWLQVQSVPA  GRRSPTSSPT
PQRRAPAVPP  ARPGSRGPAP  GPPPAGSALG  GAPPVPSRPG
ASPDPFGPPP  QVPSRPNRAP  PGVPSRSGQA  SPSRPESPRP
PFDL-864
```

(b) The sequence of dynamin2ba PRD (amino acids 745-870)

```
745–VSTPVP  PPVDDTWLQN  TSSHSPTPQR  RPVSSVHPPG
RPPAVRGPTP  GPPLIPMPVG  ATSSFSAPPI  PSRPGPQNVF
ANNDPFSAPP  QPSRPARIPP  GIPPGVPSRR  APAAPSRPTI
IRPAEPSLLD-870
```

(c) The sequence of dynamin3bab PRD (amino acids 740-859)

```
     740–V  STPAPPPVDD  SWLQHSRRSP  PPSPTTQRRL
TLSAPLPRPA  SSRGPAPAIP  SPGPHSGAPP  VPFRPGPLPP
FPNSSDSYGA  PPQVPSRPTR  APPSVPSRRP  PPSPTRPTII
RPLESSLLD-859
```

(d) The positions of dynamin1 and dynamin3 PRD splice variations that affect potential SH3 domain-binding motifs

Dyn 3 third splice forms:
c. premature stop at aa 564 removes whole PRD
a. 837RFGAVKEEA . .848 no 4th class II and 3rd class I motifs
b. 837SRRPPPSPTR . . . . . .859 4th class II and 3rd class I motifs intact

Dyn 1 second splice site forms:
a. 845SR . . . . . 864 4th class II motif intact
b. 845RI . . 851 no 4th class II motif
d. 845SQ . . . . 856 no 4th class II motif

Dyn 1 second splice site form c
premature stop codon at aa 814
removes all but 1st class I motif

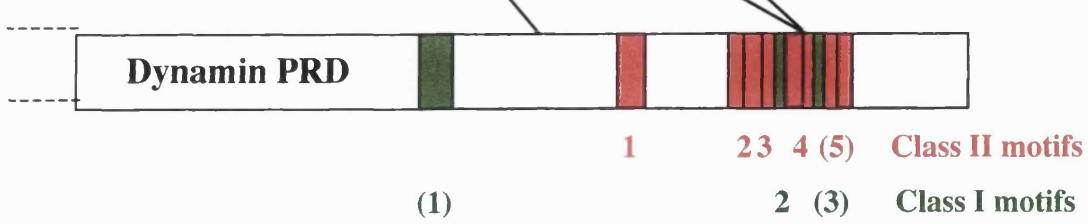

1 2 3 4 (5) Class II motifs

(1) 2 (3) Class I motifs

Figure 1.26 The proline/ arginine-rich domains of dynamins 1, 2 and 3

Dynamin1 PRD contains four class II motifs (PXXPXR), underlined in figure 1.26 (a-c), and one class I motif (RXXPXXP), bold in figure 1.26 (a-c), that are conserved in the PRD regions of dynamins 2 and 3 (compare a-c in figure 1.26). These conserved motifs may be important to the function of all three dynamins. One additional class II motif and one class I motif are present at the extreme C-terminus of dynamin2 and dynamin3 PRDs and the most N-terminal class I motif in dynamin1 PRD is not present in dynamins 2 or 3 (compare the sequences of (a), (b) and (c) in figure 1.26). Some of the splice forms of dynamins 1 and 3 affect the PRD (see figure 1.26 (d) and figure 1.23), whereas for dynamin2 only regions N-terminal to the PRD vary between splice forms (see figure 1.23). The functional significance, if any, of dynamin splice forms that lack a subset of potential SH3 domain-binding sites, or even lack the entire PRD (dynamin3 third splice site form c), and of the variations between the PRDs of dynamins 1-3 is unknown.

1.6.8 SH3 domain-containing proteins that bind to dynamin PRD

At least 14 SH3 domain-containing proteins have been found to interact with dynamin PRD: amphiphpysin1-2, endophilin1-3, intersectin1-2, syndapin1-2, Grb2, PLCγ, p85PI3K, Mlk2 and cortactin. Some of these proteins are depicted in figure 1.27 and are incorporated into the overall scheme in figure 1.20 showing protein-protein interactions within a clathrin-coated pit. Evidence that a particular SH3 domain-containing protein is a dynamin-binding protein is discussed below and ranges from *in vitro* binding to PRD constructs and pull-downs of dynamin from brain to co-localisation and an ability to interfere with dynamin function *in vivo*.

1.6.8.1 Dynamin-binding proteins implicated in synaptic transmission

Some of the dynamin-binding proteins have brain-specific or brain-enriched forms that are localised with dynamin1 at synaptic sites. For example, intersectin1 long splice form [Hussain, 1999], endophilin1/SH3p4 [Ringstad, 1997] [Micheva, Kay, 1997] and syndapin1 [Qualmann, 1999], which are all brain specific, and brain-enriched amphiphysin1 (reviewed in [Wigge, Kohler, 1997]). For endophilin1 and amphiphysin1 further *in vivo* evidence supports a role in synaptic transmission: antibodies to endophilin1 blocked synaptic vesicle recycling [Ringstad, 1999] and injection of the SH3 domain of amphiphysin1 into Lamprey neurons blocked clathrin-mediated endocytosis [Shupliakov, 1997].

Amphiphysin

There are two amphiphysin (amph) genes (1 and 2) and amphiphysin2 has at least four splice forms (termed a-d by [Ramjaun, 1999]). Amph1 is predominantly expressed in brain and at low levels in other tissues, the longest amph2 splice form (form-a) is brain-specific and the shorter amph2 splice forms are more ubiquitously expressed, reviewed in [Wigge, Kohler, 1997]. The domain structures and binding partners for amphiphysins 1 and 2 are shown schematically in figure 1.27.

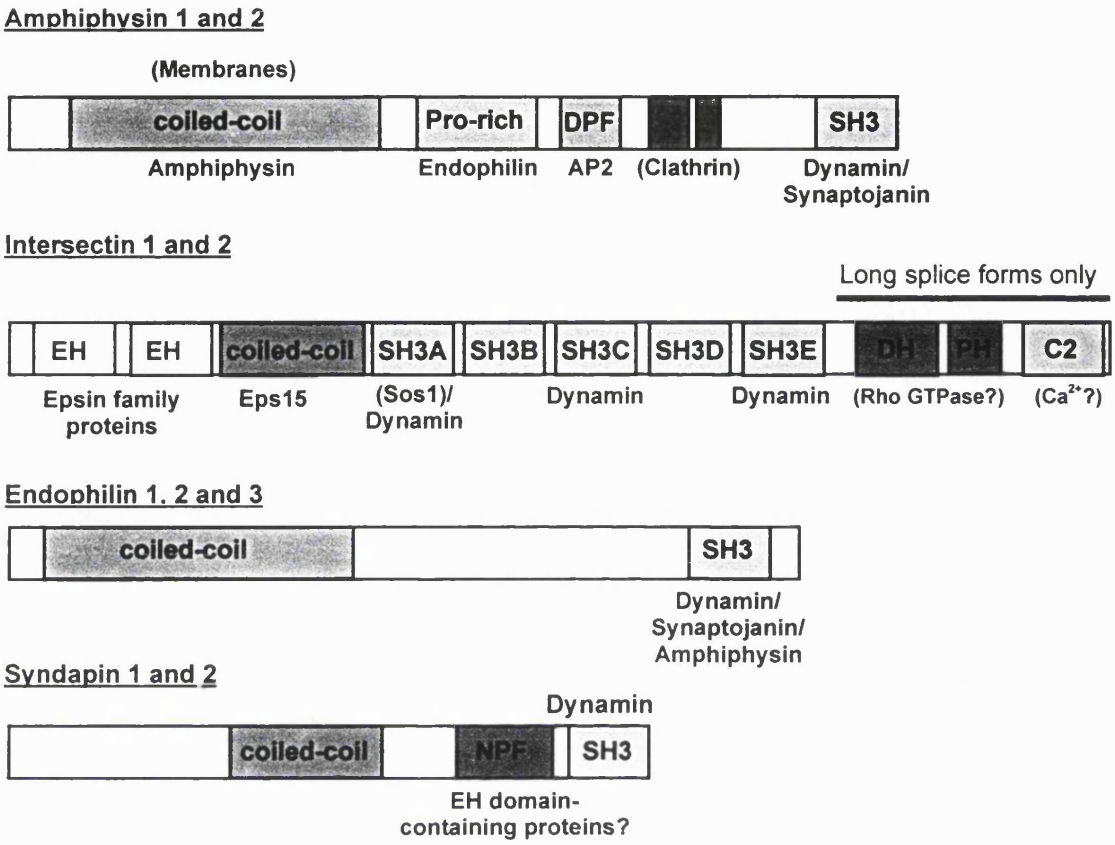

Figure 1.27 SH3 domain-containing proteins that bind to dynamin PRD

The domain structures (not to scale) and binding partners for nine of the known dynamin-binding proteins are shown. For splice form-specific interactions the name of the binding partner is shown in brackets. "?" indicates where homology with a known motif implies a function, but the protein in question has not been shown to have that function. Abbreviations: proline/arginine-rich domain (PRD); src-homology 3 (SH3); NPF and DPF are tripeptide motifs named according to the single letter amino acid code; Eps15-homology (EH).

Amphiphysins1 and 2 can form hetero- and homo-dimers through interactions of coiled-coil domains towards the N-terminus of both proteins [Wigge, Kohler, 1997] [Ramjaun, 1999]. Amphiphysin1 and two spice variants of amphiphysin2 that are expressed in brain (forms a and d) contain two neighbouring regions that bind to clathrin [Ramjaun, 1998] [Slepnev, 2000]. All amphiphysin isoforms contain an SH3 domain that binds to dynamin and synaptojanin PRDs and a region containing a DPF motif that binds to the AP2 α-ear [Wigge, Vallis, 1997] [Slepnev, 2000]. Amphiphysin2 splice forms a, c and d bind directly to membranes through an N-terminal motif that is lost in splice form-b [Ramjaun, 1999]. Amphiphysin1 can tubulate protein-free liposomes *in vitro* and can modify dynamin ring formation on these same liposomes, activities that also indicate direct membrane-association and required N-terminal regions of the protein [Takei, 1999]. These biochemical properties of amphiphysin make it an ideal candidate for the initial recruitment of dynamin to clathrin-coated pits, by association not only with dynamin but also with membranes, AP2 and clathrin.

In vivo evidence supports the idea that the PRD of dynamin, and in particular its interaction with amphiphysin, is important for dynamin recruitment to clathrin-coated pits. Analysis of plasma membranes prepared by sonication of transiently transfected adherent cells revealed that wild type dynamin was almost exclusively associated with clathrin-containing domains, whereas deletion of the PRD prevented recruitment of this mutant dynamin to clathrin-coated pits [Shpetner, 1996]. Injection of amphiphysin1 SH3 domain protein, or a peptide containing the region of dynamin1 PRD that binds to amphiphysin, into living Lamprey neurons blocked clathrin-mediated endocytosis at a step after clathrin coat recruitment but before invagination [Shupliakov, 1997]. Also transient transfection of the SH3 domain from amphiphysin1 or 2 into mammalian cells blocked endocytosis [Wigge, Vallis, 1997] [Owen, Wigge, 1998].

The SH3 domains of amphiphysins 1 and 2 are unique among known dynamin-binding SH3 domains in their ability to interfere with dynamin multimerization in solution [Owen, Wigge, 1998]. This property also appears to account for the potent inhibition of endocytosis by amphiphysin SH3 domains *in vivo* [Owen, Wigge, 1998]. Such results prompted the idea that amphiphysin may recruit dynamin to coated pits, but keep it in an un-assembled state until an unknown signal disrupts dynamin-amphiphysin interactions and allows dynamin to self-assemble into rings (discussed further in [Sever, 2000b]). In such a model amphiphysin acts as a timer to delay dynamin self-assembly while the clathrin lattice gains curvature, whilst at the same time enabling the dynamin that is required for the later stages of clathrin-coated pit constriction and fission to be recruited. This model appears at odds with the observation that amphiphysin facilitates the formation of rings and vesiculation of liposomes by dynamin [Takei, 1999]. However, as discussed above, the role of ring formation in dyanmin function itself is still a matter for debate and further analysis will be required to understand the exact role of amphiphysin in dynamin function.

Endophilin

The endophilin family was isolated by PCR using degenerate oligonucleotides based upon Grb2 SH3 domain [Giachino, 1997]. In the same year the endophilins were also found to be binding partners for synaptojanin, in yeast-two-hybrid and overlay assays, and were subsequently found also to bind to dynamin, with both interactions being mediated by their SH3 domains [de Heuvel, 1997] [Micheva, Kay, 1997] [Ringstad, 1997]. There are three endophilin family members (previously named SH3p or GL-SH3): endophilin1/SH3p4/GL-2 mRNA was only detected in brain; endophilin2 SH3p13/SH3-GL3 mRNA was detected both in brain and testis; endophilin3/SH3p8/GL-1 mRNA was more ubiquitous. The SH3 domain of endophilin1 has also been shown to mediate binding to a proline-rich region of amphiphysin [Micheva, Ramjaun, 1997].

As mentioned above, antibody-mediated disruption of endophilin1 function in a tonically stimulated synapse lead to inhibition of the invagination stage in the clathrin-coated pit cycle, see figure 1.19 [Ringstad, 1999], suggesting that an endophilin1 complex is active at this early stage in coated pit formation. One activity of endophilin1, mentioned above, that could influence to the change in curvature needed for clathrin-coated pit invagination is its LPA acyl transferase activity [Schmidt, 1999].

1.6.8.2 Signaling roles for dynamin and its PRD binding partners

Recently signalling roles, separate to its role in endocytosis, have been suggested for dynamin, in particular dynamin2. Endocytosis of some receptors, both receptor tyrosine kinases and seven-transmembrane receptors, has been shown to be required for full ERK activation, reviewed in [Di Fiore, 1999] and [Ceresa, 2000]. Dynamin has been implicated in the control of ERK activation, so may provide a link between ERK and endocytosis. K44A dynamin1 or dynamin2 were shown to inhibit ERK activation in response to EGF, LPA and phorbol ester, acting at the level of the MAPKKs MEK1 and MEK2 [Kranenburg, Verlaan, 1999a]. A study using G protein-coupled opiod receptors showed that ligands that did not induce endocytosis and receptor chimeras that were not internalised still induced ERK activation that was inhibited by K44A dynamin, suggesting that endocytosis and ERK activation are separate dynamin activities [Whistler, 1999]. A more recent study, however, has shown that another G protein-coupled receptor, the β2-adrenergic receptor, can activate ERK via transactivation of EGFRs [Maudsley, 2000]. It remains to be seen whether a similar transactivation mechanism accounts for the dynamin-dependent ERK activation seen by Whistler et al that was not dependent upon endocytosis of the opiod G protein-coupled receptors in this study. Proteins that may link dynamin to ERK activation are discussed below.

One other recent report suggested that dynamin may function as a signal-transducing GTPase. Using HeLa cells transfected with wild type dynamin2 under a tetracyclin-OFF promoter, it was shown that even a 5-fold increase in dynamin2 levels induced apoptosis [Fish, 2000]. Interestingly over-expression of dynamin1 did not induce apoptosis, which may be important to the ability of neurons to express very high levels of endogenous dynamin1. It appeared that endocytosis was dependent upon p53 and occurred only in actively proliferating cells [Fish, 2000].

<u>Dynamin-binding proteins involved in signal transduction</u>

A subset of the proteins shown to bind to dynamin are also involved in signal transduction (Grb2, PLCγ, Mlk2, p85PI3K and possibly intersectin1), so may provide interesting links between endocytosis and receptor signaling. A number of GST-SH3 domains used as bait in a screen for

SH3 domain-binding proteins were found to bind to dynamin and to increase its *in vitro* GTPase activity [Gout, 1993]. The strongest of these binding partners were the SH3 domains of phospholipase Cγ (PLCγ) and growth factor receptor-bound protein 2 (Grb2), both of which other groups later independently identified as dynamin-binding partners [Seedorf, 1994]. A weaker interaction was also seen with the SH3 domain of the p85α phosphatidylinositol-3 kinase (PI3K) regulatory subunit [Gout, 1993]. There does not appear to be any evidence that the p85 regulatory subunit of PI3K is linked to dynamin *in vivo* in mammalian cells. The only evidence for a physiological link between PLCγ, which converts PI-(3,4,5)-P_3 to DAG and IP_3, and dynamin appears to be an increase in their association in response to PDGF stimulation [Scaife, 1994].

Recently the endothelial nitric oxide synthase (eNOS) was reported to bind to dynamin2 *in vitro* and *in vivo* and to be stimulated by this interaction [Cao, S, 2000]. The regions of eNOS and dynamin that mediate this interaction were not determined.

Grb2

Grb2 contains two SH3 domains and the N-terminal domain (SH3-N) alone was sufficient for a strong interaction with dynamin [Gout, 1993] [Vidal, 1999]. Full-length Grb2, however, was more potent as an activator of dynamin GTPase activity, suggesting the involvment of additional regions of the proteins in this activity [Gout, 1993]. Grb2 SH3 domains also interact with and activate the Ras exchange factor Sos1 [Chardin, 1993] [Vidal, 1999]. Some evidence suggests that Grb2 may be an *in vivo* binding partner for dynamin. Stimulation of the interaction of Grb2 with dynamin has beeen detected in a number of cell types: (a) MDCK cells treated with EGF [Wang, 1996]; (b) insulin treatment of hepatocytes [Wada, 1998], smooth muscle cells [Karoor, 1998] or CHO-IR cells [Ando, 1994]; (c) monocytes treated with colony-stimulating factor [Kharbanda, 1995]. Although Grb2 SH3-N binds to dynamin *in vitro* and *in vivo* it did not inhibit EGFR endocytosis in transfected cells [Wang, 1996] or transferrin endocytosis in a perforated cell assay [Simpson, 1999]. Peptides from Grb2 SH2 domain or from the EGFR Grb2-binding site, however, did block EGFR internalisation [Wang, 1996]. This suggests that receptor signaling via Grb2, but not necessarily recruitment of proteins such as dynamin to the N-terminal SH3 domain of Grb2, is required for EGFR endocytosis.

Intersectins 1 and 2

Intersectin1 (also known as Ese1) was found to co-precipitate with dynamin [Hussain, 1999] and was separately identified as a dynamin binding partner in a yeast-two-hybrid screen. Intersectin2 (also known as Ese2) was more recently cloned by homology with intersectin1 and both genes have been found to produce a long and a short splice form. All forms of intersectin contain five

SH3 domains, a coiled-coil region and two EH domains (see figure 1.27). Only three of the five intersectin1 SH3 domains bind strongly enough to dynamin to deplete it from brain extracts (SH3A, C and E). SH3A was a potent inhibitor of endocytosis in a perforated cell assay and SH3A appeared to inhibit at the coated pit constriction stage, whereas SH3C or SH3E inhibited fission [Simpson, 1999]. Interestingly, SH3A (but not SH3s B-E) has been shown to mediate an interaction of intersectin with Sos1, and will compete with Grb2 for binding to Sos1 [Tong, Hussain, de Heuvel, 2000]. Over-expression of SH3A was seen to inhibit activation of Ras in a number of cell types [Tong, Hussain, Adams, 2000]. These data together suggest that the interaction of intersectin1 SH3A with Sos1, rather than with dynamin, may be important for coated pit constriction. Of the five SH3 domains SH3A in intersectin2 is the least similar to intersectin1 [Pucharcos, 2000]; it will be interesting to see whether intersectin2 also binds to Sos1 or whether this interaction is specific to intersectin1. Although Grb2 and intersectin are strong candidates to mediate dynamin activation of ERK they activate the ERK pathway at the level of Ras, which is not consistent with observations that K44A dynamin inhibited ERK activation at the level of MEK [Kranenburg, Verlaan, 1999a].

The EH domains of intersectin allow it to bind to NPF motifs in proteins such as syndapin (discussed below) and epsin and the central coiled-coil domain of intersectin facilitates binding to the coiled-coil domain of Eps15, creating a complex between these two EH domain-containing proteins [Sengar, 1999]. A similar complex occurs in yeast between the EH domain-containing proteins Pan1p and End3p and epsin family proteins [Tang, HY, 1997]. The long splice forms of intersectins 1 and 2 contain an additional C-terminal DH-PH Rho GEF motif, giving them the potential to activate Rho GTPases [Cerione, 1996], and a C2 potential Ca^{2+}-binding domain [Rizo, 1998] [Guipponi, 1998] [Pucharcos, 2000]. The long form of intersectin1 is only expressed by neurons, but the long form of intersectin2 is ubiquitous [Hussain, 1999] [Pucharcos, 2000]. In studies of the long forms of intersectins 1 and 2 analysis of the actin cytoskeleton or *in vitro* GEF assays have not yet been carried out, so it is not known which Rho GTPases are activated by intersectin's DH-PH motif. If intersectin long does have a functional GEF domain then the many actin-dependent and actin-independent processes activated by Rho GTPases (summmarised in section 1.3.2 above) could be stimulated by intersectin, possibly in response to dynamin binding.

Mlk2

Mlk2 (mixed lineage kinase) is a Rac-binding Ser/Thr protein kinase, which is a MAPKKK in the JNK MAP kinase cascade [Hirai, 1997]. Mlk2 has been reported to bind to dynamin via its SH3 domain and to increase dynamin GTPase activity *in vitro* in an SH3 domain-dependent manner [Rasmussen, 1998]. We have found that injection of full-length Mlk2 DNA into the nuclei of

Hep2 cells inhibited transferrin endocytosis (A Bishop and A Hall unpublished data). Whether this activity is dependent upon the SH3 or kinase domains of Mlk2 has not been determined.

1.6.8.3 Links between dynamin, its PRD binding partners and actin

In yeast endocytosis appears to be functionally coupled to organisation and assembly of the actin cytoskeleton [Kubler, 1993] [Moreau, 1997] [Tang, HY, 1997] [Wesp, 1997]. Attempts to discern whether there are links between actin and endocytosis in mammalian cells have produced variable results depending on the cell type and methods used. For example, both cytochalasin D and latrunculin A (latA) caused actin disassembly in perforated A431 cells, but only latA inhibited endocytosis and the actin monomer-sequestering protein thymosin β4 inhibited endocytosis at high concentrations, but enhanced it at lower concentrations (up to 0.5μM) [Lamaze, 1997]. One report showed dynamin in brain extracts to co-purify with profilin, the actin monomer-binding protein, but which region of dynamin mediates this interaction and whether it is direct is unknown [Witke, 1998]. Links between actin, Rho GTPases and endocytosis are discussed further in chapter 7 and are reviewed by [Ellis, 2000b] and [Qualmann, Kessels, 2000].

Dynamin-binding proteins with links to actin reorganization

At least five SH3 domain-containing proteins have the potential to link dynamin to actin reorganization. Intersectin 1 and 2 long forms, as discussed above, have the potential to be Rho GTPase GEFs, so may induce actin changes by activating a small GTPase. Neuronal syndapin1 and the more ubiquitous syndapin2 (which has four splice forms) both bind to N-WASP, as well dynamin and synaptojanin [Qualmann, 1999] [Qualmann and Kelly, 2000], as do the closely related proteins PACSINs 1-3 [Modregger, 2000]. The interactions of syndapins 1 and 2 and PACSINs 1-3 with dynamin are SH3 domain-dependent [Qualmann, 1999] [Qualmann and Kelly, 2000], as may be their interactions with N-WASP, which also contains multiple proline-rich sequences [Miki, 1996]. As discussed above, N-WASP can recruit the Arp2/3 complex, profilin and actin to create an actin nucleation complex, reviewed in [Mullins, 2000]. N WASP is known to be activated by Cdc42 and lipids synergistically [Prehoda, 2000], whether binding to syndapin can contribute to N-WASP activation in addition to or instead of one of these activators is unknown. The syndapins 1 and 2 or PACSINs 1-3 inhibit transferrin endocytosis in transfected HeLa cells in an SH3 domain-dependent manner [Qualmann and Kelly, 2000] [Modregger, 2000]. By using the SH3 domain of syndapin1 in a perforated cell assay, the block in endocytosis was shown to be at a stage after constriction [Simpson, 1999]. Syndapin1 was also seen to co-localise with dynamin1 at synaptic sites in cultured neurons [Qualmann, 1999]. Along with the ability of these proteins to bind to dynamin such data suggests roles for syndapin2 and syndapin1 with dynamin in receptor-mediated endocytosis and synaptic transmission respectively. Full-

length syndapins 1 and 2 were also reported to induce microspikes in HeLa cells, which were inhibited by the Arp2/3 binding domain of N-WASP, suggesting an *in vivo* link between syndapins and N-WASP [Qualmann and Kelly, 2000]. Interestingly, syndapins 1 and 2 and PACSINs 1 and 2 (but not PACSIN 3) also contain a region rich in NPF motifs, which could potentially allow binding to EH domain-containing proteins such as Eps15 and intersectin [Qualmann and Kelly, 2000].

Cortactin contains an SH3 domain, that has recently been reported to bind to dynamin [McNiven, 2000], a proline-rich region and a series of tandem repeats that form multiple F-actin-binding domains [Wu, 1993]. Endogenous cortactin and dynamin2 were seen to co-localise at cortical actin structures in the presence of PDGF [McNiven, 2000]. Using over-expressed GFP-tagged proteins this co-localisation was shown to be dependent upon the SH3 domain of cortactin and the PRD of dynamin2 [McNiven, 2000]. These co-localisations should be treated with caution, however, as many proteins that are membrane-associated can be seen to build-up in membrane ruffles induced by Rac downstream of PDGF. If deletion of dynamin's PRD reduces its membrane-association due to loss of binding to other SH3 domain-containing proteins, such as amphiphysin, then one would still see a loss of dynamin recruitment to the actin-rich membrane protrusions containing cortactin, but this would not be a due to a loss of the cortactin-dynamin interaction.

1.6.9 The PRD of synaptojanin

The inositol-5' phosphatase p145 synaptojanin1, like dynamin, contains a PRD and binds to some of the same PRD-binding partners as dynamin: Grb2, intersectin1, syndapins 1 and 2, endophilin1 and amphiphysin1 [McPherson, Czernik, 1994] [McPherson, 1996] [de Heuvel, 1997] [Micheva, Kay, 1997] [Yamabhai, 1998] [Qualmann, 1999] [Qualmann and Kelly, 2000]. It is possible that synaptojanin regulates dynamin function by competing for these binding partners. There are two synaptojanin genes that produce three gene products [Ramjaun, 1996] [Nemoto, 1997]: neuronal p145 synaptojanin1 and the more widely expressed p170 synaptojanin1 splice form and p140 synaptojanin2. The synaptojanin PRD sequences are very variable between p145 synaptojanin1 and synaptojanin2. Synaptojanin2, unlike synaptjanin1, is almost entirely membrane-bound and has been shown to bind to Grb2, but not to amphiphysin or endophilins 1-3, suggesting that there are functional differences between synaptojanins 1 and 2 that are reflected in their interactions with SH3 domains-containing proteins [Nemoto, 1997]. The C-terminal extension of p170 synaptojanin1 binds to Eps15 and clathrin (via NPF motifs) and to the AP2 α-ear (via DPF motifs), see figure 1.20, suggesting that it performs different roles in endocytosis to the shorter splice forms that can not support these interactions [Haffner, 1997] [Haffner, 2000].

CHAPTER 2
MATERIALS AND METHODS

2.1 MOLECULAR BIOLOGY

2.1.1 Agarose gels

DNA fragments were routinely visualised on TAE agarose gels (10 x TAE: 0.4M Tris acetate, 10mM EDTA) stained with 0.8μg/ml ethidium bromide, which was added when the melted gel was cool enough to pour. For DNA fragments between 500 and 5000 base pairs 1% agarose gels were used. Fragments of less than 500 base pairs were separated on 1.5-2% agarose gels. For analytical purposes normal agarose was used (Gibco BRL). Preparative gels were made using low melting point agarose (sea plaque, FMC BioProducts #50102). 0.5-2μg of High DNA Mass-Ladder (Gibco BRL) molecular weight markers were used. DNA samples were loaded in 0.167x volume of 6x loading buffer (30% glycerol (v/v), 6mM EDTA, 0.25% bromophenol blue (w/v), 0.25% xylene cyanol FF (w/v)) and electrophoresis was carried out at 100mA for about 1h.

2.1.2 Polymerase Chain Reaction

PCR reactions were carried out in a reaction volume of 50μl with 50ng of DNA template, 10pmol of each primer, 0.2mM dNTPs and with 5u Pfu polymerase (Stratagene) in the buffer systems supplied with the enzymes. Primers were synthesised by Genosys Biotechnologies or by MWG-Biotech. Cycling conditions were typically repeated 30 times, starting with denaturing at 94°C for 1 min, reannealing at the optimal temperature for the individual primer pair (usually 55-60°C) for 30s, and elongation at 72°C for 1-3min. 5μl of PCR product was loaded on an analytical gel to confirm size and purity. PCR was used to prepare fragments of POSH for ligation into various vectors. All constructs made by PCR were sequenced in order to check for mistakes made by the DNA polymerase.

2.1.3 Restriction digests and DNA fragment purification

Where PCR reactions were to be digested, prior to purification and ligation, the PfU was first removed with 1x volume phenol:chloroform:isoamyl alcohol (24:24:1) to extract protein, followed by 1x volume chloroform:isoamyl alcohol (24:1) to extract the phenol. DNA was precipitated with 0.1x volume 3M sodium acetate plus 2x volume cold ethanol. The product was washed in ice cold 80% ethanol solution, resuspended in ddH_2O and then digested. Plasmid DNA (2-5μg) and PCR products were normally digested in a volume of 30μl with 0.5μl of each restriction enzyme (New England Biolabs), using the manufacturer's buffers, for 1h at 25-37°C. Resulting digest products were run on low melting point agarose gels. Bands of interest were

excised and melted at 65°C in 400µl TE pH7.5 (10mM Tris-HCl pH7.5, 0.4mM EDTA). Agarose was extracted with 1x volume phenol equilibrated to pH8 with 0.1M Tris-HCl (Sigma). Phenol and chloroform cleaning steps, alcohol precipitation, washing and resuspension in ddH_2O were carried out as described above for removal of PfU.

Partial restriction digest

The yeast-two-hybrid bait vector pYTH9 can not autonomously replicate. In order to integrate the vector into the yeast genome it must be linearised by XbaI digestion (see yeast-two-hybrid protocols in section 2.4). In most cases the bait insert did not contain a XbaI site, however, there was one XbaI site (at base pair 45 of POSH cDNA) in the pYTH9-N POSH construct. A partial digest was carried out: XbaI was diluted 1/5 in water and 1µl of this enzyme solution was used to digest 10µg of DNA in a volume of 20µl at 37°C for 20min. The enzyme was heat-inactivated and half of the digested DNA solution was transformed into yeast.

2.1.4 Ligation of DNA fragments

Typically, ligations were carried out using a molar ratio of vector (gel-purified linear DNA) to insert of between 1:5 and 1:10. The total reaction volume was 10µl and included 4u of T4 ligase (Promega) in the buffer system supplied with the enzyme. Ligations were performed overnight at 16°C and the whole ligation was transformed into competent E. coli as described below.

2.1.5 Preparation of competent E. coli ($RbCl_2$ method)

Competent E. coli (DH5α or BL21 strains) were prepared according to a standard protocol (Maniatis) as follows. 1ml of an overnight culture of DH5 α in SOB-Mg^{2+} (SOB- Mg^{2+} is composed of L broth (5g/l bacto Yeast Extract, 10g/l bacto Tryptone, 5g/l NaCl) plus 2.5mM KCl, 10mM $MgCl_2$, 10mM $MgSO_4$) was diluted to 50ml and grown until OD_{550} 0.4-0.5. Cells were spun down in a sterile tube and resuspended in 16.6ml of RF1 pH5.8 (15% Glycerol (w/v), 100mM KCl, 50mM $MnCl_2.4H_2O$, 30mM potassium acetate, 10mM $CaCl_2.2H_2O$, pH corrected with acetic acid and filter sterilised) and placed on ice for 20min. 4ml of RF2 pH6.8 (15% Glycerol (w/v), 10mM PIPES pH6.8, 10mM KCl, 75mM $CaCl_2.2H_2O$, pH corrected with NaOH and filter sterilised) was added and cells incubated on ice for 15min. 0.5ml aliquots were snap-frozen in liquid nitrogen and stored at –80°C.

2.1.6 Transformation of E. coli

Aliquots of competent cells were thawed on ice, mixed thoroughly with 1-10µl of DNA and left to incubate on ice for 30min. Cells were then heat shocked for 90s at 42°C and chilled on ice for 2min. 0.2ml of SOC (SOB plus 20mM glucose) was added and cells were shaken at 37°C for 1h. Half of the solution, or the full solution resuspended in up to 0.1ml, was then plated onto L broth

(LB)-agar plates (LB medium plus 20g/l bacto agar) containing 100μg/ml Ampicillin for selection of transformed cells. Plates were incubated over night at 37°C and "minipreps" made from individual colonies for analysis of incorporated DNA.

2.1.7 DNA purification

"Minipreps"

A single colony of *E. coli* was grown over night in 3ml of LB-100μg/ml ampicillin in a round bottom 15ml tube (Falcon) at 37oC with vigorous agitation. DNA was prepared from 1.5ml of culture using the StrataPrep Plasmid Miniprep Kit (Stratagene #400761) according to the manufacturer's instructions. Restriction digests, were carried out to verify the identity of the DNA. 1/10 of the miniprep DNA was digested and half of this loaded on an agarose gel. DNA prepared with these kits was clean enough for sequencing.

Caesium chloride gradient plasmid purification

This method was used to create highly pure DNA required for microinjection. A 250ml over night culture of bacteria in LB-100μg/ml ampicillin was centrifuged at 4000rpm and the pellet resuspended in ice cold resuspension buffer (25mM Tris-HCl pH8.0, 10mM EDTA, 50mM glucose). On ice 20ml of fresh lysis solution (1% SDS, 0.2M NaOH) was added, the tube was inverted six times then left on ice for 10min. The solution was neutralised with 15ml potassium acetate pH5.2 (5M potassium acetate, 11.5ml acetic acid per 15ml). The solution was inverted six times and left on ice for 10min, then centrifuged at 4200rpm for 15min. The supernatant was filtered through muslin and DNA precipitated with 1x volume of cold propan-2-ol and spun centrifuged at 4200rpm for 15min. The pellet was resuspended in 3.9ml 10x TE pH8.0 and 1.05g of CsCl was added per ml of DNA solution together with 100ml of 10mg/ml ethidium bromide.

2.1.8 DNA Sequencing

Automated sequencing

Sequencing was performed on an ABI Prism instrument at Eisai Laboratories (University College, London) and using the ABI prism Dye Terminator Cycle Sequencing Ready Reaction Kit (Perkin-Elmer) according to the manufacturer's instructions.

Manual sequencing

Manual sequencing was used where problems had occurred with automated sequencing. 3-5μg of double stranded DNA per reaction was denatured in 0.2M NaOH and 0.2M EDTA in a total volume of 20μl. 2μl 2M ammonium acetate pH4.6 and 60μl cold ethanol were added and the

solution left on dry ice for 5min. The DNA was pelleted and resuspended in 6µl ddH_2O. Within 4h of denaturation sequencing was carried out using the dideoxy chain termination method with a sequencing V2.0 kit (United States Biochemical Corporation). DNA was labelled with [^{35}S]-ATP (Amersham) and reactions performed as described in the kit instructions. Samples were loaded on a 6% polyacrylamide wedge gel containing 7M Urea in TBE and electrophoresis carried out at 80W. The gel was transferred to Watman number 1 paper and dried under vacuum at 80°C for 1h. Sequences were visualised after over night exposure at –80°C on Kodak Biomax-MR film (Sigma).

2.1.9 DNA Constructs Used

Rho GTPase constructs

Rho GTPase constructs for expression in mammalian cells (L61 Rac, L61 C40Rac, L61A37Rac, N17Rac, V12Rac, L61Cdc42, L63RhoA) were all cloned into the vector pRK5myc (provided by Steve Moss) by members of the Hall laboratory. The only exception was V20RhoL, which was provided by D Montell (The Johns Hopkins University School of Medicine, Baltimore, USA).

POSH constructs

POSH constructs for expression in mammalian cells were cloned into the vectors pRK5myc and/ or pRK5flag (adapted from pRK5myc, as described in [Tapon, Nagata, 1998]). Nicolas Tapon cloned full length POSH and C-terminal POSH constructs (Y2H POSH encoding amino acids (aa) 392-892 and C POSH aa352-892) by PCR into the Bam HI/ Hind III sites of pRK5myc, as described in [Tapon, Nagata, 1998]. Full length POSH and Y2H POSH were also sub-cloned into pRK5flag (Bam HI/ Hind III). The Rac-binding domain (RBD aa292-362) was sub-cloned (5' Bam HI/ 3' Eco RI) from pGEX4T3-POSH truncation 3 (described in [Tapon, Nagata, 1998]) into pRK5myc and pRK5flag.

N-terminal fragments of POSH (N POSH encoding aa2-290, RING-SH3 1 aa2-201, SH3 1-2 aa130-290, SH3 1 aa130-201 and SH3 2 aa192-290) were cloned into the Bam HI/ Eco RI sites of pRK5myc using PCR. pRK5myc-POSH template DNA was used [Tapon, Nagata, 1998] and the PCR primers, shown in figure 2.1, incorporated Bam HI and Eco RI cloning sites at the 5' and 3' ends respectively. N POSH was then sub-cloned into both pRK5flag and pGEX4T3 (Pharmacia) using the same Bam HI/ Eco RI restriction sites.

N POSH

5'–GCCGGATCC GATGAGTCTGCCTTGTTGGAC
Bam HI codon 2
3'-AAAGAATTC CTATGAGGCAGAGGTGCTCTGCGC
Eco RI stop

RING-SH3 1

5'- as for N POSH
3'-AAAGAATTC CTAGCACTGAGGCGGGGG
Eco RI stop

SH3 1-2

5'-GCAGGATCC GTGAGGGGAATACCTCAG
Bam HI codon 130
3'- as for N POSH

SH3 1

5'- as for SH3 1-2
3'- as for RING-SH3 1

SH3 2

5'-GAAGGATCC AAACCTTTACCTCAGCCCC
Bam HI codon 192
3'- as for N POSH

Figure 2.1 PCR primers used to clone POSH fragments into pRK5myc

All primers shown here and in figure 2.2 were purchased through Genosys.

Cs POSH

5'-GCCGAATTCAGGAATGGGACCCAGGCCTGTG
Eco RI codon 432
3'-GCAGCGGCCGC TCAGATGTTTTCCACAAAGCTCCC
Not I stop

N POSH

5'-GCGGAATTCAGATGAGTCTGCCTTGTTG
Eco RI codon 2
3'-AAAGCGGCCGC TCATGAGGCAGAGGTGCTCTGCGC
Not I stop

SH3 3

5'-GCAGAATTCGCCTCAGACTCGTCCCAG
Eco RI codon 450
3'-AAAGCGGCCGC TCAGGCATTCGTCACCGCCCTTG
Not I stop

SH3 4

5'-GCAGAATTCCCGGCCTGTTGTTTGTGAAAGG
Eco RI codon 831
3'-As for Cs POSH

Inter SH3 3-4

5'-GCCGAATTCAACAAGGGCGGTGACGAATG
Eco RI codon 512
3'-GCAGCGGCCGC TCACCTTTCACAAACAACAGGCCG
Not I stop

Figure 2.2 PCR primers used to clone POSH fragments into pYTH9

A C-terminal POSH construct that was slightly shorter than C POSH (Cs POSH encoding aa432-892) was also cloned by Nicolas Tapon into pYTH9. pYTH9 is a yeast-two-hybrid system bait vector containing the Gal4 DNA-binding domain (DBD) and with an HA tag inserted between the DBD and the mutiple cloning site, kindly provided by R Brown (Glaxo Wellcome, Stevenage, UK). Shorter C-terminal fragments of POSH (SH3 3 encoding aa450-518, SH3 4 aa831-892, inter-SH3 3-4 aa512-837) and N POSH were also cloned by PCR into pYTH9. The template DNA used in all cases was pRK5myc-POSH and the PCR primers, shown in figure 2.2, incorporated Eco RI and Not I sites at the 5' and 3' ends respectively.

Dynamin constructs and other endocytosis-related constructs

Dynamin constructs, in pCMV vectors, for expression in mammalian cells were kindly donated by H McMahon (MRC LMB, Cambridge, UK): wild type dynamin1 and dynamin2; two mutants of dynamin1, S45N (described in [Herskovits, Burgess, 1993]) and R838E (described in [Vallis, 1999]). Also provided by H McMahon was pGEX4T1-amphiphysin2 SH3 domain, described in [Owen, Wigge, 1998]. pGEX2T-rat dynamin1 proline/arginine-rich domain constructs, described in [Slepnev, 1998], were provided by P De Camilli (Howard Hughes Medical Institute, Yale University School of Medicine, New Haven, USA): full-length PRD, encoding aa750-864; PRDΔC16, aa750-848; PRDΔC32, aa750-832; PRDΔC49, aa750-848.

Other DNA constructs

pMT123-HA-Ubiquitin, which is described in [Treier, 1994], was provided by D Bohmann (EMBL, Heidelberg, Germany). pCMV5-flag-JNK1 and pGEX-c-Jun were from Dr M Karin (UC San Diego) and Dr J Ham (Eisai London Research Laboratories) respectively. pBTM116-Cbl RING (amino acids 374-430), pACT2-UbcH5 and pACT2-UbcH7 are described in [Yokouchi, 1999] and were provided by M Yokouchi (Yale University School of Medicine, New Haven, USA) and A Yoshimura (Kurume University, Kurume, Japan).

2.2 CELL BIOLOGY

2.2.1 Cell lines used

COS7 is a monkey fibroblast cell line that was used for transfections. HeLa is a human cervical adenocarcinoma epithelial cell line and Hep2 cells, used for endocytosis assays, are derived from the HeLa cell line. NIH3T3 and Swiss3T3 are mouse fibroblast cell lines. Primary human keratinocytes were prepared by Vania Braga from human foreskins. MDCK (Madin-Darby Canine Kidney) is a canine kidney epithelial cell line.

2.2.2 General cell culture conditions

Cells were maintained at 37°C with 10% CO_2 in Dulbecco's Modified Eagle's medium (DMEM, Gibco) supplemented with 10% foetal calf serum (FCS, Sigma) and 1% antibiotics (Penicillin 100U/ml and Streptomycin 100μg/ml, Gibco). For passaging, cells were washed in PBS pH7.0 (1x PBS: 8g/l NaCl, 0.24g/l KH_2PO_4, 1.8g/l $Na_2HPO_4.2H_2O$, 0.2g/l KCl) then incubated in 1ml trypsin/ EDTA (Gibco) per 80cm^2 flask (Nunc) at 37°C for 1-3min. Trypsin was inactivated by addition of fresh complete medium. Cells were stored frozen in liquid nitrogen in cryotubes (Nunc) in aliquots of 5x10^6 cells in 1ml of FCS/10% DMSO. Cells were thawed quickly in a 37°C waterbath and transferred into 20ml of growth medium and placed in an 80cm^2 flask. The medium was replaced after 4-16h, once all viable cells had attached to the plastic surface of the tissue culture flask. In the case of NIH3T3 cells donor calf serum (DCS, Stratech) was used instead of FCS for both cell freezing and growth.

2.2.3 Preparation of quiescent serum-starved sub-confluent Swiss3T3 cells

2x10^5 Swiss3T3 cells were seeded on to each 6cm plate in 4ml of DMEM, 6% FCS, 1% antibiotics, were grown until quiescent (8-9 days) and were then plated on to coverslips. The coverslips used were acid washed: 5min swirl in nitric acid, 30min in running tap water, 5min swirl in ddH_20, 5min swirl in MeOH and bake to dry. These coverslips were then coated for at least 1h, at 4°C, with 20μg/ml fibronectin (Sigma) in PBS. 16h prior to injection the quiescent Swiss3T3 cells were split onto the fibronectin-coated coverslips as follows. Growth medium was decanted from the cells. The cells were washed in trypsin/EDTA then trypsinised in 0.5ml of trypsin/EDTA. The trypsin was neutralised with an equal volume of 10mg/ml soyabean trypsin inhibitor (Sigma) in serum-free (SF) medium (13.4g/l DMEM powder, 2g/l $NaHCO_3$, 1mM sodium pyruvate and 1% antibiotics). Cells were centrifuged (1,000rpm 3min) and re-suspended in 16ml SF medium. Fibronectin-coated coverslips were washed 3x in SF media and on to each coverslip was placed 1ml of cell suspension plus 50μl of conditioned medium. 16h later microinjection was carried out as described below for NIH3T3 cells, but with the cells maintained in serum-free medium throughout.

2.2.4 Immunofluorescence microscopy

After microinjection or transfection cells on coverslips were rinsed 4x in PBS pH7.0, then fixed for 10min at room temperature in 4% paraformaldehyde in PBS. Cells were rinsed extensively in PBS between each of the following steps. After fixation cells were permeabilised for 5min in 0.2% Triton X-100 in PBS. Free aldehyde groups were reduced for 10min using 15mM Glycine in PBS. Primary antibodies were applied for 1-2h at room temperature in PBS at the concentrations stated below. After washing in PBS coverslips were incubated with secondary antibodies (Jackson) for 30min at room temperature. Secondary antibodies were used at the

following final concentrations in PBS: goat anti-mouse-FITC 2μg/ml; donkey anti-rat-Cy3 3.75μg/ml; donkey anti-rat-FITC 3.75μg/ml; donkey anti-mouse-Cy5 3.75μg/ml. In some cases Alexa-streptavidin at 2μg/ml (Molecular Probes), used to detect a biotin-dextran injection marker, Hoechst 3342 (Molecular Probes) at 10μg/ml or Rhodamine-phalloidin (Sigma) at 0.1μg/ml were also included in the secondary antibody incubation. Coverslips were rinsed in ddH_2O and mounted on mowiol mountant (Calbiochem) which had been quenched with p-phenyl-diamine.

After 1h at 37°C slides were examined on a Zeiss axiophot microscope using Zeiss x63 1.4, x40 1.3 or x25 0.8 oil-immersion objectives. Pictures were taken using a Hammamatsu C5985 CCD camera and processed with OpenLab software. Alternatively, where stated, confocal images were taken using a Nikon optiphot-2 microscope and a Nikon 40x 1.0 oil-immersion objective with a Biorad MRC 1024 laser and Biorad LaserSharp confocal software system.

2.2.5 Primary antibodies used for immunofluorescence

Primary antibodies for the detection of epitope tags were used at the following final concentrations: mouse anti-myc hybridoma supernatant (9E10, prepared in house) 1/200 dilution; rat anti-myc affinity pure (JAC6, a kind gift from R Marais, ICR Chester Beatty Laboratories, London) 16μg/ml; mouse anti-flag (M2, Sigma) 5μg/ml; rat anti-HA (3F10, Boehringer) 1.3μg/ml. Primary antibodies for the detection of endogenous proteins were used at the following final concentrations: mouse anti-beta-catenin (Transduction Labs) 2.5μg/ml; mouse anti-dynamin (hudy-1, Upstate biotech.) 5μg/ml; rabbit anti-dynamin1 (kind gift from H McMahon) 7.5μg/ml; mouse anti-human Transferrin Receptor (B3/25, a kind gift from C Hopkins and I Trowbridge) 9.5μg/ml; rabbit anti-GST-N POSH antisera (UCL70, commissioned by the Hall Lab and raised by Cocalico Biological Inc, Reamstown, PA, USA) 1/500.

2.2.6 Digitonin pre-fixation permeabilisation

A digitonin permeabilisation step was used to release cytoplasmic proteins from Hep2 cells, whilst retaining membrane- and cytoskeletally-associated proteins. Cells were placed on ice, washed twice in cold premeabilisation buffer pH7.2 (25mM Hepes, 38mM K Aspartate, 38mM K Glutamate, 38mM K Gluconate, 1.5mM EGTA, 2.5mM $MgCl_2$, pH corrected with KOH). 40μg/ml digitonin (diluted from a 100mg/ml stock in DMSO) in permeabilisation buffer was added for 10min on ice. Cells were washed 2x 5min in premeabilisation buffer/1% BSA and 2x quickly in premeabilisation buffer then fixed in 4% paraformaldehyde in premeabilisation buffer. Post-permeabilisation staining steps were carried out as described above.

2.2.7 Microinjection of NIH3T3 cells for apoptosis assays

For microinjection NIH3T3 cells were plated on acid-washed 13mm diameter coverslips at a density of 8x104 cells/coverslip. 24h after plating cells were injected using an Eppendorf micromanipulator 5171 and transjector 5240 system on a Zeiss Axiovert 135M microscope in an atmosphere maintained at 10% CO2 and 37oC. DNA constructs were diluted in PBS at 0.05mg/ml, unless otherwise stated, and were injected into the nucleus of 100 cells/coverslip. Where a fluorescent injection marker was required biotin-dextran (10,000MW and lysine-fixable, Molecular Probes) was routinely used at a final concentration of 5mg/ml and was detected using Alexa-streptavidin. Coverslips were placed into a 6cm dish containing 8ml of normal growth medium during injection and were returned to their wells after injection. For apoptosis assays two coverslips were injected with each construct to be tested. One coverslip was allowed to express for 2h and the other for 7h. At these time points cells were fixed and stained for expression of the constructs and for nuclear morphology using Hoechst. Expressing non-pyknotic cells were counted and survival calculated as:

% survival = number of expressing non-pyknotic cells (7h/ 2h) x 100

2.2.8 Microinjection of Hep2 cells and Endocytosis Assays

2.2.8.1 Transferrin Endocytosis Assay

Hep2 cells were plated on to acid-washed 13mm diameter coverslips 48h prior to injection at a density of $2.5x10^4$cells/coverslip. DNA constructs were diluted to 0.1mg/ml in PBS and were injected into the nuclei of 100 cells/coverslip. Where two constructs were injected both were at 0.1mg/ml and DNA concentrations were equalised in single construct injections in the same experiment with empty vector. After 3-4h expression cells were washed 2x in serum-free medium/0.2% fatty acid-free bovine serum albumin (SF/BSA medium). Cells were then incubated for 30min at 37°C with 20μg/ml human Transferrin-Texas Red (TR-Tfn, Molecular Probes) in SF/BSA medium. Cells were washed 2x in serum-free SF/BSA medium and 2x in PBS before fixation. Cells were stained for expression of the constructs as described above. Confocal sections were taken at the level where TR-Tfn staining was maximal in uninjected cells. From these sections the percentage of expressing cells undergoing normal endocytosis, defined as >80% Tfn internalisation when compared with uninjected neighbours, was counted (a similar quantification method was used in papers such as [Owen, Wigge, 1998]).

Staining to visualise surface transferrin receptors

In order to look at surface transferrin receptor (TfnR) levels Hep2 cells were injected as above. After 3-4h expression they were washed and treated with 20μg/ml un-labelled human Tfn (Boehringer Mannheim) in SF/BSA medium for 30min. Post-fixation and quenching, but pre-

permeabilisation, cells were stained with a mouse anti-TfnR antibody, which recognises the extracellular domain of the human TfnR (B3/25). Cells were then permeabilised with Triton x-100 as described above and co-stained for expression of injected constructs with the rat anti-myc antibody.

2.2.8.2 EGF Endocytosis Assay

Hep2 cells were injected with DNA constructs as stated above. After 3-4h of expression cells were washed twice in SF/BSA medium then transferred into ice cold 1μg/ml EGF-Rhodamine (Molecular Probes) solution in Hepes buffered serum-free medium (no $NaHCO_3$, instead buffered with 10mM Hepes pH7.6) plus 0.2% fatty acid-free BSA. Binding was carried out at 4°C in the dark for 30min, followed by transfer of coverslips back to 37°C for 10min, in pre-warmed SF/BSA medium, to allow ligand internalisation. Cells were washed 2x in SF/BSA medium and 2x in PBS before fixation and then stained for expression of the constructs. Quantification of results was carried out from confocal sections as described above for Tfn endocytosis assays.

2.2.9 Maintenance and Transfection of COS7 cells

COS7 cells were plated on to six well plates at a density of $2.5x10^5$ cells/well, or on to 10cm dishes at a density of $1x10^6$ cells/plate, 16h prior to transfection. Transfection was carried out in 1ml of serum-free, antibiotic-free medium for each $2.5x10^5$ cells to be transfected, using lipofectamine reagent (Gibco) according to the manufacturer's instructions. For every $2.5x10^5$ cells the following DNA/lipofectamine mixtures were used per 1ml of serum-free transfection medium: for transfection with only one construct, 4μl of lipofectamine reagent (2mg/ml stock) and 0.5μg of DNA; for double transfections 8μl of lipofectamine and 1μg of DNA in total (0.5μg of each DNA construct); for triple transfections 10μl of lipofectamine reagent and 1.2μg of DNA in total (0.4μg of each DNA construct). Within a single experiment the same lipofectamine/DNA concentrations were maintained for single, double or triple construct transfections, using empty vector to make up the DNA concentrations. Transfection was carried out for 4-6h and was terminated by the addition of 1ml of DMEM 20% FCS plus 2x antibiotics per 1ml of transfection solution. Transfections were harvested 24h post-transfection procedure unless stated otherwise.

<u>Addition of a caspase inhibitor during transfections</u>

In cases where the general caspase inhibitor BOC-Dfmk (BOC-Asp(OMe)-CH_2F, Enzyme Systems Products) was to be included the reagent was added with the 20%FCS medium at the end of the transfection to give a final concentration of 20μM BOC-Dfmk (from a 20mM stock in DMSO). DMSO was also added, final concentration of 0.1%, to any BOC-Dfmk minus control transfections. 24h post-transfection cells were either harvested or the medium was replaced, with or without BOC-Dfmk as appropriate.

2.2.10 Treatment of cells with proteasome inhibitors

In some experiments injected NIH3T3 or Hep2 cells were treated with proteasome inhibitors for 2-7h. Synthetic lactacystin (an irreversible 20S proteasome inhibitor) and MG132 (carbobenzoxy-L-leucyl-L-leucyl-L-leucinal, a reversible inhibitor of the 26S proteasome) cell-permeable proteasome inhibitors were used (Calbiochem). After injection cells were placed back into their wells containing growth medium plus the inhibitors, taken from 10mM stocks in DMSO, to give final inhibitor concentrations of 0-20μM and a final DMSO concentration of 0.2%.

In other experiments transfected COS7 cells were treated for 0-6h with the same proteasome inhibitors, at 0-20μM with 0.2% DMSO, which was added to their normal growth medium 24-30h post-transfection.

2.3 PROTEIN BIOCHEMISTRY

2.3.1 SDS-Polyacrylamide Gel Electrophoresis (SDS-PAGE)

Protein samples were boiled for 5min in sample buffer (1x solution: 50mM Tris-HCl (pH6.8), 2% sodium dodecyl sulphate (SDS) (w/v), 10% Glycerol (v/v), 100mM dithiothreitol (DTT) 0.1% bromophenol blue (w/v)) and loaded onto a polyacrylamide gel: 4% stacking gel with 0.1% SDS in 0.125M Tris-HCl (pH6.8); 10-14% separating gel with 0.1% SDS in 0.375M Tris-HCl (pH8.8). Running buffer was 0.2M Glycine, 0.1% SDS, 25mM Tris base. Rainbow Markers (Amersham) protein molecular weight markers (range 30-220kDa) were used. Electrophoresis was performed at 100-150V. Proteins were visualised using 1% Coomassie blue in 10% acetic acid/ 12% methanol and destained in 6.5% acetic acid/ 20% ethanol. Alternatively proteins were transferred from the gel on to nitrocellulose (see Western Blotting).

2.3.2 Western Blotting

Electrotransfer on to nitrocellulose (Schleicher and Schuell, BA 85) was performed in a Biorad submerged apparatus with a Biorad PowerPak 300 at 30V overnight at 4°C in transfer buffer (0.2M Glycine, 25mM Tris-base, 5% methanol). The nitrocellulose was rinsed in PBS pH7.0 containing 0.1% Tween 20 (v/v) (PBST) then incubated for 30min in PBST 0.2% 951-Black Indian Ink (v/v) (Winsor and Newton) in order to visualise protein transfer efficiency. Excess ink was removed with repeated PBST washes and the membrane was blocked with PBST 5% low fat milk powder (w/v) (Marvel) at room temperature for 1-4h. Primary antibodies were applied overnight at 4°C or for 4h at room temperature in PBST, 2% BSA (Sigma), 0.04% NaN_3. Membranes were washed 3x quick rinse, 4x 5min and 2x 15min in PBST. Incubation with a Horseradish peroxidase (HRP)-conjugated secondary antibody (Pierce, 0.4mg/ml stocks with

50% glycerol) was carried out for 1h at room temperature, dilutions were made in PBST/ 5% milk powder as follows: goat anti mouse-HRP and goat anti rabbit-HRP 1/5000; goat anti rat-HRP and mouse anti goat-HRP 1/2500. Washes in PBST were carried out as for the primary antibody. Blots were developed using ECL (Amersham) or Supersignal (Pierce) HRP substrate reagent kits according to the manufacturer's instructions.

2.3.3 Primary antibodies used for western blotting

Primary antibodies were used for western blotting at the following concentrations: mouse anti-myc hybridoma supernatant (9E10 made in house) 1/2000 dilution; mouse anti-flag (M2, Sigma) 1.5μg/ml; rabbit anti-GST (Upstate Biotech) 1μg/ml; rat anti-HA (3F10, Boehringer) 0.5μg/ml; mouse anti-Rac (23A8, Upstate Biotech) 1μg/ml; rabbit anti-JNK1 (C-17, Santa Cruz) 1μg/ml; affinity pure rabbit anti-dynamin (pan dynamin antibody MC63) and rabbit anti-dynamin2 were both used at 0.6μg/ml (generous gifts from Mark McNiven, Mayo Cancer Clinic, Rochester, USA); goat anti-dynamin1 (C-16, Santa Cruz) 10μg/ml; rabbit anti-GST-N POSH antisera (UCL70, commissioned by the Hall Lab and raised by Cocalico Biologicals Inc., Reamstown, PA, USA) 1/1000.

2.3.4 Stripping and re-probing of western blots

Western blot membranes to be stripped and re-probed were incubated in 62.5mM Tris pH6.8, 2% SDS, 100mM β-mercaptoethanol for 30min at 50°C with occasional agitation. The blots were then washed over a 2-4h in a large excess of PBS, 10x200ml. The efficiency of stripping was checked using ECL (Amersham) HRP substrate reagent kits according to the manufacturer's instructions. Membranes were rinsed in PBS then re-blocked in PBST 5% Marvel milk powder over-night at 4°C before re-probing with a primary antibody for western blotting as described above.

2.3.5 Purification of GST-fusion proteins

The following protocol was used for the preparation of GST fusion proteins to be used in GST-fusion protein pull-down assays and *in vitro* binding assays. In most cases the pGEX DNA constructs were transformed into the DH5α strain of *E. coli.* Exceptions were the GST-amphiphysin 2 SH3 domain and GST-dynamin PRD constructs that were transformed into the BL21 strain.

Glycerol stocks of transformed bacteria were used to inoculate 100ml of LB-100μg/ml ampicillin. This was incubated over night at 37°C with 200rpm shaking. The cultures were diluted 1/10 and grown at 30°C with 250rpm shaking for 2h. GST-fusion protein expression was induced by the

addition of isopropyl β-D-thiogalactopyranoside (IPTG) to a final concentration of 0.1mM and the cultures were shaken for a further 3h at 30°C with 250rpm shaking.

The following steps were carried out at 4°C. Cells were pelleted at 4000rpm for 10min and resuspended in 20ml wash buffer (PBS pH7.0, 50mM EDTA pH8, 1mM DTT). The solution was then transferred to a 50ml Falcon tube. Cells were again pelleted and resuspended in 3ml lysis buffer (wash buffer plus protease inhibitors 1mM phenylmethylsulfonyl fluoride (PMSF), 10μg/ml leupeptin, 10μg/ml aprotinin and 0.1% triton x-100). Lysis was carried out by sonication on ice (10x10s sonications with 10s breaks between each sonication, amplitude of 12 microns). Lysed cells were centrifuged at 10,000rpm for 10min in snap top Falcon tubes. Glutathione-agarose beads (Sigma), to which the GST protein moiety will bind, were pre-soaked in buffer A for at least 30min and washed 3x prior to use. Cell lysate supernatants were decanted into 15ml Falcon tubes and rotated for 2h with 1ml 50% glutathione-agarose bead solution in lysis buffer. Beads were pelleted by centrifugation at 6000rpm for 3min with a level 6 (level 9 maximum) breaking speed. Beads were washed with 3x10ml lysis buffer (including triton x-100), 3x10ml wash buffer (no triton x-100) and 2x10ml PBS alone then resuspended in 1x volume of PBS.

Where GST-fusion proteins to be left attached to glutathione-agarose beads were to be used for pull-down assays the beads were made up to a 50% bead solution with 40% glycerol and 0.01% NaN_3 and stored at –80°C. Prior to use the beads were washed at least four times in the appropriate assay buffer.

Where proteins were to be eluted from the beads were resuspended in 250μl of elution buffer (50mM Tris pH8, 5mM reduced glutathione) and rotated for 10min. Beads were pelleted by centrifugation at 13,000rpm for 30s and the supernatant collected. Multiple rounds of 10min 250μl elutions were carried out and assessed for protein content using a quick Biorad assay (colour change judged by eye), until there was no detectable protein present. Elutions containing the protein were pooled, residual beads were removed by centrifugation at 13,000rpm for 3min. The protein solution was dialysed two times for 1h against 1 litre of 50mM Tris pH8 to remove glutathione. Protein was concentrated with centricon-10 filter units (Amicon), by centrifugation at 6500rpm in a fixed-angle rotor until the volume was about 0.2ml, then aliquoted and snap frozen in liquid nitrogen prior to storage at –80°C.

Biorad assays were used to determine the overall GST-fusion protein yield. Protein purity and concentration were also estimated by SDS PAGE separation of GST-fusion protein samples and coomassie staining of the polyacrylamide gels.

2.3.6 Assay for protein concentration (Biorad)

Concentrated protein assay solution (BioRad) was diluted 1/5 prior to use. The OD_{595} of serial dilutions of a 2mg/ml solution of BSA were plotted (mg protein over OD_{595}) to provide a standard curve from which the concentrations of other proteins could be determined. This assay was used to estimate protein concentrations for lysates and for recombinant proteins, along with visualisation of protein purity by SDS PAGE and Coomassie staining. In cases where cells were lysed directly into SDS PAGE sample buffer the Biorad assay could not be used. In these cases lysate concentrations were estimated against lysates of known concentration separated by SDS PAGE and Coomassie stained.

2.3.7 Coomassie staining of polyacrylamide gels and blots

Gels were stained in Coomassie stain (250ml MeOH, 50ml acetic acid, 0.5g Coomassie R-250, 200ml H_2O) for 1h under gentle agitation; blots were stained for only 5min. De-staining was in several changes of 7% acetic acid, 10% ethanol for gels or 7% acetic acid, 50% methanol for blots. Gels were dried onto Whatman 3M filter paper using a heated, vacuum-assisted gel drier (BioRad). Blots were air dried.

2.3.8 Silver staining of polyacrylamide protein gels

Gels were fixed and washed three times for at least 20min each in 400ml of 50% EtOH, 10% acetic acid, followed by three times 10min in 400ml H_2O. Gels were then incubated in 200ml H_2O containing 1ml $AgNO_3$ (10g / 50 ml H_2O) for 30min. After a quick rinse in H_2O, gels were developed with 200ml developer (10g Na_2CO_3, 219µl 37% formaldehyde, 400 ml H_20) for 5-15 min. After three 5min washes in H_2O, background was reduced with Farmer's Reducer (0.6 ml Farmer A, 2.4ml Farmer B, 200ml H_2O; Farmer A: 8.46g $K_3Fe(CN)_6.3H_20$, 100ml H_2O; Farmer B: 48g $Na_2S_2O_3.5H_20$, 200ml H_2O) for up to 12min. If a second round of staining was necessary, this comprised three further 5min washes in H_2O, a further incubation with $AgNO_3$, another quick rinse in H_20 followed by a second incubation with developer. Developing reactions were stopped with 200ml of 1% acetic acid. Gels were dried onto filter paper.

2.3.9 Immuno-precipitations (IPs)

The following conditions were used for the precipitation of tagged POSH constructs from transfected COS-7 cells. Transfected cells were washed 2x in cold PBS at 4°C and plates were thoroughly aspirated before lysis. Normally 250µl of IP buffer (1.5mM $MgCl_2$, 50mM Hepes pH7.5, 50mM NaCl, 0.5% Triton x 100 (v/v), 10% Glycerol (v/v), 10mM NaF, 10mM sodium pyrophosphate, 0.1mM sodium orthovanadate, 10µg/ml leupeptin, 10µg/ml aprotinin, 1mM PMSF) was used for every $2.5x10^5$ cells transfected. Lysis was carried out for 20min at 4°C, cells were then scraped from the plate and pipetted into a 1.5ml eppendorf. Nuclei and associated

debris were removed by centrifugation at 13,000rpm for 15min to create a post-nuclear supernatant to be used for precipitations.

Normally post-nuclear supernatant from $5x10^5$ transfected cells was used for each IP, unless otherwise stated. Samples of input lysate were mixed with an equal volume of 2x sample buffer and stored for SDS PAGE analysis.

For precipitation of tagged proteins the following amounts of antibody were used per IP: 3µl of mouse anti-myc hybridoma supernatant (9E10, made in house); 2µl (6µg) of affinity pure mouse anti-flag (M2, Sigma); 10µl (4µg) of affinity pure mouse anti-HA (12CA5, Boehringer). Endogenous dynamin2 was precipitated with 1µl (3µg) of rabbit anti-dynamin2 antibody (gift from Mark McNiven, Mayo Cancer Clinic, Rochester, USA) and endogenous Rac with 3µl (3µg) of mouse anti-Rac (23A8, Upstate Biotech). Primary antibody incubations were carried out for 1-4h with rotation at 4°C.

Protein G-Sepharose (Sigma) was pre-washed with 3x 1ml of IP buffer. 100µl of 50% G-sepharose bead solution was mixed with each IP for 1h with rotation at 4°C. Beads were pelleted by centrifugation at 13,000rpm for 30s. Supernatants were removed, mixed 1:1 with 2x sample buffer and saved for SDS PAGE analysis. Beads were washed with 3x 1ml of IP buffer, then resuspended in 25µl of 1x sample buffer. Precipitates and samples of lysates and supernatants were separated by SDS PAGE and western blots probed for precipitated and co-precipitated proteins.

2.3.10 GST-fusion protein pull-down assays

The following conditions were used for GST-fusion protein pull-downs of endogenous or transfected proteins from post-nuclear supernatants. Normally a lysate containing 0.5mg of protein was used for each pull-down. Cells were washed and harvested as stated above for IPs, but using a slightly different lysis buffer (as for IPs, but with more salt, 150mM NaCl, and more detergent, 1% triton x-100). GST-fusion protein beads were prepared as described above. Lysates were incubated with rotation for 2h at 4°C with 10µg of GST, or GST-fusion protein, bound to glutathione-agarose beads. Beads were pelleted by centrifugation at 13,000rpm for 30s and pull-down supernatants were saved. Pull-downs were washed with 5x 1ml of lysis buffer, then resuspended in 25µl of 1x sample buffer. Pull-downs, and samples of lysates and supernatants, were separated by SDS PAGE and western blots were probed for proteins associated with the GST-fusion baits. Membranes were stained with coomassie blue to visualise the fusion proteins.

2.3.11 JNK kinase assays

$5x10^5$ COS-7 cells were used for each transfection. Transfections were carried out using lipofectamine as described above, with 1μg pCMV5-flag-JNK1 plus 1μg of empty pRK5myc vector or of DNA encoding a potential activator protein in the pRK5myc vector. After tranfection cells were maintained in medium containing 20μM BOC-Dfmk caspase inhibitor. 24h post-transfection cells were harvested in 250μl of the following lysis buffer (20mM Tris pH8, 5mM $MgCl_2$, 10mM EGTA, 1% triton x-100, 40mM sodium pyrophosphate, 50mM sodium fluoride, 100μM sodium pervanadate, 1mM PMSF, 10μg/ml leupeptin, 10μg/ml aprotinin) and a post-nuclear supernatant was prepared. 200μl of cell lysate was added to 600μl of IP buffer (10mM Hepes pH7.6, 25mM NaCl, 1.25mM $MgCl_2$, 50μM EDTA). The remaining lysate was mixed 1:1 with 2x SDS PAGE sample buffer for future analysis of transfection input lysates. Each lysate was incubated with M2 mouse anti-flag antibody for 1.5h at 4°C with rotation. 50μl of a 50% protein G-sepharose solution in IP buffer was added to each precipitate and mixed with rotation at 4°C for 1h. Precipitates were washed with 3x 1ml wash buffer (IP buffer minus protease inhibitors). After the final wash the liquid was thoroughly removed from the protein G-sepharose beads.

Precipitates were re-suspended in 30μl of JNK kinase assay buffer: 20mM Hepes pH7.6, 20mM $MgCl_2$, 4mM sodium fluoride, 20mM para-nitrophenyl-phosphate, 0.1mM sodium pervanadate, 2mM dithiothreitol, 20μM cold ATP and for each reaction 1-2μg GST-c-jun substrate protein and 5μCi [γ-^{32}P] ATP (Amersham, 10mCi/ml). The mixture was incubated at 30°C for 20min and the reaction was stopped with 8μl of 5x SDS PAGE sample buffer. The precipitates and 1/10 input lysate samples were separated by SDS PAGE and transferred to nitrocellulose. Phosphorylated c-jun was visualised with Biomax MR film (Kodak) and was also quantified with a PhosphorImager (Biorad Molecular Imager FX) and "Quantity One" software. Relative JNK1 levels in each precipitate were assessed by probing of western blots with a rabbit anti-JNK antibody (C-17, Santa Cruz). Expression of myc-tagged proteins in samples of lysate from each transfection was visualised by probing of western blots with mouse anti-myc (9E10). The levels of JNK in each precipitate were quantified using a Biorad GS-710 calibrated Imaging Densitometer and "Quantity One" software. Results were expressed as fold activation: (phospho-c-jun signal/level of JNK) expressed relative to the empty vector/JNK control.

2.4 THE YEAST-TWO-HYBRID SYSTEM

The principals of the yeast-two-hybrid system, which was also used for screens of cDNA libraries that resulted in the cloning of POSH and the later discovery of a binding partner for POSH (siah) are outlined within the methods described below. In addition the exact protocols used to test for interactions of POSH bait constructs with specific prey constructs are detailed.

2.4.1 Yeast strains, plasmids and materials

Two *Saccharomyces cerevisiae* yeast strains were used. Y190 [*MAT*α *gal*5-542, *gal*80-538 *his*3 *trp*1-901 *ade*2-101 *ura*3-52 *leu*2-3 *URA*3::*GAL*1-*lacZ LYS*2::*GAL*1-*His*3*cyh*^{r}], a kind gift from S Elledge, was used to test Gal DNA-binding domain-containing POSH bait constructs. L40a [*MAT*a *his*3 *leu*2 *trp*1 *URA*3::*LexA-lacZ*, *LYS*2::*LexA-HIS*3], a kind gift from S Dowell (GlaxoWellcome), was used to test LexA DNA-binding domain-containing bait constructs.

For POSH constructs the bait plasmid used was pYTH9, which contains the Gal4 DNA-binding domain and Trp selection, a kind gift from R Brown (when at GlaxoWellcome). This vector cannot replicate autonomously and was therefore integrated into the yeast genome by homologous recombination within the Trp1 gene. To facilitate integration the plasmid was linearised with XbaI, which cuts within the *Trp1* gene, prior to transformation into yeast. The bait construct pBTM116-Cbl RING contained a LexA DNA-binding domain and Trp selection and can autonomously replicate. Prey constructs were in the vectors pGAD10 or pACT2 (Clontech), which both contain a Gal4 activation domain and Leu selection. pYTH9-L63RhoA together with pGAD10-Rho GAP were used for a strong positive control interaction and empty vectors were used for negative controls.

Plates used for selection were as follows. YEPD (rich medium): 20g/l peptone (Difco), 10g/l yeast extract (Difco), 20g/l agar (Difco), 2% (w/v) D-glucose. Synthetic complete (SC)-W$^-$: 6.7g yeast nitrogen base w/o amino acids, 0.62g/l drop-out mix (CSM-His-Leu-Trp, Bio101), 0.1g/l histidine, 0.2g/l leucine, 20g/l agar. SC-WL$^-$: 6.7g yeast nitrogen base w/o amino acids, 0.62g/l drop-out mix, 0.1g/l histidine, 20g/l agar. SC-WLH$^-$ 3AT: 6.7g yeast nitrogen base w/o amino acids, 0.62g/l drop-out mix, 20g/l agar, 5-25mM 3-amino triazole (3AT).

2.4.2 Transformation of bait constructs

One colony of Y190 was picked from a YEPD plate and grown in 10ml YEPD medium (as for YEPD plates, but without agar) overnight at 30°C with vigorous shaking. The culture was diluted around 1/10 to give a final OD_{600} of 0.2. The yeast were grown for a further 3-5h, until the OD_{600} was 0.7-1.0, at 30°C with vigorous shaking. Yeast were harvested by centrifugation at 2,500rpm for 2min, washed in 20ml TE pH7.5 and re-suspended in 1ml 0.1M LiAc in TE pH7.5 (LiAcTE).

After two further washes in LiAcTE the yeast were re-suspended in 500µl of LiAcTE. 20µl of boiled carrier DNA (Salmon sperm, Sigma) was added to each 1.5ml microfuge tube containing DNA to be transformed (5µg of DNA that had been digested with XbaI then heated to 65°C for 20min to inactivate the enzyme). 100µl of yeast suspension and 700µl of 44% polyethylene glycol (MW 3350) in 0.1M LiAc were added to each tube. The yeast were kept at 30°C for 30min with occasional inversion then heat shocked at 42°C for 20min. Cells were harvested by centrifugation for 20s in a microfuge, washed 2x in 1ml TE pH7.5, re-suspended in 50µl TE pH7.5 and plated on to SC-W$^-$ plates in order to select for transfected cells and grown at 30°C.

2.4.3 Co-transformation of prey constructs

The method used was the same as for transformation of bait constructs except for the following differences. The overnight culture was taken from a single colony of bait-transformed Y190 and these yeast were grown in SC-W$^-$ medium (as for plates, but without agar). Only 1µg of plasmid to transform was used and this was not digested. After transformation cells were plated on to SC-WL$^-$ plates in order to select for transformation of both bait and prey constructs.

2.4.4 Assay for histidine minus growth

In the Y190 strain the HIS3 gene is under the control of the GAL4 promoter, in a *his*3 mutant genetic background and in L40a HIS3 is under the LexA promoter. The principal of the yeast-two-hybrid system is that when a prey construct, with a Gal4 transcription-activation domain, interacts with a bait construct, with a Gal4 or LexA DNA-binding domain, then the GAL4 or LexA promoter can be activated. The Y190 *his*3 mutation is leaky meaning that low levels of functional imidazoleglycerol-phosphate dehydratase (IGPD), the product of the HIS3 gene, are present even in the absence of activation of the reporter gene by a bait-prey interaction. 3-aminotriazole (3-AT) inhibits IGPD, which increases the threshold of IGPD activity needed for growth on histidine-minus medium. For Y190 transformants 25mM 3AT was used, whereas for L40a transformants only 5mM 3AT was required to eliminate growth of negative controls. Single colonies of cells co-transformed with bait and prey constructs were re-streaked on to SC-WLH$^-$ 3AT plates and grown at 30°C for 3-4 days. Only those cells in which the bait and prey constructs interact were able to grow on these plates. Images of these plates were grabbed and processed using a Kaiser rePRO CCD camera and Adobe Photoshop software.

2.4.5 β-galactosidase filter assay

In Y190 and L40a yeast strains the *Lac*Z gene was also under the GAL4 or LexA promoter, so that the enzyme encoded by *Lac*Z (β-galactosidase) is only expressed when fusion proteins encoded by co-transformed bait and prey constructs interact with each other. Yeast cells containing bait and prey constructs to be tested were streaked on to Whatmann number 1 filter

discs (9cm), which were then dipped three times into liquid nitrogen for 30s then allowed to thaw, in order to cause cell lysis. Once thawed discs were placed on to 10cm plates containing a filter disc soaked in buffer Z (60mM $Na_2HPO_4.7H_2O$, 40mM $Na_2HPO_4.4H_2O$, 10mM KCl, 1mM MgSO4. H_2O) with 50mM β-mercaptoethanol and 0.5mg/ml 5-bromo-4-chloroindolyl-β-D-galactoside (X-gal). Positive yeast processed the X-gal to give a blue coloured product that could be seen after 1h to 16h (depending on the strength of the interaction) incubation at 30°C.

CHAPTER 3
POSH AND APOPTOSIS

3.1 INTRODUCTION

POSH was cloned using a yeast-two-hybrid screen with activated L61Rac as bait and was shown to bind *in vitro* to wild type (wt) Rac in a GTP-dependent manner [Tapon, Nagata, 1998], so fulfilling the basic requirements to be a Rac effector protein. As a Rac effector, POSH would be expected to initiate signal transduction events in response to binding of activated Rac, leading the activation of a Rac-dependent process, which is not necessarily a known activity. In common with L61Rac, transfected POSH was shown to activate the JNK MAP kinase pathway, while injected POSH induced activation of the NF-κB transcription factor, suggesting that POSH may mediate these Rac activities [Tapon, Nagata, 1998]. Furthermore, POSH was found to bind to the effector mutant A37L61Rac, that activates JNK but not actin reorganisation, but not to C40L61Rac, that induces lamellipodia but not JNK or NF-κB [Lamarche, 1996] [Tapon, Nagata, 1998]. This again suggests that POSH is involved in mediating changes in gene transcription downstream of activated Rac, but is not involved in actin reorganisation.

Unlike L61Rac, however, full-length POSH caused apoptosis when over-expressed [Tapon, Nagata, 1998]. This chapter describes further investigation of the ability of POSH to induce apoptosis, in particular characterisation of the regions of POSH required to cause apoptosis.

3.2 RESULTS

3.2.1 POSH-induced apoptosis in different cell types

Injection or transient transfection of full-length POSH DNA, into Swiss 3T3 or COS7 fibroblast cell lines, was previously shown to induce apoptosis [Tapon, Nagata, 1998]. In order to further investigate POSH-induced apoptosis a reproducible assay was required. The kinetics of POSH expression were difficult to control using transient transfection and I decided, therefore, to set up a micro-injection-based assay.

The cells tested for POSH-induced apoptosis included primary human keratinocytes, the canine epithelial cell line MDCK and the mouse fibroblast cell line NIH3T3. The results from these experiments are shown in figure 3.1. Cells were plated onto coverslips in normal growth media containing serum. Vania Braga (MRC LMCB, UCL, London) provided primary human foreskin keratinocytes, on coverslips in media that included calcium to enable the formation of cell-cell contacts. NIH3T3 cells were plated at a density of $8x10^4$cells/coverslip 24h prior to injection.

MDCK cells were plated at a density of $2x10^4$cells/coverslip 24h prior to injection. On each coverslip the nuclei of 100 cells were injected with 0.05mg/ml pRK5myc-POSH or pRK5myc-L61Rac DNA. One coverslip was fixed 2h post-injection and the others 7h or 14h post-injection. Cells were stained for myc with 9E10 and for nuclei with Hoechst, in order to visualise the pyknotic nuclear morphology (see for example expressing cells in figure 3.3 c and h) indicative of a late stage in apoptosis. In no case did cells undergo apoptosis during the first 2h post-injection. Variations in the number of expressing cells occurred due to: (a) different DNA constructs; (b) the state of the needles used in each experiment; (c) the state of the cells used in each experiment (passage number for instance); (d) the cell type. This was corrected for using the number of cells expressing at the 2h time point for each cell type and construct injected, assuming similar expression levels for the same DNA on the same day with the same cell type, so that cell survival was expressed as:

% survival = number of non-pyknotic expressing cells (nh/2h)x100

Cell Type	DNA injected	Number of non-pyknotic expressing cells at 2h	% survival	
			7h expression	14h expression
Keratinocyte	POSH	46	54	n/d
	L61Rac	54	79	n/d
	POSH	39	41	10
	L61Rac	50	n/d	64
NIH3T3	POSH	75	11	1
	L61Rac	82	88	n/d
	POSH	79	n/d	0
	L61Rac	88	n/d	76
	POSH	69	6	n/d
MDCK	POSH	58	30	n/d
	L61Rac	67	85	n/d
	POSH	56	24	6
	L61Rac	72	78	58

Figure 3.1 Table summarising POSH-induced apoptosis data for three cell types

The data from five experiments is shown. In each case 100 cells were injected with 0.05mg/ml pRK5myc-POSH or pRK5myc-L61Rac DNA. The number of cells expressing after 2h is shown, which indicates the success in injection and expression. Survival after 7h or 14h was expressed as the number of non-pyknotic expressing cells corrected for expression efficiency using the number of expressing cells at the 2h time point, when apoptosis was not yet detected. n/d, not determined

For all three cell types almost all POSH-expressing cells had undergone apoptosis after 14h expression (0-10% survival), whereas L61Rac-expressing cells were largely unaffected. Keratinocytes were the cell type most refractory to POSH-induced apoptosis, with 41-54% survival after 7h. NIH3T3 cells were the cell type most affected by POSH after 7h expression, with only 6-11% survival. The MDCK cells were somewhere in between, with 24-30% survival after 7h. These observed differences in cell death kinetics between cell types could be due to variations in expression efficiency as well as other characteristics of the cells. COS1 and Swiss 3T3 cells were previously shown to be susceptible to POSH-induced cell death, this was also the case in my own experiments with COS7 cells and with both growing and quiescent Swiss 3T3 cells (data not shown). In later experiments it was observed that Hep2 and HeLa human epithelial cell lines, primary rat embryo fibroblasts and the mouse macrophage cell line J774 are also susceptible to POSH-induced apoptosis (data not shown), suggesting that this is not a cell-type or cell species-specific phenomenon. As an apoptosis assay system I chose to use the NIH3T3 fibroblast cell line, which had a strong apoptosis response to POSH over 7h and efficiently expressed injected DNA constructs (see figure 3.1).

3.2.2 POSH N-terminus plus the Rac-binding domain induce apoptosis

To narrow down the minimal regions of POSH required to induce apoptosis POSH truncations were tested, alone or in combination, for their ability to induce apoptosis in NIH3T3 cells. Previous work had shown that a C-terminal POSH construct (C POSH) did not induce apoptosis in NIH3T3 or COS1 cells. In an NIH3T3 cell microinjection assay I tested C POSH and Y2H POSH plus the following constructs: N POSH (POSH N-terminus up to but excluding the Rac-binding domain); RING-SH3 1 (POSH N-terminus minus the second SH3 domain); SH3 1-2 (POSH N-terminus minus the RING finger); POSH RBD (Rac-binding domain). The amino acids contained in each POSH truncation and the apoptosis assay results are summarised in figure 3.2 and examples of injected cells are shown in figure 3.3.

Using the NIH3T3 cell apoptosis assay described above it was clear that full-length POSH induced apoptosis (see figure 3.2 and figure.3.3 a-c), but that none of the POSH truncations tested could induced apoptosis on their own (data is shown for C, N, Y2H and RBD POSH in figure 3.2). Various combinations of these truncations were then tested, using one myc-tagged construct and one flag-tagged construct. Surprisingly, co-injection of N POSH plus Y2H POSH induced apoptosis just as efficiently as full-length POSH (see figures 3.2 and 3.3).

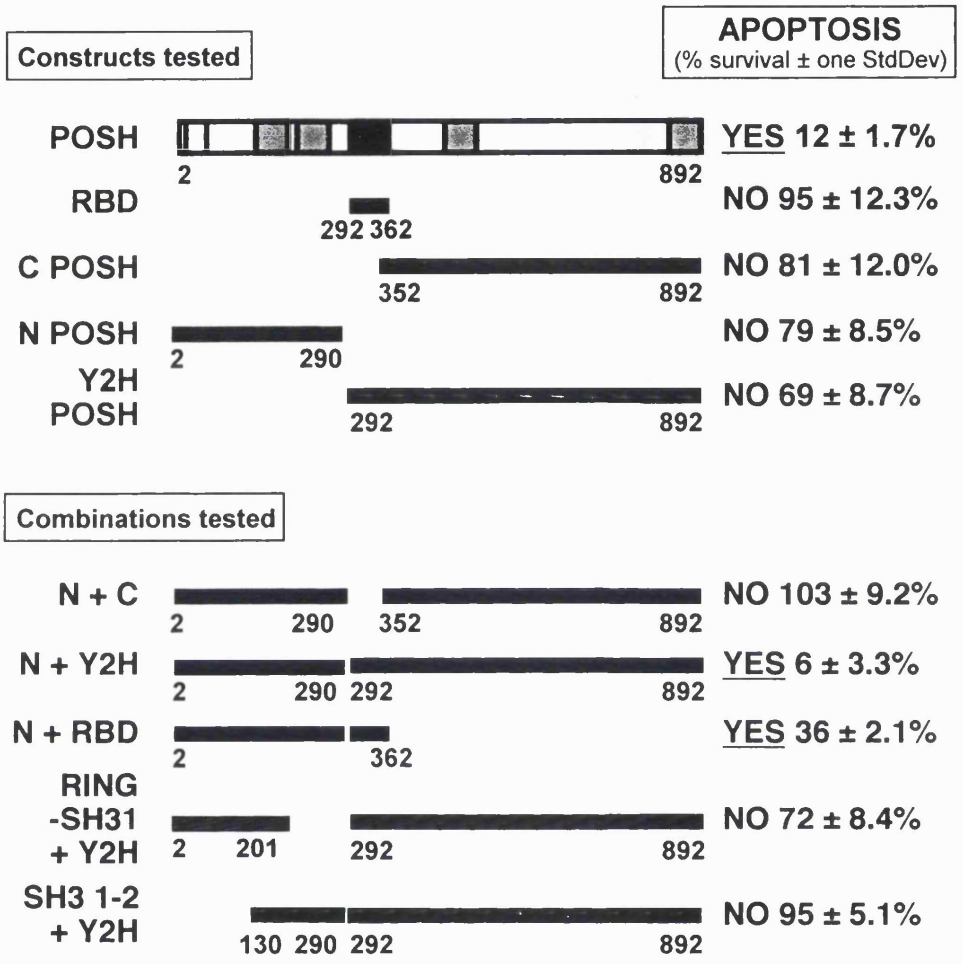

Figure 3.2 Summary of apoptosis data for various POSH constructs

The extent of each POSH construct injected is shown. The apoptosis assays were carried out as follows. 100 NIH 3T3 cells were injected/ coverslip with DNAs at 0.05mg/ml. Two coverslips were injected per DNA combination tested, one was fixed after 2h and the other after 7h. Where constructs were co-injected one was myc-tagged and the other flag-tagged. Hoechst staining was used to visualise nuclear morphology plus rat-anti-myc (JAC6) and/or mouse-anti-flag (M2) to visualise expression of myc-tagged or flag-tagged proteins respectively. Survival was expressed as (%survival = number of non-pyknotic expressing cells (7h/2h)x100). In each case average results are shown from at least three independent experiments ± one StdDev.

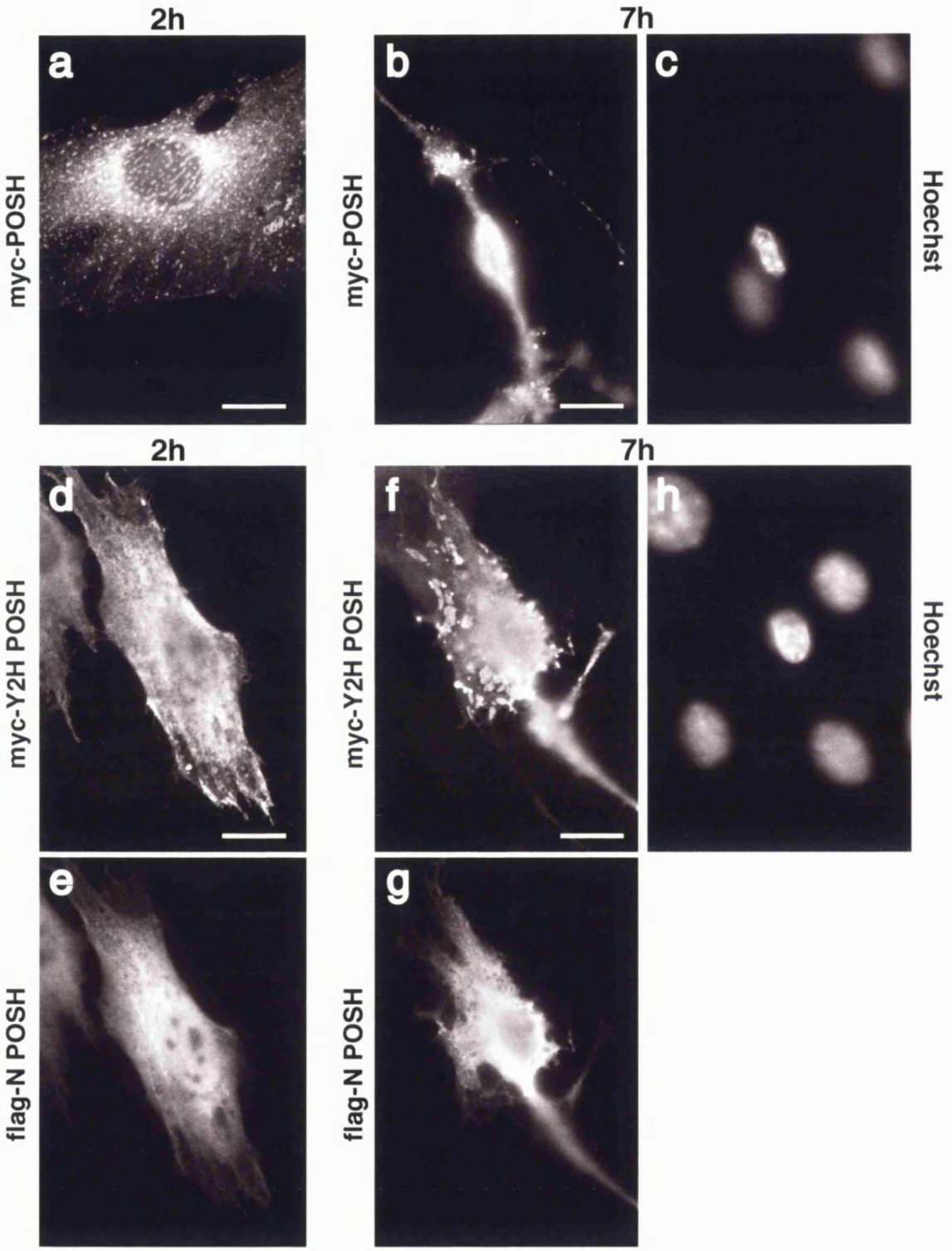

Figure 3.3 The cellular localisations of POSH constructs that induce apoptosis

NIH3T3 cells were injected with 0.05mg/ml DNAs: pRK5myc-full-length POSH/ pRK5 (a-c) or pRK5flag-N POSH/ pRK5myc-Y2H POSH (d-h). Cells were fixed 2h (a and d-e) or 7h (b-c and f-h) post-injection. Cells were stained with Hoechst, to visualise nuclear morphology (shown for 7h time point only, c and h), and rat anti-myc (JAC6) and/or mouse anti-flag M2 to visualise myc-POSH (a-b), myc-Y2H POSH (d and f) and flag-N POSH (e and g). Bars equal 30μm.

From the immunofluorescence staining myc-Y2H POSH and flag-N POSH appeared not to have exactly the same cellular distribution (see figure 3.3 d-g). N POSH was diffusely distributed in the cytoplasm, and was occasionally seen in the nucleus (see figure 3.3 e and g); Y2H POSH was also cytoplasmic but formed punctate structures not seen with N POSH, which are possibly protein aggregates and were most clearly seen at the cell periphery (see figure 3.3.d and f). Interestingly, C POSH, when at high levels (data not shown), and full-length POSH, even at quite low levels (see figure 3.3 a), have also been observed to form what appear to be cellular aggregates, suggesting that this distribution is dependent upon the C-terminus of the molecule. These data suggest that the two ends of the POSH protein (N POSH and Y2H POSH) are both required for apoptosis but do not need to be within a single molecule or to be co-localised within the cell in order to induce apoptosis. It appears, therefore, that N POSH and Y2H POSH contribute two separate activities, which together induce apoptosis.

Shorter N-terminal POSH fragments (RING-SH3 1 or SH3 1-2), in combination with Y2H POSH, could not substitute for N POSH to induce apoptosis (see figure 3.2). This suggested that the full N-terminus was needed for POSH-induced apoptosis. Removal of the Rac-binding domain from Y2H POSH (to create C POSH) completely abolished the ability of the C-terminus of POSH to complement N POSH and induce apoptosis (see figure 3.2). Finally, the RBD alone, in combination with N POSH, had a partial apoptosis-inducing effect. The RBD construct may not contain all of the amino acids required for a full apoptosis effect, or may be less stable than Y2H POSH, but did appear to be active in this apoptosis assay. These data together suggest that the RBD is the region of Y2H POSH that contributes to apoptosis. Overall, N POSH plus RBD POSH appear to be the minimal regions, which can be defined using these truncations, required for POSH-induced apoptosis.

3.2.3 Expression of POSH in COS7 cells

Previous work had revealed problems in expression of POSH in COS cell transfection assays [Tapon, Nagata, 1998]. To determine whether this was due to induction of apoptosis transfection was attempted with or without a general caspase inhibitor, BOC-Dfmk. The results of one such transfection can be seen in figure 3.4. No full-length POSH was recovered in the absence of BOC-Dfmk (figure 3.4 lane 6), whereas a small yield of protein was visible when BOC-Dfmk had been included (figure 3.4 lane 5). The yields of C POSH (figure 3.4 lanes 3-4) and N POSH (figure 3.4 lanes 1-2) were not visibly changed by the inclusion of BOC-Dfmk. This is consistent with the NIH3T3 cell injection assay showing that neither C POSH nor N POSH alone could induce apoptosis (see figure 3.2). In these experiments 48h expression times were used, whereas when 24h expression was used then a much better yield of full-length POSH was obtained even in the absence of caspase inhibitor. 24h hour expression times were, therefore, used for all of the transfections shown in the following chapters, whether or not the capase inhibitor was included.

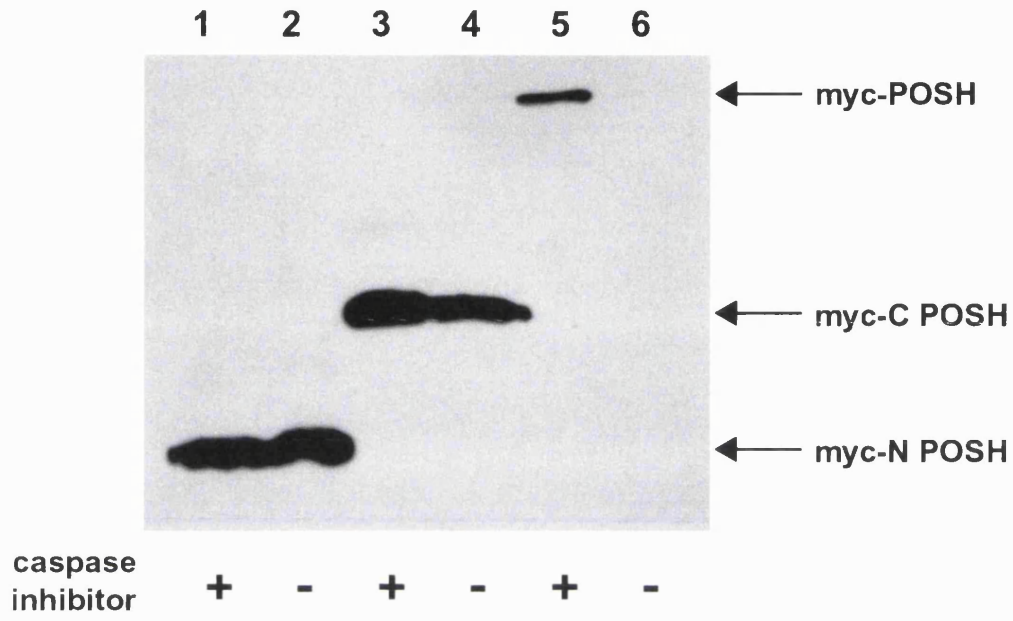

Figure 3.4 Transfection yields for full-length POSH, but not for POSH truncations, are improved by incubation with a capase inhibitor

Two wells containing $2.5x10^5$ COS-7 cells were transfected with 0.5mg of DNA encoding myc-tagged N POSH (lanes 1-2), C POSH (lanes 3-4) or full-length POSH (lanes 5-6). After a 6h incubation with the DNA/ lipofectamine mixture one well for each transfection was incubated with caspase inhibitor, 20μM BOC-Dfmk (0.2% DMSO) and the othe well was incubated just in 0.2% DMSO. The media, including DMSO or BOC-Dfmk in DMSO, was replaced 24h post-transfection. Cells were harvested 48h post-transfection and post-nuclear supernatants were prepared. 1/10 of each lysate was separated by SDS PAGE and western blots were probed with mouse anti-myc antibody (9E10) to visualise transfected myc-tagged proteins.

3.2.4 Dominant negative Rac induces apoptosis in combination with N POSH

The Rac-binding domain (RBD) was required for POSH-induced apoptosis (see above). The mechanism by which this region of POSH contributes to apoptosis when over-expressed could be to interact with and inhibit the normal activity of GTP-bound endogenous Rac. The dominant negative N17Rac mutant also inhibits endogenous Rac activity, but via a different mechanism. N17Rac forms non-productive complexes with the upstream activators of Rac, the guanine nucleotide exchange factors (GEFs), preventing them from activating endogenous Rac [Feig, 1999]. As an indication of whether inhibition of endogenous Rac was the contribution made by POSH RBD to apoptosis N POSH was tested with N17Rac for the induction of apoptosis.

Myc-N17Rac and flag-N POSH constructs were injected into NIH3T3 cells together or with empty vector. The results from three experiments are summarised in figure 3.5. N17Rac or N POSH alone did not induce significant apoptosis. The two proteins in combination potently induced apoptosis after 7h expression (see figure 3.5 A and figure 3.5 B d-f). These data show that N17Rac can substitute for ~~from~~ POSH RBD to induce apoptosis in combination with N POSH.

3.2.5 Full-length and Y2H POSH bind to activated Rac *in vivo*

POSH truncations containing the RBD (amino acids 292-362) had previously been shown to bind to the constitutively active L61Rac *in vitro* and Y2H POSH was originally cloned due to its ability to interact with L61Rac in the yeast-two-hybrid system [Tapon, Nagata, 1998]. In contrast the effector domain mutant C40L61Rac did not interact with Y2H POSH *in vitro* or using the yeast-two-hybrid system [Tapon, Nagata, 1998]. The ability of POSH constructs to bind to activated Rac had not been tested *in vivo*. If the Rac-binding domain contributes to the induction of apoptosis, in combination with N POSH, by binding to endogenous GTP-Rac then POSH and activated Rac must interact *in vivo*.

COS7 cells were transfected with flag-POSH or flag-Y2H POSH in combination with myc-tagged wtRac, L61Rac or C40L61Rac. Flag-full-length POSH was also transfected with empty vector and with myc-L61Cdc42. Flag-tagged POSH proteins were precipitated. Precipitated proteins, and samples of transfected cell lysate, were separated by SDS PAGE. Precipitated POSH proteins were visualised by probing the top of the membranes with an anti-flag antibody (figure 3.6 panel a). Co-precipitated GTPase constructs (figure 3.6 panel b), and GTPases in transfected cell lysate samples (figure 3.6 panel d), were visualised by probing of the bottom of the membranes with an anti-myc antibody. The myc blot for full-length POSH precipitates (figure 3.6 b lanes 1-6) was stripped and re-probed for endogenous Rac (figure 3.6 panel c).

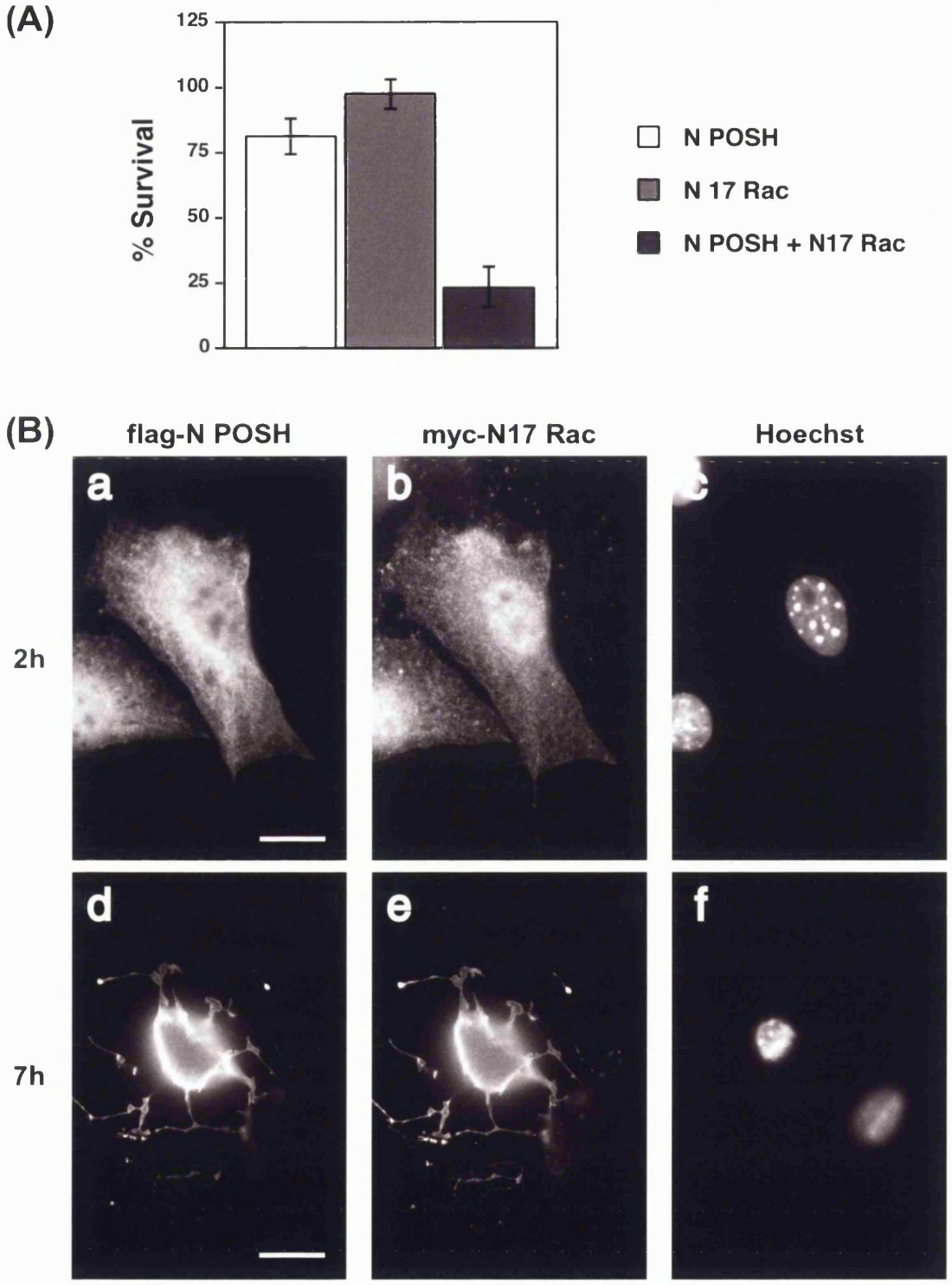

Figure 3.5 N POSH plus dominant negative N17Rac induce apoptosis

NIH3T3 cells were injected with 0.05mg/ml of the following DNAs: pRK5flag-N POSH/pRK5; pRK5myc-N17Rac/pRK5; pRK5myc-N17Rac/pRK5flag-N POSH. Cells were stained with hoechst, (B, c and f), plus rat anti myc JAC6 (b and e) and/or mouse anti-flag M2 (a and d). Combined survival data from hree independent experiments is shown in (A), average % survival (number of non-pyknotic expressing cells (7h/2h)x100) ± one StdDev. Examples of immunofluorescence staining for N17Rac/N POSH co-expressing cells after 2h (B, a-c) or 7h (B, d-f) are shown in (B). Bars equal 30μm.

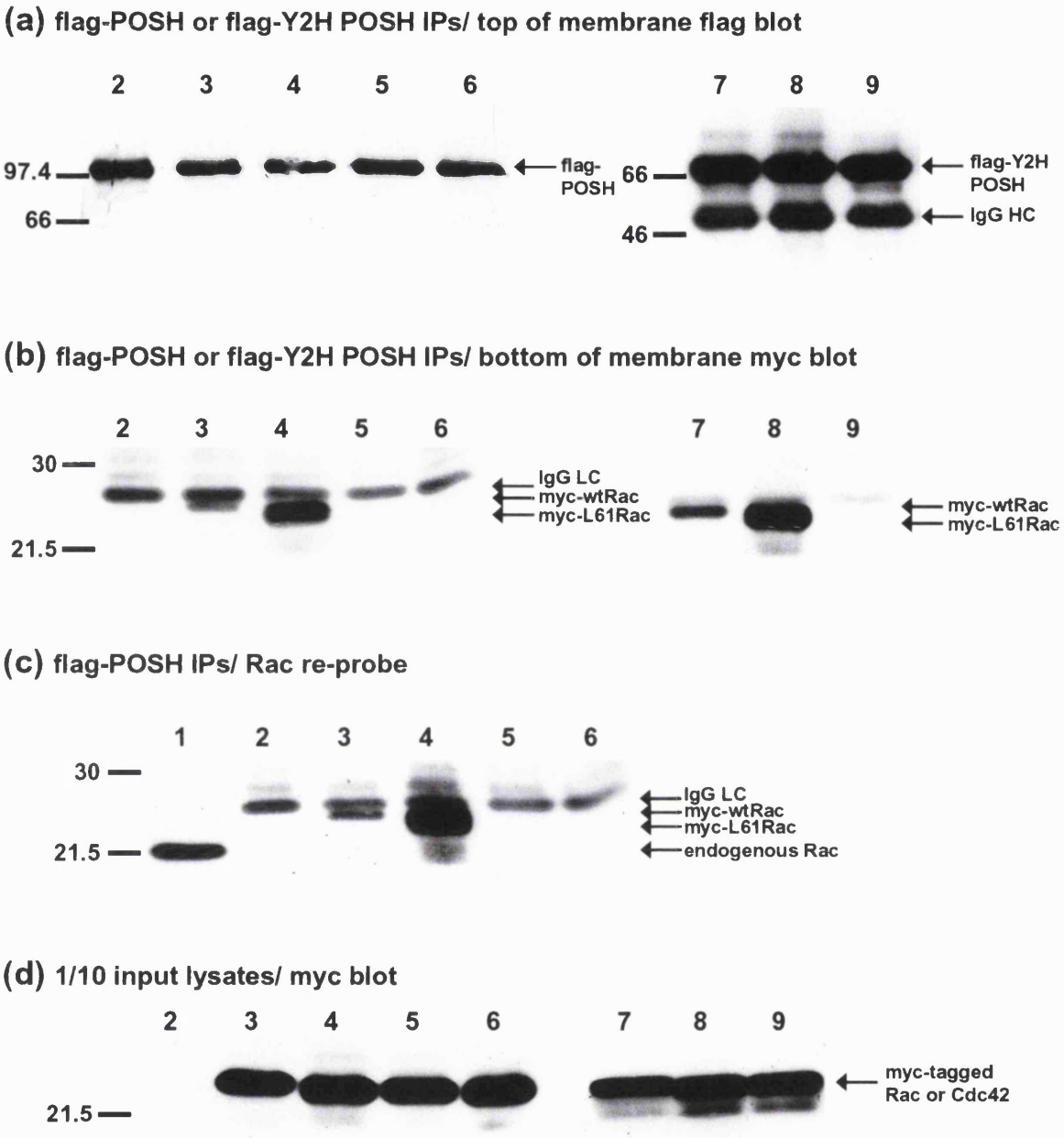

Figure 3.6 Y2H POSH and full-length POSH bind to co-transfected wild type Rac and L61Rac, but not C40L61Rac

5x10^5 COS-7 cells were mock transfected or transfected with: flag-POSH (lane 2); flagPOSH/myc-wild type (wt) Rac (lane 3); flag-POSH/myc-L61Rac (lane 4); flag-POSH/myc-C40L61Rac (lane 5); flag-POSH/ myc-L61Cdc42 (lane 6); flag-Y2HPOSH/myc-wtRac (lane 7); flag-Y2H POSH/myc-L61Rac (lane 8); flag-Y2H POSH/myc-C40L61Rac (lane 9). Cells were harvested 24h post-transfection and flag-tagged POSH proteins were precipitated with mouseanti-flag antibody (M2). Precipitates (lanes 2-9), samples of mock transfected COS7 cell lysate (panel c, lane 1), and samples of transfected cell lysates (panel d) were separated by SDS PAGE. Co-precipitated GTPases and GTPases in transfected cell lysates were visualised by probing the bottom of the western blot membranes with mouse-anti-myc antibody (9E10) (panels b and d). Precipitated POSH proteins were visualised by probing the top of the western blot membranes with M2. The myc blot of full-length POSH precipitates (panel b) was stripped and reprobed with a mouse anti-Rac (23A8) antibody to visualise endogenous Rac (panel c). Abbreviations: light chain (LC); heavy chain (HC).

All GTPase constructs were well expressed, as seen from the lysate samples (figure 3.6 panel d). L61Rac was clearly co-precipitated with both Y2H POSH (figure 3.6 (b) lane 8) and full-length POSH (figure 3.6 (b) lane 4). A small amount of wtRac, visible just below the IgG light chain, was also co-precipitated with Y2H POSH (figure 3.6 (b) lane 7) and full-length POSH (figure 3.6 (b) lane 3). This presumably represents the GTP-loaded portion of the over-expressed wtRac protein. C40L61Rac did not bind to Y2H POSH (figure 3.6 (b) lane 8) or full-length POSH (figure 3.6 (b) lane 5) and L61Cdc42 did not bind to full-length POSH *in vivo* (figure 3.6 (b) lane 6). These results indicate that Y2H POSH and full-length POSH show the same binding preferences towards the Rho GTPase proteins tested *in vivo* as Y2H POSH showed *in vitro* [Tapon, Nagata, 1998].

Endogenous Rac could be seen, running significantly lower than myc-tagged wtRac (figure 3.6 (c) lane 3), in a mock transfected cell lysate sample containing 1/10 of the amount of lysate used in the immuno-precipitations (figure 3.6 (c) lane 1). Endogenous Rac was not seen to co-precipitate with full-length POSH (figure 3.6 (c) lane 2). The amount of endogenous Rac in the GTP-bound state, to which POSH could bind, may be too small to be detected, even when the cells are stimulated by 10% serum as was the case here.

It appears from these data that full-length POSH and Y2H POSH bind *in vivo* to over-expressed activated Rac (wtRac and L61Rac), but an interaction with endogenous Rac could not be detected. As the interaction of POSH with over-expressed wtRac protein was weak but clearly visible (see figure 3.6 (b) lanes 3 and 7) it is likely that POSH interacts with endogenous activated Rac, but the levels are too low to be detected in this assay.

3.2.6 POSH Rac-binding domain inhibits L61Rac-induced ruffling

In order to determine whether POSH, via the RBD, can interact with and inhibit endogenous Rac *in vivo* the ability of POSH to interfere with L61Rac-induced ruffling was tested. This assay was carried out by injection of subconfluent quiescent serum starved Swiss3T3 cells, because they contain very little organised F-actin prior to stimulation (see figure 3.7 b). Flag-tagged L61Rac DNA was injected at a 1:2 DNA ratio with empty vector or with various different POSH constructs. The percentage of injected/expressing cells from that were ruffling for each DNA combination tested is shown in figure 3.7 (a). Representative pictures of cells expressing each construct are shown in (b-h).

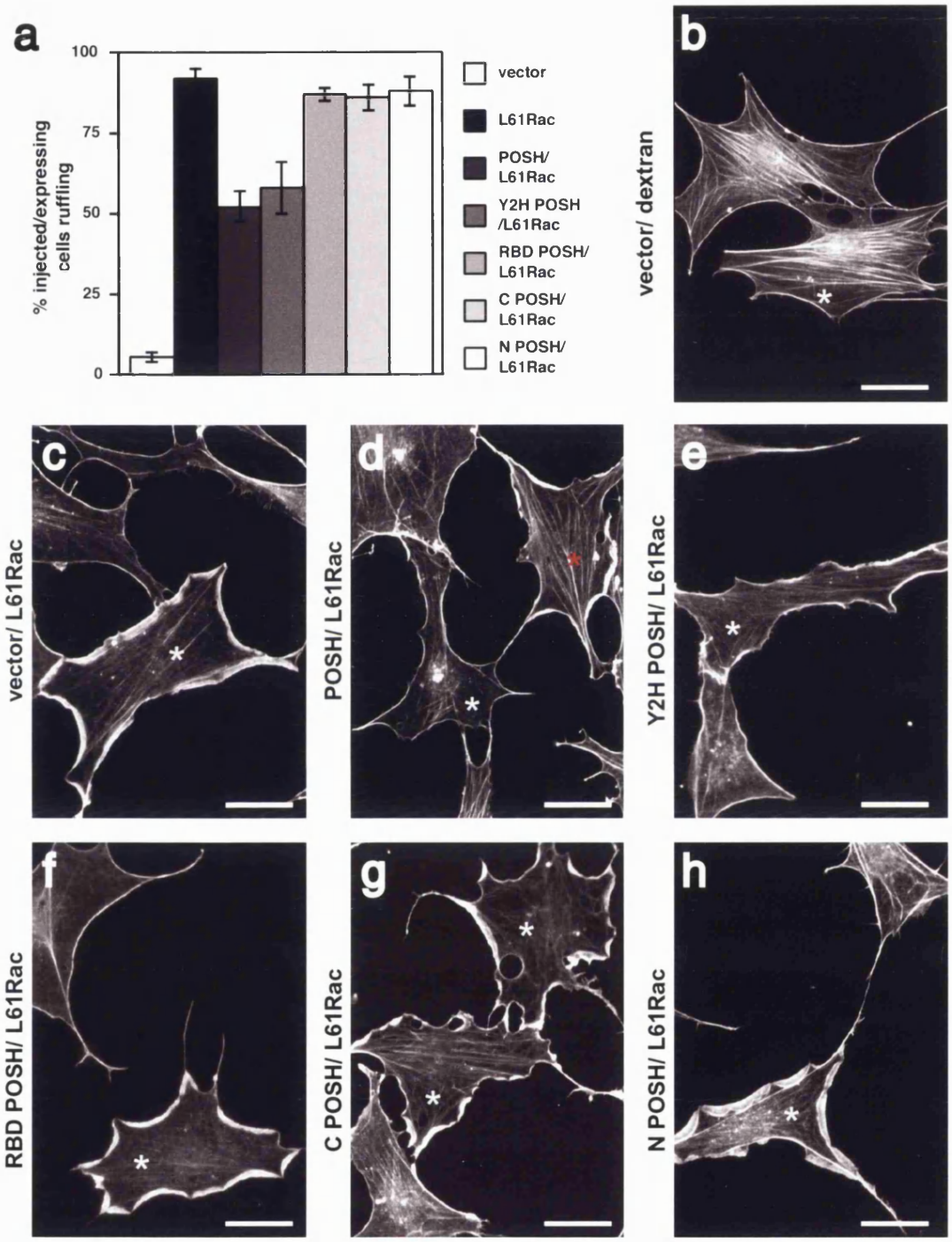

Figure 3.7 Proteins containing POSH Rac-binding domain inhibit L61Rac-induced ruffling
Sub-confluent quiescent Swiss 3T3 cells were serum starved for 16h prior to injection. 100 cells/coverslip were injected with 5mg/ml biotin-dextran plus 0.3mg/ml empty vector (b) or 0.1mg/ml pRK5flag-L61Rac plus 0.2mg/ml of the following pRK5myc constructs: empty vector (c); full-length POSH (d); Y2H POSH (e); C POSH (f); RBD POSH (g); N POSH (h). After 2h expression cells were fixed and stained for actin using rhodamine-phalloidin, for the dextran injection marker using alexa-streptavidin and for myc-tagged protein expression, where appropriate, using the mouse anti-myc antibody 9E10 and goat anti-mouse-FITC secondary antibody. **(a)** shows the average % injected/expressing cells ruffling ± one StdDev for three independent experiments. **(b-g)** show examples of the actin staining for injected/expressing cells. Injected/expressing cells are marked with a white star. A cell that was expressing Rac and extremely low levels of POSH is marked with a red star. Bars equal 60μm.

Mock-injected serum starved quiescent Swiss 3T3 cells did not show significant levels of ruffling (figure 3.7 a and b), whereas almost all L61Rac-expressing cells were ruffling (figure 3.7 a and c). N POSH (figure 3.7 a and h) and C POSH (figure 3.7 a and g) do not contain POSH RBD and did not significantly effect Rac-induced ruffling. POSH RBD alone, which had a partial effect in the apoptosis assay (see figure 3.2), did not have a significant effect upon ruffling in L61Rac-co-expressing cells (figure 3.7 a and f). Full-length POSH (figure 3.7 a and d) and Y2H POSH (figure 3.7 a and e) contain the RBD and inhibited Rac-induced ruffling in around half of the co-expressing cells. Ruffling was not inhibited in cells expressing a very low level of POSH (such as the cell marked with a red star in figure 3.7 d) or Y2H POSH, suggesting a dose-dependent effect. Attempts to increase the dose of POSH relative to Rac did not prove successful: injection of more POSH DNA resulted in a large proportion of very retracted cells even after just 2h expression; use of less Rac DNA reduced the number of cells injected with Rac alone that were ruffling, making the effects of inhibitory constructs more difficult to assess.

3.2.7 Activated Rac rescues POSH-expressing cells from apoptosis

When in excess, constructs containing the Rac-binding domain of POSH inhibited activated Rac (see figure 3.7) and this may be the activity that ~~they~~ also contributed to apoptosis (see figure 3.2). If this is the case then co-expression of an excess of activated Rac with POSH may rescue cells from POSH-induced apoptosis. To test this hypothesis the NIH3T3 cell micro-injection-based apoptosis assay system described above was used. Cells were injected with flag-tagged full-length POSH at a 1:1 DNA ratio with empty vector or with myc-tagged activated mutants of various Rho GTPases. The GTPases tested were L61Rac, L61Cdc42 and V20RhoL, all of which are constitutively active mutants. RhoL is a *Drosophila* Rho GTPase that when disrupted caused severe oogenesis defects in flies [Murphy, 1996]. When introduced into mammalian cells RhoL, like L61Rac, induced lamellipodia and caused focal contact formation, but unlike L61Rac it did not activate JNK (Nobes, Nagata and Hall unpublished data).

The results from nine apoptosis experiments, where the ability of these Rho GTPases to rescue POSH-expressing cells was assessed, are summarised in figure 3.8 (A). Each Rho GTPase was tested in at least three experiments. L61Cdc42 and V20RhoL did not themselves induce apoptosis but were unable to rescue POSH-expressing cells. In contrast L61Rac was able to rescue a significant proportion of POSH-expressing cells from apoptosis (see figure 3.8 A).

(A)

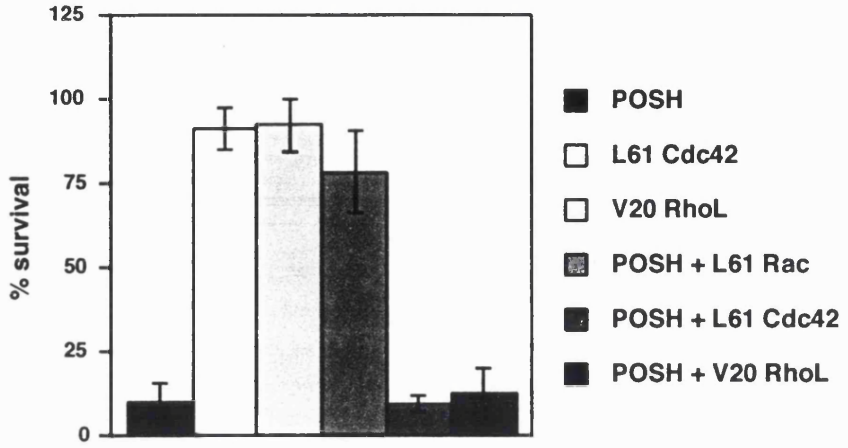

Figure 3.8 (A) Activated Rac, but not the activated mutants of other Rho GTPases, rescues POSH-expressing cells from apoptosis

This graph summarises survival data from nine apoptosis assays, each DNA combination was tested in at least three independent experiments 100 NIH 3T3 cells were injected per coverslip and in each experiment two coverslips were injected for every DNA combination tested. One coverslip was fixed 2h post-injection and the other after 7h. All constructs were injected at 0.05mg/ml of each DNA and where a single construct was injected the DNA concentration was made up to a total of 0.1mg/ml with empty vector. Rho GTPase constructs were all myc-tagged and POSH was flag-tagged. Cells were stained with hoechst to visualise nuclear morphology, plus rat anti-myc (JAC6) to visualise expression of myc-tagged proteins and mouse anti-flag (M2) to visualise expression of flag-tagged proteins. The number of expressing non-pyknotic cells were counted and survival was expressed as (%survival=number of non-pyknotic expressing cells (7h/2h)x100). The results shown are averages ± one StdDev.

(B)

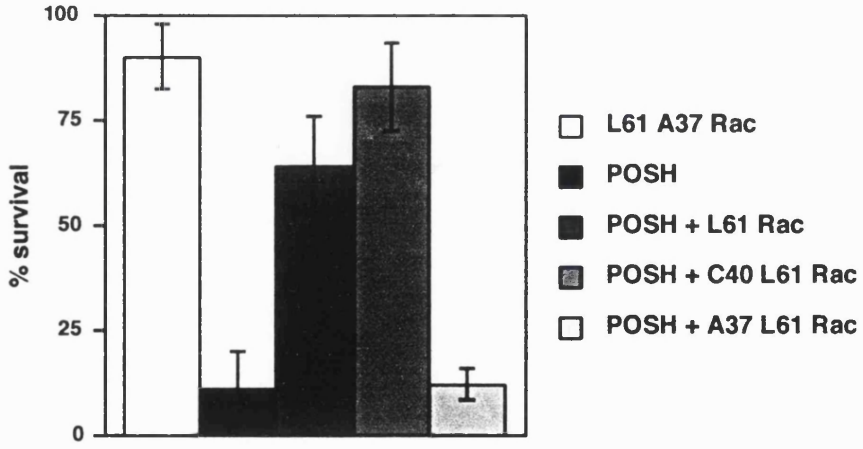

Figure 3.8 (B) Activated Rac, but not the activated mutants of other Rho GTPases, rescues POSH-expressing cells from apoptosis

This graph summarises survival data from four apoptosis assays, each DNA combination was tested in at least three independent experiments The assay to test the abiility of C40L61Rac and A37L61Rac to rescue flag-POSH-expressing cells was carried out as described in (A).

3.2.8 C40L61Rac does not bind to POSH, but still rescues POSH-expressing cells

Having found that activated L61Rac could rescue POSH-expressing cells from apoptosis we went on to test whether rescue was dependent upon an interaction between POSH and Rac. I used the A37L61Rac and C40L61Rac mutants, which do and do not bind to POSH respectively, and tested them for their ability to rescue POSH-expressing cells. The NIH3T3 cell assay was used as described ~~in~~ above. The results from four experiments, where flag-POSH was injected with empty vector or with myc-tagged Rac mutants, are summarised in figure 3.8 B.

The A37L61Rac mutant, that binds to POSH, did not induce apoptosis itself, but was not able to rescue POSH-expressing cells from apoptosis (see figure 3.8 B). Surprising the C40L61Rac mutant, that does not bind to POSH *in vitro* or *in vivo* (see figure 3.6 and [Tapon, Nagata, 1998]), was capable of rescuing POSH-expressing cells from apoptosis (see figure 3.8 B). C40L61Rac was in fact slightly more effective than L61Rac itself (see figure 3.8 B). These data suggest that Rac can provide a survival signal that is independent of binding to POSH.

3.2.9 N POSH and Y2H POSH activate the JNK kinase cascade, but not as strongly as full-length POSH

In response to many stress stimuli JNK activation accompanies apoptosis and in some cases JNK activation appears to contribute to the induction of apoptosis. In at least two cases a signaling pathway from a Rho GTPase (Cdc42) to JNK has been shown to induce apoptosis [Chuang, 1997] and [Bazenet, 1998]. It was previously shown that full-length POSH induced JNK activation, whereas C POSH did not [Tapon, Nagata, 1998]. Whether POSH-induced apoptosis was JNK-dependent was unknown. The data shown in figure 3.2 indicates that N POSH and RBD POSH are the regions of POSH required for the induction of apoptosis. I tested these regions of POSH for their ability to activate JNK. COS7 cells were transfected with flag-tagged JNK1 along with empty vector or myc-tagged L61Rac (that activates JNK), C40L61Rac (that is unable to significantly activate JNK), full-length POSH (that activates JNK) or the two POSH constructs that contribute to apoptosis, N POSH and Y2H POSH. Flag-JNK1 was precipitated from each transfected cell lysate and assayed for its ability to phosphorylate GST-c-jun substrate. The results from a representative JNK assay are shown in figure 3.9.

L61Rac, and to a slightly lesser extent full-length POSH, were seen to activate JNK (9.9 and 8.0 fold activation respectively), whereas C40L61Rac induced only modest JNK activation (3.3 fold activation), see figure 3.9. Y2H POSH and N POSH both caused significant activation of JNK (5.4 and 6.1 fold activation respectively), but neither constructs alone could reproduce the JNK activation effect of full-length POSH (8.0 fold activation), see figure 3.9.

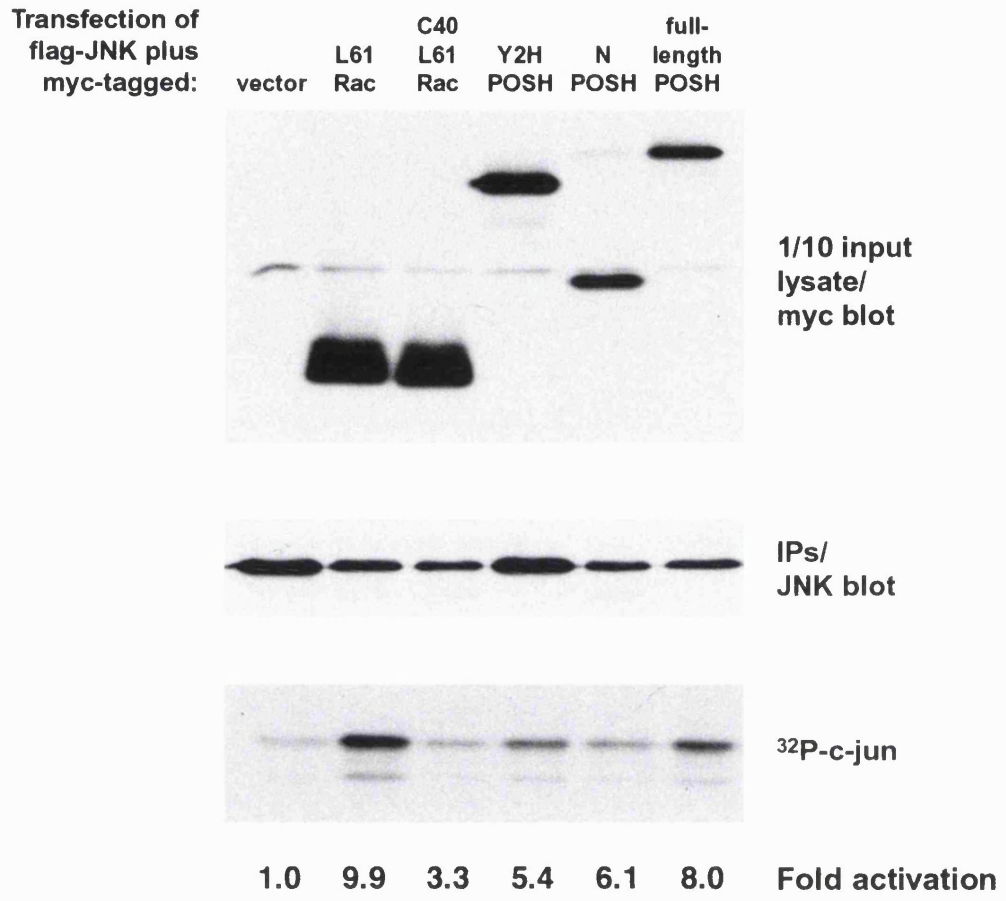

Figure 3.9 JNK activation by Rac and POSH constructs

$7x10^5$ COS7 cells were transfected, on a 10cm plate, with 2μg pCMV5-flag-JNK1 plus 2μg of empty vector (lane 1) or of DNA encoding myc-tagged: L61Rac (lane 2), C40L61Rac (lane 3), Y2H POSH (lane 4), N POSH (lane 5) or full-length POSH (lane 6). Cells were grown in the presence of 20μM BOC-Dfmk caspase inhibitor post-tranfection. Transfected cells were harvested 24h post-tranfection ~~cells~~ when the cells were only about 60% confluent (full confluency has been reported to inhibit JNK activation) . Aliquots of each lysate were separated by SDS PAGE, transferred to nitrocellulose and probed for expression of myc-tagged constructs with mouse anti-myc antibody 9E10 (top panel). Lysates were diluted into IP buffer and flag-JNK1 was precipitated using mouse anti-flag antibody M2. JNK1 activity in the precipitates was assayed using GST-c-jun as a substrate and ^{32}P-ATP labeling. After termination of the kinase reaction, immune complexes were separated by SDS PAGE and transferred to nitrocellulose. Phospho-c-jun was visualised with Biomax-MR film (bottom panel) and quantified with a phosphorimager (Biorad Molecular Imager FX and "Quantity One" software). Levels of JNK in each precipitate (middle panel) were visualised by probing of the membrane with rabbit anti-JNK antibody C-17 and were quantified using a Biorad GS-710 calibrated Imaging Densitometer and "Quantity One" software. The JNK kinase assay results were expressed as fold activation: (phospho-c-jun signal/JNK level) expressed relative to the JNK/empty vector control.

3.3 DISCUSSION

3.3.1 POSH-induced apoptosis occurs in many cell types

Having injected and transfected full-length POSH into numerous cell types, discussed above, I have come to the conclusion that POSH-induced apoptosis is not a phenomenon specific to any particular cell type or species. Interestingly both quiescent and growing Swiss 3T3 cells undergo POSH-induced apoptosis (data not shown). This suggests that an actively proliferating state is not required for cells to be susceptible to POSH-induced cell-death. At least one protein, wild type dynamin2, did require cells to be actively proliferating for apoptosis to be induced by its over-expression [Fish, 2000].

3.3.2 The apoptosis assay system

The micro-injection-based apoptosis assay system used for apoptosis assays enabled expression times to be closely controlled. Use of micro-injection, however, limited the number of cells analysed in each experiment. A better assay system may have been to create inducible stable cell lines (using the tetracyclin promoter for instance) for expression of POSH and its truncations. In this way the timing of apoptosis and the amount of protein expressed could still be closely controlled, by the addition or removal of the inducing agent, and the number of cells that could be analysed in each experiment would be much greater. This type of system has been used to analysis apoptosis responses to proteins such as c-Myc and dynamin2 [Hueber, 1997] [Fish, 2000].

3.3.3 N POSH plus POSH Rac-binding domain induce apoptosis

A schematic representation of what is known about POSH-induced apoptosis and rescue of POSH-expressing cells is shown in figure 3.10. Using truncations of POSH alone and in combination I have shown that the N-terminus of POSH, up to but not including the Rac-binding domain, plus the Rac-binding domain itself are both required in order for POSH to induce apoptosis (see figures 3.2 and 3.10). Although the activities of these two regions of POSH were both required to induce apoptosis they appeared to be able to act separately, in terms of being separate protein fragments that were not co-localised within the cell (see figure 3.3).

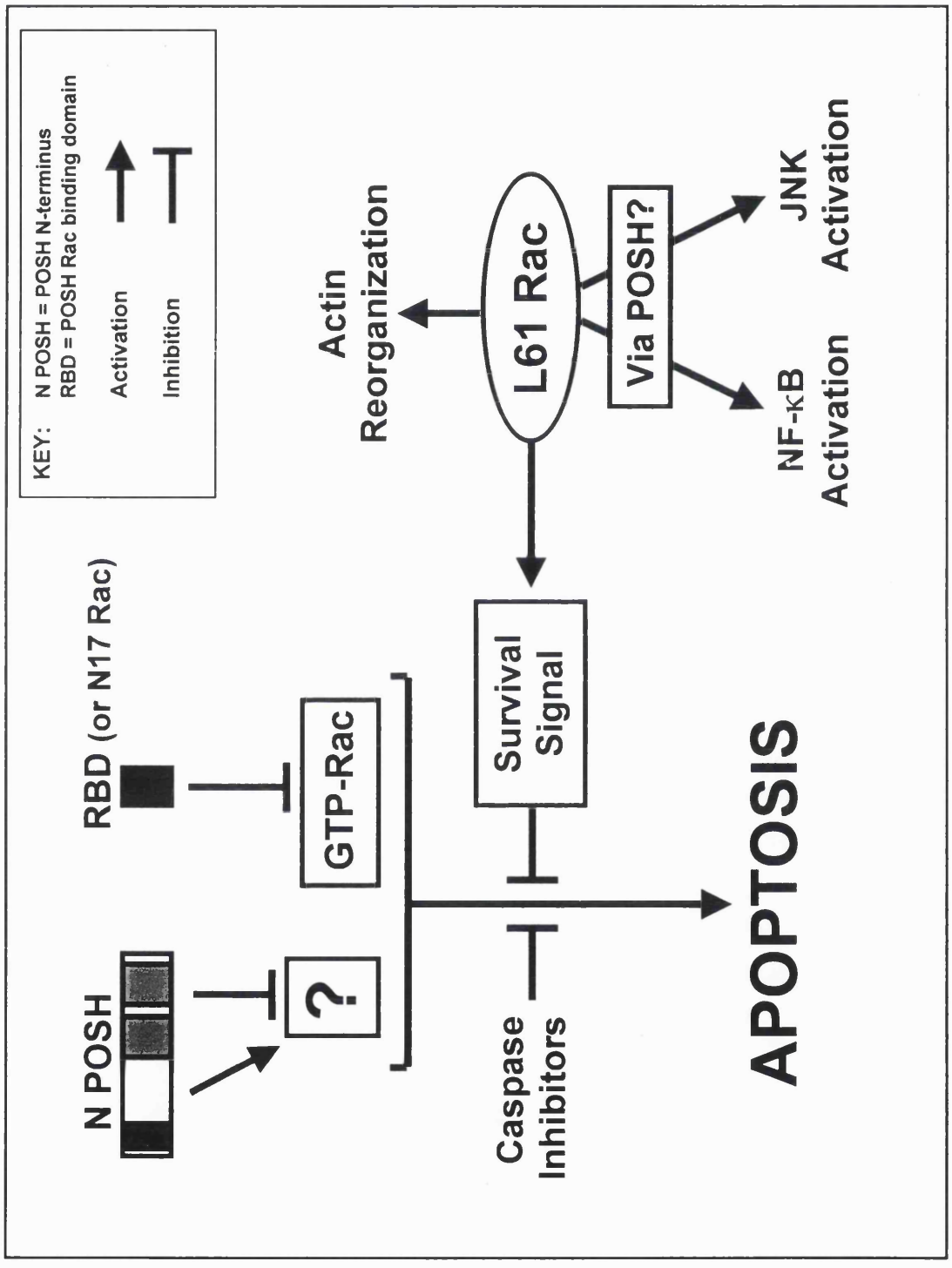

Figure 3.10 Schematic representation of what is known about POSH-induced apoptosis and rescue of POSH-expressing cells

3.3.4 JNK and POSH-induced apoptosis

Full-length POSH activates the JNK MAPK cascade. When looking for mechanisms by which the N POSH and POSH RBD together induce apoptosis JNK activation was a possible candidate. There are many examples of JNK activation that are associated with apoptosis. In most cases JNK is activated by apoptotic stimuli, but is not actually responsible for inducing apoptosis, for example in the case of detachment-induced apoptosis (termed anoikis) ~~apoptosis~~ of MDCK epithelial cells [Khwaja and Downward, 1997]). In other cases inhibition of JNK activation actually prevents apoptosis. For instance, dominant negative ASK1 prevents cisplatin (a DNA damaging agent)-induced apoptosis in human ovarian carcinoma and human kidney cells [Chen, Z, 1999].

There are at least two examples where activation of JNK by a Rho GTPase leads to apoptosis. In Jurkat cells over-expression of activated Cdc42 caused apoptosis and this Cdc42-induced cell death was inhibited by dominant negative components of the JNK pathway [Chuang, 1997]. In rat sympathetic neurons apoptosis in response to NGF withdrawal was inhibited by dominant negative Cdc42 or dominant negative components of the JNK pathway [Bazenet, 1998]. Inhibition of the JNK pathway appears to be required for the ability of Bcl-2 to suppress cell death in N18TG neuroglioma cells and c-jun over-expression antagonized the death protection activity of Bcl-2 [Park, 1997]. JNK has also been found to phosphorylate Bcl-2, and this phosphorylation was increased by co-expression of V12Rac [Maundrell, 1997]. At least one report suggests that phosphorylation inhibits Bcl-2 survival signals [Chang, 1997], therefore activation of JNK, which inactivates Bcl-2, may be a mechanism by which Rac can induce JNK-dependent cell death.

The involvement of JNK, or not, in apoptosis seems to depend upon the specific cell types and the apoptotic stimuli used. In the case of neuronal cell death following injury it has been suggested that c-jun expression is a prerequisite for the activity of other transcription factors, with which it dimerizes, that actually determine whether the cell undergoes apoptosis or survives [Herdegen, 1998]. Some groups have also suggested that the duration of the JNK response is crucial, with prolonged JNK activity being associated with apoptosis (see for instance [Roulston, 1998] and [Sanchez-Perez, 1998]).

In terms of POSH-induced apoptosis, both N POSH and Y2H POSH (which were both required for full POSH-induced apoptosis) alone caused JNK activation (see figure 3.9). Neither construct was as potent as full-length POSH (see figure 3.9). The ability of Y2H POSH to activate JNK was dependent upon the RBD, as C POSH (which is missing the RBD) showed no capacity to activate JNK in my hands (data not shown) and in previous experiments [Tapon, Nagata, 1998]. Based upon this data it is possible that an additive effect upon JNK activation by N POSH and the

Rac-binding domain of Y2H POSH contributes to POSH-induced apoptosis. This has not been tested directly by triple transfection of JNK1 with both N POSH and Y2H POSH.

Additional evidence suggests that, although the regions of POSH required to induce apoptosis can also activate JNK, activation of JNK is not essential for POSH-induced apoptosis. Firstly, Y2H POSH can be replaced by N17Rac in the apoptosis assay and N17Rac has not been shown to activate JNK. This suggests that JNK activation by the RBD of POSH is not required for POSH to induce apoptosis, or that N17Rac and Y2H POSH act via totally different mechanisms. Secondly, it was previously observed that dominant negative versions of a component of the JNK pathway (kinase dead SEK1 mutants S220A/T224L and K129R) did not rescue POSH-expressing cells from apoptosis [Tapon, Nagata, 1998]. Unless activation of a component of the JNK pathway upstream of SEK1 (which is a MAPKK) or parallel to SEK1 is the key step in POSH-induced apoptosis, this suggests that JNK activation by POSH is not essential for apoptosis [Tapon, Nagata, 1998].

If activation of JNK by N POSH and RBD POSH is not crucial for induction of apoptosis then other activities of these proteins must be considered as triggers for apoptosis. Further investigation of the binding partners and activities of N POSH is discussed in chapters 4-6. Experiments to investigate the contribution made by POSH Rac-binding domain (RBD) to apoptosis are described above and will be discussed below.

3.3.5 Inhibition of Rac by POSH RBD contributes to apoptosis

A 71 amino acid region of POSH (amino acids 292-362) containing the RBD was previously shown to be sufficient to mediate an interaction with activated Rac *in vitro* [Tapon, Nagata, 1998]. Binding to GTP-Rac was the only known activity of this region of POSH, so whether this activity of POSH RBD was responsible for its contribution to apoptosis was investigated. Four observations shown above all suggest that inhibition of Rac by POSH RBD does contribute to apoptosis:

(1) POSH RBD and full-length POSH can bind to Rac *in vivo*

I found that full-length POSH and the shorter Y2H POSH both bind to L61Rac and to activated wild type Rac *in vivo* (see figure 3.6), backing up previous *in vitro* binding studies [Tapon, Nagata, 1998]. Unfortunately, endogenous Rac was not seen to associate with POSH *in vivo*. This may be due to a lack of sensitivity in the assay and because of low levels of GTP-bound Rac, even though in this assay cells were in serum, which should activated some Rac protein. Over-expressed wild type and activated mutants of Rac were able to bind to POSH, therefore, it is still possible that the small amount of endogenous GTP-bound Rac in the cells can also bind to over-expressed POSH, but this remains to be shown directly in a biochemical assay.

(2) POSH constructs containing the RBD can inhibit L61Rac-induced lamellipodia

Full-length POSH and Y2H POSH were shown to inhibit the activity of GTP-Rac *in vivo*, using L61Rac-induced lamellipodia formation as an assay for Rac activity, in a RBD-dependent manner (see figure 3.7). POSH RBD alone was not effective in this assay, although higher levels of DNA were not tested for this construct and may prove more potent. The POSH RBD construct was also less effective than Y2H POSH or full-length POSH in the apoptosis assay (see figure 3.2). These data show a correlation between the ability to inhibit Rac and to contribute to apoptosis. N POSH is not required for binding to Rac and did not appear to induce signals that inhibit Rac-induced ruffling (see figure 3.7).

(3) N17Rac can replace POSH RBD to induce apoptosis in combination with N POSH

POSH binds GTP-Rac (see figure 3.6) and can inhibit Rac signaling (see figure 3.7), but is this what POSH RBD contributes to apoptosis? If this is the case then other Rac-inhibitors should be able to take the place of POSH RBD and, along with N POSH, induce apoptosis. This was confirmed using N17Rac, which inhibits Rac activation by inhibiting Rac GEFs, plus N POSH in apoptosis assays. Apoptosis was induced by N17Rac plus N POSH just as strongly as for full-length POSH (see figure 3.5). This suggested that POSH RBD may also contribute to apoptosis by inhibiting endogenous Rac, in this case by binding directly to Rac rather than by inhibiting Rac GEFs. In this assay it may seem more appropriate to use the Rac-binding domain from another Rac effector instead of N17Rac, but because most of the Rac effectors for which we have DNA constructs, such as PAK, also bind to Cdc42 this would complicate the assay.

(4) Adding an excess of activated Rac can rescue POSH-expressing cells

Expression of activated L61Rac, but not of other activated Rho GTPase mutants, rescued POSH-co-expressing cells (see figure 3.8). This again suggested that the activity that POSH RBD contributes to apoptosis is to inhibit activated endogenous Rac, for which excess activated Rac can compensate.

Overall, these data suggest that constructs containing POSH RBD bind to activated Rac and that this inhibits endogenous Rac activity, which contribute to apoptosis along with an unknown signal from N POSH, as depicted in figure 3.10.

3.3.6 Rescue of POSH-expressing cells by activated Rac

The discovery that C40L61Rac rescued POSH-expressing cells (see figure 3.7) was somewhat surprising, given that it had been previously shown *in vitro* [Tapon, Nagata, 1998] and is shown here *in vivo* (see figure 3.6) that this Rac effector mutant does not bind to POSH. This showed that Rac did not need to bind to POSH in order to rescue POSH-expressing cells, suggesting that C40L61Rac produces a survival signal that somehow compensates for the pro-apoptotic signals

produced by POSH without the need for a POSH-Rac interaction. The evidence discussed above suggested that the binding of POSH to Rac inhibits its activity and contributes to apoptosis, which implies that Rac activity normally has a role to play in cell survival.

One model consistent with the data is that POSH inhibits a Rac survival signal and that this, in combination with a pro-apoptotic signal from N POSH, leads to apoptosis. Models of how normal Rac signaling may relate to the induction of apoptosis by POSH and to the ability of C40L61Rac to rescue POSH-expressing cells are shown in figure 3.11. Activated endogenous Rac normally produces many signals in a controlled and balanced manner, some of which may involve endogenous POSH. When over-expressed the N-terminus of POSH may produce an excess of signals that have the potential to induce apoptosis (shown as signal A in figure 3.9). Alone this was not enough for apoptosis to be triggered under the conditions tested, when cells were in serum, 0.05mg/ml DNA was injected and expression was for 7h (see data in figure 3.2 and model in figure 3.11 a). A separate construct containing the Rac-binding domain of POSH could form a non-productive complex inhibiting signals, including any survival signals (depicted as signal B in figure 3.11), from endogenous Rac (as suggested by the data discussed in section 3.3.5). When these activities of RBD POSH and N POSH are added together apoptosis is induced (depicted in figure 3.11 b). Within full-length POSH the Rac-binding domain also allows POSH to bind to Rac and the ability of POSH to inhibit Rac-induced ruffling (see figure 3.7) suggests that this interaction can interfere with signals that require binding of Rac to other effectors *in vivo* (depicted in figure 3.11 c).

The models for POSH-induced apoptosis shown in figure 3.11 suggest that activated Rac produces signals that have the potential to induce apoptosis, such as JNK activation (discussed above) and the unknown N POSH signal (shown as signal A in figure 3.11), but also that Rac induces signals than can promote cell survival, such as signal B in figure 3.11. In a number of studies Rho GTPases have indeed been shown to have pro-apoptotic or survival effects. In one study RhoA and Rac1 were both shown to induce apoptosis in the NIH3T3 cell line that used for the apoptosis assays shown here, but only after serum starvation [Esteve, 1998]. In my hands activated Rac, in NIH3T3 cells in serum, had the opposite effect and produced a survival signal in response to the POSH apoptotic stimulus. Rac has been implicated in mediating pro-apoptotic signals in T cells, both in activated Rac2 transgenic mice [Lores, 1997] and in cultured T cells in response to activation of the Fas receptor [Brenner, 1997] [Subauste, 2000].

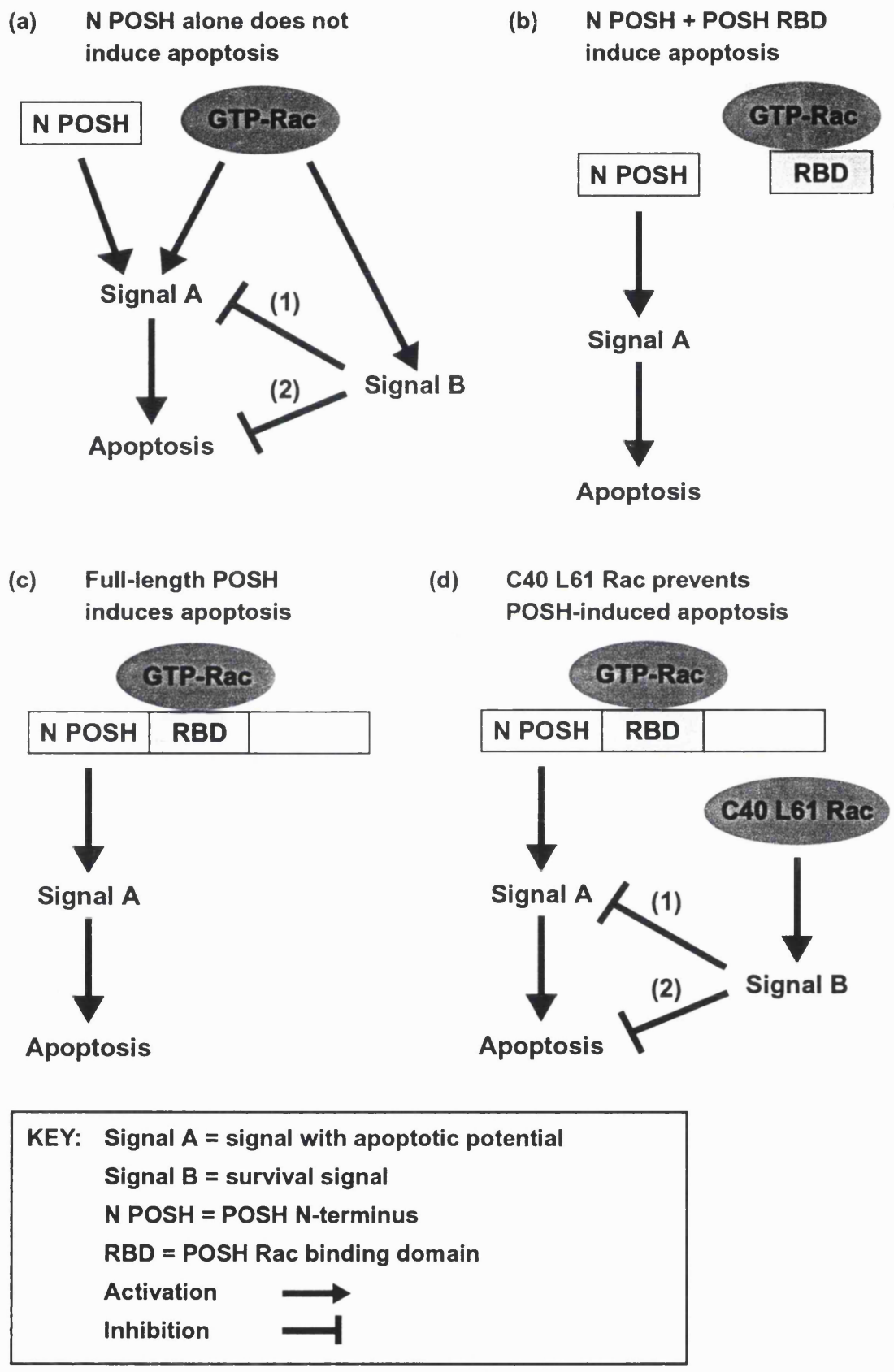

Figure 3.11 Models for the relationship between POSH-induced apoptosis and Rac survival signals (see text for discussion)

In other contexts Rac has been shown to produce pro-survival signals. For instance, after prolonged detachment from extracellular matrix fibroblasts undergo apoptosis and constitutively active Rac1 and Cdc42 were shown to rescue Balb/C3T3 fibroblasts from apoptosis induced in this way [Lassus, 2000]. Also, inhibition of Rac with dominant negative mutants transiently transfected into adherent Balb/C 3T3 fibroblasts caused p53-dependent apoptosis after 40h expression [Lassus, 2000], suggesting that activated Rac was normally required for the survival of these cells. Insulin-induced anti-apoptotic signals have also been shown to be Rac-dependent in Rat-1 cells stably expressing insulin-receptor/colony stimulating factor receptor-1 chimeras [Boehm, 1999]. Two cell types dependent upon interleukin-3 (IL3) undergo apoptosis induced by IL3 deprivation, which is inhibited by an activated Rac survival signal [Nishida, 1999] [Schurmann, 2000]

This apparently conflicting data reflects the potential of Rac to induce both pro-apoptotic and pro-survival signals and to induce signals that them selves have both pro-apoptotic and survival-inducing potential, such as JNK activation (see introduction section 1.4.4). When the normal balance of these signals is disrupted by experimental manipulations cell death or survival effects of Rac begin to be observed.

C40L61Rac or endogenous GTP Rac can produce signals (shown as signal B in figure 3.11) that somehow compensate for the apoptosis-inducing potential of the signals produced by POSH (shown as signal A in figure 3.11). These survival signals may act quite generally on the apoptosis machinery downstream of POSH (depicted as signal (2) from Rac in figure 3.11 a and d). Alternatively this survival signal may counteract more directly and specifically the signals produced by N POSH (depicted as signal (1) from Rac in figure 3.11 a and d). If the nature of the N POSH signal were known, then one could test whether C40L61Rac directly inhibits this signal, having a type (1) effect as depicted in figure 3.11 d. The ability of L61Rac to modify N POSH activities is addressed further in chapters 4-6.

The inability of by A37L61Rac, which binds to POSH, to rescue of POSH-expressing cells seemed surprising. Since carrying out these experiments it has been published that A37L61Rac as well as constitutively activating JNK and NF-κB can act as a dominant negative protein to inhibit Rac-mediated platelet-derived growth factor-induced ruffling [Schwartz, 1998]. A37L61Rac binds to POSH and may actually enhance pro-apoptotic POSH signals. Along with the observation that A37L61Rac also inhibits some of the activities of endogenous Rac it is more surprising that A37L61Rac did not itself induce apoptosis . It has, in fact, been shown that with longer expression times and more DNA than used here A37L61Rac induces membrane blebbing normally associated with apoptosis, but does not induce a full apoptosis effect [Schwartz, 1998].

3.3.7 Possible Rac survival signals

The survival signal provided by C40L61Rac (shown as signal B in figure 3.11) could be a novel signal or a known Rac signal. Of the known Rac signals there are some that have already been implicated in survival.

NF-κB

Rac can activate NF-κB [Perona, 1997] [Sulciner, 1996] and in some contexts NF-κB has been shown to act as a survival signal (reviewed in [Baichwal, 1997]). In the case of TNFα signaling, for instance, NF-κB is essential for protection against apoptosis. RelA -/- mice die on or before embryonic day 14.5 (RelA being an NF-κB subuit) as a result of massive liver apoptosis, a tissue containing high levels of TNFα [Beg, 1995]. In contrast, mice lacking both RelA and TNFα are viable with normal livers, although they are prone to infection [Doi, 1999]. The mechanisms of NF-κB-induced survival in response to stimulation by TNFα are now quite well understood. NF-κB activates the transcription of genes for TRAF1 (TNF receptor-associated factor 1), TRAF2, IAP-1 (inhibitor of apoptosis-1) and IAP-2. The products of these genes lead to inactivation of caspase 8 (also known as FLICE, FADD-like ICE), a caspase that is recruited to activated receptors such as Fas and TNFR1 [Wang, 1998]. In addition, NF-κB activates, at the level of transcription, a Bcl-2 family member called A1/Bfl-1, which appears to have pro-survival affects [Wang, 1999]. In one report Rac was shown to promote survival of Ras-transformed cells and this was dependent upon NF-κB activation [Joneson, 1999].

C40L61Rac does not activate NF-κB [Tapon, Nagata, 1998] and yet provides the survival signal that rescues POSH-expressing cells (see figure3.8 B). Also POSH itself can activate NF-κB [Tapon, Nagata, 1998], but this is sufficient to mediate survival. These points appear to rule out NF-κB activation as the Rac-induced survival signal that prevents POSH-induced apoptosis. It would be interesting to see whether the NF-κB that is activated by POSH is cleaved by caspases, also activated by POSH, to induce a dominant negative feedback loop promoting apoptosis as was shown in endothelial cells [Levkau, 1999].

Signals that induce lamellipodia formation

I tested the activated V20RhoL mutant for rescue of POSH-expressing cells because it shares many of the characteristics of C40L61Rac, being able to induce lamellipodia and associated focal complexes but not to activate JNK or NF-κB (Nobes, Nagata and Hall unpublished data). The observation that V20RhoL could not rescue POSH-expressing cells (see figure 3.8) suggests that the survival signal produced by C40L61Rac is separate from the signals that induce lamellipodia and focal contacts (as depicted schematically in figure 3.10). This assumes that Rac and RhoL

utilise the same signal transduction pathways in order to produce lamellipodia, a point that has not been addressed.

PKB/Akt activation and inactivation of the pro-apoptotic protein BAD

Rac is not the only small GTPase that can produce both pro-apoptotic signals and survival signals that have to be balanced by the cell in response to external stimuli. In fibroblasts Ras signaling through one of its effectors Raf has been reported to lead to apoptosis, whereas signaling through another Ras effector phosphatidylinositol-3-kinase (PI3K), and subsequent activation of PKB/Akt, can provide a survival signal [Kauffmann-Zeh, 1997] [Khwaja, Rodriguez-Viciana, 1997] and reviewed in [Downward, 1998]. PKB/Akt is known to prevent apoptosis by inhibition of the pro-apoptotic protein BAD (Bcl-xl/Bcl-2-associated death promoter) by phosphorylation, which inhibits its binding to other members of the Bcl-2 family and promotes its association with 14-3-3 proteins [Hsu, 1997]. The products of PI3K both activate PKB directly and activate PKD, which in turn phosphorylates PKB [Klippel, 1997]. Akt has been shown to be cleaved, and thereby inactivated, by caspases, suggesting that inactivation of Akt is important to the progression of apoptosis [Widmann, 1998].

Downstream of Ras PI3K activation leads to two separate pathways that activate Rac and PKB [Welch, 1998]. There are also some indications that PI3K may also act downstream of Rac. A direct and GTP-dependent interaction of Rac with PI3K has been reported by two groups [Bokoch, Vlahos, 1996] [Tolias, 1995]. PI3K-dependent activation of PKB/Akt has also been shown to mediate survival signals downstream of Rac that can suppress apoptosis in response to interleukin-3 depravation in BaF3 cells [Nishida, 1999] and lymphoid progenitor cells [Schurmann, 2000]. PAK, a Rac/Cdc42 effector, can also directly phosphorylate and inactivate the pro-apoptotic protein BAD [Schurmann, 2000]. In Rat-1 fibroblasts Akt/PKB, activated by Ras in a PI3K-dependent manner, has also been reported to activate PAK independently of Rac [Tang, Y, 2000]. All together these data suggest that downstream of both Rac and Ras are survival signals mediated by PI3K activation of PKB/Akt, and possibly by PAK phosphorylation of BAD. Inhibition of BAD, by PI3K activation of PKB/Akt or directly by PAK, seems to be a common survival signal induced by both Ras and Rac.

Activation of PKB/Akt is another potential Rac survival signaling pathway that could be acting to rescue POSH-expressing cells. It would be interesting to know whether the C40L61Rac mutant, which could produce a survival signal to combat POSH, is able to activate PKB/Akt. If so, then one could test whether inhibition of the PKB activator PI3K (with wortmannin or LY294002) prevents rescue of POSH-expressing cells by C40L61Rac. PAK does not bind strongly to C40L61Rac [Lamarche, 1996], so it is unlikely that direct inactivation of BAD by PAK mediates the C40L61Rac survival signal.

CHAPTER 4
THE INTERACTION OF POSH WITH DYNAMIN

4.1 INTRODUCTION

4.1.1 Searching for proteins that interact with POSH

POSH does not appear to have a catalytic site, but does contain multiple motifs that may mediate protein-protein interactions (four SH3 domains a Rac-binding region and a RING finger). This suggests that POSH is a scaffold-like protein. Scaffolds generally function by bringing together specific combinations of proteins, to which they bind directly or indirectly, into a macromolecular complex (reviewed in [Burack, 2000]). One would expect the binding partners of POSH to reflect its function *in vivo*, as appears to be the case for other scaffold proteins. For example, N-WASP binds to Cdc42-GTP, profilin, G-actin and the Arp2/3 complex, implying that it functions as a Cdc42-activated anchoring site for actin nucleation, and a large body of evidence now suggests that indeed it does (recently reviewed in [Mullins, 2000]).

Some of the POSH truncations have biological activity, indicating that they can fold correctly and are functional fragments. For instance, N POSH contributed to POSH-induced apoptosis (see chapter 3 figure 3.2), N POSH activates JNK, although not as strongly as full-length POSH, (see chapter 3 figure 3.9) and C POSH was previously shown to activate NF-κB [Tapon, Nagata, 1998]. In order to shed light upon the mechanisms by which N POSH contributes to apoptosis and activates JNK, and by which C POSH activates NF-κB, the N POSH and C POSH truncations were used to search for POSH binding partners using affinity chromatography. It was also hoped that any binding partners identified may provide clues as to the function of endogenous POSH *in vivo*.

4.1.2 Identification of dynamin2 as a binding partner for N POSH

Henrik Daub, now a former member of Alan Hall's laboratory, was screening for proteins that co-precipitate with various targets of interest to the Rho GTPase field. Henrik agreed to incorporate N POSH and C POSH into his assay and to scale-up any positive hits for identification by Mass Spectrometry (Mass Spec). The co-precipitation assay used is described in detail in figure 4.1. In summary, COS7 cells were transfected with myc-tagged constructs, tagged proteins were precipitated, washed and mixed with [^{35}S]methionine-labelled or cold cell lysates. Precipitated proteins were separated by SDS PAGE and visualised by autoradiography or silver staining respectively.

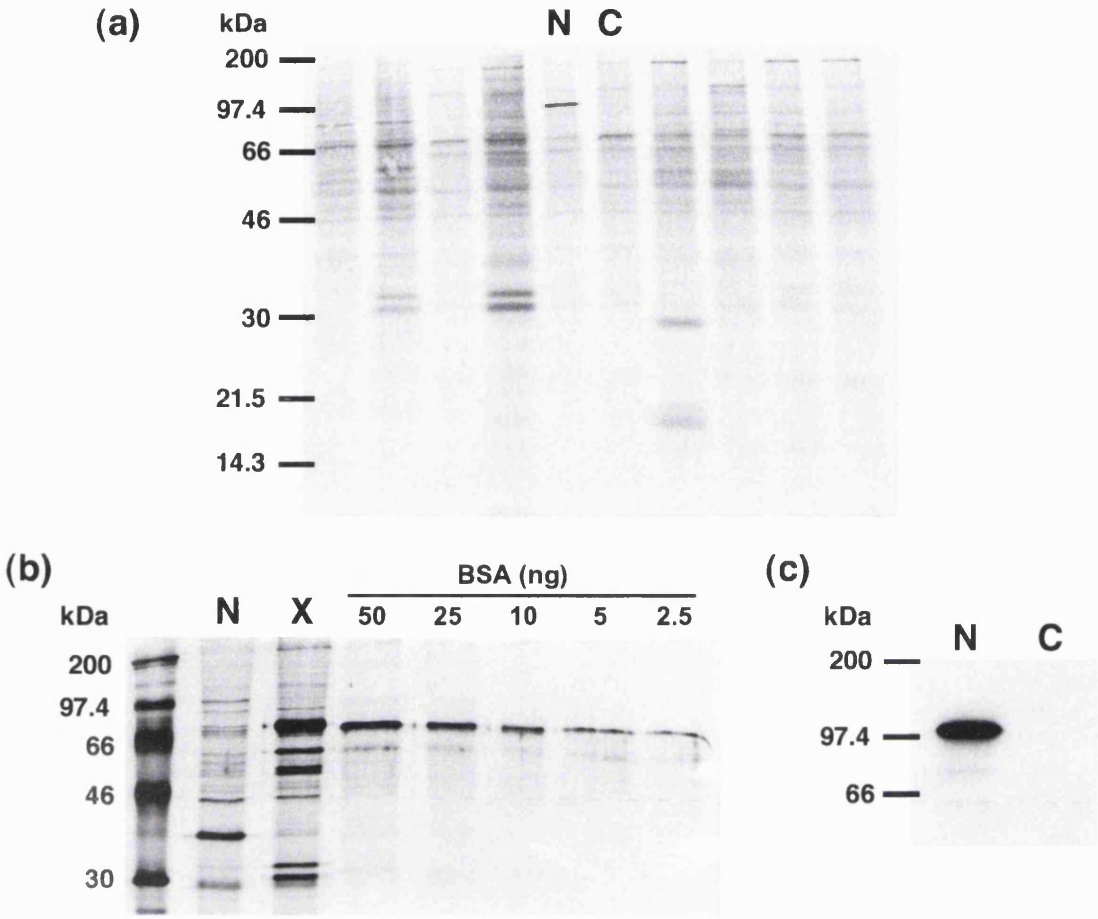

Figure 4.1 Identification of dynamin2 as a binding partner for N POSH (Henrik Daub unpublished data) **(a)** shows that N POSH (N), but not C POSH (C), binds strongly to a 100kDa protein co-precipitated from Swiss3T3 cell lysate. Additional precipitates for unrelated myc-tagged proteins are shown for comparison (unlabelled lanes). 1mg of pRK5myc-N POSH or pRK5myc-C POSH was transfected for 4h into $2x10^5$ COS7 cells. After 24h of transfection post-nuclear supernatants were prepared (lysis in 150μl of the IP lysis buffer described in the methods). Myc-tagged proteins were precipitated for 2.5h with 5μl of 9E10 that had been covalently linked to protein G-sepharose. Precipitates were washed 2x and mixed with [35S]-labelled Swiss3T3 cell lysate for 2.5h. Precipitates were again washed 2x and separated by SDS PAGE, transferred to nitrocellulose and viewed by autoradiography using Biomax MR film (Kodak). Labelled lysate was prepared as follows: 2x10cm plates of 80% confluent Swiss3T3 cells were serum-starved over night, one plate was labelled with 120mCi/ml [35S]-Met/Cys (NEN) in Met/Cys-free medium, after lysis (in 250μl lysis buffer/dish) post-nuclear supernatants were prepared, mixed together and pre-cleared with 20μl of 9E10 for 2h prior to use. **(b)** shows a silver stained gel used to estimate the yield of 100kDa N POSH-binding protein (N), as judged by comparison with BSA standards (2.5-50ng). Proteins precipitated by an unrelated myc-tagged protein (X) are shown for comparison. 14μg of pRK5myc-N POSH was transfected into $3x10^6$ COS7 cells (2x10cm dishes). Post-nuclear supernatants were prepared in 500μl of the lysis buffer/ plate and N POSH was precipitated for 2.5h with 50μl of 9E10 covalently linked to protein G-sepharose. Precipitates were washed and mixed for 2.5h with 1ml of cold HeLa cell lysate (from one 15cm dish of serum-starved 80% confluent cells), which had been pre-cleared with 9E10 for 2h. After washing 3μl from a total 35μl of co-precipitated protein was separated by SDS PAGE and viewed by silver staining (silver staining protocol described in the methods). **(c)** shows a western blot verifying that the 100kDa N POSH-binding protein is dynamin2. A section encompassing N POSH and C POSH co-precipitated proteins (lanes N and C) in the 66-200kDa range was cut from the membrane whose autoradiograph is shown in panel (a) and was probed with rabbit anti-dynamin2 antibody (provided by M McNiven, Mayo Cancer Clinic, Rochester, USA).

C POSH and N POSH each contain two SH3 domains. Any proteins that bind non-specifically to over-expressed SH3 domain-containing proteins in this assay would be expected to appear in both N POSH and C POSH precipitates, and would be treated with caution. C POSH does not contain the Rac-binding domain, so will not precipitate GTP-Rac. Additional myc-tagged constructs, unrelated to POSH, were included in the same co-precipitation experiments. These constructs provided a useful comparison to distinguish co-precipitated bands that were specific to a particular construct from non-specific background bands.

Initial experiments used radio-labelled lysates from the mouse fibroblast Swiss3T3 cell line. A typical autoradiograph from one such experiment is shown in figure 4.1 (a). No co-precipitated protein bands specific to the C POSH construct were visible (figure 4.1 (a) lane C). N POSH precipitated a strong 100kDa protein band (figure 4.1 (a) lane N), which did not appear to bind to C POSH (figure 4.1 (a) lane C) or to any of the other myc-tagged proteins included in this experiment (figure 4.1 (a) un-labelled lanes).

Lysates from the human HeLa cell line were used in subsequent experiments. Sequence information for human proteins is currently more complete than for mouse proteins, making it easier to identify human proteins after Mass Spec analysis. The co-precipitation assay was scaled-up, using cold HeLa lysate, until the 100kDa N POSH-associated band could be clearly seen by silver staining.

An example of the silver-stained results of an N POSH co-precipitation assay, using cold HeLa cell lysate, is shown in figure 4.1 (b). Only 8.5% of the total N POSH-precipitated protein was loaded onto this gel (figure 4.1 (b) lane N). Judging by the BSA standards, also shown in figure 4.1 (b), this 8.5% contained 2-5ng of the 100kDa protein. The remaining N POSH precipitate, therefore, contained 21-54ng of the 100kDa band, which was enough for Mass Spec analysis.

In Joël Vandekerckhove's laboratory in Belgium the remaining N POSH precipitated protein from the experiment described in figure 4.1 (b) underwent SDS PAGE separation and negative protein staining (with an imidazole-Zn salt-based method [Castellanos-Serra, 1999]). The 100kDa N POSH-precipitated band was excised and eluted (elution as described in [Gevaert, 1998]). Using MALDI Mass Spec and peptide fingerprinting analysis [Gevaert, 2000] Kris Gevaert identified the 100kDa N POSH-associated protein as dynamin2, a protein essential for endocytosis (see introduction section 1.6). Dynamin2 is the ubiquitous form of the protein that would be expected to be present in the HeLa cell lysate used in this experiment.

The Mass Spec result was confirmed by blotting of a section from the membrane shown in figure 4.1 (a) with a rabbit anti dynamin2 antibody. A strong dynamin2 signal was seen at 100kDa in

the N POSH precipitate (figure 4.1 (c) lane N), whereas there was no dynamin2 in the C POSH precipitate (figure 4.1 (c) lane C).

In this chapter I will describe experiments carried out to further characterise the interaction between POSH and dynamin. The ability of POSH to bind to itself, which was discovered whilst investigating the interaction between full-length POSH and dynamin, will also be discussed.

4.2 RESULTS

4.2.1. N POSH binds to dynamin2 in transfected COS7 cell lysates

From Henrik's work it appeared that N POSH, but not C POSH, expressed in COS7 cells could interact with endogenous dynamin2 from lysates derived from at least two cell types: HeLa cells, a human epithelial cell line; Swiss 3T3 cells, a mouse fibroblast cell line. I tested whether N POSH could also bind to dynamin2 directly from transfected COS7 cells.

Myc-tagged N POSH and Y2H POSH were transfected into COS7 cells. Post-nuclear supernatants were prepared and myc-tagged proteins precipitated with 9E10. Precipitates were separated by SDS PAGE and western blots were probed for endogenous dynamin2. These experiments showed that N POSH did indeed bind to endogenous dynamin2 derived from COS7 cells (figure 4.2 (a) lane 2), whereas Y2H POSH, like the shorter C POSH protein (see figure 4.1), did not bind to dynamin2 (figure 4.2 (a) lane 1).

4.2.2 Identification of the dynamin2 binding site within N POSH

Transfected N POSH was clearly able to bind to dynamin in COS7 cell lysates (see figure 4.2). This assay system was also used to test shorter regions of POSH N-terminus for binding to dynamin2. Myc-tagged constructs encoding the first two SH3 domains of POSH (SH3 1-2), minus the RING finger, or the individual N-terminal SH3 domains (SH3 1 and SH3 2) were transfected into COS7 cells. The myc-tagged proteins were precipitated, separated by SDS PAGE and the western blots probed for co-precipitated endogenous dynamin2.

Similar amounts of endogenous dynamin2 were precipitated with N POSH (figure 4.2 (a) lane 2) and with SH3 1-2 (figure 4.2 (a) lane 3). There was no dynamin2 precipitated with either of the individual N-terminal SH3 domains (figure 4.2 (a) lanes 4-5). These data indicate that both of the N-terminal SH3 domains of POSH, but not the RING finger, are required for the interaction of POSH with dynamin.

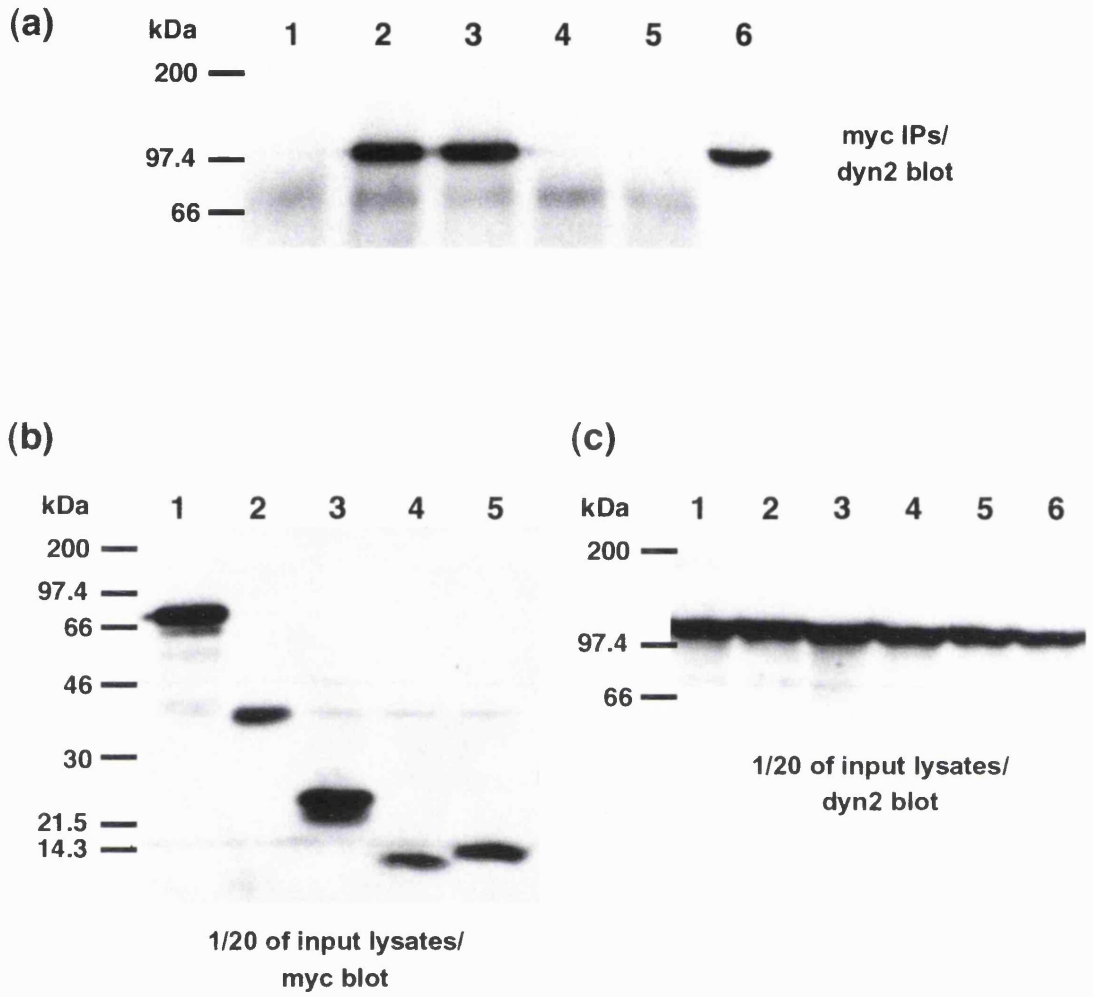

Figure 4.2 Endogenous dynamin2 is precipitated from COS7 cells with N POSH and POSH SH3 domains 1-2

$5x10^5$ COS-7 cells were transfected with 1μg of DNA encoding myc-tagged POSH truncations: Y2H POSH (1), N POSH (2), SH3 1-2 (3), SH3 1 (4), SH3 2 (5). Mock transfected COS7 cell lysate was used for comparison of dynamin levels in the precipitates (6). Transfected myc-tagged proteins were immunoprecipitated with mouse anti-myc antibody 9E10. Lysate samples (panels b and c) and precipitates (panel a) were separated by SDS PAGE. Western blots of lysate samples were probed with 9E10 (panel b), to visualise expression levels of transfected myc-tagged proteins, or with a rabbit anti dynamin2 antibody (panel c), to visualise levels of endogenous dynamin. Co-precipitated dynamin2 was visualised in myc-tagged POSH protein precipitates by probing of western blots with the rabbit anti dynamin2 antibody (panel a).

4.2.3 Binding of GST-N POSH to dynamin in rat brain lysate

The neuronal form of dynamin (dynamin1), which is specialised for its role in synaptic transmission (see introduction section 1.6), is present along with dynamin2 in whole brain lysates. We were interested to see whether N POSH could bind to endogenous dynamin1, as an indication of whether endogenous POSH could be playing a part in synaptic transmission. GST or GST-N POSH, bound to glutathione-agarose beads, were mixed with post-nuclear supernatants from adult rat brain or from Hep2 cells. Hep2 epithelial cell lysate (the cell line used for functional endocytosis assays described in chapter 5) was used as a control lysate that contains dynamin2, but not dynamin1. GST-fusion protein pull-downs, and samples of input lysate, were separated by SDS PAGE. The top of the western blots were probed with goat anti-dynamin1 (C-16, Santa Cruz) antibody (figure 4.3 panel a) to visualise endogenous dynamin and the bottom was coomassie stained to visualise GST-fusion proteins and lysate protein levels (figure 4.3 panel b).

The C-16 antibody is supposed to be specific for dynamin1, but C-16 also recognised dynamin2 from Hep2 cells (figure 4.3 (a) lanes 1 and 3). GST-N POSH bound to dynamin from both Hep2 cells (figure 4.3 (a) lane 3) and rat brain (figure 4.3 (a) lane 6), whereas GST did not (figure 4.3 (a) lanes 2 and 5). In the absence of a dynamin1-specific antibody it was not possible to conclude, from these experiments, whether the dynamin precipitated from rat brain lysate with N POSH included neuronal dynamin1.

4.2.4 Levels of POSH mRNA and protein in the brain

In the brain dynamin and a number of its binding partners are involved in the rapid endocytosis required for recovery of synaptic vesicle membranes (reviewed in [Brodin, 2000]). Dynamin1 is brain specific [Nakata, 1991] and is expressed at high levels by neurons, the cell type in which synaptic transmission occurs. There are also brain-specific or brain-enriched forms of a number of dynamin-binding proteins, for instance: intersectin1 long form [Guipponi, 1998], Syndapin1 [Qualmann, 1999] and Endophilin1 [Giachino, 1997] [Ringstad, 1997]. If POSH were involved in the specialised endocytosis involved in synaptic transmission then one would expect levels of POSH protein and mRNA to be high in the brain, and possibly for there to be brain-specific POSH isoforms.

N Tapon analysed POSH mRNA levels in adult mouse tissues by northern blotting using a cDNA fragment corresponding to base pairs 1-325 of full-length POSH, coding for POSH RING finger, as a probe [Tapon, Nagata, 1998]. A single band of POSH mRNA was detected in many tissues; levels were highest in kidney>lung>brain>testis>liver>heart, and were too low to be detect in skeletal muscle and spleen. The POSH mRNA distribution does not suggest that POSH is exclusively important in the brain, although relatively high levels are present in this tissue. There is no brain-specific splice form of POSH that can be detected by this probe.

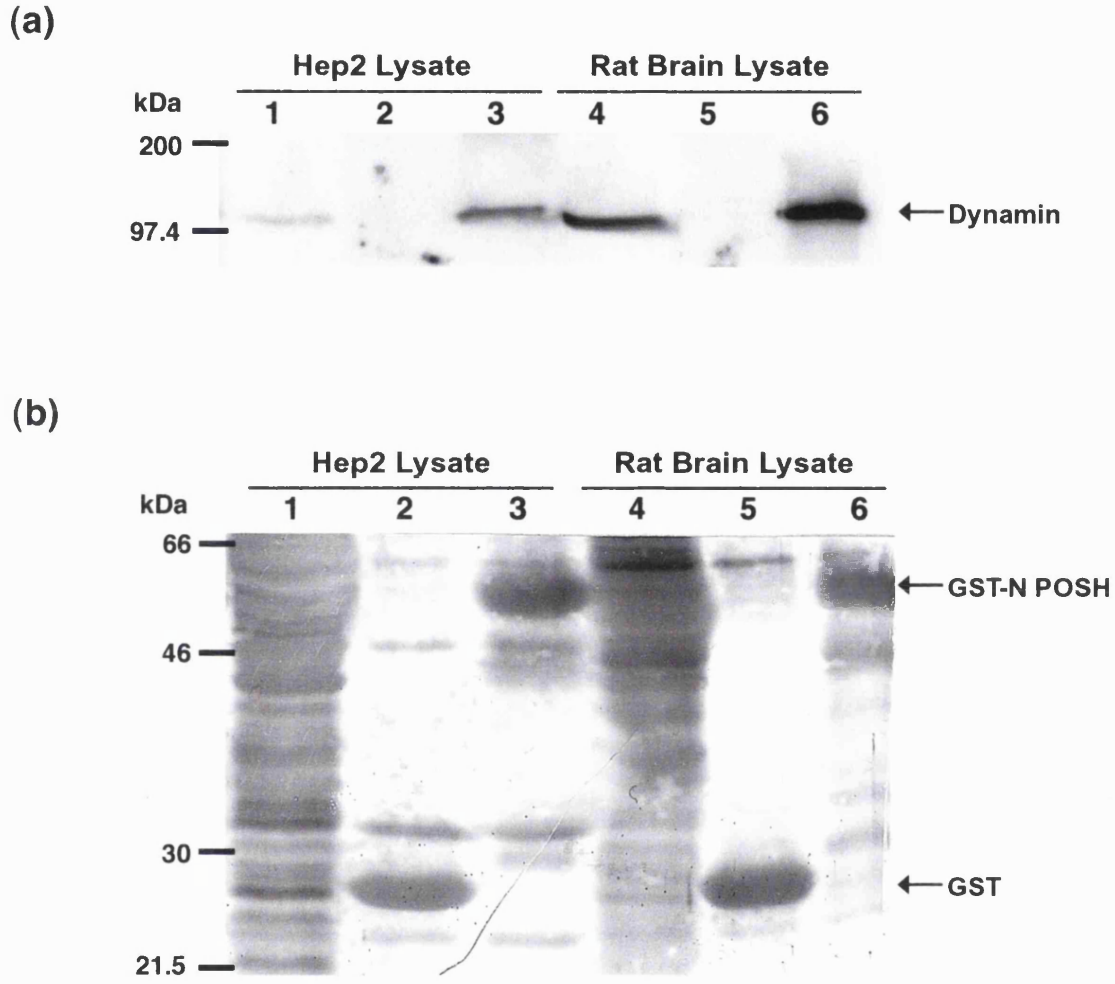

Figure 4.3 GST-N POSH binds to dynamin from adult rat brain lysate

A confluent 10cm plate of Hep2 cells was lysed in pull-down buffer and a post-nuclear supernatant was prepared. Adult rat brain post-nucelar supernatant was provided by Nic Branden (MRC LMCB, London): whole rat brains were homogenised, solubilised for 1h in a Tris-based buffer (25mMTrisHCl pH7.5, 1% NP-40, 0.5% deoxycholate, 1mM EDTA, 1mM EGTA,10mM sodium orthovanadate, protease inhibitors) and a post-nuclear supernatant was prepared. Both lysates were diluted in pull-down buffer to give a 1mg/ml protein solution. 500μl of each lysate was mixed for 2h at 4^{O}C with 20μg of GST (lanes 2 and 5) or GST-N POSH (lanes 3 and 6). Pull-downs were washed 5x in pull-down buffer and separated, along with 25ml lysate samples (lanes1 and 4), by SDS PAGE. Dynamin was visualised on western blots by probing the top of the membranes with goat-anti-dynamin1 antibody (C-16, Santa Cruz), panel a. Protein levels, in lysates and for fusion proteins, were visualised by coomassie staining of the bottom of the membranes, panel b.

Recently the Hall lab commissioned two rabbit anti-POSH antibodies (UCL69 and UCL70) to be raised against GST-N POSH by Cocalico Biologicals Inc. (Reamstown, PA, USA). UCL69 and UCL70 antisera were pre-incubated with GST or GST-N POSH and were then used to probe for endogenous POSH in rat brain lysate and various cell line lysates by western blotting. Whole cell lysates from MDCK cells (canine kidney epithelial cell line) and NIH3T3 cells (mouse fibroblast cell line), as well as adult rat brain post-nuclear supernatant, were tested for POSH-reactive protein. Lysate from COS7 cells transfected with myc-POSH provided a positive control. Western blots of the lysates were also probed with an anti-dynamin antibody that recognises dynamin1 and 2.

UCL69 and UCL70 were both able to detect over-expressed full-length myc-tagged POSH (figure 4.4 (a) and (c) lane 1) and this POSH signal was abolished by pre-blocking of the antibodies with GST-N POSH (figure 4.4 (b) and (d) lane 1). Neither the whole cell line lysates (figure 4.4 (a) and (c) lanes 3 and 4) nor the rat brain post-nuclear supernatant (figure 4.4 (a) and (c) lane 2) showed any POSH signal. Strong dynamin signals were seen in MDCK and NIH3T3 cell lysates (figure 4.4 (e) lanes 3 and 4 respectively) and even more dynamin was seen in rat brain lysate (figure 4.4 (e) lane 2).

4.2.5 N POSH binds to dynamin1, but does not require the same binding site as amphiphysin

The proline/ arginine-rich domain (PRD) of dynamin interacts with various SH3 domain-containing proteins (described in introduction section 1.6.8). POSH SH3 1-2, which is composed entirely of two SH3 domains, was sufficient to mediate the interaction of POSH with dynamin (see figure 4.2), making it likely that POSH also binds to dynamin within the SH3 domain-binding PRD region. Amphiphysins 1 and 2 require the sequence PSRPNR within dynamin1 PRD (shown in red in figure 4.6) for their interaction with dynamin [Grabs, 1997] [Owen, Wigge, 1998]. Mutation of the final arginine within this motif to glutamate (R838E) is sufficient to severely impair the interaction of dynamin with amphiphysin SH3 domain [Vallis, 1999]. H McMahon (MRC LMB, Cambridge) kindly provided us with constructs encoding wild type dynamin1 and the dynamin1 R838E mutant. These constructs were used to test the ability of GST-N POSH to bind to over-expressed dynamin1 and to determine whether POSH requires the same motif as amphiphysin for this interaction. GST-amph2 SH3, a GST fusion protein containing amphiphysin2 SH3 domain [Owen, Wigge, 1998], was used as a control (construct also provided by H McMahon).

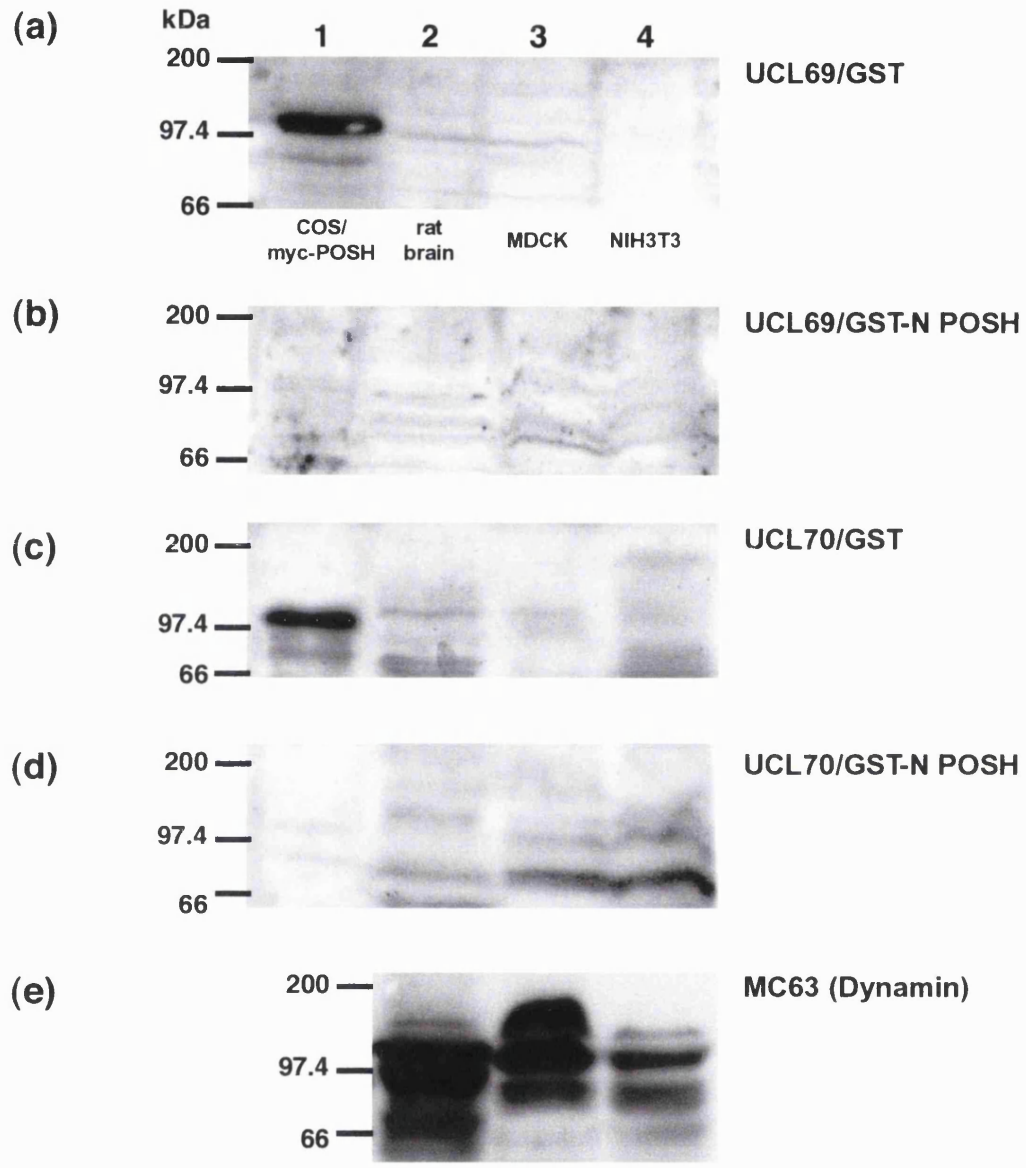

Figure 4.4 Western blots showing a lack of endogenous POSH in MDCK and NIH3T3 cell lysates and adult rat brain lysate

COS7 cells transfected with myc-POSH (1), untransfected MDCK cells (3) and NIH3T3 cells (4) were lysed directly in 1x SDS PAGE sample buffer and protein levels were estimated by running samples on SDS PAGE gels along side lysates of known protein concentration. Post-nuclear supernatant from whole adult rat brain (2) was provided by Nic Branden (MRC LMCB, London) and was prepared as described in figure 4.3. Lysate samples containing about 50μg of protein, or half as much protein for COS7 cells transfected with myc-POSH, were separated by SDS PAGE. Rabbit anti-GST-N POSH antisera, UCL69 panels (a) and (b) or UCL70 panels (c) and (d), were pre-incubated at 4°C for 1h with either GST, panels (a) and (c), or with the antigen GST-N POSH, panels (b) and (d), at a concentration of (1μl sera+5μg GST or GST-N POSH)/ml in PBS 0.05% Tween. These antibody solutions were then used to visualise, by western blotting, POSH-specific and non-specific protein bands respectively. Levels of dynamin in the lysates were detected by probing of western blots with the rabbit anti-dynamin antibody MC63, panel e, which recognises dynamin1 as well as dyanmin2.

COS7 cells were mock transfected, transfected with wild type dynamin1 or with the R838E dynamin1 mutant. Post-nuclear supernatants were prepared and aliquots of each lysate were incubated with GST, GST-amph2 SH3 or GST-N POSH, bound to glutathione-agarose beads. GST-fusion protein pull-downs, lysate samples and pull-down supernatant samples were separated by SDS PAGE. Western blots were probed for dynamin with the C16 goat-anti-dynamin antibody (top of the membranes) and for GST with a rabbit anti-GST antibody (bottom of the membranes).

Both GST-amph2 SH3 and GST-N POSH bound to endogenous dynamin2 (figure 4.5 (a) lanes 3 and 4 respectively) and over-expressed dynamin1 (figure 4.5 (b) lanes 3-4 respectively). GST did not bind to endogenous dynamin2 from mock transfected COS7 cells (figure 4.5 (a) lane 2) or to a significant amount of over-expressed dynamin1 (figure 4.5 (b) lane 2).

GST-amph2 SH3 bound to slightly more R838E dynamin1 then the GST control (figure 4.5 (f) lanes 3 and 2 respectively), indicating that this dynamin1 mutation did not totally abolish the interaction of dynamin with amphiphysin in this experiment. The amount of R838E dynamin1 bound to GST-amph2 SH3 (figure 4.5 (f) lane 3) was quite small, around the same as that in the 1/10 input lysate sample (figure 4.5 (f) lane 1). In contrast, for wild type dynamin1 a large enrichment was seen upon binding to GST-amph2 SH3 (figure 4.5 (b) lane 3) as compared with the amount of dynamin1 in the lysate sample (figure 4.5 (b) lane 1). The binding of GST-N POSH to R838E dynamin1 (figure 4.5 (b) lane 4) was not significantly reduced compared to wild type dynamin1 (figure 4.5 (f) lane 4) if expression levels are taken into account (indicated by lysate samples in figure 4.5 (f) lane 1 and (b) lane 1 respectively). The amount of dynamin1 R838E left in the pull-down supernatants further indicated that dynamin1 R838E was extracted from the lysate by binding to GST-N POSH (figure 4.5 (g) lane 3), but not by incubation with GST (figure 4.5 (g) lane 1) or GST-amph2 SH3 (figure 4.5 (g) lane 2).

These data show that N POSH is fully capable of binding to dynamin1, leaving open the possibility that POSH may have a role to play in synaptic transmission. The R838E mutation reduced binding to amphiphysin SH3 domain, but did not greatly impair the interaction of N POSH with dynamin1, suggesting that POSH does not bind to the same motif as amphiphysin within dynamin PRD.

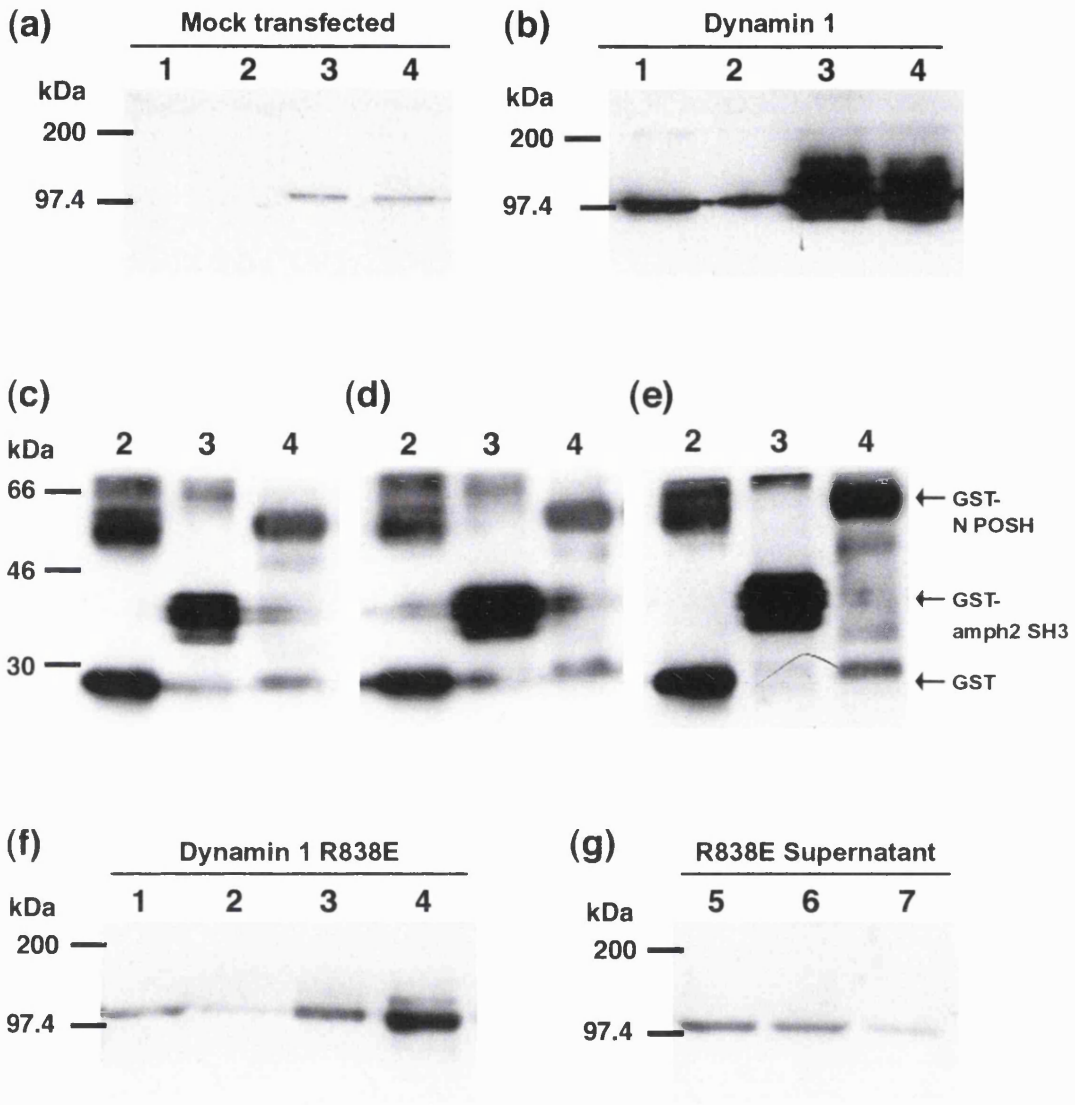

Figure 4.5 GST-N POSH binds to over-expressed wild type dynamin1 and to a dynamin1 point mutant, R838E, that has reduced binding to amphiphysin2

$2x10^6$ COS7 cells were mock transfected (panels a and c) or transfected with 4μg of DNA encoding wild type (panels b and d) or R838E mutant dynamin 1 (panels e-g). Cells were lysed in 2ml of pull-down buffer. To 500μl of each lysate was added 10μg of GST (2), GST-amph2 SH3 (3) or GST-N POSH (4), bound to glutathione-agarose beads. After 2h of mixing, and thorough washing (5x1ml), GST-fusion protein pull-downs (2-4), 50μl lysate samples (1) and 50μl pull-down supernatant samples (shown for R838E only, panel g) were separated by SDS PAGE. Dynamin was visualised, at the top of the membranes, by probing western blots with C-16 goat anti-dynamin (panels a-b and f-g). GST-fusion proteins were visualised, at the bottom of the membranes, by probing with rabbit anti GST (panels c-e).

4.2.6 Identification of the N POSH binding site within dynamin PRD

POSH SH3 domains are required for binding to dynamin (see figure 4.2), suggesting that POSH interacts with the PRD region of dynamin. To determine whether POSH really does bind to dynamin PRD, and to narrow down the POSH binding site within dynamin, we made use of GST-fusion protein constructs encoding the full dynamin1aa PRD and three shorter truncations provided by Pietro De Camilli (Yale University, USA), shown in figure 4.6. The PRD truncations are missing the final 16, 32 or 49 C-terminal amino acids, and are named GST-ΔC16 PRD and so on. Each PRD truncation removes some of the proline-rich class I and class II potential SH3 domain-binding motifs, shown in bold or underlined respectively in figure 4.5, to which POSH may bind.

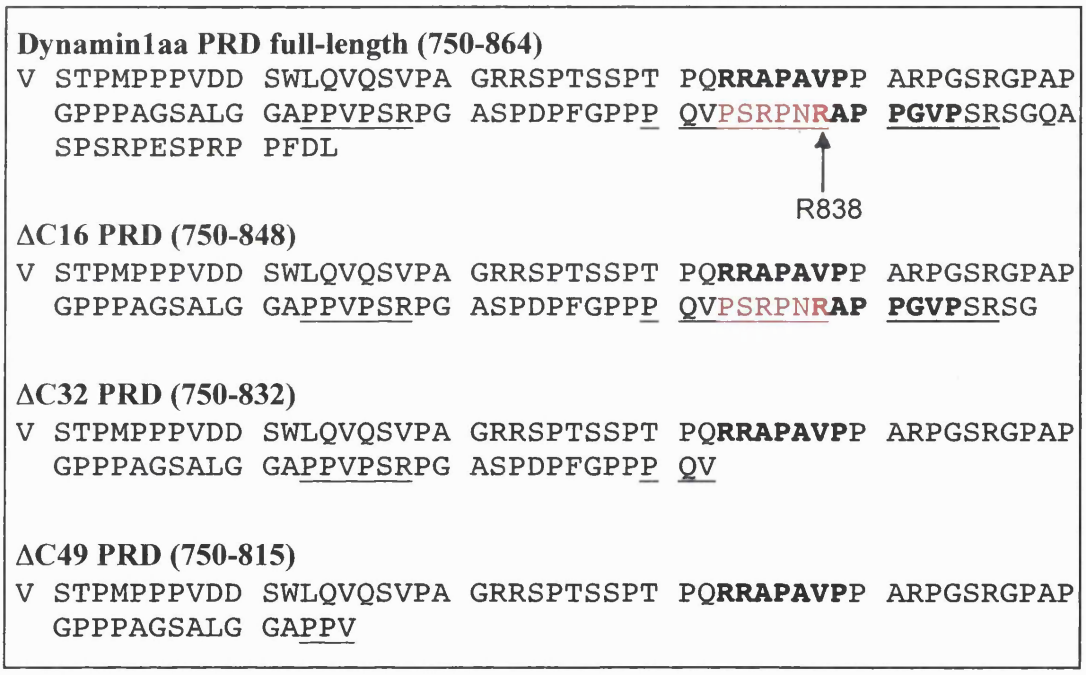

Figure 4.6 Amino acid sequences for the full dynamin1aa proline/ arginine-rich domain (PRD) and for three PRD truncations

Sequences of the full dynamin1aa proline/arginine-rich domain and of three shorter truncations. Class II SH3 domain-binding motifs (PXXPXR, where X is any amino acid) are underlined and class I motifs (RXXPXXP) are shown in bold. The amphiphysin-binding site is shown in red and the position of the R838E mutation (used for experiments described in section 4.2.5), which reduces binding to amphipysin, is noted. The four dynamin PRD protein fragments shown were made as GST-fusion proteins, from constructs provided by Pietro De Camilli (Yale University, New Haven, USA), which were used for the experiments described in section 4.2.6. Note that each truncation contains a deletion of the number of C-terminal amino acids in its name eg. ΔC32 PRD is missing the final 32 amino acids.

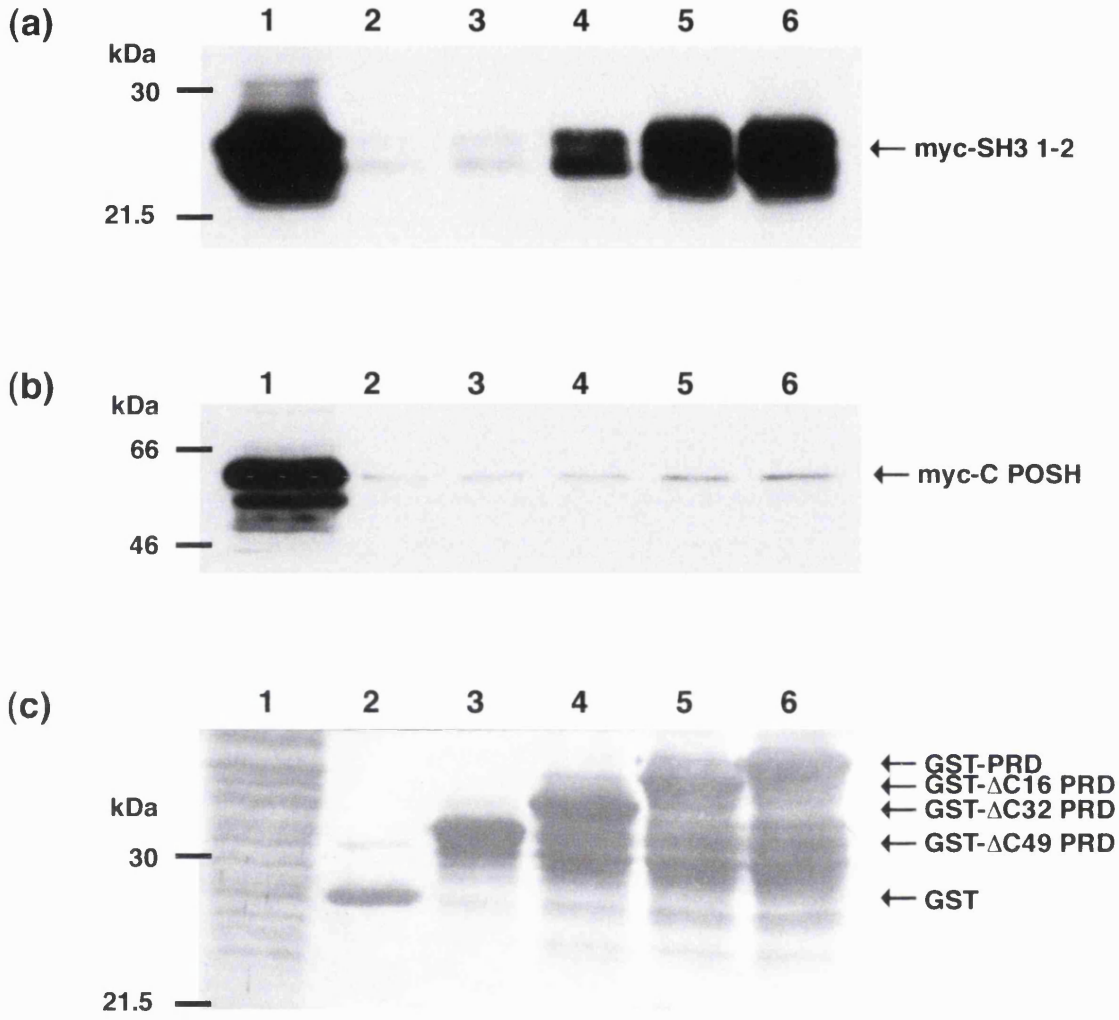

Figure 4.7 POSH SH3 domains 1-2 bind to dynamin1 proline/arginine-rich domain
$3x10^6$ COS-7 cells were transfected with 3μg of myc-tagged C POSH or SH3 1-2 DNA. Lysate samples containing about 500μg of protein were mixed with 20μg of GST (lane 2), GST-ΔC49 PRD (lane 3), GST-ΔC32 PRD (lane 4), GST-ΔC16 PRD (lane 5) or GST-PRD (lane 6). After 2h of mixing, and thorough washing (5x1ml), GST-fusion protein pull-downs (lanes 2-6) were separated, along with lysate samples containing 25μg of protein (lane 1), by SDS PAGE. SH3 1-2 and C POSH were visualised by probing of western blots with mouse anti-myc antibody (9E10) panels (a) and (b) respectively. GST-fusion proteins were visualised by indian ink staining of the membranes, panel (c).

COS7 cells were transfected with either SH3 1-2 or C POSH and post-nuclear supernatants were prepared. Aliquots from each lysate were mixed with GST-PRD, GST-ΔC16 PRD, GST- ΔC32 PRD, GST-ΔC49 PRD and GST, bound to glutathione-agarose beads. GST-fusion protein pull-downs and lysate samples were separated by SDS PAGE. The western blots were probed for myc-tagged SH3 1-2 (figure 4.7 panel a) and C POSH (figure 4.7 panel b) and the membranes were stained with indian ink in order to visualise the fusion proteins (figure 4.7 panel c).

The amount of C POSH associated with the dynamin1 PRD GST-fusion proteins was very small (figure 4.7 (b) lanes 3-6) and was little more than that associated with GST alone (figure 4.7 (b) lane 2). In contrast, large amounts of SH3 1-2 was associated with both GST-full-length PRD (figure 4.7 (a) lane 6) and with the shorter GST-ΔC16 PRD protein (figure 4.7 (a) lane 5). A smaller, but significant, amount of SH3 1-2 was seen to bind to GST-ΔC32 PRD (figure 4.7 (a) lane 4). GST-ΔC49 PRD and GST associated with insignificant amounts of SH3 1-2 (figure 4.7 (a) lanes 3 and 2 respectively). For unknown reasons the myc-SH3 1-2 protein appeared as a doublet (see figure 4.7 panel a), which is something that was also occasionally observed in other experiments (for example see figure 4.2 (b) lane 3).

These data show that the two N-terminal SH3 domains of POSH, but not the two C-terminal SH3 domains, interact with dynamin1 proline/arginine-rich domain. The ability of SH3 1-2 to bind to the different PRD truncations (figure 4.7 (a) lanes 3-6) allowed the POSH binding site within dynamin1 PRD to be mapped to the amino acids shown in figure 4.8 (b) according to the following arguments. Firstly, deletion of the final 32 amino acids (aa) of dynamin1 PRD only partially destroyed the interaction with POSH, while deletion of 49aa completely destroyed the interaction. This shows that the region of dynamin1 PRD N-terminal to, and including, amino acid 815 (the last amino acid in GST-ΔC49 PRD) is not required for the interaction of POSH with dynamin. It also suggests that an SH3 domain-binding motif (shown in red in figure 4.8 (b)), which remains intact in the 32aa truncation and is destroyed (half deleted) by truncation of 49aa, may mediate the weak interaction of SH3 1-2 with GST-ΔC32 PRD.

Secondly, the interaction of SH3 1-2 with the full GST-PRD protein was no stronger than with the 16aa truncation. This suggests that the region C-terminal to dynamin1 amino acid 848 (the last amino acid in GST-ΔC16 PRD) is not required for dynamin binding to POSH.

Finally, GST-ΔC16 PRD bound more strongly than GST-ΔC32 PRD to SH3 1-2. This suggests that amino acids 833 to 848 (shown in green in figure 4.8 (b)), which are present in GST-ΔC16 PRD and not in GST-ΔC32 PRD, are required for strong binding of POSH to dynamin. The amphiphysin-binding site lies within this region, double underlined in figure 4.8 (b), but

experiments using the R838E mutant to destroy this site (described in section 4.2.5 above) suggested that this particular motif is not essential for binding of POSH to dynamin. The only class I SH3 domain-binding motif (shown in bold in figure 4.8 b) within the region that is present in GST-ΔC16 PRD and not in GST-ΔC32 PRD (shown in green in figure 4.8 b) should also be destroyed by the R838E mutation. It is, therefore, unlikely that this particular motif is essential for binding of POSH to dynamin.

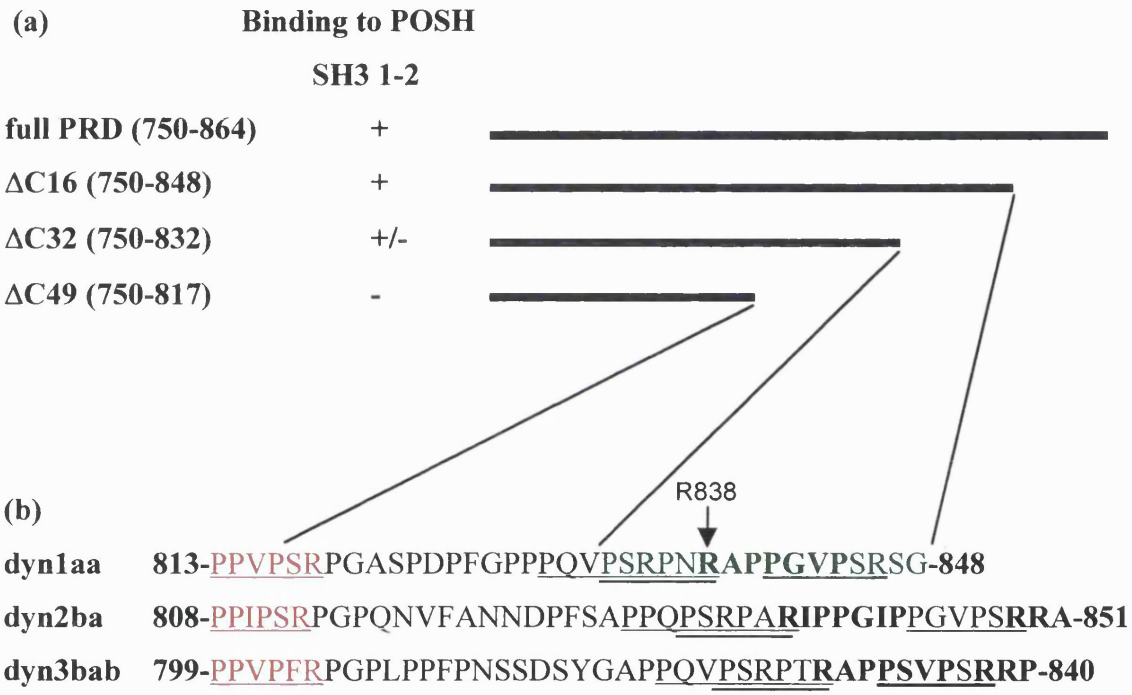

Figure 4.8 Summary of the regions of dynamin1 PRD required for binding to POSH

(a) Schematic summary of the data shown in figure 4.7, for the binding of POSH SH3 domains 1-2 to dynamin1aa PRD GST-fusion protein constructs. (+) positive interaction; (+/-) weak interaction; (-) no interaction. The full sequences of these constructs are shown in figure 4.6.

(b) The amino acid sequence of the region of dynamin1aa PRD that encompasses the motifs required for binding to POSH SH3 1-2. The equivalent regions of dynamin2ba and dynamin 3bab PRDs are also shown. Class II SH3 domain-binding motifs, (PXXPXR, where X is any amino acid) are underlined and class I motifs (RXXPXXP) are shown in bold. The one motif still present in GST-ΔC32 PRD, to which SH3 1-2 bound weakly, but half deleted in GST-ΔC49 PRD, to which SH3 1-2 did not bind, is shown in red. The region that appears to be required for the strong binding of POSH to dynamin PRD is shown in green. The amphiphysin-binding site (PSRPNR), double underlined, does not appear to bind to POSH (according to experiments using the R838E mutant discussed in section 4.2.5).

4.2.7 Co-precipitation of dynamin2 with full-length POSH

Having found that truncations of POSH containing the N-terminal two SH3 domains could bind to dynamin we went on to test whether myc-tagged full-length POSH could also bind to endogenous dynamin2. As discussed in chapter 3, full-length POSH induces apoptosis. Despite this, with relatively short expression times (24-30h) a reasonable yield of transfected POSH protein could be recovered. Addition of a general caspase inhibitor, BOC-Dfmk, to the media also helped to increase protein yields, especially with longer expression times (see chapter 3).

COS7 cells were transfected with myc-tagged full-length POSH or N POSH, with or without BOC-Dfmk. Cells were harvested after 24h and post-nuclear supernatants were prepared and myc-tagged proteins were precipitated. Precipitates were separated by SDS PAGE and co-precipitated dynamin was visualised by probing of western blots with the rabbit anti-dynamin2 antibody. The membranes were stripped and re-probed with a mouse-anti-myc antibody in order to visualise precipitated POSH constructs.

In the absence of the caspase inhibitor very little endogenous dynamin2 could be precipitated with myc-POSH (figure 4.9 (a) lane 2). An increase in dynamin2 precipitated with full-length POSH was seen when BOC-Dfmk was included (figure 4.9 (a) lane 3). A much larger amount of dynamin2 was co-precipitated with N POSH, with or without the caspase inhibitor (figure 4.9 (a) lanes 4-5), than with full-length POSH.

From these data it appears that full-length POSH can bind to dynamin2 and that this interaction is slightly increased by the addition of a caspase inhibitor. Even so, the interaction of full-length POSH with dynamin2 is weak compared with that of the N POSH truncation.

4.2.8 Evidence for a POSH homophilic interaction

For many Rho GTPase effector proteins their inactive state is maintained by autoinhibitory homophilic interactions, as discussed in the introduction. We were interested in whether POSH can also interact with itself, especially as this may inhibit its interaction with other proteins and could explain the observed weak interaction of full-length POSH, as compared with the N POSH truncation, with dynamin (see figure 4.9).

The ability of full-length POSH and various POSH truncations, co-transfected into COS7 cells, to bind to themselves and to each other was tested. The results from two experiments are shown in figure 4.10. In the first experiment (figure 4.10 panels a and b) the ability of full-length POSH to bind to itself was tested by co-transfection of myc- and flag-tagged POSH constructs. In addition flag-Y2H POSH was co-expressed with myc-Y2H POSH and with the shorter myc-C POSH construct.

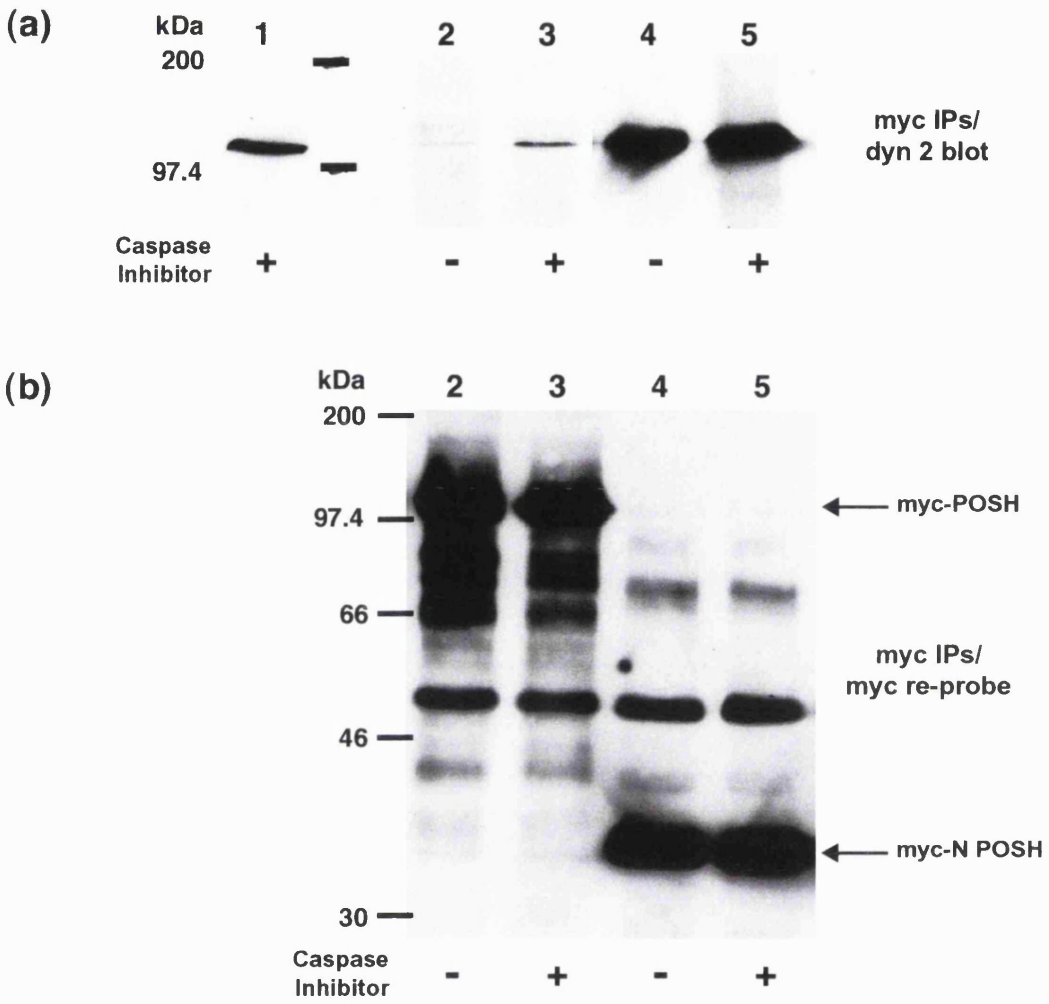

Figure 4.9 Caspase inhibitors increase co-precipitation of endogenous dynamin2 with full-length POSH

$5x10^5$ COS7 cells were mock transfected with empty vector. 2x ($5x10^5$) COS7 cells were transfected either with myc-full length POSH or myc-N POSH. For the mock transfected cells, and for one dish from each transfection, the general caspase inhibitor BOC-Dfmk (20μM final concentration, from a 20mM stock in DMSO) was added to the post-transfection media. For all cells the media was made up to 0.1% DMSO. 24h post-transfection post-nuclear supernatants were prepared and transfected proteins were precipitated with mouse anti-myc antibody 9E10. Precipitates from transfections treated with BOC-Dfmk (lanes 3 and 5) or just with DMSO (lanes 2 and 4) and samples of mock transfected cell lysate (lane 1) were separated by SDS PAGE. Dynamin2 in mock transfected lysate (lane 1) and co-precipitated with POSH constructs (lanes 2-5) was visualised by western blotting with rabbit anti-dynamin2 antibody (panel a). Blots were stripped and re-probed with 9E10 in order to visualise precipitated POSH constructs (panel b).

In the second experiment (figure 4.10 panels c and d) myc-C POSH was again co-transfected with flag-Y2H POSH, but also with flag-N POSH. In all cases the myc-tagged protein was precipitated. In the first experiment, as some co-expressed proteins were the same size, precipitates were split in half before separation by SDS PAGE and probing of western blots with either anti myc or mouse anti-flag antibodies. For the second experiment precipitates, and their supernatants, were separated by SDS PAGE and western blots were probed with a mixture of anti-myc and anti-flag antibodies to visualise proteins with either tag.

Only a small amount of myc-tagged full-length POSH was present in the precipitate (figure 4.11 (b) lane 1), even so this myc-POSH protein was seen to bind to a small amount of flag-POSH (figure 4.11 (a) lane 1). The C-terminal POSH construct, myc-Y2H POSH, bound to a flag-tagged version of itself (figure 4.11 (a) lane 2) and to the shorter myc-C POSH protein, lacking the Rac-binding domain, (figure 4.11 (a) lane 3 and (c) lane 2). In contrast, the N-terminal POSH fragment, N POSH, was not co-precipitated with C POSH (figure 4.11 (c) lane 1), but remained in the supernatant (figure 4.11 (c) lane 1).

These data show that full-length POSH can interact with itself and that this is mediated by regions within POSH C-terminus. Y2H POSH, which contains the Rac-binding domain, is able to bind to C POSH, which lacks this domain. This shows that the Rac-binding domain is not required on both sides of the POSH-POSH interface in order to mediate the POSH-POSH homophilic interaction.

4.2.9 Rac does not increase the binding of POSH to dynamin

Full-length POSH bound very weakly to dynamin when compared with the N POSH truncation (see figure 4.9). One explanation for this could be that steric hindrance of the POSH-dynamin interaction is caused by the POSH-POSH homophilic interaction, see section 4.2.8 above. The Y2H POSH truncation undergoes a homophilic interaction (see section 4.2.8) and contains the POSH Rac-binding domain. In some cases the binding of an activated Rho GTPase to an effector protein has been shown to relieve autoinhibitory homophilic interactions, for example this is true of the Cdc42 effector WASP [Kim, 2000] and the Rac and Cdc42 effector PAK1 [Tu, 1999]. In a similar way it was possible that binding of activated Rac to Y2H POSH could inhibit its homophilic interaction and may increase the accessibility of full-length POSH SH3 domains 1 and 2 to dynamin.

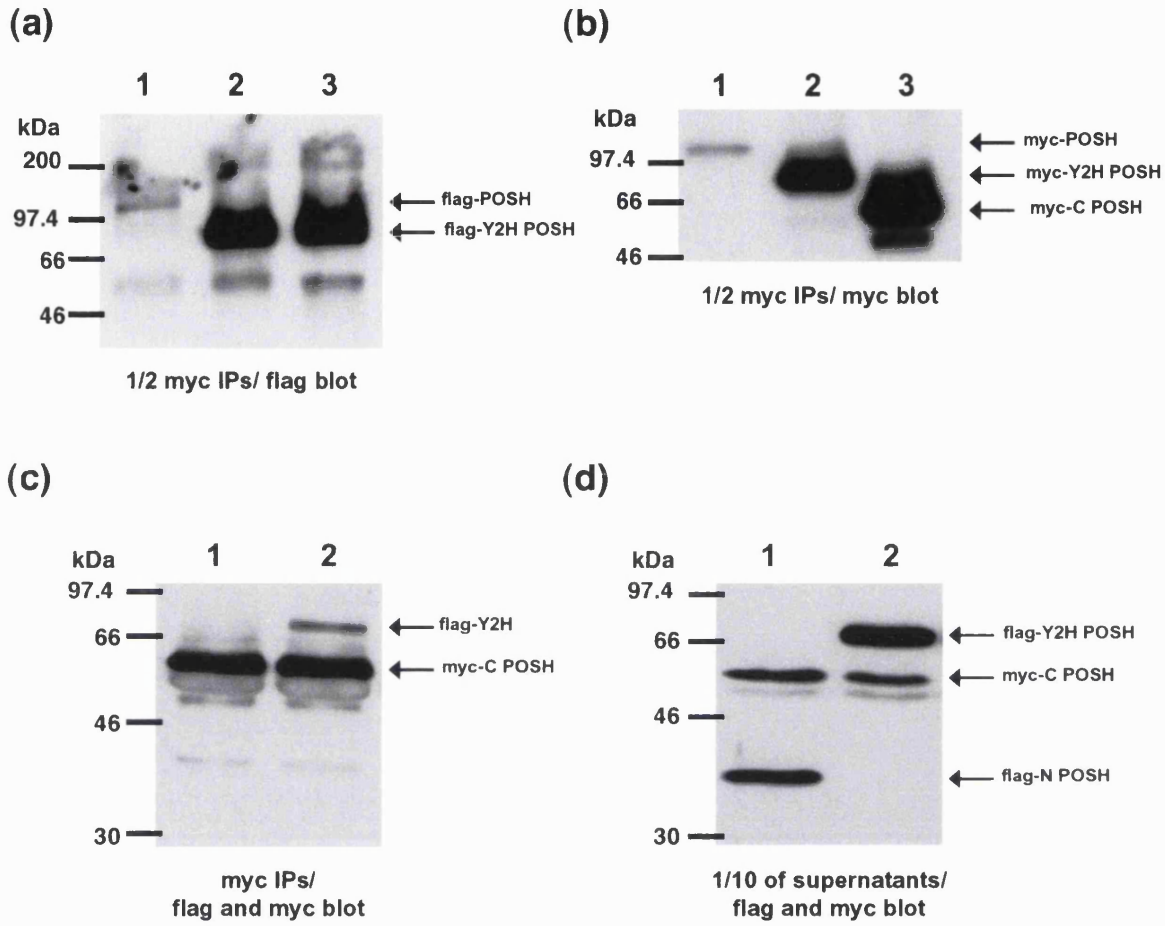

Figure 4.10 C-terminal POSH constructs, Y2H POSH and C POSH, and full-length POSH bind to each other and not to N POSH

(a) and **(b)** $5x10^5$ COS-7 cells were co-transfected with: myc and flag-tagged full-length POSH (POSH, lane 1); myc-Y2H POSH and flag-Y2H POSH (Y2H, lane 2); myc-C POSH (C) and flag-Y2H POSH (lane 3). Myc-tagged proteins were precipitated with 9E10 covalently linked to protein G-sepharose, kindly provided by Sonja Krugman (Hall lab). Precipitates were split in half and separated by SDS PAGE. Precipitated myc-tagged proteins were visualised by probing of western blots with mouse anti-myc, 9E10, (panel b) and co- precipitated flag-tagged proteins by blotting with mouse anti-flag, M2, (panel a).

(c) and **(d)** $2.5x10^5$ COS-7 cells were co-transfected with flag-N POSH and myc-C POSH (lane 1) or flag-Y2H POSH and myc-C POSH (lane 2). myc-C POSH was precipitated with 9E10. Precipitates (panel c) and precipitate supernatant samples (panel d) were separated by SDS PAGE. Myc and flag-tagged proteins were visualised by probing of western blots with 9E10 + M2.

To test whether active Rac could increase binding of POSH to dynamin COS7 cells were co-transfected with flag-tagged POSH alone or with myc-tagged wild type (wt) Rac or L61 Rac. Control transfections of proteins that do or do not bind to dynamin, flag-N POSH and flag-Y2H POSH respectively, were also included. Post-nuclear supernatants were prepared and flag-tagged POSH proteins were precipitated. Precipitates and lysate samples were separated by SDS PAGE and transferred to nitrocellulose. The top of each membrane was probed for co-precipitated endogenous dynamin2 (figure 4.11 a) and the bottom of the membranes were probed for co-precipitated myc-tagged Rac proteins (figure 4.11 c). Precipitated flag-tagged POSH proteins were visualised by stripping of the dynamin2 blot and re-probing for flag (figure 4.11 b). Myc-tagged Rac proteins in lysate samples were also visualised by probing of the bottom of the membranes for myc (figure 4.11 d).

In control transfections N POSH was seen to bind to dynamin2 (figure 4.11 (a) lane 2) and Y2H POSH did not bind to any dynamin2 (figure 4.11 (a) lane 3), as shown previously (see figure 4.2). In this experiment there was no detectable dynamin2 bound to full-length POSH (figure 4.11 (a) lane 4). The two Rac constructs co-expressed with POSH were both present at high levels in the transfected cell lysates (figure 4.11 (d) lanes 5-6). A small amount of wt Rac (presumable the GTP-bound portion) and a larger amount of L61 Rac were seen to be co-precipitated with POSH (figure 4.11 (c) lanes 5 and 6). Co-expression of wt Rac or L61 Rac with POSH did not increase the amount of endogenous dynamin2 bound to POSH (figure 4.11 (a) lanes 5 and 6 respectively).

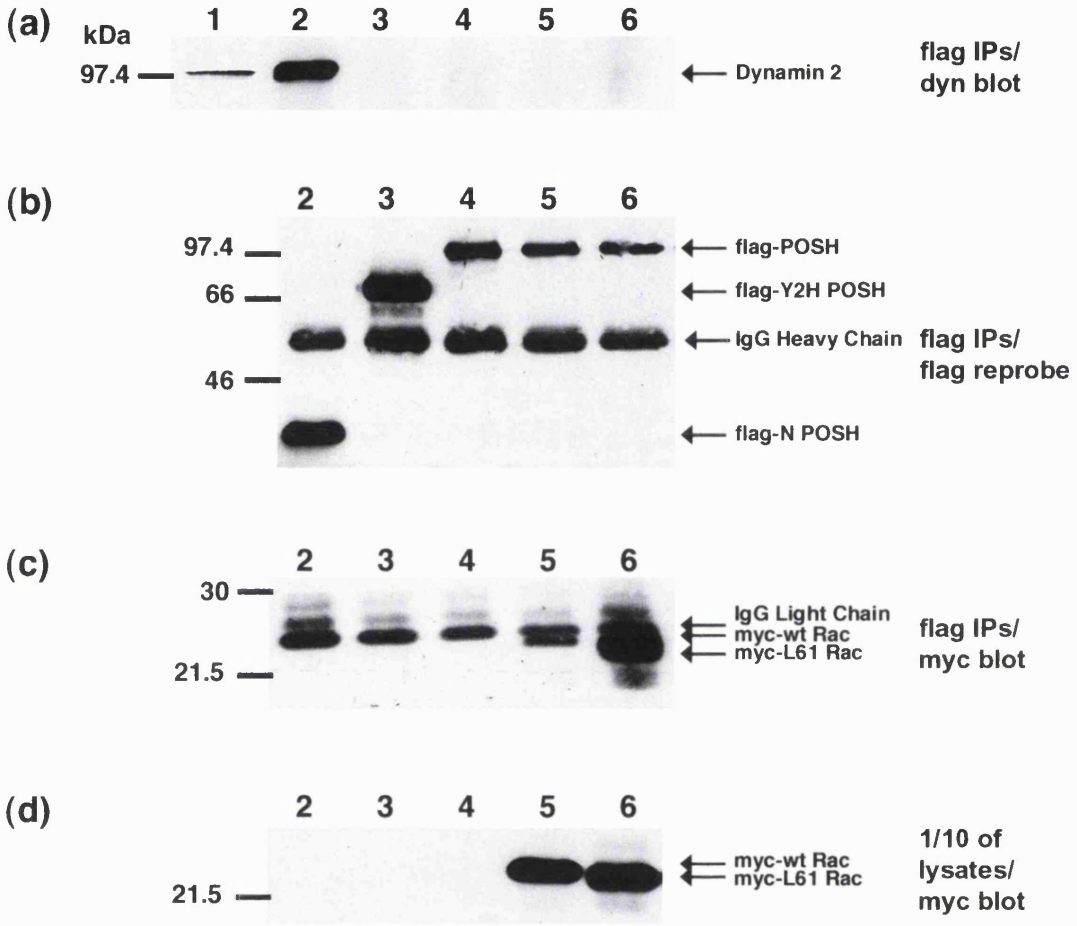

Figure 4.11 Co-expression of L61Rac does not increase binding of full-length POSH to endogenous dynamin2

5x10^5 COS-7 cells were mock transfected or transfected with the following pRK5 DNA constructs: flag-N POSH (lane 2); flag-Y2H POSH (lane 3); flag-POSH (lane 4); flag POSH and myc-wild type (wt) Rac (lane 5); flag-POSH and myc-L61 Rac (lane 6). flag-tagged POSH proteins were precipitated with mouse anti-flag antibody M2. Immunoprecipitates (panels a-c, lanes 2-6), samples of mock transfected COS7 cell lysate (panel a, lane 1), and samples of transfected cell lysates (panel d) were separated by SDS PAGE and transferred to nitrocellulose. Co-precipitated endogenous dynamin2 was visualised at the top of the membrane and Rac at the bottom of the membrane by probing of western blots with rabbit anti-dynamin2 (panel a) or mouse anti-myc, 9E10, (panel c) antibodies respectively. The dynamin blot was stripped and precipitated flag-tagged POSH proteins were visualised by reprobing with M2 (panel b). myc-tagged Rac proteins in lysate samples were also visualised by probing of western blots with 9E10 (panel d).

4.3 DISCUSSION

4.3.1 The interaction of POSH N-terminal SH3 domains with dynamin

The major binding partner for N POSH in HeLa and Swiss 3T3 cell lysates appeared to be dynamin2 (Henrik Daub and Kris Gevaert unpublished data, see figure 4.1). Results shown here confirm that both transfected myc-N POSH and GST-N POSH fusion protein interact with endogenous dynamin2 derived from a number of cell line lysates and from whole rat brain lysate (see figures 4.2 and 4.3). Within N POSH the two SH3 domains alone were sufficient for POSH to bind to dynamin (see figure 4.2). The individual SH3 domains, as myc-tagged transfected proteins, did not bind to detectable levels of endogenous dynamin2 (see figure 4.2).

It is possible that the individual POSH N-terminal SH3 domains interacted too weakly with dynamin to be detected with the relatively low endogenous levels of dynamin in COS7 cells. In order to clarify whether POSH SH3 1 or SH3 2 individually are able to bind even weakly to dynamin at least two approaches could be used. Firstly, GST-fusion proteins of individual POSH SH3 domains could be used to probe brain lysate, where dynamin levels are high, or could be tested for binding to recombinant dynamin protein. Probing of brain lysate, as a rich source of dynamin, with SH3 domain GST-fusion proteins has proved a successful combination to detect an interaction between dynamin and the individual SH3 domains of other binding partners (see for instance [Gout, 1993] [Grabs, 1997] and [Yamabhai, 1998]). Secondly, point mutations could be made within pRK5myc-SH3 1-2 that destroy the function of each SH3 domain individually. These mutants could be transfected into COS7 cells and tested for binding to endogenous dynamin2 or to dynamin1 PRD GST-fusion protein. Such an approach has been used to demonstrate that other proteins require their single SH3 domains to bind to dynamin; for example, Mlk2 W59A [Rasmussen, 1998], syndapin1 P434L [Qualmann, 1999] and amphiphysin1 G684R/P687L [Grabs, 1997] (residues shown in red in figure 4.12) no longer bind to dynamin. These are all mutations of relatively conserved hydrophobic residues within the SH3 domain motif, shown in bold in figure 4.12. Such conserved residues would be good choices for point mutations to destroy the function of POSH SH3 domains; for example, mPOSH SH3 1 should be disrupted with G181R/P184L mutations and SH3 2 with G247R/P250L mutations (also indicated in red in figure 4.12).

It is not every SH3 domain that binds to dynamin *in vitro*, but POSH is certainly not the only SH3 domain-containing protein to bind to dynamin (see introduction section 1.6.8). C POSH and the longer Y2H POSH, like N POSH, contain two SH3 domains, but unlike N POSH they do not bind to dynamin (see figures 4.1 and 4.2). Gout et al screened fourteen SH3 domain-GST fusion proteins for their ability to bind to dynamin from rat brain extract [Gout, 1993].

Figure 4.12 Alignment of POSH N-terminal SH3 domains with other dynamin-binding SH3 domains

Hydrophobic amino acids conserved in all SH3 domains are shown in bold. Positions of amino acid point mutations that have been used to destroy the function of SH3 domains for Mlk2, syndapin1 and amphiphysin1 (discussed in the text) and similar mutations that could be made within mPOSH SH3 1 and SH3 2 are shown in red. Inserts that extend the n-Src loop and the distal loop (nomenclature derived from [Noble, 1993] and [Wu, 1995]) of amphiphysin1 and 2 SH3 domains are shown in grey [Owen, 1998]. Interestingly Mlk2, and to a lesser extent POSH SH3 2, also appear to have extended n-Src loops, also shown in grey. Negatively charged amino acids present in the extended n-Src loop of amphiphysins1 and 2, which may contribute to selective binding of amphiphysin to a dynamin motif containing two R residues (PSRPNR) [Owen, 1998] are underlined and in grey. Abbreviations: human (h); mouse (m); rat (r); *Drosophila* (d); N-terminal SH3 domain (N); Plenty of SH3s (POSH); mixed lineage kinase 2 (Mlk2); growth factor receptor-bound protein 2 (Grb2); endophilin (Endo); amphiphysin (Amph). Accession numbers for the proteins whose SH3 domain sequences are shown: mPOSH AAC40070; dPOSH AAF37265; hMlk2 Q02779; hGrb2 NP_002077; rPLCγ1, NP_037319; mEndo1 NP_062408; rSyndapin1 NP_058990; hAmph1 longer splice form, NP_001626; hAmph2 splice form a, AAC51345.

Gout et al found that two SH3 domains bound strongly to dynamin (Grb2 (N) and PLCγ), two bound with intermediate strength (p85α and Grb2 (C)) and three showed a very weak interaction (src, fyn, fgr and p67phox (C)) [Gout, 1993]. The other seven SH3 domains tested (rasGAP, n-src p47phox (C), p67phox (N), Crk, α-spectrin and Csk) and GST alone did not show any detectable interaction with dynamin [Gout, 1993]. The SH3 domains of amphiphysins1 and 2 [Grabs, 1997] [Owen, Wigge, 1998], endophilins1-3 [Ringstad, 1997], syndapins1 and 2 [Qualmann, 1999] [Qualmann and Kelly, 2000], intersectins1 and 2 [Yamabhai, 1998], Mlk2 [Rasmussen, 1998] and cortactin [McNiven, 2000] have also been found to be strong dynamin binding partners.

My data suggest that neither SH3 1 nor SH3 2 of POSH individually bind to dynamin, making POSH the only protein to require more than one SH3 domain for binding to dynamin PRD. Most of the dynamin-binding proteins only contain one SH3 domain. Grb2 contains two SH3 domains, the N-terminal one being the stronger binding partner for dynamin [Gout, 1993], and intersectin contains five SH3 domains, three of which will individually bind to dynamin [Yamabhai, 1998]. For Grb2 the interaction with dynamin does not appear to be stronger with both SH3 domains than with just the N terminal one [Gout, 1993], for intersectin this has not been directly tested.

4.3.2 The dynamin PRD binding site for POSH

The two N-terminal SH3 domains of POSH, like the SH3 domains of other dynamin-binding proteins, interact with the isolated proline/arginine rich domain (PRD) of dynamin (see figure 4.7). For POSH it remains to be formerly proven that this interaction is direct, although the observation that a construct containing just two SH3 domains of POSH will bind to fusion proteins containing just dynamin PRD strongly suggest that this is the case. The exact motifs within dynamin PRD required for the binding of POSH SH3 domains can not be conclusively determined using the PRD truncations shown in figure 4.6. They do, however, allow the region required for binding of POSH to dynamin to be narrowed down to the 36 amino acid sequence shown in figure 4.8 (b). All of the classic SH3 domain-binding motifs within this POSH-binding region of dynamin1 PRD are conserved in the PRDs of dynamin2 and dynamin3, as shown in figure 4.8. This is consistent with the observation that POSH can bind to both dynamin2 (see figure 4.2) and dynamin1 (see figures 4.5 and 4.7).

The data suggests that POSH requires its two N-terminal SH3 domains for its interaction with dynamin (as discussed above in section 4.3.2). The region of dynamin PRD required for binding of POSH (shown in figure 4.8 b) also contains multiple potential SH3 domain binding sites (four class II motifs, underlined in figure 4.8 (b) and one class I motif, bold in figure 4.8 b). The two

SH3 domains within N POSH may bind to different motifs within this region of dynamin PRD in order to form a stable POSH-dynamin complex.

The strong interaction of SH3 1-2 with GST-ΔC16 PRD may represent an interaction of both of the POSH N-terminal SH3 domains with dynamin (probably requiring motifs shown in green and red in figure 4.8 b). The observed weaker interaction of POSH SH3 1-2 with the shorter GST-ΔC32 PRD protein may represent the binding of just one of the two SH3 domains to dynamin (probably requiring the motif shown in red in figure 4.8 b). These possibilities could be further investigated using point mutations to destroy the function of each of the SH3 domains individually (appropriate mutations are discussed above and are indicated in red in figure 4.12). These mutants could then be tested for binding to the dynamin1aa PRD constructs, in an attempt to determine whether each of the two SH3 domains mediate a separate interaction with dynamin.

In order to identify exactly which PRD sequences mediate the interaction of POSH with dynamin one could make PRD point mutations to knock-out specific class I or II motifs (for instance by mutation of critical R residues N- or C-terminal to the PXXP motifs respectively). Alternatively, peptides containing the individual PRD class I or class II motifs implicated in the POSH-dynamin interaction could be tested for their ability to inhibit binding of POSH SH3 domains 1-2 to dynamin. Both PRD mutagenesis and PRD peptide approaches have proved fruitful in the analysis of amphiphysin binding to dynamin PRD [Owen, Wigge, 1998] [Vallis, 1999].

4.3.3 Dynamin PRD motifs utilised by other SH3 domain-containing proteins

The binding sites within dynamin PRD have been narrowed down for a number of SH3 domain-containing proteins and these are summarised in figure 4.13. The majority of SH3 domain-containing proteins found to bind to dynamin appear to utilise regions within the PRD that are conserved between dynamin isoforms (discussed in introductory section 1.6.7 and shown in figure 1.26).

Only amphiphysin has been shown to interact with the 4th class II motif of dynamin PRD (PSRPNR) [Grabs, 1997] [Owen, Wigge, 1998]. The interaction of amphiphysin1 with dynamin is impaired by a point mutation (R838E) within this motif [Vallis, 1999]. Mlk2 was found to bind to a region encompassing both the amphiphysin-binding site and the most C-terminal class I and class II motifs in dynamin1aa PRD [Rasmussen, 1998]. Grb2 appears to bind to the 3rd class II motif, which overlaps with the 4th: Grb2 binding to dynamin can be blocked by a peptide containing amino acids 827–838 (GPPPQVPSRPNR) [Vidal, 1998], but unlike amphiphysin Grb2 can not bind to a truncation of dynamin PRD that contains the PSRPNR motif [Okamoto, 1997].

Studies using dynamin1 PRD truncations indicated that amino acids 809-826, a region that includes the 1st class II motif, was required for binding of dynamin1 to both p85α and PLCγ SH3 domains [Okamoto, 1997]. This was consistent with a previous study showing that amino acids 812-820 of dynamin1 (APPVPSRPG), a region that encompasses the 1st class II motif (underlined), was involved in binding of PLCγ SH3 domain to dynamin [Seedorf, 1994]. Using dynamin1 PRD truncations a region containing the first class I motif, which is only present in neuronal dynmain1 PRD, and stopping half way though the first class II motif was implicated in binding to endophilin1 [Slepnev, 1998].

Identification of the exact sites within dynamin PRD required for the POSH interaction could allow predictions to be made as to whether POSH would compete with these other dynamin-binding partners. The dynamin1 PSRPNR motif, which is the binding site for amphiphysins1 and 2, lies within the POSH-binding region of dynamin (see figure 4.13), but does not appear to be essential for the interaction of dynamin PRD with POSH (see figure 4.5).

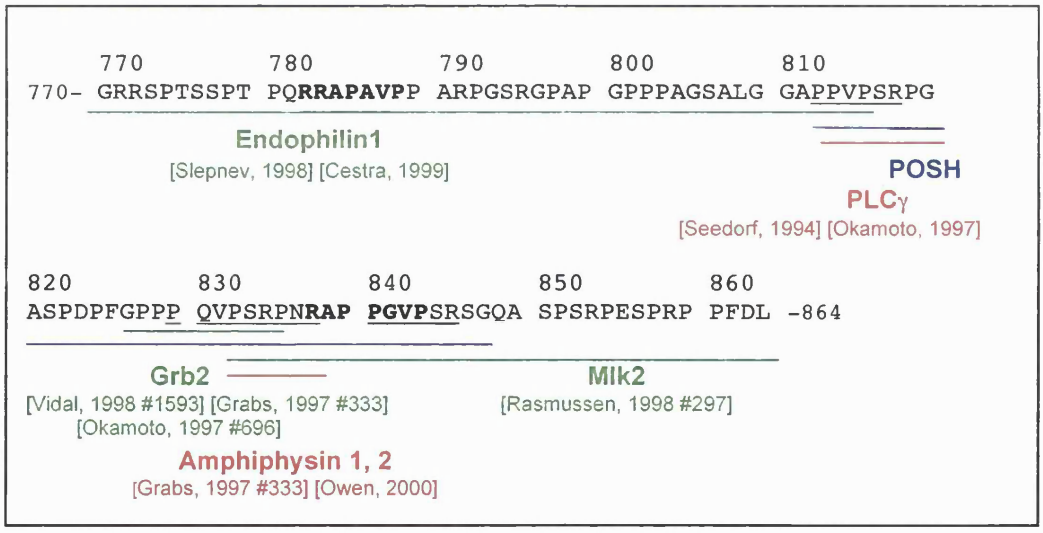

Figure 4.13 Regions of dyanmin PRD that interact with SH3 domain-containing proteins

The region of dynamin1aa proline/arginine-rich domain (PRD) that appears to bind to POSH, according to the experiments using PRD truncations discussed in section 4.2.6, is shown in blue. Regions shown to mediate binding to other SH3 domain-containing proteins are shown in red and green. Class I (bold) and class II (underlined) potential SH3 domain-binding motifs are indicated. For amphiphysin1 and 2, PLCγ and Grb2 have their binding sites been narrowed down, using combinations of PRD truncations and peptides, to single SH3 domain-binding motifs (see references and text for details). The other interaction domains indicated are not minimal binding sites, but are regions identified using PRD truncations, point mutants and peptides, which form part the interface of each protein with dynamin (see references and text for details).

Only Endophilin1 appears to have dynamin binding site totally outside of the POSH-binding region of dynamin PRD (see figure 4.13), so is more likely than the other dynamin binding partners shown in figure 4.13 to bind to dynamin at the same time as POSH. *In vitro* competition studies between the SH3 domains of other dynamin-binding proteins and N POSH could be used to determine whether POSH can compete with other binding partners for dynamin PRD. *In vivo* other regulatory factors may influence the dynamics of these interactions, such as phosphorylation events and lipid binding (see introduction sections 1.5.6 and 1.5.7).

Certain splice forms of dynamins 1 and 3 change the potential SH3 domain-binding sites present within the PRD (as shown in introductory figure 1.26). These splice forms may bind to different SH3 domain-containing proteins. Two dynamin1 second splice site variants (b and d) and a dynamin 3 third splice site variant (a) have alternative tails that destroy the 4th dynamin1 class II SH3 domain-binding motif (PGVPSR), as shown in figure 1.26 (d). This SH3 domain-binding motif lies within the potential POSH-binding region shown in figure 4.8 (b). The significance of such variations to the functions of dynamins 1 and 3, compared with the invariant tail of dynmain 2, is presently unclear.

4.3.4 The functional significance of POSH binding to dynamin

When it was discovered that POSH binds to dynamin we were searching for N POSH binding partners in order to gain and insight into how N POSH contributes to apoptosis. Experiments examining the relationship between apoptosis, dynamin and endocytosis are discussed in chapter 6. It was also hoped that some understanding of the function of endogenous POSH would be gained from identifying N POSH or C POSH binding partners. Having identified dynamin as an N POSH binding protein possible roles for POSH, and its other binding partner Rac, in endocytosis must be considered. Evidence for a functional link between POSH and dynamin in endocytosis, indicated by the ability of over-expressed POSH to interfere with endocytosis, is discussed in chapter 5.

4.3.4.1 POSH and synaptic transmission

Dynamin1 plays a specialised role in the rapid endocytosis required for synaptic vesicle membrane retrieval. In this chapter the question of whether POSH can bind to dynamin1 as well as dynamin2 was addressed, as an indication of whether POSH could potentially be involved, with dynamin1, in synaptic transmission. Evidence suggests that some of the other known dynamin-binding partners (intersectin1, endophilin1 and amphiphysin1) do have roles to play in this function of dynamin (reviewed in [Brodin, 2000] and discussed in introduction section 1.6.8.2).

N POSH was capable of binding to endogenous dynamin from brain extracts (see figure 4.3) and to transfected neuronal dynamin1 (see figure 4.5), opening up the possibility that POSH could be involved with dynamin1 in synaptic transmission. On the other hand, endogenous POSH protein could not be detected in rat brain post-nuclear supernatant (figure 4.4), although POSH mRNA levels in mouse brain were quite high [Tapon, Nagata, 1998]. It is still possible that a brain-specific mammalian POSH gene exists, although only one POSH gene could be detected in the human genome. If the N-terminus of an alternative form of POSH were very different to the ubiquitious form then it would not be detected with the probe used to look at POSH mRNA distribution or with the anti-POSH antibodies (UCL69 and UCL70) used for blotting of rat brain extract (figure 4.4).

4.3.4.2 Additional *in vitro* assays to test the functional relevance of the POSH-dynamin interaction

Additional *in vitro* assays could provide information about the functional relevance of the interaction of POSH with dynamin. These include the ability of POSH N-terminal SH3 domains to affect dynamin GTPase activity and oligomerization (two processes that are tightly linked) and their ability to interfere with specific steps in the endocytic pathway in a perforated cell assay.

SH3 domains that can induce dynamin GTPase activity

A few of the SH3 domains that bind strongly to dynamin have been shown to increase dynamin GTPase activity, such as full-length Grb2 [Gout, 1993] and Mlk2 [Rasmussen, 1998]. Dynamin's GTPase activity certainly forms part of the cycle of dynamin activity that facilitates endocytosis, although the exact role played by dynamin GTP hydrolysis remains a matter for debate (see models in figure 1.25). Interestingly, Grb2 full-length is a much stronger activator of dynamin GTPase activity than Grb2 N-terminal SH3 domain, although the interaction with dynamin only appears to require the N-terminal SH3 domain [Gout, 1993]. For N POSH it appears that both SH3 domains are important for binding to dynamin, but their ability to effect dynamin GTPase has not been assessed.

SH3 domains that can prevent dynamin oligomerization

Another *in vitro* assay that gave interesting results for amphiphysin (amph) showed that amph1 and 2 SH3 domains, but not Grb2 (N) or spectrin SH3 domains, can prevent dynamin oligomerization [Owen, Wigge, 1998].

The SH3 domains of amph1 and 2 appear to have special features revealed by the structure of amph2 SH3 domain and functional analysis of amph1 and 2 SH3 domains *in vitro* and *in vivo* [Owen, Wigge, 1998]. (1) These SH3 domains contain extensions to the n-src and distal loops, shown in grey in figure 4.12. The n-src loop extension appears to be required, but not sufficient, for their ability to inhibit dynamin oligomerization *in vitro* and for inhibition of endocytosis *in*

vivo [Owen, Wigge, 1998]. (2) Amph1 and 2 SH3 domains also contain an extra patch of negative charge to which residues in the extended src loop (grey and underlined in figure 4.12) and residues from the RT loop contribute. This extra negatively charged patch may provide amph1 and 2 SH3 domains with their specificity for binding to proline-rich motifs containing two positively charged residues, such as the dynamin1 PSRPNR motif.

The combination of binding to a particular C-terminal motif within dynamin PRD plus the presence of extended loops has been suggested to provide amph1 and 2 SH3 domains with a special ability to interfere with dynamin oligomerization. Interestingly, Mlk2, and to a lesser extent POSH SH3 2, also appear to contain a longer n-src loop (shown in grey in figure 4.12) than the SH3 domains from the other dynamin-binding proteins shown in figure 4.12. These n-src loop extensions do not contain negatively charged residues, for POSH SH3 domain 2 there are in fact positively charged residues (arginines) in the src loop extension. This may reflect binding of Mlk2 and POSH to different motifs within dynamin PRD to the PSRPNR motif that binds to amphiphysin. Whether Mlk2 SH3 or POSH SH3 2 are capable of inhibiting dymamin oligomerization and whether this contributes to their ability to interfere with dynamin function (shown for POSH in chapter 5 and for Mlk2 in A Bishop and A Hall unpublished data) remains to be seen.

SH3 domains that inhibit specific stages in coated pit formation

Sandra Schmid's lab in California routinely use a perforated cell assay (with snap frozen A431 cells or more recently undifferentiated 3T3-L1 cells) to look quantitatively at the uptake of biotinylated transferrin (Tfn) [Yamabhai, 1998]. They can detect different stages in coated pit formation. The initial open pit is accessible to exogenously added avidin. The constricted pit is inaccessible to avidin, but is still attached to the plasma membrane and accessible to a small membrane impermeable reducing agent the sodium salt of 2-mercaptoethane sulphonic acid (MesNa). The detached coated pit has undergone membrane fission to release the vesicle and is MesNa and avidin inaccessible. Using this type of assay both pit constriction and fission appear to be dynamin-dependent events (discussed in introduction section 1.6.2).

This assay has been used to determine the effects upon Tfn endocytosis of pre-incubation with GST-fusion proteins of different SH3 domains. Those that do not bind to dynmain, such as Abl SH3 domain, had no effect in this assay [Simpson, 1999]. Grb2 N-terminal SH3 domain, despite being a strong binding partner for dynamin was only weakly inhibitory in this assay [Simpson, 1999]. Maybe this reflects a need for both Grb2 SH3 domains that was observed in the dynamin GTPase activity assay [Gout, 1993]. Endophilin1, amphiphysin2 and syndapin1 SH3 domains all inhibited the formation of detached coated pits [Simpson, 1999]. For endophilin synaptojanin is a major binding partner in addition to dynamin (see for instance [de Heuvel, 1997]), so the effects

of this SH3 domain may be due to inhibition of synaptojanin as well as dynamin. Intersectin SH3A, out of its five SH3 domains three of which bind with significant strength to dynamin (A, C and E) [Yamabhai, 1998], had the greatest effect upon Tfn endocytosis. Intersectin SH3A was unusual in blocking the early pit constriction events [Simpson, 1999]. This unusual property could be due to a distinct role for intersectin with dynamin in endocytosis or due to binding of SH3A to partners other than dynamin (such as Sos1 [Tong, Hussain, de Heuvel, 2000]). It would be interestingly to see whether GST-N POSH can interfere with early or late stages of Tfn endocytosis in this assay system.

4.3.5 Does POSH bind to synaptojanin?

As mentioned in section 1.6.9, synaptojanin also contains a PRD and binds to some of the same SH3 domain-containing proteins as dynamin. The synaptojanin1 145kDa form is only expressed in brain [McPherson, Takei, 1994], whereas the longer 170kDa splice form of synaptojanin1 [Ramjaun, 1996] and synaptojanin2 are more ubiquitous [Nemoto, 1997]. Endophilins1-3 are found bound mainly to synaptojanin1 in brain, and to a lesser extent to dynamin1 [de Heuvel, 1997]. Amphiphysin1 also bind strongly to synaptojanin, but in a separate complex from endophilin1 [Micheva, Kay, 1997]. Intersectin1 SH3 domains bind strongly to synaptojanin1 long and short forms from rat brain as well as to dynamin1 [Yamabhai, 1998].

Although no bands of the more ubiquitous forms of synaptojanin, 170kDa synaptojanin1 or 145kDa syjaptojanin2, were seen associated with N POSH from radiolabelled ~~HeLa~~ S3T3 cell lysates (figure 4.1 (a) lane N) POSH may still bind to synaptojanin as well as to dynamin. If POSH binds less strongly to synaptojanin and the levels of synaptojanin are lower than dynamin in ~~HeLa~~ S3T3 cell lysates then an interaction may have been overlooked. Also, the large size of the synaptojanins may make them more difficult to resolve by SDS PAGE. GST-fusion proteins containing synaptojainin PRD could be used to test whether synaptojanin can bind to POSH in the same way as ~~POSH~~ was shown for dynamin PRD (see figure 4.7).

4.3.6 The interaction of full-length POSH with dynamin

Full-length POSH binds very weakly to endogenous dynmain2 compared with the N POSH truncation (see figure 4.9 a). The introduction of a caspase inhibitor slightly increased the amount of dynamin co-precipitated (see figure 4.9 a lanes 2 and 3). This increase in bound dynamin2 did not seem to be due to an increase in the amount of POSH in the precipitate, as the levels of precipitated POSH protein were quite similar with or without the caspase inhibitor (see figure 4.9 b lanes 2 and 3). The dynamin interaction with full-length POSH, even in the presence of a caspase inhibitor was clearly weak compared with the N POSH truncation. Possible explanations for why full-length POSH binds weakly to dynamin include the following.

(1) Does the POSH-POSH interaction mask the dynamin binding site?

A POSH-POSH homophilic interaction mediated by C-terminal regions of the proteins was observed (see figure 4.10). Although these interactions do not directly involve the dynamin-binding N-terminal SH3 domains it was possibility that this homophilic interaction could make full-length POSH less accessible to dynamin than the N POSH truncation.

For other Rho GTPase effector proteins that contain autoinhibitory domains binding of an activated Rho GTPase has been observed to disrupt autoinhibitory interactions, making binding sites for other proteins accessible (discussed in introductory section 1.2.6.1). Initial attempts to test whether activated Rac can disrupt POSH-POSH interactions using triple transfections were not successful (data not shown). An *in vitro* assay using recombinant proteins, which has been successful in studies of PAK autoinhibition [Tu, 1999], may prove more fruitful.

Co-expression of L61 Rac with POSH did not increase the binding of full-length POSH to dynamin (see figure 4.11). This suggests that either GTP-Rac, or at least GTP-Rac alone, does not unmask N-terminal POSH sequences required for binding to dynamin or that the weak interaction of full-length POSH with dynamin compared with N POSH is not due to autoinhibitory interactions.

(2) Is the POSH-dynamin interaction regulated by phosphorylation?

It is possible that only a small sub-population of full-length POSH is somehow competent for binding to dynamin, a phosphorylated or de-phosphorylated portion for instance. If the N POSH truncation were not affected by such a control mechanism then all the N POSH protein could bind to dynamin, giving a higher yield as observed (figure 4.10 (a) compare lanes 2 and 4). In cells expressing the very highest levels of myc-tagged POSH protein more of the POSH protein that is competent for dynamin-binding may be present. It is these high expressing cells that are most likely to die from apoptosis during transfections. When these cells are kept alive with caspase inhibitors this may result in the observed small increase in dynamin co-precipitated with POSH (figure 4.10 (a) compare lanes 2 and 3).

It is also possible that the interaction of full-length POSH, but not that of N POSH, is sensitive to dynamin phosphorylation. In the case of amphiphysin in nerve terminals its binding to dynamin is inhibited by Serine/Threonine phosphorylation of dynamin1, by kinases that include PKC [Slepnev, 1998]. In non-neuronal cells dynamin2 has been reported to be Tyrosine phosphorylated by Src, in response to stimuli such as insulin and LPA [Baron, 1998] [Kranenburg, Verlaan, 1999b].

Whether phosphorylation of dynamin, or of POSH itself, could account for inhibition of dynamin binding to full-length POSH in COS cell lysates, whilst not affecting binding to N POSH, has not been directly investigated. However, in all the experiments shown above the cells were grown in serum prior to harvesting, so would receive many potential kinase pathway-stimulating signals. Also, precipitations were carried out in the presence of phosphatase inhibitors, which should maintain any dynamin or POSH phosphorylations during the immuno-precipitation procedure. To look at serine/threonine phosphorylation of dynamin and POSH precipitated from COS7 cells in serum one could label cells with [γ-^{32}P]-ATP. The phosphorylation state of membrane-associated and cytosolic fractions of these proteins could be analysed separately. In neurons membrane-bound dynamin is de-phosphorylated, whereas the cytoplasmic pool is mainly phosphorylated [Liu, Powell, 1994]. Using cell cracking and a 100,000g spin of the post-nuclear supernatant to pellet membranes transfected myc-POSH was seen by western blotting in both membrane-associated and cytosolic fractions (data not shown).

4.3.7 The POSH homophilic interaction

POSH was found to bind to itself via regions towards the C-terminus of the protein (see figure 4.10). The RBD, which is present in full-length and Y2H POSH, is not required on both sides of the POSH-POSH interface, as Y2H POSH will bind to the C POSH truncation that lacks this region. C POSH has not been tested for binding to itself, which would determine whether the RBD is required for the POSH-POSH interaction, as is the case for PAK and WASP (reviewed in [Hoffman and Cerione, 2000]). Shorter truncations of POSH and point mutations, SH3 domain mutations and mutations of the partial CRIB domain (shown in figure 1.15) if the RBD is part of the interface, could be used to determine exactly which regions within Y2H are essential for the POSH-POSH interaction.

To define the regions of POSH that interact with each other would be useful for the design of a dominant negative POSH construct to use in analysis of the functions of endogenous POSH. Regions of the N-terminus bind to dynamin and the RBD binds to Rac, so truncations containing these regions interfere indiscriminately with the functions of these binding partners rather than just with those pathways that involve POSH (see data in chapters 3 and 5). If a part of the C-terminus of POSH outside of the RBD could be found that binds to other POSH molecules then this may be able to inhibit endogenous POSH more specifically. Such an approach proved successful for PAK autoinhibitory domain constructs that act as dominant negative proteins to inhibit endogenous PAK function [Frost, 1998].

An interesting correlation exists between POSH constructs that associate with each other in precipitates (full-length POSH, Y2H POSH and C POSH, see figure 4.10) and those that often form patches of protein when over-expressed and observed by immunofluorescence (see for

instance figure 5.1 (A) a and c). Whether these patches of protein are aggregates may be determined by EM analysis. Whether this aggregation is dependent upon POSH homophilic interactions may be determined using mutants, that have yet to be identified, that do not self-associate. Certainly the N-terminus of POSH that is not involved in the homophilic interactions does not form intracellular aggregates (see for instance figure 5.1 (A) e).

CHAPTER 5
POSH AND ENDOCYTOSIS

5.1 INTRODUCTION

In chapter 4 the ability of POSH to bind to dynamin's proline/arginine-rich domain, requiring two N-terminal SH3 domains, was discussed. The next question to address was whether this interaction was functionally relevant *in vivo*. In this chapter data is presented showing that POSH constructs containing the dynamin-binding domain can interfere with clathrin-dependent endocytosis *in vivo*. Further evidence suggesting that this effect of POSH is dynamin-dependent is also described.

5.2 RESULTS

5.2.1 POSH constructs containing the dynamin-binding domain inhibit transferrin endocytosis

In order to see whether the binding of POSH to dynamin had functional consequences *in vivo* endocytosis assays were carried out using texas-red labelled transferrin (Tfn-TR). At the plasma membrane (PM) the transferrin receptor (TfnR) is constitutively localised to clathrin-coated pits and is recycled back to the PM after endocytosis. Endocytic vesicles and the recycling compartment can be labelled by incubation of cells at 37°C with Tfn-TR. Hep2 cells were used for this assay because they have high levels of transferrin receptors and are human cells, which bind well to the human recombinant transferrin used to make the Tfn-TR probe.

In order to look at the effects of POSH DNA constructs upon Tfn uptake Hep2 cells were injected with 0.1mg/ml myc-tagged POSH constructs. After 3-4h of expression Tfn-TR was applied for 30min at 37°C. Cells were fixed and stained for expression of myc-tagged proteins. Injection was used for these endocytosis assays, rather than transient transfection, because it is easier to control expression levels using microinjection, which allowed full-length POSH to be expressed at low levels and avoid the induction of apoptosis (see Chapter 3).

To assess transferrin uptake confocal sections were taken through expressing cells (visualised by myc staining) and their uninjected neighbours. Note that surface transferrin was not stripped from the cells in these assays and can be seen in some of the confocal sections (see for instance figure 5.1 (A) h). From these sections the percentage of expressing cells undergoing normal endocytosis (defined as >80% Tfn internalisation when compared with uninjected neighbours) was counted for at least three independent experiments for each construct tested, a similar quantification method was used in papers such as [Owen, Wigge, 1998].

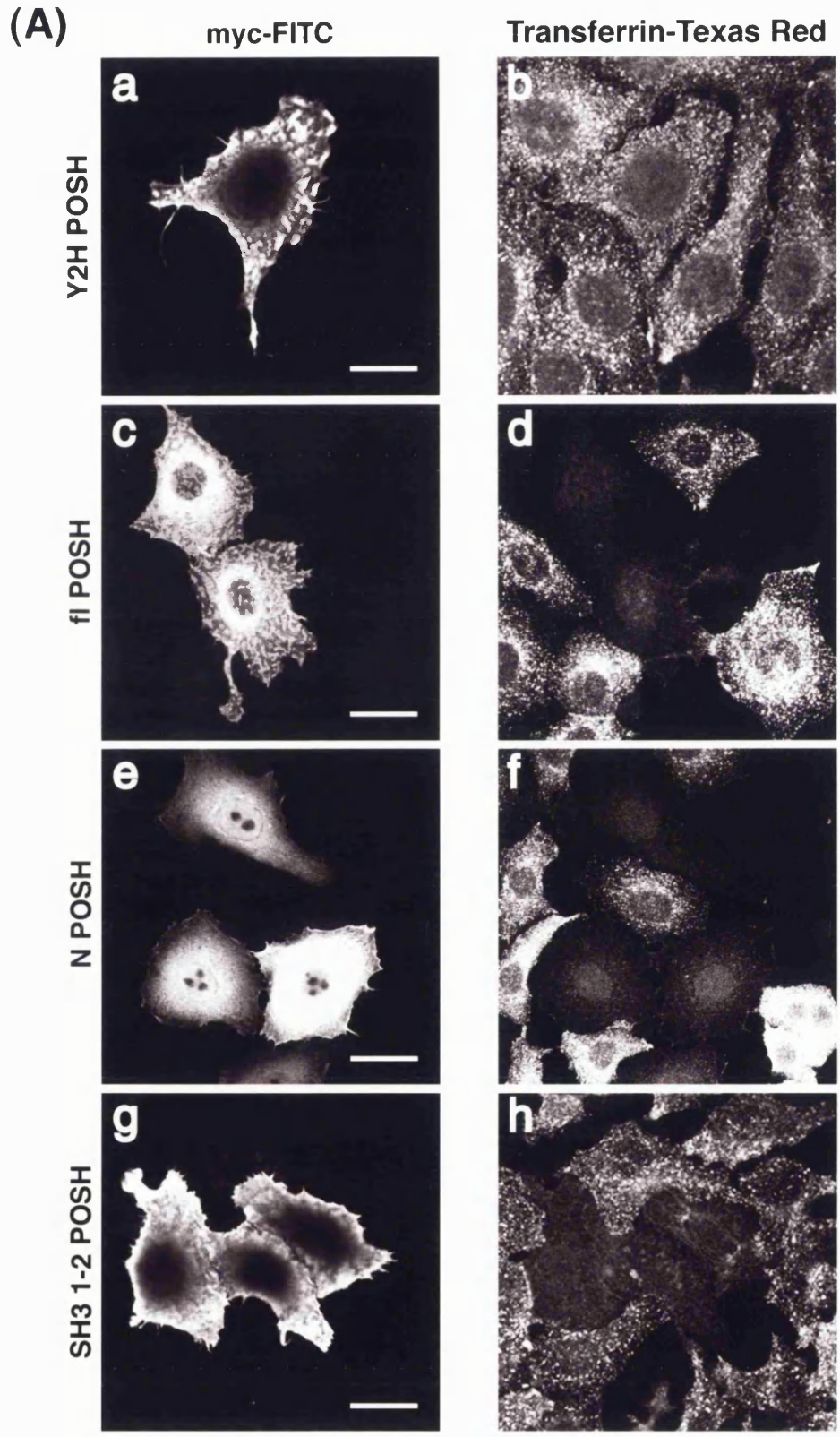

Figure 5.1 Overexpression of full-length POSH constructs containing the dynamin-binding domain inhibits transferrin (Tfn) endocytosis

(B)

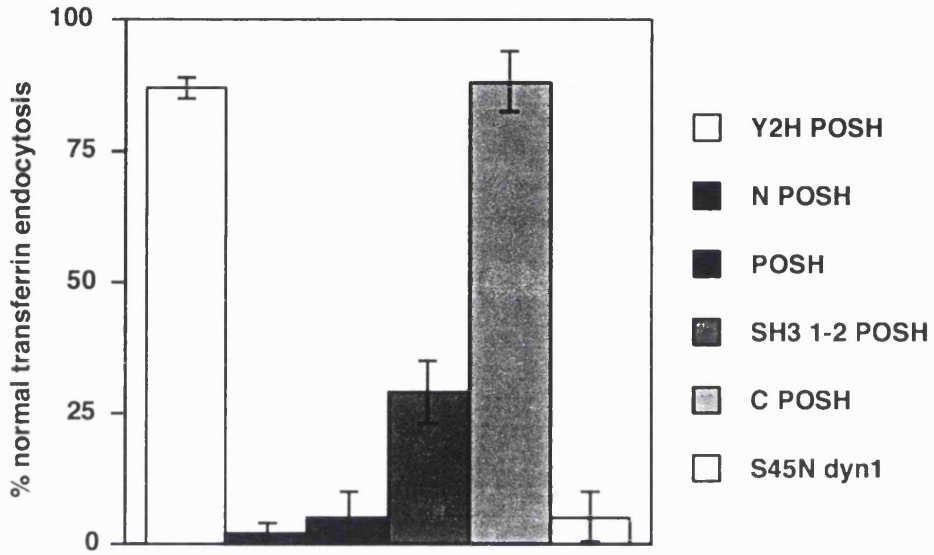

Figure 5.1 Over-expression of POSH constructs containing the dynamin-binding domain inhibits transferrin (Tfn) endocytosis

(A) Hep2 cells were injected with 0.1mg/ml DNA for myc-tagged POSH constructs: Y2H POSH (a and b); full-length POSH (c and d), N POSH (e and f) and SH3 1-2 (g and h). 3-4h post-injection cells were washed twice in serum-free media/0.2% fatty acid-free BSA (SF/BSA media) then treated for 30min at 37°C with 20μg/ml Tfn-TR in SF/BSA media (shown in panels b, d, f and h). Cells were washed, fixed and stained for expression with mouse anti-myc antibody 9E10 (shown in panels a, c, e and g). Confocal microscopy was used to visualised the cells; examples of confocal sections taken through expressing cells and their uninjected neighbours are shown. These sections were taken just below the centre of the cells for Tfn, where Tfn levels were highest in uninjected cells, and 1μm higher for myc, where myc staining was maximal. Bars equal 38μm (a-b), 60μm (c-d) and 50μm (e-h).

(B) Graph showing quantified Tfn endocytosis results from five independent experiments (C POSH and S45N dynamin1 were tested in only three of these experiments). Hep2 cells were injected with 0.1mg/ml myc-tagged POSH constructs or S45N dynamin 1 (dyn1) and were treated as in (A). From confocal sections, such as those shown in (A), the number of expressing cells showing normal Tfn endocytosis were counted. Normal endocytosis was defined as internalisation of at least 80% of the Tfn seen to be internalised by uninjected neighbouring cells. Error bars±one StdDev.

A number of myc-tagged POSH DNA constructs were tested in this way for their ability to interfere with Tfn endocytosis. Three POSH constructs containing the N-terminal two SH3 domains, that bind to dynamin, were able to inhibit Tfn endocytosis: full-length POSH (figure 5.1 (A) c and d), N POSH (figure 5.1 (A) e and f) and SH3 1-2 (figure 5.1 (A) g and h). The Y2H POSH construct, which contains POSH C-terminus from the Rac-binding domain to the end of the protein, had no significant effect upon Tfn endocytosis (figure 5.1 (A) a and b). Individual SH3 domain constructs (SH3 1 or SH3 2), which did not bind to dynamin when precipitated from transfected COS7 cells (see figure 4.2), were also tested alone or mixed together (0.1mg/ml of each DNA) and were found not to inhibit endocytosis (data not shown).

Quantified results from five Tfn endocytosis assays, where each DNA construct was tested in at least three independent experiments, are shown in figure 5.1 (B). In addition to those constructs for which photographs are shown in figure 5.1 (A) a dominant negative dynamin mutant (S45N dynamin1) was also used as an endocytosis-inhibiting control. Upon quantification it became clear that S45N dynamin1, full-length POSH and N POSH all inhibited transferrin endocytosis to a similar extent, with more than 90% of cells unable to internalise Tfn (see figure 5.1 (B)). SH3 1-2 POSH was not as potent an inhibitor of endocytosis as the longer N POSH construct (% normal endocytosis 29±6 and 3±2 respectively, see figure 5.1 (B)). Closer inspection of cells expressing SH3 1-2 revealed that the expression level appeared to dictated whether or not endocytosis was inhibited; cells with bright myc staining were inhibited, whereas those whose myc staining was weak were not. S45N dynamin, N POSH and full-length POSH appeared to inhibit endocytosis even when expressed at low levels.

The results for C POSH, a shorter C-terminal POSH construct than Y2H POSH missing the Rac-binding domain, are also shown in figure 5.1 (B). C POSH was tested for effects upon endocytosis because it does not bind to active Rac or dynamin (figure 4.1 and [Tapon, Nagata, 1998]), but does bind to other POSH constructs (see figure 4.10) so could potentially act as a dominant negative protein to specifically interfere with endogenous POSH. C POSH, however, like the longer Y2H POSH, did not inhibit endocytosis of Tfn (see figure 5.1 (B)).

5.2.2 POSH constructs containing the dynamin-binding domain inhibit EGF endocytosis

The effects of expression of POSH DNA constructs upon endocytosis of Rhodamine-labelled EGF (EGF-rhod) were also assessed. The EGF Receptor (EGFR), unlike the TfnR, only enters clathrin-coated pits after ligand binding and is largely lysosomaly degraded after endocytosis. Hep2 cells have high levels of EGFRs and bind well to the human EGF-rhodamine (EGF-rhod) used for the assay, so were good cells in which to look at endocytosis of both Tfn and EGF ligands. As the EGFR is degraded after endocytosis in this assay EGF was bound for 1/2h at 4°C

and then allowed to internalise for just 10min at 37°C. Cells were again microinjected with POSH constructs, allowed to express for 3-4h and then treated with the EGF-rhod. Cells were fixed and stained for myc-tagged protein expression and were analysed for EGF internalisation using confocal microscopy as described above for the Tfn endocytosis assay.

Representative photographs and quantitative data from three independent experiments are shown in figures 5.2 (A) and (B) respectively. The EGF endocytosis assay gave essentially the same results as seen for Tfn. Full-length POSH (shown in figure 5.2 (A) c and d), N POSH (figure 5.2 (A) e and f) and S45N dynamin1 were highly inhibitory, even at low levels of expression, while SH3 1-2 only partially inhibited endocytosis (figure 5.2 (A) g and h). Inhibition of EGF endocytosis by SH3 1-2 was slightly less efficient than for Tfn endocytosis (% normal endocytosis 29±6 for Tfn and 55±7 for EGF). Y2H POSH (figure 5.2 (B) and (A) a and b) did not have a significant affect upon EGF endocytosis, as was the case for Tfn endocytosis.

5.2.3 Surface transferrin receptor levels are not down-regulated in cells expressing inhibitory POSH constructs

From the above endocytosis assays it was clear that POSH constructs containing the dynamin-binding domain could interfere with endocytosis. One way to inhibit internalisation of receptors would be to inhibit their presence at the surface of the cell, by down-regulating expression or increasing degradation. During the 3-4h of expression prior to incubation with EGF or Tfn loss of surface receptors for these ligands, induced by POSH constructs, could account for the inhibition of endocytosis. Levels of surface transferrin receptors (TfnR) on POSH-expressing cells were tested using the same injection-based protocol as described above for TR-Tfn endocytosis assays, but treating the cells with un-labelled Tfn. Fixed Hep2 cells were stained prior to permeabilisation with a mouse anti-TfnR antibody, B3/25, which recognises the external domain of the TfnR. Cells were then permeabilised and co-stained for expression of injected myc-tagged POSH constructs. Expressing cells were analysed by confocal microscopy for TfnR levels in the centre and on the surface of the cells.

Cells expressing POSH, N POSH or SH3 1-2, which all inhibited endocytosis of Tfn (see figures 5.1 and 5.2), showed a significant increase in surface TfnR levels and certainly did not show any signs of receptor down-regulation (see figure 5.3 A and B). No such increase was seen for cells expressing Y2H POSH (data not shown).

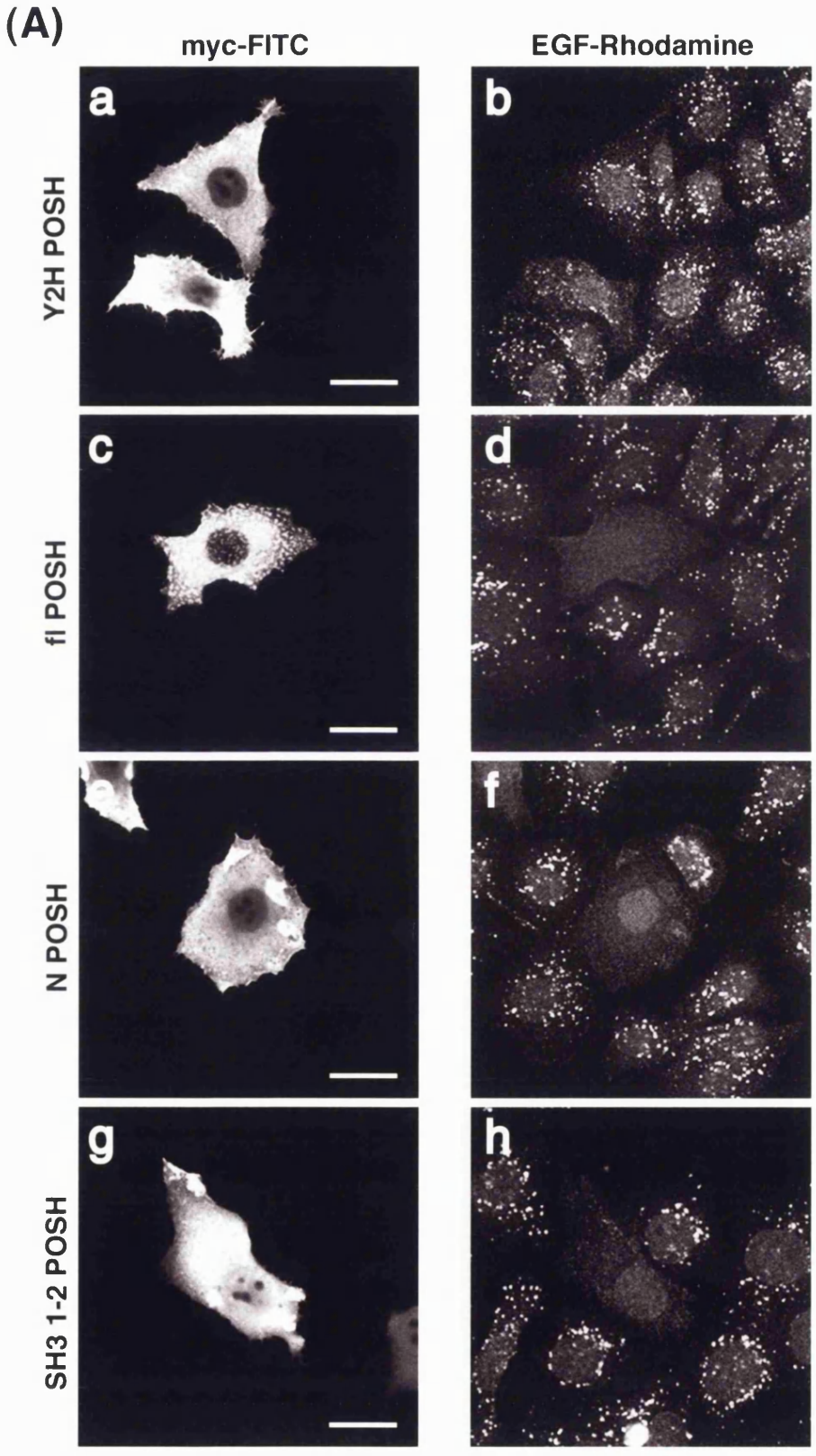

Figure 5.2 Over-expression of POSH constructs containing the dynamin-binding domain inhibits EGF endocytosis

(B)

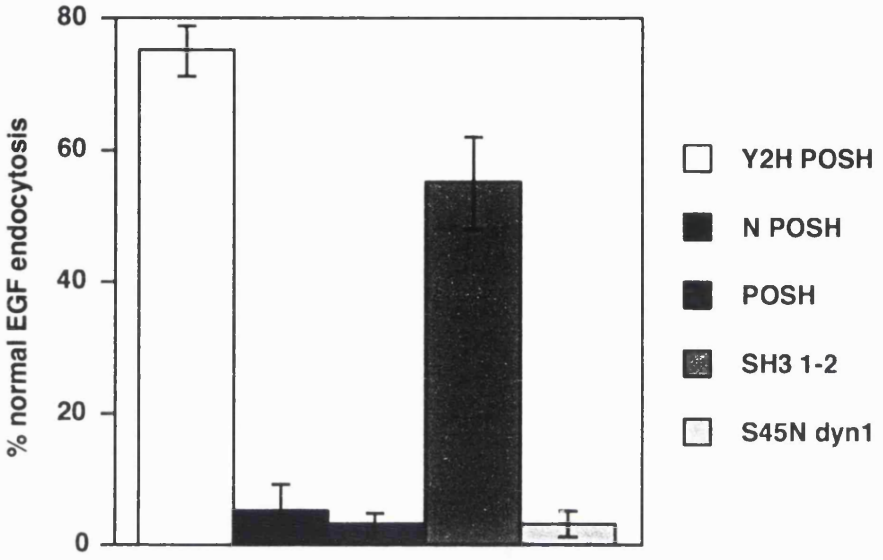

Figure 5.2 Over-expression of POSH constructs containing the dynamin-binding domain inhibits EGF endocytosis

(A) Hep2 cells were injected with 0.1mg/ml DNA encoding myc-tagged POSH constructs: Y2H POSH (a and b); full-length POSH (c and d), N POSH (e and f) and SH3 1-2 (g and h). 3-4h post-injection cells were washed twice with serum-free media/0.2% fatty acid-free BSA (SF/BSA media), treated for 30min at 4°C with 1mg/ml EGF-Rhodamine in Hepes buffered (10mM Hepes pH7.6) SF/BSA media then returned to 37°C into pre-warmed SF/BSA media for 10min to allow EGF internalisation (EGF-Rhodamine is shown in panels b, d, f and h). Cells were washed 2x in SF/BSA media and 2x in PBS, fixed and stained for expression with the mouse anti-myc antibody 9E10 (see panels a, c, e and g). Examples of confocal sections taken through expressing cells and their uninjected neighbours are shown. These sections were taken just below the centre of the cells for EGF, where EGF-Rhodamine levels were highest in uninjected cells, and 1μm higher in the z-axis for myc, where myc staining was maximal. Bars equal 60μm (a-d), 50μm (e-f) and 43μm (g-h).

(B) Graph showing quantified EGF endocytosis results from three independent experiments. Hep2 cells were injected with myc-tagged POSH constructs and were treated as in (A). From confocal sections, such as those shown in (A), the number of expressing cells showing normal EGF endocytosis were counted; normal endocytosis was defined as internalisation of at least 80% of the EGF seen to be internalised by uninjected neighbouring cells.
Error bars±one StdDev.

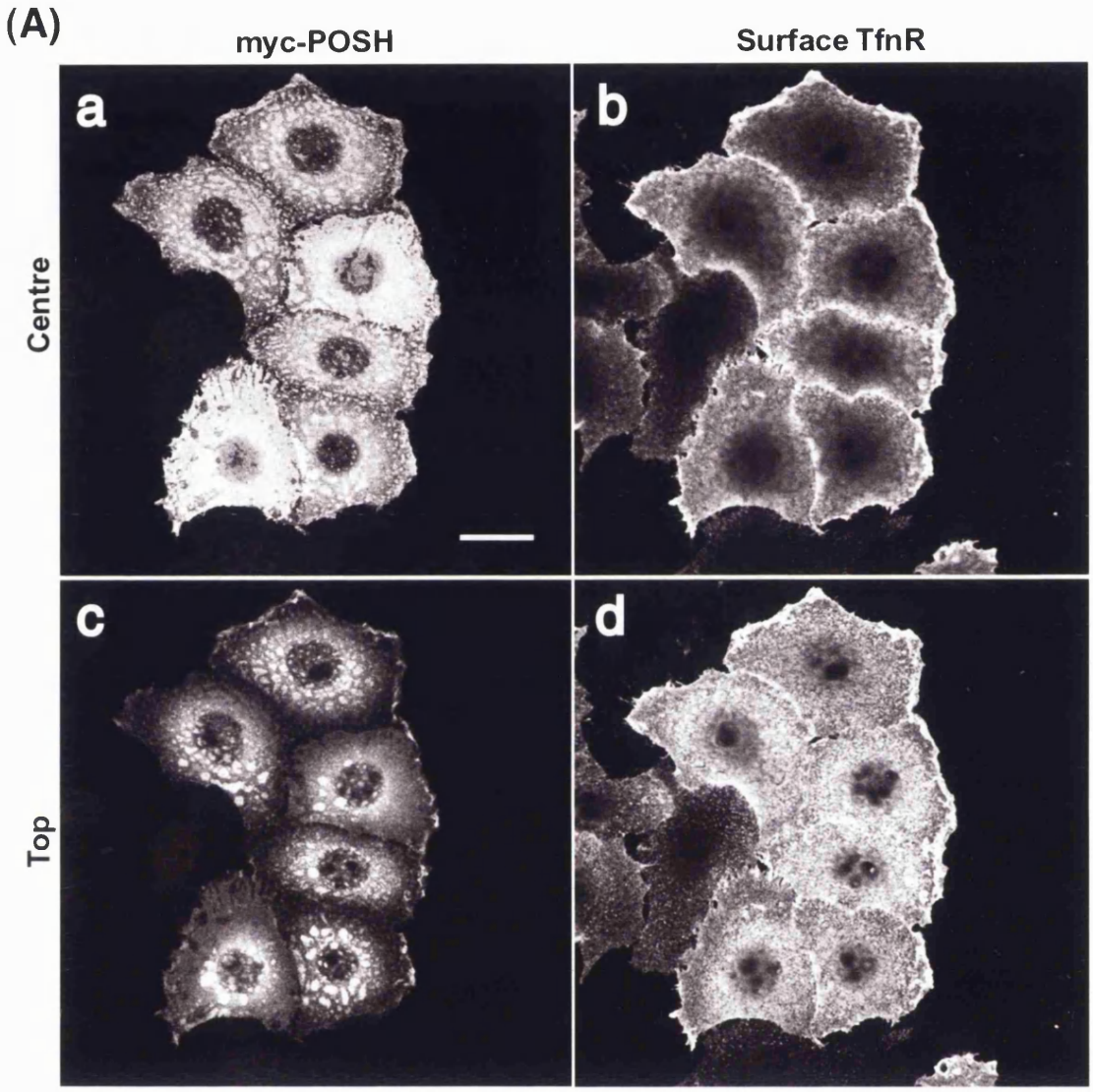

Figure 5.3 Overexpression of POSH constructs containing the dynamin-binding domain causes a build-up of surface transferrin receptors

(A) Full-length POSH

Hep2 cells were injected with 0.1mg/ml myc POSH. 3-4h post-injection cells were treated for 30min with 20μg/ml human transferrin then fixed. Cells were stained for surface transferrin receptors (TfnR) (b and d), using the B3/25 mouse antibody that recognises the extracellular domain of the TfnR (b and d), permeabilised and stained for expression with the rat anti-myc antibody, JAC6 (a and c). Confocal sections were taken near the centre (a and b) and near the top (1.5μm higher, c and d) of the cells. Bar equals 50μm.

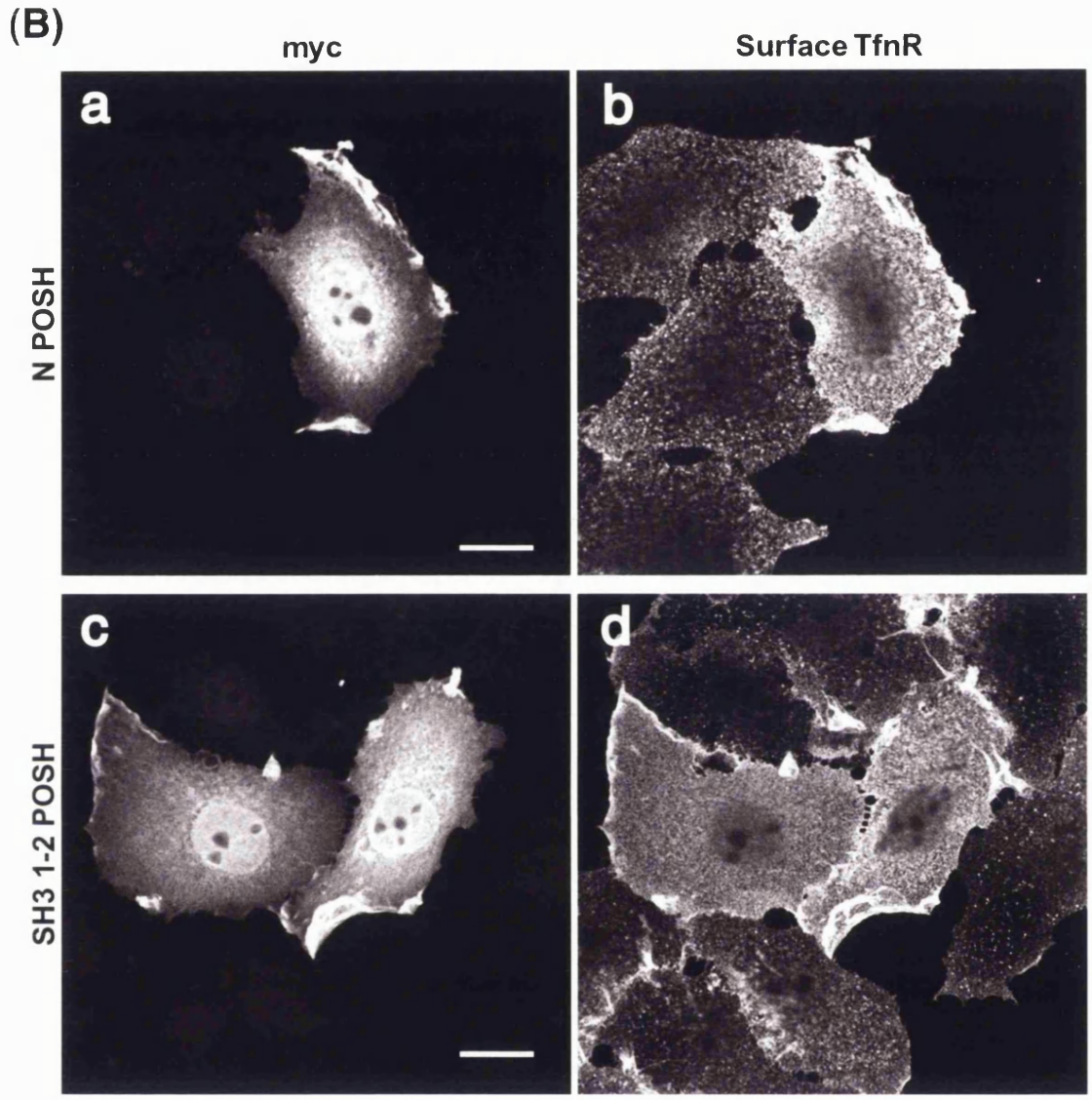

Figure 5.3 Over-expression of POSH constructs containing the dynamin-binding domain causes a build-up of surface transferrin receptors

(B) N POSH and SH3 1-2

Hep2 cells were injected with 0.1mg/ml myc-N POSH (a and b) or myc-SH31-2 POSH (c and d). 3-4h post-injection cells were treated for 30min with 20μg/ml human transferrin and fixed. Cells were stained for surface transferrin receptor (TfnR) (b and d), using the B3/25 mouse antibody that recognises the extracellular domain of the TfnR, permeabilised and then stained for expression with the rat anti-myc antibody JAC6 (a and c). Confocal sections were taken near the top of the cells. Bars equal 30μm.

At the centre of the cells, in the z-axis, (see for instance figure 5.3 (A) a and b) a high level of PM TfnR staining was seen at the edges of endocytosis-inhibited cells, when compared with their un-injected neighbours. Nearer the top of expressing cells a high level of TfnR staining covering the cell surface was also seen (see figure 4.17 (B) and (A) c and d). This increase in surface TfnR staining seen in cells expressing endocytosis-inhibiting POSH constructs is consistent with a build-up of receptors as they recycled to the surface and were unable to be endocytosed. TfnR staining on endocytosis-inhibited cells included many punctate spots, also seen in the un-injected cells, suggesting that at least some of the receptors are present within clathrin-coated pits. The build-up of surface receptors that are unable to be endocytosed may have saturated coated-pit components, which could account for the more diffuse background TfnR staining in cells expressing inhibitory POSH constructs.

5.2.4 Over-expression of dynamin2 rescues POSH-expressing cells from their block in transferrin or EGF endocytosis

Only constructs containing the two SH3 domains of POSH that bound to dynamin were able to inhibit EGF and transferrin endocytosis. This suggested that inhibition of dynamin was the mechanism by which POSH inhibited endocytosis. To test whether this was the case wild type dynamin2 was co-expressed with POSH constructs to see whether endocytosis of Tfn or EGF could be rescued. Endocytosis assays were carried out as described above for Tfn and EGF, but with each POSH construct injected with an equal concentration of empty vector or wild type dynamin2.

Figure 5.4 (A) and (B) show examples of triple-stained confocal sections (stained for Tfn-TR, myc and dynamin) for cells injected with POSH (A) or N POSH (B) with or without co-expression of dynamin2. The levels of staining for myc-tagged POSH proteins along with dynamin2 appeared to be comparable with the inhibited POSH-only controls (compare a and d in figures 5.4 (A) and (B)). There did not appear to be an obvious co-localisation of over-expressed POSH or N POSH with endogenous dynamin (see a and b in figures 5.4 (A) and (B)) or over-expressed dynamin2 (see d and e in figures 5.4 (A) and (B)).

From data such as that shown in figure 5.4 (A) and (B) it appeared that co-expression of dynamin2 with POSH or N POSH, at a 1:1 DNA ratio, restored endocytosis of Tfn. Quantified data from three experiments for Tfn endocytosis and three for EGF endocytosis are shown in figure 5.5. Cells expressing POSH, N POSH or POSH SH3 1-2 constructs were inhibited in endocytosis of Tfn and EGF, as shown previously (figures 5.1 and 5.2 respectively). Dynamin2 co-expression rescued endocytosis of both Tfn and EGF in combination with all three inhibitory POSH constructs (see figure 5.5).

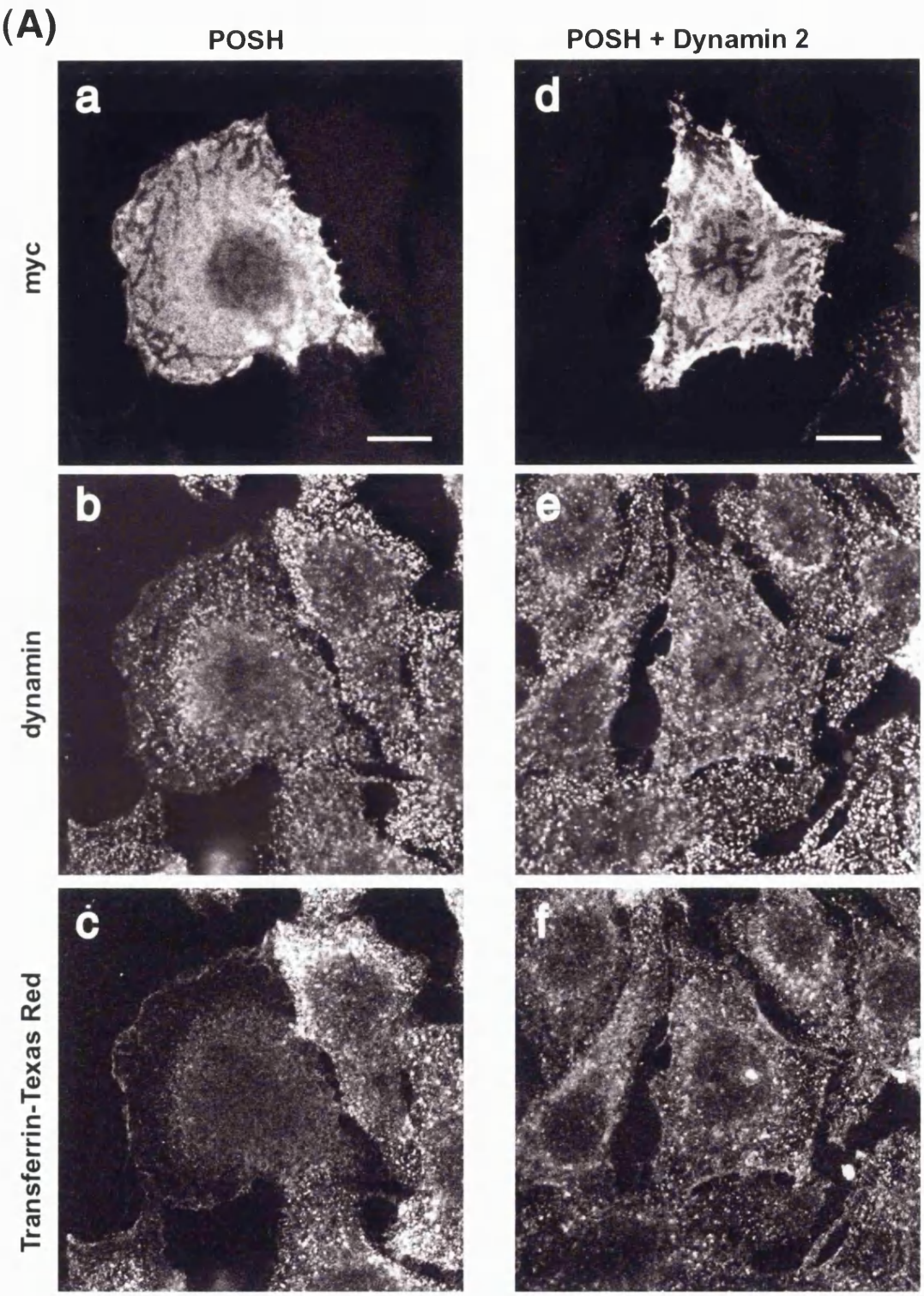

Figure 5.4 Co-expression of wild type dynamin2 with POSH constructs containing the dynamin-binding domain rescues transferrin endocytosis

Hep2 cells were injected with 0.1mg/ml myc-tagged POSH **(A)** or N POSH **(B)** 1:1 with empty vector (a-c) or with wild type dynamin2 DNA (d-f). After 3-4h expression cells were treated with Tfn-TR as described in figure 5.1. Cells were stained for myc-POSH constructs with rat-anti-myc (JAC6), with a FITC secondary antibody, and for dynamin with mouse-anti-dynamin (hudy-1), with a Cy5 secondary antibody. Confocal sections were taken just below the centre of the cells were Tfn levels were highest (in this case the three sections shown are from the same point in the z-axis). (A) Bars equal 25μm. (B) Bars equal 30μm.

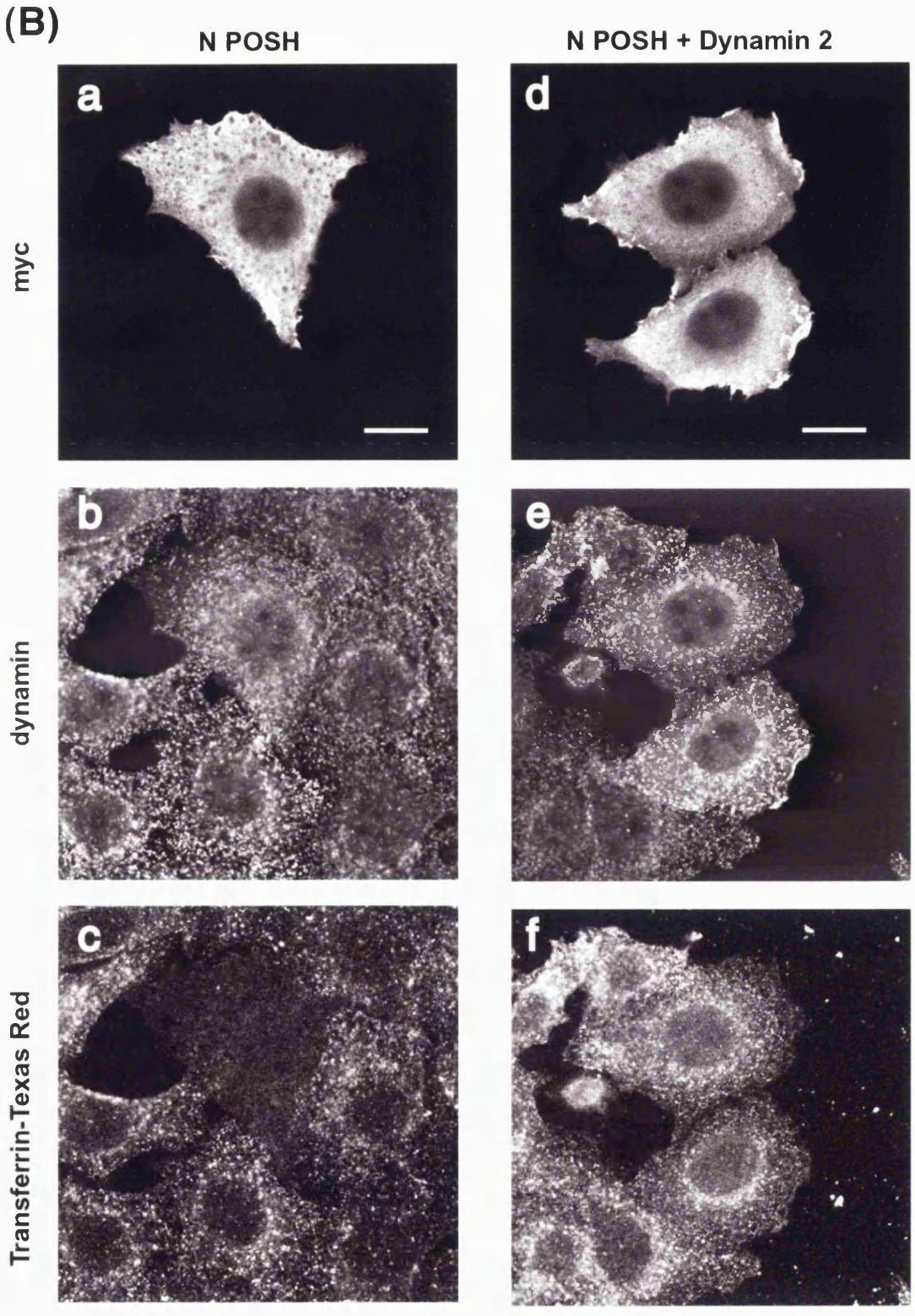

Figure 5.4 Co-expression of wild type dynamin2 with POSH constructs containing the dynamin-binding domain rescues transferrin endocytosis

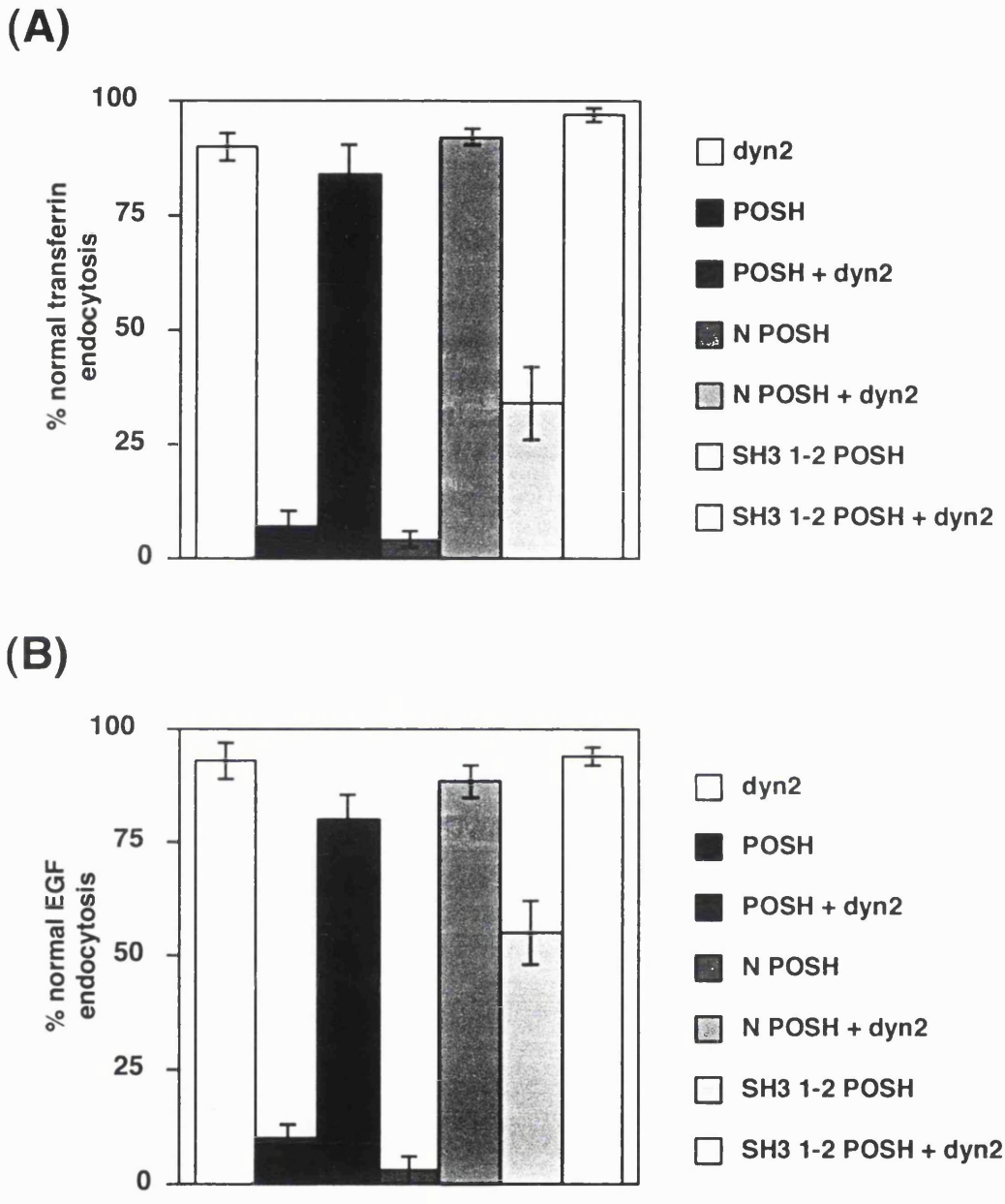

Figure 5.5 Co-expression of wild-type dynamin2 with POSH constructs containing the dynamin-binding domain rescues transferrin and EGF endocytosis

Graphs showing quantified Tfn (A) and EGF (B) endocytosis assay results, each for three experiments. Hep2 cells were injected with myc-tagged POSH constructs 1:1 with empty vector or with wild type dynamin2 DNA, or with dynamin2 1:1 with empty vector and 2.5mg/ml FITC-dextran. Endocytosis assays were carried out and quantified as described in figures 5.1 and 5.2. POSH and dynamin constructs were visualised as described in figure 5.4. FITC-dextran was included in injections of dynamin2 alone to aid the detection of expressing cells above the staining of endogenous dynamin2. Error bars±one StdDev.

Wild type dynamin2 alone was used as a control in the above rescue experiments and had no visible affect upon Tfn or EGF endocytosis (see figure 5.5). Transfection of wild type dynamin2, but not dynamin1, under an inducible promoter has been reported to cause p53-dependent apoptosis in dividing cells [Fish, 2000]. Apoptosis was not seen in response to over-expression of wild type dynamin2 alone or in combination with POSH, which itself induces apoptosis after longer expression times, over the 3-4h of expression used in these experiments.

5.2.5 A portion of over-expressed POSH is membrane or cytoskeletally-associated

Full-length POSH, N POSH and SH3 1-2 all inhibited endocytosis in a dynamin-dependent manner (see section 5.2.4). This suggests that POSH either interferes with dynamin at its site of action, the PM, or sequesters dynamin in the cytoplasm, preventing it from reaching its site of action. To act via the first mechanism some of the POSH protein must be recruited to the PM..

Confocal sections taken near the top of Hep2 cells expressing N POSH or SH3 1-2 often showed enriched myc-tagged POSH protein staining, compared with general cytoplasmic levels, in ruffles at the edge or on top of the cell. See for instance, N POSH-expressing cells shown in figure 5.1 A (e), figure 5.2 A (e) and figure 5.3 B (a) and SH3 1-2-expressing cells shown in figure 5.2 A (g) and figure 5.3 B (c). This staining pattern suggests that N POSH and SH3 1-2 are membrane-associated and may possibly be specifically enriched in ruffles, although any membrane-associated protein will be seen enriched in these folds of membrane to a certain extent.

To get an indication of whether a portion of the over-expressed full-length POSH protein was membrane or cytoskeletally-associated Hep2 cells were permeabilised with digitonin prior to fixation, which selectively removed the cytoplasmic pool of POSH. Cells were injected with pRK5myc-POSH, after 3-4h of expression cells were either fixed and permeabilised with triton-X100 (see figure 5.6 a) or were permeabilised at 4°C with digitonin prior to fixation (figure 5.6 b and c) and stained with anti-POSH antibody. Digitonin treatment removed the cytoplasmic pool of over-expressed POSH to reveal a membrane or cytoskeletally-associated fraction (see figure 5.6 b and c) that was obscured in cells fixed and then permeablised with triton-X100 (see figure 5.6 a). Lines of POSH staining were seen in digitonin permeabilised cells (figure 5.6 b and c) that are reminiscent of mitochondrial staining. Interestingly, there are dynamin-like proteins associated with mitochondria [Smirnova, 1998] [Wong, 2000]. Co-staining of NIH3T3 cells for over-expressed POSH (using UCL69 anti-POSH antibody) and mitochondria (using treatment of live cells with mitotracker), however, did not reveal any co-localisation (data not shown), although in this experiment digitonin permeabilisation was not used to remove cytoplasmic protein pools.

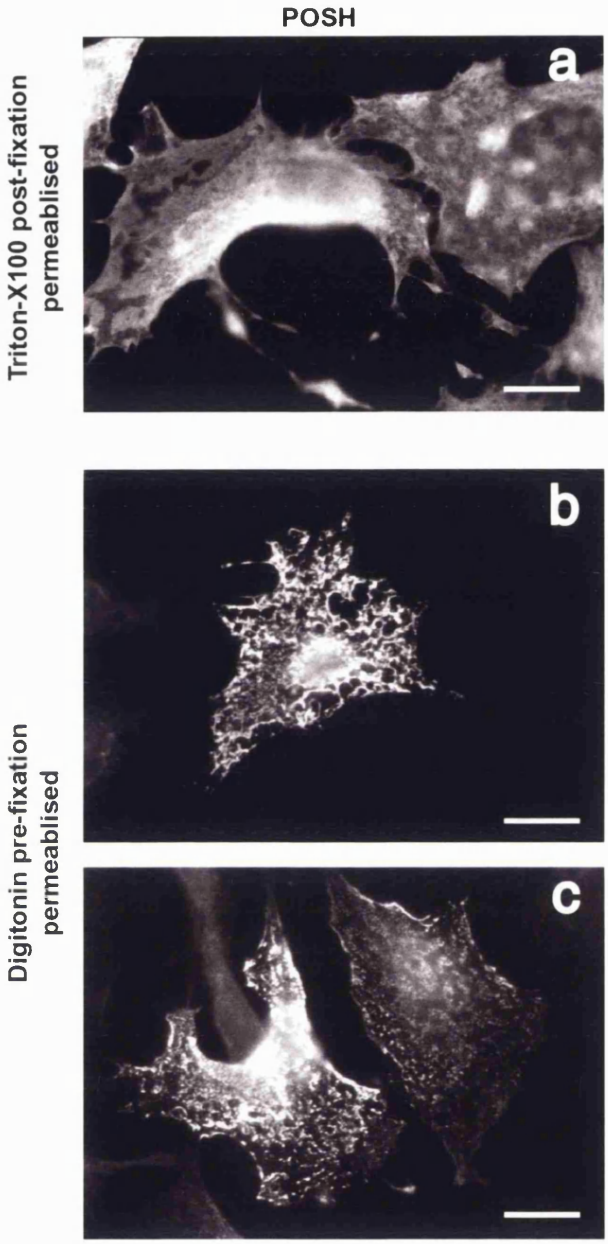

Figure 5.6 Digitonin permeabilisation prior to fixation reveals a portion of POSH that is membrane-associated

Hep2 cells were injected with 0.1mg/ml pRK5myc-POSH. 3-4h post-injection cells some coverslips were fixed, permeablised with triton-X100 and then stained with a rabbit anti-POSH antibody (UCL69) (a). Other cells were placed on ice, washed in cold permeabilisation buffer pH7.2 (25mM Hepes, 38mM K Aspartate, 38mM K Glutamate, 38mM K Gluconate, 1.5mM EGTA, 2.5mM MgCl2, pH corrected with KOH) then treated with 40μg/ml digitonin in permeabilisation buffer for 10min. Cells were washed 2x 5min in premeabilisation buffer/1% BSA and 2x quickly in premeabilisation buffer then fixed in 4% paraformaldehyde in premeabilisation buffer. All cells were stained with rabbit anti-POSH antibody UCL69. Bars equal 25μm (a), 40μm (b and c).

5.3 DISCUSSION

5.3.1 POSH constructs containing the dynamin-binding site inhibit endocytosis

The ability of POSH to affect dynamin function *in vivo* was tested as an indication of whether the binding of POSH to dynamin represents a functional relationship between these two proteins. Any POSH construct containing the first two SH3 domains, which are sufficient for POSH binding to dynamin (see section 4.2.2), was found to inhibit endocytosis of Tfn and EGF.

There was not a perfect correlation between the ability of a POSH construct to bind to dynamin, in COS7 cell precipitates (see figures 4.2 and 4.10), and the ability to inhibit endocytosis in Hep2 cells (see figures 5.1 and 5.2). For instance, even though full-length POSH did not bind strongly to endogenous dynamin2 (see figure 4.10), it strongly inhibited transferrin endocytosis (see figures 5.1 and 5.2). This discrepancy may be due to the fact that the endocytosis assays were carried out with shorter expression times, and in a different cell type, to the transfections used for binding studies. It may also be that a pool of POSH-associated dynamin that is active in the intact cell endocytosis assays was lost during binding experiments due to factors such as POSH-induced apoptosis over the transfection period. Alternatively full-length POSH may inhibit endocytosis via a mechanism that does not require strong binding to dynamin. SH3 1-2, on the other hand, bound very strongly to endogenous dynamin2 (see figures 4.2 and 4.7), but is not quite as potent as N POSH at inhibiting endocytosis (see figures 5.1 and 5.2). This suggests that the RING finger, present within N POSH but not SH3 1-2, may contribute to the ability of POSH to inhibit endocytosis, although it was not required for the binding of dynamin to POSH. The ability of full-length POSH to inhibit endocytosis may also require some activity of the RING finger that does not depend upon strong binding to dynamin. POSH RING finger is discussed further in chapter 6.

It should be pointed out that, although over-expression of full-length POSH inhibited endocytosis this does not mean that endogenous POSH has a role in inhibiting endocytosis *in vivo*. For instance, in the case of intersectin1 (known as Ese1) the protein appears to have a positive role to play in endocytosis (see for example [Simpson, 1999]). Even so, over-expression of the full-length wild type intersectin1 protein inhibits endocytosis [Sengar, 1999], possibly by sequestration of physiological binding partners into non-productive complexes due to the excess of protein.

5.3.2 POSH inhibition of endocytosis is dynamin-dependent

Staining for transferrin receptors on the surface of cells expressing endocytosis-inhibiting POSH constructs showed an increase in surface receptor levels (see figure 5.3). This showed that down-

regulation of receptor expression could not account for the inhibition of endocytosis observed in POSH-expressing cells.

Endocytosis was rescued in N POSH or SH3 1-2-expressing cells by dynamin2, suggesting that inhibition of endocytosis by these constructs is dynamin-dependant (see figures 5.4 and 5.5). Although full-length POSH does not bind strongly to dynamin, over-expression of wild type dynamin2 was still sufficient to compensate for POSH inhibition of endocytosis. Maybe POSH only requires a transient or indirect interaction with dynamin in order to exert its inhibitory effect.

A portion of full-length POSH protein appears to be membrane or cytoskeletally-associated, according to staining of cells after digitonin permeabilisation (see figure 5.6). POSH was also seen to be associated with membranes upon probing of western blots of post-nuclear supernatant cytoplasmic and membrane fractionations (supernatant or pellet respectively from a 100,000g centrifugation) from COS7 cells expressing myc-POSH (data not shown). N POSH and SH3 1-2 also appeared to be enriched in membrane structures, in particular surface actin-rich ruffles (see examples in figures 5.1-5.3). These data suggest that excess POSH has the potential to interfere with dynamin function at the PM. These data also suggest that endogenous POSH may associate with membranes, possibly via binding to dynamin or GTP-Rac.

A clearer understanding of the mechanism by which POSH inhibits dynamin function could be gained from assays discussed in chapter 4. For instance, *in vitro* analysis of the effects of POSH upon dynamin oligomerization and GTPase activity and assessment of the stage at which coated pit assembly is blocked using large and small probes in a perforated cell assay. Immunofluorescence and EM analysis of various components of coated pits in POSH-expressing cells (AP2 and TfnR for instance) could also help to determine whether coated pits are formed, but are stuck at the PM, or whether coated pit formation itself is blocked. Punctate regions of transferrin receptor staining, seen amongst the generally elevated levels of transferrin receptor on the surface of POSH-expressing cells (see figure 5.3), may represent coated pits that are present in these cells, but are stuck at the PM. This could be clarified using EM analysis.

5.3.3 A possible role for POSH in signaling by dynamin

Levels of wild type dynamin2 protein just 5 fold above that of the endogenous protein (produced using stable transfectants containing an inducible dynmain2 construct) have been reported to induce apoptosis in dividing cells in p53-dependent manner [Fish, 2000]. In my experiments wild type dynamin2 was found to rescue inhibition of endocytosis by POSH and was not seen to induce apoptosis alone or in combination with any of the POSH constructs (see figures 5.4 and 5.5). After 4h expression POSH alone kills very few Hep2 cells; Hep2 cells undergo apoptosis with kinetics very similar to the MDCK cells mentioned in chapter 3 section 3.2.1 (data not

shown). Co-expression of dynamin2 with full-length POSH, each of which alone can induce apoptosis, did not appear (in Hep2 cells after 3-4h expression) to augment the apoptosis-inducing activity of POSH. In many cells the level of over-expressed dynamin2 appeared, by immuno-fluorescence, to be only slightly higher than endogenous dynamin (see e in figure 5.4 (A) and (B)). It may be that although the level of dynamin2 expression in these experiments was sufficient to rescue endocytosis it was not enough to induce apoptosis, or there may not have been enough dividing injected cells to see the apoptosis effect.

As mentioned in chapter 3, POSH very strongly induces apoptosis in quiescent Swiss3T3 fibroblasts (data not shown), which suggests that POSH induction of apoptosis, unlike that of dynamin2, is not dependent upon cell division. Apoptosis induced by wt dynamin2 was also p53-dependent, something that has not been directly tested for POSH-induced apoptosis. NIH3T3 cells, in which most of the apoptosis work was carried out, express normal levels of p53 (see for instance [Meek, 1988]). HeLa cells (from which the Hep2 cell line was derived) have severely reduced p53 expression [Scheffner, 1991], but were still sensitive to POSH-induced apoptosis (data not shown). If POSH-induced apoptosis does not share any of the characteristics of dynamin2-induced apoptosis then it is unlikely that POSH and dynamin lie in the same signaling pathway leading to apoptosis. The observation that dynamin2 may have the capacity to induce endocytosis-independent signals opens up the possibility that endogenous POSH does not act with dynamin in endocytosis at all, but is recruited to dynamin in order to induce signal transduction pathways. Over-expression of POSH constructs may interfere with, or even enhance, dynamin2-induced signaling pathways, as well inhibiting the action of dynamin in endocytosis. Over-expressed POSH constructs may inhibit endocytosis due to high and unregulated protein levels and not because endogenous POSH is involved, along with dynamin, in endocytosis.

5.3.4 Rac and POSH inhibition of endocytosis

L61Rac binds to POSH *in vitro* [Tapon, Nagata, 1998] and *in vivo* (see figure 3.6), but did not increase binding of full-length POSH to dynamin (see figure 4.11) and did not rescue endocytosis in POSH-expressing cells (data not shown). L61Rac was reported itself to inhibit endocytosis of TR-Tfn when transiently transfected into HeLa cells (>95% of expressing cells were reported to be inhibited in transferrin endocytosis) [Lamaze, 1996]. In the same paper Schmid et al used a perforated A431 cell assay as a quantitative method to measure Tfn-HRP endocytosis. With this assay L61Rac protein was shown to inhibit Tfn endocytosis (by around 40%) and addition of Rho-GDI, that inhibits Rho GTPases, recovered endocytosis [Lamaze, 1996]. It was possible, therefore, that POSH and Rac could be acting together to inhibit endocytosis via a common pathway. Using Hep2 cells and micro-injection significant inhibition of transferrin endocytosis

by L61Rac could not be detected (data not shown), making it impossible to address a possible role for POSH in Rac inhibition of endocytosis using this assay system.

With the perforated cell assay Schmid et al attempted to show that the effects of L61Rac upon endocytosis were not due to actin reorganisation by L61Rac. They showed that treatment with up to 10μg/ml cytochalasin D (which destabilises actin filaments) or phalloidin (which stabilises polymerised actin) did not stop L61Rac from inhibiting endocytosis, neither did these agents inhibit endocytosis themselves [Lamaze, 1996]. Lamaze et al, however, later found that agents that sequester actin monomers, such as thymosin β4, increase Tfn endocytosis at low levels (0.25μM) and inhibit Tfn endocytosis at higher levels (10μM) in the perforated A431 cell assay [Lamaze, 1997]. A more recent report shows actin to play a variable, but not obligatory, role in receptor-mediated endocytosis in mammalian cells [Fujimoto, 2000]. It has been suggested, but still remains to be proved, that activated Rac exerts inhibitory effects upon endocytosis due to its ability to induce the formation of an actin meshwork just below the PM (lamellipodia), which may prevent release of coated pits. POSH has not been linked to actin-reorganisation by Rac (see introduction section 1.4.3.1). If the effects of L61Rac upon endocytosis observed by Schmid et al do prove to be actin-dependent then it is unlikely that POSH is involved in this Rac activity.

CHAPTER 6
POSH, APOPTOSIS AND ENDOCYTOSIS

6.1 INTRODUCTION

6.1.1 Links between POSH-induced apoptosis and inhibition of endocytosis

POSH both induces apoptosis (see chapter 3) and inhibits endocytosis (see chapter 5). It remained to be determined how, if at all, these two activities of POSH were linked. In this chapter evidence is presented which, along with that in the previous three results chapters, shows that inhibition of endocytosis combined with inhibition of Rac is not sufficient to induce apoptosis, but that both the RING finger and the dynamin-binding SH3 domains within N POSH are required.

Data presented in chapters 5 and 3 shows firstly, that inhibition of endocytosis by SH3 1-2 is not as potent as inhibition by N POSH (see figures 5.1 and 5.2) and secondly, that SH3 1-2 is not sufficient to replace N POSH in order to induce apoptosis (see figure 3.2). Such data, along with experiments described in sections 6.21 and 6.22 below, suggests that POSH RING finger is essential for the apoptosis-inducing potential of POSH and increases the efficiency of endocytosis inhibition by POSH. We decided to investigate possible functions of POSH RING finger. A number of RING finger proteins have been shown to act as E3 ubiquitin ligases (reviewed in [Freemont, 2000]), leading us to question whether POSH is also an E3 enzyme.

6.1.2 Introduction to E3 ubiquitin ligases

The ubiquitination process (shown schematically in figure 6.1) leads to formation of a thioester bond between the C-terminus of the 76 amino acid polypeptide ubiquitin (Ub) and a number of lysine residue side chains within target substrate proteins (reviewed in [Hershko, 1998]). Additional ubiquitin polypeptides can be added to lysines within ubiquitin itself, usually at ubiquitin lysine residue 48, to create multi-ubiquitinated proteins. Once multi-ubiquitinated proteins are targeted for degradation by a multi-catalytic protease complex called the 26S proteasome (reviewed in [Bochtler, 1999] and [Coux, 1996]). Only one mammalian E1 ubiquitin-activating enzyme has been identified, whereas there are at least seventeen E2 ubiquitin-conjugating enzymes in mammalian cells [Jensen, 1995]. E3 ubiquitin ligases are the most varied component in the ubiquitination pathway and are responsible, alone or as a complex with other proteins (see examples in figure 6.2), for recruiting both an E2 ubiquitin-conjugating enzyme and specific protein substrates to be ubiquitinated. In addition to the scheme shown in figure 6.1, E4 components facilitate the addition of one ubiquitin to another to form a multi-ubiquitin chain [Koegl, 1999].

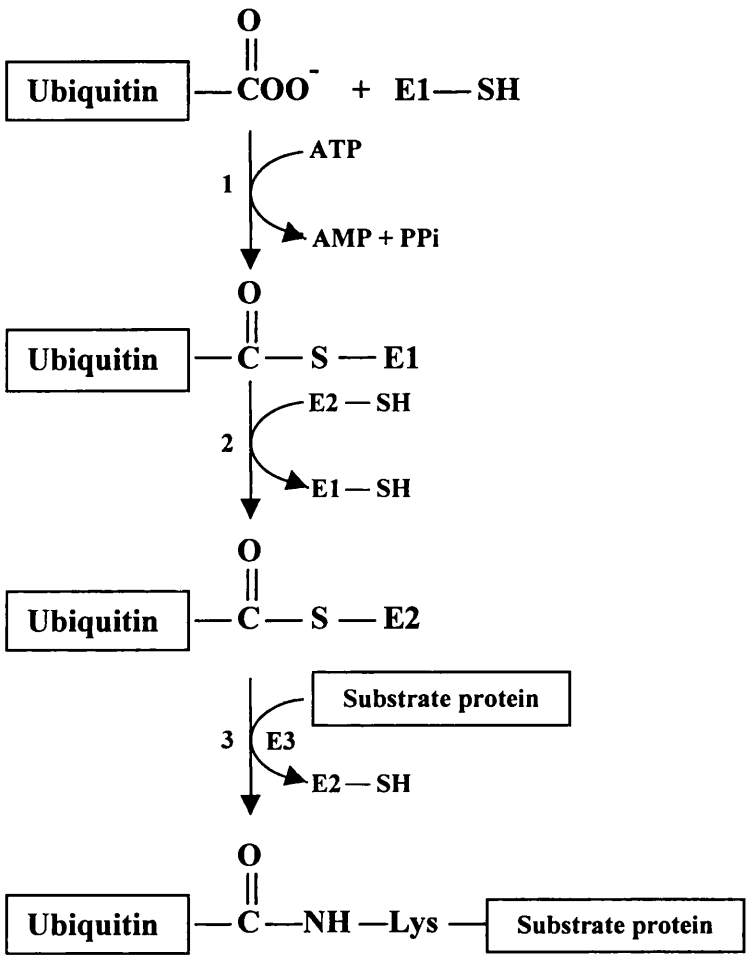

Figure 6.1 Reactions involved in the attachment of ubiquitin to a protein

(1) The terminal carboxyl group of ubiquitin is joined, via a thioester linkage, to the ubiquitin-activating enzyme (E1), which is a dimer of two identical 105kDa subunits, in an ATP-dependent reaction. (2) Activated ubiquitin is transferred to a sulfhydryl group of one of several small (25-70kDa) ubiquitin-conjugating enzymes (E2). (3) A ubiquitin ligase (E3) transfers activated ubiquitin from the E2 enzyme to a lysine on a target substrate protein, forming an isopeptide linkage between ubiquitin C-terminal glycine and the lysine ε-amino group. The ubiquitin moiety may be ligated to additional ubiquitin polypeptides, usually via the ε-amino group of ubiquitin lysine 48, to form a branched chain.

There are two broad groups of E3 enzymes identified to date, the HECT (homologous to E6-AP COOH-terminus) domain-containing E3s [Huibregtse, 1995] and the RING finger-containing E3s [Freemont, 2000]. E6-AP (E6-associated protein), which ubiquitinates p53 in the presence of E6 proteins from certain strains of human papiloma virus [Scheffner, 1994], was the first HECT domain-containing E3 to be identified [Huibregtse, 1993]. Like all HECT family proteins E6-AP binds to E2s, from which it accepts Ub in the form of a thioester linkage to a conserved cysteine within its HECT domain, and then catalyses the formation of stable Ub-substrate conjugates [Hatakeyama, 1997].

RING finger E3s do not appear to form thioesters with Ub. These E3s bring E2-Ub together with substrate and position them correctly for Ub transfer, but exactly how the transfer occurs is unclear (see for instance [Zheng, 2000]). The first RING finger-containing E3 to be identified was the N-end rule E3 in yeast, Ubr1p, which selectively induces the degradation of proteins with certain N-terminal residues. Ubr1p was later found to require its RING finger for this activity, although not for E2 enzyme (Ubc2p) binding [Xie, 1999]. In other cases the RING finger has been shown to be essential for E3 binding to an E2 enzyme as well as being required for ubiquitination activity, reviewed in [Freemont, 2000].

Regions outside of the E3 enzyme RING finger domain, or entirely separate proteins, can determine the substrate specificity of an E3 ubiquitin ligase. For example, as depicted in figure 6.2 (B), an SH2 domain within the E3 ubiquitin ligase Cbl allows it to be recruited to activated tyrosine-phosphorylated receptors, which are its ubiquitination targets [Joazeiro, 1999] and reviewed in [Barinaga, 1999]. In other cases a complex of proteins that includes a RING finger component act together to perform the functions of an E3 enzyme, (reviewed in [Laney, 1999] and [Tyers, 1999]). For example, the SCF (Skp1-Cdc53/Cul1-F-box protein) that is involved in the degradation of proteins such as G1 cyclins [Skowyra, 1999] and IκB [Karin, 2000] contains a RING finger protein called Rbx1. Figure 6.2 (A) shows how Rbx1 binds simultaneously to an E2 enzyme called Cdc34, an adaptor called Cdc53/CUL1 and F-box proteins that each recruit specific substrate(s) for ubiquitination, reviewed in [Tyers, 1999]. Many RING finger proteins, alone or in combination with other proteins, are now known to be acting as E3 ubiquitin ligases. Preliminary evidence suggesting that POSH may be involved in the ubiquitination process is described below.

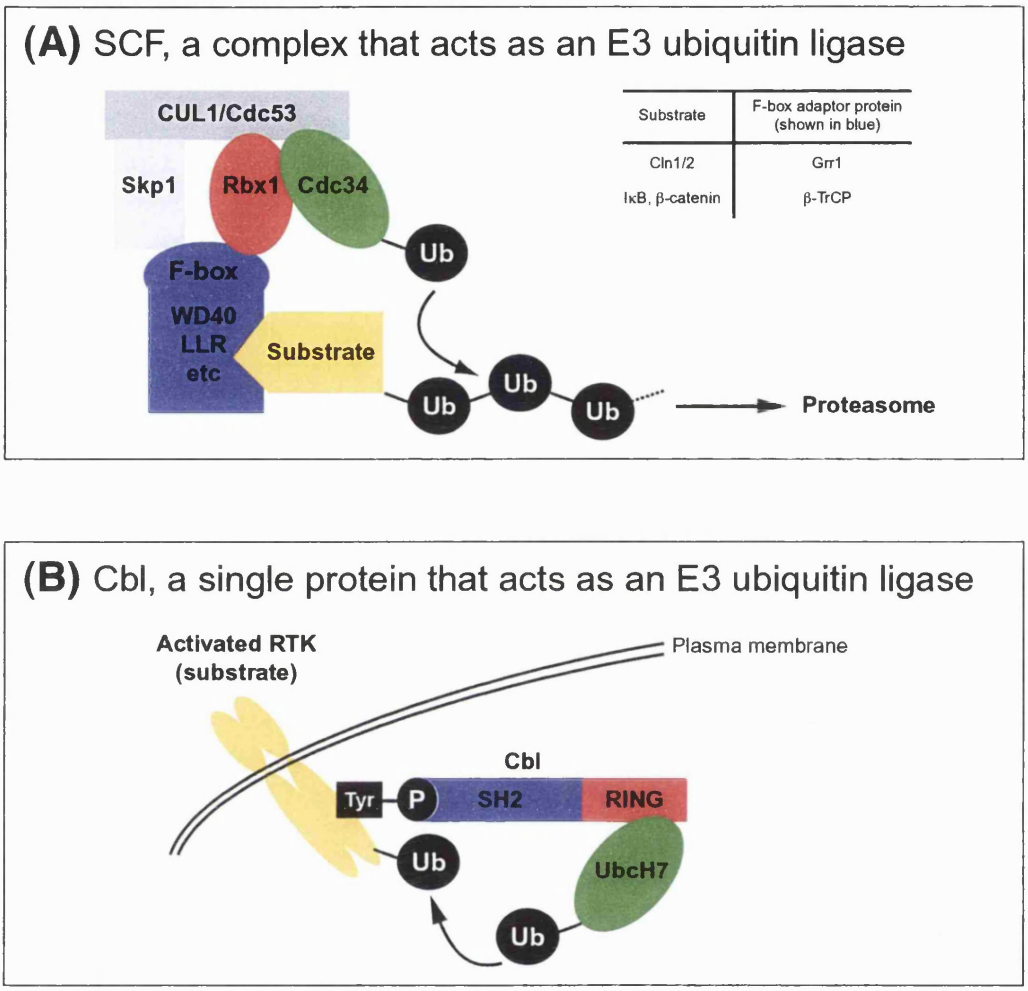

Figure 6.2 Two examples of E3 ubiquitin ligases that contain a RING finger domain protein **(A)** shows the structure of SCF (Skp1-Cdc53/CUL1-F-box) E3 ubiquitin ligases. SCFs are complexes of proteins that together facilitate the transfer of ubiquitin (Ub) from an E2 ubiquitin-conjugating enyme (in green) to a substrate protein (in yellow). The core ubiquitin ligase complex is composed of two adaptor proteins (Cdc53/CUL1 and Skp1) and an E2 enzyme (Cdc34) as well as a RING finger protein (Rbx1, in red) that lies at the heart of the complex. A number of proteins (in blue) containing an F-box domain, through which they bind to both Skp1 and Rbx1, can recruit different substrate proteins into the SCF complex via additional domains such as WD40 repeats or leucine-rich repeats (LLR). Two examples of F-box proteins that associate with the SCF complex, and the substrates that they recruit, are shown to the right. Based upon [Tyers, 1999]. **(B)** shows the ubiquitinating complex formed by Cbl, a single protein that alone can act as E3 ubiquitin ligase. Cbl is targeted to phospho-tyrosine-containing motifs within a number of activated receptor tyrosine kinases (RTKs), which are the targets for Cbl-mediated ubiquitination, via an SH2 domain. The SH2 domain (in blue), therefore, plays an analogous role to F-box proteins in SCF complexes (also blue in A), that being substrate recognition. Cbl, like Rbx1 (red in A), binds to an E2 enzyme, UbcH7 (in green), an interaction that is mediated by Cbl RING finger (also in red). Based upon [Barinaga, 1999].

6.2 RESULTS

6.2.1 Dominant negative dynamin does not induce apoptosis in combination with inhibitors of Rac

In chapter 3 data was presented showing that POSH N-terminus plus the Rac-binding domain are required for POSH to induce apoptosis (see figure 3.2). N17Rac could replace POSH RBD in this assay to induce apoptosis in combination with N POSH (see figure 3.5). SH3 1-2 could not substitute for N POSH, in combination with Y2H POSH, to induce apoptosis (see figure 3.2). This suggests that inhibition of endocytosis, caused by high levels of SH3 1-2 protein (see figures 5.1 and 5.2), is not sufficient to induce apoptosis in combination inhibition of Rac. SH3 1-2, however, is less potent than N POSH as an endocytosis inhibitor (see figures 5.1 and 5.2). The dominant negative S45N mutant of dynamin1 (described in [Herskovits, Burgess, 1993]) inhibited endocytosis just as strongly as N POSH in my hands (see figures 5.1 and 5.2 B).

S45N dynamin1 was tested, in combination with Y2H POSH or N17Rac, which both inhibit Rac (see [Feig, 1999] and figure 3.7), to see whether as a strong inhibitor of endocytosis S45N dynamin1 could contribute to apoptosis in place of N POSH. NIH3T3 cells were injected with S45N dynamin1 DNA plus empty vector, myc-N17Rac or myc-Y2H POSH. Flag-N POSH was also injected with N17Rac or Y2H POSH as a control that induces apoptosis. Quantified results from three experiments using Y2H POSH to inhibit Rac, and three experiments using N17Rac, are shown in figures 6.2 (A) and (B) respectively. Photographs showing examples of cells injected with Y2H POSH with S45N dynamin1 or N POSH are shown in figure 6.3 (C).

S45N dynamin1 alone or in combination with the two inhibitors of endogenous GTP-Rac (Y2H POSH or N17Rac) did not induce apoptosis after 7h expression (figures 6.2 and 6.3 a-f). In contrast N POSH strongly induced apoptosis in combination with Y2H POSH or N17Rac (figure 6.3 and 6.3 g-l), as seen in previous experiments (see figures 4.2 and 3.5). In some cases cells expressing Y2H POSH plus S45N dynamin were seen to be retracted after 7h expression (see for instance figure 6.3 (C) j-k), but the nuclei in such cells were not pyknotic (see figure 6.3 (C) f). This was also seen in some cells expressing high levels of Y2H POSH alone after 7h expression (data not shown). It was mentioned in chapter 3 that Y2H POSH forms cytoplasmic punctate structures (see for instance figure 6.3 (C) b, e, h and k) that are not formed by N POSH (see for instance figure 6.3 (C) g and j). After 7h expression of Y2H plus N POSH, in the few cells that were still spread, the N POSH protein appeared to be excluded from Y2H POSH-stained structures (see figure 6.3 (C) j and k). This was not seen so dramatically after just 2h expression (see for instance figure 3.3 d-e and figure 6.3 (C) g-h) or after 7h expression in cells that were badly retracted (see figure 3.3 f and g).

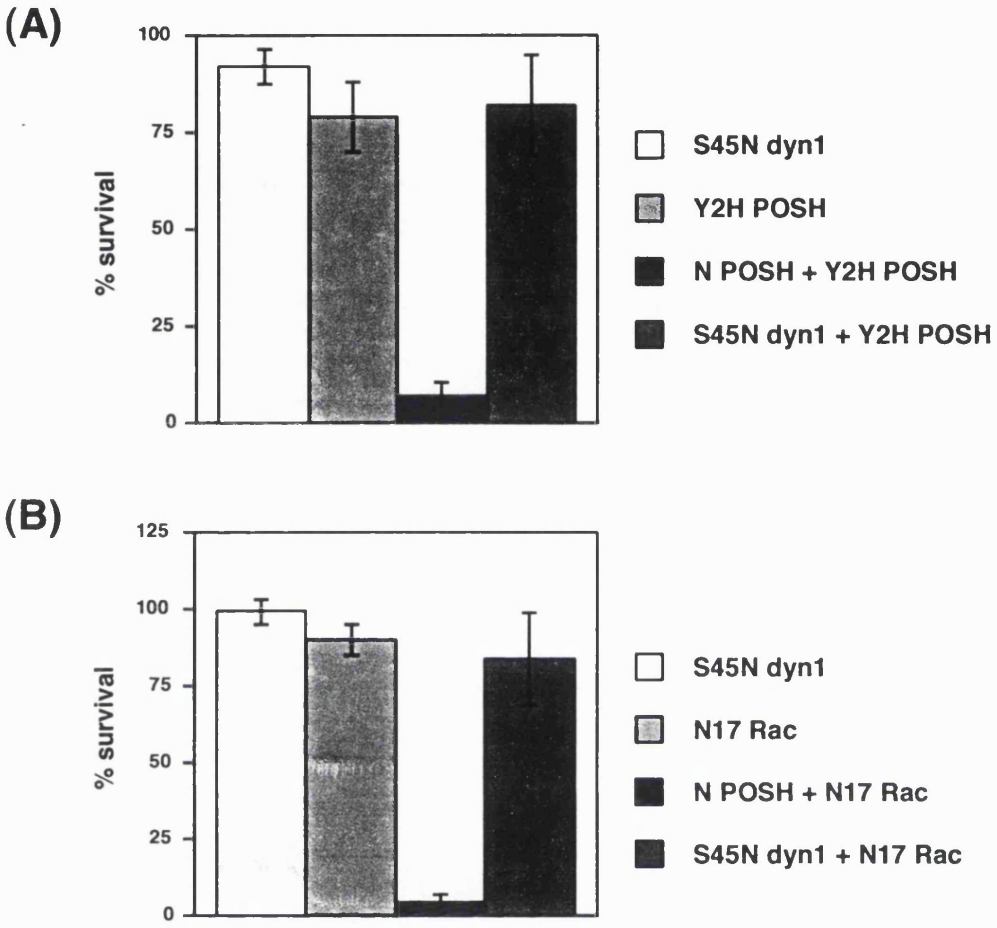

Figure 6.3 Dominant negative S45N dynamin, unlike N POSH, does not induce apoptosis in combination with Y2H POSH or N17 Rac

NIH3T3 cells were injected with 0.05mg/ml of the following DNAs: **(A)** S45Ndyanmin1 (dyn1)/pRK5, myc-Y2H POSH/pRK5, flag-N POSH/myc-Y2H POSH, S45Ndyn1/ myc-Y2H POSH; **(B)** S45Ndyanmin1 (dyn1)/pRK5, myc-N17Rac/pRK5, flag-N POSH/ myc-N17Rac, S45Ndyn1/myc-N17Rac. Two coverslips were injected with each DNA combination, one was fixed after 2h and the other after 7h. Expression of S45N dynamin1 was visualised with a mouse anti-dynamin1 antibody (hudy-1), myc-tagged proteins were visualised with a rat anti-myc antibody (JAC6) and flag-tagged proteins with a mouse anti-flag antibody (M2). Nuclear morphology was visualised with Hoechst staining. The number of non-pyknotic expressing cells was counted and survival expressed as: (% survival = number of non-pyknotic expressing cells (7h/2h)x100). The results shown in **(A)** and **(B)** are each averages from three experiments ± one StdDev.

(C) Immunofluorescence images are shown for NIH3T3 cells injected with 0.05mg/ml DNAs encoding myc-Y2H POSH and flag–N POSH (g-l) or myc-Y2H POSH and S45N dyn1 (a-f) after 2h (a-c and g-i) or 7h (d-f and j-l) expression. Bars equal 30μm.

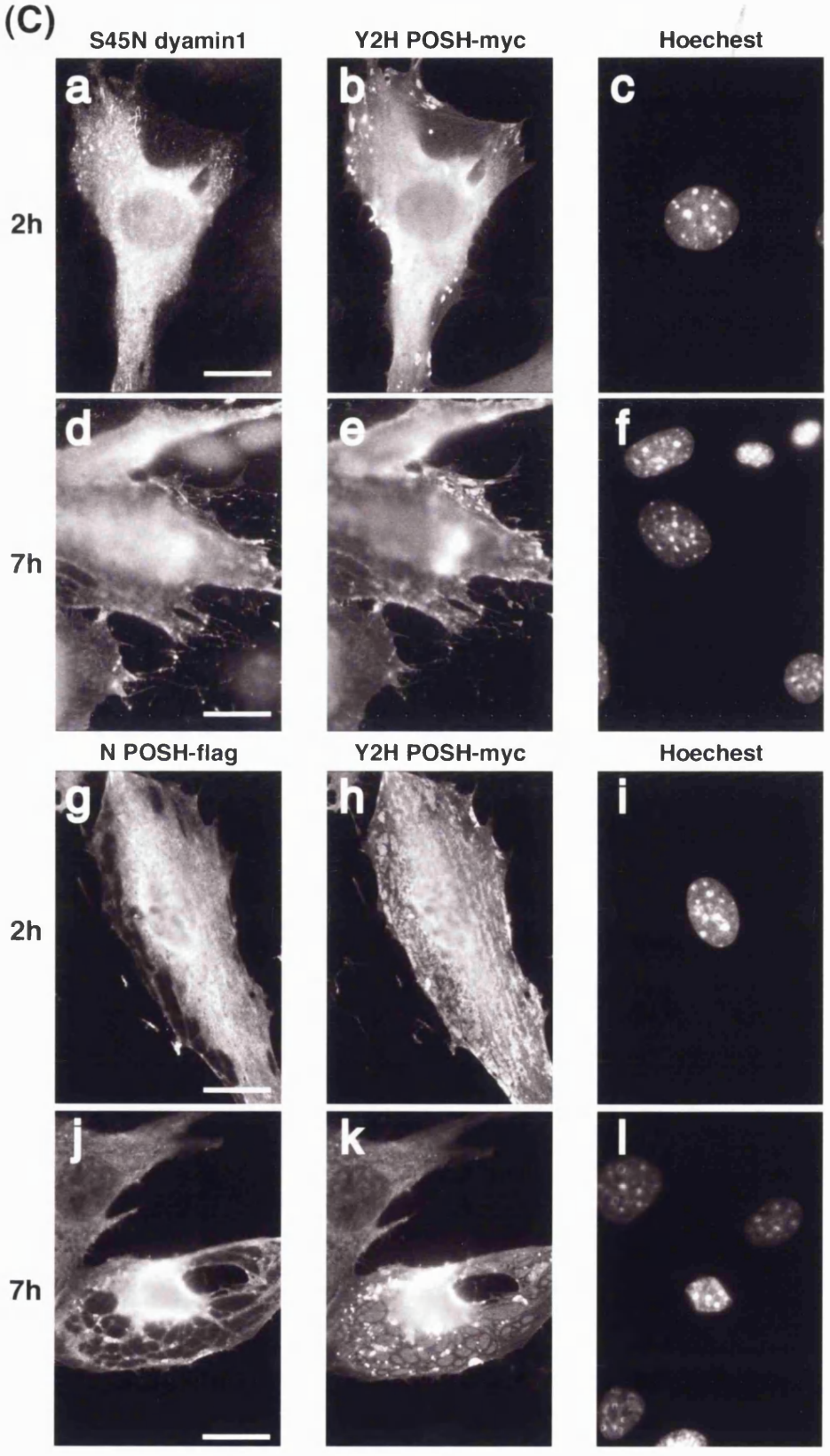

Figure 6.3 Dominant negative S45N dynamin, unlike N POSH, does not induce apoptosis in combination with Y2H POSH or N17 Rac

6.2.2 N POSH inhibits endocytosis in NIH3T3 cells

Experiments described above investigating links between endocytosis inhibition and POSH-induced apoptosis assume that S45N dynamin1, N POSH and to a lesser extent POSH SH3 1-2, inhibit endocytosis in NIH3T3 cells (used for apoptosis assays) as they did in Hep2 cells (used for endocytosis assays, see figure 5.1 and 5.2). For N POSH this was tested directly by injection of pRK5myc-N POSH into NIH3T3 cells. After 4h expression cells were treated with Tfn-TR. Empty vector and pRK5myc-C POSH injections were used as controls. Confocal sections taken through expressing cells and their uninjected neighbours are shown in figure 6.4.

The Tfn-TR signal was not as high using NIH3T3 mouse fibroblasts (figure 6.4 b, d and f) as it was with Hep2 epithelia-like human cells (see for instance figure 5.1A b). Even so, internalised Tfn could be detected in uninjected NIH3T3 cells and at similar levels in cells injected with empty vector (figure 6.4 a-b) or expressing myc-C POSH (figure 6.4 c-d). Almost all NIH3T3 cells expressing N POSH were inhibited in their ability to internalise Tfn (see for example figure 6.4 e-f).

6.2.3 Proteasome inhibitors rescue POSH-expressing cells

POSH RING finger is essential for POSH-induced apoptosis and a number of RING finger proteins are E3 ubiquitin ligases (see above). It seemed possible, therefore, that POSH is also an E3 enzyme and that POSH RING finger contributes to apoptosis by facilitating the degradation of a protein needed for cell survival. To begin to test this hypothesis the ability of inhibitors of the proteasome to rescue cells from POSH-induced apoptosis was assessed. Two inhibitors were tested: Lactacystin, a fungal metabolite that irreversibly inhibits peptidases in the 20S proteasome core by covalent modification [Fenteany, 1995] [Dick, 1996]; MG132, a peptide inhibitor (Z-Leu-Leu-Leu-CHO) that is thought to compete with ubiquitinated substrates for binding to the active site of proteases in the outer subunits of the 26S complex [Chadebech, 1999] [Tsukamoto, 1999].

NIH3T3 cells were injected with POSH DNA. After injection cells were treated with various concentrations of MG132 or Lactacystin. Cells were stained for POSH expression, for nuclear morphology and also for endogenous β-catenin. β-catenin staining was used to determine whether the proteasome inhibitors had worked; β-catenin protein builds-up when its degradation by the proteasome is inhibited and this is most clearly seen as an increase in nuclear protein [Aberle, 1997].

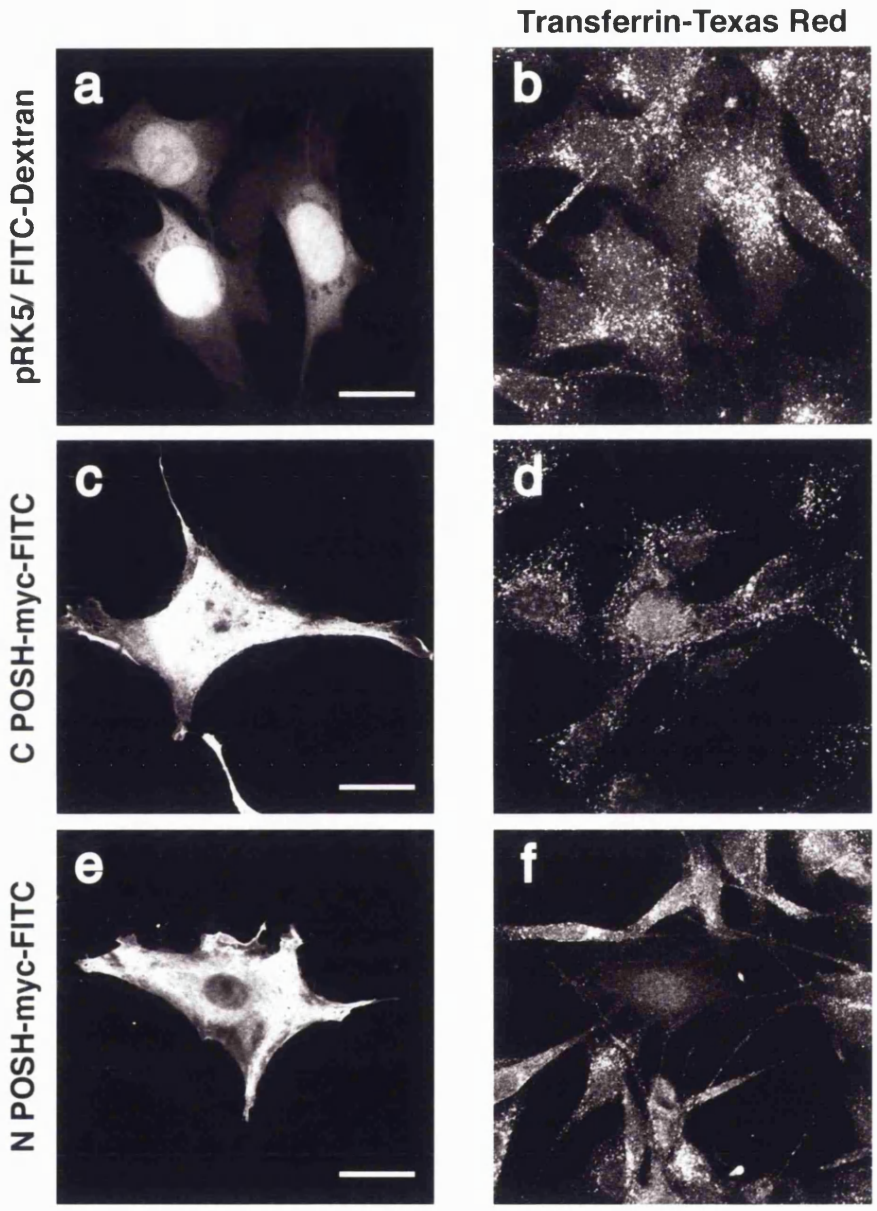

Figure 6.4 N POSH inhibits transferrin endocytosis in NIH3T3 cells
NIH 3T3 cells were injected with 2.5mg/ml FITC-Dextran plus 0.05mg/ml pRK5 (a-b) or with 0.05mg/ml pRK5myc-C POSH (c-d) or pRK5myc-N POSH (e-f). After 4h expression the cells were treated with 20μg/ml transferrin-texas red for 30min. Cells were washed, fixed and mounted strainght away, in the case of vector/FITC-dextran-injected cells, or permeabilised and stained with mouse anti-myc antibody 9E10, in the case of C-POSH and N-POSH DNA-injected cells. The confocal sections shown were taken at levels in the z-axis where myc and TR-Tfn levels were highest.
Bars equal a-b 37μm, c-d 50μm, e-f 66μm.

Average survival results from four experiments are shown in figure 6.5 (A) and representative immunofluorescence images are shown in figure 6.5 (B). The majority of untreated POSH-expressing cells had undergone apoptosis after 7h (see figure 6.5 A). After 7h uninjected cells and POSH-expressing cells that were not yet apoptotic had very low levels of endogenous β-catenin in the nucleus (see for instance figure 6.5 B a-c). Treatment with 1μM MG132 or with 10μM or 20μM MG132 or Lactacystin rescued more than 50% of POSH-expressing cells from apoptosis (see figure 6.5 A) and could be seen to cause a build-up of nuclear β-catenin in injected and uninjected cells (see figure 6.5 B d-i). At a concentration of 1μM Lactacystin did not cause a visible change in β-catenin distribution (data not shown) and did not rescue POSH-expressing cells from apoptosis (see figure 6.5 A).

6.2.4 Inhibition of endocytosis by POSH is not affected by proteasome inhibition

If ubiquitin-dependent protein degradation is important for POSH inhibition of endocytosis, as well as POSH-induced apoptosis (see section 6.2.3 above), then proteasome inhibitors may rescue endocytosis in POSH-expressing cells. To determine whether this was the case myc-POSH, myc-N POSH or empty vector were injected into Hep2 cells, which were treated for 3-4h with just DMSO, or MG132 in DMSO and then with Tfn-TR. POSH-injected cells were stained for myc-expression (FITC-dextran marked empty vector-injected cells) and viewed by confocal microscopy. In parallel, coverslips of uninjected Hep2 cells were also treated with DMSO alone or with MG132 in DMSO and were stained for β-catenin, to determine whether the proteasome inhibitor had worked.

An increase in nuclear β-catenin was seen for Hep2 cells treated with MG132 (figure 6.6 b) compared with cells treated with DMSO alone (figure 6.6 a). In three independent experiments MG132 was seen to have no visible effect on the ability of POSH (figure 6.6 e-f) or N POSH (figure 6.6 g-h) to inhibit transferrin endocytosis. Neither did MG132 itself appear to inhibit normal transferrin endocytosis in uninjected cells or empty vector-injected cells (figure c-d).

6.2.5 POSH does not bind to the E2 enzymes UbcH5 and UbcH7

If POSH can act as an E3 ubiquitin ligase then it must bind to an E2 enzyme. N POSH was tested in the yeast-two-hybrid system for binding to two E2 enzymes (UbcH7 and UbcH5). UbcH7 is an E2 enzyme that binds to Cbl RING finger in the two-hybrid system [Yokouchi, 1999] and with which HHARI and H7-AP1 interact *in vitro* in a RING finger-dependent manner [Moynihan, 1999]. UbcH5 is an E2 enzyme to which Cbl, HHARI and H7-AP1 do not bind, but which interacts with the HECT protein E6-AP [Scheffner, 1994] and with a number of RING-finger containing E3 enzymes [Lorick, 1999].

(A)

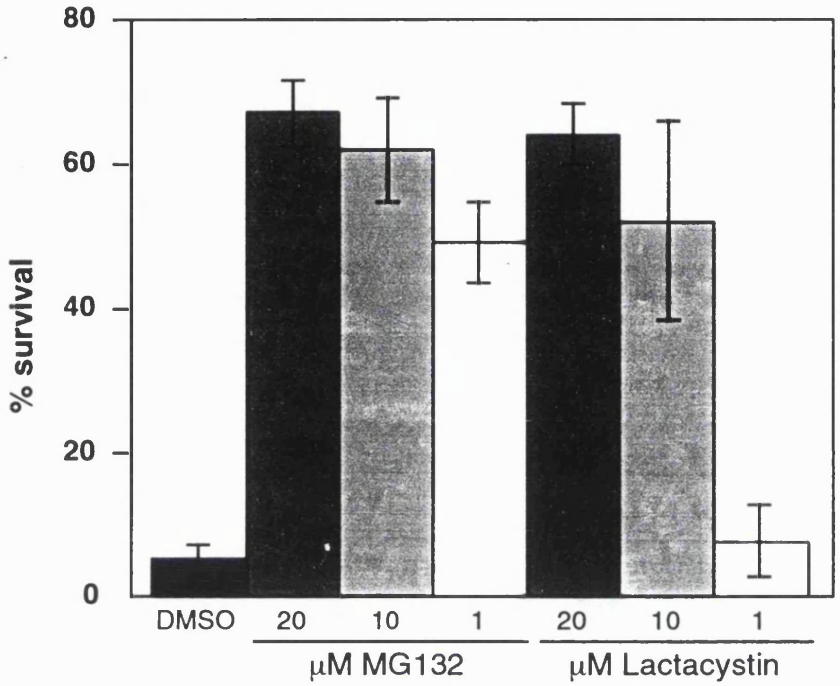

Figure 6.5 Proteasome inhibitors rescue POSH-expressing cells from apoptosis
100 NIH 3T3 cells per coverslip were injected with 0.05mg/ml pRK5myc-POSH. After injection coverslips were placed into normal growth media supplemented with just 0.2% DMSO or with the proteasome inhibitors MG132 or lactacystin in DMSO, at final concentrations of 20μM, 10μM or 1μM as indicated and made up to 0.2% DMSO in each case. One DMSO-treated coverslip was fixed after 2h expression. Proteasome inhibitor-treated coverslips and a second DMSO-treated coverslip were fixed after 7h. Expression of myc-POSH was visualised by staining with the rat anti-myc antibody JAC6 (B a, d and g) and nuclear morphology was visualised with Hoechst (B c, f and i). The localisation of endogenous β-catenin was also visualised using a mouse anti-β-catenin antibody (B b, e and h). This was to check that the proteasome inhibitors had worked; β-catenin degradation is blocked by proteasome inhibitors causing its protein levels to build-up, which is most clearly seen as an increase in nuclear β-catenin. The numbers of non-pyknotic expressing cells on each coverslip were counted and survival expressed as (% survival = number of non-pyknotic expressing cells (7h/2h)x100). The results shown in (A) are averages from four experiments ± one StdDev. Immunofluorescence pictures of representative cells after 7h POSH expression are shown for cells treated with DMSO alone (B a-c), with 10μM MG132 (B d-f) or with 10μM lactacystin (B g-i). Bars in (B) equal 30μm.

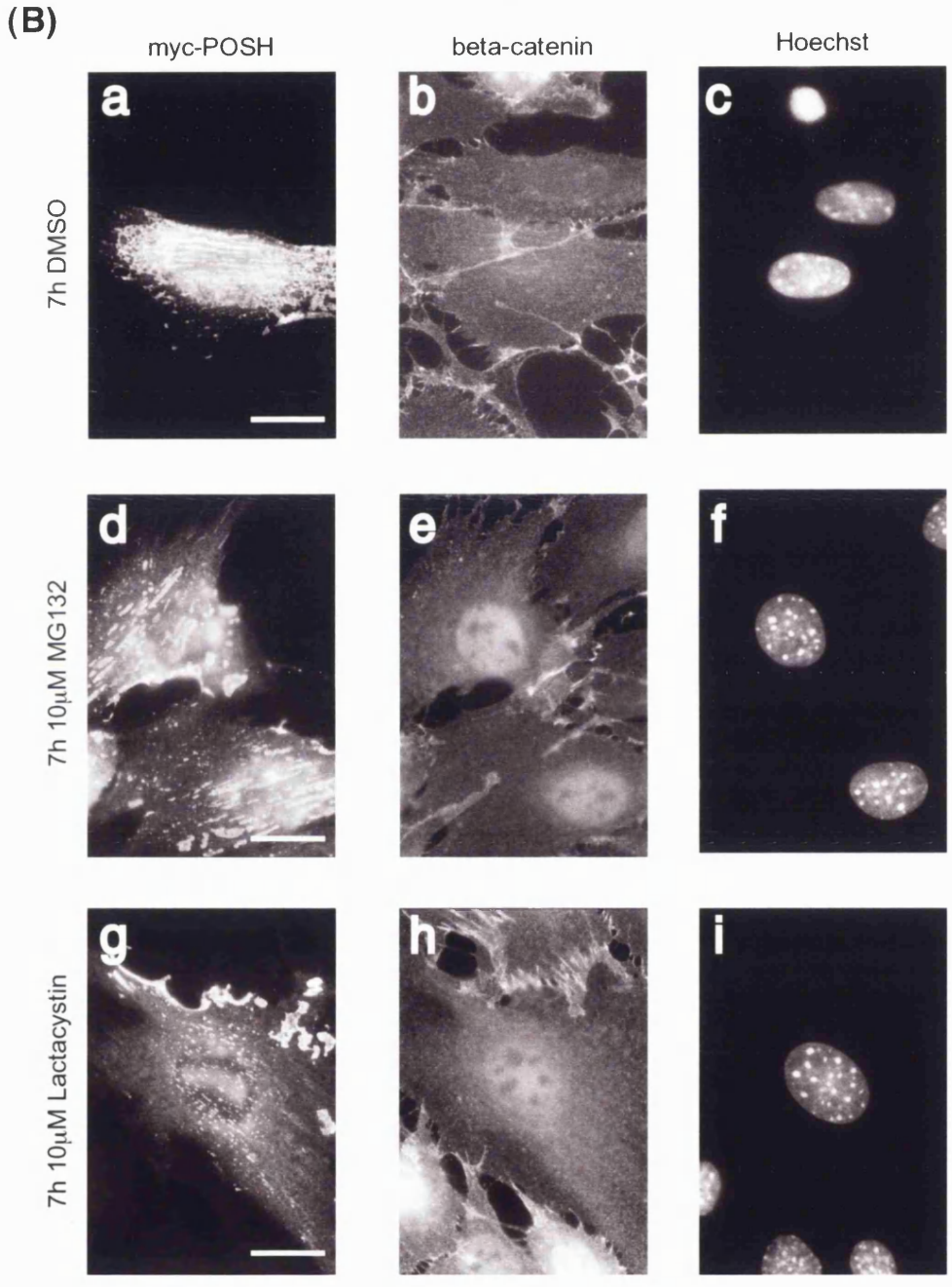

Figure 6.5 Proteasome inhibitors rescue POSH-expressing cells from apoptosis

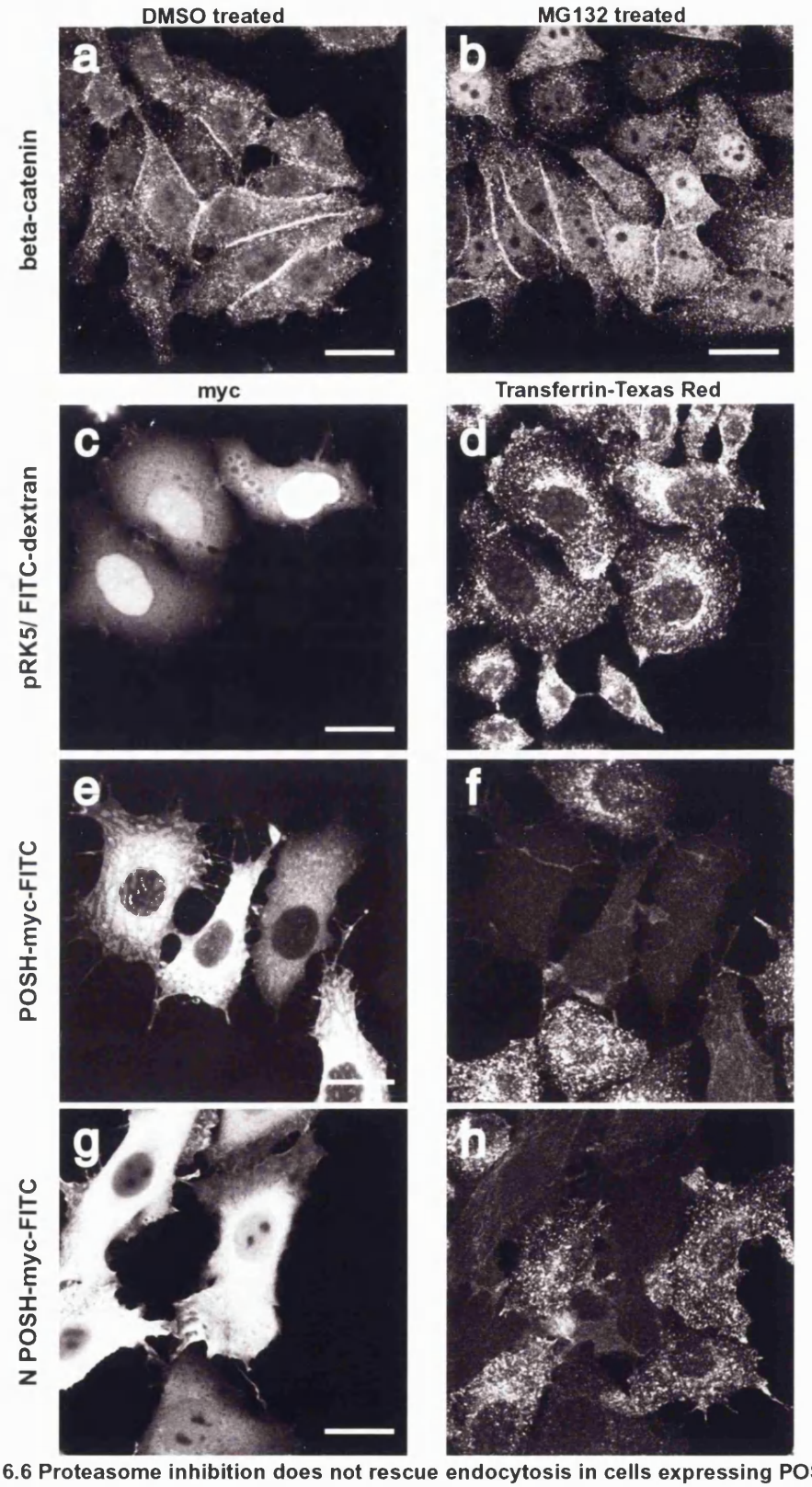

Figure 6.6 Proteasome inhibition does not rescue endocytosis in cells expressing POSH

100 Hep2 cells were injected/coverslip with 0.1mg/ml empty vector plus 2.5mg/ml FITC-dextran (c-d) or with 0.1mg/ml myc-POSH (e-f) or myc-N POSH (g-h) DNA. Injected cells, and coverslips of uninjected cells, were treated for 3-4h with 0.2% DMSO (a) or 10μM MG132/0.2% DMSO (b-h). Coverslips of uninjected DMSO or MG132 treated cells (a-b) were fixed and stained with a mouse anti β-catenin antibody. Injected cells were treated for 15min with 20μM Tfn-TR, still in the presence of DMSO or MG132/DMSO, washed and fixed. POSH and N POSH-injected cells were stained for myc tagged protein expression and cells were viewed with confocal microscopy. Bars equal: a-b 60μm, c-d 40μm, e-h 45μm.

As a positive yeast-two-hybrid control the pBTM116-Cbl RING finger (amino acids 374-430) construct was kindly provided, along with pACTII-UbcH5 and pACTII-UbcH7, by M Yokouchi (Yale University School of Medicine, New Haven, USA) and A Yoshimura (Kurume University, Kurume, Japan), these constructs are all described in [Yokouchi, 1999]. The yeast-two-hybrid systems for pBTM116 (LexA DNA-binding domain) and pYTH9 (Gal4 DNA-binding domain) required different yeast strains for analysis. Use of the yeast-two-hybrid system is described in methods section 2.4

The control construct pBTM116-Cbl RING, in the yeast strain L40a, was tested against pACTII-UbcH7 and pACTII-UbcH5 and was found to bind to the former but not the latter, as shown previously in [Yokouchi, 1999] (data not shown). pYTH9-N POSH was integrated into yeast strain Y190 and was tested against empty vector, pACTII-UbcH7 and pACTII-UbcH5. N POSH did not interact with UbcH7 or UbcH5 (data not shown). The same results were gained using two assays: (1) growth on histidine minus 3AT (3-amino triazole) plates (5mM 3AT for L40a and 25mM for Y190); (2) expression of β-galactosidase detected with X-gal.

6.2.6 Over-expressed POSH is ubiquitinated and N POSH associates with a ubiquitinated protein

The observation that proteasome inhibitors were able to rescue POSH-expressing cells lead us to further investigate a possible link between POSH and ubiquitination. A number of RING-type E3 enzymes have been reported to be ubiquitinated themselves (see for instance [Lorick, 1999] and [Honda, 2000]). We set out to test whether POSH itself was ubiquitinated and to visualise other ubiquitinated proteins (E2 enzymes or substrate proteins) with which POSH could associate.

In order to visualise ubiquitinated proteins an HA-tagged ubiquitin construct (HA-Ub), kindly provided by D Bohmann (EMBL, Heidelberg, Germany), was transfected along with POSH constructs into COS7 cells. Results from a representative experiment, where myc-tagged POSH, C-POSH, N POSH and SH3 1-2 were transfected with HA-Ub or with empty vector, and treated for 4h with either DMSO alone or MG132 in DMSO, are shown in figure 6.7. Myc-tagged proteins were precipitated, precipitates were split in half and separated by SDS PAGE. Half of each precipitate was probed for HA-tagged ubiquitinated proteins (figure 6.7 b and d) and half for precipitated myc-tagged POSH proteins (figure 6.7 a and c).

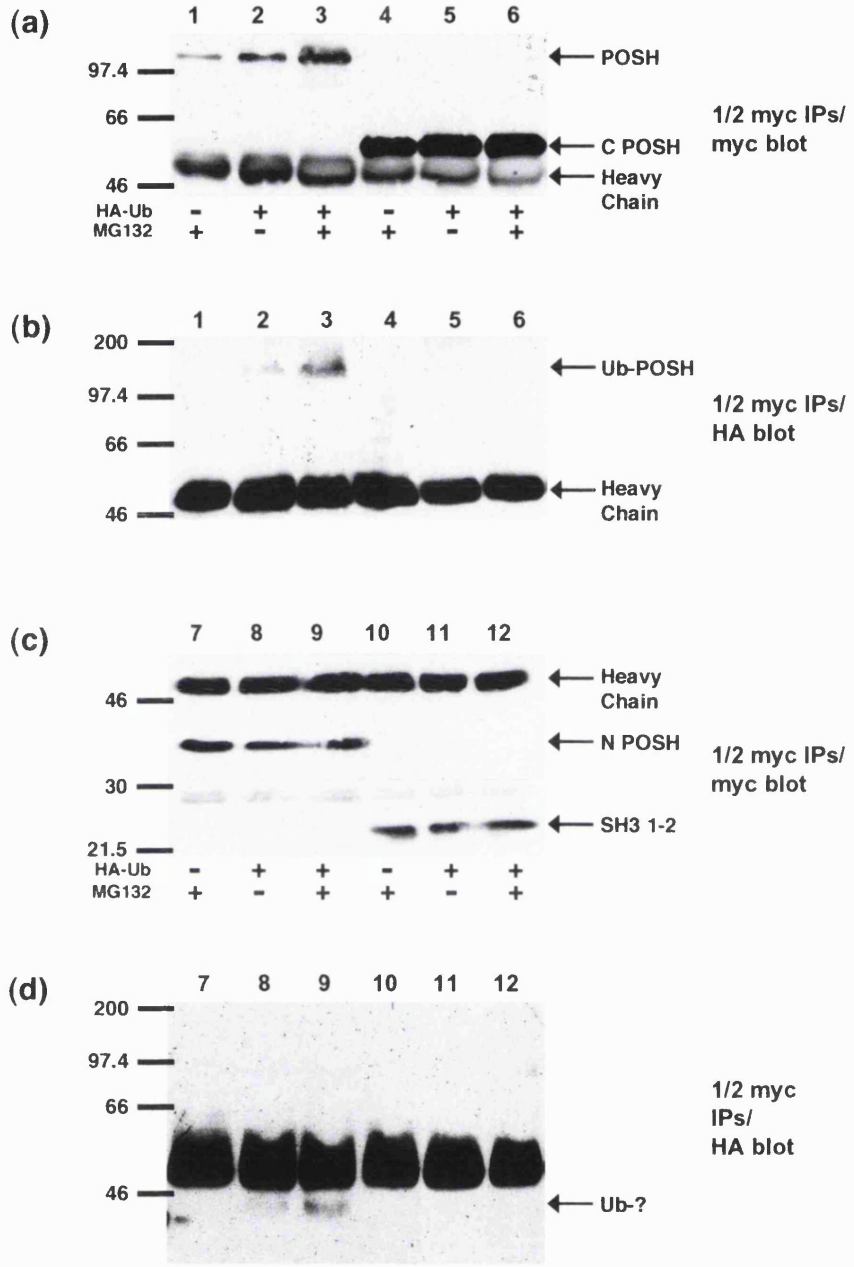

Figure 6.7 Full-length POSH is itself ubiquitinated and N POSH associates with a ubiquitinated protein of around 42kDa

Three lots of $5x10^5$ COS-7 cells were each transfected with 1μg of DNA encoding myc-tagged full-length POSH (1-3), C POSH (4-6), N POSH (7-9) or SH3 1-2 (10-12). In each case two plates were co-transfected with 1μg of DNA encoding HA-Ubiquitin (Ub) and the third with 1μg of empty vector. 24h post-transfection for each POSH construct an HA-Ub co-transfected plate and an empty vector control plate were treated for 4h with 10μM MG132 and for all plates the medium was made up to 0.1% DMSO. Post-nuclear supernatants were prepared and myc-tagged proteins were precipitated for 4h with mouse anti-myc antibody 9E10. Precipitates were split in half and separated by SDS PAGE. For half of the precipitates myc-tagged proteins were visualised by probing of western blots with 9E10 (a and c) and for the other half ubiquitinated proteins were visualised by probing of western blots with the rat anti-HA antibody 3F10 (b and d).

The overall amount of full-length POSH seen in the presence of both MG132 and HA-Ub was greater and the band of myc-tagged protein extended to a slightly higher molecular weight (figure 6.7 (a) lane 3) compared with either MG132 or HA-Ub alone (figure 6.7 (a) lanes 1 and 2). This suggests that the combination of an excess of ubiquitin and inhibition of the proteasome together stabilised POSH, and in particular a higher molecular form of POSH. Both the overall increase in protein and the spread in molecular weight were only seen in experiments where the level of POSH protein was not too high and where the MG132 was freshly prepared. No change in levels or molecular weight were visible for C POSH ((a) lanes 4-6), N POSH ((c) lanes 7-9) or SH3 1-2 ((c) lanes 10-12).

At a slightly higher molecular weight than the major precipitated myc-POSH band a ubiquitinated protein was seen in full-length POSH precipitates in the presence of the HA-Ub construct (figure 6.7 (b) lanes 2 and 3), but not in the absence of HA-Ub (figure 6.7 (b) lane 1). This band is either ubiquitinated full-length POSH or a ubiquitinated protein of similar molecular weight that is co-precipitated with POSH. The amount of ubiquitinated protein in POSH precipitates was increased by the addition of MG132 (figure 6.7 (b) compare lanes 2 and 3). This correlates with the observed increase in overall protein levels and molecular weight seen in myc-blots to detect precipitated POSH protein (figure 6.7 (a) compare lanes 2 and 3), suggesting that the ubiquitinated protein is POSH itself.

There was no ubiquitin associated with precipitated C POSH, N POSH or SH3 1-2 (data not shown), but an HA-tagged ubiquitinated protein (shown as Ub-? in figure 6.7) was detected at around 42kDa specifically in N POSH precipitates in the presence of HA-Ub (figure 6.7 (d) lanes 8 and 9). Treatment with MG132 caused an increase in the amount of this unknown ubiquitinated protein (figure 6.7 (d) compare lanes 8 and 9). Using Lactacystin instead of MG132 ubiquitination of full-length POSH and association of N POSH with a 42kDa ubiquitinated protein were similarly enhanced (data not shown).

SH3 1-2 did not associate with the ubiquitinated 42kDa protein seen in N POSH precipitates (figure 6.7 (d) lanes 10-12). To see whether the RING finger of N POSH, missing from the SH3 1-2 construct, alone was sufficient for association with this unknown ubiquitinated protein RING-SH3 1 and RING alone were compared with N POSH using the same assay as that described in figure 6.7. Neither of these shorter RING finger-containing proteins bound to the ubiquitinated 42kDa protein seen in N POSH precipitates or to any other ubiquitinated proteins in this assay (data not shown).

6.2.7 Dynamin and L61Rac do not appear to be ubiquitinated

If POSH acts as an E3 enzyme then the two proteins already known to bind to POSH, activated Rac and dynamin, could be targets of POSH-dependent ubiquitination. This possibility was tested in the following experiments.

Dynamin precipitated by N POSH is not ubiquitinated

Endogenous dynamin2 (the "aa" splice form is 870 amino acids long) runs slightly lower than myc-full-length POSH (892 amino acids plus myc tag) at around 100kDa. In experiments such as that shown in figure 6.7 HA blots were stripped and re-probed for dynamin2.

The results of re-probing the same blots shown in figure 6.7 (b) and (d) in order to visualise endogenous dynamin2 precipitated by each POSH construct are shown in figure 6.8 (A). There was a large amount of dynamin, both in the presence and absence of proteasome inhibitors, associated with precipitates of both N POSH (figure 6.8 (b) lanes 7-9) and SH3 1-2 (figure 6.8 (b) lanes 10-12). This precipitated dynamin2 was not ubiquitinated, as determined by probing for HA-tagged Ub (figure 6.7 d). No dynamin was detected in full-length POSH (figure 6.8 (a) 1-3) or C POSH (figure 6.8 (a) 4-6) precipitates.

Precipitated dynamin is not ubiquitinated with or without expression of POSH

If dynamin were ubiquitinated in the presence of full-length POSH, but not in the presence of the N POSH truncation, then ubiquitinated dynamin would not be detected in experiments such as that shown in figures 6.7 and 6.8 (A) because it does not stably associate with full-length POSH. Further experiments were carried out to address whether full-length POSH can induce ubiquitination of dynamin although the two proteins are not stably associated.

Myc-POSH was expressed in COS7 cells along with HA-Ub, or HA-Ub was expressed alone, in the presence or absence of MG132 (as described in figure 6.7). Either myc-POSH or endogenous dynamin2 were precipitated and precipitates were probed for the presence of HA-tagged ubiquitinated proteins. These HA blots were stripped and re-probed for precipitated POSH or dynamin2.

In two such experiments myc-POSH precipitates were seen, as shown in previous studies, to contain ubiquitinated protein of a molecular weight just above that of the majority of myc-tagged POSH protein (data not shown). There were no HA-ubiquitin-tagged proteins visible in precipitates of dynamin2 from COS7 cells expressing HA-Ub alone or from COS7 cells expressing myc-POSH, with or without MG132 treatment and with or without HA-Ub, although the precipitates contained large and similar amounts of dynamin2 (data not shown).

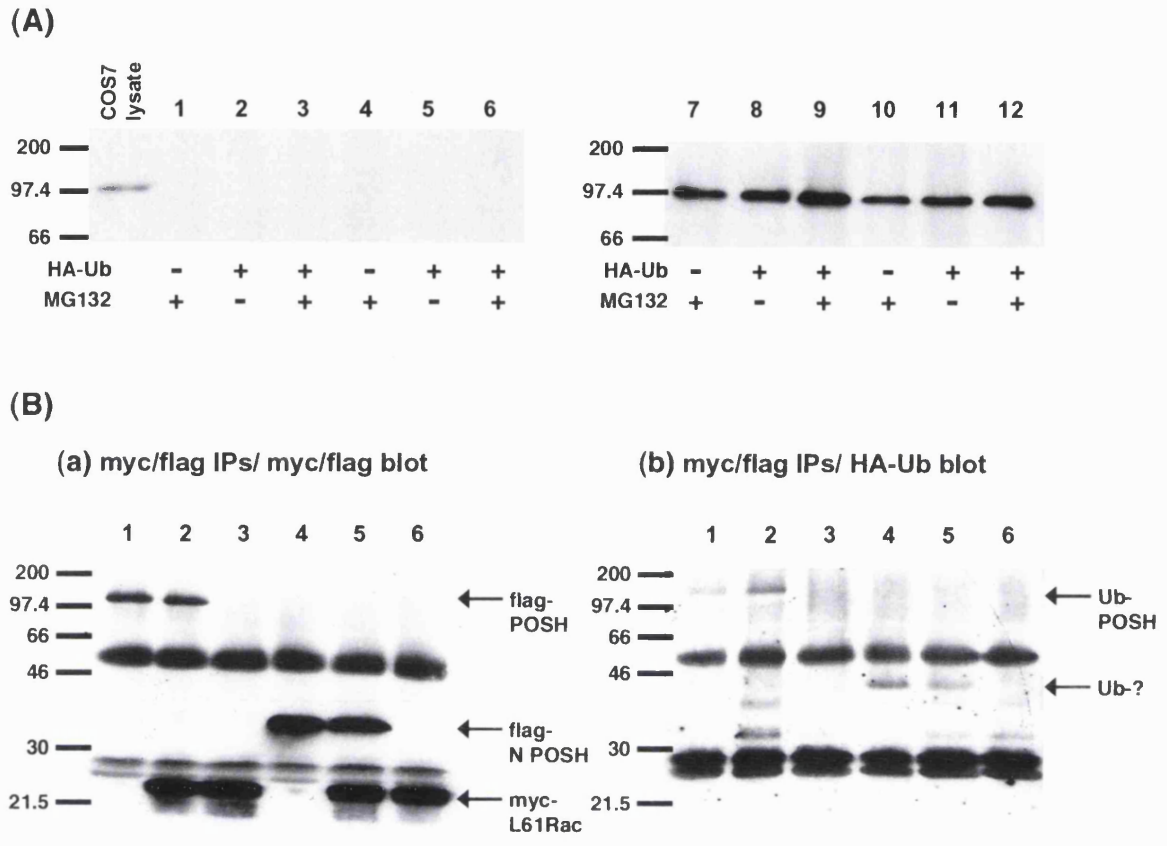

Figure 6.8 Dynamin and L61Rac are not ubiquitinated by POSH

(A) shows that N POSH and SH3 1-2 precipitate dynmain2, but this dynamin was not ubiquitinated (data not shown). The anti-HA blots of precipitated myc-tagged full-length POSH (1-3), C POSH (4-6), N POSH (7-9) and SH3 1-2 (10-12) shown in figure 6.7 (b) and (d) were stripped and re-probed with rabbit anti-dynamin2 antibody, and the results are shown here. Although a large amount of endogenous dynmain2 was associated with precipitated N POSH and SH3 1-2 (lanes 7-12) this dynamin was not ubiquitinated according to HA blotting (see figure 6.7 d). Full-length POSH (lanes 1-3) and C POSH (lanes 4-6) did not bind to dynamin2 in this assay.

(B) shows that POSH, but not Rac, is ubiquitinated upon co-expression of activated Rac with POSH. $5x10^5$ COS7 cells were transfected with 0.8μg of DNA encoding HA-Ub plus 0.8μg of the following pRK5 vector DNAs: flag-POSH/empty vector (1); flag-POSH/myc-L61Rac (2); myc-L61Rac/empty vector (3 and 6); flag-N POSH/empty vector (4); flag-N POSH/myc-L61Rac (5). For the last 4h of transfection the cells were treated with 10μM MG132 (proteasome inhibitor). Post-nuclear supernatants were prepared and both flag and myc-tagged proteins were precipitated for 4h at 4°C using monoclonal antibodies M2 and 9E10, which were added to all samples. The whole of each precipitate was separated by SDS PAGE and western blots were probed first with rat anti-HA antibody JAC6 (b), then stripped and re-probed with M2 plus 9E10 (a).

L61Rac is not ubiquitinated by POSH, but increases POSH ubiquitination

To investigate ubiquitination of Rac, HA-Ub was expressed with myc-L61Rac and/or flag-tagged POSH or N POSH. In all cases the cells were treated with MG132 and both myc and flag-tagged proteins were precipitated. Precipitates were probed for HA-ubiquitin (figure 6.8 (B) b) and these western blots were stripped and re-probed for precipitated myc and flag tagged proteins (figure 6.8 (B) a).

In such experiments, as seen before, POSH was associated with a band of ubiquitinated protein that is probably POSH itself, both in the presence (figure 6.8 (B) b lane 2) or absence (figure 6.8 (B) b lane 1) of L61Rac. N POSH, as shown in figure 6.7, was associated with a 42kDa ubiquitinated protein, both in the presence (figure 6.8 (B) b lane 5) or absence (figure 6.8 (B) b lane 4) of L61Rac. L61Rac itself did not appear to be associated with ubiquitin (figure 6.8 (B) b lanes 2-3 and 5-6), but if a large shift in the molecular weight of Rac was caused by multi-ubiquitination then this ubiquitinated protein would be obscured by the IgG light chain. Additional bands of ubiquitinated proteins (at around 30kDa and 35kDa) seen in lysates containing L61Rac (figure 6.8 B lanes 2-3 and 5-6) in this particular experiment were not seen in subsequent experiments.

6.2.8 The region between POSH SH3 domains 3 and 4 binds to an E3 ubiquitin ligase

A yeast-two-hybrid screen was carried out in the Hall laboratory using a C-terminal region of POSH as bait (amino acids 432-892), called here Cs POSH because it was slightly shorter than the C POSH construct used for expression in mammalian cells (amino acids 352-892). The library screened was the same NIH3T3 cell cDNA library, in pGAD10 vector, from which POSH was originally cloned [Tapon, Nagata, 1998]. One clone that gave positive results in both histidine minus growth and β-galactosidase assays, and proved positive upon DNA extraction and re-transformation into the bait strain, coded for a C-terminal region of an E3 ubiquitin ligase called seven in abstentia homolog 2 (siah-2) (Tapon and Hall unpublished data).

Siah2 is related to *Drosophila* seven in abstentia (sina), which is involved in R7 cell fate determination [Carthew, 1990]. Sina acts by association with an E2 enzyme, UBCD1, which allows it to induce ubiquitination and degradation of the transcription repressor tramtrack (TTK88) to which it also binds [Tang, AH, 1997]. Two types of mammalian sina homologue genes have been identified, the siah1 group of four closely related genes and siah2 [Della, 1993].

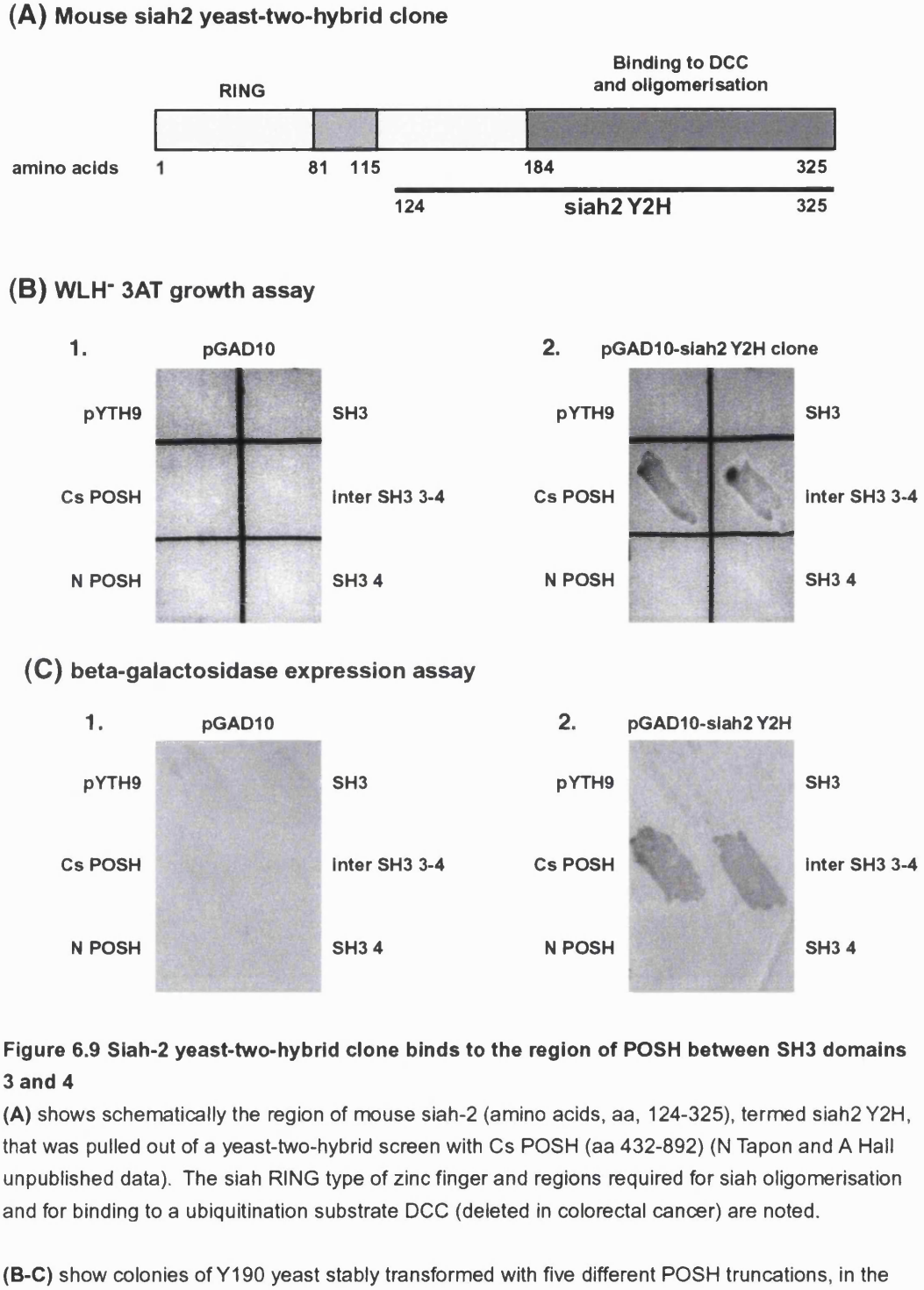

Figure 6.9 Siah-2 yeast-two-hybrid clone binds to the region of POSH between SH3 domains 3 and 4

(A) shows schematically the region of mouse siah-2 (amino acids, aa, 124-325), termed siah2 Y2H, that was pulled out of a yeast-two-hybrid screen with Cs POSH (aa 432-892) (N Tapon and A Hall unpublished data). The siah RING type of zinc finger and regions required for siah oligomerisation and for binding to a ubiquitination substrate DCC (deleted in colorectal cancer) are noted.

(B-C) show colonies of Y190 yeast stably transformed with five different POSH truncations, in the bait vector pYTH9, or with empty pYTH9, and co-transformed with empty pGAD10 prey vector (1 in B and C) or pGAD10siah2 Y2H (2 in B and C). Protocols for yeast transformations and yeast-two-hybrid analysis of protein-protein interactions are described in methods section 2.4. Growth on tryptophan/leucine/histidine minus (WLH^-) plates (B) and expression of β-galactosidase (C) were tested as indications that a protein-protein interaction had occured. The Gal4 activation domain alone (empty pGAD10 vector) showed no interaction with the Gal4 DNA-binding domain alone (empty pYTH9 vector) or fused to any of the POSH constructs tested in either assay (B and C 1). Siah2 Y2H did not bind to the Gal4 DNA-binding domain alone or fused to N POSH (aa 2-292), SH3 3 (aa 450-518) or SH3 4 (aa 831-892). Siah2 Y2H (B and C 2) was seen to interact with the Cs POSH control construct and with the region of POSH between SH3 domains 3 and 4, inter SH3 3-4,(aa 512-837).

Like POSH, siah proteins contain a RING finger. Siah1 (A-D) and siah2 have variable protein sequences at the extreme N-terminus, but are almost identical from the RING finger to the C-terminus of the protein (see siah2 domain structure in figure 6.9 A). Mammalian siah, like sina, has been shown to be an E3 ubiquitin ligase. Siah requires its RING finger for ubiquitination activity and E2 enzyme binding and acts to ubiquitinate at least one known substrate, the netrin receptor DCC (deleted in colorectal cancer) [Hu, 1997] [Hu, 1999]. A C-terminal region of mouse siah-2 (amino acids 124-325) was pulled-out of the yeast-two-hybrid screen with Cs POSH. This construct, termed siah2 Y2H, mediates oligomerization of siah and contains the binding site for DCC, but does not contain the N-terminal RING finger required for E3 enzyme activity, [Hu, 1999] (see figure 6.9 A).

The sequence elements within Cs POSH required for an interaction with the siah-2 yeast-two-hybrid clone (siah2 Y2H) were assessed using shorter POSH truncations in pYTH9. pYTH9 alone, SH3 3, SH3 4 and the inter-SH3 3-4 region (inter-SH3) were stably integrated into the Y190 yeast strain and tested against empty vector and pGAD10-siah2 Y2H. Yeast were tested both for growth on histidine minus/ 25mM 3AT plates and expression of β-galactosidase as assays for protein-protein interactions (see methods for a description of the principals and use of the yeast-two-hybrid system). In both cases empty pGAD10 did not appear to interact with any of the POSH truncations tested (see figure 6.9 B and C 1). The siah2 Y2H clone was found to interact in both assays with the Cs POSH control and with the inter-SH3 domains 3-4 region of POSH (see figure 6,9 B and C 2).

6.3 DISCUSSION

6.3.1 POSH-induce apoptosis and inhibition of endocytosis

Over many years scientists have inhibited endocytosis using methods such as intracellular potassium depletion [Larkin, 1986], treatment with hypertonic media [Heuser, JE, 1989] or acidification [Heuser, J, 1989], and more recently using dominant negative mutants of dynamin and other coated pit components (including dynamin-binding proteins). Out of all these reports I can find only one case where apoptosis is induced by any endocytosis-inhibiting treatment, that is over-expression of the dynamin-binding protein Mlk2. Over-expressed Mlk2 induces apoptosis [Nagata, 1998], although it is much less potent than POSH (data not shown), and inhibits transferrin endocytosis in Hep2 cells (data not shown). Mlk2 also strongly activates JNK and (like POSH) is a Rac-binding protein, both of which may make additional contributions to the induction of apoptosis by this kinase. Consistent with the idea that inhibition of endocytosis alone does not induce apoptosis, POSH or S45N dynamin1, although sufficient to inhibit

endocytosis (see figures 5.1 and 5.2), do not induce apoptosis in NIH3T3 cells (see figure 3.2). N POSH combined with inhibitors of Rac, however, does induce apoptosis (see chapter 3). The following data indicates that inhibition of endocytosis is not the only contribution made by N POSH to apoptosis, although it does appear to play some part, and that the RING finger is essential for POSH-induced apoptosis.

N POSH inhibits endocytosis in NIH3T3 cells

For inhibition of endocytosis by N POSH to make any contribution to apoptosis N POSH would have to inhibit endocytosis in the NIH3T3 cells used for apoptosis assays in the same way as it did in Hep2 cells (see figures 5.1 and 5.2). The Tfn-TR uptake signal was weaker using NIH3T3 cells than Hep2 cells, but Tfn endocytosis could still be visualised, and N POSH was seen to inhibit transferrin endocytosis (see figure 6.4). Inhibition of endocytosis could, therefore, theoretically be involved in POSH-induced apoptosis in the NIH3T3 cell assay.

Inhibition of endocytosis plus inhibition of Rac does not cause apoptosis

Although N POSH inhibits endocytosis in NIH3T3 cells, inhibition of endocytosis by other proteins, in combination with inhibitors of Rac, did not cause apoptosis (summarised in the table shown in figure 6.10). SH3 1-2 or S45N dynamin1, which is a stronger inhibitor of endocytosis than SH3 1-2 in Hep2 cells (see figures 5.1 and 5.2), were used to inhibit endocytosis. Neither protein could induce apoptosis in combination with inhibitors of Rac, Y2H POSH or N17Rac, (see figure 3.2, figure 6.3 and summary in figure 6.10). These data suggest that the RING finger within N POSH, which is not present in SH3 1-2 and is not required for binding to dynamin, is essential for POSH to induce apoptosis. These data do not rule out some contribution to apoptosis from the dynamin-binding SH3 domains of POSH, but suggest that inhibition of dynamin is not the only contribution made by N POSH to apoptosis. One result presented in chapter 3 suggests that the dynamin-binding SH3 domains of POSH do make some contribution to apoptosis. A POSH RING-SH3 1 construct, lacking the second SH3 domain present in N POSH, could neither bind to dynamin and inhibit endocytosis (data not shown) nor replace N POSH to induce apoptosis (see figure 3.2 and summary table in figure 6.10).

Protein	Binding to dynamin	Inhibition of endocytosis	Induction of apoptosis when combined with inhibitors of Rac:	
			+Y2H POSH	+ N17Rac
N POSH	+	+	+	+
SH3 1-2 POSH	+	+/-	-	-
Zn-SH3 1 POSH	-	-	-	-
S45N dynamin1	n/a	+	-	-

Figure 6.10 Table summarising the effects of POSH truncations and a dominant negative dynamin mutant (S45N) upon endocytosis and apoptosis

(+) indicates an effect, (-) indicates no effect; (+/-) indicates a partial effect; n/a, not applicable.

6.3.2 POSH and ubiquitination

POSH RING finger is essential for the contribution of N POSH to apoptosis and increases the potency of POSH inhibition of endocytosis (compare N POSH with SH3 1-2, lacking the RING finger, in figures 5.1 and 5.2 and in the summary table in figure 6.10). Many other RING finger proteins have been shown to act as E3 ubiquitin ligases (introduced above and reviewed in [Freemont, 2000]). The following observations suggest that POSH may also act as an E3 ubiquitin ligase, or at least that POSH in some way is linked to the process of ubiquitination.

Proteasome inhibitors prevent POSH-induced apoptosis

POSH-induced apoptosis appears to be proteasome-dependent, as inhibition of the proteasome with Lactacystin or MG132 rescued POSH-expressing NIH3T3 cells (see figure 6.5). Apoptosis in general is highly influenced by proteasome activity. For example, proteasome activity controls the activity of transcription factors with roles in survival and apoptosis, such as NF-κB [Karin, 2000] and c-jun [Treier, 1994] (see introduction section 1.4.4 and discussion in chapter 3). The proteasome also degrades key apoptosis regulators, such as ubiquitinated pools of p53 [Soussi, 2000] and Bcl-2 [Chadebech, 1999].

Inhibition of the proteasome by Lactacystin has itself been reported to induce apoptosis in a number of cell types, such as human chronic lymphocytic leukaemia lymphocytes [Delic, 1998] [Masdehors, 1999] and cerebellar granule cells [Pasquini, 2000]. NIH3T3 cell fibroblasts, after 7h proteasome inhibition, did not undergo apoptosis, rather these treatments actually rescued POSH-expressing cells from apoptosis. These results suggest either that POSH (directly or indirectly) induces ubiquitination of something required for cell survival, and that this is important to the ability of POSH to induce apoptosis, or that the proteasome inhibitors have an anti-apoptotic effect unrelated to POSH.

It is not unheard of for proteasome inhibition to prevent apoptosis, although most reports show a pro-apoptotic effect of proteasome inhibitors such as Lactacystin. For instance, it has been reported that proteasome inhibition blocks death of thymocytes in response to a number of pro-apoptotic stimuli [Grimm, 1996] and that activation of interleukin-1β converting enzyme (ICE) family caspases was blocked, in both sympathetic neurons and macrophages, by Lactacystin [Sadoul, 1996]. The ability of Lactacystin and MG132 to prevent apoptosis of NIH3T3 cells in response to agents other than POSH has not been tested, but may help to determine the specificity of the effect.

Unlike apoptosis, endocytosis is not rescued in POSH-expressing cells by proteasome inhibition (see figure 6.6). This shows that ubiquitin-dependent degradation events are not essential for POSH to inhibit endocytosis. SH3 1-2 is able to inhibit endocytosis alone, but the RING finger

of N POSH (which is probably be the region of POSH involved in ubiquitination) does increase the potency of POSH inhibition of endocytosis (see figures 5.1 and 5.2). A RING finger-dependent, possibly ubiquitination-dependent, event, therefore, increase the ability of POSH to inhibit endocytosis although, unlike POSH-induced apoptosis, it is not essential for POSH inhibition of endocytosis.

Full-length POSH is ubiquitinated

POSH contains a RING finger, as do many proteins known to be E3 ubiquitin ligases. POSH itself, when over-expressed with HA-Ub, appears to be ubiquitinated and the amount of ubiquitinated POSH detected is increased by proteasome inhibitors (see figures 6.7 and 6.8). For HECT domain E3 enzymes modification with ubiquitin is part of the ubiquitin transfer process [Hatakeyama, 1997]. This does not appear to be the case for RING finger E3s, but ubiquitination of a number of these E3s has also been observed both *in vitro* and *in vivo*, for Mdm2 [Honda, 2000] and A07 [Moynihan, 1999] for instance. In the case of Mdm2 evidence suggests that ubiquitination of the E3 enzyme regulates its activity: Mdm2 modification with the ubiquitin-like peptide, SUMO-1, prevents ubiquitination of Mdm2 itself and increases its ubiquitination activity towards p53 [Buschmann, 2000].

Although full-length POSH ubiquitination is not inconsistent with a role for POSH as an E3 enzyme it may be that POSH is just a substrate for another E3-E2 enzyme complex. Siah, to which POSH binds in the yeast-two-hybrid system (see figure 6.9), has been shown to act as an E3 enzyme [Hu, 1997] [Hu, 1999] and is a possible candidate, in addition to POSH itself, to mediate POSH ubiquitination. It may even be that POSH and siah somehow co-operate to mediate ubiquitination of the same or different substrates (possibly including each other) in a higher order complex, although this has not been shown for other E3 enzymes. It would be interesting to see whether POSH ubiquitination could be blocked by co-expression of constructs encoding the C-terminal region of siah that binds to POSH in the yeast-two-hybrid system.

A possible PEST site within POSH

It is difficult to predict simply from amino acid sequence whether a protein is likely to be ubiquitinated. One or more lysine residues, to which the ubiquitin can actually be conjugated, are of course required. Beyond this there does appear to be general preference for ubiquitination of proteins containing what are called PEST (proline, glutamate, serine, threonine-rich) sequences. PEST sequences make a protein more likely to be targeted for ubiquitination, but do not have to contain the actual ubiquitinated lysine residues. The PEST algorithm, formulated by Rogers et al [Rogers, 1986], has proved powerful in predicting proteins subject to rapid turnover. Sequences that are bounded by basic residues (K, R or H) and that include at least one proline and one acidic

residue score as PEST hits with this algorithm. The strength of the PEST score depends mainly upon the proportion of P, D, E, S or T amino acids within the interval.

Using the Rogers algorithm to analyse POSH one potential PEST site was identified, amino acids 268-291, which has a lysine at either end and contains 55% P, D, E, S or T (shown in figure 6.11). This mPOSH potential PEST sequence is present and 67% identical in the human POSH clone, but the equivalent region of *Drosophila* POSH does not contain the bounding K, R or H residues typical of a PEST site. The final K within the potential PEST sequence of mPOSH is not present within the N POSH truncation, which terminates at amino acid 290. If POSH requires both the RING finger, to recruit an E2 enzyme, and the PEST site to be ubiquitinated itself then this may explain why full-length POSH, but not the N POSH truncation, is ubiquitinated.

The POSH potential PEST sequence	% PDEST
mPOSH 268-**K** P P V P G V D T A E C P S A T A Q S T S A S **K**-291	55
hPOSH 270-**K** P P V P G V D A G E C S S A A A Q S S T A P **K**-293	50
dPOSH 270-L **H** T H P L C H P P K Q Q G Q R A L P P V P V I-293	n/a

Figure 6.11 A putative PEST site in POSH

The region of full-length mouse (m) POSH that scores most highly with the Rogers et al PEST algorithm [Rogers, 1986] and the equivalent regions of human (h) and *Drosophila* (d) POSH are shown. K, R or H residues bounding each PEST sequence are shown in bold and PDEST residues between them are underlined. The % PDEST within each PEST site is shown. n/a = not applicable, and indicates the incomplete PEST site in dPOSH.

Some proteins, such as IκB, β-catenin and the G1 cyclins, have to be serine phosphorylated in order for E3 enzymes to recognise them as ubiquitination substrates. For IκB two lysines (residues 21 and 22) are the major ubiquitin conjugation sites, but are not needed for E3 enzyme recruitment, reviewed in [Karin, 2000]. E3 recruitment, in this case the SCF^{-TrCP} complex depicted in figure 6.2, requires two phosphorylated serines (residues 33 and 36); a phospho-peptide of amino acids 28-39 will inhibit IκB ubiquitination in cell-free extracts [Yaron, 1997]. For Cbl ubiquitination of its receptor substrates relies upon recognition of phospho-tyrosine motifs by its SH2 domain (shown in figure 4.2 and reviewed in [Barinaga, 1999]). It is possible that targeting of POSH for ubiquitination, either by a separate E3 enzyme (such as siah) or by POSH itself, is similarly regulated by phosphorylation.

POSH and binding to E2 ubiquitin-conjugating enzymes

If POSH is an E3 enzyme then it must bind to an E2 enzyme, of which there are at least 17 in mammalian cells [Jensen, 1995]. Two E2 enzymes, UbcH5 and UbcH7, known to bind to other RING finger-containing E3 enzymes [Lorick, 1999] [Moynihan, 1999] [Yokouchi, 1999], were tested against N POSH in the yeast-two-hybrid system, but no interaction was seen (data not shown). We attempted to visualise ubiquitinated proteins, E2 enzymes or substrates, physically associated with precipitated full-length POSH and N POSH using over-expressed HA-Ub as a marker. Binding of endogenous E2 enzymes to over-expressed precipitated RING-finger proteins has been observed previously for A07 with UbcH5 in COS-7 cells [Lorick, 1999] and for HHARI with UbcH7 in HeLa cells [Moynihan, 1999], but using anti-E2 antibodies rather than ubiquitin to visualise the co-precipitated E2 enzymes.

With full-length POSH only a band of ubiquitinated protein that appears to be POSH itself was seen (see figures 6.7 and 6.8). N POSH was seen to associate with a ubiquitinated protein of around 42kDa (see figures 6.7 and 6.8) and this was dependent upon the presence of the RING finger (SH3 1-2 did not bind to this protein, see figure6.7 c-d). UbcH5 and UbcH7, which did not bind to N POSH in the yeast-two-hybrid system (data not shown) are both a lot smaller than 42kDa, but other E2 enzymes exist of molecular weight up to 70kDa. This N POSH-associated protein at 42kDa could, therefore, be an E2 enzyme. Probing of N POSH precipitates with anti-E2 antibodies or extraction of the 42kDa band and Mass Spec analysis could determine the identity of this protein bound to N POSH.

If the 42kDa protein bound to N POSH were an E2 enzyme, and if N POSH can not ubiquitinate itself or substrate proteins, then it may become stuck to the E2 enzyme, allowing the protein to be visualised in N POSH precipitates. It may be that full-length POSH associates only transiently with the 42kDa putative E2 enzyme, prior to ubiquitination of itself or substrate proteins, and this is why it is not found stably associated with the 42kDa ubiquitinated protein.

Shorter POSH truncations containing the RING finger did not bind to the 42kDa protein (data not shown). For the E3 enzyme Cbl the RING finger alone will bind to the E2 enzyme UbcH7 in the yeast-two-hybrid system, but the interaction is increased when additional regions of the protein are included [Yokouchi, 1999]. A crystal structure of Cbl with UbcH7 also revealed that the majority of contacts between the two proteins are mediated by Cbl RING finger, but that additional contacts were formed by an α-helical region N-terminal to the RING finger [Zheng, 2000]. The 42kDa N POSH-associated protein, although unable to bind to POSH RING finger alone, may still be an E2 enzyme that requires other regions within N POSH in addition to the RING finger for a strong interaction.

6.3.3 Possible links between POSH, Rac, dynamin and ubiquitination

If POSH is an E3 enzyme then it may act upon Rac or dynamin themselves, to which it binds directly, or it may be involved in the ubiquitination of other proteins associated with Rac or dynamin. Candidate proteins that are involved in Rac or dynamin function and are known to be ubiquitinated, so may be targets for POSH are as follows.

Rac-associated proteins and ubiquitination

Our attempts to detect any ubiquitinated Rac were hampered by the fact that Rac runs just below the light chain on SDS PAGE gels. However, initial experiments suggest that activated L61Rac, in the presence of POSH and/or HA-Ub, is not ubiquitinated (see figure 6.8). So far there is no evidence from our work or that of others to suggest that Rac is a target for ubiquitination.

Only one known Rho GTPase target is known to be ubiquitinated, as a means to control the timing of its activity, which is the yeast Cdc42 effector protein Gic-2p [Jaquenoud, 1998]. POSH appears, therefore, to be only the second known ubiquitination-controlled Rho GTPase effector.

In terms of ubiquitination of proteins that bind to and regulate Rac activity, none of the Rho GTPase GAPs or RhoGDIs are known to be ubiquitinated. A family of related GEFs (mammalian Tiam-1 and Stef and *Drosophila* Sif) that act upon Rac have been shown to contain potential PEST sites that are important for their stability, although ubiquitination of these proteins has not been shown directly, reviewed in [Stam, 1999]. These GEFs are, therefore, potential Rac-related proteins that could be targets for POSH-induced ubiquitination.

Dynamin and ubiquitination

To my knowledge dynamin, like Rac, has not been shown to be ubiquitinated. In experiments described above, neither endogenous dynamin2 co-precipitated with N POSH (see figures 6.7 and 6.8) nor dynamin2 precipitated from lysates with or without transfected full-length POSH (data not shown) was seen to be ubiquitinated. The evidence so far suggests that dynamin itself is not the target for POSH-dependent ubiquitination, which indicates that N POSH does not contribute to apoptosis, or more potently inhibit endocytosis that SH3 1-2, by inducing dynamin degradation.

There are at least two types of endocytosis-related protein that may be targets for POSH-induced ubiquitination. Firstly, a number of activated receptors are ubiquitinated and secondly the coated pit component Eps15 (shown within the coated pit protein-protein interactions scheme in figure 1.20) is also ubiquitinated, as discussed in introduction section 1.5.8.

The functional significance of Eps15 ubiquitination remains uncertain and the ubiquitin ligase that mediates Eps15 ubiquitination has not been identified. Interestingly, in terms of being a possible ubiquitination substrate for POSH, Eps15 contains proline-rich motifs, one of which has been shown to bind to the adaptor protein Crk, so could potentially bind to POSH SH3 domains [Schumacher, 1995]. Eps15 is around 100kDa, a very similar size to dynamin and POSH itself. If Eps15 were to bind to full-length POSH, but not to the N POSH or C POSH truncations, or if it were to bind weakly or transiently to N POSH or C POSH, then an interaction of POSH with Eps15 may have missed by the assay for N POSH and C POSH binding proteins shown in figure 4.1. If Eps15 were the target for POSH ubiquitination, then this could be the contribution made by the N POSH RING finger to apoptosis and possibly to full endocytosis inhibition.

The membrane-bound receptors recruited to clathrin-coated pits may be another possible target for POSH-dependent ubiquitination. In yeast ubiquitination of a number of receptors, including the G protein-coupled pheromone receptors STE2 [Hicke, 1996] and STE3 [Roth, 1998], has been shown to be required for their internalisation and subsequent vacuolar degradation (reviewed in [Hicke, 1999]). In mammalian cells a number of receptors appear to be ubiquitinated, many of which are receptor tyrosine kinases, such as PDGF receptor [Mori, 1995] and EGF receptor [Stang, 2000], and some of which are ion channels, such as the epithelial Na^+ channel, ENaC, [Staub, Gautschi, 1997]. In contrast to studies in yeast, in mammalian cells no cases of seven-transmembrane receptor ubiquitination have been reported.

Ubiquitination of EGF receptor [Yokouchi, 1999] and of colony stimulating factor receptor [Lee, PS, 1999] are dependent upon the E3 enzyme Cbl, whose SH2 domain allows it to bind to phospho-tyrosines within the cytoplasmic tails of these activated receptors and recruit an E2 enzyme (as shown in figure 6.2). ENaC binds to Nedd4, a HECT type of E3 enzyme, via WW domains of Nedd4 and proline/tyrosine-rich sequences in the ENaC cytoplasmic tail [Staub, Yeger, 1997]. Interestingly, siah, to which POSH can bind, appears to target another receptor, DCC, for ubiquitination [Hu, 1997]. POSH may act as an E3 enzyme to target other receptors, possibly receptors that lead to the activation of Rac, for ubiquitination.

Mono-ubiquitination was found to be sufficient to facilitate endocytosis of STE2 [Terrell, 1998]. In mammalian cells mono-ubiquitination, or addition of small numbers of ubiquitin polypeptides sometimes with unusual lysine 46 ubiquitin-ubiquitin links, also results in a modification that is not efficiently recognised by the proteasome, reviewed in [Strous, 1999]. This type of ubiquitination may instead have a signalling role in which proteins like POSH could be involved.

CHAPTER 7
SUMMARY AND FUTURE DIRECTIONS

POSH is a modular, scaffold-like protein with multiple binding partners. The known activities and binding partners for POSH are summarised in figure 7.1. The experiments described in chapters 3-6 have used full-length POSH and truncations to show that POSH binds not only to the small GTPase Rac, but also to the larger GTPase dynamin, and that POSH may be involved in (or at least is controlled by) ubiquitination. In terms of future experiments, the creation of a number of point mutants within POSH could enable the regions required for POSH activities and interactions to be narrowed down further, examples of possible POSH mutants that might be informative are shown in figure 7.2 and are discussed below. The key outstanding question, however, is the physiological role of POSH. Possible lines for further investigation, where links between Rac, actin, endocytosis, dynamin and ubiquitination have been reported, into the role of POSH are outlined below.

7.1 POSH binding partners

Binding of POSH to activated Rac

POSH was originally cloned due to its ability to bind to activated Rac in the yeast-two-hybrid system [Tapon, Nagata, 1998] and here is shown also to bind to activated Rac *in vivo* (see figure 3.6). A 71 amino acid region of POSH was found to be sufficient for binding to Rac [Tapon, Nagata, 1998] and constructs containing this region are able to inhibit Rac-induced ruffling *in vivo* (see figure3.7). Whether the partial CRIB motif (identified by myself and S Krugman and shown in figure 1.15) or putative TPR regions (identified by [Koga, 1999] and shown in figure 1.14) are required for this interaction remains to be seen. Mutations that would destroy the CRIB motif, allowing its contribution to binding of Rac to be determined, are shown in figure 7.2.

Binding of POSH to dynamin PRD

Using affinity chromatography the major binding partner for the N-terminus of POSH (in Swiss3T3 and HeLa cell lysates) was found to be dynamin2 (see figure 4.1). Data presented in this thesis shows that the two N-terminal SH3 domains of POSH (see figure 4.2) and the PRD of dynamin (see figure 4.7), specifically a PRD region of 36 amino acids shown in figure 4.8 b, are sufficient to mediate this interaction. Mutations that could destroy the functions of POSH SH3 domains 1 or 2 are shown in figure 7.2 and would be used to determine more precisely the contributions made by each of these SH3 domains to the interface of N POSH with dynamin PRD. Recombinant or *in vitro* translated POSH and dynamin proteins would be required to formally verify *in vitro* that the POSH-dynamin interaction is direct.

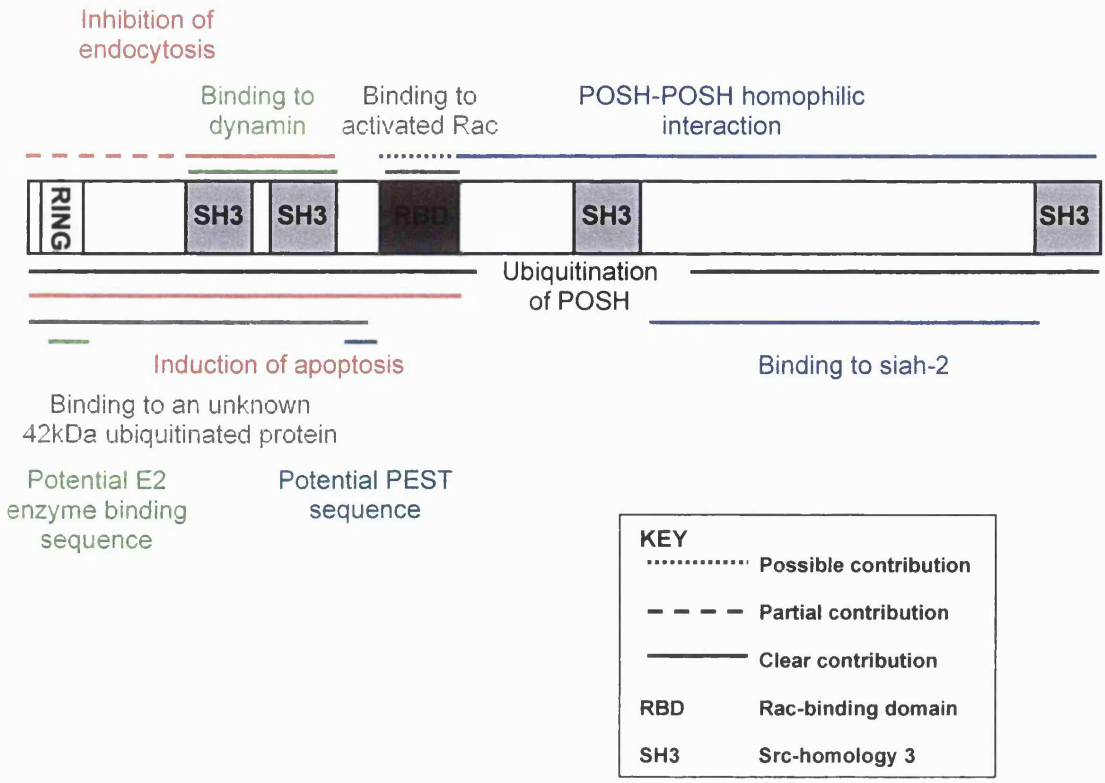

Figure 7.1 Regions of POSH shown to have certain binding partners or activities

Multiple binding partners for POSH have now been identified, suggesting that it is truly a scaffold protein. The minimal regions of POSH required for binding to the following proteins are shown: dynamin (see figure 4.2); activated Rac ([Tapon, Nagata, 1998] and see figure 3.6); ubiquitin (only full-length, see figures 6.7 and 6.8); a 42kDa ubiquitinated protein (see figures 6.7 and 6.8); siah-2 (Tapon and Hall unpublished data and see figure 6.9); POSH itself (see figure 4.10). A potential binding site for an E2 ubiquitin-conjugating enzyme (the RING finger) and a possible PEST site that may contribute to the ubiquitination of POSH are also shown. In addition, the regions of POSH required for the induction of apoptosis and for inhibition of endocytosis are indicated.

Domain	RING finger	SH3 1	SH3 2	PEST	CRIB
Mutations	C12A/C14A or C49A/C52A	G181R/ P184L	G247R/ P250L	K291G	I326A/S327A/ P329A

Figure 7.2 POSH point mutations that could be made as tools to further probe the functions of individual domains

Amino acids are shown according to the single letter code and numbered as in mouse POSH (accession number AAC40070).

The relatively weak interaction of full-length POSH with dynamin compared with the N POSH truncation (see figure 4.9) may be due to the need for addition or removal of post-translational modifications of POSH or dynamin. For instance, ubiquitinated POSH may not bind to dynamin or phosphorylated dynamin may not bind to POSH. It would be interesting to look at the phosphorylation states of transfected POSH, and of the dynamin to which it and N POSH bind, by [γ-^{32}P] ATP labelling of cells and precipitation of POSH proteins.

POSH homophilic interactions

The C-terminal region of POSH can interact with itself (see figure 4.10), though the exact sequences required have not been determined. The Rac-binding domain (RBD) does not appear to be required on both sides of the POSH-POSH interface, as indicated in figure 7.1.

Ubiquitination

Full-length POSH, but none of the truncations tested, was found to be ubiquitinated (see figure 6.7 and 6.8). The covalent modification of POSH with one or more ubiquitin molecules could require a PEST-like sequence, which in other short-lived proteins is required for ubiquitination. Mutation of the final lysine within the potential PEST region of POSH should indicate whether this region is required for ubiquitination (figure 7.2). If the loss of this one amino acid prevented ubiquitination then its absence in the N POSH truncation would account for the lack of ubiquitination of this construct (see figures 6.7 and 6.8).

Binding of POSH to a 42kDa ubiquitinated protein and to Siah-2

The presence of a RING finger within POSH suggests that POSH itself may recruit an E2 ubiquitin-conjugating enzyme, as suggested in figure 7.1 and discussed in chapter 6, and facilitate the ubiquitination of a substrate. My data suggests that this substrate is not dynamin or Rac (see chapter 6 section 6.2.7). Whether a ubiquitinated protein of unknown identity, and around 42kDa molecular weight, that associates with N POSH (see figures 6.7 and 6.8) is a substrate for POSH or an E2 enzyme remains to be seen.

The C-terminus of POSH, the region between SH3 domains 3 and 4, which contains no identifiable motifs and is not conserved between mouse and *Drosophila* POSH (see figure 1.13), binds to another RING finger-containing protein, siah-2. Siah family members in *Drosophila* [Tang, AH, 1997] and in mammals [Hu, 1997] have been proposed to act as E3 ubiquitin ligases. This raises the possibilities that POSH ubiquitination may require siah ubiquitin ligase activity and also that siah and POSH may somehow act in concert to ubiquitinate the same or different substrates. The one known substrate of mammalian siah is DCC, an axon guidance receptor [Hu, 1997]. Given that dynamin is recruited to sites of receptor-mediated endocytosis the complex formed by binding of POSH to dynamin, siah to DCC and POSH to siah could be imagined to

play some role *in vivo* in the regulation of DCC endocytosis (POSH and axon guidance are discussed further below). The ability of siah to induce POSH ubiquitination in an *in vitro* assay, or of C-terminal regions of siah (that bind to POSH) to inhibit POSH ubiquitination *in vivo*, could be tested as an indication of whether siah is required for POSH ubiquitination. Alternatively, POSH RING finger may recruit an E2 enzyme and in the absence of another substrate this complex may ubiquitinate POSH itself. The role of the RING finger in full-length POSH ubiquitination could be assessed using RING finger mutants such as those suggested in figure 7.2.

7.2 POSH-induced apoptosis

The body of evidence presented in chapters 3 and 6 suggests that three regions of POSH are required to reconstitute the potent apoptosis-inducing effect of full-length POSH. These are the Rac-binding domain, the dynamin-binding double SH3 domain motif and the RING finger. The contributions of each of these domains to POSH-induced apoptosis that has been determined using truncations could be further verified using full-length POSH containing the point mutations suggested in figure 7.2 to destroy the functions of one or more domains.

It is interesting to note that Mlk2, which also binds to both dynamin and Rac but does not contain a RING finger, also induces apoptosis [Nagata, 1998], although the effect is less potent for Mlk2 compared to POSH (data not shown). This suggests that there may be some similarities between the apoptosis-inducing potentials of POSH and Mlk2. It was assumed that Mlk2 requires its kinase activity in order to induce apoptosis, but this was not tested. Apoptosis has been detected in response to an excess of wild type dynamin2 [Fish, 2000]. It would be interesting to see whether regions of POSH that do not bind directly to dynamin could interfere with dynamin2-induced apoptosis, suggesting that POSH lies downstream of dynamin2 in a pathway leading to apoptosis.

7.3 POSH-induced apoptosis reveals a Rac survival signal

The ability of over-expressed POSH to induce apoptosis has provided an assay system with which to probe not only the activities of POSH, but also those of its binding partner Rac. It was found that over-expression of activated Rac could rescue POSH-expressing cells from apoptosis (see figure 3.8). Surprisingly this did not depend upon the ability of Rac to bind to POSH, as the C40L61Rac mutant that does not bind to POSH *in vivo* (see figure 3.6) rescues POSH-expressing cells even more efficiently than L61Rac (see figure 3.8 B).

The survival signal produced by Rac could act specifically to combat POSH-induced apoptosis signals or could act more generally downstream of these signals to prevent apoptosis (as depicted in the summary model in figure 3.11). There are a number of known Rac-induced signals that could promote cell survival, the major ones being NF-κB activation and PKB/Akt

phosphorylation (discussed in section 3.3.7). Whether or not these signals can be induced by the C40L61Rac mutant provides an indication of whether they could be the mechanism by which Rac rescues cells. It is already known that NF-κB is not activated by C40L61 Rac [Tapon, Nagata, 1998] and it remains to be seen whether C40L61Rac can activate PKB/Akt.

7.4 Possible physiological roles for POSH

Clathrin-dependent endocytosis, actin and Rac

A number of reports suggest roles for actin in clathrin-dependent endocytosis in yeast ([Munn, 1995], [Tang, HY, 2000]) and in mammalian cells ([Durrbach, 1996] [Lamaze, 1997], [Merrifield, 1999], [Fujimoto, 2000]). Some of the other dynamin-binding proteins are involved in actin dynamics (cortactin or profilin) or signal transduction downstream of Rho GTPases (Mlk2 and syndapin/PACSIN family proteins that bind to N-WASP), see introduction section 1.6.8.2. There has been only one report of Rac itself modulating clathrin-mediated endocytosis [Lamaze, 1996]. In yeast there appears to be a clear requirement both for actin and ubiquitination in endocytosis (reviewed in [Riezman, 1996]), whereas in mammalian cells the roles played by actin and ubiquitination in clathrin-dependent endocytosis are less clear. Such reports, however, do suggest that there could be a role for POSH co-ordinating Rac and dynamin, and possibly ubiquitination, in clathrin-dependent endocytosis.

There are a small number of examples where links between Rac and clathrin-independent endocytosis, or between dynamin itself and actin, have been reported. These are discussed below, as they are also processes in which a role for POSH could be investigated.

Actin and dynamin in podosomes

In the structures called podosomes a link between dynamin function and the stability of these actin-rich structures has been reported [Ochoa, 2000]. Podosomes have been described as zones of close contact to the substratum, consisting of an actin-rich core, where actin-associated regulatory proteins are also found, and surrounded by a ring of vinculin-containing focal complexes [Tarone, 1985]. The core of the podosome also often contains a narrow tubular invagination of the plasma membrane remarkably similar to tubules seen when synaptic membranes are treated with GTPγS to inhibit dynamin [Ochoa, 2000]. Podosomes occur naturally in macrophages and lymphocytes, where they play a role in migration [Wolosewick, 1984] [Linder, 1999] and in osteoclasts, where they mediate attachment and motility and generate the sealed compartment where bone marrow resorption takes place [Tarone, 1985] [Zambonin-Zallone, 1988]. Similar structures can also be induced in cells such as fibroblasts by over-activity of Src [Tarone, 1985]. The actin-rich region of podosomes contains proteins including dynmain2aa, Cdc42 and the Cdc42 effector protein WASP [Linder, 1999] [Ochoa, 2000].

Podosomes are disrupted in Wiscott-Aldrich syndrome patients and can be disrupted by constitutively active Cdc42 [Linder, 1999] or by GTPase-deficient dynamin2aa mutants [Ochoa, 2000]. Although, unlike Cdc42, Rac has not been localised to podosomes or shown to effect podosome structure this is an interesting context in which to look for POSH.

None of the cells used in my assays to date contain podosomes, so any localisation of POSH to these structures has not ~~have~~ been addressed. Interestingly, the dynamin2 in podosomes could not be detected by the hudy-1 anti-dynmain antibody that I used to detect dynamin by immunofluorescence (see for instance figure 5.4 B b and e). Podosome-associated dynamin was detected by the anti-dynmain2 antibody used here for western blotting (for instance, see figure 4.2 and [Jones, SM, 1998]). In BHK21 cells dramatic localisation of dynamin2 to ruffles was seen using the dynamin2-specific antibody [Ochoa, 2000], whereas in my hands N POSH was much more clearly seen than endogenous dynamin detected using the hudy-1 antibody in Hep2 cell ruffles (see figure 5.4 B d and e). It is possible that a pool of dynamin that co-localises with POSH was not detected with hudy-1, but may be seen with other antibodies and possibly in other cell types (such as those containing podosomes).

Phagocytosis, Rac and dynamin

As mentioned in the introduction section 1.3.3.4, professional phagocytes require Rac for phagocytosis in response to binding of IgG-opsinised particles to the Fc-γ receptor [Caron, 1998]. Early phagosomes were also shown to be associated with dynamin2 and Fc-γ receptor-dependent phagocytosis could be impaired by dominant negative K44A dyanmin2, but interestingly not by K44A dynamin1 [Gold, 1999]. This suggests that both Rac and dynamin2 may have a role to play in phagocytosis, although, like the podosome structures above, phagocytosis is not a clathrin-dependent endocytic event. Initial investigations by E Caron into a possible role for POSH in Fc-γ receptor-dependent phagocytosis indicated that N POSH and full-length POSH, but not the C POSH fragment, can inhibit phagocytosis (data not shown). This backs-up the report that dynamin is required for phagocytosis, but does not prove a specific role for POSH.

Macropinocytosis and Rac

Like phagocytosis macropinocytosis, also introduced in section 1.3.3.4, is an actin-dependent and clathrin-independent endocytic event. Antigen-presenting cells, such as dendritic cells, require a high level of macropinocytosis type of endocytosis to internalise antigens for processing and class II major histocompatibility complex presentation. Two recent papers point to roles for the small GTPases Rac and Cdc42 in endocytosis control in dendritic cells [Garrett, 2000] [West, 2000]. The relationship between dynamin and these clathrin-independent endocytic events in dendritic

cells has not been established, but the link with Rac makes it another context in which co-ordination of dynamin and Rac by POSH could be required, so may warrant further investigation.

Ubiquitination, Rho GTPases and endocytosis during axon guidance

Rac has been implicated in growth cone collapse during axon guidance in response to the semaphorin3A/collapsin-1 axon guidance cue [Jin, 1997] [Kuhn, 1999] [Vastrik, 1999] and has been shown to associate with the cytoplasmic domain of plexin-B1, a semaphorin (sema) co-receptor [Vikis, 2000]. Interestingly, dynamin localises with actin in growth cones and disruption of dynamin or its binding partner amphiphysin impairs growth cone collapse [Torre, 1994] [Mundigl, 1998]. In addition, sema3A appears to increase endocytosis and to co-ordinately redistribute actin, neuropilin-1 (a sema3A-binding glycoprotein), plexin co-receptors and Rac1, suggesting a close relationship between the collapse of actin structures and receptor internalisation in response to this ligand [Fournier, 2000]. Added to this interesting relationship between Rac, actin and endocytosis during growth cone collapse, another binding partner for POSH, siah, mediates ubiquitination of an axon guidance receptor DCC [Hu, 1997]. The possibility that POSH plays a role in co-ordinating receptor ubiquitination with Rac and dynamin activities during growth cone collapase is being further investigated by K Nobes.

7.5 Final conclusions

To conclude, it seems that the Rac-binding protein POSH also binds to dynamin and can interfere with endocytosis, so linking Rac signaling to endocytosis. Siah-2, another RING finger protein, also binds to POSH. POSH itself is ubiquitinated and contains a RING finger that may provide a docking site for an E2 ubiquitin-conjugating enzyme. POSH is, therefore, a potential ubiquitin ligase whose substrates have yet to be identified. Much of this work stemmed from the observation that POSH induces apoptosis and this activity appears to require inhibition of endogenous Rac by POSH Rac-binding domain, binding of POSH to dynamin and some activity of the RING finger, possibly related to ubiquitination. The study of POSH-induced apoptosis has also lead to the detection of a Rac-induced survival signal. Unfortunately, the inability to detect endogenous POSH has hampered investigation of the physiological role of POSH, but various contexts in which Rac and dynamin have both been shown to be required, described above, may in the future yield information about the *in vivo* role of POSH.

ACKNOWLEDGMENTS

Unending thanks to Duncan for sorting out formatting problems, for putting up with mountains of papers in the living room and for being generally wonderful. Thanks to Mum and Dad for listening, even when I go on about POSH, to my sister Paula for always bringing life back into perspective and to all my mates for providing a POSH-free zone and being there for me.

Thanks and big hugs to past and present members of the LMCB, in particular: Nic for giving me POSH (the protein and the doll) and for champagne when I really needed it. Henrik for being my longest serving bench mate and for the dynamin connection! Emmanuelle for reading not only my introduction, but even the methods, and for checking on my well being more times than I can count. Nathalie for teaching me so much in such a short time. Anja for last minute yeast transformations (love those yeasty-beasties and they will love you too). Richard for pointing out what I didn't always want to hear (you'll be a great group leader). John for the job advice (what will the Housman Rooms do without you, me and Richard?). Sonja for trying to make me more concise (it didn't work) and for many outrageous chats. Lars for review writing advice (if you'll be my up-stream boy I'll be your down-stream girl!). Jay for the pleasure of seeing your perfectly ironed self across the bench every day. Martha for being one of the most lovely people I know. Laura Machesky for giving me confidence that an excellent scientist can still be wild. David for the loin cloth moment. Koh-ichi for trying to find Charing Cross Hospital at Charing Cross. Laura Turner for a shoulder when I needed it. Myrto and Sandrine for cheering me up with the silliest Christmas decorations known to man. Annette, my Mum's really great and lots of fun, I hope you forgive me. Karen for the proteins, even if you did chuck most of them out in a moment of hormonal imbalance. Kate for blushing so easily and for taking POSH to a better place, the axon! Dan for gorgeous Swiss cells. Vania for being amazingly positive whatever life brings. Mariette for sound advice on life and love. Josef and Paul for being my favourite boys, it was a pleasure spending four years with you guys, keep in touch.

Thanks to Mark Marsh, Dan Cutler, Colin Hopkins, Harvey McMahon, Pietro De Camilli and Mark McNiven for advice and reagents when I entered the strange world of endocytosis. Special thanks to Mark for helpful discussion and for reading my introduction. Thanks also to Kris Gevaert in Joël Vandekerckhove's laboratory for Mass Spec. expertise. Last, but certainly not least, many thanks to my supervisor, Alan, for making the Hall lab an inspirational place to work, for being enthusiastic (even about endocytosis) and for patience during the longest thesis incubation in Hall lab history.

This research was primarily supported by the Medical Research Council; additional sponsorship was provided by Glaxo Wellcome.

REFERENCES

Abdul-Manan, N, et al. (1999). "Structure of Cdc42 in complex with the GTPase-binding domain of the 'Wiskott-Aldrich syndrome' protein." Nature **399** (6734): 379.

Abe, K, et al. (2000). "Vav2 is an activator of Cdc42, Rac1, and RhoA." J Biol Chem **275** (14): 10141.

Aberle, H, et al. (1997). "beta-catenin is a target for the ubiquitin-proteasome pathway." Embo J **16** (13): 3797.

Abo, A, et al. (1992). "Reconstitution of neutrophil NADPH oxidase activity in the cell-free system by four components: p67-phox, p47-phox, p21rac1, and cytochrome b-245." J Biol Chem **267** (24): 16767.

Abo, A, et al. (1991). "Activation of the NADPH oxidase involves the small GTP-binding protein p21rac1." Nature **353** (6345): 668.

Abo, A, et al. (1998). "PAK4, a novel effector for Cdc42Hs, is implicated in the reorganization of the actin cytoskeleton and in the formation of filopodia." Embo J **17** (22): 6527.

Achiriloaie, M, Barylko, B and Albanesi, JP (1999). "Essential role of the dynamin pleckstrin homology domain in receptor- mediated endocytosis." Mol Cell Biol **19** (2): 1410.

Adams, JC and Schwartz, MA (2000). "Stimulation of fascin spikes by thrombospondin-1 is mediated by the GTPases Rac and Cdc42." J Cell Biol **150** (4): 807.

Adamson, P, et al. (1992). "Post-translational modifications of p21rho proteins." J Biol Chem **267** (28): 20033.

Adamson, P, Paterson, HF and Hall, A (1992). "Intracellular localization of the P21rho proteins." J Cell Biol **119** (3): 617.

Adra, CN, et al. (1997). "RhoGDIgamma: a GDP-dissociation inhibitor for Rho proteins with preferential expression in brain and pancreas." Proc Natl Acad Sci U S A **94** (9): 4279.

Ahmed, S, et al. (1991). "The cysteine-rich domain of human proteins, neuronal chimaerin, protein kinase C and diacylglycerol kinase binds zinc. Evidence for the involvement of a zinc-dependent structure in phorbol ester binding." Biochem J **280** (Pt 1): 233.

Ahmed, S, et al. (1993). "A novel functional target for tumor-promoting phorbol esters and lysophosphatidic acid. The p21rac-GTPase activating protein n-chimaerin." J Biol Chem **268** (15): 10709.

Ahn, S, et al. (1999). "Src-mediated tyrosine phosphorylation of dynamin is required for beta2- adrenergic receptor internalization and mitogen-activated protein kinase signaling." J Biol Chem **274** (3): 1185.

Aktories, K, Schmidt, G and Hofmann, F (2000). GTPases targetted by bacterial toxins. GTPases. A Hall. Oxford, Oxford University Press: 311.

Aktories, KaK, G. (1997). Clostridium botulinum ADP-ribosyltransferase C3. Bacterial toxins: tools in cell biology and pharmacology. K Aktories. Weinheim, Chapman and Hall: 61.

Alam, MR, et al. (1997). "Kalirin, a cytosolic protein with spectrin-like and GDP/GTP exchange factor-like domains that interacts with peptidylglycine alpha-amidating monooxygenase, an integral membrane peptide-processing enzyme." J Biol Chem **272** (19): 12667.

Alberts, AS, Geneste, O and Treisman, R (1998). "Activation of SRF-regulated chromosomal templates by Rho family GTPases requires a signal that also induces H4 hyperacetylation." Cell **92** (4): 475.

Allen, WE, et al. (1998). "A role for Cdc42 in macrophage chemotaxis." J Cell Biol **141** (5): 1147.

Altschuler, Y, et al. (1998). "Redundant and distinct functions for dynamin-1 and dynamin-2 isoforms." J Cell Biol **143** (7): 1871.

Amano, M, et al. (1996). "Phosphorylation and activation of myosin by Rho-associated kinase (Rho-kinase)." J Biol Chem **271** (34): 20246.

Anafi, M, et al. (1997). "SH2/SH3 adaptor proteins can link tyrosine kinases to a Ste20-related protein kinase, HPK1." J Biol Chem **272** (44): 27804.

Anderson, RG (1998). "The caveolae membrane system." Annu Rev Biochem **67**: 199.

Anderson, RG, Goldstein, JL and Brown, MS (1977). "A mutation that impairs the ability of lipoprotein receptors to localise in coated pits on the cell surface of human fibroblasts." Nature **270** (5639): 695.

Ando, A, et al. (1994). "A complex of GRB2-dynamin binds to tyrosine-phosphorylated insulin receptor substrate-1 after insulin treatment." Embo J **13** (13): 3033.

Araki, N, Johnson, MT and Swanson, JA (1996). "A role for phosphoinositide 3-kinase in the completion of macropinocytosis and phagocytosis by macrophages." J Cell Biol **135** (5): 1249.

Arber, S, et al. (1998). "Regulation of actin dynamics through phosphorylation of cofilin by LIM- kinase." Nature **393** (6687): 805.

Aronheim, A, et al. (1998). "Chp, a homologue of the GTPase Cdc42Hs, activates the JNK pathway and is implicated in reorganizing the actin cytoskeleton." Curr Biol **8** (20): 1125.

Ashby, MN, King, DS and Rine, J (1992). "Endoproteolytic processing of a farnesylated peptide in vitro." Proc Natl Acad Sci U S A **89** (10): 4613.

Aspenstrom, P, Lindberg, U and Hall, A (1996). "Two GTPases, Cdc42 and Rac, bind directly to a protein implicated in the immunodeficiency disorder Wiskott-Aldrich syndrome." Curr Biol **6** (1): 70.

Aspenstrom, P and Olson, MF (1995). "Yeast two-hybrid system to detect protein-protein interactions with Rho GTPases." Methods Enzymol **256**: 228.

Atfi, A, et al. (1997). "Evidence for a role of Rho-like GTPases and stress-activated protein kinase/c-Jun N-terminal kinase (SAPK/JNK) in transforming growth factor beta-mediated signaling." J Biol Chem **272** (3): 1429.

Awasaki, T, et al. (2000). "The Drosophila trio plays an essential role in patterning of axons by regulating their directional extension." Neuron **26** (1): 119.

Azuma, Y and Dasso, M (2000). "The role of Ran in nuclear function." Curr Opin Cell Biol **12** (3): 302.

Baba, Y, et al. (1999). "Involvement of wiskott-aldrich syndrome protein in B-cell cytoplasmic tyrosine kinase pathway." Blood **93** (6): 2003.

Bae, CD, et al. (1998). "Determination of interaction sites on the small G protein RhoA for phospholipase D." J Biol Chem **273** (19): 11596.

Bagrodia, S and Cerione, RA (1999). "Pak to the future." Trends Cell Biol **9** (9): 350.

Bagrodia, S, Derijard, B, et al. (1995). "Cdc42 and PAK-mediated signaling leads to Jun kinase and p38 mitogen-activated protein kinase activation." J Biol Chem **270** (47): 27995.

Bagrodia, S, Taylor, SJ, et al. (1995). "Identification of a mouse p21Cdc42/Rac activated kinase." J Biol Chem **270** (39): 22731.

Baichwal, VR and Baeuerle, PA (1997). "Activate NF-kappaB or die?" Curr Biol **7** (2): 94.

Baldwin, AS, Jr. (1996). "The NF-kappa B and I kappa B proteins: new discoveries and insights." Annu Rev Immunol **14**: 649.

Bamburg, JR, McGough, A and Ono, S (1999). "Putting a new twist on actin: ADF/cofilins modulate actin dynamics." Trends Cell Biol **9** (9): 364.

Bar-Sagi, D and Hall, A (2000). "Ras and Rho GTPases: a family reunion." Cell **103** (2): 227.

Barbacid, M (1987). "ras genes." Ann. Rev. Biochem. **56**: 779.

Barfod, ET, et al. (1993). "Cloning and expression of a human CDC42 GTPase-activating protein reveals a functional SH3-binding domain." J Biol Chem **268** (35): 26059.

Barinaga, M (1999). "A New Finger on the Protein Destruction Button." Science **286**: 223.

Baron, V, Alengrin, F and Van Obberghen, E (1998). "Dynamin associates with Src-Homology Collagen (Shc) and becomes tyrosine phosphorylated in response to insulin." Endocrinology **139** (6): 3034.

Barr, FA and Shorter, J (2000). "Membrane traffic: do cones mark sites of fission?" Curr Biol **10** (4): R141.

Barylko, B, et al. (1998). "Synergistic activation of dynamin GTPase by Grb2 and phosphoinositides." J Biol Chem **273** (6): 3791.

Bateman, J, Shu, H and Van Vactor, D (2000). "The guanine nucleotide exchange factor trio mediates axonal development in the Drosophila embryo." Neuron **26** (1): 93.

Bauerfeind, R, Takei, K and De Camilli, P (1997). "Amphiphysin I is associated with coated endocytic intermediates and undergoes stimulation-dependent dephosphorylation in nerve terminals." J Biol Chem **272** (49): 30984.

Bazenet, CE, Mota, MA and Rubin, LL (1998). "The small GTP-binding protein Cdc42 is required for nerve growth factor withdrawal-induced neuronal death." Proc Natl Acad Sci U S A **95** (7): 3984.

Beck, KA and Keen, JH (1991). "Interaction of phosphoinositide cycle intermediates with the plasma membrane-associated clathrin assembly protein AP-2." J Biol Chem **266** (7): 4442.

Beg, AA, et al. (1995). "Embryonic lethality and liver degeneration in mice lacking the RelA component of NF-kappa B." Nature **376** (6536): 167.

Bellanger, J, et al. (2000). "The Rac1- and RhoG-specific GEF domain of Trio targets filamin to remodel cytoskeletal actin." Nat Cell Biol **2** (12).

Benard, V, Bohl, BP and Bokoch, GM (1999). "Characterization of rac and cdc42 activation in chemoattractant- stimulated human neutrophils using a novel assay for active GTPases." J Biol Chem **274** (19): 13198.

Benmerah, A, et al. (1996). "The ear of alpha-adaptin interacts with the COOH-terminal domain of the Eps 15 protein." J Biol Chem **271** (20): 12111.

Benmerah, A, et al. (1998). "AP-2/Eps15 interaction is required for receptor-mediated endocytosis." J Cell Biol **140** (5): 1055.

Beraud, C, Henzel, WJ and Baeuerle, PA (1999). "Involvement of regulatory and catalytic subunits of phosphoinositide 3- kinase in NF-kappaB activation." Proc Natl Acad Sci U S A **96** (2): 429.

Billadeau, DD, et al. (1998). "The Vav-Rac1 pathway in cytotoxic lymphocytes regulates the generation of cell-mediated killing." J Exp Med **188** (3): 549.

Bilodeau, D, et al. (1999). "Regulation of Rho protein binding to membranes by rhoGDI: inhibition of releasing activity by physiological ionic conditions." Biochem Cell Biol **77** (1): 59.

Bishop, AL and Hall, A (2000). "Rho GTPases and their effector proteins." Biochem J **348 Pt 2**: 241.

Blake, TJ, Heath, KG and Langdon, WY (1993). "The truncation that generated the v-cbl oncogene reveals an ability for nuclear transport, DNA binding and acute transformation." Embo J **12** (5): 2017.

Blangy, A, et al. (2000). "TrioGEF1 controls Rac- and Cdc42-dependent cell structures through the direct activation of rhoG." J Cell Sci **113** (Pt 4): 729.

Bochtler, M, et al. (1999). "The proteasome." Annu Rev Biophys Biomol Struct **28**: 295.

Bock, BC, et al. (2000). "Cdc42-induced activation of the mixed-lineage kinase SPRK in vivo. Requirement of the Cdc42/Rac interactive binding motif and changes in phosphorylation." J Biol Chem **275** (19): 14231.

Boehm, JE, Chaika, OV and Lewis, RE (1999). "Rac-dependent Anti-apoptotic Signaling by the Insulin Receptor Cytoplasmic Domain." J Biol Chem **274** (40): 28632.

Bokoch, GM, Bohl, BP and Chuang, T-H (1994). "Guanine nucleotide exchange regulates membrane translocation of rac/rho GTP-binding proteins." J Biol Chem **269** (50): 31674.

Bokoch, GM, Vlahos, CJ, et al. (1996). "Rac GTPase interacts specifically with phosphatidylinositol 3-kinase." Biochem J **315** (Pt 3): 775.

Bokoch, GM, Wang, Y, et al. (1996). "Interaction of the Nck adapter protein with p21-activated kinase (PAK1)." J Biol Chem **271** (42): 25746.

Booker, GW, et al. (1993). "Solution structure and ligand-binding site of the SH3 domain of the p85 alpha subunit of phosphatidylinositol 3-kinase." Cell **73** (4): 813.

Borden, KL, et al. (1995). "The solution structure of the RING finger domain from the acute promyelocytic leukaemia proto-oncoprotein PML." Embo J **14** (7): 1532.

Bos, JL (1989). "ras oncogenes in human cancer: a review [published erratum appears in Cancer Res 1990 Feb 15;50(4):1352]." Cancer Res **49** (17): 4682.

Bourmeyster, N and Vignais, PV (1996). "Phosphorylation of Rho GDI stabilizes the Rho A-Rho GDI complex in neutrophil cytosol." Biochem Biophys Res Commun **218** (1): 54.

Bourne, HR, Sanders, DA and McCormick, F (1991). "The GTPase superfamily: conserved structure and molecular mechanism." Nature **349** (6305): 117.

Bowtell, D, et al. (1992). "Identification of murine homologues of the Drosophila son of sevenless gene: potential activators of ras." Proc Natl Acad Sci U S A **89** (14): 6511.

Braga, V (2000a). "The crossroads between cell-cell adhesion and motility." Nat Cell Biol **2** (10): E182.

Braga, V (2000b). "Epithelial cell shape: cadherins and small GTPases." Exp Cell Res **261** (1): 83.

Braga, VM, et al. (2000). "Activation of the small GTPase rac is sufficient to disrupt cadherin-dependent cell-cell adhesion in normal human keratinocytes." Mol Biol Cell **11** (11): 3703.

Braga, VMM (1999). "Small GTPases and regulation of cadherin dependent cell-cell adhesion." Molecular Pathology **52** (4): 197.

Brenner, B, et al. (1997). "Fas- or ceramide-induced apoptosis is mediated by a Rac1-regulated activation of Jun N-terminal kinase/p38 kinases and GADD153." J Biol Chem **272** (35): 22173.

Bresnick, AR (1999). "Molecular mechanisms of nonmuscle myosin-II regulation." Curr Opin Cell Biol **11** (1): 26.

Brill, S, et al. (1996). "The ras GTPase-activating-protein-related human protein IQGAP2 harbors a potential actin binding domain and interacts with calmodulin and rho family GTPases." Mol Cell Biol **16** (9): 4869.

Brodin, L, Low, P and Shupliakov, O (2000). "Sequential steps in clathrin-mediated synaptic vesicle endocytosis." Curr Opin Neurobiol **10** (3): 312.

Brown, AM, O'Sullivan, AJ and Gomperts, BD (1998). "Induction of exocytosis from permeabilized mast cells by the guanosine triphosphatases Rac and Cdc42." Mol Biol Cell **9** (5): 1053.

Brown, JL, et al. (1996). "Human Ste20 homologue hPAK1 links GTPases to the JNK MAP kinase pathway." Curr Biol **6** (5): 598.

Bucci, C, et al. (1992). "The small GTPase rab5 functions as a regulatory factor in the early endocytic pathway." Cell **70** (5): 715.

Buchsbaum, R, et al. (1996). "The N-terminal pleckstrin, coiled-coil, and IQ domains of the exchange factor Ras-GRF act cooperatively to facilitate activation by calcium." Mol Cell Biol **16** (9): 4888.

Burack, WR and Shaw, AS (2000). "Signal transduction: hanging on a scaffold." Curr Opin Cell Biol **12** (2): 211.

Burbelo, PD, Drechsel, D and Hall, A (1995). "A conserved binding motif defines numerous candidate target proteins for both Cdc42 and Rac GTPases." J Biol Chem **270** (49): 29071.

Burger, KNJ (2000). "Greasing Membrane Fusion and Fission Machineries." Traffic **1**: 605.

Buschmann, T, et al. (2000). "SUMO-1 modification of Mdm2 prevents its self-ubiquitination and increases Mdm2 ability to ubiquitinate p53." Cell **101** (7): 753.

Cadavid, AL, Ginzel, A and Fischer, JA (2000). "The function of the Drosophila fat facets deubiquitinating enzyme in limiting photoreceptor cell number is intimately associated with endocytosis." Development **127** (8): 1727.

Cao, H, Garcia, F and McNiven, MA (1998). "Differential distribution of dynamin isoforms in mammalian cells." Mol Biol Cell **9** (9): 2595.

Cao, H, et al. (2000). "Disruption of golgi structure and function in mammalian cells expressing a mutant dynamin." J Cell Sci **113** (Pt 11): 1993.

Cao, S, et al. (2000). "Direct interaction between endothelial nitric oxide synthase and dynamin-2: Implications for nitric oxide synthase function." J Biol Chem.

Cao, T, et al. (1998). "Ret finger protein is a normal component of PML nuclear bodies and interacts directly with PML." J Cell Sci **111** (Pt 10): 1319.

Caron, E and Hall, A (1998). "Identification of two distinct mechanisms of phagocytosis controlled by different Rho GTPases." Science **282** (5394): 1717.

Carr, JF and Hinshaw, JE (1997). "Dynamin assembles into spirals under physiological salt conditions upon the addition of GDP and gamma-phosphate analogues." J Biol Chem **272** (44): 28030.

Carter, LL, et al. (1993). "Multiple GTP-binding proteins participate in clathrin-coated vesicle- mediated endocytosis." J Cell Biol **120** (1): 37.

Carthew, RW and Rubin, GM (1990). "seven in absentia, a gene required for specification of R7 cell fate in the Drosophila eye." Cell **63** (3): 561.

Casimir, C, et al. (1992). "Identification of the defective NADPH-oxidase component in chronic granulomatous disease: a study of 57 European families." Eur J Clin Invest **22** (6): 403.

Castellanos-Serra, L, et al. (1999). "Proteome analysis of polyacrylamide gel-separated proteins visualized by reversible negative staining using imidazole-zinc salts." Electrophoresis **20** (4-5): 732.

Ceresa, BP and Schmid, SL (2000). "Regulation of signal transduction by endocytosis." Curr Opin Cell Biol **12** (2): 204.

Cerione, RA and Zheng, Y (1996). "The Dbl family of oncogenes." Curr Opin Cell Biol **8** (2): 216.

Chadebech, P, et al. (1999). "Phosphorylation and proteasome-dependent degradation of Bcl-2 in mitotic-arrested cells after microtubule damage." Biochem Biophys Res Commun **262** (3): 823.

Chamberlain, CE, Kraynov, VS and Hahn, KM (2000). "Imaging spatiotemporal dynamics of Rac activation in vivo with FLAIR." Methods Enzymol **325**: 389.

Chang, BS, et al. (1997). "Identification of a novel regulatory domain in Bcl-X(L) and Bcl-2." Embo J **16** (5): 968.

Chardin, P, et al. (1993). "Human Sos1: a guanine nucleotide exchange factor for Ras that binds to GRB2." Science **260** (5112): 1338.

Chau, V, et al. (1989). "A multiubiquitin chain is confined to specific lysine in a targeted short-lived protein." Science **243** (4898): 1576.

Chaudhary, A, et al. (2000). "Phosphatidylinositol 3-kinase regulates Raf1 through Pak phosphorylation of serine 338." Curr Biol **10** (9): 551.

Chavrier, P and Goud, B (1999). "The role of ARF and Rab GTPases in membrane transport." Curr Opin Cell Biol **11** (4): 466.

Chen, H, et al. (1999). "The interaction of epsin and Eps15 with the clathrin adaptor AP-2 is inhibited by mitotic phosphorylation and enhanced by stimulation- dependent dephosphorylation in nerve terminals." J Biol Chem **274** (6): 3257.

Chen, MS, et al. (1991). "Multiple forms of dynamin are encoded by shibire, a Drosophila gene involved in endocytosis." Nature **351** (6327): 583.

Chen, Z, et al. (1999). "ASK1 mediates apoptotic cell death induced by genotoxic stress." Oncogene **18** (1): 173.

Chen, ZJ, Parent, L and Maniatis, T (1996). "Site-specific phosphorylation of IkappaBalpha by a novel ubiquitination- dependent protein kinase activity." Cell **84** (6): 853.

Cheng, JD, et al. (1998). "Functional redundancy of the nuclear factor kappa B inhibitors I kappa B alpha and I kappa B beta." J Exp Med **188** (6): 1055.

Cherfils, J and Chardin, P (1999). "GEFs: structural basis for their activation of small GTP-binding proteins." Trends Biochem Sci **24** (8): 306.

Chou, MM and Blenis, J (1995). "The 70 kDa S6 kinase: regulation of a kinase with multiple roles in mitogenic signalling." Curr Opin Cell Biol **7** (6): 806.

Chou, MM and Blenis, J (1996). "The 70 kDa S6 kinase complexes with and is activated by the Rho family G proteins Cdc42 and Rac1." Cell **85** (4): 573.

Chow, C-W, et al. (1997). "Nuclear accumulation of NFAT4 opposed by the JNK signal transduction pathway." Science **278** (5343): 1638.

Christofori, G and Semb, H (1999). "The role of the cell-adhesion molecule E-cadherin as a tumour-suppressor gene." Trends Biochem Sci **24** (2): 73.

Chuang, TH, Bohl, BP and Bokoch, GM (1993). "Biologically active lipids are regulators of Rac.GDI complexation." J Biol Chem **268** (35): 26206.

Chuang, TH, et al. (1997). "The small GTPase Cdc42 initiates an apoptotic signaling pathway in Jurkat T lymphocytes." Mol Biol Cell **8** (9): 1687.

Chuang, TH, et al. (1995). "Abr and Bcr are multifunctional regulators of the Rho GTP-binding protein family." Proc Natl Acad Sci U S A **92** (22): 10282.

Chung, J, et al. (1994). "PDGF- and insulin-dependent pp70S6k activation mediated by phosphatidylinositol-3-OH kinase." Nature **370** (6484): 71.

Cicchetti, P, et al. (1995). "3BP-1, an SH3 domain binding protein, has GAP activity for Rac and inhibits growth factor-induced membrane ruffling in fibroblasts." Embo J **14** (13): 3127.

Clarke, S (1992). "Protein isoprenylation and methylation at carboxyl-terminal cysteine residues." Annu Rev Biochem **61**: 355.

Coda, L, et al. (1998). "Eps15R is a tyrosine kinase substrate with characteristics of a docking protein possibly involved in coated pits-mediated internalization." J Biol Chem **273** (5): 3003.

Cohen, GB, Ren, R and Baltimore, D (1995). "Modular binding domains in signal transduction proteins." Cell **80** (2): 237.

Collawn, JF, et al. (1990). "Transferrin receptor internalization sequence YXRF implicates a tight turn as the structural recognition motif for endocytosis." Cell **63** (5): 1061.

Confalonieri, S, et al. (2000). "Tyrosine phosphorylation of eps15 is required for ligand-regulated, but not constitutive, endocytosis." J Cell Biol **150** (4): 905.

Cook, T, Mesa, K and Urrutia, R (1996). "Three dynamin-encoding genes are differentially expressed in developing rat brain." J Neurochem **67** (3): 927.

Cook, TA, Urrutia, R and McNiven, MA (1994). "Identification of dynamin 2, an isoform ubiquitously expressed in rat tissues." Proc Natl Acad Sci U S A **91** (2): 644.

Corvera, S, D'Arrigo, A and Stenmark, H (1999). "Phosphoinositides in membrane traffic." Curr Opin Cell Biol **11** (4): 460.

Coso, OA, et al. (1995). "The small GTP-binding proteins Rac1 and Cdc42 regulate the activity of the JNK/SAPK signaling pathway." Cell **81** (7): 1137.

Coux, O, Tanaka, K and Goldberg, AL (1996). "Structure and functions of the 20S and 26S proteasomes." Annu Rev Biochem **65**: 801.

Cox, AD and Der, CJ (1992). "Protein prenylation: more than just glue?" Curr Opin Cell Biol **4** (6): 1008.

Cox, D, et al. (1997). "Requirements for both Rac1 and Cdc42 in membrane ruffling and phagocytosis in leukocytes." J Exp Med **186** (9): 1487.

Cremona, O and De Camilli, P (1997). "Synaptic vesicle endocytosis." Curr Opin Neurobiol **7** (3): 323.

Cremona, O, et al. (1999). "Essential role of phosphoinositide metabolism in synaptic vesicle recycling." Cell **99** (2): 179.

Crespo, P, et al. (1996). "Rac-1 dependent stimulation of the JNK/SAPK signaling pathway by Vav." Oncogene **13** (3): 455.

Crespo, P, et al. (1997). "Phosphotyrosine-dependent activation of Rac-1 GDP/GTP exchange by the vav proto-oncogene product." Nature **385** (6612): 169.

D'Souza-Schorey, C, Boettner, B and Van Aelst, L (1998). "Rac regulates integrin-mediated spreading and increased adhesion of T lymphocytes." Mol Cell Biol **18** (7): 3936.

D'Souza-Schorey, C, et al. (1997). "A role for POR1, a Rac1-interacting protein, in ARF6-mediated cytoskeletal rearrangements." Embo J **16** (17): 5445.

Dallery, E, et al. (1995). "TTF, a gene encoding a novel small G protein, fuses to the lymphoma- associated LAZ3 gene by t(3;4) chromosomal translocation." Oncogene **10** (11): 2171.

Damke, H, et al. (1995). "Clathrin-independent pinocytosis is induced in cells overexpressing a temperature-sensitive mutant of dynamin." J Cell Biol **131** (1): 69.

Damke, H, et al. (1994). "Induction of mutant dynamin specifically blocks endocytic coated vesicle formation." J Cell Biol **127** (4): 915.

Daniels, RH, Hall, PS and Bokoch, GM (1998). "Membrane targeting of p21-activated kinase 1 (PAK1) induces neurite outgrowth from PC12 cells." Embo J **17** (3): 754.

Davis, RJ and Ip, YT (1998). "Signal transduction by the c-Jun N-terminal kinase (JNK) - from inflammation to development." Curr Opin Cell Biol **10** (2): 205.

De Deken, X, et al. (2000). "Cloning of two human thyroid cDNAs encoding new members of the NADPH oxidase family." J Biol Chem **275** (30): 23227.

de Heuvel, E, et al. (1997). "Identification of the major synaptojanin-binding proteins in brain." J Biol Chem **272** (13): 8710.

Debant, A, et al. (1996). "The multidomain protein Trio binds the LAR transmembrane tyrosine phosphatase, contains a protein kinase domain, and has separate rac- specific and rho-specific guanine nucleotide exchange factor domains." Proc Natl Acad Sci U S A **93** (11): 5466.

del Pozo, MA, et al. (2000). "Adhesion to the extracellular matrix regulates the coupling of the small GTPase Rac to its effector PAK." Embo J **19** (9): 2008.

Delic, J, et al. (1998). "The proteasome inhibitor lactacystin induces apoptosis and sensitizes chemo- and radioresistant human chronic lymphocytic leukaemia lymphocytes to TNF-alpha-initiated apoptosis." Br J Cancer **77** (7): 1103.

Della, NG, Senior, PV and Bowtell, DD (1993). "Isolation and characterisation of murine homologues of the Drosophila seven in absentia gene (sina)." Development **117** (4): 1333.

Derry, JM, Ochs, HD and Francke, U (1994). "Isolation of a novel gene mutated in Wiskott-Aldrich syndrome [published erratum appears in Cell 1994 Dec 2;79(5):following 922]." Cell **78** (4): 635.

Desagher, S and Martinou, JC (2000). "Mitochondria as the central control point of apoptosis." Trends Cell Biol **10** (9): 369.

DeTulleo, L and Kirchhausen, T (1998). "The clathrin endocytic pathway in viral infection." Embo J **17** (16): 4585.

Dharmawardhane, S, et al. (1997). "Localization of p21-activated kinase 1 (PAK1) to pinocytic vesicles and cortical actin structures in stimulated cells." J Cell Biol **138** (6): 1265.

Di Fiore, PP and Gill, GN (1999). "Endocytosis and mitogenic signaling." Curr Opin Cell Biol **11** (4): 483.

Diaz-Meco, MT, et al. (1996). "Lambda-interacting protein, a novel protein that specifically interacts with the zinc finger domain of the atypical protein kinase C isotype lambda/iota and stimulates its kinase activity in vitro and in vivo." Mol Cell Biol **16** (1): 105.

Dick, LR, et al. (1996). "Mechanistic studies on the inactivation of the proteasome by lactacystin: a central role for clasto-lactacystin beta-lactone." J Biol Chem **271** (13): 7273.

Diekmann, D, et al. (1994). "Interaction of Rac with p67phox and regulation of phagocytic NADPH oxidase activity." Science **265** (5171): 531.

Diekmann, D, et al. (1991). "Bcr encodes a GTPase-activating protein for p21rac." Nature **351** (6325): 400.

Diekmann, D, et al. (1995). "Rac GTPase interacts with GAPs and target proteins through multiple effector sites." Embo J **14** (21): 5297.

Diener, K, et al. (1997). "Activation of the c-Jun N-terminal kinase pathway by a novel protein kinase related to human germinal center kinase." Proc Natl Acad Sci U S A **94**: 9687.

Doi, TS, et al. (1999). "Absence of tumor necrosis factor rescues RelA-deficient mice from embryonic lethality." Proc Natl Acad Sci U S A **96** (6): 2994.

Downward, J (1998). "Ras signalling and apoptosis." Curr Opin Genet Dev **8** (1): 49.

Drake, MT, Downs, MA and Traub, LM (2000). "Epsin binds to clathrin by associating directly with the clathrin- terminal domain. Evidence for cooperative binding through two discrete sites." J Biol Chem **275** (9): 6479.

Drechsel, DN, et al. (1997). "A requirement for Rho and Cdc42 during cytokinesis in Xenopus embryos." Curr Biol **7** (1): 12.

Driessens, MH, et al. (2001). "Plexin-B semaphorin receptors interact directly with active Rac and regulate the actin cytoskeleton by activating Rho." Curr Biol **11** (5): 339.

Dunham, I, et al. (1999). "The DNA sequence of human chromosome 22." Nature **402** (6761): 489.

Duprez, E, et al. (1999). "SUMO-1 modification of the acute promyelocytic leukaemia protein PML: implications for nuclear localisation." J Cell Sci **112** (Pt 3): 381.

Durrbach, A, Louvard, D and Coudrier, E (1996). "Actin filaments facilitate two steps of endocytosis." J Cell Sci **109** (Pt 2): 457.

Earnshaw, WC, Martins, LM and Kaufmann, SH (1999). "Mammalian caspases: structure, activation, substrates, and functions during apoptosis." Annu Rev Biochem **68**: 383.

Edwards, DC, et al. (1999). "Activation of LIM-kinase by Pak1 couples Rac/Cdc42 GTPase signalling to actin cytoskeletal dynamics." Nat Cell Biol **1** (5): 253.

Ellis, S and Mellor, H (2000a). "The novel rho-family GTPase rif regulates coordinated actin-based membrane rearrangements." Curr Biol **10** (21): 1387.

Ellis, S and Mellor, H (2000b). "Regulation of endocytic traffic by rho family GTPases." Trends Cell Biol **10** (3): 85.

Erickson, JW, Cerione, RA and Hart, MJ (1997). "Identification of an actin cytoskeletal complex that includes IQGAP and the Cdc42 GTPase." J Biol Chem **272** (39): 24443.

Estes, PS, et al. (1996). "Traffic of dynamin within individual Drosophila synaptic boutons relative to compartment-specific markers." J Neurosci **16** (17): 5443.

Esteve, P, et al. (1998). "Rho-regulated signals induce apoptosis in vitro and in vivo by a p53- independent, but Bcl2 dependent pathway." Oncogene **17** (14): 1855.

Everett, R, et al. (1995). "Point mutations in the herpes simplex virus type 1 Vmw110 RING finger helix affect activation of gene expression, viral growth, and interaction with PML-containing nuclear structures." J Virol **69** (11): 7339.

Everett, RD, et al. (1993). "A novel arrangement of zinc-binding residues and secondary structure in the C3HC4 motif of an alpha herpes virus protein family." J Mol Biol **234** (4): 1038.

Fadok, VA, et al. (2000). "A receptor for phosphatidylserine-specific clearance of apoptotic cells." Nature **405** (6782): 85.

Fanger, GR, et al. (1997). "MEKKS, GCKs, MLKs, PAKs, TAKs and TPLs: upstream regulators of the c-Jun amino-terminal kinases." Curr Opin Genet Dev **7**: 67.

Fanger, GR, Johnson, NL and Johnson, GL (1997). "MEK kinases are regulated by EGF and selectively interact with Rac/Cdc42." Embo J **16** (16): 4961.

Fazioli, F, et al. (1993). "eps15, a novel tyrosine kinase substrate, exhibits transforming activity." Mol Cell Biol **13** (9): 5814.

Feig, LA (1999). "Tools of the trade: use of dominant-inhibitory mutants of Ras-family GTPases." Nat Cell Biol **1** (2): E25.

Feig, LA, et al. (1986). "Isolation of ras GTP-binding mutants using an in situ colony-binding assay." Proc Natl Acad Sci U S A **83** (13): 4607.

Feng, S, et al. (1994). "Two binding orientations for peptides to the Src SH3 domain: development of a general model for SH3-ligand interactions." Science **266** (5188): 1241.

Fenteany, G, et al. (1995). "Inhibition of proteasome activities and subunit-specific amino-terminal threonine modification by lactacystin." Science **268** (5211): 726.

Ferguson, SS, et al. (1996). "G-protein-coupled receptor regulation: role of G-protein-coupled receptor kinases and arrestins." Can J Physiol Pharmacol **74** (10): 1095.

Finlin, BS and Andres, DA (1997). "Rem is a new member of the Rad- and Gem/Kir Ras-related GTP-binding protein family repressed by lipopolysaccharide stimulation." J Biol Chem **272** (35): 21982.

Fish, KN, Schmid, SL and Damke, H (2000). "Evidence that dynamin-2 functions as a signal-transducing GTPase." J Cell Biol **150** (1): 145.

Floyd, S and De Camilli, P (1998). "Endocytosis proteins and cancer: a potential link?" Trends Cell Biol **8** (8): 299.

Foster, R, et al. (1996). "Identification of a novel human Rho protein with unusual properties: GTPase deficiency and in vivo farnesylation." Mol Cell Biol **16** (6): 2689.

Fournier, AE, et al. (2000). "Semaphorin3A enhances endocytosis at sites of receptor-F-actin colocalization during growth cone collapse." J Cell Biol **149** (2): 411.

Freemont, PS (2000). "RING for destruction?" Curr Biol **10** (2): R84.

Fritz, G and Kaina, B (1997). "rhoB encoding a UV-inducible Ras-related small GTP-binding protein is regulated by GTPases of the Rho family and independent of JNK, ERK, and p38 MAP kinase." J Biol Chem **272** (49): 30637.

Frost, JA, et al. (1998). "Differential effects of PAK1-activating mutations reveal activity- dependent and - independent effects on cytoskeletal regulation." J Biol Chem **273** (43): 28191.

Frost, JA, et al. (1997). "Cross-cascade activation of ERKs and ternary complex factors by Rho family proteins." Embo J **16** (21): 6426.

Fu, Y and Galan, JE (1999). "A salmonella protein antagonizes Rac-1 and Cdc42 to mediate host-cell recovery after bacterial invasion." Nature **401** (6750): 293.

Fujimoto, LM, et al. (2000). "Actin Assembly Plays a Variable, but not Obligatory Role in Receptor-Mediated Endocytosis in Mammalian Cells." Traffic **1**: 161.

Fukata, M, et al. (1997). "Regulation of cross-linking of actin filament by IQGAP1, a target for Cdc42." J Biol Chem **272** (47): 29579.

Fukata, M, et al. (1999). "Cdc42 and Rac1 regulate the interaction of IQGAP1 with beta-catenin." J Biol Chem **274** (37): 26044.

Gaidarov, I, et al. (1996). "A functional phosphatidylinositol 3,4,5-trisphosphate/phosphoinositide binding domain in the clathrin adaptor AP-2 alpha subunit. Implications for the endocytic pathway [published erratum appears in J Biol Chem 1996 Oct 25;271(43):27188]." J Biol Chem **271** (34): 20922.

Gaidarov, I, Krupnick, JG, et al. (1999). "Arrestin function in G protein-coupled receptor endocytosis requires phosphoinositide binding." Embo J **18** (4): 871.

Gaidarov, I, Santini, F, et al. (1999). "Spatial control of coated-pit dynamics in living cells." Nat Cell Biol **1** (1): 1.

Galisteo, ML, et al. (1996). "The adaptor protein Nck links receptor tyrosine kinases with the serine-threonine kinase Pak1." J Biol Chem **271** (35): 20997.

Gallusser, A and Kirchhausen, T (1993). "The beta 1 and beta 2 subunits of the AP complexes are the clathrin coat assembly components." Embo J **12** (13): 5237.

Gao, LY and Kwaik, YA (2000). "The modulation of host cell apoptosis by intracellular bacterial pathogens." Trends Microbiol **8** (7): 306.

Garrett, WS, et al. (2000). "Developmental control of endocytosis in dendritic cells by Cdc42." Cell **102** (3): 325.

Gauthier-Rouviere, C, et al. (1998). "RhoG GTPase controls a pathway that independently activates Rac1 and Cdc42Hs." Mol Biol Cell **9** (6): 1379.

Gerwins, P, Blank, JL and Johnson, GL (1997). "Cloning of a novel mitogen-activated protein kinase kinase kinase, MEKK4, that selectively regulates the c-Jun amino terminal kinase pathway." J Biol Chem **272**: 8288.

Gevaert, K, et al. (1998). "Sample preparation procedures for ultrasensitive protein identification by PSD-MALDI-TOF mass spectrometry." J Protein Chem **17** (6): 560.

Gevaert, K and Vandekerckhove, J (2000). "Protein identification methods in proteomics." Electrophoresis **21** (6): 1145.

Ghoda, L, Lin, X and Greene, WC (1997). "The 90-kDa ribosomal S6 kinase (pp90rsk) phosphorylates the N-terminal regulatory domain of IkappaBalpha and stimulates its degradation in vitro." J Biol Chem **272** (34): 21281.

Giachino, C, et al. (1997). "A novel SH3-containing human gene family preferentially expressed in the central nervous system." Genomics **41** (3): 427.

Gille, P, Strahl, T and Shaw, PE (1995). "Activation of ternary complex factor Elk-1 by stress-activated protein kinases." Curr Biol **5**: 1191.

Gilmore, AP and Burridge, K (1996). "Regulation of vinculin binding to talin and actin by phosphatidyl-inositol-4-5-bisphosphate." Nature **381** (6582): 531.

Gizachew, D, et al. (2000). "Structure of the complex of Cdc42Hs with a peptide derived from P-21 activated kinase." Biochemistry **39** (14): 3963.

Gjoerup, O, et al. (1998). "Rac and Cdc42 are potent stimulators of E2F-dependent transcription capable of promoting retinoblastoma susceptibility gene product hyperphosphorylation." J Biol Chem **273** (30): 18812.

Glise, B and Noselli, S (1997). "Coupling of Jun amino-terminal kinase and Decapentaplegic signaling pathways in Drosophila morphogenesis." Genes Dev **11** (13): 1738.

Gold, ES, et al. (1999). "Dynamin 2 is required for phagocytosis in macrophages." J Exp Med **190** (12): 1849.

Goldstein, JC, et al. (2000). "The coordinate release of cytochrome c during apoptosis is rapid, complete and kinetically invariant." Nat Cell Biol **2** (3): 156.

Goldstein, JL, et al. (1985). "Receptor-mediated endocytosis: concepts emerging from the LDL receptor system." Annu Rev Cell Biol **1**: 1.

Goodman, OB, Jr., et al. (1997). "Arrestin/clathrin interaction. Localization of the arrestin binding locus to the clathrin terminal domain." J Biol Chem **272** (23): 15017.

Goodman, OB, Jr., et al. (1996). "Beta-arrestin acts as a clathrin adaptor in endocytosis of the beta2-adrenergic receptor." Nature **383** (6599): 447.

Gorvel, JP, et al. (1998). "Differential properties of D4/LyGDI versus RhoGDI: phosphorylation and rho GTPase selectivity." FEBS Lett **422** (2): 269.

Gosser, YQ, et al. (1997). "C-terminal binding domain of Rho GDP-dissociation inhibitor directs N-terminal inhibitory peptide to GTPases." Nature **387** (6635): 814.

Gout, I, et al. (1993). "The GTPase dynamin binds to and is activated by a subset of SH3 domains." Cell **75** (1): 25.

Govers, R, et al. (1997). "Linkage of the ubiquitin-conjugating system and the endocytic pathway in ligand-induced internalization of the growth hormone receptor." Embo J **16** (16): 4851.

Grabs, D, et al. (1997). "The SH3 domain of amphiphysin binds the proline-rich domain of dynamin at a single site that defines a new SH3 binding consensus sequence." J Biol Chem **272** (20): 13419.

Grigliatti, TA, et al. (1973). "Temperature-sensitive mutations in Drosophila melanogaster. XIV. A selection of immobile adults." Mol Gen Genet **120** (2): 107.

Grimm, LM, et al. (1996). "Proteasomes play an essential role in thymocyte apoptosis." Embo J **15** (15): 3835.

Gu, X and Verma, DP (1997). "Dynamics of phragmoplastin in living cells during cell plate formation and uncoupling of cell elongation from the plane of cell division." Plant Cell **9** (2): 157.

Guinamard, R, et al. (1998). "Tyrosine phosphorylation of the Wiskott-Aldrich syndrome protein by Lyn and Btk is regulated by CDC42." FEBS Lett **434** (3): 431.

Guipponi, M, et al. (1998). "Two isoforms of a human intersectin (ITSN) protein are produced by brain-specific alternative splicing in a stop codon." Genomics **53** (3): 369.

Gumbiner, BM (1996). "Cell adhesion: the molecular basis of tissue architecture and morphogenesis." Cell **84** (3): 345.

Guo, W, et al. (1998). "Identification of the binding surface on Cdc42Hs for p21-activated kinase." Biochemistry **37** (40): 14030.

Gupta, S, et al. (1995). "Transcription factor ATF2 regulation by the JNK signal transduction pathway." Science **267**: 389.

Haataja, L, Groffen, J and Heisterkamp, N (1997). "Characterization of RAC3, a novel member of the Rho family." J Biol Chem **272** (33): 20384.

Habets, GG, et al. (1994). "Identification of an invasion-inducing gene, Tiam-1, that encodes a protein with homology to GDP-GTP exchangers for Rho-like proteins." Cell **77** (4): 537.

Haffner, C, et al. (2000). "Direct interaction of the 170 kDa isoform of synaptojanin 1 with clathrin and with the clathrin adaptor AP-2." Curr Biol **10** (8): 471.

Haffner, C, et al. (1997). "Synaptojanin 1: localization on coated endocytic intermediates in nerve terminals and interaction of its 170 kDa isoform with Eps15." FEBS Lett **419** (2-3): 175.

Hall, A (1994). "Small GTP-binding proteins and the regulation of the actin cytoskeleton." Annu Rev Cell Biol **10**: 31.

Hall, A (1998). "Rho GTPases and the actin cytoskeleton." Science **279** (5350): 509.

Hall, A, et al. (1983). "Identification of transforming gene in two human sarcoma cell lines as a new member of the ras gene family located on chromosome 1." Nature **303** (5916): 396.

Hammond, SM, et al. (1997). "Characterization of two alternately spliced forms of phospholipase D1. Activation of the purified enzymes by phosphatidylinositol 4,5- bisphosphate, ADP-ribosylation factor, and Rho family monomeric GTP- binding proteins and protein kinase C-alpha." J Biol Chem **272** (6): 3860.

Han, J, et al. (1997). "Lck regulates Vav activation of members of the Rho family of GTPases." Mol Cell Biol **17** (3): 1346.

Han, J, et al. (1998). "Role of substrates and products of PI 3-kinase in regulating activation of Rac-related guanosine triphosphatases by Vav." Science **279** (5350): 558.

Han, JS, et al. (1998). "The potential role for CDC42 protein from rat brain cytosol in phospholipase D activation." Biochem Mol Biol Int **45** (6): 1089.

Hancock, JF, et al. (1991). "A CAAX or a CAAL motif and a second signal are sufficient for plasma membrane targeting of ras proteins." Embo J **10** (13): 4033.

Hancock, JF, et al. (1989). "All ras proteins are polyisoprenylated but only some are palmitoylated." Cell **57** (7): 1167.

Hannah, MJ, Schmidt, AA and Huttner, WB (1999). "Synaptic vesicle biogenesis." Annu Rev Cell Dev Biol **15**: 733.

Hao, W, et al. (1997). "Regulation of AP-3 function by inositides. Identification of phosphatidylinositol 3,4,5-trisphosphate as a potent ligand." J Biol Chem **272** (10): 6393.

Harden, N, et al. (1995). "A dominant inhibitory version of the small GTP-binding protein Rac disrupts cytoskeletal structures and inhibits developmental cell shape changes in Drosophila." Development **121** (3): 903.

Harris, TW, et al. (2000). "Mutations in synaptojanin disrupt synaptic vesicle recycling." J Cell Biol **150** (3): 589.

Hart, MJ, et al. (1996). "IQGAP1, a calmodulin-binding protein with a rasGAP-related domain, is a potential effector for cdc42Hs." Embo J **15** (12): 2997.

Hart, MJ, et al. (1994). "Cellular transformation and guanine nucleotide exchange activity are catalyzed by a common domain on the dbl oncogene product." J Biol Chem **269** (1): 62.

Hart, MJ, et al. (1998). "Direct stimulation of the guanine nucleotide exchange activity of p115 RhoGEF by Galpha13." Science **280** (5372): 2112.

Hartwig, JH, et al. (1995). "Thrombin receptor ligation and activated Rac uncap actin filament barbed ends through phosphoinositide synthesis in permeabilized human platelets." Cell **82** (4): 643.

Hatakeyama, S, Jensen, JP and Weissman, AM (1997). "Subcellular localization and ubiquitin-conjugating enzyme (E2) interactions of mammalian HECT family ubiquitin protein ligases." J Biol Chem **272** (24): 15085.

Haucke, V and De Camilli, P (1999). "AP-2 recruitment to synaptotagmin stimulated by tyrosine-based endocytic motifs." Science **285** (5431): 1268.

Haucke, V, et al. (2000). "Dual interaction of synaptotagmin with &mgr;2- and alpha-adaptin facilitates clathrin-coated pit nucleation." Embo J **19** (22): 6011.

Hawkins, PT, et al. (1995). "PDGF stimulates an increase in GTP-Rac via activation of phosphoinositide 3-kinase." Curr Biol **5** (4): 393.

Henley, JR, et al. (1998). "Dynamin-mediated internalization of caveolae." J Cell Biol **141** (1): 85.

Herdegen, T, et al. (1998). "Lasting N-terminal phosphorylation of c-Jun and activation of c-Jun N-terminal kinases after neuronal injury." J Neurosci **18** (14): 5124.

Hershko, A and Ciechanover, A (1998). "The ubiquitin system." Annu Rev Biochem **67**: 425.

Herskovits, JS, Burgess, CC, et al. (1993). "Effects of mutant rat dynamin on endocytosis." J Cell Biol **122** (3): 565.

Herskovits, JS, Shpetner, HS, et al. (1993). "Microtubules and Src homology 3 domains stimulate the dynamin GTPase via its C-terminal domain." Proc Natl Acad Sci U S A **90** (24): 11468.

Hess, JA, et al. (1997). "Role of Rho family proteins in phospholipase D activation by growth factors." J Biol Chem **272** (3): 1615.

Heuser, J (1989). "Effects of cytoplasmic acidification on clathrin lattice morphology." J Cell Biol **108** (2): 401.

Heuser, JE and Anderson, RG (1989). "Hypertonic media inhibit receptor-mediated endocytosis by blocking clathrin-coated pit formation." J Cell Biol **108** (2): 389.

Heuser, JE and Keen, J (1988). "Deep-etch visualization of proteins involved in clathrin assembly." J Cell Biol **107** (3): 877.

Heuser, JE, et al. (1987). "Deep-etch visualization of 27S clathrin: a tetrahedral tetramer." J Cell Biol **105** (5): 1999.

Hewlett, LJ, Prescott, AR and Watts, C (1994). "The coated pit and macropinocytic pathways serve distinct endosome populations." J Cell Biol **124** (5): 689.

Heyworth, PG, et al. (1994). "Rac translocates independently of the neutrophil NADPH oxidase components p47phox and p67phox. Evidence for its interaction with flavocytochrome b558." J Biol Chem **269** (49): 30749.

Hicke, L (1999). "Gettin' down with ubiquitin: turning off cell-surface receptors, transporters and channels." Trends Cell Biol **9** (3): 107.

Hicke, L and Riezman, H (1996). "Ubiquitination of a yeast plasma membrane receptor signals its ligand-stimulated endocytosis." Cell **84** (2): 277.

Hildebrand, JD, Taylor, JM and Parsons, JT (1996). "An SH3 domain-containing GTPase-activating protein for Rho and Cdc42 associates with focal adhesion kinase." Mol Cell Biol **16** (6): 3169.

Hill, CS, Wynne, J and Treisman, R (1995). "The Rho family GTPases RhoA, Rac1, and CDC42Hs regulate transcriptional activation by SRF." Cell **81** (7): 1159.

Hill, E, et al. (2001). "The Role of Dynamin and Its Binding Partners in Coated Pit Invagination and Scission." J Cell Biol **152** (2): 309.

Hing, H, et al. (1999). "Pak functions downstream of Dock to regulate photoreceptor axon guidance in Drosophila." Cell **97** (7): 853.

Hinshaw, JE (2000). "Dynamin and Its Role in Membrane Fission." Annu Rev Cell Dev Biol **16**: 483.

Hinshaw, JE and Schmid, SL (1995). "Dynamin self-assembles into rings suggesting a mechanism for coated vesicle budding." Nature **374** (6518): 190.

Hirai, S, et al. (1997). "MST/MLK2, a member of the mixed lineage kinase family, directly phosphorylates and activates SEK1, an activator of c-Jun N-terminal kinase/stress-activated protein kinase." J Biol Chem **272**: 15167.

Hirao, M, et al. (1996). "Regulation mechanism of ERM (ezrin/radixin/moesin) protein/plasma membrane association: possible involvement of phosphatidylinositol turnover and Rho-dependent signaling pathway." J Cell Biol **135** (1): 37.

Hoffman, GR and Cerione, RA (2000). "Flipping the switch: the structural basis for signaling through the CRIB motif." Cell **102** (4): 403.

Hoffman, GR, Nassar, N and Cerione, RA (2000). "Structure of the Rho family GTP-binding protein Cdc42 in complex with the multifunctional regulator RhoGDI." Cell **100** (3): 345.

Holstein, SE, Ungewickell, H and Ungewickell, E (1996). "Mechanism of clathrin basket dissociation: separate functions of protein domains of the DnaJ homologue auxilin." J Cell Biol **135** (4): 925.

Honda, A, et al. (1999). "Phosphatidylinositol 4-phosphate 5-kinase alpha is a downstream effector of the small G protein ARF6 in membrane ruffle formation." Cell **99** (5): 521.

Honda, R and Yasuda, H (2000). "Activity of MDM2, a ubiquitin ligase, toward p53 or itself is dependent on the RING finger domain of the ligase." Oncogene **19** (11): 1473.

Hori, Y, et al. (1991). "Post-translational modifications of the C-terminal region of the rho protein are important for its interaction with membranes and the stimulatory and inhibitory GDP/GTP exchange proteins." Oncogene **6** (4): 515.

Hoshino, M, et al. (1999). "Identification of the stef gene that encodes a novel guanine nucleotide exchange factor specific for Rac1." J Biol Chem **274** (25): 17837.

Houssa, B, et al. (1999). "Diacylglycerol kinase theta binds to and is negatively regulated by active RhoA." J Biol Chem **274** (11): 6820.

Hsu, SY, et al. (1997). "Interference of BAD (Bcl-xL/Bcl-2-associated death promoter)-induced apoptosis in mammalian cells by 14-3-3 isoforms and P11." Mol Endocrinol **11** (12): 1858.

Hu, G and Fearon, ER (1999). "Siah-1 N-terminal RING domain is required for proteolysis function, and C-terminal sequences regulate oligomerization and binding to target proteins." Mol Cell Biol **19** (1): 724.

Hu, G, et al. (1997). "Mammalian homologs of seven in absentia regulate DCC via the ubiquitin-proteasome pathway." Genes Dev **11** (20): 2701.

Huang, Y, Baker, RT and Fischer-Vize, JA (1995). "Control of cell fate by a deubiquitinating enzyme encoded by the fat facets gene." Science **270** (5243): 1828.

Hueber, AO, et al. (1997). "Requirement for the CD95 receptor-ligand pathway in c-Myc-induced apoptosis." Science **278** (5341): 1305.

Hughes, WE, Cooke, FT and Parker, PJ (2000). "Sac phosphatase domain proteins." Biochem J **350 Pt 2**: 337.

Huibregtse, JM, et al. (1995). "A family of proteins structurally and functionally related to the E6-AP ubiquitin-protein ligase." Proc Natl Acad Sci U S A **92** (11): 5249.

Huibregtse, JM, Scheffner, M and Howley, PM (1993). "Cloning and expression of the cDNA for E6-AP, a protein that mediates the interaction of the human papillomavirus E6 oncoprotein with p53." Mol Cell Biol **13** (2): 775.

Hung, TJ and Kemphues, KJ (1999). "PAR-6 is a conserved PDZ domain-containing protein that colocalizes with PAR-3 in Caenorhabditis elegans embryos." Development **126** (1): 127.

Hussain, NK, et al. (1999). "Splice variants of intersectin are components of the endocytic machinery in neurons and nonneuronal cells." J Biol Chem **274** (22): 15671.

Huttenlocher, A, et al. (1998). "Integrin and cadherin synergy regulates contact inhibition of migration and motile activity." J Cell Biol **141** (2): 515.

Huxford, T, et al. (1998). "The crystal structure of the IkappaBalpha/NF-kappaB complex reveals mechanisms of NF-kappaB inactivation." Cell **95** (6): 759.

Hyman, J, et al. (2000). "Epsin 1 undergoes nucleocytosolic shuttling and its eps15 interactor NH(2)-terminal homology (ENTH) domain, structurally similar to Armadillo and HEAT repeats, interacts with the transcription factor promyelocytic leukemia Zn(2)+ finger protein (PLZF)." J Cell Biol **149** (3): 537.

Ihara, K, et al. (1998). "Crystal structure of human RhoA in a dominantly active form complexed with a GTP analogue." J Biol Chem **273** (16): 9656.

Illenberger, D, et al. (1998). "Stimulation of phospholipase C-beta2 by the Rho GTPases Cdc42Hs and Rac1." Embo J **17** (21): 6241.

Inouye, C, Dhillon, N and Thorner, J (1997). "Ste5 RING-H2 domain: role in Ste4-promoted oligomerization for yeast pheromone signaling." Science **278** (5335): 103.

Jacobson, MD, Weil, M and Raff, MC (1997). "Programmed cell death in animal development." Cell **88** (3): 347.

Jahner, D and Hunter, T (1991). "The ras-related gene rhoB is an immediate-early gene inducible by v-Fps, epidermal growth factor, and platelet-derived growth factor in rat fibroblasts." Mol Cell Biol **11** (7): 3682.

Janmey, PA and Stossel, TP (1987). "Modulation of gelsolin function by phosphatidylinositol 4,5-bisphosphate." Nature **325** (6102): 362.

Jaquenoud, M, et al. (1998). "The Cdc42p effector Gic2p is targeted for ubiquitin-dependent degradation by the SCFGrr1 complex." Embo J **17** (18): 5360.

Jenkins, GH, Fisette, PL and Anderson, RA (1994). "Type I phosphatidylinositol 4-phosphate 5-kinase isoforms are specifically stimulated by phosphatidic acid." J Biol Chem **269** (15): 11547.

Jensen, DE, et al. (1998). "BAP1: a novel ubiquitin hydrolase which binds to the BRCA1 RING finger and enhances BRCA1-mediated cell growth suppression." Oncogene **16** (9): 1097.

Jensen, JP, et al. (1995). "Identification of a family of closely related human ubiquitin conjugating enzymes." J Biol Chem **270** (51): 30408.

Jin, Z and Strittmatter, SM (1997). "Rac1 mediates collapsin-1-induced growth cone collapse." J Neurosci **17** (16): 6256.

Joazeiro, CA, et al. (1999). "The tyrosine kinase negative regulator c-Cbl as a RING-type, E2- dependent ubiquitin-protein ligase." Science **286** (5438): 309.

Joberty, G, et al. (2000). "The cell-polarity protein Par6 links Par3 and atypical protein kinase C to Cdc42." Nat Cell Biol **2** (8): 531.

Johnson, DI (1999). "Cdc42: An essential Rho-type GTPase controlling eukaryotic cell polarity." Microbiol Mol Biol Rev **63** (1): 54.

Jones, GE, Allen, WE and Ridley, AJ (1998). "The Rho GTPases in macrophage motility and chemotaxis." Cell Adhes Commun **6** (2-3): 237.

Jones, SM, et al. (1998). "Role of dynamin in the formation of transport vesicles from the trans- Golgi network." Science **279** (5350): 573.

Joneson, T and Bar-Sagi, D (1998). "A Rac1 effector site controlling mitogenesis through superoxide production." J Biol Chem **273** (29): 17991.

Joneson, T and Bar-Sagi, D (1999). "Suppression of Ras-induced apoptosis by the Rac GTPase." Mol Cell Biol **19** (9): 5892.

Joneson, T, et al. (1996). "RAC regulation of actin polymerization and proliferation by a pathway distinct from Jun kinase [published erratum appears in Science 1997 Apr 11;276(5310):185]." Science **274** (5291): 1374.

Jost, M, et al. (1998). "Phosphatidylinositol-4,5-bisphosphate is required for endocytic coated vesicle formation." Curr Biol **8** (25): 1399.

Jou, TS and Nelson, WJ (1998). "Effects of regulated expression of mutant RhoA and Rac1 small GTPases on the development of epithelial (MDCK) cell polarity." J Cell Biol **142** (1): 85.

Jou, TS, Schneeberger, EE and Nelson, WJ (1998). "Structural and functional regulation of tight junctions by RhoA and Rac1 small GTPases." J Cell Biol **142** (1): 101.

Joyal, JL, et al. (1997). "Calmodulin modulates the interaction between IQGAP1 and Cdc42. Identification of IQGAP1 by nanoelectrospray tandem mass spectrometry." J Biol Chem **272** (24): 15419.

Kaibuchi, K, et al. (1999). "Regulation of cadherin-mediated cell-cell adhesion by the Rho family GTPases." Curr Opin Cell Biol **11** (5): 591.

Karin, M and Ben-Neriah, Y (2000). "Phosphorylation meets ubiquitination: the control of NF-[kappa]B activity." Annu Rev Immunol **18**: 621.

Kariya, K, et al. (2000). "Regulation of complex formation of POB1/epsin/adaptor protein complex 2 by mitotic phosphorylation." J Biol Chem **275** (24): 18399.

Karoor, V, et al. (1998). "Insulin stimulates sequestration of beta-adrenergic receptors and enhanced association of beta-adrenergic receptors with Grb2 via tyrosine 350." J Biol Chem **273** (49): 33035.

Katzav, S, Martin-Zanca, D and Barbacid, M (1989). "vav, a novel human oncogene derived from a locus ubiquitously expressed in hematopoietic cells." Embo J **8** (8): 2283.

Kauffmann-Zeh, A, et al. (1997). "Suppression of c-Myc-induced apoptosis by Ras signalling through PI(3)K and PKB." Nature **385** (6616): 544.

Kaufmann, N, Wills, ZP and Van Vactor, D (1998). "Drosophila Rac1 controls motor axon guidance." Development **125** (3): 453.

Kawano, Y, et al. (1999). "Phosphorylation of myosin-binding subunit (MBS) of myosin phosphatase by Rho-kinase in vivo." J Cell Biol **147** (5): 1023.

Kawasaki, Y, et al. (2000). "Asef, a link between the tumor suppressor APC and G-protein signaling." Science **289** (5482): 1194.

Keen, JH, et al. (1991). "Clathrin domains involved in recognition by assembly protein AP-2." J Biol Chem **266** (12): 7950.

Keep, NH, et al. (1997). "A modulator of rho family G proteins, rhoGDI, binds these G proteins via an immunoglobulin-like domain and a flexible N-terminal arm." Structure **5** (5): 623.

Keller, HU (1990). "Diacylglycerols and PMA are particularly effective stimulators of fluid pinocytosis in human neutrophils." J Cell Physiol **145** (3): 465.

Kessell, I, Holst, BD and Roth, TF (1989). "Membranous intermediates in endocytosis are labile, as shown in a temperature-sensitive mutant." Proc Natl Acad Sci U S A **86** (13): 4968.

Kharbanda, S, et al. (1995). "Stimulation of human monocytes with macrophage colony-stimulating factor induces a Grb2-mediated association of the focal adhesion kinase pp125FAK and dynamin." Proc Natl Acad Sci U S A **92** (13): 6132.

Khwaja, A and Downward, J (1997). "Lack of correlation between activation of Jun-NH2-terminal kinase and induction of apoptosis after detachment of epithelial cells." J Cell Biol **139** (4): 1017.

Khwaja, A, et al. (1997). "Matrix adhesion and Ras transformation both activate a phosphoinositide 3-OH kinase and protein kinase B/Akt cellular survival pathway." Embo J **16** (10): 2783.

Kiefer, F, et al. (1996). "HPK1, a hematopoietic protein kinase activating the SAPK/JNK pathway." Embo J **15**: 7013.

Kim, AS, et al. (2000). "Autoinhibition and activation mechanisms of the Wiskott-Aldrich syndrome protein." Nature **404**: 151.

King, AJ, et al. (1998). "The protein kinase Pak3 positively regulates Raf-1 activity through phosphorylation of serine 338 [published erratum appears in Nature 2000 Jul 27;406(6794):439]." Nature **396** (6707): 180.

Kirchhausen, T (1999). "Adaptors for clathrin-mediated traffic." Annu Rev Cell Dev Biol **15**: 705.

Kirchhausen, T, Harrison, SC and Heuser, J (1986). "Configuration of clathrin trimers: evidence from electron microscopy." J Ultrastruct Mol Struct Res **94** (3): 199.

Kirchhausen, T and Rosen, FS (1996). "Disease mechanism: unravelling Wiskott-Aldrich syndrome." Curr Biol **6** (6): 676.

Kiyokawa, E, et al. (1998). "Activation of Rac1 by a Crk SH3-binding protein, DOCK180." Genes Dev **12** (21): 3331.

Kjoller, L and Hall, A (1999). "Signaling to Rho GTPases." Exp Cell Res **253** (1): 166.

Klein, DE, et al. (1998). "The pleckstrin homology domains of dynamin isoforms require oligomerization for high affinity phosphoinositide binding." J Biol Chem **273** (42): 27725.

Klippel, A, et al. (1997). "A specific product of phosphatidylinositol 3-kinase directly activates the protein kinase Akt through its pleckstrin homology domain." Mol Cell Biol **17** (1): 338.

Klug, A and Rhodes, D (1987). "Zinc fingers: a novel protein fold for nucleic acid recognition." Cold Spring Harb Symp Quant Biol **52**: 473.

Knaus, UG, et al. (1991). "Regulation of phagocyte oxygen radical production by the GTP-binding protein Rac 2." Science **254** (5037): 1512.

Kobayashi, K, et al. (1998). "p140Sra-1 (specifically Rac1-associated protein) is a novel specific target for Rac1 small GTPase." J Biol Chem **273** (1): 291.

Koegl, M, et al. (1999). "A novel ubiquitination factor, E4, is involved in multiubiquitin chain assembly." Cell **96** (5): 635.

Koenig, JH and Ikeda, K (1989). "Disappearance and reformation of synaptic vesicle membrane upon transmitter release observed under reversible blockage of membrane retrieval." J Neurosci **9** (11): 3844.

Koga, H, et al. (1999). "Tetratricopeptide repeat (TPR) motifs of p67(phox) participate in interaction with the small GTPase Rac and activation of the phagocyte NADPH oxidase." J Biol Chem **274** (35): 25051.

Kolluri, R, et al. (1996). "Direct interaction of the Wiskott-Aldrich syndrome protein with the GTPase Cdc42." Proc Natl Acad Sci U S A **93** (11): 5615.

Kosaka, T and Ikeda, K (1983a). "Possible temperature-dependent blockage of synaptic vesicle recycling induced by a single gene mutation in Drosophila." J Neurobiol **14** (3): 207.

Kosaka, T and Ikeda, K (1983b). "Reversible blockage of membrane retrieval and endocytosis in the garland cell of the temperature-sensitive mutant of Drosophila melanogaster, shibirets1." J Cell Biol **97** (2): 499.

Kozasa, T, et al. (1998). "p115 RhoGEF, a GTPase activating protein for Galpha12 and Galpha13." Science **280** (5372): 2109.

Kozlov, MM (1999). "Dynamin: possible mechanism of "Pinchase" action." Biophys J **77** (1): 604.

Kozma, R, et al. (1995). "The Ras-related protein Cdc42Hs and bradykinin promote formation of peripheral actin microspikes and filopodia in Swiss 3T3 fibroblasts." Mol Cell Biol **15** (4): 1942.

Kozma, R, et al. (1996). "The GTPase-activating protein n-chimaerin cooperates with Rac1 and Cdc42Hs to induce the formation of lamellipodia and filopodia." Mol Cell Biol **16** (9): 5069.

Kozma, R, et al. (1997). "Rho family GTPases and neuronal growth cone remodelling: relationship between increased complexity induced by Cdc42Hs, Rac1, and acetylcholine and collapse induced by RhoA and lysophosphatidic acid." Mol Cell Biol **17** (3): 1201.

Kranenburg, O, et al. (1999). "Activation of RhoA by lysophosphatidic acid and Galpha12/13 subunits in neuronal cells: induction of neurite retraction." Mol Biol Cell **10** (6): 1851.

Kranenburg, O, Verlaan, I and Moolenaar, WH (1999a). "Dynamin is required for the activation of mitogen-activated protein (MAP) kinase by MAP kinase kinase." J Biol Chem **274** (50): 35301.

Kranenburg, O, Verlaan, I and Moolenaar, WH (1999b). "Gi-mediated tyrosine phosphorylation of Grb2 (growth-factor-receptor- bound protein 2)-bound dynamin-II by lysophosphatidic acid." Biochem J **339** (Pt 1): 11.

Kraynov, VS, et al. (2000). "Localized rac activation dynamics visualized in living cells." Science **290** (5490): 333.

Krupnick, JG, et al. (1997). "Arrestin/clathrin interaction. Localization of the clathrin binding domain of nonvisual arrestins to the carboxy terminus." J Biol Chem **272** (23): 15011.

Kubler, E and Riezman, H (1993). "Actin and fimbrin are required for the internalization step of endocytosis in yeast." Embo J **12** (7): 2855.

Kuhn, TB, et al. (1999). "Myelin and collapsin-1 induce motor neuron growth cone collapse through different pathways: inhibition of collapse by opposing mutants of rac1." J Neurosci **19** (6): 1965.

Kumar, A, et al. (1997). "Deficient cytokine signaling in mouse embryo fibroblasts with a targeted deletion in the PKR gene: role of IRF-1 and NF-kappaB." Embo J **16** (2): 406.

Kuroda, S, et al. (1996). "Identification of IQGAP as a putative target for the small GTPases, Cdc42 and Rac1." J Biol Chem **271** (38): 23363.

Kuroda, S, et al. (1998). "Role of IQGAP1, a target of the small GTPases Cdc42 and Rac1, in regulation of E-cadherin- mediated cell-cell adhesion." Science **281** (5378): 832.

Kwon, T, et al. (2000). "Akt protein kinase inhibits Rac1-GTP binding through phosphorylation at serine 71 of Rac1." J Biol Chem **275** (1): 423.

Kyriakis, JM and Avruch, J (1996). "Sounding the alarm: protein kinase cascades activated by stress and inflammation." J Biol Chem **271**: 24313.

Lacy, P, et al. (1999). "Expression and translocation of Rac2 in eosinophils during superoxide generation." Immunology **98** (2): 244.

Lamarche, N and Hall, A (1994). "GAPs for rho-related GTPases." Trends Genet **10** (12): 436.

Lamarche, N, et al. (1996). "Rac and Cdc42 induce actin polymerization and G1 cell cycle progression independently of p65PAK and the JNK/SAPK MAP kinase cascade." Cell **87** (3): 519.

Lamaze, C, et al. (1996). "Regulation of receptor-mediated endocytosis by Rho and Rac." Nature **382** (6587): 177.

Lamaze, C, et al. (1997). "The actin cytoskeleton is required for receptor-mediated endocytosis in mammalian cells." J Biol Chem **272** (33): 20332.

Lambeth, JD, et al. (2000). "Novel homologs of gp91phox." Trends Biochem Sci **25** (10): 459.

Laney, JD and Hochstrasser, M (1999). "Substrate targeting in the ubiquitin system." Cell **97** (4): 427.

Lang, P, et al. (1996). "Protein kinase A phosphorylation of RhoA mediates the morphological and functional effects of cyclic AMP in cytotoxic lymphocytes." Embo J **15** (3): 510.

Laporte, SA, et al. (1999). "The beta2-adrenergic receptor/betaarrestin complex recruits the clathrin adaptor AP-2 during endocytosis." Proc Natl Acad Sci U S A **96** (7): 3712.

Lapouge, K, et al. (2000). "Structure of the TPR Domain of p67(phox) in Complex with Rac.GTP." Mol Cell **6** (4): 899.

Larkin, JM, Donzell, WC and Anderson, RG (1986). "Potassium-dependent assembly of coated pits: new coated pits form as planar clathrin lattices." J Cell Biol **103** (6 Pt 2): 2619.

Lassus, P, et al. (2000). "Extinction of rac1 and Cdc42Hs signalling defines a novel p53-dependent apoptotic pathway." Oncogene **19** (20): 2377.

Leberer, E, et al. (1992). "The protein kinase homologue Ste20p is required to link the yeast pheromone response G-protein beta gamma subunits to downstream signalling components." Embo J **11** (13): 4815.

Leberer, E, Thomas, DY and Whiteway, M (1997). "Pheromone signalling and polarized morphogenesis in yeast." Curr Opin Genet Dev **7** (1): 59.

Lebowitz, PF, Du, W and Prendergast, GC (1997). "Prenylation of RhoB is required for its cell transforming function but not its ability to activate serum response element-dependent transcription." J Biol Chem **272** (26): 16093.

Lee, A, et al. (1999). "Dominant-negative inhibition of receptor-mediated endocytosis by a dynamin-1 mutant with a defective pleckstrin homology domain." Curr Biol **9** (5): 261.

Lee, FS, et al. (1997). "Activation of the IkappaB alpha kinase complex by MEKK1, a kinase of the JNK pathway." Cell **88** (2): 213.

Lee, PS, et al. (1999). "The Cbl protooncoprotein stimulates CSF-1 receptor multiubiquitination and endocytosis, and attenuates macrophage proliferation." Embo J **18** (13): 3616.

Leeuwen, FN, et al. (1997). "The guanine nucleotide exchange factor Tiam1 affects neuronal morphology; opposing roles for the small GTPases Rac and Rho." J Cell Biol **139** (3): 797.

Leevers, SJ, Vanhaesebroeck, B and Waterfield, MD (1999). "Signalling through phosphoinositide 3-kinases: the lipids take centre stage." Curr Opin Cell Biol **11** (2): 219.

Leffers, H, et al. (1993). "Identification of two human Rho GDP dissociation inhibitor proteins whose overexpression leads to disruption of the actin cytoskeleton." Exp Cell Res **209** (2): 165.

Lehrman, MA, et al. (1985). "Internalization-defective LDL receptors produced by genes with nonsense and frameshift mutations that truncate the cytoplasmic domain." Cell **41** (3): 735.

Lei, M, et al. (2000). "Structure of PAK1 in an autoinhibited conformation reveals a multistage activation switch." Cell **102** (3): 387.

Lelias, JM, et al. (1993). "cDNA cloning of a human mRNA preferentially expressed in hematopoietic cells and with homology to a GDP-dissociation inhibitor for the rho GTP- binding proteins." Proc Natl Acad Sci U S A **90** (4): 1479.

Leonard, DA, et al. (1997). "Use of a fluorescence spectroscopic readout to characterize the interactions of Cdc42Hs with its target/effector, mPAK-3." Biochemistry **36** (5): 1173.

Lerm, M, et al. (1999). "Deamidation of Cdc42 and Rac by Escherichia coli cytotoxic necrotizing factor 1: activation of c-Jun N-terminal kinase in HeLa cells." Infect Immun **67** (2): 496.

Leung, T, et al. (1993). "Germ cell beta-chimaerin, a new GTPase-activating protein for p21rac, is specifically expressed during the acrosomal assembly stage in rat testis." J Biol Chem **268** (6): 3813.

Levkau, B, et al. (1999). "Apoptosis overrides survival signals through a caspase-mediated dominant-negative NF-kappa B loop." Nat Cell Biol **1** (4): 227.

Li, G, et al. (1997). "Uncoupling of membrane ruffling and pinocytosis during Ras signal transduction." J Biol Chem **272** (16): 10337.

Li, N and Karin, M (1998). "Ionizing radiation and short wavelength UV activate NF-kappaB through two distinct mechanisms." Proc Natl Acad Sci U S A **95** (22): 13012.

Li, N and Karin, M (2000). "Signaling pathways leading to nuclear factor-kappa B activation." Methods Enzymol **319**: 273.

Li, R, et al. (1999). "Localization of the PAK1-, WASP-, and IQGAP1-specifying regions of Cdc42." J Biol Chem **274** (42): 29648.

Lin, D, et al. (2000). "A mammalian PAR-3-PAR-6 complex implicated in Cdc42/Rac1 and aPKC signalling and cell polarity." Nat Cell Biol **2** (8): 540.

Lin, HC, et al. (1998). "Sequestration of the G protein beta gamma subunit complex inhibits receptor-mediated endocytosis." Proc Natl Acad Sci U S A **95** (9): 5057.

Lin, HC and Gilman, AG (1996). "Regulation of dynamin I GTPase activity by G protein betagamma subunits and phosphatidylinositol 4,5-bisphosphate." J Biol Chem **271** (45): 27979.

Linder, S, et al. (1999). "Wiskott-Aldrich syndrome protein regulates podosomes in primary human macrophages." Proc Natl Acad Sci U S A **96** (17): 9648.

Ling, L, Cao, Z and Goeddel, DV (1998). "NF-kappaB-inducing kinase activates IKK-alpha by phosphorylation of Ser- 176." Proc Natl Acad Sci U S A **95** (7): 3792.

Liu, JP, et al. (1994). "Dynamin I is a Ca(2+)-sensitive phospholipid-binding protein with very high affinity for protein kinase C." J Biol Chem **269** (33): 21043.

Liu, JP, Sim, AT and Robinson, PJ (1994). "Calcineurin inhibition of dynamin I GTPase activity coupled to nerve terminal depolarization." Science **265** (5174): 970.

Liu, JP, et al. (1997). "Molecular interactions between dynamin and G-protein betagamma-subunits in neuroendocrine cells." Mol Cell Endocrinol **132** (1-2): 61.

Liu, JP, et al. (1996). "Calcium binds dynamin I and inhibits its GTPase activity." J Neurochem **66** (5): 2074.

Liu, X, et al. (1998). "NMR structure and mutagenesis of the N-terminal Dbl homology domain of the nucleotide exchange factor Trio." Cell **95** (2): 269.

Longenecker, K, et al. (1999). "How RhoGDI binds Rho." Acta Crystallogr D Biol Crystallogr **55** (Pt 9): 1503.

Lores, P, et al. (1997). "Enhanced apoptosis in the thymus of transgenic mice expressing constitutively activated forms of human Rac2GTPase." Oncogene **15** (5): 601.

Lorick, KL, et al. (1999). "RING fingers mediate ubiquitin-conjugating enzyme (E2)-dependent ubiquitination." Proc Natl Acad Sci U S A **96** (20): 11364.

Lovering, R, et al. (1993). "Identification and preliminary characterization of a protein motif related to the zinc finger." Proc Natl Acad Sci U S A **90** (6): 2112.

Lu, W, et al. (1997). "Activation of Pak by membrane localization mediated by an SH3 domain from the adaptor protein Nck." Curr Biol **7** (2): 85.

Luo, L, Jan, LY and Jan, YN (1997). "Rho family GTP-binding proteins in growth cone signalling." Curr Opin Neurobiol **7** (1): 81.

Luo, Z, et al. (1997). "An intact Raf zinc finger is required for optimal binding to processed Ras and for ras-dependent Raf activation in situ." Mol Cell Biol **17** (1): 46.

Lupas, A (1996). "Coiled coils: new structures and new functions." Trends Biochem Sci **21** (10): 375.

Mabuchi, I, et al. (1993). "A rho-like protein is involved in the organisation of the contractile ring in dividing sand dollar eggs." Zygote **1** (4): 325.

Machesky, LM and Gould, KL (1999). "The Arp2/3 complex: a multifunctional actin organizer." Curr Opin Cell Biol **11** (1): 117.

Machesky, LM and Insall, RH (1998). "Scar1 and the related Wiskott-Aldrich syndrome protein, WASP, regulate the actin cytoskeleton through the Arp2/3 complex." Curr Biol **8** (25): 1347.

Machesky, LM, et al. (1999). "Scar, a WASp-related protein, activates nucleation of actin filaments by the Arp2/3 complex." Proc Natl Acad Sci U S A **96** (7): 3739.

Mackay, JP and Crossley, M (1998). "Zinc fingers are sticking together." Trends Biochem Sci **23** (1): 1.

Maekawa, M, et al. (1999). "Signaling from Rho to the actin cytoskeleton through protein kinases ROCK and LIM-kinase." Science **285** (5429): 895.

Maguire, J, et al. (1994). "Gem: an induced, immediate early protein belonging to the Ras family." Science **265** (5169): 241.

Mahaffey, DT, et al. (1990). "Clathrin-coated pits contain an integral membrane protein that binds the AP-2 subunit with high affinity." J Biol Chem **265** (27): 16514.

Malcolm, KC, Elliott, CM and Exton, JH (1996). "Evidence for Rho-mediated agonist stimulation of phospholipase D in rat1 fibroblasts. Effects of Clostridium botulinum C3 exoenzyme." J Biol Chem **271** (22): 13135.

Malecz, N, et al. (2000). "Synaptojanin 2, a novel rac1 effector that regulates clathrin-mediated endocytosis." Curr Biol **10** (21): 1383.

Malinin, NL, et al. (1997). "MAP3K-related kinase involved in NF-kappaB induction by TNF, CD95 and IL-1." Nature **385** (6616): 540.

Malosio, ML, et al. (1997). "Differential expression of distinct members of Rho family GTP-binding proteins during neuronal development: identification of Rac1B, a new neural-specific member of the family." J Neurosci **17** (17): 6717.

Manser, E, et al. (1995). "Molecular cloning of a new member of the p21-Cdc42/Rac-activated kinase (PAK) family." J Biol Chem **270** (42): 25070.

Manser, E, et al. (1993). "A non-receptor tyrosine kinase that inhibits the GTPase activity of p21cdc42." Nature **363** (6427): 364.

Manser, E, et al. (1994). "A brain serine/threonine protein kinase activated by Cdc42 and Rac1." Nature **367** (6458): 40.

Manser, E, et al. (1998). "PAK kinases are directly coupled to the PIX family of nucleotide exchange factors." Mol Cell **1** (2): 183.

Mao, J, et al. (1998). "Guanine nucleotide exchange factor GEF115 specifically mediates activation of Rho and serum response factor by the G protein alpha subunit Galpha13." Proc Natl Acad Sci U S A **95** (22): 12973.

Marks, B, et al. (2001). "GTPase activity of dynamin and resulting conformation change are essential for endocytosis." Nature **410** (6825): 231.

Marks, PW and Kwiatkowski, DJ (1996). "Genomic organization and chromosomal location of murine Cdc42." Genomics **38** (1): 13.

Marsh, M and McMahon, HT (1999). "The structural era of endocytosis." Science **285** (5425): 215.

Marshall, CJ (1994). "MAP kinase kinase kinase, MAP kinase kinase and MAP kinase." Curr Opin Genet Dev **4** (1): 82.

Marshall, CJ (1996). "Ras effectors." Curr Opin Cell Biol **8** (2): 197.

Masdehors, P, et al. (1999). "Increased sensitivity of CLL-derived lymphocytes to apoptotic death activation by the proteasome-specific inhibitor lactacystin." Br J Haematol **105** (3): 752.

Massol, P, et al. (1998). "Fc receptor-mediated phagocytosis requires CDC42 and Rac1." Embo J **17** (21): 6219.

Maudsley, S, et al. (2000). "The beta(2)-adrenergic receptor mediates extracellular signal-regulated kinase activation via assembly of a multi-receptor complex with the epidermal growth factor receptor." J Biol Chem **275** (13): 9572.

Maundrell, K, et al. (1997). "Bcl-2 undergoes phosphorylation by c-Jun N-terminal kinase/stress- activated protein kinases in the presence of the constitutively active GTP-binding protein Rac1." J Biol Chem **272** (40): 25238.

Mayer, BJ (1999). "Endocytosis: EH domains lend a hand." Curr Biol **9** (2): R70.

McCallum, SJ, Wu, WJ and Cerione, RA (1996). "Identification of a putative effector for Cdc42Hs with high sequence similarity to the RasGAP-related protein IQGAP1 and a Cdc42Hs binding partner with similarity to IQGAP2." J Biol Chem **271** (36): 21732.

McLauchlan, H, et al. (1998). "A novel role for Rab5-GDI in ligand sequestration into clathrin-coated pits." Curr Biol **8** (1): 34.

McMahon, HT (1999). "Endocytosis: an assembly protein for clathrin cages." Curr Biol **9** (9): R332.

McMahon, HT, Wigge, P and Smith, C (1997). "Clathrin interacts specifically with amphiphysin and is displaced by dynamin." FEBS Lett **413** (2): 319.

McNiven, MA, et al. (2000). "Regulated interactions between dynamin and the actin-binding protein cortactin modulate cell shape." J Cell Biol **151** (1): 187.

McPherson, PS, et al. (1994). "Interaction of Grb2 via its Src homology 3 domains with synaptic proteins including synapsin I." Proc Natl Acad Sci U S A **91** (14): 6486.

McPherson, PS, et al. (1996). "A presynaptic inositol-5-phosphatase." Nature **379** (6563): 353.

McPherson, PS, et al. (1994). "p145, a major Grb2-binding protein in brain, is co-localized with dynamin in nerve terminals where it undergoes activity-dependent dephosphorylation." J Biol Chem **269** (48): 30132.

Medley, QG, et al. (2000). "The Trio Guanine Nucleotide Exchange Factor Is a RhoA Target. binding of Rhoa to the trio immunoglobulin-like domain." J Biol Chem **275** (46): 36116.

Meek, DW and Eckhart, W (1988). "Phosphorylation of p53 in normal and simian virus 40-transformed NIH 3T3 cells." Mol Cell Biol **8** (1): 461.

Mercurio, F and Manning, AM (1999). "Multiple signals converging on NF-kappaB." Curr Opin Cell Biol **11** (2): 226.

Mercurio, F, et al. (1997). "IKK-1 and IKK-2: cytokine-activated IkappaB kinases essential for NF-kappaB activation." Science **278** (5339): 860.

Merrifield, CJ, et al. (1999). "Endocytic vesicles move at the tips of actin tails in cultured mast cells." Nat Cell Biol **1** (1): 72.

Messmer, UK and Pfeilschifter, J (2000). "New insights into the mechanism for clearance of apoptotic cells." Bioessays **22** (10): 878.

Micheva, KD, Kay, BK and McPherson, PS (1997). "Synaptojanin forms two separate complexes in the nerve terminal. Interactions with endophilin and amphiphysin." J Biol Chem **272** (43): 27239.

Micheva, KD, et al. (1997). "SH3 domain-dependent interactions of endophilin with amphiphysin [published erratum appears in FEBS Lett 1997 Dec 8;419(1):150]." FEBS Lett **414** (2): 308.

Michiels, F, et al. (1995). "A role for Rac in Tiam1-induced membrane ruffling and invasion." Nature **375** (6529): 338.

Michiels, F, et al. (1997). "Regulated membrane localization of Tiam1, mediated by the NH2-terminal pleckstrin homology domain, is required for Rac-dependent membrane ruffling and C-Jun NH2-terminal kinase activation." J Cell Biol **137** (2): 387.

Miki, H, Miura, K and Takenawa, T (1996). "N-WASP, a novel actin-depolymerizing protein, regulates the cortical cytoskeletal rearrangement in a PIP2-dependent manner downstream of tyrosine kinases." Embo J **15** (19): 5326.

Miki, H, et al. (1998). "Induction of filopodium formation by a WASP-related actin- depolymerizing protein N-WASP." Nature **391** (6662): 93.

Miki, H, Suetsugu, S and Takenawa, T (1998). "WAVE, a novel WASP-family protein involved in actin reorganization induced by Rac." Embo J **17** (23): 6932.

Miki, H and Takenawa, T (1998). "Direct binding of the verprolin-homology domain in N-WASP to actin is essential for cytoskeletal reorganization." Biochem Biophys Res Commun **243** (1): 73.

Miki, H, et al. (2000). "IRSp53 is an essential intermediate between Rac and WAVE in the regulation of membrane ruffling." Nature **408**: 732 .

Miller, WE, et al. (2000). "beta-arrestin1 interacts with the catalytic domain of the tyrosine kinase c-SRC. Role of beta-arrestin1-dependent targeting of c-SRC in receptor endocytosis." J Biol Chem **275** (15): 11312.

Minden, A, et al. (1995). "Selective activation of the JNK signaling cascade and c-Jun transcriptional activity by the small GTPases Rac and Cdc42Hs." Cell **81** (7): 1147.

Mira, JP, et al. (2000). "Endogenous, hyperactive Rac3 controls proliferation of breast cancer cells by a p21-activated kinase-dependent pathway." Proc Natl Acad Sci U S A **97** (1): 185.

Modregger, J, et al. (2000). "All three PACSIN isoforms bind to endocytic proteins and inhibit endocytosis." J Cell Sci **113 Pt 24**: 4511.

Moore, MS, et al. (1987). "Assembly of clathrin-coated pits onto purified plasma membranes." Science **236** (4801): 558.

Moreau, V, et al. (1997). "The yeast actin-related protein Arp2p is required for the internalization step of endocytosis." Mol Biol Cell **8** (7): 1361.

Mori, S, et al. (1995). "Degradation process of ligand-stimulated platelet-derived growth factor beta-receptor involves ubiquitin-proteasome proteolytic pathway." J Biol Chem **270** (49): 29447.

Morinaka, K, et al. (1999). "Epsin binds to the EH domain of POB1 and regulates receptor-mediated endocytosis." Oncogene **18** (43): 5915.

Morreale, A, et al. (2000). "Structure of Cdc42 bound to the GTPase binding domain of PAK." Nat Struct Biol **7** (5): 384.

Mott, HR, et al. (1999). "Structure of the small G protein Cdc42 bound to the GTPase-binding domain of ACK." Nature **399** (6734): 384.

Moynihan, TP, et al. (1999). "The ubiquitin-conjugating enzymes UbcH7 and UbcH8 interact with RING finger/IBR motif-containing domains of HHARI and H7-AP1." J Biol Chem **274** (43): 30963.

Muhlberg, AB, Warnock, DE and Schmid, SL (1997). "Domain structure and intramolecular regulation of dynamin GTPase." Embo J **16** (22): 6676.

Muller, RT, et al. (1997). "The rat myosin myr 5 is a GTPase-activating protein for Rho in vivo: essential role of arginine 1695." Mol Biol Cell **8** (10): 2039.

Mullins, RD (2000). "How WASP-family proteins and the Arp2/3 complex convert intracellular signals into cytoskeletal structures." Curr Opin Cell Biol **12** (1): 91.

Mundigl, O, et al. (1998). "Amphiphysin I antisense oligonucleotides inhibit neurite outgrowth in cultured hippocampal neurons." J Neurosci **18** (1): 93.

Munemitsu, S, et al. (1990). "Molecular cloning and expression of a G25K cDNA, the human homolog of the yeast cell cycle gene CDC42." Mol Cell Biol **10** (11): 5977.

Munn, AL, et al. (1995). "end5, end6, and end7: mutations that cause actin delocalization and block the internalization step of endocytosis in Saccharomyces cerevisiae." Mol Biol Cell **6** (12): 1721.

Murphy, AM and Montell, DJ (1996). "Cell type-specific roles for Cdc42, Rac, and RhoL in Drosophila oogenesis." J Cell Biol **133** (3): 617.

Murphy, JE and Keen, JH (1992). "Recognition sites for clathrin-associated proteins AP-2 and AP-3 on clathrin triskelia." J Biol Chem **267** (15): 10850.

Nagata, K, et al. (1998). "The MAP kinase kinase kinase MLK2 co-localizes with activated JNK along microtubules and associates with kinesin superfamily motor KIF3." Embo J **17** (1): 149.

Nakashima, S, et al. (1999). "Small G protein Ral and its downstream molecules regulate endocytosis of EGF and insulin receptors." Embo J **18** (13): 3629.

Nakata, T, et al. (1991). "Predominant and developmentally regulated expression of dynamin in neurons." Neuron **7** (3): 461.

Nakata, T, Takemura, R and Hirokawa, N (1993). "A novel member of the dynamin family of GTP-binding proteins is expressed specifically in the testis." J Cell Sci **105** (Pt 1): 1.

Nassar, N, et al. (1998). "Structures of Cdc42 bound to the active and catalytically compromised forms of Cdc42GAP." Nat Struct Biol **5** (12): 1047.

Nemoto, Y, et al. (1997). "Synaptojanin 2, a novel synaptojanin isoform with a distinct targeting domain and expression pattern." J Biol Chem **272** (49): 30817.

Nesterov, A, et al. (1999). "Inhibition of the receptor-binding function of clathrin adaptor protein AP-2 by dominant-negative mutant mu2 subunit and its effects on endocytosis." Embo J **18** (9): 2489.

Newsome, TP, et al. (2000). "Trio combines with dock to regulate Pak activity during photoreceptor axon pathfinding in Drosophila." Cell **101** (3): 283.

Nicotera, P, Leist, M and Ferrando-May, E (1999). "Apoptosis and necrosis: different execution of the same death." Biochem Soc Symp **66**: 69.

Nimnual, AS, Yatsula, BA and Bar-Sagi, D (1998). "Coupling of Ras and Rac guanosine triphosphatases through the Ras exchanger Sos." Science **279** (5350): 560.

Nishida, K, Kaziro, Y and Satoh, T (1999). "Anti-apoptotic function of Rac in hematopoietic cells." Oncogene **18** (2): 407.

Nisimoto, Y, et al. (1997). "Rac binding to p67(phox). Structural basis for interactions of the Rac1 effector region and insert region with components of the respiratory burst oxidase." J Biol Chem **272** (30): 18834.

Nobes, C and Marsh, M (2000). "Dendritic cells: new roles for Cdc42 and Rac in antigen uptake?" Curr Biol **10** (20): R739.

Nobes, CD and Hall, A (1995). "Rho, rac, and cdc42 GTPases regulate the assembly of multimolecular focal complexes associated with actin stress fibers, lamellipodia, and filopodia." Cell **81** (1): 53.

Nobes, CD and Hall, A (1999). "Rho GTPases control polarity, protrusion, and adhesion during cell movement." J Cell Biol **144** (6): 1235.

Nobes, CD, et al. (1995). "Activation of the small GTP-binding proteins rho and rac by growth factor receptors." J Cell Sci **108** (Pt 1): 225.

Nobes, CD, et al. (1998). "A new member of the Rho family, Rnd1, promotes disassembly of actin filament structures and loss of cell adhesion." J Cell Biol **141** (1): 187.

Noble, ME, et al. (1993). "Crystal structure of the SH3 domain in human Fyn; comparison of the three-dimensional structures of SH3 domains in tyrosine kinases and spectrin." Embo J **12** (7): 2617.

Nomanbhoy, TK, Erickson, JW and Cerione, RA (1999). "Kinetics of Cdc42 membrane extraction by Rho-GDI monitored by real-time fluorescence resonance energy transfer." Biochemistry **38** (6): 1744.

Noren, NK, et al. (2000). "p120 catenin regulates the actin cytoskeleton via Rho family GTPases." J Cell Biol **150** (3): 567.

Norman, JC, et al. (1996). "The small GTP-binding proteins, Rac and Rho, regulate cytoskeletal organization and exocytosis in mast cells by parallel pathways." Mol Biol Cell **7** (9): 1429.

O'Sullivan, AJ, et al. (1996). "Purification and identification of FOAD-II, a cytosolic protein that regulates secretion in streptolysin-O permeabilized mast cells, as a rac/rhoGDI complex." Mol Biol Cell **7** (3): 397.

Obermeier, A, et al. (1998). "PAK promotes morphological changes by acting upstream of Rac." Embo J **17** (15): 4328.

Ochoa, GC, et al. (2000). "A functional link between dynamin and the actin cytoskeleton at podosomes." J Cell Biol **150** (2): 377.

Ohga, N, et al. (1989). "Rabbit intestine contains a protein that inhibits the dissociation of GDP from and the subsequent binding of GTP to rhoB p20, a ras p21-like GTP-binding protein." Biochem Biophys Res Commun **163** (3): 1523.

Ohno, H, et al. (1995). "Interaction of tyrosine-based sorting signals with clathrin-associated proteins." Science **269** (5232): 1872.

Okamoto, PM, Herskovits, JS and Vallee, RB (1997). "Role of the basic, proline-rich region of dynamin in Src homology 3 domain binding and endocytosis." J Biol Chem **272** (17): 11629.

Oldridge, J and Marsh, M (1998). "Nef--an adaptor adaptor?" Trends Cell Biol **8** (8): 302.

Olofsson, B (1999). "Rho guanine dissociation inhibitors: pivotal molecules in cellular signalling." Cell Signal **11** (8): 545.

Olson, MF, Ashworth, A and Hall, A (1995). "An essential role for Rho, Rac, and Cdc42 GTPases in cell cycle progression through G1." Science **269** (5228): 1270.

Olson, MF and Marais, R (2000). "Ras protein signalling." Semin Immunol **12** (1): 63.

Olson, MF, et al. (1996). "Faciogenital dysplasia protein (FGD1) and Vav, two related proteins required for normal embryonic development, are upstream regulators of Rho GTPases." Curr Biol **6** (12): 1628.

Owen, D, et al. (2000). "Residues in Cdc42 that specify binding to individual CRIB effector proteins." Biochemistry **39** (6): 1243.

Owen, DJ and Evans, PR (1998). "A structural explanation for the recognition of tyrosine-based endocytotic signals." Science **282** (5392): 1327.

Owen, DJ, et al. (2001). "A Third Specificity-Determining Site in μ2 Adaptin for Sequences Upstream of Yxxφ Sorting Motifs." Traffic **2**: 105.

Owen, DJ, et al. (1999). "A structural explanation for the binding of multiple ligands by the alpha-adaptin appendage domain." Cell **97** (6): 805.

Owen, DJ, et al. (1998). "Crystal structure of the amphiphysin-2 SH3 domain and its role in the prevention of dynamin ring formation." Embo J **17** (18): 5273.

Oyama, T, et al. (1994). "A truncated beta-catenin disrupts the interaction between E-cadherin and alpha-catenin: a cause of loss of intercellular adhesiveness in human cancer cell lines." Cancer Res **54** (23): 6282.

Page, LJ and Robinson, MS (1995). "Targeting signals and subunit interactions in coated vesicle adaptor complexes." J Cell Biol **131** (3): 619.

Palfrey, HC and Artalejo, CR (1998). "Vesicle recycling revisited: rapid endocytosis may be the first step." Neuroscience **83** (4): 969.

Park, J, et al. (1997). "Activation of c-Jun N-terminal kinase antagonizes an anti-apoptotic action of Bcl-2." J Biol Chem **272** (27): 16725.

Pasquini, LA, et al. (2000). "Lactacystin, a specific inhibitor of the proteasome, induces apoptosis and activates caspase-3 in cultured cerebellar granule cells." J Neurosci Res **59** (5): 601.

Pawson, T and Gish, GD (1992). "SH2 and SH3 domains: from structure to function." Cell **71** (3): 359.

Pearse, BM, Smith, CJ and Owen, DJ (2000). "Clathrin coat construction in endocytosis." Curr Opin Struct Biol **10** (2): 220.

Peeler, JS, Donzell, WC and Anderson, RG (1993). "The appendage domain of the AP-2 subunit is not required for assembly or invagination of clathrin-coated pits." J Cell Biol **120** (1): 47.

Perez-Alvarado, GC, et al. (1994). "Structure of the carboxy-terminal LIM domain from the cysteine rich protein CRP." Nat Struct Biol **1** (6): 388.

Perona, R, et al. (1997). "Activation of the nuclear factor-kappaB by Rho, CDC42, and Rac-1 proteins." Genes Dev **11** (4): 463.

Peter, M, et al. (1996). "Functional analysis of the interaction between the small GTP binding protein Cdc42 and the Ste20 protein kinase in yeast." Embo J **15** (24): 7046.

Pitcher, JA, et al. (1995). "Pleckstrin homology domain-mediated membrane association and activation of the beta-adrenergic receptor kinase requires coordinate interaction with G beta gamma subunits and lipid." J Biol Chem **270** (20): 11707.

Post, PL, Bokoch, GM and Mooseker, MS (1998). "Human myosin-IXb is a mechanochemically active motor and a GAP for rho." J Cell Sci **111** (Pt 7): 941.

Powell, KA, et al. (2000). "Phosphorylation of dynamin I on Ser-795 by protein kinase C blocks its association with phospholipids." J Biol Chem **275** (16): 11610.

Prehoda, KE, et al. (2000). "Integration of multiple signals through cooperative regulation of the N-WASP-Arp2/3 complex." Science **290** (5492): 801.

Prendergast, GC, et al. (1995). "Critical role of Rho in cell transformation by oncogenic Ras." Oncogene **10** (12): 2289.

Price, LS, et al. (1998). "Activation of Rac and Cdc42 by integrins mediates cell spreading." Mol Biol Cell **9** (7): 1863.

Price, LS, et al. (1995). "The small GTPases Rac and Rho as regulators of secretion in mast cells." Curr Biol **5** (1): 68.

Prigmore, E, et al. (1995). "A 68-kDa kinase and NADPH oxidase component p67phox are targets for Cdc42Hs and Rac1 in neutrophils." J Biol Chem **270** (18): 10717.

Proud, CG (1996). "p70 S6 kinase: an enigma with variations." Trends Biochem Sci **21** (5): 181.

Pucharcos, C, Estivill, X and de la Luna, S (2000). "Intersectin 2, a new multimodular protein involved in clathrin-mediated endocytosis." FEBS Lett **478** (1-2): 43.

Puls, A, et al. (1999). "Activation of the small GTPase Cdc42 by the inflammatory cytokines TNF(alpha) and IL-1, and by the Epstein-Barr virus transforming protein LMP1." J Cell Sci **112** (Pt 17): 2983.

Pulverer, BJ, et al. (1991). "Phosphorylation of c-jun mediated by MAP kinases." Nature **353**: 670.

Qiu, RG, et al. (1997). "Cdc42 regulates anchorage-independent growth and is necessary for Ras transformation." Mol Cell Biol **17** (6): 3449.

Qiu, RG, Abo, A and Steven Martin, G (2000). "A human homolog of the C. elegans polarity determinant Par-6 links Rac and Cdc42 to PKCzeta signaling and cell transformation." Curr Biol **10** (12): 697.

Qiu, RG, et al. (1995). "An essential role for Rac in Ras transformation." Nature **374** (6521): 457.

Qualmann, B and Kelly, RB (2000). "Syndapin isoforms participate in receptor-mediated endocytosis and actin organization." J Cell Biol **148** (5): 1047.

Qualmann, B, Kessels, MM and Kelly, RB (2000). "Molecular links between endocytosis and the actin cytoskeleton." J Cell Biol **150** (5): F111.

Qualmann, B, et al. (1999). "Syndapin I, a synaptic dynamin-binding protein that associates with the neural wiskott-aldrich syndrome protein." Mol Biol Cell **10** (2): 501.

Quilliam, LA, et al. (1996). "Isolation of a NCK-associated kinase, PRK2, an SH3-binding protein and potential effector of Rho protein signaling." J Biol Chem **271** (46): 28772.

Quinn, MT, et al. (1993). "Translocation of Rac correlates with NADPH oxidase activation. Evidence for equimolar translocation of oxidase components." J Biol Chem **268** (28): 20983.

Racoosin, EL and Swanson, JA (1992). "M-CSF-induced macropinocytosis increases solute endocytosis but not receptor-mediated endocytosis in mouse macrophages." J Cell Sci **102** (Pt 4): 867.

Radhakrishna, H, et al. (1999). "ARF6 requirement for Rac ruffling suggests a role for membrane trafficking in cortical actin rearrangements." J Cell Sci **112** (Pt 6): 855.

Radhakrishna, H and Donaldson, JG (1997). "ADP-ribosylation factor 6 regulates a novel plasma membrane recycling pathway." J Cell Biol **139** (1): 49.

Rameh, LE, et al. (1997). "A comparative analysis of the phosphoinositide binding specificity of pleckstrin homology domains." J Biol Chem **272** (35): 22059.

Ramjaun, AR and McPherson, PS (1996). "Tissue-specific alternative splicing generates two synaptojanin isoforms with differential membrane binding properties." J Biol Chem **271** (40): 24856.

Ramjaun, AR and McPherson, PS (1998). "Multiple amphiphysin II splice variants display differential clathrin binding: identification of two distinct clathrin-binding sites." J Neurochem **70** (6): 2369.

Ramjaun, AR, et al. (1999). "The N terminus of amphiphysin II mediates dimerization and plasma membrane targeting." J Biol Chem **274** (28): 19785.

Rasmussen, RK, et al. (1998). "Mixed-lineage kinase 2-SH3 domain binds dynamin and greatly enhances activation of GTPase by phospholipid." Biochem J **335** (Pt 1): 119.

Read, MA, et al. (1997). "TNFalpha induced E-selectin expression is activated by the NF-kB and JNK/p38 MAP kinase pathways." J Biol Chem **272**: 2753.

Reid, T, et al. (1999). "Identification and characterization of hPEM-2, a guanine nucleotide exchange factor specific for Cdc42." J Biol Chem **274** (47): 33587.

Ren, XD, et al. (1996). "Physical association of the small GTPase Rho with a 68-kDa phosphatidylinositol 4-phosphate 5-kinase in Swiss 3T3 cells." Mol Biol Cell **7** (3): 435.

Renshaw, MW, Lea-Chou, E and Wang, JY (1996). "Rac is required for v-Abl tyrosine kinase to activate mitogenesis." Curr Biol **6** (1): 76.

Ridley, A (2000). "Rho GTPases. Integrating integrin signaling." J Cell Biol **150** (4): F107.

Ridley, AJ (2000). Rho. GTPases. A Hall. Oxford, Oxford University Press: 89.

Ridley, AJ and Hall, A (1992). "The small GTP-binding protein rho regulates the assembly of focal adhesions and actin stress fibers in response to growth factors." Cell **70** (3): 389.

Ridley, AJ, et al. (1992). "The small GTP-binding protein rac regulates growth factor-induced membrane ruffling." Cell **70** (3): 401.

Riezman, H, et al. (1996). "Actin-, myosin- and ubiquitin-dependent endocytosis." Experientia **52** (12): 1033.

Rimm, DL, et al. (1995). "Alpha 1(E)-catenin is an actin-binding and -bundling protein mediating the attachment of F-actin to the membrane adhesion complex." Proc Natl Acad Sci U S A **92** (19): 8813.

Ringstad, N, et al. (1999). "Endophilin/SH3p4 is required for the transition from early to late stages in clathrin-mediated synaptic vesicle endocytosis." Neuron **24** (1): 143.

Ringstad, N, Nemoto, Y and De Camilli, P (1997). "The SH3p4/Sh3p8/SH3p13 protein family: binding partners for synaptojanin and dynamin via a Grb2-like Src homology 3 domain." Proc Natl Acad Sci U S A **94** (16): 8569.

Rittinger, K, Walker, PA, Eccleston, JF, Nurmahomed, K, et al. (1997). "Crystal structure of a small G protein in complex with the GTPase- activating protein rhoGAP." Nature **388** (6643): 693.

Rittinger, K, Walker, PA, Eccleston, JF, Smerdon, SJ, et al. (1997). "Structure at 1.65 A of RhoA and its GTPase-activating protein in complex with a transition-state analogue." Nature **389** (6652): 758.

Rivero-Lezcano, OM, et al. (1995). "Wiskott-Aldrich syndrome protein physically associates with Nck through Src homology 3 domains." Mol Cell Biol **15** (10): 5725.

Rizo, J and Sudhof, TC (1998). "C2-domains, structure and function of a universal Ca2+-binding domain." J Biol Chem **273** (26): 15879.

Robinson, PJ, et al. (1994). "Phosphorylation of dynamin I and synaptic-vesicle recycling." Trends Neurosci **17** (8): 348.

Robinson, PJ, et al. (1993). "Dynamin GTPase regulated by protein kinase C phosphorylation in nerve terminals." Nature **365** (6442): 163.

Rodriguez, MM, et al. (1999). "RACK1, a protein kinase C anchoring protein, coordinates the binding of activated protein kinase C and select pleckstrin homology domains in vitro." Biochemistry **38** (42): 13787.

Rodriguez-Viciana, P, et al. (1994). "Phosphatidylinositol-3-OH kinase as a direct target of Ras." Nature **370** (6490): 527.

Rodriguez-Viciana, P, et al. (1996). "Activation of phosphoinositide 3-kinase by interaction with Ras and by point mutation." Embo J **15** (10): 2442.

Rogers, S, Wells, R and Rechsteiner, M (1986). "Amino acid sequences common to rapidly degraded proteins: the PEST hypothesis." Science **234** (4774): 364.

Rohatgi, R, et al. (1999). "The interaction between N-WASP and the Arp2/3 complex links Cdc42-dependent signals to actin assembly." Cell **97** (2): 221.

Ron, D, et al. (1989). "The N-terminal region of proto-dbl down regulates its transforming activity." Oncogene **4** (9): 1067.

Ron, D, et al. (1988). "Molecular cloning and characterization of the human dbl proto-oncogene: evidence that its overexpression is sufficient to transform NIH/3T3 cells." Embo J **7** (8): 2465.

Roth, AF, Sullivan, DM and Davis, NG (1998). "A large PEST-like sequence directs the ubiquitination, endocytosis, and vacuolar degradation of the yeast a-factor receptor." J Cell Biol **142** (4): 949.

Rothe, M, et al. (1995). "The TNFR2-TRAF signaling complex contains two novel proteins related to baculoviral inhibitor of apoptosis proteins." Cell **83** (7): 1243.

Roulston, A, et al. (1998). "Early activation of c-Jun N-terminal kinase and p38 kinase regulate cell survival in response to tumor necrosis factor alpha." J Biol Chem **273** (17): 10232.

Rouse, J, et al. (1994). "A novel kinase cascade triggered by stress and heat shock that stimulates MAPKAP kinase-2 and phosphorylation of the small heat shock proteins." Cell **78**: 1027.

Roux, P, et al. (1997). "The small GTPases Cdc42Hs, Rac1 and RhoG delineate Raf-independent pathways that cooperate to transform NIH3T3 cells." Curr Biol **7** (9): 629.

Rozelle, AL, et al. (2000). "Phosphatidylinositol 4,5-bisphosphate induces actin-based movement of raft-enriched vesicles through WASP-Arp2/3." Curr Biol **10** (6): 311.

Rudolph, MG, et al. (1998). "The Cdc42/Rac interactive binding region motif of the Wiskott Aldrich syndrome protein (WASP) is necessary but not sufficient for tight binding to Cdc42 and structure formation." J Biol Chem **273** (29): 18067.

Rudolph, MG, et al. (1999). "Biochemical analysis of SopE from Salmonella typhimurium, a highly efficient guanosine nucleotide exchange factor for RhoGTPases." J Biol Chem **274** (43): 30501.

Sadoul, R, et al. (1996). "Involvement of the proteasome in the programmed cell death of NGF-deprived sympathetic neurons." Embo J **15** (15): 3845.

Sahai, E, Alberts, AS and Treisman, R (1998). "RhoA effector mutants reveal distinct effector pathways for cytoskeletal reorganization, SRF activation and transformation." Embo J **17** (5): 1350.

Sakisaka, T, et al. (1997). "Phosphatidylinositol 4,5-bisphosphate phosphatase regulates the rearrangement of actin filaments." Mol Cell Biol **17** (7): 3841.

Salcini, AE, et al. (1997). "Binding specificity and in vivo targets of the EH domain, a novel protein-protein interaction module." Genes Dev **11** (17): 2239.

Salim, K, et al. (1996). "Distinct specificity in the recognition of phosphoinositides by the pleckstrin homology domains of dynamin and Bruton's tyrosine kinase." Embo J **15** (22): 6241.

Sanchez-Perez, I, Murguia, JR and Perona, R (1998). "Cisplatin induces a persistent activation of JNK that is related to cell death." Oncogene **16** (4): 533.

Sander, EE, et al. (1999). "Rac downregulates Rho activity: reciprocal balance between both GTPases determines cellular morphology and migratory behavior." J Cell Biol **147** (5): 1009.

Sander, EE, et al. (1998). "Matrix-dependent Tiam1/Rac signaling in epithelial cells promotes either cell-cell adhesion or cell migration and is regulated by phosphatidylinositol 3-kinase." J Cell Biol **143** (5): 1385.

Sanders, LC, et al. (1999). "Inhibition of myosin light chain kinase by p21-activated kinase." Science **283** (5410): 2083.

Sansonetti, PJ (2000). "Phagocytosis, a cell biology view." J Cell Sci **113** (Pt 19): 3355.

Saurin, AJ, et al. (1996). "Does this have a familiar RING?" Trends Biochem Sci **21** (6): 208.

Scaife, R, et al. (1994). "Growth factor-induced binding of dynamin to signal transduction proteins involves sorting to distinct and separate proline-rich dynamin sequences." Embo J **13** (11): 2574.

Schaeffer, HJ, et al. (1998). "MP1: a MEK binding partner that enhances enzymatic activation of the MAP kinase cascade." Science **281** (5383): 1668.

Schafer, DA, D'Souza-Schorey, C and Cooper, JA (2000). "Actin Assembly at Membranes Controlled by ARF6." Traffic **1**: 892.

Scheffner, M, Huibregtse, JM and Howley, PM (1994). "Identification of a human ubiquitin-conjugating enzyme that mediates the E6-AP-dependent ubiquitination of p53." Proc Natl Acad Sci U S A **91** (19): 8797.

Scheffner, M, et al. (1991). "The state of the p53 and retinoblastoma genes in human cervical carcinoma cell lines." Proc Natl Acad Sci U S A **88** (13): 5523.

Scheffzek, K, Ahmadian, MR and Wittinghofer, A (1998). "GTPase-activating proteins: helping hands to complement an active site." Trends Biochem Sci **23** (7): 257.

Scherle, P, Behrens, T and Staudt, LM (1993). "Ly-GDI, a GDP-dissociation inhibitor of the RhoA GTP-binding protein, is expressed preferentially in lymphocytes." Proc Natl Acad Sci U S A **90** (16): 7568.

Scheufler, C, et al. (2000). "Structure of TPR domain-peptide complexes: critical elements in the assembly of the Hsp70-Hsp90 multichaperone machine." Cell **101** (2): 199.

Schmeichel, KL and Beckerle, MC (1997). "Molecular dissection of a LIM domain." Mol Biol Cell **8** (2): 219.

Schmid, SL (1997). "Clathrin-coated vesicle formation and protein sorting: an integrated process." Annu Rev Biochem **66**: 511.

Schmid, SL and Carter, LL (1990). "ATP is required for receptor-mediated endocytosis in intact cells." J Cell Biol **111** (6 Pt 1): 2307.

Schmidt, A, et al. (1997). "The yeast phosphatidylinositol kinase homolog TOR2 activates RHO1 and RHO2 via the exchange factor ROM2." Cell **88** (4): 531.

Schmidt, A, et al. (1999). "Endophilin I mediates synaptic vesicle formation by transfer of arachidonate to lysophosphatidic acid." Nature **401** (6749): 133.

Schmidt, G, et al. (1997). "Gln 63 of Rho is deamidated by Escherichia coli cytotoxic necrotizing factor-1." Nature **387** (6634): 725.

Schouten, GJ, et al. (1997). "IkappaB alpha is a target for the mitogen-activated 90 kDa ribosomal S6 kinase." Embo J **16** (11): 3133.

Schreck, R, Rieber, P and Baeuerle, PA (1991). "Reactive oxygen intermediates as apparently widely used messengers in the activation of the NF-kappa B transcription factor and HIV-1." Embo J **10** (8): 2247.

Schuebel, KE, et al. (1996). "Isolation and characterization of murine vav2, a member of the vav family of proto-oncogenes." Oncogene **13** (2): 363.

Schumacher, C, et al. (1995). "The SH3 domain of Crk binds specifically to a conserved proline-rich motif in Eps15 and Eps15R." J Biol Chem **270** (25): 15341.

Schurmann, A, et al. (2000). "p21-activated kinase 1 phosphorylates the death agonist bad and protects cells from apoptosis." Mol Cell Biol **20** (2): 453.

Schwartz, MA, Meredith, JE and Kiosses, WB (1998). "An activated Rac mutant functions as a dominant negative for membrane ruffling." Oncogene **17** (5): 625.

Seabra, MC, et al. (1991). "Protein farnesyltransferase and geranylgeranyltransferase share a common alpha subunit." Cell **65** (3): 429.

Seaman, MN, Ball, CL and Robinson, MS (1993). "Targeting and mistargeting of plasma membrane adaptors in vitro." J Cell Biol **123** (5): 1093.

Seedorf, K, et al. (1994). "Dynamin binds to SH3 domains of phospholipase C gamma and GRB-2." J Biol Chem **269** (23): 16009.

Segal, AW and Abo, A (1993). "The biochemical basis of the NADPH oxidase of phagocytes." Trends Biochem Sci **18** (2): 43.

Sells, MA, Boyd, JT and Chernoff, J (1999). "p21-activated kinase 1 (Pak1) regulates cell motility in mammalian fibroblasts." J Cell Biol **145** (4): 837.

Sells, MA, et al. (1997). "Human p21-activated kinase (Pak1) regulates actin organization in mammalian cells." Curr Biol **7** (3): 202.

Sengar, AS, et al. (1999). "The EH and SH3 domain Ese proteins regulate endocytosis by linking to dynamin and Eps15." Embo J **18** (5): 1159.

Settleman, J (1999). "Rho GTPases in development." Prog Mol Subcell Biol **22**: 201.

Sever, S, Damke, H and Schmid, SL (2000a). "Dynamin:GTP controls the formation of constricted coated pits, the rate limiting step in clathrin-mediated endocytosis." J Cell Biol **150** (5): 1137.

Sever, S, Damke, H and Schmid, SL (2000b). "Garrotes, Springs, Ratchets and Whips: Putting Dynamin Models to the Test." Traffic **1**: 385.

Sever, S, Muhlberg, AB and Schmid, SL (1999). "Impairment of dynamin's GAP domain stimulates receptor-mediated endocytosis." Nature **398** (6727): 481.

Sheikh, MS and Fornace, AJ, Jr. (2000). "Role of p53 family members in apoptosis." J Cell Physiol **182** (2): 171.

Shibasaki, Y, et al. (1997). "Massive actin polymerization induced by phosphatidylinositol-4- phosphate 5-kinase in vivo." J Biol Chem **272** (12): 7578.

Shih, W, Gallusser, A and Kirchhausen, T (1995). "A clathrin-binding site in the hinge of the beta 2 chain of mammalian AP-2 complexes." J Biol Chem **270** (52): 31083.

Shirsat, NV, et al. (1990). "A member of the ras gene superfamily is expressed specifically in T, B and myeloid hemopoietic cells." Oncogene **5** (5): 769.

Shpetner, HS, Herskovits, JS and Vallee, RB (1996). "A binding site for SH3 domains targets dynamin to coated pits." J Biol Chem **271** (1): 13.

Shpetner, HS and Vallee, RB (1989). "Identification of dynamin, a novel mechanochemical enzyme that mediates interactions between microtubules." Cell **59** (3): 421.

Shpetner, HS and Vallee, RB (1992). "Dynamin is a GTPase stimulated to high levels of activity by microtubules." Nature **355** (6362): 733.

Shupliakov, O, et al. (1997). "Synaptic vesicle endocytosis impaired by disruption of dynamin-SH3 domain interactions." Science **276** (5310): 259.

Simpson, F, et al. (1999). "SH3-domain-containing proteins function at distinct steps in clathrin- coated vesicle formation." Nat Cell Biol **1** (2): 119.

Skowyra, D, et al. (1999). "Reconstitution of G1 cyclin ubiquitination with complexes containing SCFGrr1 and Rbx1." Science **284** (5414): 662.

Slepnev, VI, et al. (2000). "Tandem arrangement of the clathrin and AP-2 binding domains in amphiphysin 1 and disruption of clathrin coat function by amphiphysin fragments comprising these sites." J Biol Chem **275** (23): 17583.

Slepnev, VI, et al. (1998). "Role of phosphorylation in regulation of the assembly of endocytic coat complexes." Science **281** (5378): 821.

Smirnova, E, et al. (1999). "A model for dynamin self-assembly based on binding between three different protein domains." J Biol Chem **274** (21): 14942.

Smirnova, E, et al. (1998). "A human dynamin-related protein controls the distribution of mitochondria." J Cell Biol **143** (2): 351.

Smith, CJ, Grigorieff, N and Pearse, BM (1998). "Clathrin coats at 21 A resolution: a cellular assembly designed to recycle multiple membrane receptors." Embo J **17** (17): 4943.

Somsel Rodman, J and Wandinger-Ness, A (2000). "Rab GTPases coordinate endocytosis." J Cell Sci **113 Pt 2**: 183.

Sone, M, et al. (1997). "Still life, a protein in synaptic terminals of Drosophila homologous to GDP-GTP exchangers [published erratum appears in Science 1997 Mar 7;275(5305):1405]." Science **275** (5299): 543.

Song, J, et al. (1998). "Localization of endogenous ARF6 to sites of cortical actin rearrangement and involvement of ARF6 in cell spreading." J Cell Sci **111** (Pt 15): 2257.

Sontag, JM, et al. (1994). "Differential expression and regulation of multiple dynamins." J Biol Chem **269** (6): 4547.

Soussi, T (2000). "The p53 tumor suppressor gene: from molecular biology to clinical investigation." Ann N Y Acad Sci **910**: 121.

Spaargaren, M and Bos, JL (1999). "Rab5 induces Rac-independent lamellipodia formation and cell migration." Mol Biol Cell **10** (10): 3239.

Stam, JC and Collard, JG (1999). "The DH protein family, exchange factors for Rho-like GTPases." Prog Mol Subcell Biol **22**: 51.

Stang, E, et al. (2000). "Polyubiquitination of the epidermal growth factor receptor occurs at the plasma membrane upon ligand-induced activation." J Biol Chem **275** (18): 13940.

Staub, O, Gautschi, I, et al. (1997). "Regulation of stability and function of the epithelial Na+ channel (ENaC) by ubiquitination." Embo J **16** (21): 6325.

Staub, O, Yeger, H, et al. (1997). "Immunolocalization of the ubiquitin-protein ligase Nedd4 in tissues expressing the epithelial Na+ channel (ENaC)." Am J Physiol **272** (6 Pt 1): C1871.

Stenmark, H and Aasland, R (1999). "FYVE-finger proteins--effectors of an inositol lipid." J Cell Sci **112** (Pt 23): 4175.

Stowell, MH, et al. (1999). "Nucleotide-dependent conformational changes in dynamin: evidence for a mechanochemical molecular spring." Nat Cell Biol **1** (1): 27.

Strous, GJ and Govers, R (1999). "The ubiquitin-proteasome system and endocytosis." J Cell Sci **112** (Pt 10): 1417.

Su, YC, et al. (1997). "NIK is a new Ste20-related kinase that binds NCK and MEKK1 and activates the SAPK/JNK cascade via a conserved regulatory domain." Embo J **1997** (16): 1279.

Su, YC, Treisman, JE and Skolnik, EY (1998). "The Drosophila Ste20-related kinase misshapen is required for embryonic dorsal closure and acts through a JNK MAPK module on an evolutionarily conserved signaling pathway." Genes Dev **12** (15): 2371.

Subauste, MC, et al. (2000). "Rho family proteins modulate rapid apoptosis induced by cytotoxic T lymphocytes and Fas." J Biol Chem **275** (13): 9725.

Suetsugu, S, Miki, H and Takenawa, T (1998). "The essential role of profilin in the assembly of actin for microspike formation." Embo J **17** (22): 6516.

Suh, YA, et al. (1999). "Cell transformation by the superoxide-generating oxidase Mox1." Nature **401** (6748): 79.

Sulciner, DJ, et al. (1996). "rac1 regulates a cytokine-stimulated, redox-dependent pathway necessary for NF-kappaB activation." Mol Cell Biol **16** (12): 7115.

Sweitzer, SM and Hinshaw, JE (1998). "Dynamin undergoes a GTP-dependent conformational change causing vesiculation." Cell **93** (6): 1021.

Symons, M, et al. (1996). "Wiskott-Aldrich syndrome protein, a novel effector for the GTPase CDC42Hs, is implicated in actin polymerization." Cell **84** (5): 723.

Takahashi, K, et al. (1997). "Direct interaction of the Rho GDP dissociation inhibitor with ezrin/radixin/moesin initiates the activation of the Rho small G protein." J Biol Chem **272** (37): 23371.

Takahashi, T, et al. (1999). "Plexin-neuropilin-1 complexes form functional semaphorin-3A receptors." Cell **99** (1): 59.

Takei, K, et al. (1998). "Generation of coated intermediates of clathrin-mediated endocytosis on protein-free liposomes." Cell **94** (1): 131.

Takei, K, et al. (1995). "Tubular membrane invaginations coated by dynamin rings are induced by GTP-gamma S in nerve terminals." Nature **374** (6518): 186.

Takei, K, et al. (1999). "Functional partnership between amphiphysin and dynamin in clathrin- mediated endocytosis." Nat Cell Biol **1** (1): 33.

Takeuchi, M, Rothe, M and Goeddel, DV (1996). "Anatomy of TRAF2. Distinct domains for nuclear factor-kappaB activation and association with tumor necrosis factor signaling proteins." J Biol Chem **271** (33): 19935.

Tamagnone, L, et al. (1999). "Plexins are a large family of receptors for transmembrane, secreted, and GPI-anchored semaphorins in vertebrates." Cell **99** (1): 71.

Tan, EC, et al. (1993). "The human active breakpoint cluster region-related gene encodes a brain protein with homology to guanine nucleotide exchange proteins and GTPase-activating proteins." J Biol Chem **268** (36): 27291.

Tang, AH, et al. (1997). "PHYL acts to down-regulate TTK88, a transcriptional repressor of neuronal cell fates, by a SINA-dependent mechanism." Cell **90** (3): 459.

Tang, HY, Munn, A and Cai, M (1997). "EH domain proteins Panlp and End3p are components of a complex that plays a dual role in organization of the cortical actin cytoskeleton and endocytosis in Saccharomyces cerevisiae." Mol Cell Biol **17** (8): 4294.

Tang, HY, Xu, J and Cai, M (2000). "Panlp, End3p, and S1a1p, three yeast proteins required for normal cortical actin cytoskeleton organization, associate with each other and play essential roles in cell wall morphogenesis." Mol Cell Biol **20** (1): 12.

Tang, TK, et al. (1998). "Proteolytic cleavage and activation of PAK2 during UV irradiation- induced apoptosis in A431 cells." J Cell Biochem **70** (4): 442.

Tang, Y, et al. (1997). "Kinase-deficient Pak1 mutants inhibit Ras transformation of Rat-1 fibroblasts." Mol Cell Biol **17** (8): 4454.

Tang, Y, Yu, J and Field, J (1999). "Signals from the Ras, Rac, and Rho GTPases converge on the Pak protein kinase in Rat-1 fibroblasts." Mol Cell Biol **19** (3): 1881.

Tang, Y, et al. (2000). "The Akt proto-oncogene links Ras to Pak and cell survival signals." J Biol Chem **275** (13): 9106.

Tapon, N (1998a). Identification of New Targets for the Rho and Rac GTPases. Biochemistry. London, University College London: 131.

Tapon, N (1998b). Identification of New Targets for the Rho and Rac GTPases. Biochemistry. London, University College London: 128.

Tapon, N, et al. (1998). "A new rac target POSH is an SH3-containing scaffold protein involved in the JNK and NF-kappaB signalling pathways." Embo J **17** (5): 1395.

Tarone, G, et al. (1985). "Rous sarcoma virus-transformed fibroblasts adhere primarily at discrete protrusions of the ventral membrane called podosomes." Exp Cell Res **159** (1): 141.

Teramoto, H, et al. (1996). "Signaling from the small GTP-binding proteins Rac1 and Cdc42 to the c- Jun N-terminal kinase/stress-activated protein kinase pathway. A role for mixed lineage kinase 3/protein-tyrosine kinase 1, a novel member of the mixed lineage kinase family." J Biol Chem **271** (44): 27225.

Terrell, J, et al. (1998). "A function for monoubiquitination in the internalization of a G protein- coupled receptor." Mol Cell **1** (2): 193.

Thompson, G, et al. (1998). "Delineation of the Cdc42/Rac-binding domain of p21-activated kinase." Biochemistry **37** (21): 7885.

Tolias, KF, Cantley, LC and Carpenter, CL (1995). "Rho family GTPases bind to phosphoinositide kinases." J Biol Chem **270** (30): 17656.

Tolias, KF, et al. (1998). "Characterization of a Rac1- and RhoGDI-associated lipid kinase signaling complex." Mol Cell Biol **18** (2): 762.

Tolias, KF, et al. (2000). "Type ialpha phosphatidylinositol-4-phosphate 5-kinase mediates rac- dependent actin assembly." Curr Biol **10** (3): 153.

Tong, XK, Hussain, NK, Adams, AG, et al. (2000). "Intersectin can regulate the Ras/MAP kinase pathway independent of its role in endocytosis." J Biol Chem **275** (38): 29894.

Tong, XK, Hussain, NK, de Heuvel, E, et al. (2000). "The endocytic protein intersectin is a major binding partner for the Ras exchange factor mSos1 in rat brain." Embo J **19** (6): 1263.

Torre, E, McNiven, MA and Urrutia, R (1994). "Dynamin 1 antisense oligonucleotide treatment prevents neurite formation in cultured hippocampal neurons." J Biol Chem **269** (51): 32411.

Touhara, K, et al. (1994). "Binding of G protein beta gamma-subunits to pleckstrin homology domains." J Biol Chem **269** (14): 10217.

Treier, M, Staszewski, LM and Bohmann, D (1994). "Ubiquitin-dependent c-Jun degradation in vivo is mediated by the delta domain." Cell **78** (5): 787.

Treisman, R (1996). "Regulation of transcription by MAP kinase cascades." Curr Opin Cell Biol **8** (2): 205.

Trenkle, T, et al. (2000). "Major transcript variants of VAV3, a new member of the VAV family of guanine nucleotide exchange factors." Gene **245** (1): 139.

Trowbridge, IS, Collawn, JF and Hopkins, CR (1993). "Signal-dependent membrane protein trafficking in the endocytic pathway." Annu Rev Cell Biol **9**: 129.

Tsukamoto, T and Nigam, SK (1999). "Cell-cell dissociation upon epithelial cell scattering requires a step mediated by the proteasome." J Biol Chem **274** (35): 24579.

Tu, H and Wigler, M (1999). "Genetic evidence for Pak1 autoinhibition and its release by Cdc42." Mol Cell Biol **19** (1): 602.

Tuma, PL and Collins, CA (1994). "Activation of dynamin GTPase is a result of positive cooperativity." J Biol Chem **269** (49): 30842.

Tuma, PL and Collins, CA (1995). "Dynamin forms polymeric complexes in the presence of lipid vesicles. Characterization of chemically cross-linked dynamin molecules." J Biol Chem **270** (44): 26707.

Tuma, PL, Stachniak, MC and Collins, CA (1993). "Activation of dynamin GTPase by acidic phospholipids and endogenous rat brain vesicles." J Biol Chem **268** (23): 17240.

Tung, RM and Blenis, J (1997). "A novel human SPS1/STE20 homologue, KHS, activates Jun N-terminal kinase." Oncogene **14**: 653.

Turner, CE, et al. (1999). "Paxillin LD4 motif binds PAK and PIX through a novel 95-kD ankyrin repeat, ARF-GAP protein: A role in cytoskeletal remodeling." J Cell Biol **145** (4): 851.

Turner, KM, Burgoyne, RD and Morgan, A (1999). "Protein phosphorylation and the regulation of synaptic membrane traffic." Trends Neurosci **22** (10): 459.

Tyers, M and Willems, AR (1999). "One ring to rule a superfamily of E3 ubiquitin ligases." Science **284** (5414): 601.

Ungewickell, E, et al. (1995). "Role of auxilin in uncoating clathrin-coated vesicles." Nature **378** (6557): 632.

Vallis, Y, et al. (1999). "Importance of the pleckstrin homology domain of dynamin in clathrin- mediated endocytosis." Curr Biol **9** (5): 257.

Van Aelst, L and D'Souza-Schorey, C (1997). "Rho GTPases and signaling networks." Genes Dev **11** (18): 2295.

Van Aelst, L, Joneson, T and Bar-Sagi, D (1996). "Identification of a novel Rac1-interacting protein involved in membrane ruffling." Embo J **15** (15): 3778.

van Delft, S, Govers, R, et al. (1997). "Epidermal growth factor induces ubiquitination of Eps15." J Biol Chem **272** (22): 14013.

van Delft, S, Schumacher, C, et al. (1997). "Association and colocalization of Eps15 with adaptor protein-2 and clathrin [published erratum appears in J Cell Biol 1997 Apr 7;137(1):259]." J Cell Biol **136** (4): 811.

van der Bliek, AM and Meyerowitz, EM (1991). "Dynamin-like protein encoded by the Drosophila shibire gene associated with vesicular traffic." Nature **351** (6325): 411.

van der Bliek, AM, et al. (1993). "Mutations in human dynamin block an intermediate stage in coated vesicle formation." J Cell Biol **122** (3): 553.

van Leeuwen, FN, et al. (1999). "Rac regulates phosphorylation of the myosin-II heavy chain, actinomyosin disassembly and cell spreading." Nat Cell Biol **1** (4): 242.

van Leeuwen, FN, et al. (1995). "Oncogenic activity of Tiam1 and Rac1 in NIH3T3 cells." Oncogene **11** (11): 2215.

Vastrik, I, et al. (1999). "Sema3A-induced growth-cone collapse is mediated by Rac1 amino acids 17- 32." Curr Biol **9** (18): 991.

Vidal, M, et al. (1999). "Molecular and cellular analysis of Grb2 SH3 domain mutants: interaction with Sos and dynamin." J Mol Biol **290** (3): 717.

Vidal, M, et al. (1998). "Differential interactions of the growth factor receptor-bound protein 2 N-SH3 domain with son of sevenless and dynamin. Potential role in the Ras-dependent signaling pathway." J Biol Chem **273** (9): 5343.

Vigers, GP, Crowther, RA and Pearse, BM (1986). "Location of the 100 kd-50 kd accessory proteins in clathrin coats." Embo J **5** (9): 2079.

Vignal, E, et al. (2000). "Characterization of TCL, a New GTPase of the Rho Family related to TC10 and Cdc42." J Biol Chem **275** (46): 36457.

Vikis, HG, et al. (2000). "The semaphorin receptor plexin-B1 specifically interacts with active rac in a ligand-dependent manner." Proc Natl Acad Sci U S A **97** (23): 12457.

Vincent, S, Jeanteur, P and Fort, P (1992). "Growth-regulated expression of rhoG, a new member of the ras homolog gene family." Mol Cell Biol **12** (7): 3138.

Vincent, S and Settleman, J (1997). "The PRK2 kinase is a potential effector target of both Rho and Rac GTPases and regulates actin cytoskeletal organization." Mol Cell Biol **17** (4): 2247.

Von Pawel-Rammingen, U, et al. (2000). "GAP activity of the Yersinia YopE cytotoxin specifically targets the Rho pathway: a mechanism for disruption of actin microfilament structure." Mol Microbiol **36** (3): 737.

Wada, S, et al. (1998). "Involvement of growth factor receptor-bound protein-2 in rat hepatocyte growth." J Gastroenterol Hepatol **13** (6): 635.

Wang, CY, et al. (1999). "NF-kappaB induces expression of the Bcl-2 homologue A1/Bfl-1 to preferentially suppress chemotherapy-induced apoptosis." Mol Cell Biol **19** (9): 5923.

Wang, CY, et al. (1998). "NF-kappaB antiapoptosis: induction of TRAF1 and TRAF2 and c-IAP1 and c-IAP2 to suppress caspase-8 activation." Science **281** (5383): 1680.

Wang, DS, et al. (1995). "Binding of pleckstrin homology domains to WD40/beta-transducin repeat containing segments of the protein product of the Lis-1 gene." Biochem Biophys Res Commun **209** (2): 622.

Wang, Z and Moran, MF (1996). "Requirement for the adapter protein GRB2 in EGF receptor endocytosis." Science **272** (5270): 1935.

Warnock, DE, Baba, T and Schmid, SL (1997). "Ubiquitously expressed dynamin-II has a higher intrinsic GTPase activity and a greater propensity for self-assembly than neuronal dynamin-I." Mol Biol Cell **8** (12): 2553.

Warnock, DE, Hinshaw, JE and Schmid, SL (1996). "Dynamin self-assembly stimulates its GTPase activity." J Biol Chem **271** (37): 22310.

Warnock, DE, Terlecky, LJ and Schmid, SL (1995). "Dynamin GTPase is stimulated by crosslinking through the C-terminal proline-rich domain." Embo J **14** (7): 1322.

Waterman, H, et al. (1999). "The RING finger of c-Cbl mediates desensitization of the epidermal growth factor receptor." J Biol Chem **274** (32): 22151.

Waterman-Storer, CM, Salmon, WC and Salmon, ED (2000). "Feedback interactions between cell-cell adherens junctions and cytoskeletal dynamics in newt lung epithelial cells." Mol Biol Cell **11** (7): 2471.

Wei, Y, et al. (1997). "Crystal structure of RhoA-GDP and its functional implications [letter]." Nat Struct Biol **4** (9): 699.

Weissbach, L, et al. (1994). "Identification of a human rasGAP-related protein containing calmodulin-binding motifs." J Biol Chem **269** (32): 20517.

Weissman, AM (1997). "Regulating protein degradation by ubiquitination." Immunol Today **18** (4): 189.

Welch, H, et al. (1998). "Protein kinase B and rac are activated in parallel within a phosphatidylinositide 3OH-kinase-controlled signaling pathway." J Biol Chem **273** (18): 11248.

Welch, MD (1999). "The world according to Arp: regulation of actin nucleation by the Arp2/3 complex." Trends Cell Biol **9** (11): 423.

Werbonat, Y, et al. (2000). "Essential role of dynamin in internalization of M2 muscarinic acetylcholine and angiotensin AT1A receptors." J Biol Chem **275** (29): 21969.

Wesp, A, et al. (1997). "End4p/Sla2p interacts with actin-associated proteins for endocytosis in Saccharomyces cerevisiae." Mol Biol Cell **8** (11): 2291.

West, MA, Bright, NA and Robinson, MS (1997). "The role of ADP-ribosylation factor and phospholipase D in adaptor recruitment." J Cell Biol **138** (6): 1239.

West, MA, et al. (2000). "Rac is required for constitutive macropinocytosis by dendritic cells but does not control its downregulation." Curr Biol **10** (14): 839.

Westphal, RS, et al. (1999). "Identification of kinase-phosphatase signaling modules composed of p70 S6 kinase-protein phosphatase 2A (PP2A) and p21-activated kinase-PP2A." J Biol Chem **274** (2): 687.

Westwick, JK, et al. (1997). "Rac regulation of transformation, gene expression, and actin organization by multiple, PAK-independent pathways." Mol Cell Biol **17** (3): 1324.

Westwick, JK, et al. (1998). "Transforming potential of Dbl family proteins correlates with transcription from the cyclin D1 promoter but not with activation of Jun NH2-terminal kinase, p38/Mpk2, serum response factor, or c-Jun." J Biol Chem **273** (27): 16739.

Whistler, JL and von Zastrow, M (1999). "Dissociation of functional roles of dynamin in receptor-mediated endocytosis and mitogenic signal transduction." J Biol Chem **274** (35): 24575.

Whitehead, IP, et al. (1997). "Dbl family proteins." Biochim Biophys Acta **1332** (1): F1.

Whitmarsh, AJ, et al. (1998). "A mammalian scaffold complex that selectively mediates MAP kinase activation." Science **281** (5383): 1671.

Whitmarsh, AJ and Davis, RJ (1998). "Structural organization of MAP-kinase signaling modules by scaffold proteins in yeast and mammals." Trends Biochem Sci **23** (12): 481.

Whitmarsh, AJ, et al. (1995). "Integration of MAP Kinase Signal Transduction Pathways at the Serum Response Element." Science **269**: 403.

Whitmarsh, AJ, et al. (1997). "Role of p38 and JNK MAP kinases in the activation of ternary complex factors." Mol Cell Biol **17**: 2360.

Widmann, C, Gibson, S and Johnson, GL (1998). "Caspase-dependent cleavage of signaling proteins during apoptosis. A turn-off mechanism for anti-apoptotic signals." J Biol Chem **273** (12): 7141.

Wigge, P, et al. (1997). "Amphiphysin heterodimers: potential role in clathrin-mediated endocytosis." Mol Biol Cell **8** (10): 2003.

Wigge, P and McMahon, HT (1998). "The amphiphysin family of proteins and their role in endocytosis at the synapse." Trends Neurosci **21** (8): 339.

Wigge, P, Vallis, Y and McMahon, HT (1997). "Inhibition of receptor-mediated endocytosis by the amphiphysin SH3 domain." Curr Biol **7** (8): 554.

Wilde, A, et al. (1999). "EGF receptor signaling stimulates SRC kinase phosphorylation of clathrin, influencing clathrin redistribution and EGF uptake." Cell **96** (5): 677.

Witke, W, et al. (1998). "In mouse brain profilin I and profilin II associate with regulators of the endocytic pathway and actin assembly." Embo J **17** (4): 967.

Wittinghofer, A and Nassar, N (1996). "How Ras-related proteins talk to their effectors." Trends Biochem Sci **21** (12): 488.

Wolosewick, JJ (1984). "Distribution of actin in migrating leukocytes in vivo." Cell Tissue Res **236** (3): 517.

Wong, ED, et al. (2000). "The dynamin-related GTPase, Mgm1p, is an intermembrane space protein required for maintenance of fusion competent mitochondria." J Cell Biol **151** (2): 341.

Wong, WT, et al. (1995). "A protein-binding domain, EH, identified in the receptor tyrosine kinase substrate Eps15 and conserved in evolution." Proc Natl Acad Sci U S A **92** (21): 9530.

Worthylake, DK, Rossman, KL and Sondek, J (2000). "Crystal structure of Rac1 in complex with the guanine nucleotide exchange region of Tiam1." Nature **408**: 682 .

Wu, H and Parsons, JT (1993). "Cortactin, an 80/85-kilodalton pp60src substrate, is a filamentous actin-binding protein enriched in the cell cortex." J Cell Biol **120** (6): 1417.

Wu, X, et al. (1995). "Structural basis for the specific interaction of lysine-containing proline-rich peptides with the N-terminal SH3 domain of c-Crk." Structure **3** (2): 215.

Xia, Y, et al. (2000). "MEK kinase 1 is critically required for c-Jun N-terminal kinase activation by proinflammatory stimuli and growth factor-induced cell migration." Proc Natl Acad Sci U S A **97** (10): 5243.

Xie, Y and Varshavsky, A (1999). "The E2-E3 interaction in the N-end rule pathway: the RING-H2 finger of E3 is required for the synthesis of multiubiquitin chain." Embo J **18** (23): 6832.

Yamabhai, M, et al. (1998). "Intersectin, a novel adaptor protein with two Eps15 homology and five Src homology 3 domains." J Biol Chem **273** (47): 31401.

Yang, D, et al. (1997). "Absence of exitotoxicity-induced apoptosis in the hippocampus of mice lacking the JNK3 gene." Nature **389**: 865.

Yang, N, et al. (1998). "Cofilin phosphorylation by LIM-kinase 1 and its role in Rac-mediated actin reorganization." Nature **393** (6687): 809.

Yao, L, et al. (1999). "Pleckstrin homology domains interact with filamentous actin." J Biol Chem **274** (28): 19752.

Yap, AS, Brieher, WM and Gumbiner, BM (1997). "Molecular and functional analysis of cadherin-based adherens junctions." Annu Rev Cell Dev Biol **13**: 119.

Yaron, A, et al. (1997). "Inhibition of NF-kappa-B cellular function via specific targeting of the I-kappa-B-ubiquitin ligase." Embo J **16** (21): 6486.

Yaron, A, et al. (1998). "Identification of the receptor component of the IkappaBalpha-ubiquitin ligase." Nature **396** (6711): 590.

Yasuda, J, et al. (1999). "The JIP group of mitogen-activated protein kinase scaffold proteins." Mol Cell Biol **19** (10): 7245.

Ye, W, et al. (1995). "Inhibition of clathrin assembly by high affinity binding of specific inositol polyphosphates to the synapse-specific clathrin assembly protein AP-3." J Biol Chem **270** (4): 1564.

Yokouchi, M, et al. (1999). "Ligand-induced ubiquitination of the epidermal growth factor receptor involves the interaction of the c-Cbl RING finger and UbcH7." J Biol Chem **274** (44): 31707.

Yoshii, S, et al. (1999). "alphaPIX nucleotide exchange factor is activated by interaction with phosphatidylinositol 3-kinase." Oncogene **18** (41): 5680.

Yu, H, et al. (1994). "Structural basis for the binding of proline-rich peptides to SH3 domains." Cell **76** (5): 933.

Zalcman, G, et al. (1996). "RhoGDI-3 is a new GDP dissociation inhibitor (GDI). Identification of a non-cytosolic GDI protein interacting with the small GTP-binding proteins RhoB and RhoG." J Biol Chem **271** (48): 30366.

Zhang, G, et al. (1995). "Crystal structure of the cys2 activator-binding domain of protein kinase C delta in complex with phorbol ester." Cell **81** (6): 917.

Zhang, JZ, et al. (1994). "Synaptotagmin I is a high affinity receptor for clathrin AP-2: implications for membrane recycling." Cell **78** (5): 751.

Zhang, Q, et al. (1999). "ARF6 is required for growth factor- and rac-mediated membrane ruffling in macrophages at a stage distal to rac membrane targeting." Mol Cell Biol **19** (12): 8158.

Zhang, Q, et al. (1998). "A requirement for ARF6 in Fcgamma receptor-mediated phagocytosis in macrophages." J Biol Chem **273** (32): 19977.

Zhang, S, et al. (1995). "Rho family GTPases regulate p38 mitogen-activated protein kinase through the downstream mediator Pak1." J Biol Chem **270** (41): 23934.

Zhao, ZS, et al. (1998). "A conserved negative regulatory region in alphaPAK: inhibition of PAK kinases reveals their morphological roles downstream of Cdc42 and Rac1." Mol Cell Biol **18** (4): 2153.

Zhao, ZS, Manser, E and Lim, L (2000). "Interaction between PAK and nck: a template for Nck targets and role of PAK autophosphorylation." Mol Cell Biol **20** (11): 3906.

Zhao, ZS, et al. (2000). "Coupling of PAK-interacting exchange factor PIX to GIT1 promotes focal complex disassembly." Mol Cell Biol **20** (17): 6354.

Zheng, N, et al. (2000). "Structure of a c-Cbl-UbcH7 complex: RING domain function in ubiquitin- protein ligases." Cell **102** (4): 533.

Zheng, Y, Bagrodia, S and Cerione, RA (1994). "Activation of phosphoinositide 3-kinase activity by Cdc42Hs binding to p85." J Biol Chem **269** (29): 18727.

Zheng, Y, Fischer, DJ, et al. (1996). "The faciogenital dysplasia gene product FGD1 functions as a Cdc42Hs- specific guanine-nucleotide exchange factor." J Biol Chem **271** (52): 33169.

Zheng, Y, Zangrilli, D, et al. (1996). "The pleckstrin homology domain mediates transformation by oncogenic dbl through specific intracellular targeting." J Biol Chem **271** (32): 19017.

Zhong, S, et al. (2000). "Role of SUMO-1-modified PML in nuclear body formation." Blood **95** (9): 2748.

Zong, H, et al. (1999). "Loop 6 of RhoA confers specificity for effector binding, stress fiber formation, and cellular transformation." J Biol Chem **274** (8): 4551.